ELISA VON GROLL

TAXONOMY, HOST ASSOCIATIONS, AND COLLECTING METHODS OF SHINING FUNGUS BEETLES (COLEOPTERA: STAPHYLINIDAE: SCAPHIDIINAE) IN FRAGMENTS OF THE ATLANTIC FOREST IN MINAS GERAIS, SOUTHEASTERN BRAZIL

Tese apresentada à Universidade Federal de Viçosa, como parte das exigências do Programa de Pós-Graduação em Biologia Animal, para obtenção do título de *Doctor Scientiae.*

Orientador: Cristiano Lopes Andrade

VIÇOSA - MINAS GERAIS

2024

Ficha catalográfica elaborada pela Biblioteca Central da Universidade Federal de Viçosa - Campus Viçosa

T
G875t
2024

Groll, Elisa von, 1988-
Taxonomy, host associations, and collecting methods of shining fungus beetles (Coleoptera: Staphylinidae: Scaphidiinae) in fragments of the Atlantic Forest in Minas Gerais, southeastern Brazil / Elisa von Groll. – Viçosa, MG, 2024.
1 tese eletrônica (327f.): il. (algumas color.).

Orientador: Cristiano Lopes Andrade.
Tese (doutorado) - Universidade Federal de Viçosa, Departamento de Biologia Animal, 2024.
Inclui bibliografia.
DOI: https://doi.org/10.47328/ufvbbt.2024.120
Modo de acesso: World Wide Web.

1. Besouro. 2. Besouro - Morfologia. 3. Biodiversidade. 4. Fungos. I. Andrade, Cristiano Lopes, 1980-. II. Universidade Federal de Viçosa. Departamento de Biologia Animal. Programa de Pós-graduação em Biologia Animal. III. Título.

CDD 22. ed. 595.7642

Bibliotecário(a) responsável: Advania Elza da Silva CRB-6/3263

ELISA VON GROLL

TAXONOMY, HOST ASSOCIATIONS, AND COLLECTING METHODS OF SHINING FUNGUS BEETLES (COLEOPTERA: STAPHYLINIDAE: SCAPHIDIINAE) IN FRAGMENTS OF THE ATLANTIC FOREST IN MINAS GERAIS, SOUTHEASTERN BRAZIL

Tese apresentada à Universidade Federal de Viçosa, como parte das exigências do Programa de Pós-Graduação em Biologia Animal, para obtenção do título de *Doctor Scientiae.*

APROVADA: 15 janeiro 2024.

Assentimento:

gov.br Documento assinado digitalmente
ELISA VON GROLL
Data: 26/03/2024 14:30:55-0300
Verifique em https://validar.iti.gov.br

Elisa von Groll

Autora

gov.br Documento assinado digitalmente
CRISTIANO LOPES ANDRADE
Data: 08/04/2024 19:08:42-0300
Verifique em https://validar.iti.gov.br

Cristiano Lopes Andrade

Orientador

Para o meu afilhado Miguel, pois esses
quatro anos em que estive distante
jamais poderiam ter sido em vão.

AGRADECIMENTOS

Expresso minha profunda gratidão a todos que me apoiaram ao longo da minha jornada acadêmica. Inúmeras pessoas, algumas das quais talvez desconheçam a importância de suas contribuições, foram fundamentais para o meu percurso. Desde gestos pequenos até grandes atos, cada um desempenhou um papel crucial, permitindo-me avançar, apesar dos contra tempos.

Embora eu desejasse mencionar individualmente cada pessoa que me ajudou, por razões excepcionais, optei por não o fazer. Contudo, é muito importante que todos saibam que a conclusão deste doutorado não teria sido possível sem o encorajamento e o apoio constante de cada um que me incentivou, impedindo-me de desistir ou sucumbir.

Expresso minha profunda gratidão ao The Field Museum of Natural History e à The Coleopterists Society pelas verbas que possibilitaram minha estadia temporária no FMNH. Realizar uma experiência no exterior sempre foi um sonho, e foi somente dessa maneira que pude concretizá-lo. A imersão na coleção de Scaphidiinae no museu foi de extrema importância para uma compreensão mais profunda da diversidade desse grupo.

Agradeço à Coordenação de Aperfeiçoamento de Pessoal de Nível Superior (CAPES) pela concessão da bolsa de estudos. Minha gratidão se estende aos profissionais da Divisão Psicossocial e da Divisão de Saúde da Universidade Federal de Viçosa (UFV), cujo suporte foi fundamental para minha recuperação. Por fim, agradeço ao Departamento de Biologia Animal da UFV por conceder a estrutura necessária para a realização deste trabalho.

RESUMO

VON GROLL, Elisa, D.Sc., Universidade Federal de Viçosa, janeiro de 2024. **Taxonomia, associação com hospedeiros e métodos de coleta de besouros Scaphidiinae (Coleoptera: Staphylinidae) em fragmentos de Floresta de Mata Atlântica em Minas Gerais, sudeste do Brasil.** Orientador: Cristiano Lopes Andrade.

A subfamília Scaphidiinae, que até 1997 abrigava pouco mais de 1000 espécies, agora registra mais de 2000 espécies, indicando um contínuo aumento que não mostra sinais de estabilização iminente. Apesar de sua maior diversidade se concentrar nos trópicos, a Região Neotropical permanece pouco estudada em relação a essa subfamília. Portanto, o objetivo desta tese é preencher a lacuna no conhecimento existente sobre esses besouros. Para isso, foram conduzidas coletas, dissecções, redescrições e descrições de novas espécies. A pesquisa resultou em quatro artigos já publicados, e um quinto está em processo de publicação. No primeiro artigo, uma nova espécie (*Scaphisoma pandemum* von Groll & Lopes-Andrade, 2021) é descrita para o Brasil. No segundo artigo, um novo método para a coleta de besouros em cogumelos é apresentado. No terceiro, cinco novas espécies do gênero *Cyparium* Erichson, 1845 são descritas, além de apresentar duas redescrições. O quarto artigo traz um novo registro para o Brasil: *S. nigrofasciatum* Pic, 1915, uma espécie originaria da Ásia foi registrada para Minas Gerais, Brasil. No quinto artigo, ainda a ser publicado, 20 novas espécies são descritas, estando distribuídas nos seguintes cinco gêneros: *Cyparium*, *Alexidia* Reitter, 1880, *Baeocera* Erichson, 1845, *Scaphisoma* Leach, 1815, and *Toxidium* LeConte, 1860. Todos os artigos de cunho taxonômico incluem, sempre que possível, ilustrações da morfologia externa e interna de machos e fêmeas, acompanhadas de dados relacionados ao hospedeiro. Além dos resultados taxonômicos, as coletas realizadas em Minas Gerais ampliaram significativamente a Coleção Entomológica do Laboratório de Sistemática e Biologia de Coleoptera da Universidade Federal de Viçosa (CELC), tornando-a a maior coleção de Scaphidiinae no Brasil, com mais de 1800 espécimes, facilitando, assim, a continuidade das pesquisas sobre esse grupo.

Palavras-chave: Biodiversidade; fungos; morfologia; Região Neotropical.

ABSTRACT

VON GROLL, Elisa, D.Sc., Universidade Federal de Viçosa, January, 2024. **Taxonomy, host associations, and collecting methods of shining fungus beetles (Coleoptera: Staphylinidae: Scaphidiinae) in fragments of the Atlantic Forest in Minas Gerais, southeastern Brazil.** Advisor: Cristiano Lopes Andrade.

The subfamily Scaphidiinae, which included just over 1000 species until 1997, now records over 2000 species, indicating a continuous increase that shows no signs of imminent stabilization. Despite its greatest diversity being concentrated in the tropics, the Neotropical Region remains understudied concerning this subfamily. Therefore, the objective of this thesis is to fill the existing knowledge gap about these insects. To achieve this goal, collections, dissections, redescriptions, and descriptions of new species were conducted. The research has resulted in four already published articles, with a fifth in the process of publication. In the first article, a new species (*Scaphisoma pandemum* von Groll & Lopes-Andrade, 2021) is described for Brazil. The second article introduces a new method for collecting beetles in fungi. The third article describes five new species of the genus *Cyparium* Erichson, 1845, and redescribes two species. The fourth article brings a new record for Brazil: *S. nigrofasciatum* Pic, 1915, original from Asia was collected in Minas Gerais. The fifth article, yet to be published, presents 20 new species distributed across five genera: *Cyparium*, *Alexidia* Reitter, 1880, *Baeocera* Erichson, 1845, *Scaphisoma* Leach, 1815, and *Toxidium* LeConte, 1860. All taxonomic papers include, whenever possible, illustrations of the external and internal morphology of males and females, accompanied by data related to the host. In addition to taxonomic results, the collections made in Minas Gerais have significantly expanded the Entomological Collection of the Laboratory of Systematics and Biology of Coleoptera at the Federal University of Viçosa (CELC), making it the largest collection of Scaphidiinae in Brazil, with more than 1800 specimens, enabling the continuation of research on this group.

Keywords: Biodiversity; fungi; morphology; Neotropical Region.

SUMARY

1. INTRODUCTION

1.1 Scaphidiinae Latreille, 1806

Shining fungus beetles are small beetles (≅0.84–14.0 mm long) worldwide distributed (LÖBL & OGAWA, 2016; TANG *et al.*, 2014). They are diverse and abundant in most terrestrial ecosystems, especially tropical and subtropical forests (LESCHEN & LÖBL, 1995). These beetles are typically collected on fungi, slime molds, through sifting litter, or by flight intercept traps (LAWRENCE & NEWTON, 1980; NEWTON, 1984; LESCHEN, 1994; STEPHENSON *et al.*, 1994; LÖBL & LESCHEN, 2003a; TANG *et al.*, 2014; LÖBL, 2018; LÖBL *et al.*, 2021).

Most studies on Scaphidiinae focus on describing new species, usually providing descriptions of the external morphology and the male aedeagus. Some papers illustrate larvae and/or describe the larval biology of certain species (KASULE, 1968; ASHE, 1984; KOMPANTSEV & POTOTSKAYA, 1987; NEWTON, 1991; LESCHEN, 1994; HANLEY 1996). Only two phylogenetic studies have been conducted specificity on scaphidiines: (1) to define tribes and generic limits (LESCHEN & LÖBL, 1995), and (2) to examine the Scaphisomatini Casey, 1893 status (LESCHEN & LÖBL, 2005).

There is a significant gap in the biological and taxonomical information on Neotropical Scaphidiinae. No specialist on scaphidiines has been resident in South America, and a comprehensive taxonomic revision of Neotropical species has not been undertaken until now. The limited works exclusively or primarily dedicated to Neotropical scaphidiines were conducted by Fierros-López (1998; 2002; 2005; 2006a; 2006b; 2010) on Mexican species, Löbl and Leschen (2003b) on the neotropical genus *Alexidia* Reitter, 1880, and Löbl (1974) on the Brazilian genus *Amalocera* Erichson, 1845.

Within the Neotropical region (*sensu* MORRONE, 2015), the Brazilian scaphidiine fauna is one of the least known, with only 32 species and subspecies, distributed in seven genera, recorded in the country so far (LÖBL, 2018; von GROLL & LOPES-ANDRADE, 2021; 2022). This is inconsistent with the expected diversity of these organisms in such a vast territory with different biomes and a wide availability of fungi and slime molds.

Taxonomic history

Scaphidiinae Latreille, 1807 (Coleoptera, Staphylinidae) was initially described as a family (Scaphidiidae) to include the so-called “shining fungus beetles”, characterized by the compact,

oval, and curved body, long legs, 1–2 exposed abdominal segments, antennae on frons, between eyes, among other features. However, while studying beetle larvae from different subfamilies of Staphylinidae and closely related groups, Kasule (1966) concluded that the larva of ‘Scaphidiidae’ were morphologically similar to the larvae of Staphylinidae. Therefore, Kasule (1966) downgraded to a subfamily status: Scaphidiinae. Although it took some time for coleopterists to accept this new classification (LÖBL & LESCHEN, 2003a), it is now widely recognized. Scaphidiinae was then placed in the Oxyteline group of Staphylinidae (LAWRENCE & NEWTON, 1982; NEWTON & THAYER, 1992).

Over the years, the number of Scaphidiinae species has considerably increased. Previously considered a taxon with low diversity, it now encompasses approximately 1800 described species organized into 36 genera and four tribes: Cypariini Achard, 1924, Scaphiini Achard, 1924, Scaphidiini Latreille, 1806, and Scaphisomatini Casey, 1893 (LÖBL, 2018). The first catalog, published 61 years after the establishment of this group, included 51 valid species and nine genera (GEMMINGER & HAROLD, 1868). The second catalog increased the number of species to 241 and 19 genera (CSIKI, 1908), while the third catalog included only 245 described species and 21 genera (CSIKI, 1910). The fourth catalog reported a significant jump, with 1287 species in 45 genera (LÖBL, 1997).

Based on undescribed material housed in museums, it is known that the diversity of Scaphidiinae in tropical and subtropical regions is significantly greater than what has been reported in the scientific literature (LESCHEN & LÖBL, 1995). However, only 171 species and 12 subspecies are recorded from the Neotropical region (Löbl, 2018; von GROLL & LOPES-ANDRADE, 2021; 2022). It is plausible to assume that the number of Neotropical Scaphidiinae is much higher than currently known.

1.2 Phylogenetic relationships and classification

Initially, the classification of Scaphidiinae was based on Achard's work (1914). Nonetheless, the tribes and their subdivisions were not proposed following Linnaean classification principles (LESCHEN & LÖBL, 2005). In this sense, relationships among tribes and genera of shining fungus beetles began to be better understood through a phylogenetic analysis that included 69 characters representing all Scaphidiinae tribes and genera of Cypariini and Scaphidiini (Leschen & Löbl, 1995). This analysis was further developed by Löbl in 1997.

The position of Scaphidiinae within the family Staphylinidae and other Staphylinoidea was more elucidated by a phylogeny that included families within Staphylinoidea (Scaphidiinae was still considered a family in this study). As a result, Hansen (1997) suggested that Scaphidiinae forms a highly monophyletic group and is more likely to be placed between 'Scydmaenidae' and 'Empelidae' (both of which are now considered subfamilies of Staphylinidae).

In 2005, a cladistics analysis was performed to examine the status of the tribes of Scaphisomatini (LESCHEN & LÖBL, 2005). This analysis included 47 terminal taxa and 110 adult characters and revealed that the Scaphisomatini subtribes were paraphyletic, leading to their synonymy under Scaphisomatini.

Subsequent studies that analyzed the position of Scaphidiinae within Staphylinidae also supported the strong monophyly of Scaphidiinae (GREBENNIKOV & NEWTON, 2012; MCKENNA *et al*., 2014). The current position of Scaphidiinae is part of the Oxitelinae group: “Scaphidiinae + (Oxytelinae + Osoriinae + Piestinae)” (Grebennikov & Newton, 2012).

1.3 Interactions with fungi and slime molds, and development

Although Scaphidiinae beetles belong to the predominantly saprophagous and predatory group Oxyteline (Staphylinidae), both the larvae and adults of these beetles feed on a variety of fungi and slime molds, particularly wood-rooting Basidiomycete fungi (LAWRENCE & NEWTON, 1980; NEWTON, 1984). The feeding habits of scaphidiines vary between genera, but in general, most of them feed on hyphae of Polyporales. Beetles of the genus *Cyparium* Erichson, 1845 show a strong affinity for the Agaricales order, while *Baeocera* Erichson, 1845 beetles primarily feed on slime mold basidiomes (LAWRENCE & NEWTON, 1980; NEWTON, 1984). Additionally, scaphidiine larvae possess morphological adaptations in their oral system that are likely related to their feeding habits (LAWRENCE & NEWTON, 1980; LESCHEN & LÖBL, 2005).

Larvae are typically found on the gills of fungi, but it is not well known where these beetles complete their pupal development (ASHE, 1984). The duration of complete development varies considerably. For example, in the case of *Scaphisoma commune* Löbl, 1997 which is found in *Auriporia aurea* (Peck) Ryvarden, 1973 (Polyporaceae), the development period was observed to be 21–25 days, with pupation lasting between 9–12 days (HANLEY, 1996; as *S. castaneum* Motschulsky, 1845). On the other hand, the pupation of *S. americanum* Löbl, 1987 lasts 5–7 days (ASHE, 1984; as *S. terminata*). It is expected that beetles feeding on ephemeral gilled

mushrooms, such as *Cyparium*, undergo more rapid development (ASHE, 1984). Larvae that feed on Basidiomycetes are known to construct fragile canopies from digested food, the function of which is still unknown but is likely for protection (HANLEY, 1996; LESCHEN & LÖBL, 2005).

2. OBJECTIVES

The absence of basic knowledge about the distribution, biology, abundance, and diversity of beetles from the Scaphidiinae family significantly obstructs any subsequent study, whether in phylogeny, interaction networks, molecular, morphological, or fauna surveys. In this regard, the main objective of this thesis is to take the first step in filling the significant knowledge gap concerning Scaphidiinae beetles in Brazil, focused in the state of Minas Gerais, southeast.

As specific objectives, this thesis is focused on (1) investigating the fauna of Scaphidiinae in selected areas; (2) creating an inventory of shining fungus beetles and their hosts; (3) describing species and, (4) redescribing poorly known species previously described.

3. RESULTS

The results are presented in five chapters:

CAPÍTULO 1

***Scaphisoma pandemum* sp. nov. (Coleoptera: Staphylinidae: Scaphidiinae) from the Atlantic Forest of Southeast Brazil** – In this chapter, a new species of Scaphidiinae was described for Brazil. The majority of the material used for the description was collected during this thesis. Descriptions and images of the internal and external structures of males and females were published. Additionally, images of the beetles on their host fungus were included. This article represents the first study exclusively focused on Scaphidiinae in Brazil and has been published in the scientific journal Zootaxa.

CAPÍTULO 2

A simple, low-cost device for collecting mushroom-dwelling Scaphidiinae (Coleoptera, Staphylinidae) – In this chapter, a straightforward and practical methodology for collecting beetles on mushrooms was introduced. This technique was applied to gather a substantial portion of the beetles included in this thesis. It is worth noting that this methodology is not

confined solely to the collection of Scaphidiinae but is also valuable for collecting any other beetle associated with mushrooms. The chapter has been published in the scientific journal Zootaxa, as a scientific note.

CAPÍTULO 3

Contributions to the taxonomy of Neotropical *Cyparium* Erichson (Coleoptera: Staphylinidae: Scaphidiinae), with the description of five new species – In this chapter, an exclusive study dedicated to the genus *Cyparium* Erichson, 1845, was conducted, encompassing the description of five new species and the redescriptions of two previously known species. The descriptions and redescriptions include illustrations of the internal and external morphology of both males and females. Additionally, illustrations of other beetles from the Neotropical Region were presented, based on photographs provided by museums and/or original descriptions. This work was presented during the Qualifying Exam and was published in the European Journal of Taxonomy.

CAPÍTULO 4

Rediscovery and redescription of *Scaphisoma nigrofasciatum* Pic (Coleoptera: Staphylinidae: Scaphidiinae): a remarkable new record from a distant continent– In this chapter, a new record for the Asian species *Scaphisoma nigrofasciatum* is provided. The new locality is in Minas Gerais, Brazil. Specimens from both India and Brazil were compared. The paper provides images of the external and internal morphology of males and females. The main hypothesis is that the beetles came along with their host fungi. However, a molecular analysis is suggested to compare specimens. The article was published in the scientific journal Zootaxa.

CAPÍTULO 5

New species of Scaphidiinae (Coleoptera: Staphylinidae) from remnants of the Atlantic Forest in Minas Gerais, southeastern Brazil, with host associations, and an illustrated key to the Brazilian genera – In this chapter, 20 new species of shining fungus beetles, distributed across five genera, are described: *Cyparium* Erichson, 1845 (1 new specie), *Alexidia* Reitter, 1880 (2), *Baeocera* Erichson, 1845 (6), *Scaphisoma* Leach, 1815 (4), and *Toxidium* LeConte, 1860 (7). The descriptions are based on males and/or females internal and external morphology. Illustrative plates are provided in order to better understand the

morphology of this group. Also, notes on the host are also provided for all species. Additionally, a key to the Brazilian Scaphidiinae genera is presented. As a result, the recorded number of Scaphidiinae species in Brazil increases from 42 to 62. This manuscript is in process of publication in the European Journal of Taxonomy.

CAPÍTULO 1 – *Scaphisoma pandemum* sp. nov. (Coleoptera: Staphylinidae: Scaphidiinae) from the Atlantic Forest of Southeast Brazil

Publicado na revista *Zootaxa* 4999(2): 143–156.

https://doi.org/10.11646/zootaxa.4999.2.4

Zootaxa 4999 (2): 143–156
https://www.mapress.com/j/zt/

Article

ISSN 1175-5326 (print edition)
ZOOTAXA
ISSN 1175-5334 (online edition)

https://doi.org/10.11646/zootaxa.4999.2.4
http://zoobank.org/urn:lsid:zoobank.org:pub:C9A3640C-0297-4E3D-9210-AD3C5FC5F9B8

Scaphisoma pandemum sp. nov. (Coleoptera: Staphylinidae: Scaphidiinae) from the Atlantic Forest of Southeast Brazil

ELISA VON GROLL[1,2*] & CRISTIANO LOPES-ANDRADE[2]
[1]*Programa de Pós-Graduação em Biologia Animal, Universidade Federal de Viçosa, Av. Peter Henry Rolfs, s/n, 36570-900, Viçosa, MG, Brasil*
[2]*Laboratório de Sistemática e Biologia de Coleoptera, Departamento de Biologia Animal, Universidade Federal de Viçosa, Av. Peter Henry Rolfs, s/n, 36570-900, Viçosa, MG, Brasil.* https://orcid.org/0000-0001-9652-1369
**Corresponding author.* elisavgroll@gmail.com; https://orcid.org/0000-0002-6563-8684

Abstract

Scaphidiinae (Coleoptera, Staphylinidae) comprises more than 1800 described species in 46 genera. With 766 described species and subspecies, *Scaphisoma* Leach is the most diverse genus of this subfamily and is distributed almost worldwide. A total of 38 species are recorded from the Neotropical region and only six are known from Brazil. In this paper, *Scaphisoma pandemum* von Groll & Lopes-Andrade, **sp. nov**. is described on the basis of 44 specimens collected from polyporoid fungi in two Atlantic Forest remnants in Viçosa, Minas Gerais, Southeast Brazil. We provide images of adult male and female and their dissected parts, information and photographs of host fungi and comparative notes.

Key words: Shining fungus beetles, Neotropical, morphology, taxonomy, genitalia

Introduction

The shining fungus beetles (Coleoptera: Staphylinidae: Scaphidiinae) are highly diverse in tropical and subtropical regions (Leschen & Löbl 1995) and are usually found in bracket fungi, mushrooms and slime molds (Löbl & Leschen 2003). The whole subfamily comprises more than 1800 described species in 46 genera (Löbl 2018a,b; Löbl 2019), most known only from adult specimens collected from a single or a few localities. The most diverse genus is *Scaphisoma* Leach, which includes 766 described species and subspecies (Löbl 2018 a,b; Löbl 2019; Löbl *et al*. 2021) distributed almost worldwide, being absent from Chile, southern Argentina and the tundra of the northern American continent (Löbl & Leschen 2003).

Scaphisoma beetles are easily collected anywhere in the neotropics, especially within forested areas, but remain poorly known in the region. A total of 38 described species of *Scaphisoma* are known from the Neotropical region (sensu Morrone 2014), but only six of these are reported from Brazil, as follows (type locality *ipsis litteris* between parentheses): *S. brunneipenne* Pic, 1916:19 ("Brésil"); *S. elongatum* Waterhouse, 1879:533 ("Rio de janeiro"); *S. phalacroide* Pic, 1920b:96 ("Brésil: Santos"); *S. rubripes* Pic, 1920a:5 ("Brésil"); *S. testaceiventre* Pic, 1928:76 ("Sao Paulo"); and *S. tropicum andreinii* Pic, 1920b:96 ("Brésil: Santos").

Two great impediments for taxonomic studies, especially for micro-Coleoptera and in particular *Scaphisoma*, is the lack of identified specimens in national collections and the high costs for travelling to examine type specimens deposited in European museums (Löbl 2018b). A further impediment to their study is the bureaucracy and risk of receiving and sending material through the mail that impose serious limitations for conducting taxonomic works in the country. For groups like Scaphidiinae that were never studied by Brazilian researchers, the hurdles to document biodiversity is insurmountable.

During this study, we had been collecting scaphidiines in the Atlantic Forest of Southeast Brazil as part of a long-term study of the fungus-dwelling beetles, but our research was drastically affected by restrictions imposed by the covid-19 pandemic. Based on material amassed thus far, field collections have revealed a huge diversity of scaphidiines, most belonging to new species. Our objective in this work is to describe one of these, *Scaphisoma pandemum* **sp. nov.**, providing images of adult male and female bodies and dissected parts, information on its host fungi and comparative notes to a few morphologically similar Neotropical species of *Scaphisoma*.

Accepted by J. Klimaszewski: 14 Jun. 2021; published: 9 Jul. 2021

Material and methods

Specimens of the new species were collected at two Atlantic Forest remnants in Viçosa, state of Minas Gerais, Southeast Brazil: "Mata da Biologia" (-20°48'05"S, 42°51'58"W), with 75 hectares and located within the campus of the Federal University of Viçosa; and "Estação de Pesquisa, Treinamento e Educação Ambiental Mata do Paraíso" (-20°45'32"S, 42°51'49"W), with 194 hectares and located about 4 Km south of the campus, but under the care of the university. A total of 44 adults of the new species were found (21 males, 15 females, 8 with sex undetermined), while actively searching for scaphidiines on fungi.

Two females and six males were dissected, comprising the two collection sites, three different fungi, and the full range of color morphs. These specimens were first boiled in water to soften their tissues, and then the structures of interest were extracted and immersed in a saturated KOH solution for maceration of soft tissues, then immersed in a solution of 10% acetic acid for a few minutes to neutralize any remaining KOH, and finally cleaned in water. More delicate structures were dissected immediately after this process. Measurements were taken under a Zeiss Stemi 2000C stereomicroscope equipped with 2x objective lens and an ocular micrometer. Photographs were taken using a Zeiss Discovery V20 stereomicroscope equipped with a Zeiss AxioCam 506 and a Zeiss AxioLab compound microscope equipped with a Zeiss AxioCam MRc or a Canon EOS 1000D digital câmera; all photos were taking using the technic of focus-staking. Photographs in the field were taken using a Canon EOS 5D camera + Canon MP-E 65mm macro lens, a Nikon D810 camera + Nikon Micro-Nikkor 105mm macro lens, and smartphones.

Terminology follows Friedrich & Beutel (2006), Hübler & Klass (2013), Löbl & Leschen (2003) and Naomi (1989a,b), and the examined characters were mostly those provided in the phylogenetic study by Leschen & Löbl (2005). Unless otherwise specified in the text (between square brackets), labels are printed on white paper. Pin label transcriptions are placed within quotation marks, with each label separated by a backslash. The number and gender of specimens bearing these labels are stated immediately before the label data.

Six males (including the holotype) and six females were measured (Figs 1A–D); however, sometimes a few structures were concealed and could not be measured. The following abbreviations are used for measurements (in mm): TL (total body length, not including head and abdomen; Fig. 1A), PL (pronotal length along the midline; Fig. 1A), PA (pronotal width at the anterior margin; Fig. 1A), PB (pronotal width at the posterior margin; Fig. 1A), EL (elytral length in the midline, including the scutellar shield; Fig. 1A), EI (length of the inner margins of elytra; Fig. 1A), EW (greatest right elytron width; Fig. 1A), EH (elytral height in lateral view; Fig. 1B), HW (maximum width of the head including eyes; Fig. 1C), SY (shortest width between eyes above the antennae; Fig. 1C), GY (greatest width between eyes, in the center; Fig. 1C), WA (width between antennae; Fig. 1C), MC (mesothorax length in the midline; Fig. 1C), MB (mesothorax length between fore and middle legs, not including mesocoxal areas; Fig. 1D), VL (length of ventrite I in the midline; Fig. 1D), ML (length of mesocoxal area; Fig. 1D), MA (length of metacoxal area; Fig. 1D).

Acronyms of scientific collections are as follows:

CAMB	Coleção Ayr de Moura Bello (Rio de Janeiro, state of Rio de Janeiro, Brazil)
CELC	Coleção Entomológica do Laboratório de Sistemática e Biologia de Coleoptera da Universidade Federal de Viçosa (Viçosa, Minas Gerais, Brazil)
FMNH	Field Museum of Natural History (Chicago, Illinois, USA)

Taxonomy

Scaphisoma pandemum von Groll & Lopes-Andrade, sp. nov.

Figs 1–9

Type locality. Mata da Biologia, Universidade Federal de Viçosa, Viçosa, state of Minas Gerais, Southeast Brazil.

Type material. HOLOTYPE: ♂ (CELC) "Brasil: MG, Viçosa 'Mata da Biologia', 26.i.2017, S. Aloquio & W. Gomes leg. \ *Scaphisoma pandemum* von Groll & Lopes-Andrade HOLOTYPUS [red paper]". PARATYPES: 20♂♂, 15♀♀, 8 with sex undetermined as follows: ♂, ♀, 1 ex. (CELC), same data as holotype; 2♂♂ (CELC; one ♂ genitalia dissected and stored in glycerin), 4♀♀ (2 CELC, 1 CAMB, 1 FMNH) "BRASIL: MG, Viçosa 'Mata do

Paraíso', 11.ii.2015, S. Aloquio, A. Orsetti, C. Lopes-Andrade & M. Bento leg."; ♀, ♂, 1 ex. (CELC; ♂ genitalia dissected and stored in glycerin) "BRASIL: MG, Viçosa, Mata do Paraíso, 25.v.2016, A. Orsetti, C. Lopes-Andrade & Pecci-Maddalena leg. \ casca de tronco"; ♂, ♀ (CELC) "BRASIL: MG, Viçosa, EPTEA Mata do Paraíso, 21.xi.2019, Leg. LabCol Fungo 10 \ Em *Steccherinum undigerum*"; 2♂♂, 4♀♀, 1 ex. (CELC, 4♀♀ (2♀♀: genitalia dissected and stored in glycerin); 2♂♂: completely dissected and stored in glycerin, 1 ex.) "BRASIL: MG, Viçosa, UFV, 'Mata da Biologia', 26.vi.2019, Leg. E. von Groll & A. Orsetti \ Em *Geesterania* cf. *carneola* (Steccherinaceae)"; 5♂♂, ♀ (CELC, 5♂♂ (1♂ genitalia dissected and stored in glycerin), ♀) "BRASIL: MG, Viçosa, Mata da Biologia, 02.ix.2020 Leg. G.L.N. Martins & I.S.C. Pecci-Maddalena \ Em *Geesterania* cf. *carneola* (Steccherinaceae)"; 3♂♂, ♀ (CELC) "Mata da Biologia, 08.ix.2020, Leg. E. von Groll & A. Orsetti \ Fungo 05, Em *Geesterania* cf. *carneola*"; ♂ (CELC; genitalia dissected and stored in glycerin), "Mata da Biologia, 08.ix.2020, Leg. E. von Groll & A. Orsetti \ Fungo 12, Em *Schizopora paradoxa*"; 3♂♂ (1 CELC, 1 CAMB, 1 FMNH), 2♀♀, 5exs (CELC), "BRASIL: MG, Viçosa, Mata da Biologia, 12.ix.2020, Leg. G.L.N. Martins & G.J. Figueiredo \ Em *Geesterania* cf. *carneola*"; ♂ (CELC), "BRASIL: MG, Viçosa, Recanto das Cigarras (Mata da Biol.), 20.xi.2019, Leg. LabCol, Fungo 25 \ Em *Geesterania* cf. *carneola* (Steccherinaceae)". All paratypes additionally labelled "*Scaphisoma pandemum* von Groll & Lopes-Andrade PARATYPUS [yellow paper]".

Diagnosis. TL: 1.38–1.56 mm in males and 1.50–1.64 mm in females. Elytral apex and sometimes the humeral areas yellow (Figs 2A–C). First abdominal ventrite dark anteriorly and yellow at apex (Fig. 2D, 6F). Metaventrite densely pubescence on disc, but sparsely pubescent laterally (Fig. 4D). Mesocoxal lines arcuate, impunctate (Fig 4D); submetacoxal lines convex and punctate (Fig. 6F). Aedeagus with internal sac simple (Figs 7F, G), with conspicuous denticular structure (Figs 7H).

Description. **Coloration**: brown to dark brown (Figs 2A–F). Head castaneous (Fig. 2G); antennae pale yellow to yellow (Fig. 2H); mouth parts pale yellow (Figs 2I; 3A–E). Thorax light brown to brown ventrally (Fig. 2D); pronotum castaneous to brown (Figs 3G,H); coxae and legs yellow (Fig. 2D). Elytra mostly brown, with apical 1/4 yellow (Figs 2A–C); humeral areas with or without yellow band extending to apex, more conspicuous in teneral specimens (Fig. 2C). Abdomen mostly yellow; anterior portion of first segment dark (Fig. 2D).

Head (Fig. 2G). Subcylindrical, glossy and smooth; frons with fine and sparse punctation, pubescent. Labral setae present (Fig. 2I). Mandibles unidentate (Figs 3A,B), subapical serrations on left mandible very small, barely visible. Maxillae with aciculate palps (each apical palpomere narrower than the precedent), palpomere II with two apical setae (Fig. 3C); galea wide, radulate (Fig. 3C); lacinia with long and sparse lateral setae (Fig. 3C). Hypopharynx setose (Figs 3D,E). Labium with curved palps; palpomere I and II with one subapical seta each (Fig. 3D). Mentum rectangular and setose (Fig. 3D). Submentum with trapezoidal apex (Fig. 3F). Gula not reaching submentum (Fig. 3F), without pores (Fig. 3F). Eyes notched anteriorly by antennal insertions (Fig. 2G). Antennae filiform (Fig. 2H), with measurements as follows (left antenna, from base to apex, in mm): 0.06, 0.07, 0.03, 0.05, 0.07, 0.08, 0.11, 0.09, 0.12, 0.11, 0.12.

Prothorax. Pronotum trapezoidal, glossy; punctation dense, fine and somewhat deep; each puncture with one seta as long as interspace of two punctures (Figs 3G,H); lateral margins rounded (Figs 3G,H), with prominent carinae visible when seen from above, each carina with punctate lateral stria alongside. Posterior pronotal angle acuate, partially concealed bellow elytra (Fig. 2F). Prosternum in front of procoxae (Fig. 4A) shorter than procoxal cavity; prosternal process sickleform (Fig. 4B). Hypomera smooth, glabrous (Figs 2D, 4A), completely visible in lateral view (Figs 2E,F); apex not extended beyond posterior margin of pronotum. Profurca (Fig. 4C) with stalk longer than apex; apex rounded.

Mesothorax. Mesoventral space (prepectus) absent. Procoxal rests subrounded (Figs 4D,E). Mesoventral lines present, short, impunctate (Figs 4D,E). Secondary lines absent. Mesoventral process paxillate, elongate-oval in lateral view (Fig. 4F). Median lines short, connected to mesoventral process (Fig. 4E). Mesanepisterna smooth, shinning; punctures, sparse; pubescence, fine (Fig. 4E). Mesepimera shinning, smooth, about 1/2 the length of anapleural suture and 5 times as long as wide (Fig. 4E). Distance between mesocoxae slightly shorter than width of each coxa (Fig. 4E).

Metathorax. Metaventrite (Fig. 4E) smooth, shinning; punctation dense and coarse on disc, fine and sparse laterally; pubescence dense and thick on disc, fine and sparse laterally. Metaventrite fused to mesoventrite. Mesocoxal lines arcuate, not punctate (Fig. 4D,E). Primary setae setose (Fig. 4D). Premetacoxal lines and discrimen absent. Metepimera expanding gradually posteriorly; metepimeral suture impunctate. Metanepisterna narrowed anteriorly (Figs 2F, 4E,F). Metendosternite with short stalk and well-developed arms (Fig. 5A).

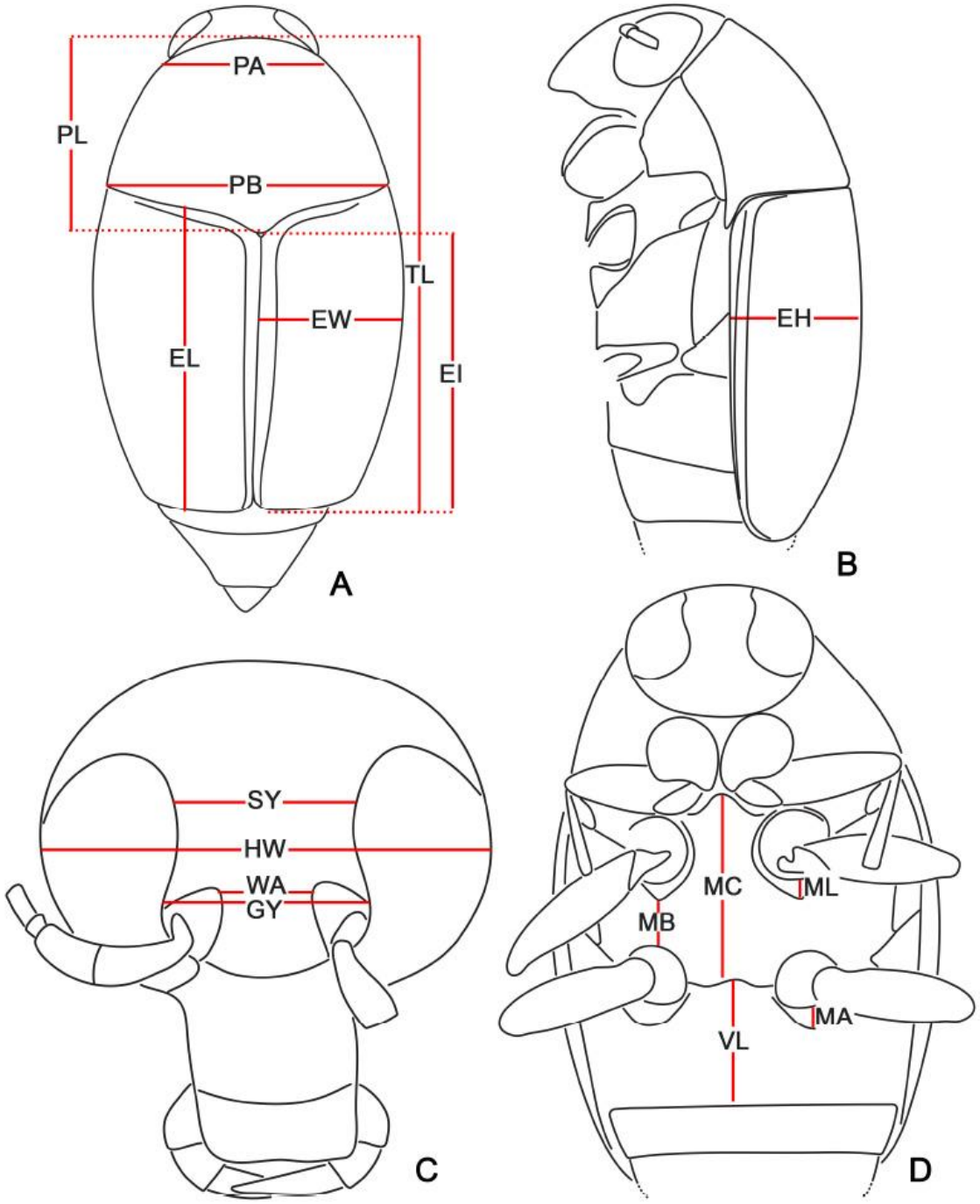

FIGURE 1. *Scaphisoma pandemum* **sp. nov.**, measurements taken: A, dorsal view; B, lateral view; C, head, frontal view; D, ventral view. Abbreviations: EH, elytral height in lateral view; EI, length of the inner margins of elytra; EL, elytral length in the midline; EW, greatest right elytron width; GY, greatest width between eyes, in the center; HW, maximum width of the head including eye; MA, length of metacoxal area; MB, mesothorax length between fore and middle legs, not including mesocoxal areas; MC, mesothorax length in the midline; ML, length of mesocoxal area; PA, pronotal width at the anterior margin; PB, pronotal width at the posterior margin; PL, pronotal length; SY, shortest width between eyes above the antennae; TL, total body length; VL, length of ventrite I in the midline; WA, width between antennae.

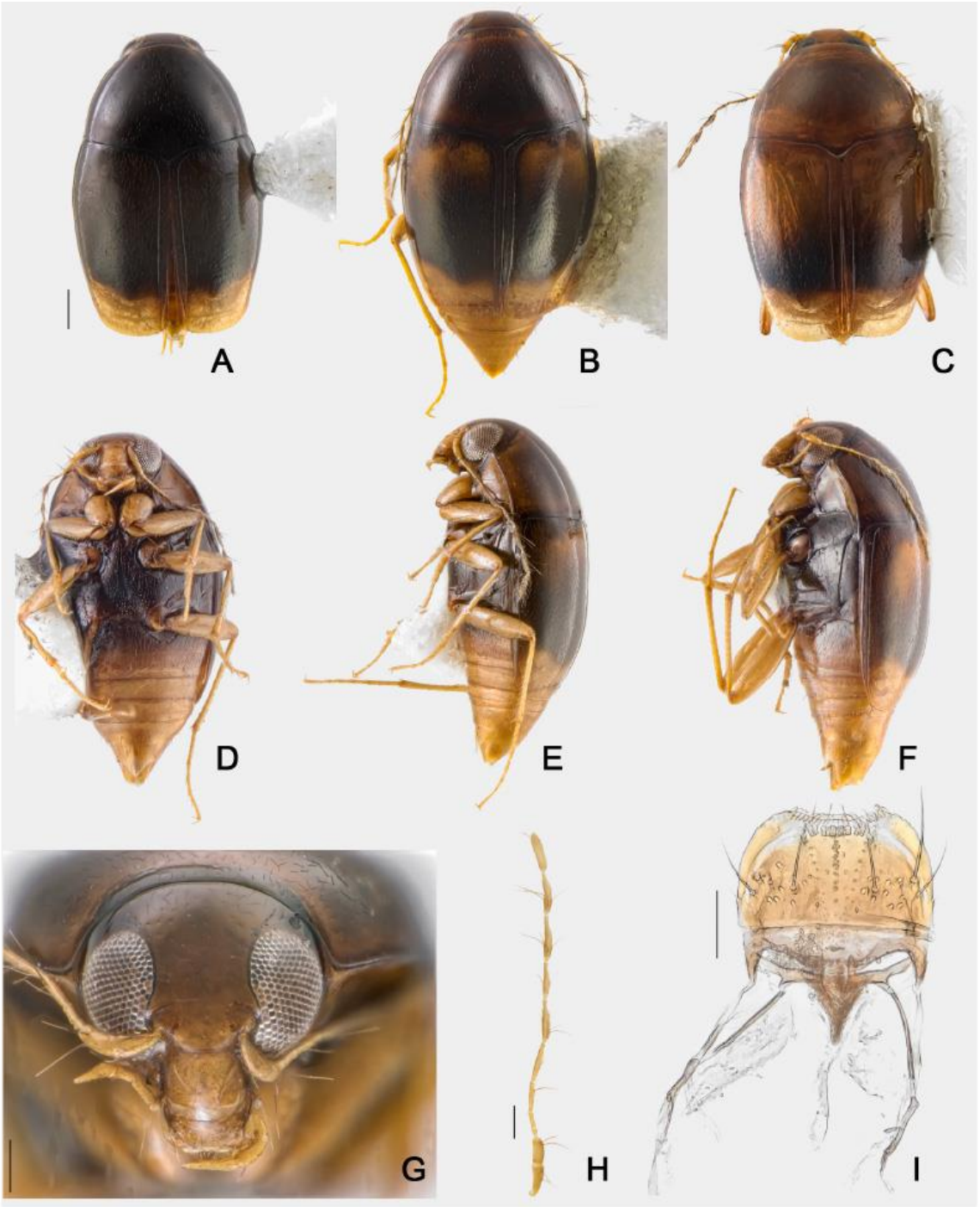

FIGURE 2. *Scaphisoma pandemum* **sp. nov.** Dorsal view: A, female, Mata do Paraíso"; B, holotype, male, "Mata da Biologia"; C, female, Mata da Biologia; holotype, male "Mata da Biologia": D, ventral view; E, lateral view; F, male, "Mata da Biologia", lateral view; holotype, male "Mata da Biologia": G, head, frontal view; H, antenna, I, labrum. Scale bars: A–F, 0.2 mm; G,H, 0.1 mm, I, 0.05 mm.

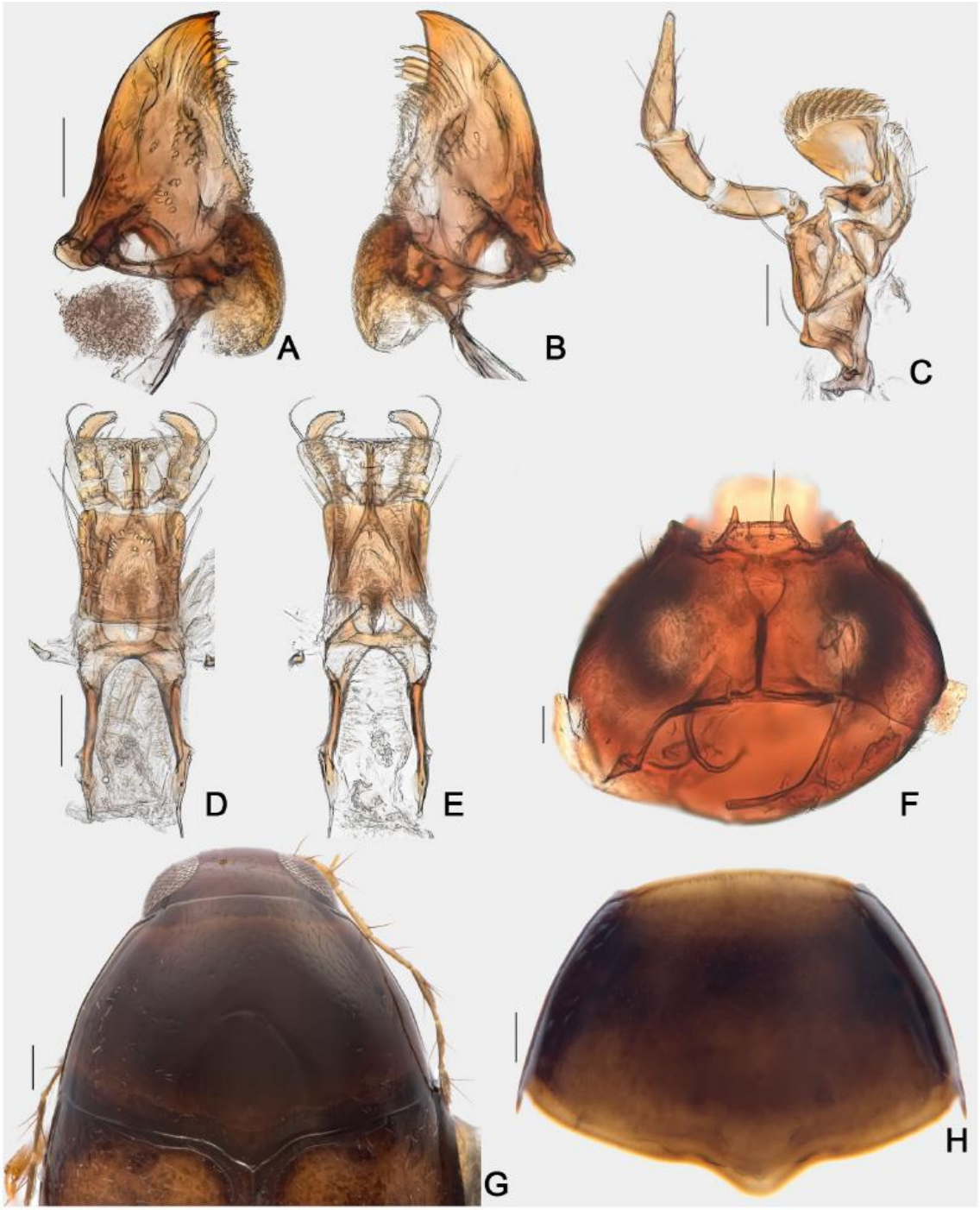

FIGURE 3. *Scaphisoma pandemum* **sp. nov.** Male, "Mata da Biologia": A,B, mandibles; C, maxilla; D, labium; E, hypopharynx; F, head; ventral view; pronotum: G, holotype, male, "Mata da Biologia"; H, male, "Mata da Biologia". Scale bars: A–F, 0.05 mm; G, H, 0.1 mm.

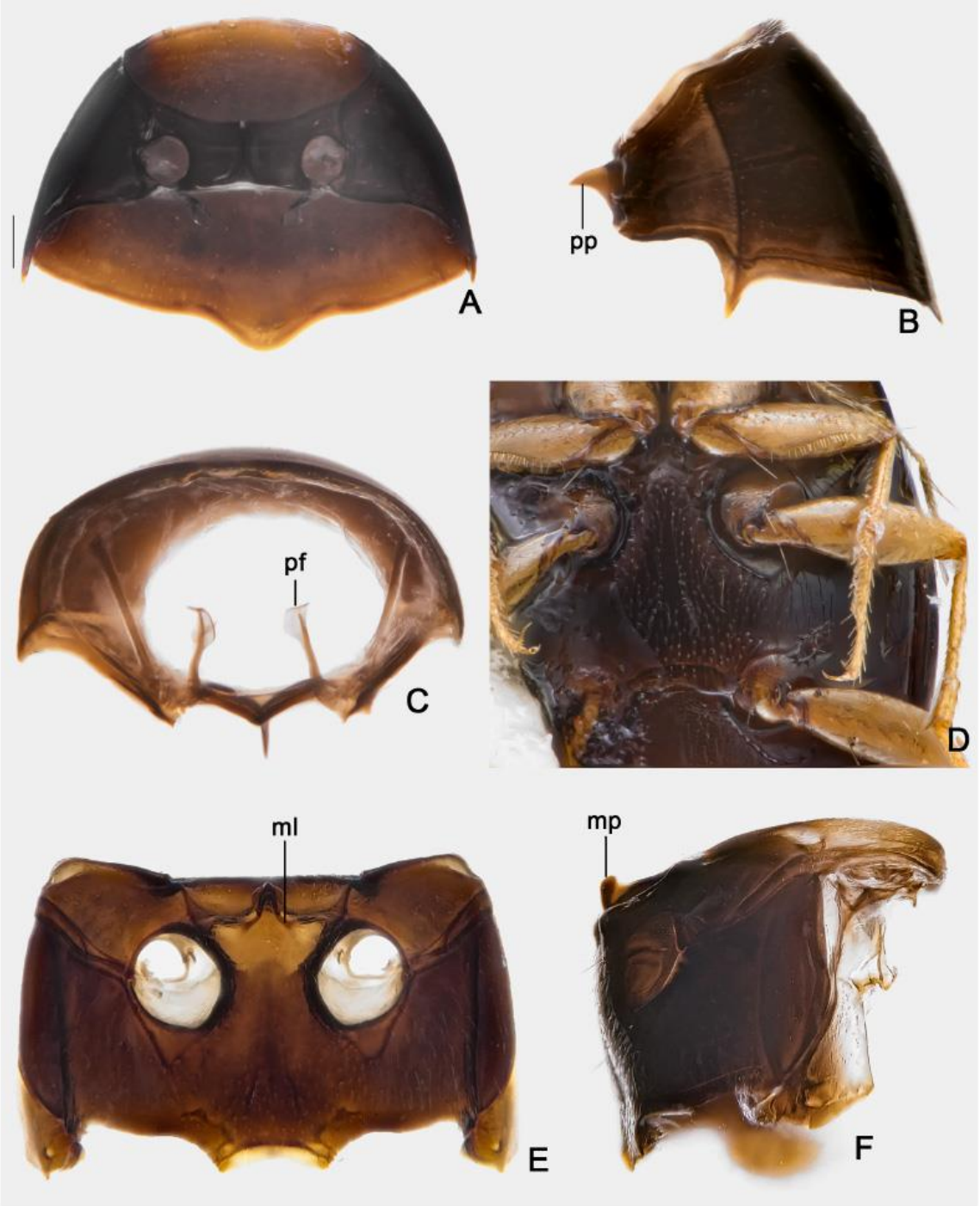

FIGURE 4. *Scaphisoma pandemum* **sp. nov.** Male, "Mata da Biologia": prothorax: A, ventral view; B, lateral view; C, inner view; metathorax, ventral view: D, holotype, male, "Mata da Biologia"; E, male, "Mata da Biologia"; metathorax, lateral view: male, "Mata da Biologia" (ml, median line; mp, mesoventral process; pf, profurca; pp, prosternal process). Scale bars: A–F, 0.1 mm.

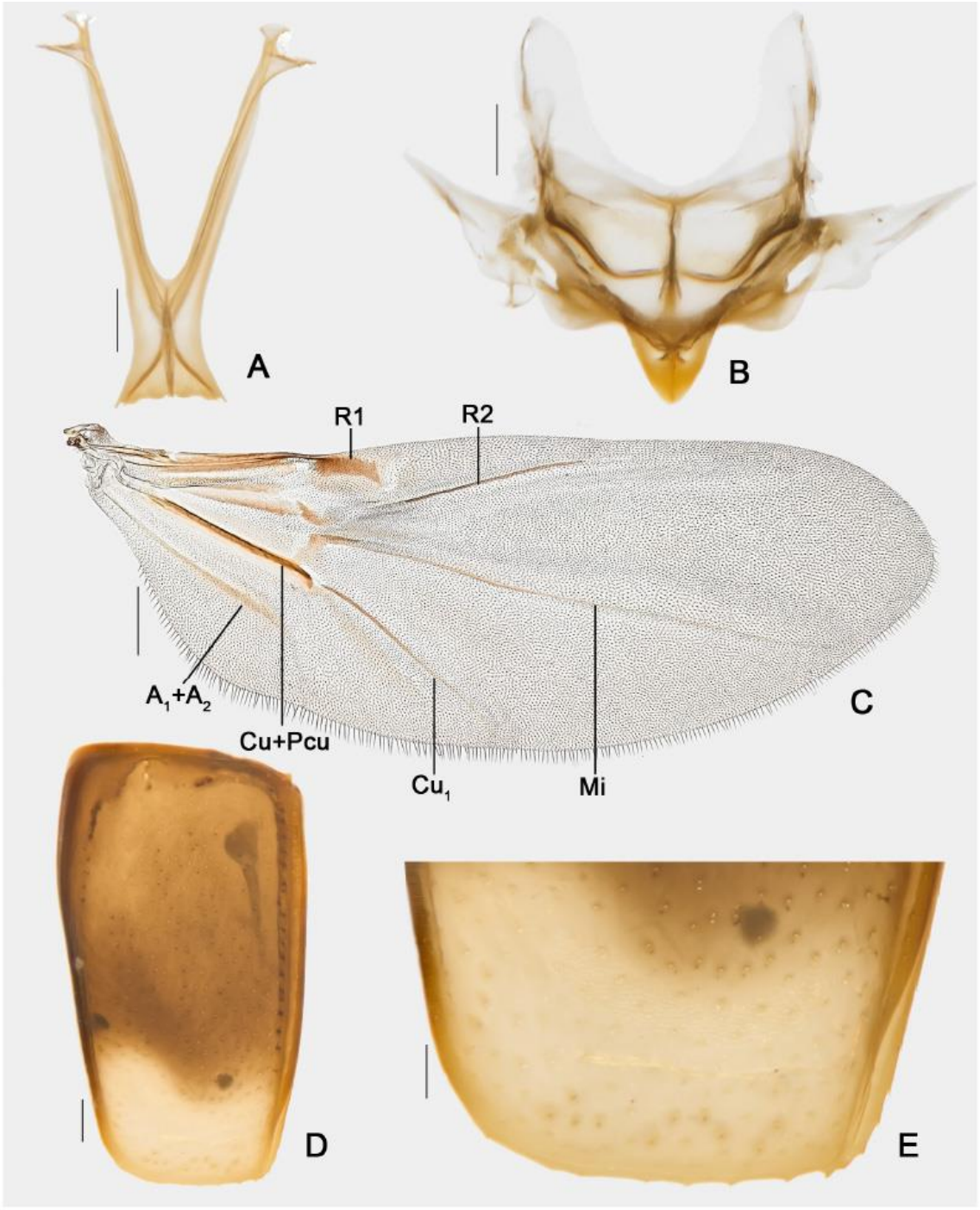

FIGURE 5. *Scaphisoma pandemum* **sp. nov.** Male, "Mata da Biologia": A, metendosternite; B, scutellar plate; C, wing; D, elytron; E, elytron, apex. Scale bars: A,D, 0.1 mm; B,E, 0.05 mm; C, 0.2 mm.

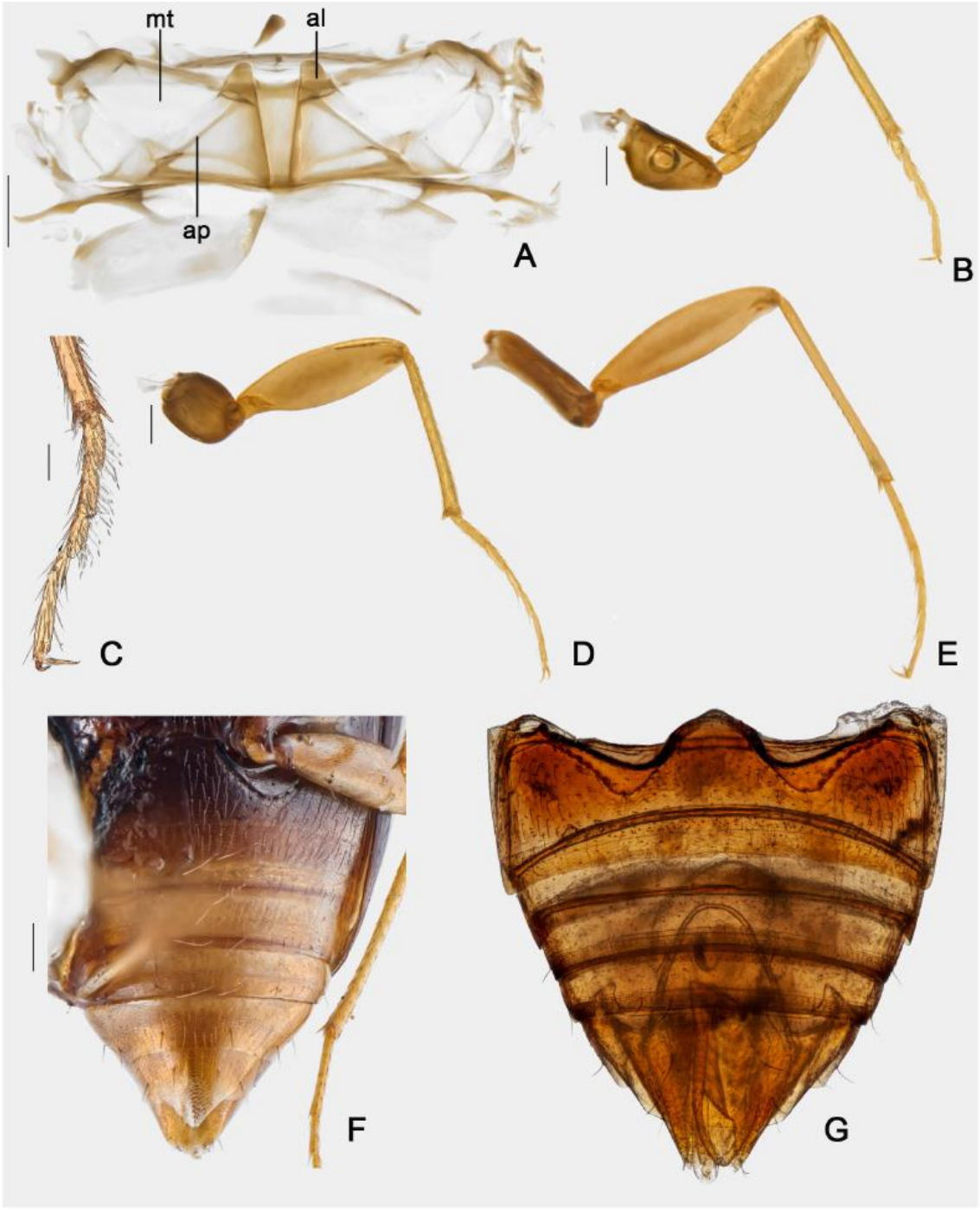

FIGURE 6. *Scaphisoma pandemum* **sp. nov.** Male, "Mata da Biologia": A, metanotum; B, fore leg; C, pretarsus; D, middle leg; E, hind leg; abdomen: F, holotype, male, "Mata da Biologia"; G, male, "Mata da Biologia" (al, alacristae; ap, apodeme; mt, metascutum). Scale bars: A,B,D–G, 0.1 mm; C, 0.05 mm.

Pterothorax. Tip of scutellar shield exposed; tip width about one third the length of the pteronotum; scutellar suture trapezoidal (Fig. 5B). Hind wings fully developed; R1 small, R2, M1 and Cu_1 thin, Cu+Pcu slightly thickened, A_1+A_2 faint (Fig. 5C). Elytra convex (Figs 2A–C, E-F, 5D); carinae of lateral margin visible in dorsal view;

apical margins somewhat rounded; sutural striae somewhat expanding to disc and tapering to apex (Figs 2A–C); basal striae reaching 2/3 of elytra, joined to sutural striae forming a curve (Figs 2A–C, 3G); adsutural area with single row of punctures, each puncture bearing a seta (Figs 2A–C); lateral stria punctate; apical edge serrate (Fig. 5E). Metanotum (Fig. 6A) with alacristae trapezoidal; sides subrounded; metascutum, large; apodeme, oblique.

Legs (Figs 6B–E). Profemora with ctenidium (Fig. 4D). Mesofemora rounded in cross-section; subapical seta not sclerotized. Tibiae smooth, with spinose apex (Figs 6B,D,E). Coxae, trochanters and femora with striate microsculpture.

Abdomen (Figs 6F,G). Microsculpture transversely striate, densely pubescent; punctation fine, shallow; variable number of primary setae on disc of ventrites. Submetacoxal lines convex, punctate; submetacoxal areas finely microsculptured. Pygidium smooth dorsally.

Males. Pro- and mesotarsomeres widened, with tenent setae (Figs 6B,C). Abdominal ventrites 1–3 each with six thick primary setae, 4–5 each with two setae (variation may be due to loss of setae) (Fig. 6F). Sternum IX long, narrow (Fig. 7E). Tergite IX with broad ventral struts (Fig. 7A). Aedeagus (Figs 7B-D) symmetrical; basal bulb weakly sclerotized; apex well sclerotized, somewhat twisted, with subapical denticles (Fig. 7B); parameres slightly arcuate and widened, overlapping apically; internal sac simple, with wide curved flagellum (Figs 7F,G) and denticular structure bearing a row of teeth (Figs 7H).

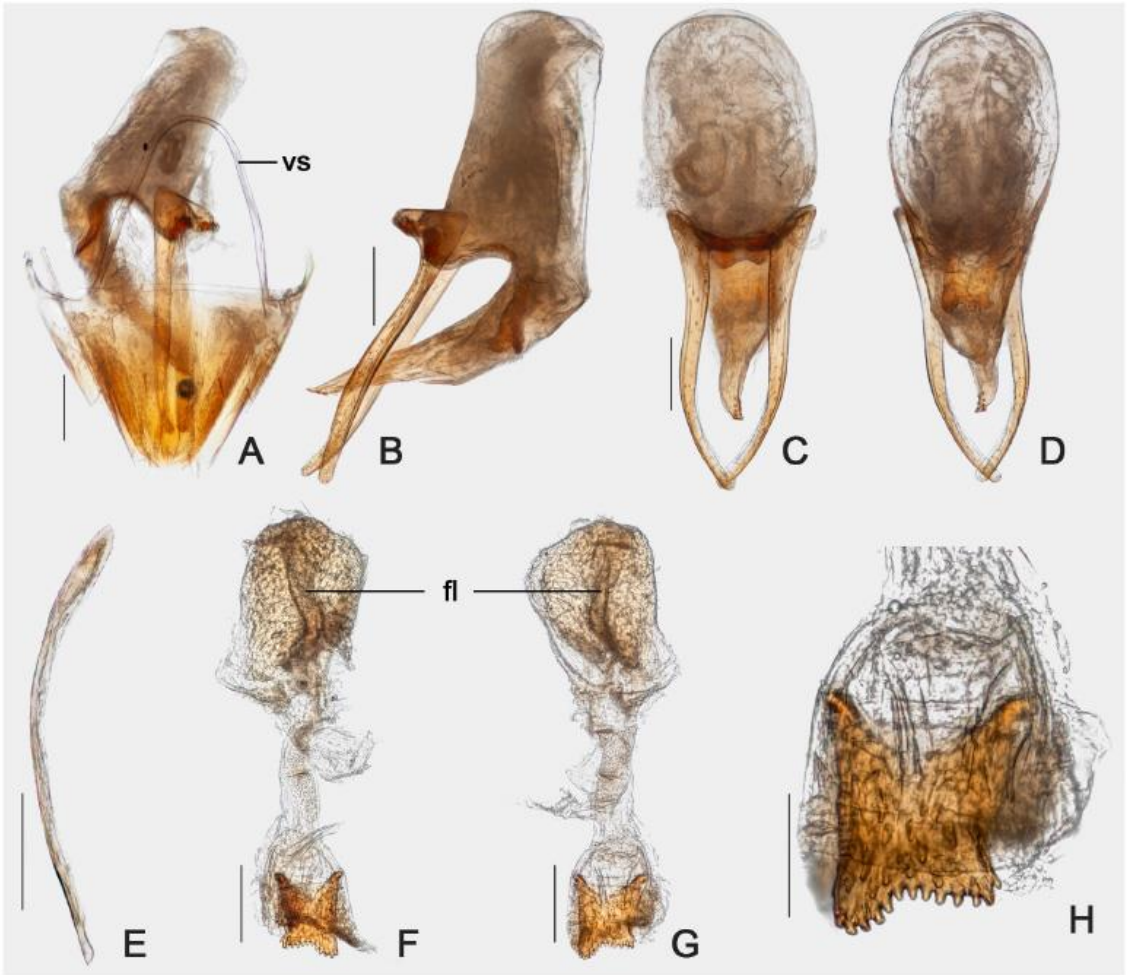

FIGURE 7. *Scaphisoma pandemum* **sp. nov.** Male, "Mata da Biologia": A, abdominal terminalia. Aedeagi: B, lateral view, C, frontal view; D, dorsal view; E, Sternum IX; internal sac, male "Mata da Biologia": F, frontal view, G, dorsal view, H, denticular structure of the internal sac (fl, flagellum; vs, ventral struts). Scale bars: A–G, 0.1 mm; H, 0.05 mm.

Females. Each abdominal ventrite with one pair of primary setae on disc, usually thinner than those of males. Ovipositor simple (Figs 8A–C): distal gonocoxites elongated, with slender gonostyli; bursa copulatrix small, membranous (Fig. 8A,B); spermatheca not detected.

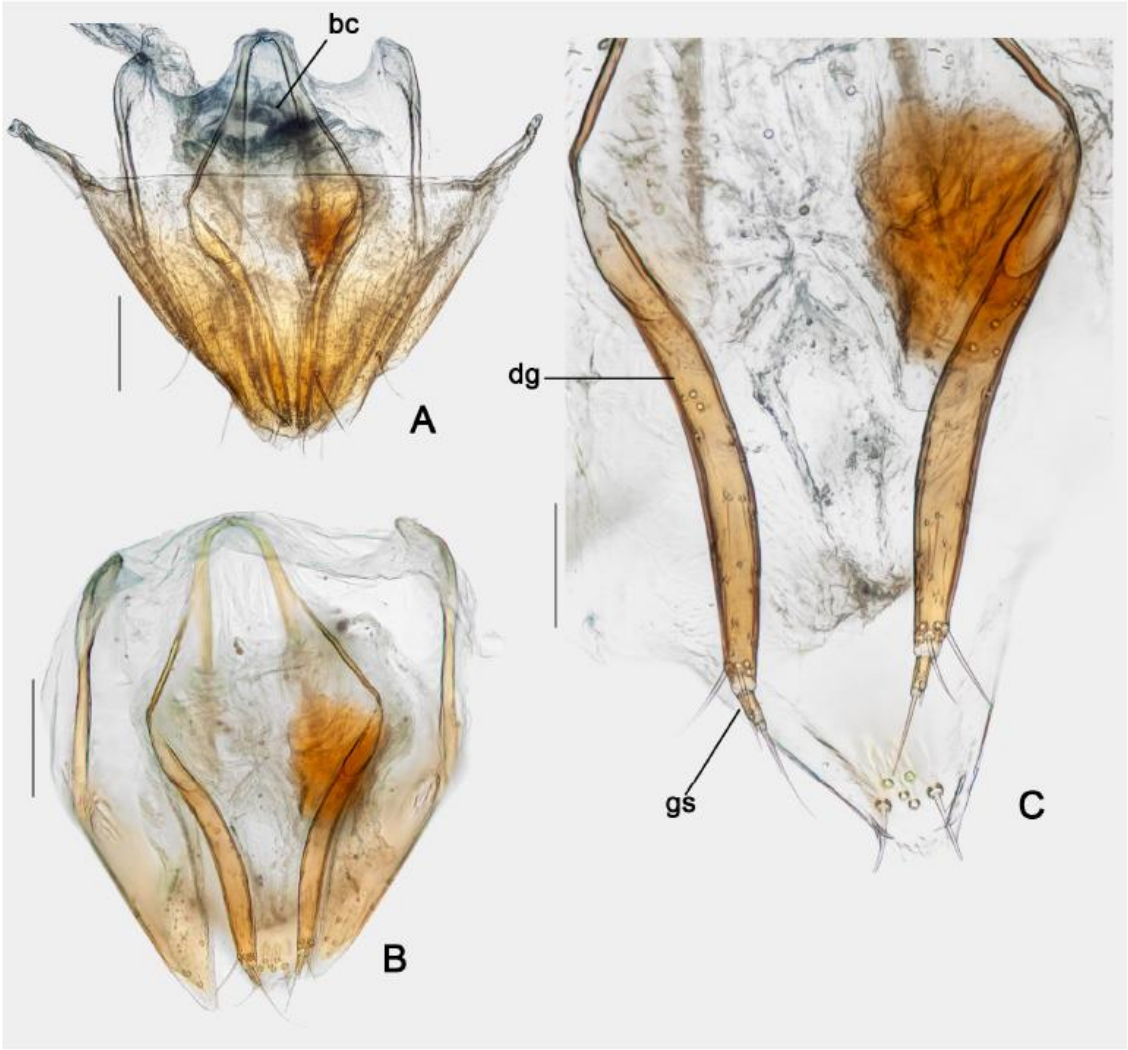

FIGURE 8. *Scaphisoma pandemum* **sp. nov.** A, Female, "Mata da Biologia", terminalia and abdomen; female, "Mata da Biologia": B, female genitalia, C, ovipositors (bc, bursa copulatrix; dg, distal gonocoxites; gs, gonostyli). Scale bars: A,B, 0.1 mm; C, 0.05 mm.

Measurements. Males (n=6, unless otherwise specified; in mm): TL 1.38–1.56 (mean = 1.50, standard deviation ± 0.06), PL 0.56–0.65 (0.61 ± 0.03), PA 0.47–0.52 (0.50 ± 0.02), PB 0.84–0.92 (0.86 ± 0.03), EL 0.94–1.05 (1.00 ± 0.04), EI 0.76–0.93 (0.90 ± 0.06), EW 0.43–0.52 (0.47 ± 0.03), EH 0.35–0.42 (0.37 ± 0.03), HW 0.43–0.49 (0.46 ± 0.02), SY 0.17–0.18 (0.18 ± 0.01), GY 0.21–0.24 (0.22 ± 0.01), WA 0.10–0.12 (0.11 ± 0.01), MC (n=2) 0.15–0.47 (0.31 ± 0.23), MB (n=5) 0.13–0.15 (0.14 ± 0.01), VL (n= 5) 0.24–0.32 (0.28 ± 0.04), ML 0.05–0.09 (0.06 ± 0.02), MA 0.05–0.07 (0.06 ± 0.01). **Females** (n= 6, unless otherwise specified; in mm): TL 1.50–1.64 (mean=1.57, standard deviation ± 0.05), PL 0.62–0.66 (0.64 ± 0.01), PA 0.51–0.54 (0.52 ± 0.01), PB 0.86–0.95 (0.90 ± 0.03), EL 0.98–1.05 (1.02 ± 0.02), EI 0.91–0.97 (0.93 ± 0.02), EW 0.43–0.52 (0.49 ± 0.03), EH 0.36–0.43 (0.39 ± 0.03), HW 0.46–0.50 (0.48 ± 0.02), SY 0.18–0.21 (0.20 ± 0.01), GY 0.22–0.25 (0.23 ± 0.01), WA 0.10–0.15 (0.12 ± 0.02), MC (n= 4) 0.15–0.52 (0.40 ± 0.17), MB (n= 5) 0.15–0.19 (0.16 ± 0.02), VL 0.26–0.32 (0.30 ± 0.03), ML 0.05–0.07 (0.05 ±0.01), MA 0.05–0.07 (0.05 ± 0.01).

Host fungi. Adult specimens were collected six times from *Geesterania* cf. *carneola* (Bres.) Westphalen & Rajchenberg (Steccherinaceae; Figs 9A–C). Adults were also collected once in *Steccherinum undigerum* (Berk. & M.A. Curtis) (Steccherinaceae; Fig. 9D) and in *Schizopora paradoxa* (Schrad.) Donk (Schizoporaceae; Figs 9E–F).

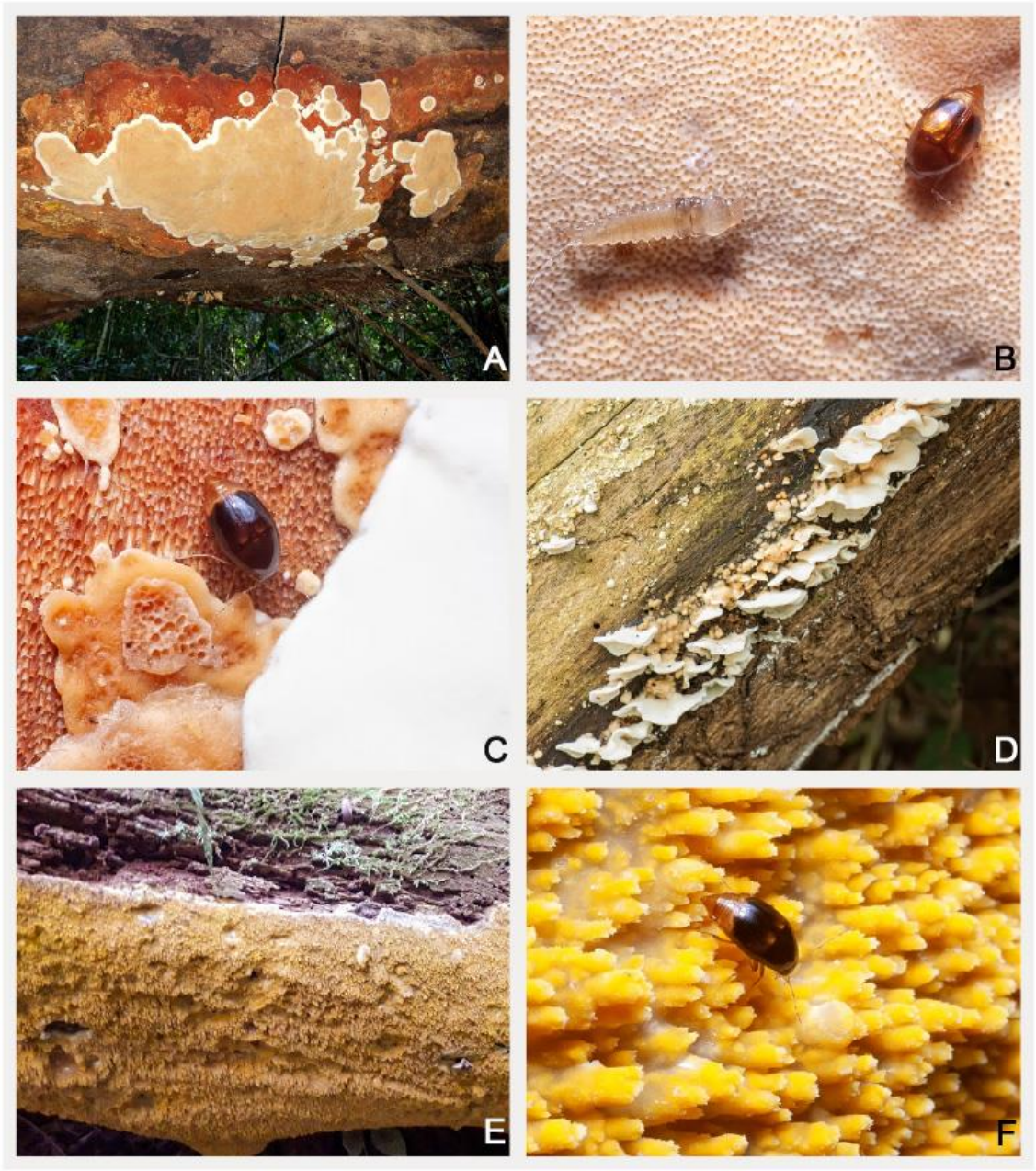

FIGURE 9. A, host fungus *Geesterania* cf. *carneola*; adult of *Scaphisoma pandemum* **sp. nov.** in *Geesterania* cf. *carneola*: B, with the large yellow humeral band, and C, with just a small yellow humeral band ; D, host fungus *Steccherinum undigerum*; E, host fungus *Schizopora paradoxa*; F, *Scaphisoma pandemum* **sp. nov.** in the same host fungus.

Etymology. From the Latin "pandemus", derived from the Ancient Greek πάνδημος and meaning "affecting all the people", in the neuter nominative singular, in reference to the fact that the present article was written during the pandemic of covid-19, who drastically affected our ongoing works on the Atlantic Forest scaphidiines.

Remarks. *Scaphisoma pandemum* has been frequently collected in two sites: "Mata da Biologia" and "Mata do Paraíso", both in Viçosa, Minas Gerais. The basidiomes identified as *Geesterania* cf. *carneola*, mentioned in the type material, correspond to a single fungus species, which was the most common host species for *Scaphisoma pandemum* and in which all color morphs were found. In order to make sure that the color morphs belong to a single species, two males from "Mata do Paraíso" and four males from "Mata da Biologia" were dissected. The dissected specimens from "Mata do Paraíso" were of different colors: one with the yellow humeral band and the other without it; they were found in different fungus species as well. Three males from "Mata da Biologia" were devoid of yellow humeral band, two of them collected in *Geesterania* cf. *carneola* and the other in *Schizopora paradoxa*. The fourth male had the humeral yellow band and was collected in *Geesterania* cf. *carneola*. We considered the observed color variation of the body as intraspecific variation of a single species.

Scaphisoma pandemum is similar to *Scaphisoma lunatum* (Matthews, 1888) from Nicaragua and Costa Rica. Both have similar coloration, but different mesocoxal lines: *S. lunatum* has parallel mesocoxal lines (Fierros-López, 2006), while *S. pandemum* has arcuate lines. *Scaphisoma pandemum* is also comparatively smaller (1.38–1.64 mm; while *S. lunatum* is 1.75 mm). Their aedeagi are similar, but Fierros-López (2006) did not mention whether there is a denticular structure in the internal sac, present in S. *pandemum*; parameres in *S. pandemum* are thinner and straighter than in *S. lunatum*. *Scaphisoma pandemum* is also similar to *S. rubripes*, but they have different body coloration: the body of *S. rubripes* is mostly black, and its antennae, labrum, tarsi and abdominal apex are red (Pic, 1920a); while *S. pandemum* is brown to dark brown, its labrum, antennae and tarsi are pale yellow, and its abdomen and elytral apex are yellow. No specimen of *S. pandemum* examined by us had red body parts. Their body lengths are also different: *S. pandemum* is 1.38–1.64 mm long, while *S. rubripes* is 2 mm long.

Acknowledgments

We thank Artur Orsetti for the photo of the fungus *Geesterania* cf. *carneola* in the field and Igor de S. Gonçalves and Angelico Asenjo for the bibliography provided. We would also like to thank all the staff of Laboratório de Sistemática e Biologia de Coleoptera (LabCol, Universidade Federal de Viçosa), especially for the support in field collections. We thank the reviewers for the corrections and suggestions that helped to improve our work. Financial support was provided by Fundação de Amparo à Pesquisa do Estado de Minas Gerais (FAPEMIG; Edital 02/2018—Programa Pesquisador Mineiro XII—PPM-00314-18) and Conselho Nacional de Desenvolvimento Científico e Tecnológico (CNPq; research grant number 308432/2018-5 to the junior author). This study was financed in part by Coordenação de Aperfeiçoamento de Pessoal de Nível Superior—Brasil (CAPES; Finance Code 001; doctorate degree grant to the senior author).

References

Fierros-López, H.E. (2006) Coleoptera: Datos nuevos de distribución de algunas especies de Scaphidiinae Neotropicales (Coleoptera: Staphylinidae). *Dugesiana*, 13 (1), 39–43.

Friedrich, F., & Beutel, R.G. (2006) The pterothoracic skeletomuscular system of Scirtoidea (Coleoptera: Polyphaga) and its implications for the high-level phylogeny of beetles. *Journal of Zoological Systematics and Evolutionary Research*, 44 (4), 290–315.
https://doi.org/10.1111/j.1439-0469.2006.00369.x

Hübler, N., & Klass, K.-D. (2013) The morphology of the metendosternite and the anterior abdominal venter in Chrysomelinae (Insecta: Coleoptera: Chrysomelidae). *Arthropod Systematics & Phylogeny*, 71 (1), 3–41.

Leschen, R.A.B., & Lobl, I. (1995) Phylogeny of Scaphidiinae with redefinition of tribal and generic limits (Coleoptera: Staphylinidae). *Revue suisse de Zoologie*, 102 (2), 425–474.
https://doi.org/10.5962/bhl.part.80472

Leschen, R.A.B. & Löbl, I. (2005) Phylogeny and classification of Scaphisomatini Staphylinidae: Scaphidiinae with notes on mycophagy, termitophily, and functional morphology. *Coleopterists Society Monographs*, 3, 1–63.
https://doi.org/10.1649/0010-065X(2005)059[0001:PACOSS]2.0.CO;2

Löbl, I. (2018a) A review of Scaphisomatini from Sulawesi, with descriptions of ten new species (Coleoptera: Staphylinidae: Scaphidiinae). *Acta Entomologica Musei Nationalis Pragae*, 58 (1), 151–165.
https://doi.org/10.2478/aemnp-2018-0013

Löbl, I. (2018b). *Coleoptera: Staphylinidae: Scaphidiinae*. Brill, Leiden, 418 pp.

https://doi.org/10.1163/9789004375956
Löbl, I. (2019) New Species and Records of *Scaphisoma* Leach (Coleoptera: Staphylinidae: Scaphidiinae) from the People's Republic of China. *Annales Zoologici*, 69 (2), 241–292.
https://doi.org/10.3161/00034541ANZ2019.69.2.002
Löbl, I. & Leschen, R.A.B. (2003) Scaphidiinae (Insecta: Coleoptera: Staphylinidae). *Fauna of New Zealand*, 48, 1–94.
Löbl, I., Leschen, R.A.B & Warner, W.B. (2021) Scaphisomatine of Arizona (Coleoptera, Staphylinidae, Scaphidiinae) collected by V-Flight Intercept traps. *Revue suisse de Zoologie*, 128 (1), 173–185.
https://doi.org/10.35929/RSZ.0043
Morrone, J.J. (2014) Biogeographical regionalisation of the Neotropical region. *Zootaxa*, 3782 (1), 1–110.
https://doi.org/10.11646/zootaxa.3782.1.1
Naomi, S. (1989a) Comparative Morphology of the Staphylinidae and the Allied Groups (Coleoptera, Staphylinoidea): VII. Metendosternite and Wings. *Japanese journal of entomology*, 57 (1), 82–90.
Naomi, S. (1989b) Comparative Morphology of the Staphylinidae and the Allied Groups (Coleoptera, Staphylinoidea): X. Eighth to 10th Segments of Abdomen. *Japanese journal of entomology*, 57 (4), 720–733.
Pic, M. (1916) Diagnoses spécifiques. *Mélanges Exotico-Entomologiques* 17, 8–20.
Pic, M. (1920a) Nouveautés diverses. *Mélanges Exotico-entomologiques*, 32, 1–28.
Pic, M. (1920b) Scaphidiides nouveaux de diverses origines. *Annali del Museo civico di Storia naturale di Genova*, 9 (3), 93–97.
Pic, M. (1928) Nové druhy koleopter z Brasilie. Nouveaux coléoptères du Brésil. *Sborník entomologického oddělení Národního musea v Praze*, 6, 74–76.
Waterhouse, F.H. (1879) Descriptions of new Coleoptera of geographical interest, collected by Charles Darwin, Esq. *Zoological Journal of the Linnean Society*, 14 (78), 530–534.
https://doi.org/10.1111/j.1096-3642.1879.tb02449.x

CAPÍTULO 2 – A simple, low-cost device for collecting mushroom-dwelling Scaphidiinae (Coleoptera, Staphylinidae)

Publicado na revista *Zootaxa* 5071(2): 296–298.

https://doi.org/10.11646/zootaxa.5071.2.9

Zootaxa 5071 (2): 296–298
https://www.mapress.com/j/zt/

Correspondence

ISSN 1175-5326 (print edition)
ZOOTAXA
ISSN 1175-5334 (online edition)

https://doi.org/10.11646/zootaxa.5071.2.9
http://zoobank.org/urn:lsid:zoobank.org:pub:08EC974D-09E0-4B35-AC72-2BFBA4ADD2AC

A simple, low-cost device for collecting mushroom-dwelling Scaphidiinae (Coleoptera, Staphylinidae)

ELISA VON GROLL[1,2*], SERGIO ALOQUIO[2,3] & CRISTIANO LOPES-ANDRADE[2,4]
[1]*Programa de Pós-Graduação em Biologia Animal, Universidade Federal de Viçosa, Av. Peter Henry Rolfs, s/n, 36570-900, Viçosa, MG, Brasil.*
[2]*Laboratório de Sistemática e Biologia de Coleoptera, Departamento de Biologia Animal, Universidade Federal de Viçosa, Av. Peter Henry Rolfs, s/n, 36570-900, Viçosa, MG, Brasil.*
[3] *https://orcid.org/0000-0003-2361-6943*
[4] *https://orcid.org/0000-0001-9652-1369*
**Corresponding author.* *elisavgroll@gmail.com;* *https://orcid.org/0000-0002-6563-8684*

The shining fungus beetles (Coleoptera: Staphylinidae: Scaphidiinae) comprise more than 1800 described species, which are usually small (≅0.84–14.30 mm long) (Tang *et al.* 2014 ; Löbl & Ogawa 2016) and found on bracket and resupinate fungi, mushrooms and slime molds (Newton 1984; Löbl & Leschen 2003; Löbl 2018). They are known to be diverse in forests of tropical and subtropical regions, which contrast to the low number of species currently known from Brazil: only 34 species and two subspecies from seven genera (Löbl 2018; von Groll & Lopes-Andrade, 2021). Any active search for Scaphidiinae in the Brazilian Atlantic forest reveals a considerable abundance and diverse of these organisms (pers. obs.), but they disperse rapidly if disturbed, and the success of field collections relies on the collectors' skills, luck and collecting techniques and devices. The most common methods and devices for collecting shinning fungus beetles are sifting leaf litter, rotten wood and fungi, flight intercept (FIT) and V-flight intercept (V-FIT) traps, aspirators, sweeping, and hand collecting (Löbl & Leschen 2003; Tang *et al.* 2014; Löbl *et al.* 2021). Hand collecting is considered the best method, because the host fungi and larvae can be collected together to make associations (Löbl & Leschen 2003).

The aspirator is a good device for collecting shining fungus beetles from bracket and resupinate fungi, and slime molds, usually used for species in the genera *Baeocera* Erichson, 1845, *Scaphisoma* Leach, 1815, and *Toxidium* LeConte, 1860, especially because they run to get away instead of flying (pers. obs.). On the other hand, scaphidiines of the genera *Scaphidium* Olivier,1790 and *Cyparium* Erichson, 1845 can be found associated with mushrooms (Ashe 1984; Newton 1984). These latter genera are hardly collected using aspirators, because they stay mainly on the gills and close to the stalk, not easily accessed by aspirators due to the proximity to the floor. Another problem while using aspirators is the risk of aspirating fungal spores, which may cause allergic rhinitis and allergic asthma, and the smallest spores (less than 10 µm) may even penetrate the lower airways of the lung and mediate allergic reactions (Kurup *et al.* 2000). Collecting them by hand is not always efficient, because some mushrooms can hold many beetles that can easily fly away. These beetles are very good flyers and can escape very rapidly. To circumvent these problems, we developed a more efficient, low-cost device for collecting mushroom-dwelling shining fungus beetles, which minimizes the loss of beetles and do not expose collectors to fungal spores.

The device consists of a hinged, sturdy container, with edges sharp enough to cut a fungus stalk, preferable transparent or translucent. The container is armed with an Eppendorf vial fulfilled with cotton soaked with ethyl acetate, in order to kill or faint the beetles. We used cheap plastic onion keeper as the container, which costs about R$ 15,00 each (~US$ 2.75). In order to evaluate the efficacy of this collecting device, we performed eleven field trips between July and December 2019. We did not intend to conduct any controlled experiment, but simply to attest if the device would help to collect more individuals in comparison to our previous attempts using aspirators, because we need large series of each species for our ongoing morphological and taxonomical studies. Field trips were made to two Atlantic Forest remnants in Viçosa, state of Minas Gerais, Southeast Brazil, each lasting about four hours in the morning

Some mushrooms held a large number of beetles, and sometimes it was possible to see them from afar. But most of the time, each mushroom held one to three beetles hidden mainly on or between the gills. As they could escape rapidly, it is important to approach slowly with a small mirror (Fig. 1) and examine the underside carefully. Shinning fungus beetles are usually darker than the mushroom and so easily seen with the mirror. But more care shall be taken in mushrooms with dark spores, which usually darken the gills and let beetles inconspicuous.

 Accepted by H.-Z. Zhou: 10 Nov. 2021; published: 23 Nov. 2021

Beetles and host fungi can be collected together, in one movement, encapsulating the entire mushroom with the device (Fig. 2), cutting the stalk with the edge of the lid, collecting the whole mushroom without the risk of losing the beetles. After a few minutes (Fig. 3), the dead or fainted beetles (Fig. 4) can be transferred to Falcon tubes or any other vial, and then information and photos of the fungus can be taken without the risk of losing beetles. It is advisable to keep the tubes in freezer for a few hours to certify that the beetles are dead before mounting them. In our attempts we collected 192 individuals of the genus *Cyparium*, discriminated in 10 morphospecies, from 44 mushrooms, and two specimens of *Scaphidium* in one mushroom. The large number of beetles of the genus *Cyparium* was not a surprise, as these beetles are the most common associated with gilled mushrooms (Newton 1984). Although Neotropical *Cyparium* can be efficiently collected in SNV-FITs (Löbl *et al.* 2021), that does not allow host fungi recording. The simple device described here enables a fast survey of mushroom-dwelling scaphidiines, reduces escaping risk, allows gathering information on their host fungi and does not expose collectors directly to fungal spores. Our main aim with the collection field trips was to collect scaphidiines beetles from mushrooms, but we have also captured several other mushroom-dwelling beetles, especially Erotylidae, Nitidulidae, other Staphylinidae subfamilies and Tenebrionidae.

The tropical and subtropical shinning fungus beetles are sometimes barely studied and poorly represented in scientific collections (Leschen & Löbl 1995), as is true to the Brazilian fauna. We hope that the low-cost, simple and efficient device showed here will encourage other researchers in including mushroom-dwelling scaphidiines in faunistic and ecological surveys, and help to improve the knowledge on these biologically interesting beetles.

FIGURES 1–4. Method proposed here for collecting mushroom-dwelling beetles, especially the Scaphidiinae. **1.** Examining the gills with a mirror. **2.** Encapsuling the mushroom. **3.** Waiting for the beetles to stop moving. **4.** Fainted beetles before being transferred to Falcon tubes.

Acknowledgments

We thank the staff of Laboratório de Sistemática e Biologia de Coleoptera (UFV) for the assistance in field collections, especially Artur Orsetti who kindly helped Elisa to take the photographs. Financial support was provided by Conselho Nacional de Desenvolvimento Científico e Tecnológico (CNPq; research grant number 308432/2018-5 to C.L.-A.), Coordenação de Aperfeiçoamento de Pessoal de Nível Superior—Brasil (CAPES; Finance Code 001; doctorate degree grant to the senior author) and Fundação de Amparo à Pesquisa do Estado de Minas Gerais (FAPEMIG; doctorate grant to S.A. and financial support to C.L.-A. through the "Edital 02/2018—Programa Pesquisador Mineiro XII—PPM-00314-18").

References

Ashe, J.S. (1984) Description of the larva and pupa of *Scaphisoma terminatum* Melsh. and the larva of *Scaphium castanipes* Kirby with notes on their natural history (Coleoptera: Scaphidiidae). *The Coleopterists Bulletin*, 38, 361–373.

Kurup, V.P., Shen, H.D. & Banerjee, B. (2000) Respiratory fungal allergy. *Microbes and infection*, 2 (9), 1101–1110. https://doi.org/10.1016/S1286-4579(00)01264-8

Leschen, R.A.B. & Löbl, I. (1995) Phylogeny of Scaphidiinae with redefinition of tribal and generic limits (Coleoptera: Staphylinidae). *Revue suisse de Zoologie*, 102 (2), 425–474. https://doi.org/10.5962/bhl.part.80472

Löbl, I. (2018) *Coleoptera: Staphylinidae: Scaphidiinae*. Brill, Leiden, 418 pp. https://doi.org/10.1163/9789004375956

Löbl, I. & Leschen, R.A.B. (2003) Scaphidiinae (Insecta: Coleoptera: Staphylinidae). *Fauna of New Zealand*, 48, 1–94.

Löbl, I., Leschen, R.A.B & Warner, W.B. (2021) Scaphisomatini of Arizona (Coleoptera, Staphylinidae, Scaphidiinae) collected by V-Flight Intercept traps. *Revue suisse de Zoologie*, 128 (1), 173–185. https://doi.org/10.35929/RSZ.0043

Löbl, I. & Ogawa, R. (2016) On the Scaphisomatini (Coleoptera, Staphylinidae, Scaphidiinae) of the Philippines, IV: the genera *Sapitia* Achard and *Scaphisoma* Leach. *Linzer biologische Beiträge*, 48 (2), 1339–1492.

Newton, A.F. Jr. (1984) Mycophagy in Staphylinoidea (Coleopetra). *In*: Wheeler, Q. & Blackwell, M. (Eds.), *Fungus/insect relationships. Perspectives in ecology and evolution*. Columbia University Press, New York, New York, pp. 302–353.

Tang, L., Li, L.-Z. & He, W.-J. (2014) The genus *Scaphidium* Olivier in East China (Coleoptera, Staphylinidae, Scaphidiinae). *ZooKeys*, 403, 47–96. https://doi.org/10.3897/zookeys.403.7220

von Groll, E. & Lopes-Andrade, C. (2021) *Scaphisoma pandemum* sp. nov. (Coleoptera: Staphylinidae: Scaphidiinae) from the Atlantic Forest of Southeast Brazil. *Zootaxa*, 4999 (2), 143–156. https://doi.org/10.11646/zootaxa.4999.2.4

CAPÍTULO 3 – Contributions to the taxonomy of Neotropical *Cyparium* Erichson (Coleoptera: Staphylinidae: Scaphidiinae), with the description of five new species

Publicado na revista European Journal of Taxonomy 835: 1–97

https://doi.org/10.5852/ejt.2022.835.1909

European Journal of Taxonomy 835: 1–97
https://doi.org/10.5852/ejt.2022.835.1909
ISSN 2118-9773
www.europeanjournaloftaxonomy.eu
2022 · von Groll E. & Lopes-Andrade C.

Monograph

urn:lsid:zoobank.org:pub:8B8432B1-C714-4179-8687-66902F4CBF53

Contributions to the taxonomy of Neotropical *Cyparium* Erichson (Coleoptera: Staphylinidae: Scaphidiinae), with the description of five new species

Elisa VON GROLL [1,*] & Cristiano LOPES-ANDRADE [2]

[1,2]Programa de Pós-Graduação em Biologia Animal, Universidade Federal de Viçosa, Av. Peter Henry Rolfs, s/n, 36570-900, Viçosa, MG, Brasil.
[1,2]Laboratório de Sistemática e Biologia de Coleoptera, Departamento de Biologia Animal, Universidade Federal de Viçosa, Av. Peter Henry Rolfs, s/n, 36570-900, Viçosa, MG, Brasil.

*Corresponding author: elisavgroll@gmail.com
[2]Email: ciidae@gmail.com

[1]urn:lsid:zoobank.org:author:DC564233-82A9-4939-8B7A-F02C994BBA29
[2]urn:lsid:zoobank.org:author:525ABCB9-3334-407E-9084-F0784968D290

Abstract. The genus *Cyparium* Erichson, 1845 (Staphylinidae, Scaphidiinae, Cyparіini) comprises 55 species, distributed mainly in the Neotropical and Oriental regions. Twenty-four species are known from the Neotropical region, but only eight species are reported from Brazil. In this paper we describe five new species and redescribe two species of Brazilian *Cyparium*, as follows: *Cyparium achardi* sp. nov., *C. lescheni* sp. nov., *C. loebli* sp. nov., *C. newtoni* sp. nov., *C. pici* sp. nov.; *Cyparium collare* Pic, 1920; and *Cyparium oberthueri* Pic, 1956. We provide images of adult males and females and their dissected parts, and information on host fungi whenever available. We also provide a comparative plate of dorsal colour patterns of Neotropical *Cyparium*.

Keywords. Insects, morphology, shining fungus beetles, Brazil, records.

von Groll E. & Lopes-Andrade C. 2022. Contributions to the taxonomy of Neotropical *Cyparium* Erichson (Coleoptera: Staphylinidae: Scaphidiinae), with the description of five new species. *European Journal of Taxonomy* 835: 1–97. https://doi.org/10.5852/ejt.2022.835.1909

Introduction

The shining fungus beetles (Coleoptera: Staphylinidae: Scaphidiinae Latreille, 1806) include over 1800 species and subspecies in 46 genera and four tribes: Cyparіini Achard, 1924, Scaphiini Achard, 1924, Scaphidiini Latreille, 1806, and Scaphisomatini Casey, 1893 (Löbl 2018a). They are small beetles (≈ 0.84–14.0 mm long) (Tang *et al.* 2014; Löbl & Ogawa 2016), distributed worldwide, diverse and abundant in most terrestrial ecosystems, especially subtropical and tropical forests (Leschen & Löbl 1995). They are usually collected on fungi, slime moulds, by sifting litter or using flight intercept traps (Lawrence & Newton 1980; Newton 1984; Leschen 1994; Stephenson *et al.* 1994; Löbl & Leschen 2003; Tang *et al.* 2014; Löbl 2018a; Löbl *et al.* 2021).

The genus *Cyparium* Erichson, 1845 (Staphylinidae, Scaphidiinae, Cyparіini), the only genus of Cyparіini, comprises 55 species, distributed mainly in the Neotropical and Oriental regions (Leschen & Löbl 1995; Löbl 2018a). It is absent from oceanic islands, northern Africa, Australia, Europe, Madagascar, New Guinea and Chile (Leschen & Löbl 1995). Twenty-four species are known from the Neotropical region, but only eight species are reported from Brazil, as follows: *C. collare* Pic, 1920; *C. ferrugineum* Pic, 1920; *C. grilloi* Pic, 1920; *C. grouvellei* Pic, 1920; *C. oberthueri* Pic, 1956; *C. pygidiale* Achard, 1922; *C. ruficolle* Achard, 1922; and *C. rufohumerale* Pic, 1931.

Species of *Cyparium* are easily distinguished from other scaphidiines by their robust body, non-emarginate eyes, compact antennal club with only slightly flattened antennomeres, pronotum widest posteriorly, and spinose pro- and mesotibiae (Leschen & Löbl 1995; Newton *et al.* 2001). They are usually found in basidiomes of Agaricales Underw., 1899 (Newton 1984; Kompantsev & Pototskaya 1987), but there are also records from coral fungi (Clavaraceae (Chevall., 1826)) and tooth fungi (Hydnaceae Chevall., 1826) (Newton 1984; Leschen & Löbl 1995). As feeders on ephemeral gilled mushrooms, it is expected that *Cyparium* beetles will have a faster development than other scaphidiines (Ashe 1984).

The number of described Neotropical species of *Cyparium* is quite low, considering that they are probably easy to collect using SNV-FITs traps (Löbl *et al.* 2021) or manually (von Groll *et al.* 2021), and that the region has a vast territory and heterogeneity of tropical and subtropical terrestrial ecosystems. This low number may be due to actual low diversity, or a result of the few studies on the Neotropical Scaphidiinae. The second alternative is the most likely, considering that the faunas of some tropical and subtropical areas are virtually undescribed (Leschen & Löbl 1995), and that von Groll *et al.* (2021) were able to collect ten morphospecies and 192 individuals of *Cyparium* with low collection effort in two small forest remnants of the Brazilian Atlantic biome.

In the first detailed phylogenetic study including *Cyparium*, eight species from the Nearctic, Asian, Palearctic and Neotropical regions were examined (Leschen & Löbl 1995). *Cyparium* was recovered as monophyletic, supported by the prosternum in front of the procoxae reduced to a length less than that of the procoxa, the width of the mesoventral process more than that of the metacoxal process, abdominal sternite VIII with anteriorly projecting process, and the gonostyli long (Leschen & Löbl 1995). However, the position of Cyparіini within Scaphidiinae was not well resolved. Sometimes it was placed as sister group of the remaining Scaphidiinae, or it formed a clade with Scaphiini Achard, 1924. They concluded that more data (from larvae and adults, based on better preserved specimens) were necessary to improve the results. Subsequent studies have faced the same problems. Grebennikov & Newton (2012), which included larvae and a member of Scaphiini, recovered *Cyparium* as sister to the remaining Scaphidiinae. On the other hand, McKenna *et al.* (2014) recovered *Cyparium* as the sister group of *Scaphidium* Olivier, 1790 (Scaphidiini), and them together as the sister group of *Scaphium* Kirby, 1837 (Scaphiini). When studying the phylogeny of Scaphisomatini (Scaphidiinae, Staphylinidae), Leschen & Löbl (2005) included both sexes of *Cyparium flavipes* LeConte, 1860 (synonym of *Cyparium concolor* (Fabricius, 1801)) as the outgroup. Their matrix included 110 characters and provided detailed information on the internal and external morphology of males and females of this genus.

Some of the original descriptions are remarkably complete (e.g., *Cyparium navarretei* Fierros-López, 2002), but most of them are too general and lack information necessary for accurate identifications (e.g., *C. nigronotatum* Pic, 1931 and *C. collare*), which can cause difficulties when studying these beetles, especially because it is not always easy to access type material (Löbl 2020). Regarding morphology, important contributions on coloration (Márquez 2007) and female terminalia (Ogawa & Sakai 2011) were made. Nonetheless, by studying specimens of *Cyparium*, we noticed that there are more structures to explore.

In this work we describe five new species of *Cyparium* and redescribe *C. collare* and *C. oberthueri*, all occurring in Brazil. We provide detailed morphological descriptions of adult males and females, including images of dissected structures, and host fungi data whenever possible. We also provide a comparative plate of dorsal colour patterns of Neotropical *Cyparium*.

Material and methods

Specimens collected in "Viçosa" were found at two Atlantic Forest remnants in Viçosa, state of Minas Gerais, Southeast Brazil: "Mata da Biologia" (20°45′32″ S, 42°51′49″ W), with 75 hectares and located within the campus of the Federal University of Viçosa; and "Estação de Pesquisa, Treinamento e Educação Ambiental Mata do Paraíso" (20°48′05″ S, 42°51′58″ W), with 194 hectares and located about 4 km south of the campus, but under the care of the university.

Specimens collected in 2019 followed the manual colleting method of von Groll *et al.* (2021). Fungi were photographed with a smartphone or a Nikon D810 camera, kept in a paper bag and dehydrated in a dry heat sterilizer. Beetles were kept in a freezer for a few hours and then mounted using double mounting.

For the dissections, beetles were boiled in water to soften the tissues. Then the larger parts were separated and boiled in saturated KOH solution for maceration of the tissues and cleaning. Then they were immersed in 10% acetic acid for a few minutes to neutralize any remaining KOH, and finally cleaned in water. More delicate structures were dissected after this process.

The structures were observed in glycerin and photographed in KY®. Male aedeagui were passed through a battery concentration until they were immersed in KY®: alcohol 40%, 70%, 80%; glycerin 40%, 70%, 100%; otherwise, the structure was crushed by the pressure of the 100% glycerin or KY®. Permanent slide preparations of hind wings were made using PVLG (polyvinyl alcohol-lactic acid-glycerol) (Omar *et al*. 1979). Photographs were taken using a Zeiss Discovery V20 stereo microscope equipped with a Zeiss AxioCam 506, a Zeiss AxioLab compound microscope equipped with a Zeiss AxioCam MRc or a Canon EOS 1000D digital camera; all photos were taken using the technique of focus-staking.

Antennomere measurements were taken using editing software. Body measurements were taken under a Zeiss Stemi 2000C stereo microscope equipped with a 2× objective lens and an ocular micrometer. Range, mean and standard deviation values were estimated using PAST. The following abbreviations are used for measurements (in mm):

EH = elytral height in lateral view (Fig. 1C)
EI = length of the inner margins of elytra; not including the scutellar shield (Fig. 1A)
EL = elytral length at the midline (Fig. 1A)
EW = greatest right elytron width (Fig. 1A)
HW = maximum width of the head including eyes (Fig. 1D)
IS = interocular space (Fig. 1D)
MB = mesothorax length between fore and middle legs (Fig. 1B)
MC = mesothorax length at the midline (Fig. 1B)
PA = pronotal width at the anterior margin (Fig. 1A)
PB = pronotal width at the posterior margin (Fig. 1A)
PL = pronotal length along the midline (Fig. 1A)
SL = scutellar shield length (Fig. 1A)
SW = scutellar shield width (Fig. 1A)
TL = total body length, not including head and abdomen (Fig. 1A)
VL = length of ventrite 1 in the midline (Fig. 1B)
WA = width between antennae (Fig. 1D)

To see if elytra were wider than long the following comparison was performed: EW*2 vs EL.

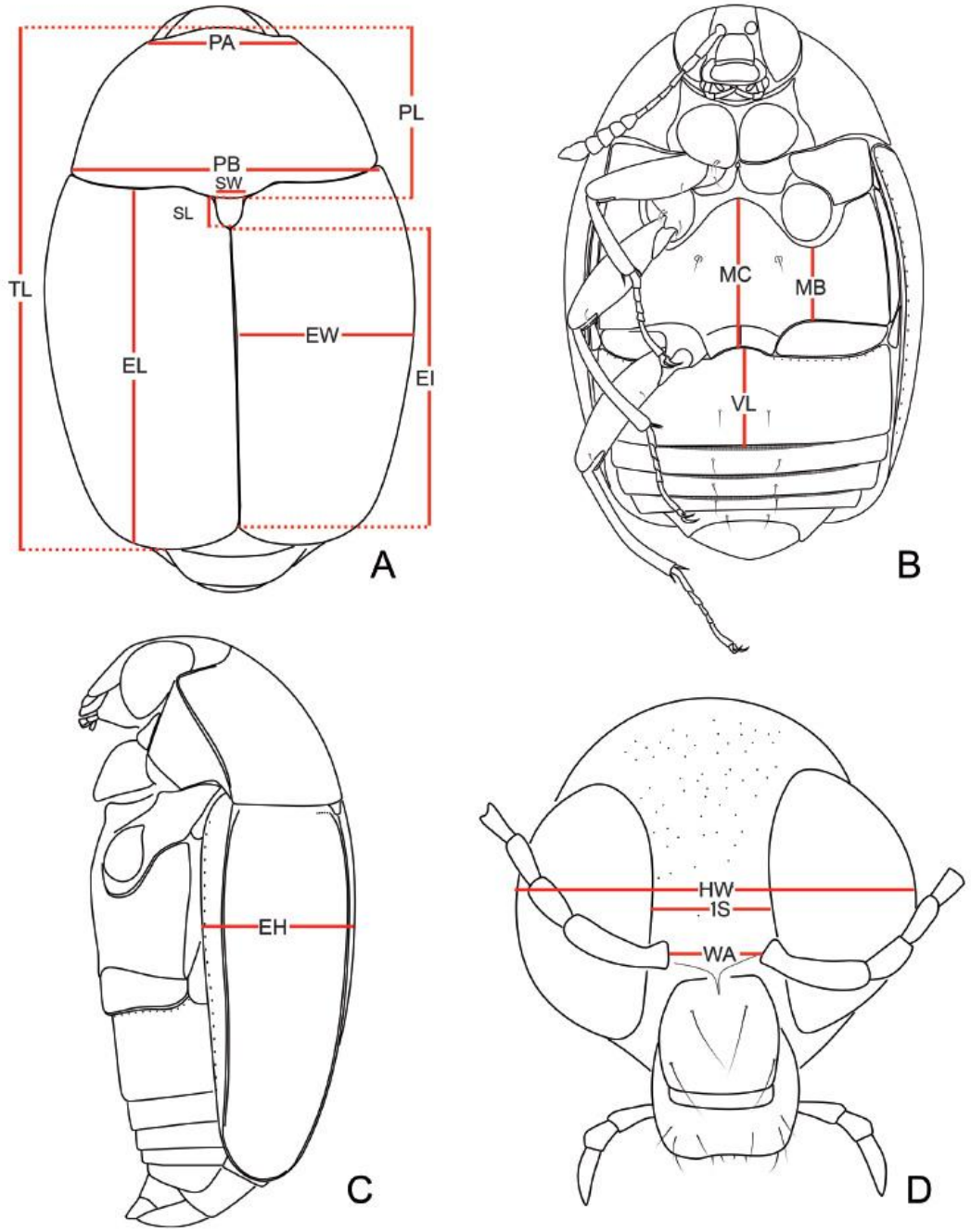

Fig. 1. *Cyparium collare* Pic, 1920. Measurements taken. **A**. Dorsal view. **B**. Ventral view. **C**. Lateral view. **D**. Head in frontal view. Abbreviations: EH = elytral height in lateral view; EI = length of the inner margins of elytra, not including the scutellar shield; EL = elytral length in the midline; EW = greatest right elytron width; HW = maximum width of the head including eyes; IS = interocular space; MB = mesothorax length between fore and middle legs; MC = mesothorax length in the midline; PA = pronotal width at the anterior margin; PB = pronotal width at the posterior margin; PL = pronotal length along the midline; SL = scutellar shield length; SW = scutellar shield width; TL = total body length, not including head and abdomen; VL = length of ventrite 1 in the midline; WA = width between antennae.

Unless otherwise specified, each description was based on the respective male holotype; descriptions of dissected parts were based on paratypes. Terminology follows Ogawa & Löbl (2013) for external morphology, and male and female terminalia; Naomi (1988a, 1988b), Leschen *et al*. (1990), Leschen & Löbl (2005) and Lawrence & Ślipiński (2013) for external morphology; Harris (1979) for microsculpture; Jałoszyński (2012) for the internal structure of the prothorax; Friedrich & Beutel (2006) for the mesonotum; Lawrence *et al.* (2021) for the hind wing venation; Crowson (1938), Naomi (1989a) and Hübler & Klass (2013) for the metendosternite; Naomi (1989b) for the abdominal segments; Naomi (1990) for male terminalia (Figs 2–3). Not all structures of scaphidiine metendosternites are well illustrated; therefore, at this moment, we adopted the term 'stalk ridge' for the suture present on the stalk

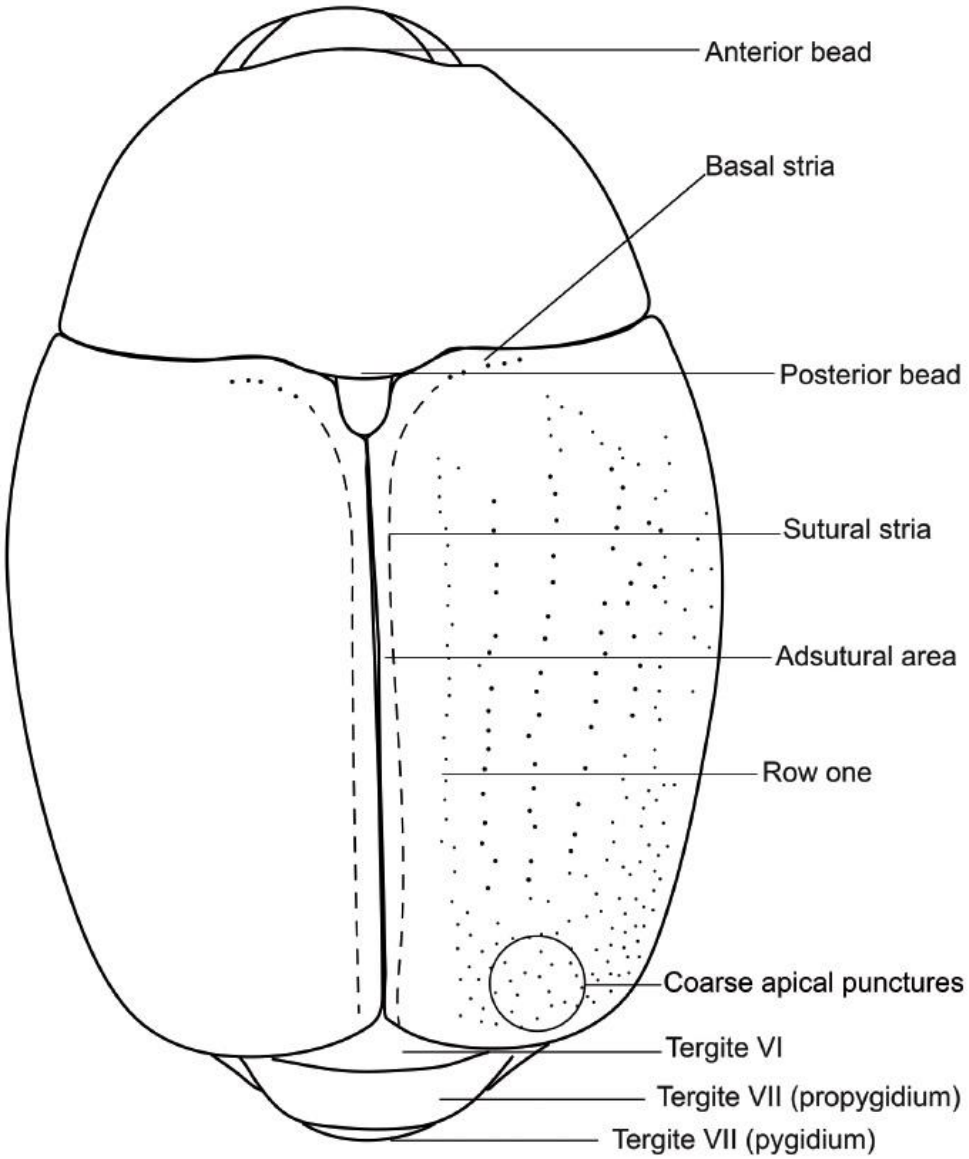

Fig. 2. Dorsal terminology. Model: *Cyparium collare* Pic, 1920.

(Fig. 10A). We call the parameral view of median lobe as 'ventral view' and the opposite view of it as 'dorsal view' even though the median lobe stays somewhat turned to the side when it is at rest.

Unless otherwise specified in the text (between square brackets), labels are printed on white paper. Each label is separated by a backslash. The number and gender of specimens bearing these labels are stated immediately before the label data.

Due to restrictions for loaning historical or type specimens to Brazilian researchers by a few museums, to the increasing Brazilian bureaucracy, risks for receiving and sending museum specimens, and high costs for visiting foreign museums, it was not possible to examine type series and historical

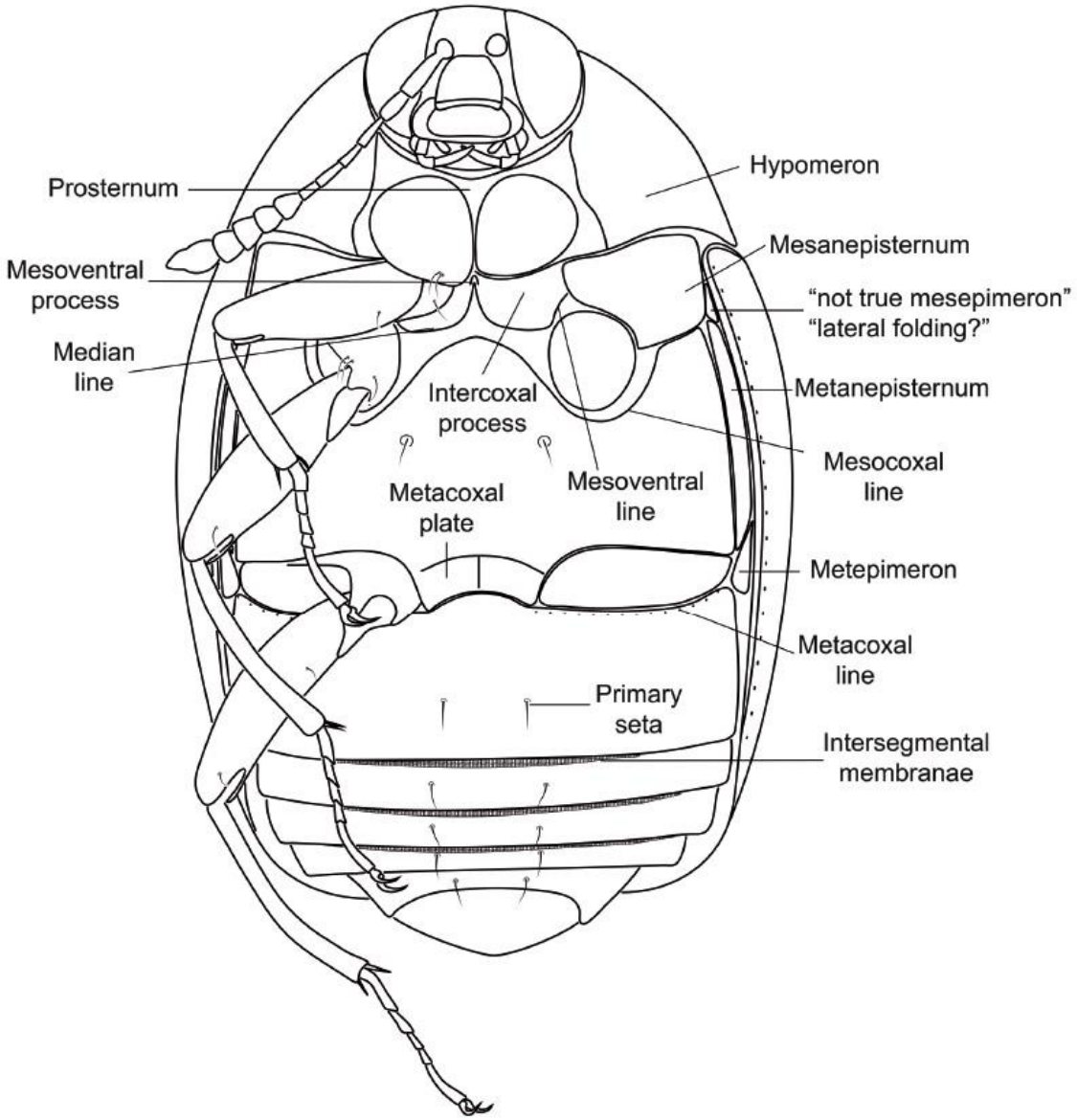

Fig. 3. Ventral terminology. Model: *Cyparium collare* Pic, 1920.

material of previously described species. Therefore, comparisons with previously described species and identification of specimens were made by consulting original descriptions, and by examining photographs kindly provided by the staff of the MNHN (Muséum national d'histoire naturelle, Paris) and the NMCZ (Natural History Museum, Prague).

Illustrations of the Neotropical species of *Cyparium* (Figs 4–5) were made using colour and length information extracted from the original descriptions, and the available photographs of type specimens (Fig. 6). Since the purpose was only to show the colour and length patterns, the shape does not represent the species. Species illustrations are displayed in alphabetical order and in proportional size (considering the anterior margin of the pronotum to elytral apex).

Supplementary material includes labels of the holotypes of the new species (Supp. file 1); figures of female terminalia of *C. lescheni* sp. nov. and *C. collare* (Supp. file 2B); and photos of habitus and male terminalia of *C. collare* from two different localities (Supp. file 3 (Figs 1A–4H)).

Acronyms of scientific collections:

CAMB	=	Coleção Ayr de Moura Bello, Rio de Janeiro, RJ, Brazil
CELC	=	Coleção Entomológica do Laboratório de Sistemática e Biologia de Coleoptera da UFV, Viçosa, MG, Brazil
CEMT	=	Seção de Entomologia da Coleção Zoológica, Departamento de Biologia e Zoologia, Instituto de Biociências, Universidade Federal de Mato Grosso, Cuiabá, MT, Brazil
CERPE	=	Coleção Entomológica da Universidade Federal Rural de Pernambuco, Recife, PE, Brazil
CZUG	=	Centro de Estudios Zoología, Universidad de Guadalajara, Jalisco, Mexico
FZCH	=	Fernando de Zayas Collection, Habana, Cuba
MCNZ	=	Museu de Ciências Naturais, Secretaria do Meio Ambiente e Infraestrutura, Porto Alegre, RS, Brazil
MCSN	=	Museo Civico di Storia Naturale, Genova, Italy
MNHN	=	Muséum national d'histoire naturelle, Paris, France
NHML	=	The Natural History Museum, London, UK (former British Museum (Natural History))
NMPC	=	Národní Muzeum, Entomologické oddělení, Praha, Czech Republic
SNSD	=	Senckenberg Naturhistorische Sammlungen Dresden, Dresden, Germany
ZMUB	=	Zoologisches Museum, Museum für Naturkunde, Berlin, Germany

As the diversity of Neotropical *Cyparium* is certainly much higher than we could access at this moment, providing a key to the described Brazilian or Neotropical species would not be useful here. Moreover, we have examined only photos of some species, which do not provide enough information for including them in an identification key.

Results

Catalogue of Neotropical species

The Neotropical *Cyparium* are barely studied and the species may have a much broader geographic distribution than currently known. At this moment we shall consider the possibility that any of the previously described Neotropical *Cyparium* may occur in Brazil. Because of this, and as a support for subsequent works, below we list all Neotropical *Cyparium* species and subspecies, based mostly on Löbl (2018a). In Figs 4–5 we provide a comparative plate of their dorsal colour patterns.

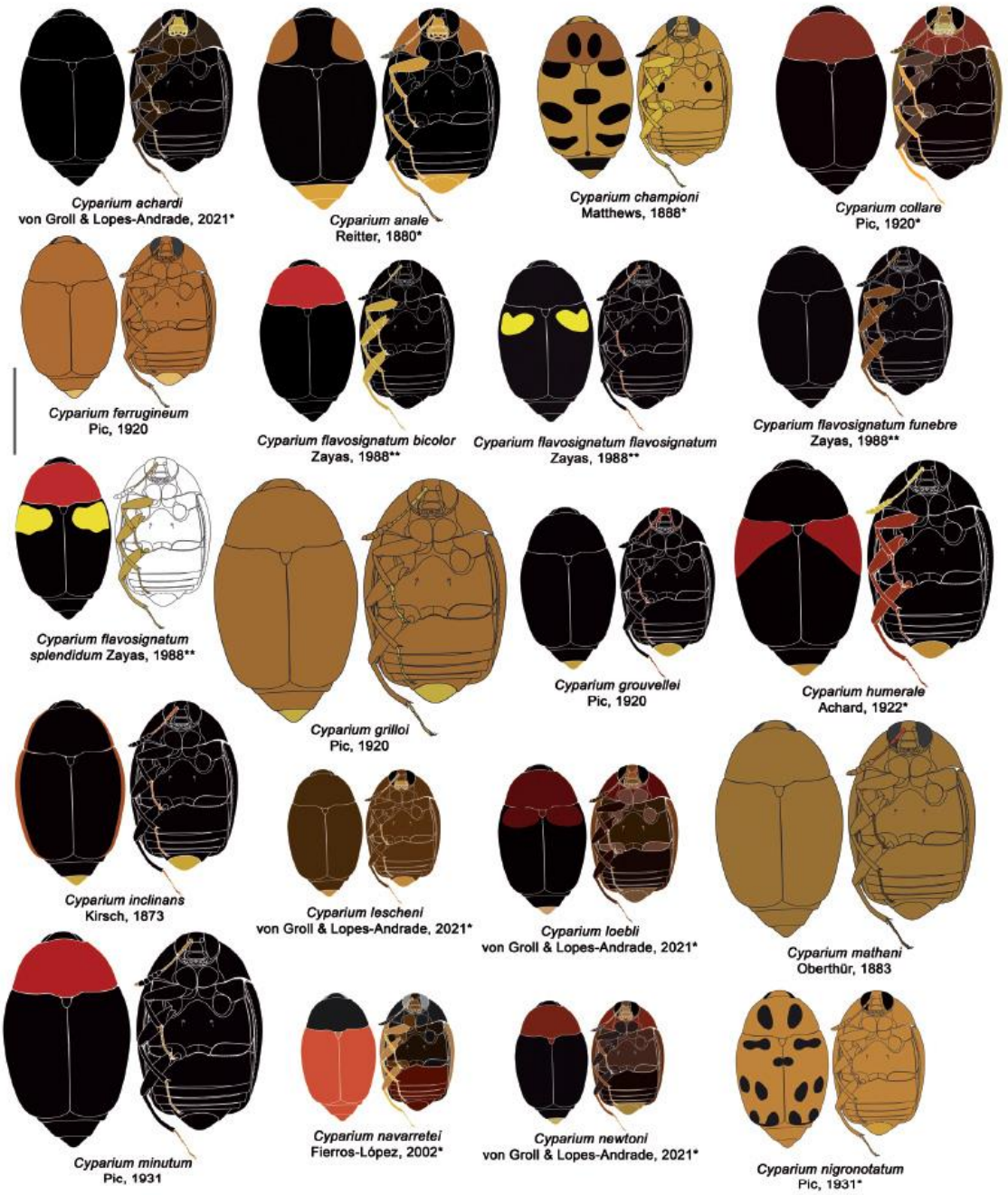

Fig. 4. *Cyparium* Erichson, 1845. Neotropical species. Illustrations based on the original descriptions. *Illustrations made based on photographs, specimens, or illustrations made by other authors; **size not provided in original description. Model: *Cyparium collare* Pic, 1920. Scale bar = 2 mm.

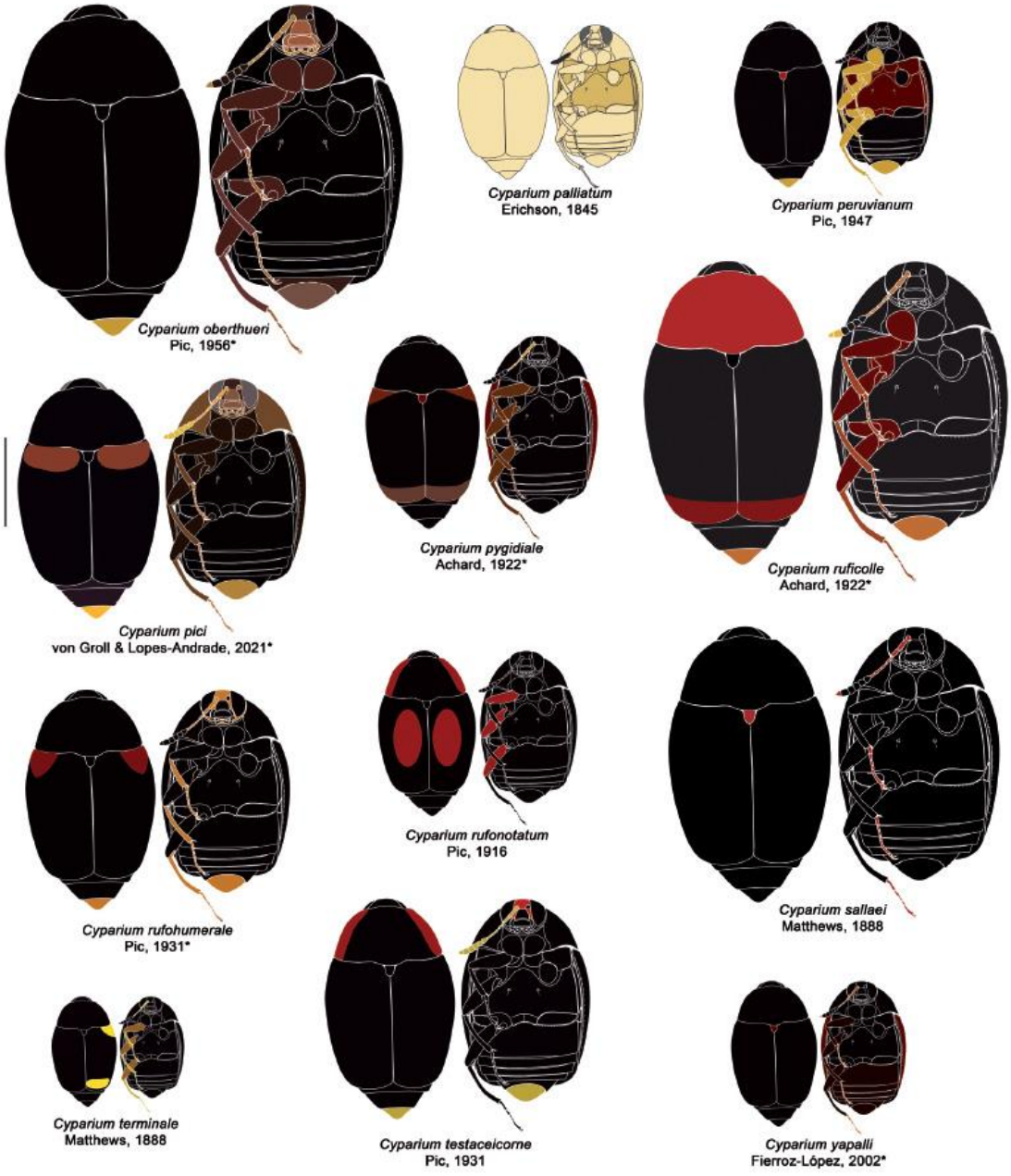

Fig. 5. *Cyparium* Erichson, 1845. Neotropical species. Illustrations based on the original descriptions. *Illustrations made based on photographs, specimens, or illustrations made by other authors. Model: *Cyparium collare* Pic, 1920. Scale bar = 2 mm.

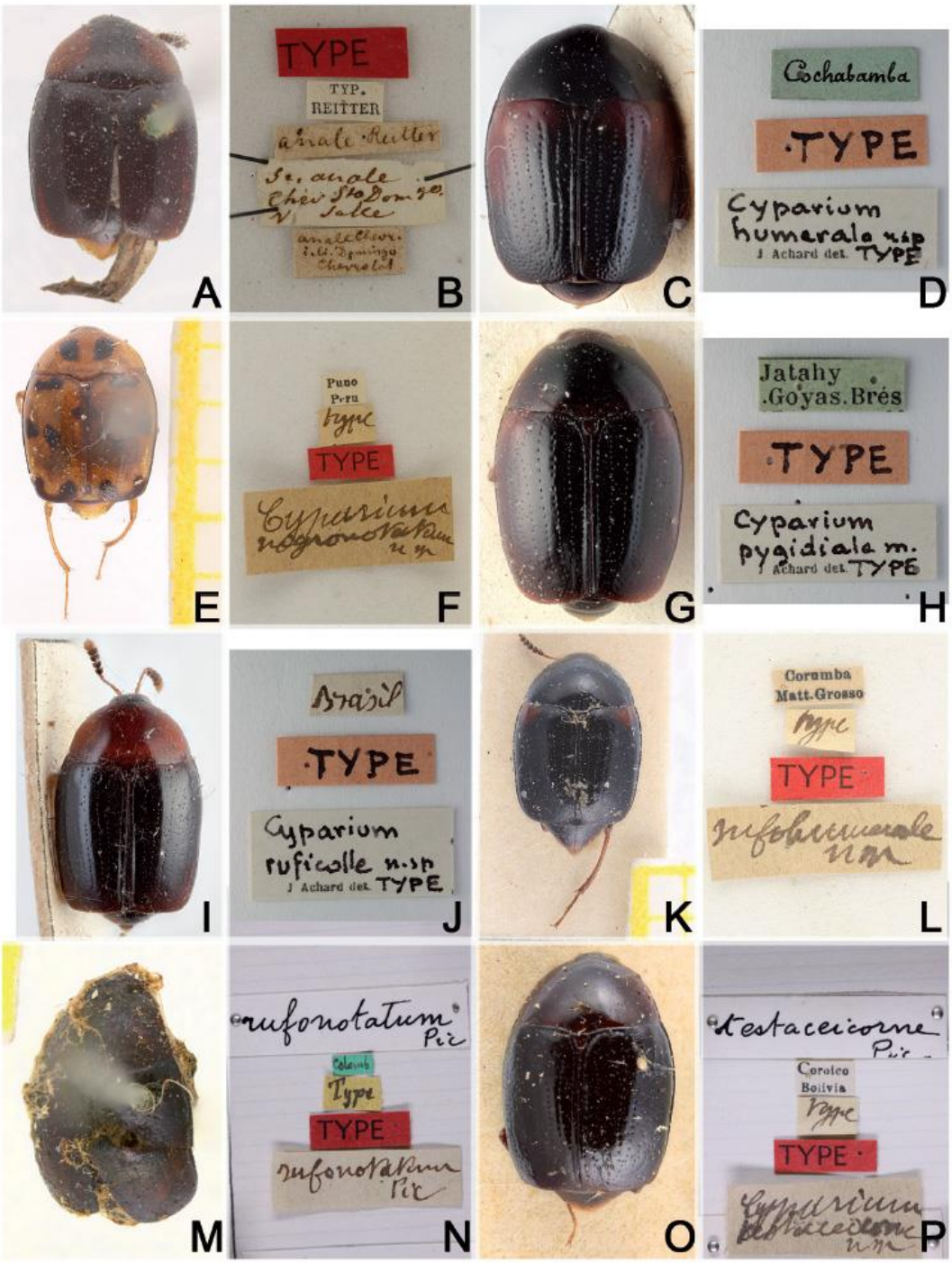

Fig. 6. Syntypes. **A–B**. *Cyparium anale* Reitter, 1880 (MNHN). **A**. Habitus. **B**. Labels. **C–D**. *C. humerale* Achard, 1992 (NMPC). **C**. Habitus. **D**. Labels. **E–F**. *C. nigronotatum* Pic, 1931 (MNHN). **E**. Habitus. **F**. Labels. **G–H**. *C. pygidiale* Achard, 1922 (NMPC collection-Prague). **G**. Habitus. **H**. Labels. **I–J**. *C. ruficolle* Achard, 1922 (NMPC). **I**. Habitus. **J**. Labels. **K–L**. *C. rufohumerale* Pic, 1931 (MNHN). **K**. Habitus. **L**. Labels. **M–N**. *C. rufonotatum* Pic, 1916 (MNHN). **M**. Habitus. **N**. Labels. **O–P**. *C. testaceicorne* Pic, 1931 (MNHN). **O**. Habitus. **P**. Labels.

Class Insecta Linnaeus, 1758
Order Coleoptera Linnaeus, 1758
Family Staphylinidae Latreille, 1802
Subfamily Scaphidiinae Latreille, 1806
Tribe Cypariini Achard, 1924
Genus *Cyparium* Erichson, 1845

Cyparium anale Reitter, 1880
Figs 4, 6A–B

Cyparium anale Reitter, 1880: 42. Syntypes, MNHN; type locality: St. Domingo.
Cyparium submetallicum Reitter, 1880: 43. Syntypes, MNHN; type locality: "India or.?". [syn.].

Cyparium anale – Achard, 1921: 86 (synonymy of *C. submetallicum* with *C. anale*).

Distribution

Dominican Republic.

Cyparium championi Matthews, 1888
Fig. 4

Cyparium championi Matthews, 1888: 167, pl. 4 fig. 9. Holotype, NHML; type locality: Panama: Bugaba.

Distribution

Bolivia; Costa Rica; Ecuador; Nicaragua; Panama; Suriname.

Cyparium collare Pic, 1920
Figs 4, 47–55, Supp. file 2B, Supp. file 3 (Figs 1A–4H)

Cyparium collare Pic, 1920a: 4. Syntypes, MNHN; type localities: "Brésil" [Matu Sinhos, Minas; Matto Grosso; Pery-Pery, Pernambuco; right bank of Parahyba].

Distribution

Brazil.

Cyparium ferrugineum Pic, 1920
Fig. 4

Cyparium ferrugineum Pic, 1920a: 5. Syntypes, MNHN; type locality: Brazil [Pery-Pery, Pernambuco, Matto Grosso].

Distribution

Brazil.

Cyparium flavosignatum Zayas, 1988
Cyparium flavosignatum flavosignatum Zayas, 1988
Fig. 4

Cyparium flavosignata Zayas, 1988: 23, fig. 13. Syntypes, FZCH; type locality: Cuba.

Distribution

Cuba.

Cyparium flavosignatum bicolor Zayas, 1988
Fig. 4

Cyparium flavosignata bicolor Zayas, 1988: 24, fig. 15. Syntypes, FZCH; type locality: Cuba.

Distribution

Cuba.

Cyparium flavosignatum funebre Zayas, 1988
Fig. 4

Cyparium flavosignata funebris Zayas, 1988: 24, fig. 14. Syntypes, FZCH; type locality: Cuba.

Distribution

Cuba.

Cyparium flavosignatum splendidum Zayas, 1988
Fig. 4

Cyparium flavosignata splendidum Zayas, 1988: 25, fig. 16. Syntypes, FZCH; type locality: Cuba.

Distribution

Cuba.

Cyparium grilloi Pic, 1920
Fig. 4

Cyparium grilloi Pic, 1920b: 94. Syntypes, MCSN; type locality: Brazil: Paranà, Palmeira.

Distribution

Brazil.

Cyparium grouvellei Pic, 1920
Fig. 4

Cyparium grouvellei Pic, 1920a: 5. Syntypes, MNHN; type locality: Brazil.

Distribution

Brazil.

Cyparium humerale Achard, 1922
Figs 4, 6C–D

Cyparium humerale Achard, 1922: 40. Syntypes, NMPC; type locality: Bolivia: Cochabamba.

Distribution

Bolivia.

Cyparium inclinans Kirsch, 1873
Fig. 4

Cyparium inclinans Kirsch, 1873: 135. Syntypes, SNSD; type locality: Peru.

Distribution

Peru.

Cyparium mathani Oberthür, 1883
Fig. 4

Cyparium mathani Oberthür, 1883: 12. Syntypes, MNHN; type localities: Peru: Iquitos and Amazones.

Distribution

Peru.

Cyparium minutum Pic, 1931
Fig. 4

Cyparium minutum Pic, 1931: 2. Syntypes, MNHN; type locality: Jamaica: Jackson Town.

Distribution

Jamaica.

Cyparium navarretei Fierros-López, 2002
Fig. 4

Cyparium navarretei Fierros-López, 2002: 8, figs 1, 3–5. Holotype male, CZUG; type locality: Mexico: Veracruz, Cerro Acatlán, Naolinco.

Distribution

Mexico.

Cyparium nigronotatum Pic, 1931
Figs 4, 6E–F

Cyparium nigronotatum Pic, 1931: 2. Syntypes, MNHN; type locality: Peru: [Puno].

Distribution

Peru.

Cyparium oberthueri Pic, 1856
Fig. 5, 56–64

Cyparium oberthüri Pic, 1956: 175. Syntypes, MNHN; type locality: Brazil: Matto Grosso.

Distribution

Brazil.

Cyparium palliatum Erichson, 1845
Fig. 5

Cyparium palliatum Erichson, 1845: 4. Syntypes ZMUB [single female, labelled as holotype]; type locality: Mexico.

Distribution

Mexico.

Cyparium peruvianum Pic, 1947
Fig. 5

Cyparium peruvianum Pic, 1947: 7. Syntypes, MNHN; type locality: Peru.

Distribution

Peru.

Cyparium pygidiale Achard, 1922
Figs 4, 6G–H

Cyparium pygidiale Achard, 1922: 40. Syntypes, NMPC; type localities: Brazil: Goyaz, Jatahy.

Distribution

Brazil.

Cyparium ruficolle Achard, 1922
Figs 4, 6I–J

Cyparium ruficolle Achard, 1922: 39. Syntypes, NMPC; type locality: Brazil [Corumba, Matto Grosso].

Distribution

Brazil.

Cyparium rufohumerale Pic, 1931
Figs 4, 6K–L

Cyparium rufohumerale Pic, 1931: 2. Syntypes, MNHN; type locality: Brazil.

Distribution

Brazil.

Cyparium rufonotatum Pic, 1916
Figs 5, 6M–N

Cyparium rufonotatum Pic, 1916: 18. Holotype, MNHN; type locality: Colombia.

Distribution

Colombia.

Cyparium sallaei Matthews, 1888
Fig. 5

Cyparium sallaei Matthews, 1888: 166, pl. 4 fig. 10. Syntypes, NHML; type locality: Mexico: Cordoba.

Distribution

Mexico.

Cyparium terminale Matthews, 1888
Fig. 5

Cyparium terminale Matthews, 1888: 167, pl. 4 fig. 9. Syntypes, NHML; type localities: Mexico: Jalapa, Cordoba; Guatemala, Zapote, Capetillo, San Juan in Vera Paz; Panama, Bugaba.

Distribution

Guatemala; Mexico; Panama.

Cyparium testaceicorne Pic, 1931
Figs 5, 6O–P

Cyparium testaceicorne Pic, 1931: 2. Syntypes, MNHN; type locality: Bolivia: [Coroico].

Distribution

Bolivia.

Remarks

We received photos of the dorsal view and labels of the type (MNHN), but the specimen shown in the photos does not match the original description. The pronotum of this specimen is entirely reddish brown and 3 mm long, while in the description Pic (1931) wrote "capite antice et thorace lateraliter rufis (…) Long. 4 mill. (…) Voisin de anale Reitt.". The specimen on the photo better fits the description of *C. collare*, by its coloration (pronotum reddish brown) and length of 3 mm. We could not locate the syntypes of *C. collare*. The illustration of *C. testaceicorne* (Fig. 5) provided here was based on the original description and not on the specimen shown in the available photos (Fig. 6O).

Cyparium yapalli Fierros-López, 2002
Fig. 5

Cyparium yapalli Fierros-López, 2002: 9, figs 2, 6–7, 9, 11. Holotype male, CZUG; type locality: Mexico: Oaxaca, Km 164 carr. Sola de Vega-Puerto Escondido.

Distribution

Mexico.

Descriptions of new species

Cyparium achardi sp. nov.
urn:lsid:zoobank.org:act:ABFE4E1F-DB31-46C1-BDC7-BDD1C4FF81E3
Figs 4, 7–13, 46; Supp. file 1A

Diagnosis

TL: 3.00–3.28 mm in males and 3.32–3.40 mm in females. Entirely black, with lateral areas of some ventral sclerites lighter (Fig. 7A–C). Eyes long (Fig. 7D). Hypomeron and metaventrite smooth. Metanepisternum and metepimeron with imbricate microsculpture. Tergite VIII of males coarsely punctate (Fig. 11D). Aedeagus strongly sclerotized (Fig. 12A–C); apex and parameres short (Fig. 12A). Distal gonocoxites of females straight and thick (Fig. 13C, E).

Etymology

In homage to the entomologist Julien Achard (1881–1925) for his significant contribution on the Neotropical Scaphidiinae.

Material examined

Holotype

BRAZIL • ♂; Minas Gerais, Viçosa, EPTEA Mata do Paraíso; 19 Nov. 2019; LabCol leg.; "Fungo 27 \\ Em *Leucoagaricus* sp. \\ *Cyparium achardi* von Groll & Lopes-Andrade HOLOTYPUS" [red paper]; CELC. (Supp. file1A).

Paratypes

BRAZIL • 3 ♂♂, 1 ♀ (1 ♂ entirely dissected, preserved in glycerin); same collection data as for holotype; "T. do Pesquisador"; 8 Nov. 2016; C. Lopes-Andrade *et al.* leg.; "\\ Em *Marasmiellus volvatus*"; CELC • 2 ♀♀ (1 ♀, abdomen dissected, preserved in glycerin); same collection data as for holotype; 14 Nov. 2019; "Fungo 22 \\ Em *Marasmiellus* sp."; CELC • 1 ♀; same collection data as for holotype; "Fungo 26 \\ Em *Hygrocybe* sp."; CELC • 1 ♂; same collection data as for holotype; "Fungo 28 \\ Em *Leucocoprinus ianthinus*"; CELC • 1 ♂; same collection data as for holotype; "Fungo 12 \\ Em *Marasmius haematocephalus*"; CELC • 1 ♀; same collection data as for holotype; 26 Nov. 2019; LabCol leg.; "Fungo 53 \\ Em *Leucocoprinus* sp."; CELC • 1 spec.; Viçosa, Recanto das Cigarras, Mata da Biol.; 20 Nov. 2019; LabCol leg; "Fungo 19 \\ Em *Leucocoprinus cepistipes*"; CELC.

All paratypes additionally labelled "*Cyparium achardi* von Groll & Lopes-Andrade PARATYPUS [yellow paper]".

Description

Measurements (holotype, in mm). TL 3.12, PL 1.31, PA 0.80, PB 1.90, EW 1.20, EL 2.17, IS 0.18, HW 0.80.

Coloration. Black; iridescent (Fig. 7A–C). Clypeus yellowish-brown; mouth parts yellowish (Fig. 7D); antennomeres I–VI and apical half of XI yellow; VII–X dark yellow (Fig. 7D–F). Hypomeron, epipleuron, and metepimeron brown to black, lighter laterally (Fig. 7B). Thorax and abdomen brown to black, lighter laterally (Fig. 7B). Coxae and femora light to chestnut brown, lighter posteriorly in some specimens; tibiae light to dark brown; tarsi yellow (Fig. 7B–C).

Head. Punctation dense, fine (Fig. 7D). Eyes tapered apically (Fig. 7D). Labrum transverse; lateral areas rounded, smoothly delimited apically; central margin slightly curved; sclerotized portion rounded with a row of short setae; lateral setae slightly exceeding margins of labrum; slightly porose centrally (Fig. 7G). Mandibles curved, subapical serrations on left mandible conspicuous (Fig. 7H–I). Maxillae with palpomere II thickened; galea and lacinia densely pubescent, narrow (Fig. 7J). Mentum with sides distinctly angulated, curved apically (Fig. 8A). Setae of labial palpomere II exceeding palpomere III; palpomere III thick, with long apical setae (Fig. 8A). Hypopharynx with sclerotized plate cup-shaped (Fig. 8A–B). Postgena with strigulate microsculpture; gular pores sparse; gula small and rounded at anterior region (Fig. 7C). Antennae variable in size between males and females (Fig. 7E–F).

Prothorax. Pronotum smooth, shining; punctation somewhat dense, fine; pubescence short, fine (Fig. 8D–E); somewhat squared, lateral areas curved, forming an obtuse angle at lateral areas of posterior margin (Fig. 8E). Hypomeron smooth (Fig. 8F). Notosternal suture straight, inward-directed (Fig. 8F). Profurca elongated, exceeding half of foramen (Fig. 8G). Prosternal process acute apically (Fig. 9A).

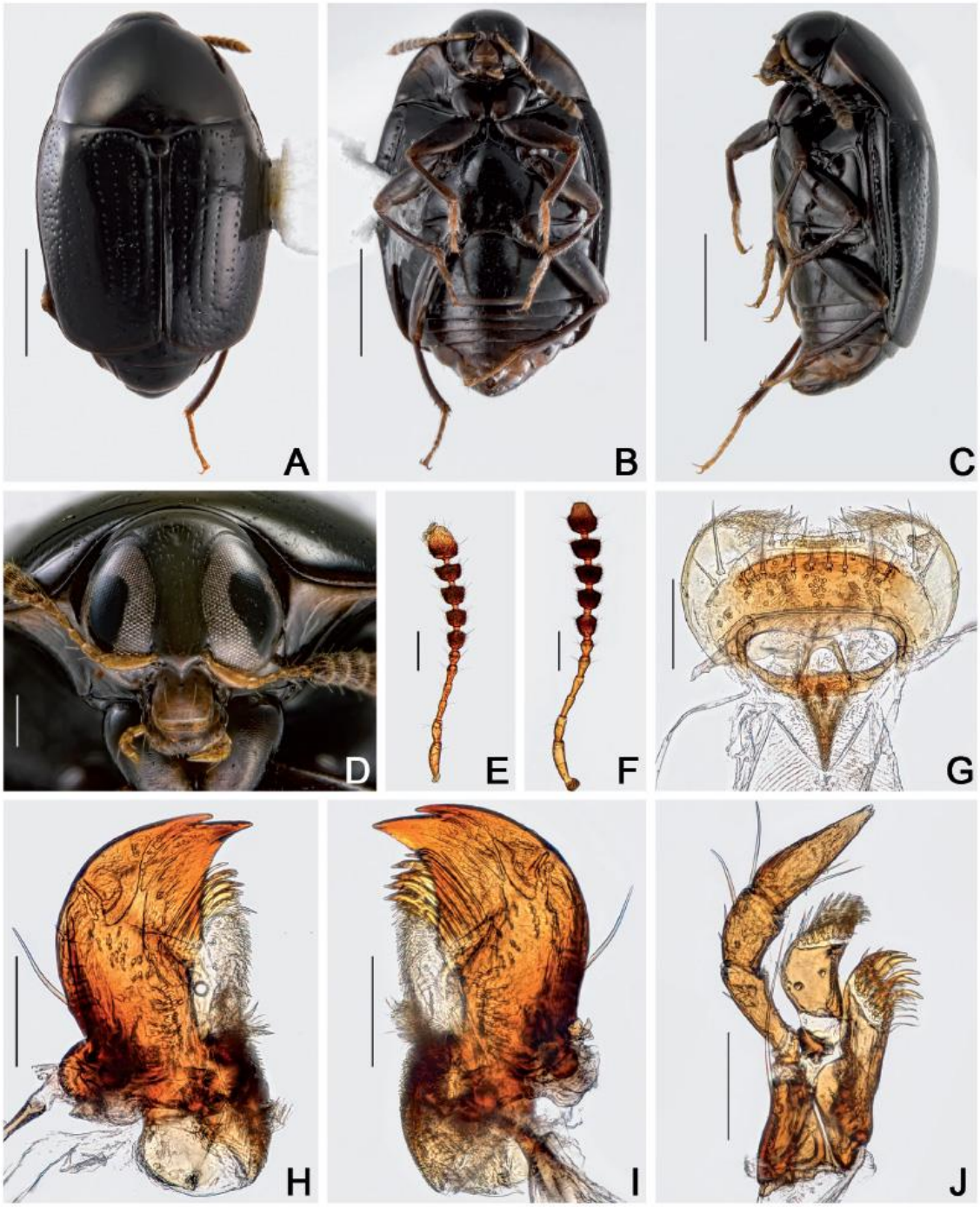

Fig. 7. *Cyparium achardi* sp. nov. **A–D**. Holotype, ♂ (CELC). **A**. Dorsal view. **B**. Ventral view. **C**. Lateral view. **D**. Frontal view. **E–F**. Antennae, paratype, ♂ (CELC) (E) and paratype, ♀ (CELC) (F). **G–J**. Paratype, ♂ (CELC). **G**. Labrum. **H–I**. Mandible. **H**. Left. **I**. Right. **J**. Maxilla. Specimens collected at Mata do Paraíso, Viçosa (MG, Brazil). Scale bars: A–C = 1.0 mm; D–F = 0.2 mm; G–J = 0.1.

Mesothorax. Mesonotum with prescutellar suture (= scutellar lines, Leschen & Löbl, 2005) almost straight (Fig. 9B). Scutellum rounded posteriorly (Fig. 9B). Anterior phragma wide, slightly curved (Fig. 9C). Mesanepisternum smooth (Fig. 9D). Procoxal rest rounded, curved posteriorly (Fig. 9D). Mesoventral line rounded; median line moderately curved; area between median line and mesocoxal line longer laterally (Fig. 9D). Mesoventral process large and straight at base in lateral view (Fig. 9E).

Metathorax. Metanotum with wide alacrista, rounded and somewhat turned to the posterior end; scutoscutellar suture slightly straight; median membranous area wide and very short (Fig. 9F). Metaventrite smooth; punctation sparse, fine; some specimens with faint lateral imbricate microsculpture (Fig. 9D). Mesocoxal line forming an open angle next to each coxal cavity and finely punctate under coxal cavity (Fig. 9D). Metanepisternum and metepimeron (Figs 7B–C, 9D) with imbricate microsculpture, but almost inconspicuous in some specimens. Intercoxal plates smooth (Fig. 7B). Metendosternite with straight furcal arms; 'stalk ridge' not exceeding half of stalk length (Fig. 10A); ventral longitudinal flange flat in lateral view (Fig. 10B).

Wings. Elytra slightly longer than wide, partially covering tergite VI (Fig. 7A); basal and lateral lines punctate (Fig. 8D); sutural line dashed; adsutural area with a row of short setae (Fig. 7A); six rows of coarse punctures (not including sutural line), but row 5 and 6 somewhat intermixed (Figs 7A, 10C); apical coarse punctation moderately sparse; apical serrations moderately large, well visible (Fig. 10D); pubescence short, fine, denser on disc. Epipleuron with a row of punctures (poorly marked in some specimens). Hind wings fully developed (Fig. 10E).

Legs. Pro-, meso- and metacoxae, and femora with strigulate microsculpture. Pro- and mesofemora somewhat fusiform (Fig. 10F–G); punctation moderately sparse and coarse. Metafemora straight, finely punctate (Fig. 10H). Mesotibiae densely spinose, spines fine (Fig. 10G). Metatibiae sparsely spinose, spines fine (Fig. 10H).

Abdomen. Tergites VI–VIII with imbricate microsculpture (Fig. 11A). Tergite VII trapezoidal; punctation dense, coarse; pubescence sparse, fine (Fig. 11A). Ventrite 1 sparsely and coarsely punctate; pubescence sparse, fine; strigulate microsculpture (Fig. 11B–C). Metacoxal lines finely punctate. Ventrites 2–5 sparsely and finely punctate; pubescence sparse, fine; imbricate microsculpture anteriorly and with strigulate microsculpture middle-posteriorly.

Males

Measurements (n = 1, paratype; in mm). Antennomeres (length(width)): 0.18(0.06), 0.11(0.05), 0.10(0.04), 0.09(0.04), 0.10(0.05), 0.07(0.06), 0.09(0.10), 0.09(0.11), 0.10(0.12), 0.10(0.13), 0.17(0.14); (n = 5, including the holotype; in mm): TL 3.00–3.28 (mean = 3.14, standard deviation ± 0.10), PL 1.20–1.31 (1.25 ± 0.04), PA 0.80–0.97 (0.89 ± 0.06), PB 1.72–2.07 (1.93 ± 0.13), SL 0.13–0.17 (0.14 ± 0.01), SW 0.15–0.20 (0.18 ± 0.02), EI 1.72–1.92 (1.81 ± 0.07), EL 2.07–2.32 (2.18 ± 0.09), EW 1.07–1.25 (1.19 ± 0.07), EH 0.70–0.80 (0.75 ± 0.05), HW 0.74–0.83 (0.78 ± 0.03), IS 0.15–0.24 (0.17 ± 0.03), WA 0.14–0.17 (0.16 ± 0.01), MC 0.72–0.92 (0.81 ± 0.08), MB 0.42–0.50 (0.46 ± 0.04), VL 0.62–0.70 (0.64 ± 0.03).

Antennae almost reaching level of mesanepisternum, smaller than in females (Fig. 7E). Pro- and mesotarsomeres I–III enlarged, with tenent setae (Fig. 10F). Tergite VIII triangular; punctation dense, coarse, subglabrous (Fig. 11D). Tergite IX with rectangular ventral struts (Fig. 11E,F). Sternite VIII rectangular, longish; finely punctate and with strigulate microsculpture (Fig. 11G). Sternite IX thicker posteriorly and triangular anteriorly (Fig. 11F). Aedeagus strongly sclerotized, enlarged and darker basely and narrowed apically, apex of median lobe short (Fig. 12A,B); openings in dorsal view somewhat enlarged, forming an acute angle (Fig. 12C); internal sac with irregular sclerites, with two hooks (Fig. 12D,E), parameres short, somewhat enlarged apically (Fig. 12A).

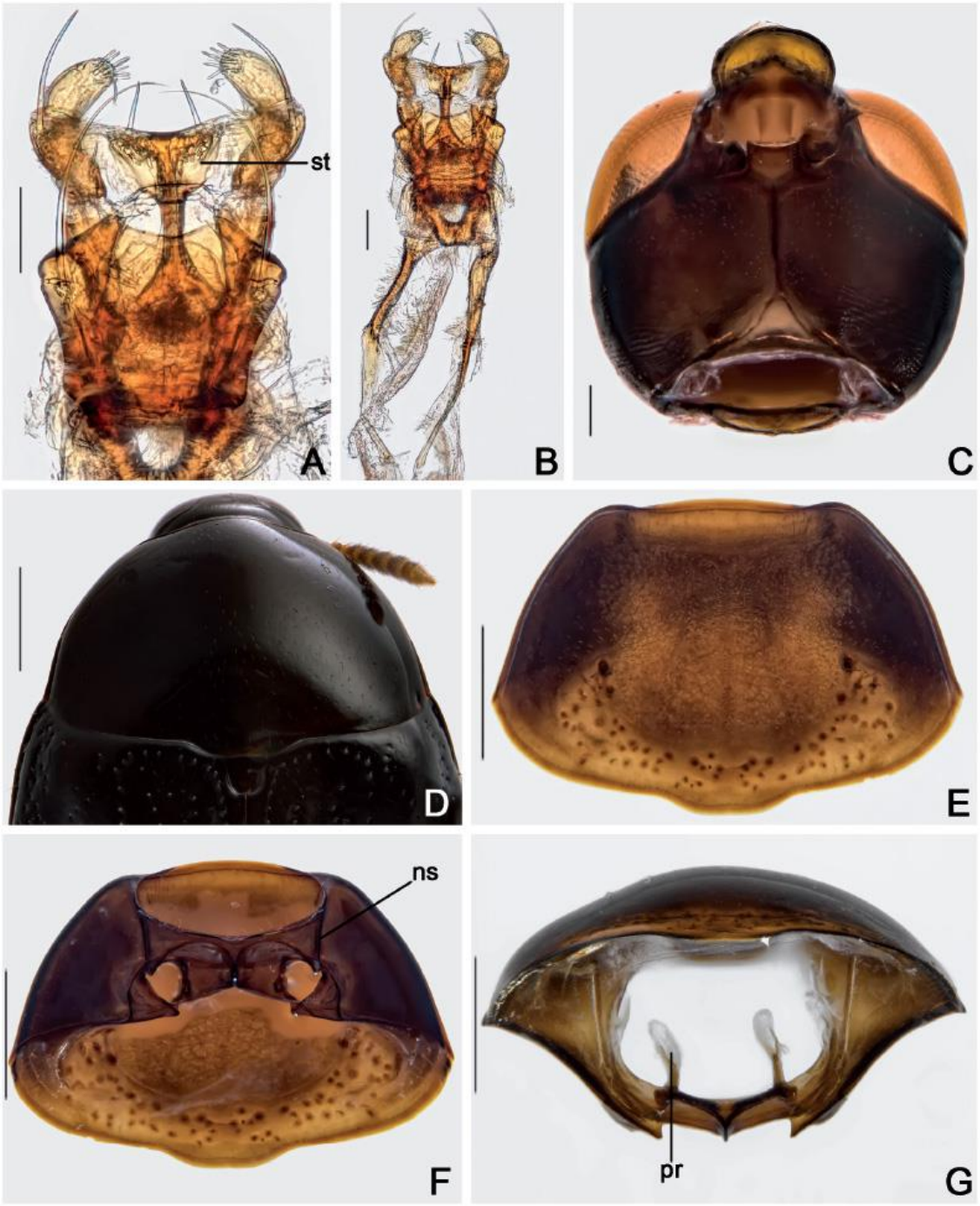

Fig. 8. *Cyparium achardi* sp. nov. **A–C.** Paratype, ♂ (CELC). **A**. Labium. **B**. Hypopharynx. **C**. Head, ventral view. **D**. Holotype, ♂ (CELC), pronotum, dorsal view. **E–G**. Paratype, ♂ (CELC), prothorax. **E**. Frontal view. **F**. Ventral view. **G**. Inner view. Specimens collected at Mata do Paraíso, Viçosa (MG, Brazil). Abbreviations: ns = notosternal suture; pr = profurca; st = sclerotized plate. Scale bars: A–B = 0.05 mm; C = 0.1 mm; D–G = 0.5 mm.

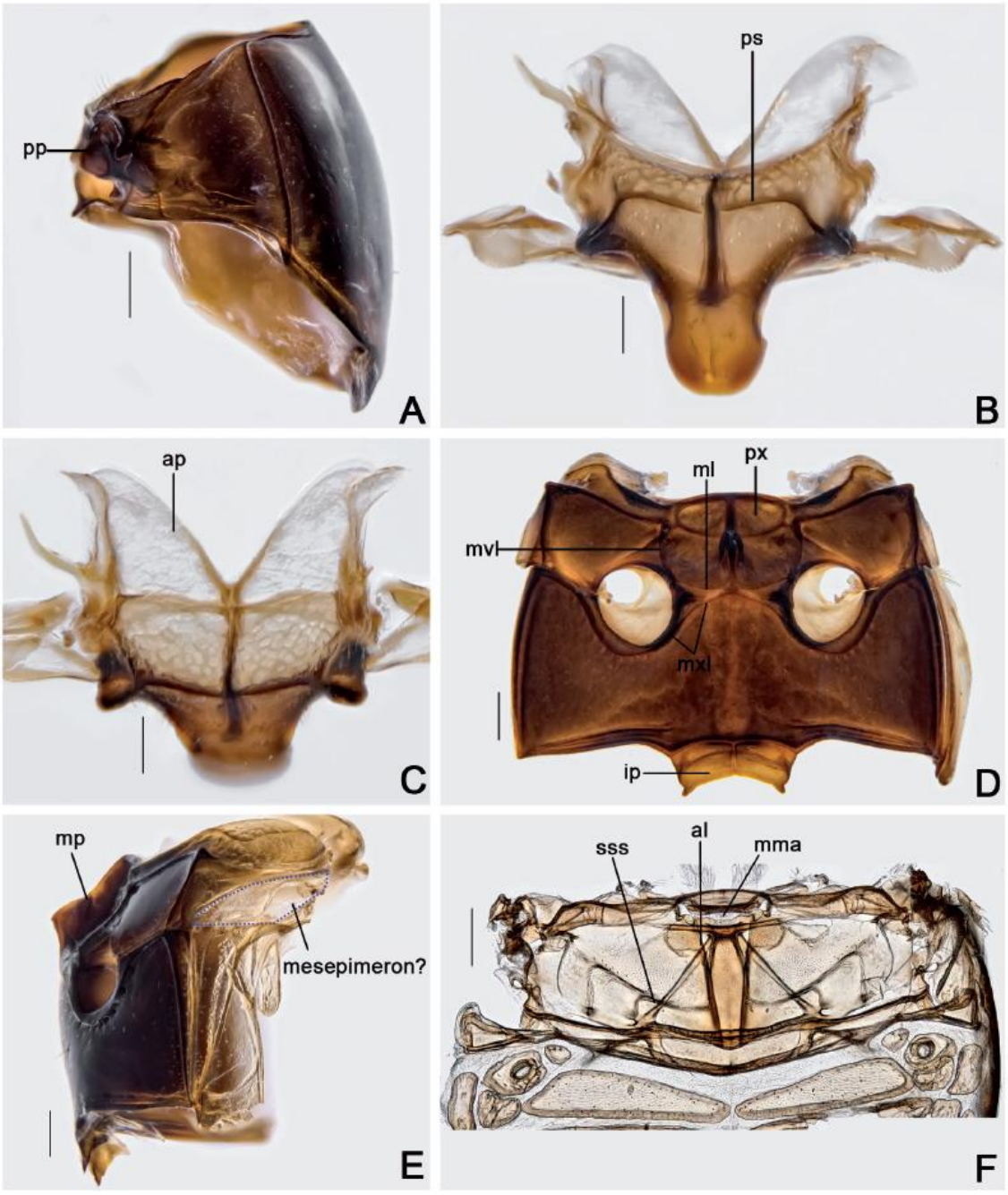

Fig. 9. *Cyparium achardi* sp. nov., paratype, ♂ (CELC). **A**. Prothorax, lateral view. **B–C**. Scutellar plate. **B**. Dorsal view. **C**. Apically slanted view. **D–E**. Meso- and metathorax. **D**. Ventral view. **E**. Lateral view. **F**. Metanotum. Specimen collected at Mata do Paraíso, Viçosa (MG, Brazil). Abbreviations: al = alacrista; ap = anterior phragma; ip = intercoxal plate; ml = median line; mma = median membranous area; mp = mesoventral process; mvl = mesoventral line; mxl = mesocoxal line; pp = prosternal process; ps = prescutellar line; px = procoxal rest; sss = scutoscutellar suture. Scale bars: A, D–F = 0.2 mm; B–C = 0.1 mm.

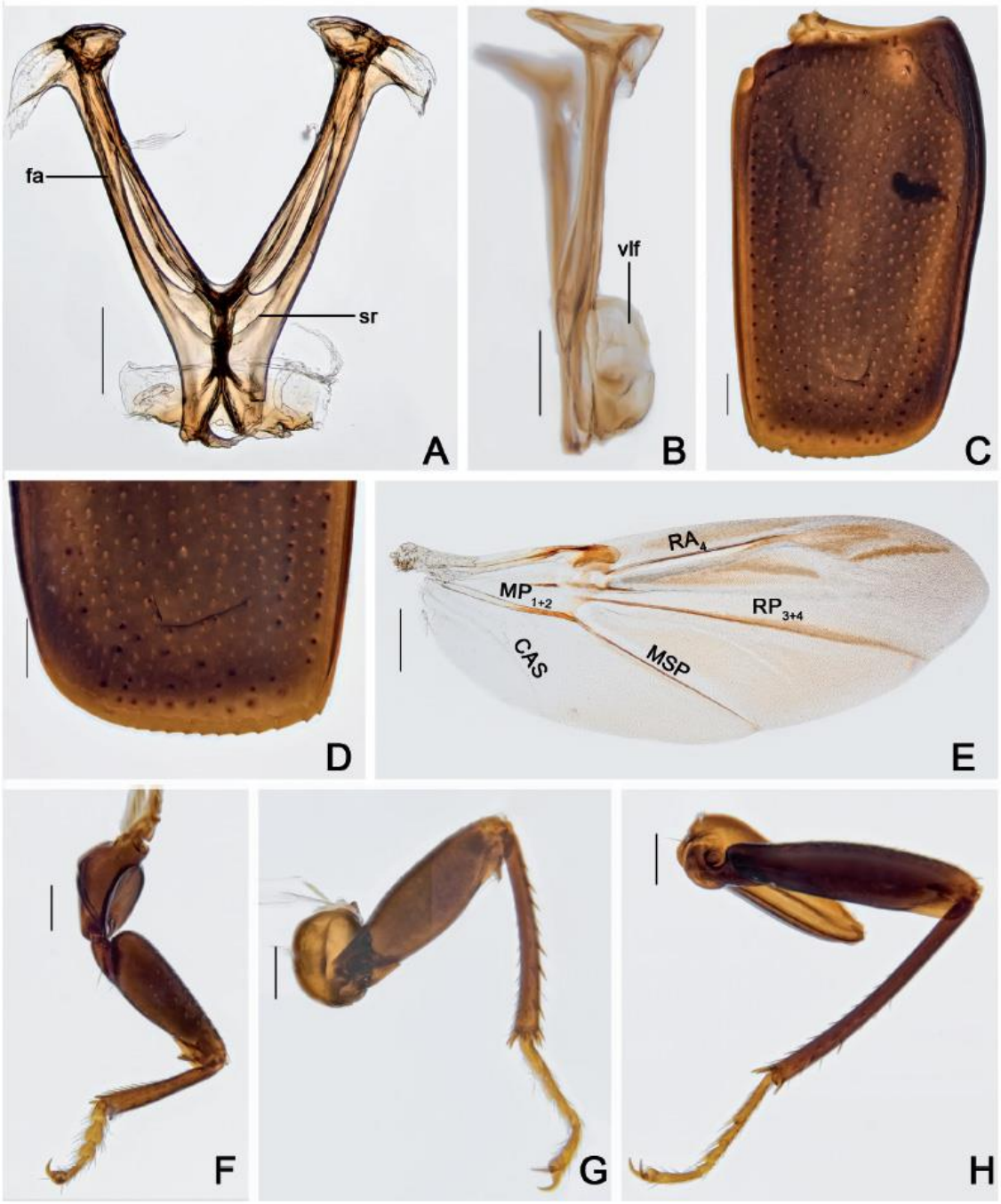

Fig. 10. *Cyparium achardi* sp. nov., paratype, ♂ (CELC). **A**–**B**. Metendosternite. **A**. Dorsal view. **B**. Lateral view. **C**–**D**. Elytron. **C**. Entire. **D**. Apex. **E**. Hind wing. **F**–**H**. Legs. **F**. Fore. **G**. Middle. **H**. Hind. Specimen collected at Mata do Paraíso, Viçosa (MG, Brazil). Abbreviations: CAS = cubitoanal strut; fa = furcal arms; MP_{1+2} = medial field; MSP = medial spur; RA_4 = radius anterior; RP_{3+4} = radius posterior; sr = 'stalk ridge'; vlf = ventral longitudinal flange. Scale bars: A–D, F–H = 0.2 mm; E = 0.5 mm.

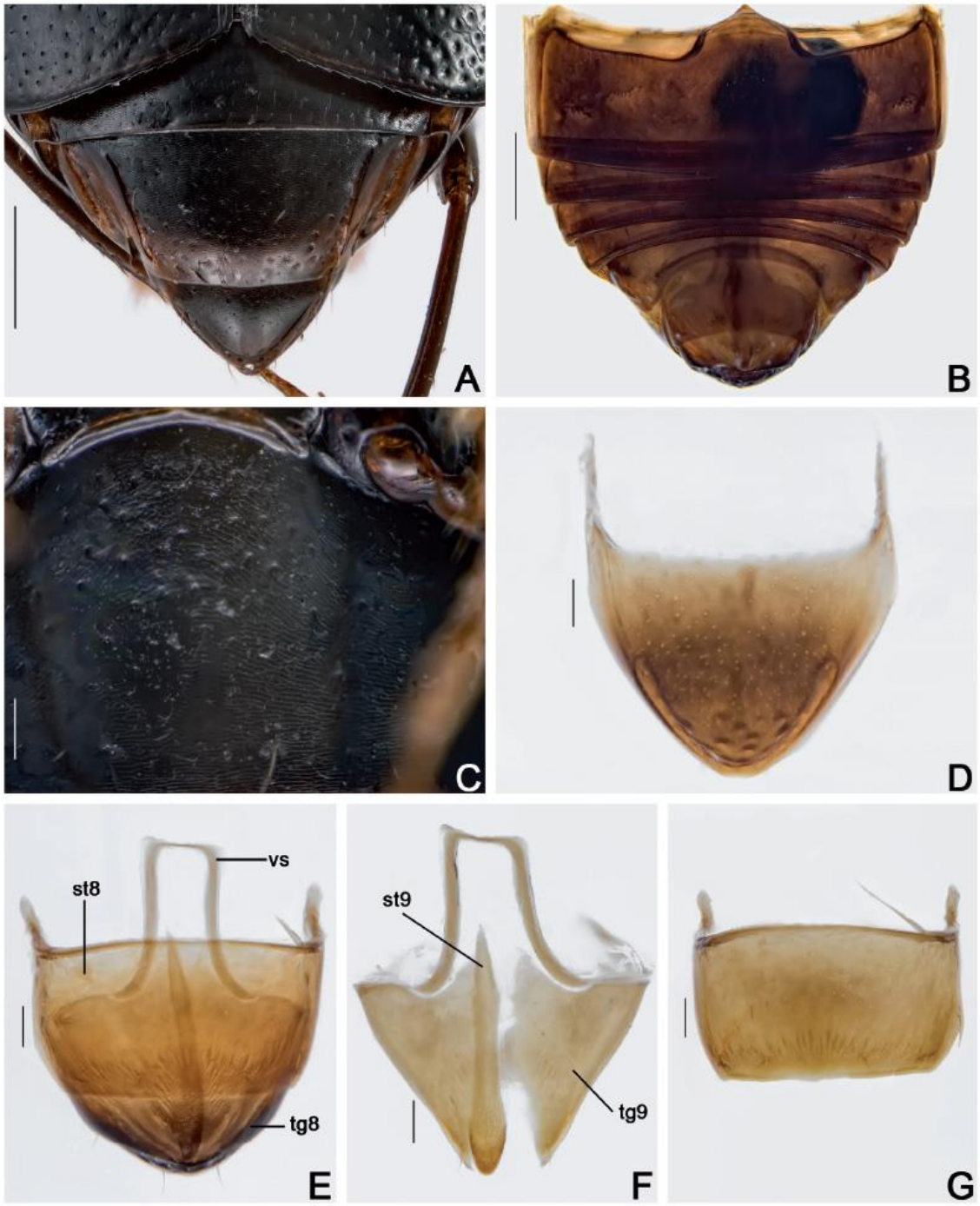

Fig. 11. *Cyparium achardi* sp. nov. **A, C**. Holotype, ♂ (CELC). **B, D–G**. Paratype ♂ (CELC). **A–B**. Abdomen, dorsal view (A) and ventral view (B). **C**. Ventrite 1. **D**. Tergite VIII. **E**. Terminalia. **F**. Tergite IX. **G**. Sternite VIII. Specimens collected at Mata do Paraíso, Viçosa (MG, Brazil). Abbreviations: st = sternite; tg = tergite; vs = ventral strut. Scale bars: A–B = 0.4 mm; C–G = 0.1 mm.

Fig. 12. *Cyparium achardi* sp. nov., paratype, ♂ (CELC): aedeagi. **A**. Lateral view. **B**. Frontal view. **C**. Dorsal view. **D**. Internal sac, frontal view. **E**. Internal sac, dorsal view. Specimen collected at Mata do Paraíso, Viçosa (MG, Brazil). Abbreviations: hk = hook; op = opening; pa = parameres. Scale bars = 0.2 mm.

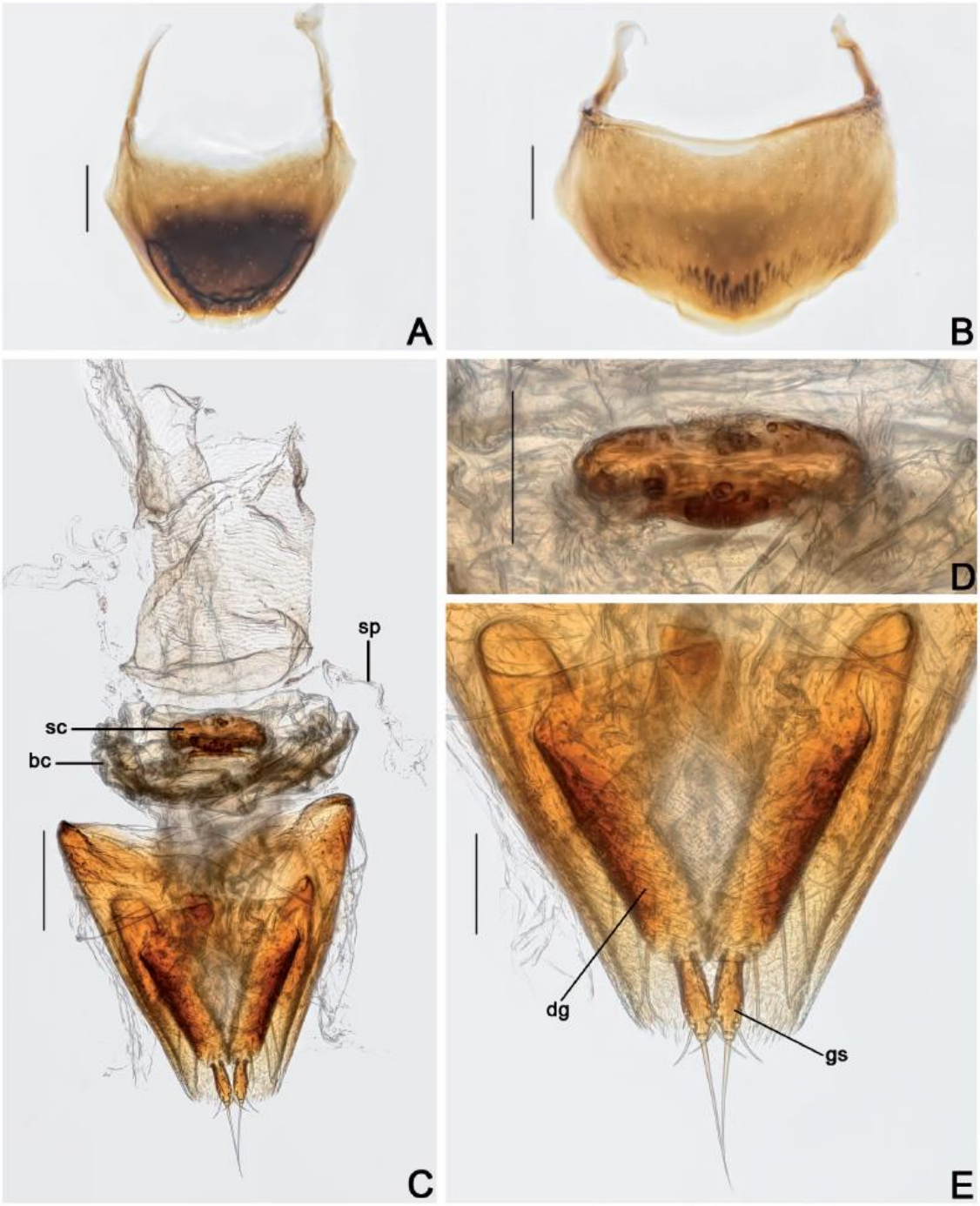

Fig. 13. *Cyparium achardi* sp. nov., paratype, ♀ (CELC). **A**. Tergite VIII. **B**. Sternite VIII. **C**. Terminalia. **D**. Sclerite of vaginal plate. **E**. Ovipositor. Specimen collected at Mata do Paraíso, Viçosa (MG, Brazil). Abbreviations: bc = bursa copulatrix; dg = distal gonocoxites; gs = gonostyli; sc = sclerite; sp = spermatheca. Scale bars: A–C = 0.2 mm; D–E = 0.1 mm.

Females

MEASUREMENTS (n = 1, paratype; in mm). Antennomeres (length(width)): 0.20(0.06), 0.13(0.05), 0.11(0.04), 0.12(0.05), 0.11(0.06), 0.08(0.07), 0.11(0.11), 0.10(0.13), 0.11(0.14), 0.10(0.16), 0.16(0.15); (n = 4, paratype; in mm): TL 3.32–3.40 (mean = 3.37, standard deviation ± 0.04), PL 1.23–1.39 (1.33 ± 0.07), PA 0.97–1.05 (1.01 ± 0.04), PB 2.05–2.17 (2.10 ± 0.05), SL 0.18–0.21 (0.19 ± 0.01), SW 0.17–0.20 (0.19 ± 0.01), EI 1.90–2.00 (1.94 ± 0.05), EL 2.27–2.40 (2.35 ± 0.05), EW 1.25–1.27 (1.25 ± 0.01), EH 0.80–1.00 (0.88 ± 0.09), HW 0.81–0.84 (0.84 ±0.02), IS 0.16–0.25 (0.20 ±0.04), WA 0.15–0.21 (0.18 ± 0.02), MC 0.87–0.95 (0.90 ± 0.03), MB 0.42–0.52 (0.46 ± 0.04), VL 0.67–0.75 (0.71 ± 0.03).

Antennae longer than in males, surpassing mesanepisternum (Fig. 7F). Tergite VIII triangular, rounded posteriorly; punctation dense, coarse (inconspicuous in some specimens); subglabrous (Fig. 13A). Sternite VIII rectangular with strigulate microsculpture (Fig. 13B). Vagina and bursa copulatrix membranous; vaginal plate with an apical sclerite and a pair of spermatheca at base of oviduct (Fig. 13C–D). Distal gonocoxites parallel, straight and thick; gonostyli larger at apex (Figs 13C, E).

Host fungi

Adults were collected from *Marasmiellus volvatus* Singer (Agaricales, Omphalotaceae) (1 record, 4 individuals), *Marasmiellus* sp. Murrill (1, 2), *Marasmius haematocephalus* (Mont.) Fr. (Agaricales, Marasmiaceae) (1, 1), *Leucocoprinus ianthinus* (Sacc.) P.Mohr (Agaricales, Agaricaceae) (1, 1), *L. cepistipes* (Sowerby) Pat. (1, 1), *Leucoprinus* sp. (1, 1), *Hygrocybe* sp. (Agaricales, Hygrophoraceae) (1, 1), *Leucoagaricus* sp. (Agaricales, Agaricaceae) (1, 1).

Remarks

Similar to *C. pygidiale*, which occurs in Jataí, Goiás, Brazil (1174 km from the collection site of *C. achardi* sp. nov.), but they differ in the humeral and apical region of the elytra, and in the scutellar shield (blackish in *C. achardi* and reddish in *C. pygidiale*); elytral punctation is also different: rows 1–3 are coarser in *C. pygidiale* and the remainder are coarser in *C. achardi*; furthermore, rows 1–3 are somewhat outward directed, while they are inward directed in *C. pygidiale*.

Distribution

Known only from Mata da Biologia, campus of the Universidade Federal de Viçosa, Viçosa, state of Minas Gerais, Southeast Brazil (Fig. 46).

Cyparium lescheni sp. nov.
urn:lsid:zoobank.org:act:8A653AB2-6DEF-4FA6-A885-438BDAF11D5F
Figs 4, 14–21, 46; Supp. file 1B, Supp. file 2A

Diagnosis

TL: 2.07–2.25 mm in males and 2.10–2.35 mm in females. Brown (Fig. 14A). Hypomeron, metaventrite and intercoxal plates with strigulate microsculpture. Metaventrite coarsely punctate above intercoxal plates (Figs 14B, 17D). Tergite VIII in males triangular (Fig. 19D). Openings of aedeagus in dorsal view forming an acute angle (Fig. 20C); internal sac with drop-like sclerites (Fig. 20D–E). Tergite VIII of females with a posterior invagination (Fig. 21A).

Etymology

In homage to Dr Richard A.B. Leschen (New Zealand Arthropod Collection) for his great contributions to the systematics of Coleoptera, especially regarding Scaphidiinae.

Material examined

Holotype

BRAZIL • ♂; Minas Gerais, Viçosa, EPTEA Mata do Paraíso; 19 Nov. 2019; LabCol leg.; "Fungo 30 \\ em *Agaricus sylvaticus* \\ *Cyparium lescheni* von Groll & Lopes-Andrade HOLOTYPUS" [red paper]; CELC. (Supp. file 1B)

Paratypes

BRAZIL • 1 ♂, 4 ♀♀; same collection data as for holotype, "T. dos Gigantes"; 15 Feb. 2015; S. Aloquio, A. Orsetti and M. Bento leg.; CELC • 1 ♀; same collection data as for holotype, "T. da Madeira"; 27 Feb. 2015; I.S.C. Pecci-Maddalena *et al.* leg.; CELC • 1 ♂; same collection data as for holotype; 13 Mar. 2015; S. Aloquio, A. Orsetti, C. Lopes-Andrade and M. Bento leg.; CELC • 1 ♂; same collection data as for holotype; 9 Nov. 2016; I. Pecci-Maddalena and C. Lopes-Andrade leg.; "\\ ex *Psathyrella candolleana*"; CELC • 5 ♂♂, 7 ♀♀ (2 ♂♂, 1 ♀, entirely dissected, preserved in glycerin; 1 ♂, 2 ♀♀, abdomen dissected, preserved in glycerin); same collection data as for holotype; CELC • 1 ♂; 1 ♀; same collection data as for holotype; CAMB • 1 ♂; 1 ♀; same collection data as for holotype; CERPE • 2 ♂♂; 1 ♀, 1 spec.; same collection data as for holotype; 21 Nov. 2019; LabCol leg.; "Fungo 06 \\ Em *Agaricus dulcidulus* e *Leucocoprinus brebissoni*"; CELC • 2 ♀♀; Viçosa, Recanto das Cigarras, Mata da Biol.; 20 Nov. 2019; LabCol leg.; "Fungo 29 \\ Em *Entoloma* (*Inocephalus*) sp."; CELC • 8 ♂♂, 3 ♀♀ (1 ♂, entirely dissected, preserved in glycerin; 2 ♂♂, 1 ♀, abdomen dissected, preserved in glycerin); same collection data as for preceding; "Fungo 08; CELC \\ Em *Psathyrella* sp."; CELC • 6 ♂♂, 11 ♀♀, 1 spec.; Viçosa, Mata da Biologia; 15 Oct. 2021; E. von Groll and A. Orsetti leg.; "Fungo 20 \\ Em *Agaricus* sp."; CELC.

All paratypes additionally labelled "*Cyparium lescheni* von Groll & Lopes-Andrade PARATYPUS [yellow paper]".

Description

Measurements (holotype, in mm). TL 2.32, PL 0.76, PA 0.70, PB 1.40, EW 0.86, EL 1.62, IS 0.20, HW 0.62.

Coloration. Iridescent. Brown; antennomeres I–VI, clypeus, mouthparts, tarsi yellow (Figs 14A, 15A). Variation: few paratypes with pronotum and hypomeron reddish brown (Fig. 14D–F); scutellum reddish brown or black (Fig. 14D); meso- and metathorax reddish brown, each sclerite lighter laterally (Fig. 14E); elytra blackish (Fig. 14D); epipleuron dark ochre; coxae and trochanters dark ochre; femora dark ochre, apex lighter; tibiae dark ochre, lighter anteriorly and posteriorly; tarsi yellow (Fig. 14E); tergite VI and VII blackish; tergite VIII yellow; ventrite 1 dark ochre, 2–4 dark yellow, 5 and 6 yellow (Fig. 14E).

Head. Punctation dense, fine (Fig. 15A). Eyes long (Fig. 15A). Labrum sub-rectangular, lateral margins smoothly rounded, not well delimited apically; central margin sub-straight; sclerotized portion inwardly curved; lateral setae considerably extending from the margins of the labrum; densely porose centrally (Fig. 15D). Mandibles strongly curved; subapical serrations on left mandible conspicuous (Fig. 15E–F). Maxillary palps, galea and lacinia moderate pubescent, elongated (Fig. 15G). Mentum straight apically and rounded laterally; sides well delimited (Fig. 16A). Setae of labial palpomere II extending palpomere III; palpomere III longish with long apical setae (Fig. 16A). Hypopharynx with narrow and rounded sclerotized-plate (Fig. 16A–B). Post gena microsculptured with transversal lines; gular pores sparse; gula long and sharp (Fig. 16C). Antennal club very distinct; antennomere XI longish, hexagonal, more or less rounded apically; remarkably different between sexes (Fig. 15B–C).

PROTHORAX. Pronotum smooth, shining; punctuation dense, fine; pubescence short, fine (Fig. 16D–E); transverse, sub-straight laterally, forming an obtuse angle at lateral areas of posterior margin (Fig. 16E). Hypomeron with strigulate microsculpture. Notosternal suture straight, inward directed (Fig. 16F). Profurca somewhat thick and elongated, slightly extending half length of foramen (Fig. 16G). Prosternal process acuminated (Fig. 17A).

MESOTHORAX. Mesonotum with prescutellar suture (= scutellar lines, Leschen & Löbl 2005) strongly wavy (Fig. 17B). Anterior phragma large and straight (Fig. 17C). Mesanepisternum with strigulate microsculpture. Procoxal rests triangular; slightly curved posteriorly (Fig. 17D). Mesoventral lines wavy and obtuse; median lines moderately wavy; area between median and mesoventral lines thin (Fig. 17D). Mesoventral process long, slightly curved at top and base, forming a not well marked ridge (Fig. 17E).

Fig. 14. *Cyparium lescheni* sp. nov. **A–C**. Holotype, ♂ (CELC). **D–F**. Paratype, ♂ (CELC). **A**. Dorsal view. **B**. Ventral view. **C**. Lateral view. **D**. Dorsal view. **E**. Ventral view. **F**. Lateral view. Specimens collected at Mata do Paraíso, Viçosa (MG, Brazil). Scale bars = 1.0 mm.

METATHORAX. Metanotum with alacrista somewhat enlarged anteriorly and turned to anterior portion; scutoscutellar suture very strongly curved; median membranous area remarkably wide, and short (Fig. 17F). Metaventrite with strigulate microsculpture; punctuation sparse, fine; coarsely punctate above intercoxal plates (Fig. 17D). Mesocoxal line forming a smooth angle between coxal cavities (Fig. 17D). Metanepisternum and metepimeron with imbricate microsculpture. Intercoxal plates with strigulate microsculpture. Metendosternite with curved furcal arms; 'stalk ridge' exceeding half length of stalk (Fig. 18A); ventral longitudinal flange long and narrow in lateral view (Fig. 18B).

WINGS. Elytra slightly wider than long, partially covering tergite VI (Fig 14A); basal and lateral lines punctate (Fig. 16D); sutural lines dashed; adsutural area with a row of setae; six rows of coarse punctures (not including sutural line) (Figs 14A, D, 18C); apical coarse punctation sparse; apical fine punctation dense (Fig. 18D); apical serrations almost inconspicuous (Fig. 18D); pubescence short and fine. Epipleuron with a line of coarse punctures. Hind wings fully developed (Fig. 18E).

LEGS. Pro-, meso- and metacoxae, and femora with strigulate microsculpture. Femora strongly fusiform (Fig. 18F–H). Profemora with inconspicuous punctuation; mesofemora with sparse and coarse punctuation; metafemora with fine and shallow punctuation. Mesotibiae densely spinose, spines fine; metatibiae sparsely spinose, spines fine.

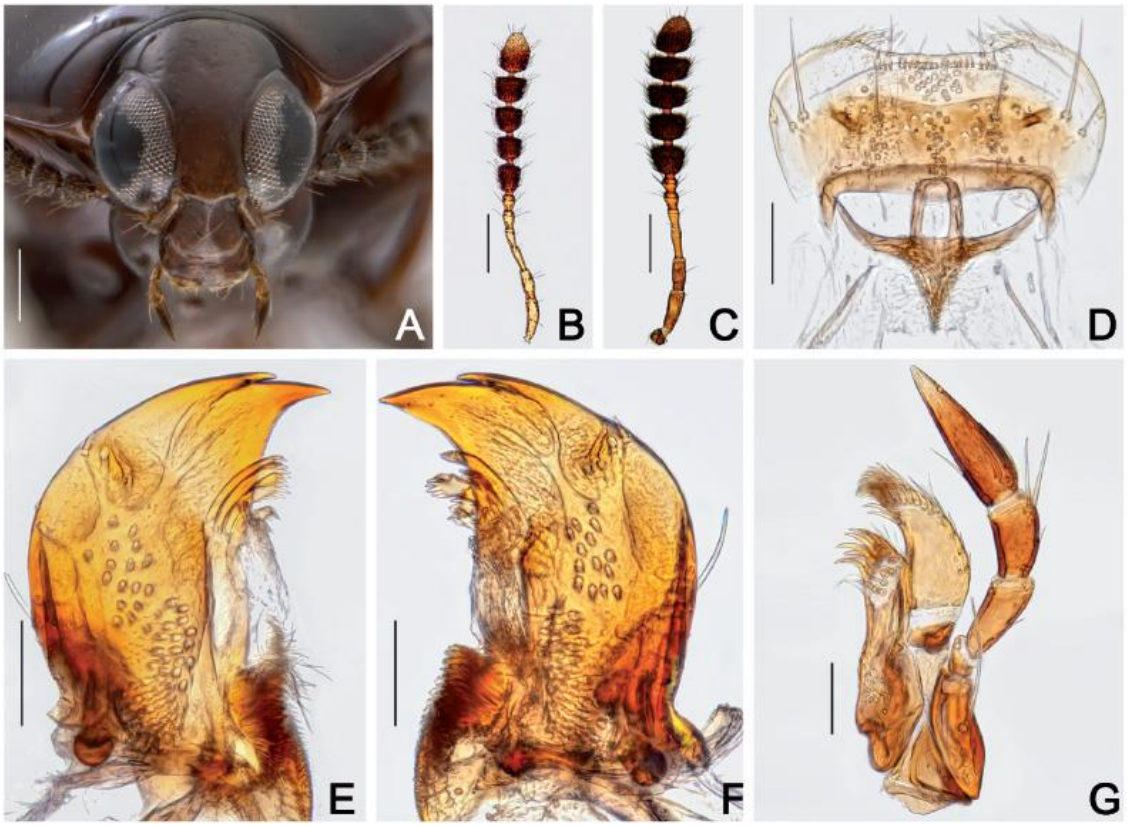

Fig. 15. *Cyparium lescheni* sp. nov. **A**. Holotype, ♂ (CELC), frontal view. **B**. Paratype, ♂ (CELC), antennae. **C**. Paratype, ♀ (CELC), antennae. **D–G**. Paratype, ♂ (CELC). **D**. Labrum. **E**. Left mandible. **F**. Right mandible. **G**. Maxilla. Specimens collected at Mata do Paraíso, Viçosa (MG, Brazil). Scale bars: A–C = 0.2 mm; D–G = 0.05 mm.

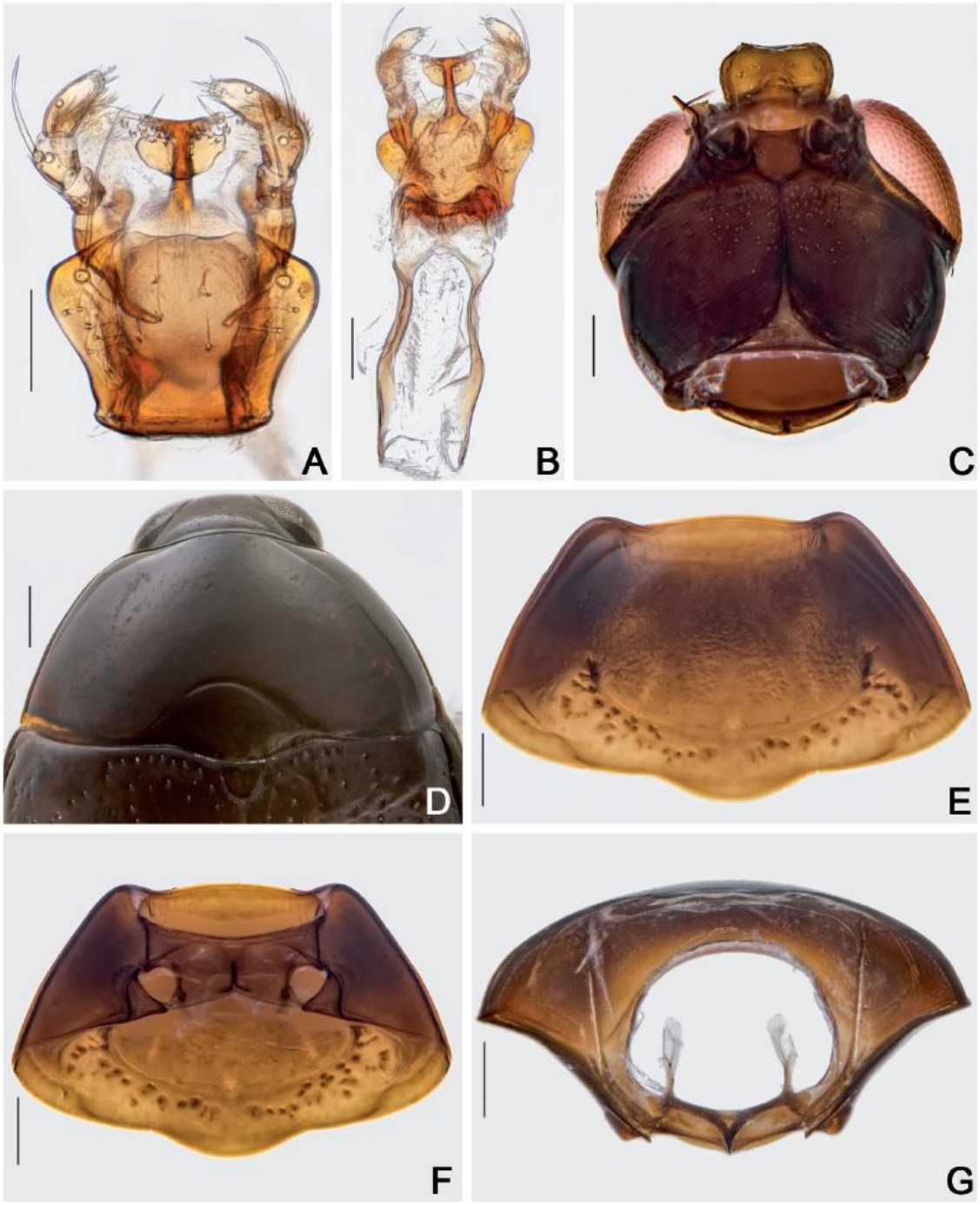

Fig. 16. *Cyparium lescheni* sp. nov. **A–C**. Paratype, ♂ (CELC). **A**. Labium. **B**. Hypopharynx. **C**. Head, ventral view. **D–E**. Pronotum, dorsal view. **D**. Holotype, ♂ (CELC). **E**. Paratype, ♂ (CELC). **F–G**. Paratype, ♂ (CELC), prothorax. **F**. Ventral view. **G**. Inner view. Specimens collected at Mata do Paraíso, Viçosa (MG, Brazil). Scale bars: A–B = 0.05 mm; C = 0.1 mm; D–G = 0.2 mm.

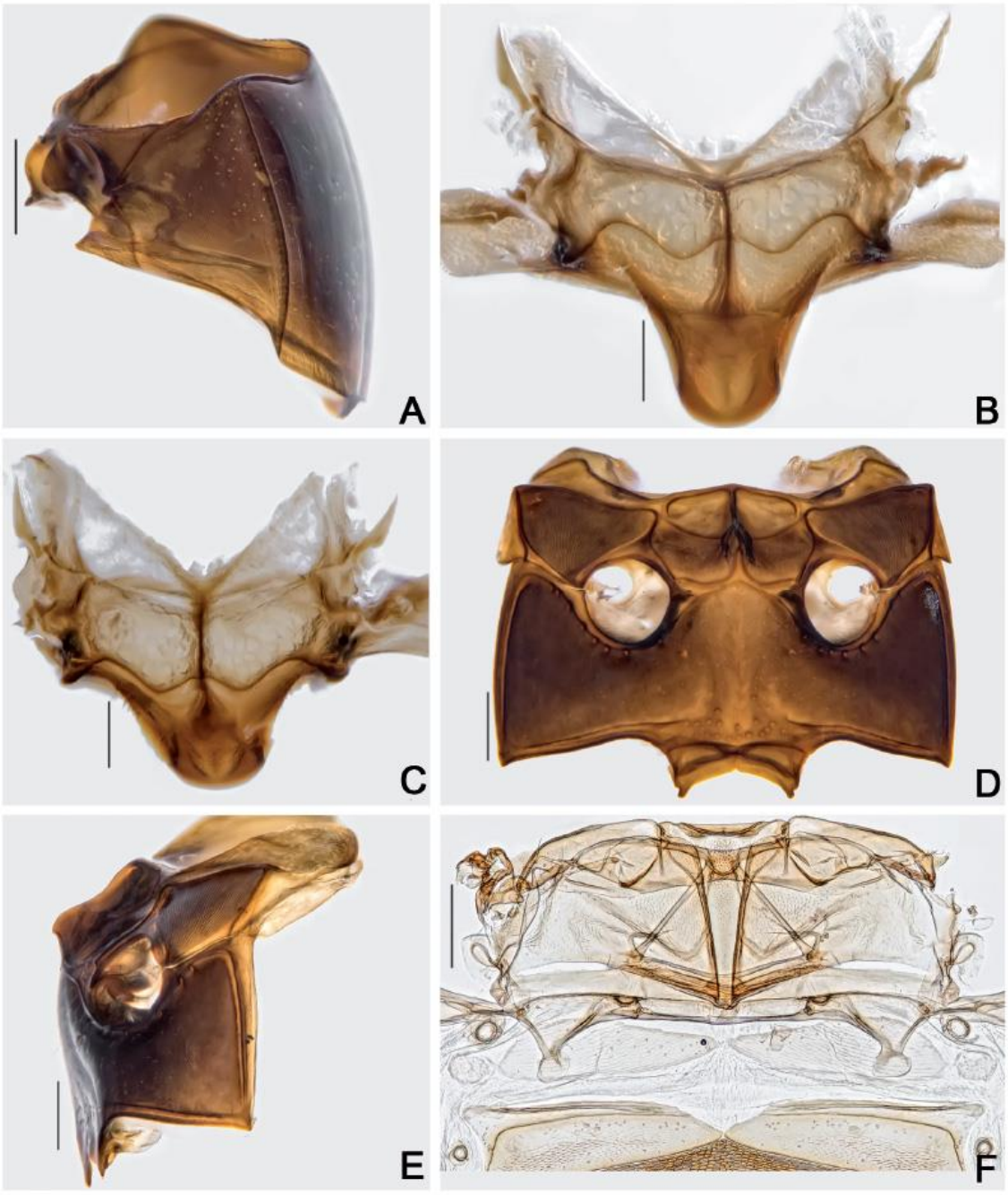

Fig. 17. *Cyparium lescheni* sp. nov., paratypes, ♂ (CELC). **A**. Prothorax, lateral view **B–C**. Scutellar plate. **B**. Dorsal view. **C**. Apically slanted view. **D–E**. Meso- and metathorax. **D**. Ventral view. **E**. Lateral view. **F**. Metanotum. Specimens collected at Mata do Paraíso, Viçosa (A–E) and Mata da Biologia (F), Viçosa (MG, Brazil). Scale bars: A, D–F = 0.2 mm; B–C = 0.1 mm.

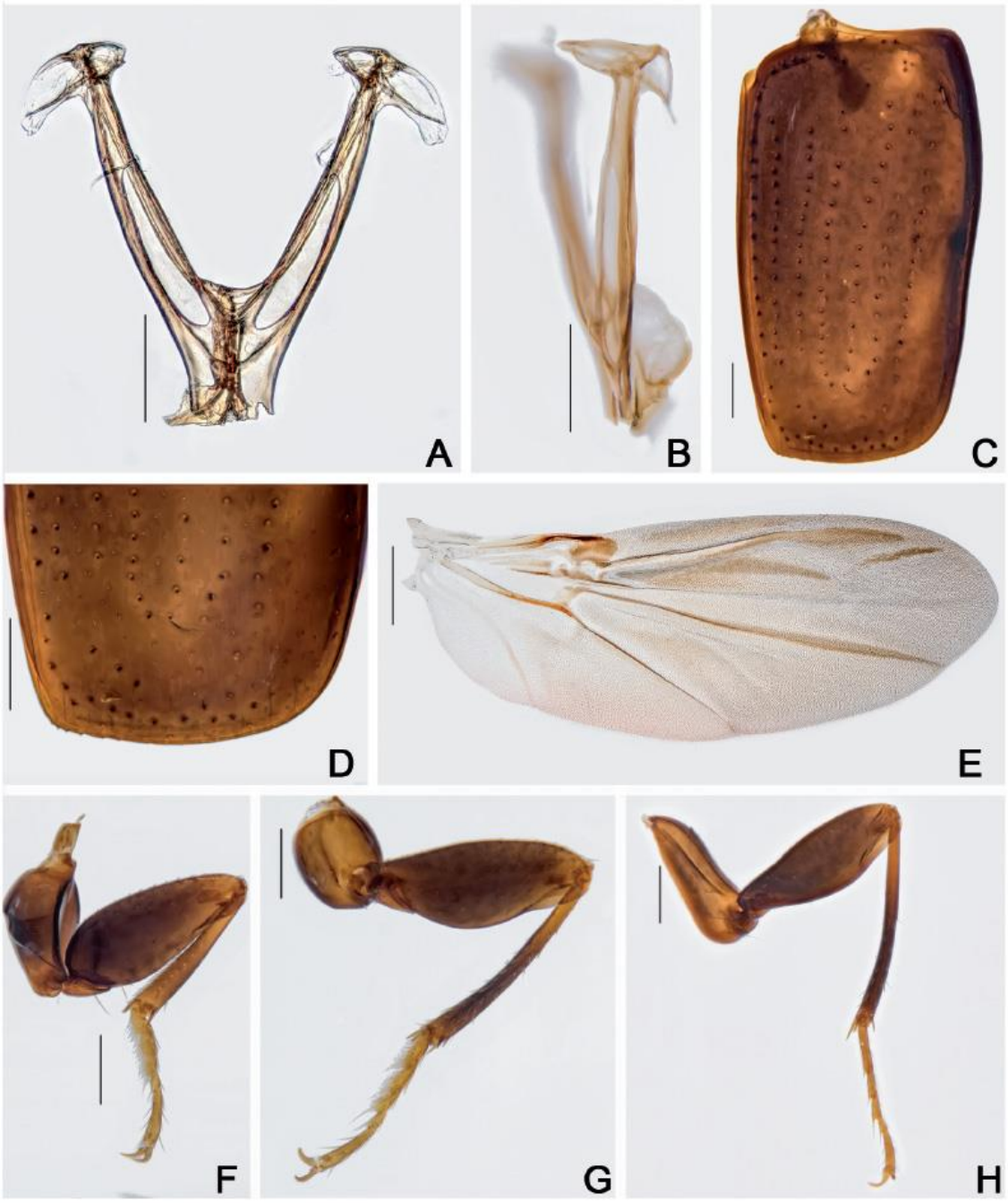

Fig. 18. *Cyparium lescheni* sp. nov., paratype, ♂ (CELC). **A–B**. Metendosternite. **A**. Dorsal view. **B**. Lateral view. **C–D**. Elytron. **C**. Entire. **D**. Apex. **E**. Hind wing. **F–H**. Legs. **F**. Fore. **G**. Middle. **H**. Hind. Specimen collected at Mata do Paraíso, Viçosa (MG, Brazil). Scale bars: A–D, F–H = 0.2 mm; E = 0.5 mm.

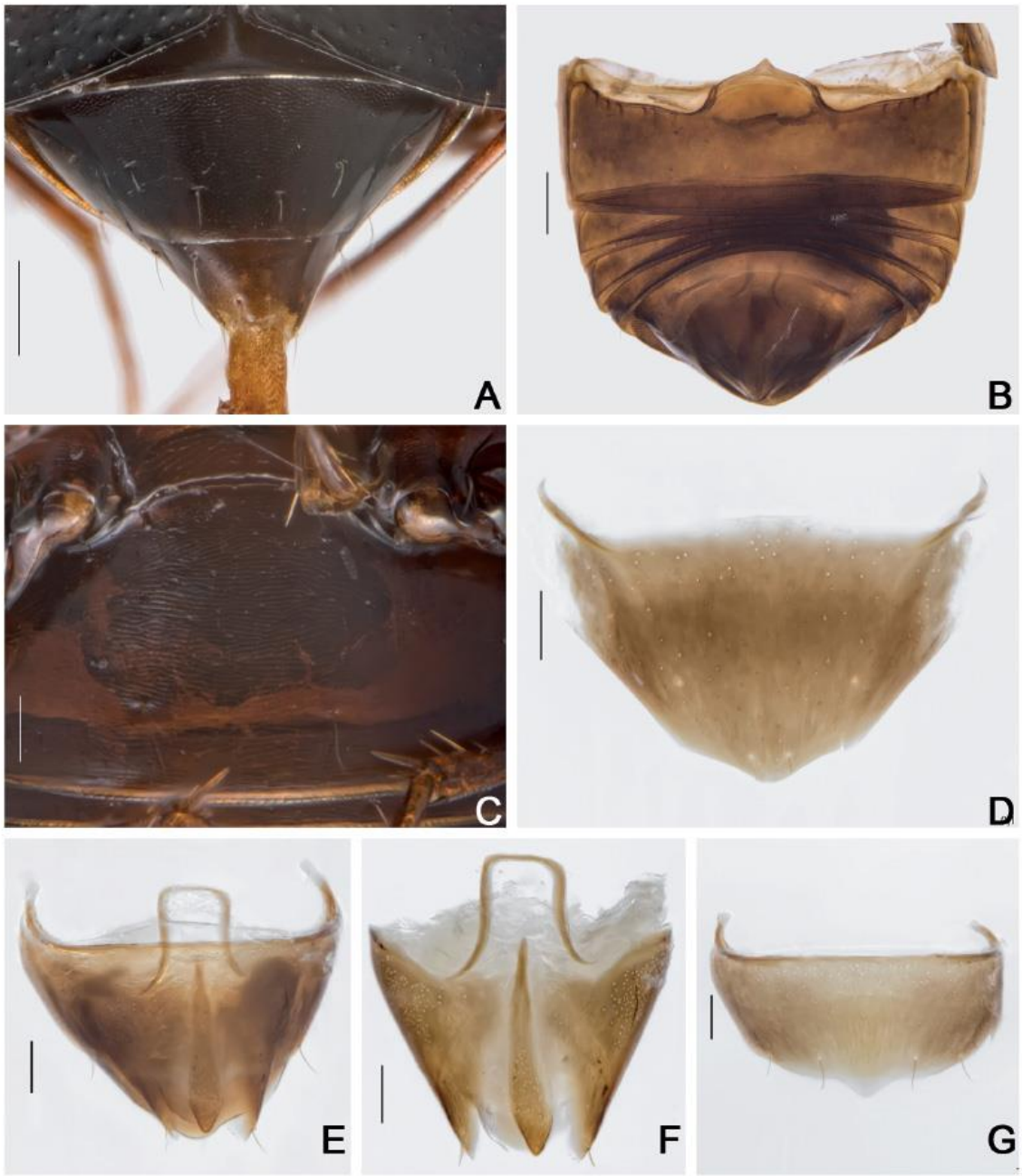

Fig. 19. *Cyparium lescheni* sp. nov. **A**–**C**. Holotype, ♂ (CELC). **D**–**G**. Paratype ♂ (CELC). **A**. Abdomen, dorsal view. **B**. Abdomen, ventral view. **C**. Ventrite 1. **D**. Tergite VIII. **E**. Terminalia. **F**. Tergite IX. **G**. Sternite VIII. Specimens collected at Mata do Paraíso, Viçosa (A–C) and Mata da Biologia (D–G), Viçosa (MG, Brazil). Scale bars: A–B = 0.2 mm; C–G = 0.1 mm.

Fig. 20. *Cyparium lescheni* sp. nov., paratype, ♂ (CELC). **A–C**. Aedeagi. **A**. Lateral view. **B**. Frontal view. **C**. Dorsal view. **D–E**. Internal sac. **D**. Frontal view. **E**. Dorsal view. Specimen collected at Mata da Biologia, Viçosa (MG, Brazil). Scale bars = 0.1 mm.

Abdomen. Tergite VI and VII with imbricate microsculpture (Fig. 19A). Tergite VII trapezoidal (Fig. 19A), triangular in some paratypes with tergite VIII not exposed; punctation sparse, fine; pubescence sparse, fine. Ventrites 1–5 sparsely and finely punctate; pubescence sparse, fine; with strigulate microsculpture (Fig. 19B–C). Metacoxal lines finely punctate.

Males

Measurements (n = 1, paratype; in mm). Antennomeres (length(width)): 0.14(0.05), 0.10(0.04), 0.08(0.03), 0.07(0.04), 0.06(0.04), 0.06(0.05), 0.09(0.08), 0.08(0.08), 0.09(0.10), 0.09(0.11), 0.14(0.10); (n = 8, including the holotype, unless otherwise specified; in mm): TL 2.07–2.32 (mean = 2.18, standard deviation ± 0.08), PL 0.74–0.80 (0.78 ± 0.02), PA 0.66–0.70 (0.69 ± 0.02), PB 1.30–1.40 (1.36 ± 0.04), SL (n = 7) 0.07–0.15 (0.11 ± 0.02), SW (n = 7) 0.09–0.14 (0.11 ± 0.02), EI 1.24–1.36 (1.30 ± 0.04), EL 1.44–1.62 (1.53 ± 0.08), EW 0.76–0.86 (0.81 ± 0.03), EH 0.50–0.62 (0.55 ± 0.04), HW 0.59–0.65 (0.62 ± 0.02), IS 0.15–0.20 (0.17 ± 0.02), WA 0.12–0.19 (0.14 ± 0.02), MC 0.55–0.64 (0.60 ± 0.03), MB 0.23–0.30 (0.27 ± 0.02), VL 0.40–0.49 (0.45 ± 0.03).

Antennae shorter than in females; club less distinct than in females (Fig. 15B). Pro- and mesotarsomeres I–III enlarged, with tenet setae (Fig. 18F–G). Tergite VIII heptagonal, acuminated posteriorly; punctuation inconspicuous; subglabrous (Fig. 19D). Tergite IX with rectangular ventral struts (Fig. 19E–F). Sternite VIII rectangular, with a projection (Fig. 19G). Sternite IX straight, constricted centrally and thicker apically (Fig. 19F). Aedeagus sclerotized, apex of median lobe short; openings in dorsal view forming an acute angle (Fig. 20A–C); internal sac with weak irregular sclerites, with drop-like sclerites (Fig. 20D–E); parameres short, enlarged apically in lateral view (Fig. 20A).

Females

Measurements (n = 1, paratype; in mm). Antennomeres (length(width)): 0.14(0.05), 0.11(0.05), 0.11(0.04), 0.06(0.04), 0.06(0.05), 0.05(0.06), 0.10(0.11), 0.09(0.13), 0.07(0.13), 0.08(0.14), 0.12(0.12); (n = 7, paratypes; in mm): TL 2.10–2.35 (mean = 2.26, standard deviation ± 0.09), PL 0.76–0.86 (0.81 ± 0.04), PA 0.66–0.74 (0.71 ± 0.02), PB 1.34–1.50 (1.43 ± 0.06), SL 0.09–0.13 (0.11 ± 0.01), SW 0.12–0.14 (0.13 ± 0.01), EI 1.30–1.40 (1.35 ± 0.04), EL 1.48–1.66 (1.58 ± 0.06), EW 0.76–0.84 (0.81 ± 0.03), EH 0.52–0.65 (0.60 ± 0.04), HW 0.61–0.66 (0.63 ± 0.02), IS 0.18–0.20 (0.18 ± 0.01), WA 0.13–0.15 (0.14 ± 0.00), MC 0.57–0.65 (0.62 ± 0.03), MB 0.25–0.32 (0.30 ± 0.02), VL 0.43–0.52 (0.50 ± 0.03).

Antennae larger than in males; antennal club more distinct (Fig. 15C). Tergite VIII hexagonal, with a posterior invagination; punctuation inconspicuous; subglabrous (Fig. 21A). Sternite VIII rectangular with a projection (Fig. 21B). Vagina membranous; bursa copulatrix with sclerites on wall (Fig. 21C, Supp. file 2A). Vaginal plate with an apical sclerite, more or less developed (Fig. 21C–D, Supp. file 2A). Two filiform spermatheca (Supp. file 2A). Distal gonocoxites straight, thin (Fig. 21C–E); gonostyli long, somewhat thick, and parallel (Fig. 21C–E).

Host fungi

Adults were collected from *Psathyrella candolleana* (Fr.) Maire (Agaricales, Psathyrellaceae) (1 record, 1 individual), *Psathyrella* sp. (1, 11), *Agaricus* sp. (1, 18; von Groll *et al.* 2021: figs 1–4), *A. dulcidulus* Schulzer (1, 4), *A. sylvaticus* Schaeff. (1, 20) and *Entoloma* (*Inocephalus*) sp. (Agaricales, Entolomataceae) (1, 2).

Remarks

Measurements similar to those of *C. newtoni*, except for the comparatively longer antennae. It was found co-occurring with *C. newtoni* in the same host fungi. However, they differ at first view by the coloration: *C. lescheni* sp. nov. is brown with few individuals of the same coloration as *C. newtoni* (pronotum reddish brown and elytra black); a few individuals of *C. newtoni* are brown, but darker than *C. lescheni*. They also differ by the microsculpture of the metaventrite: present in *C. lescheni* and absent

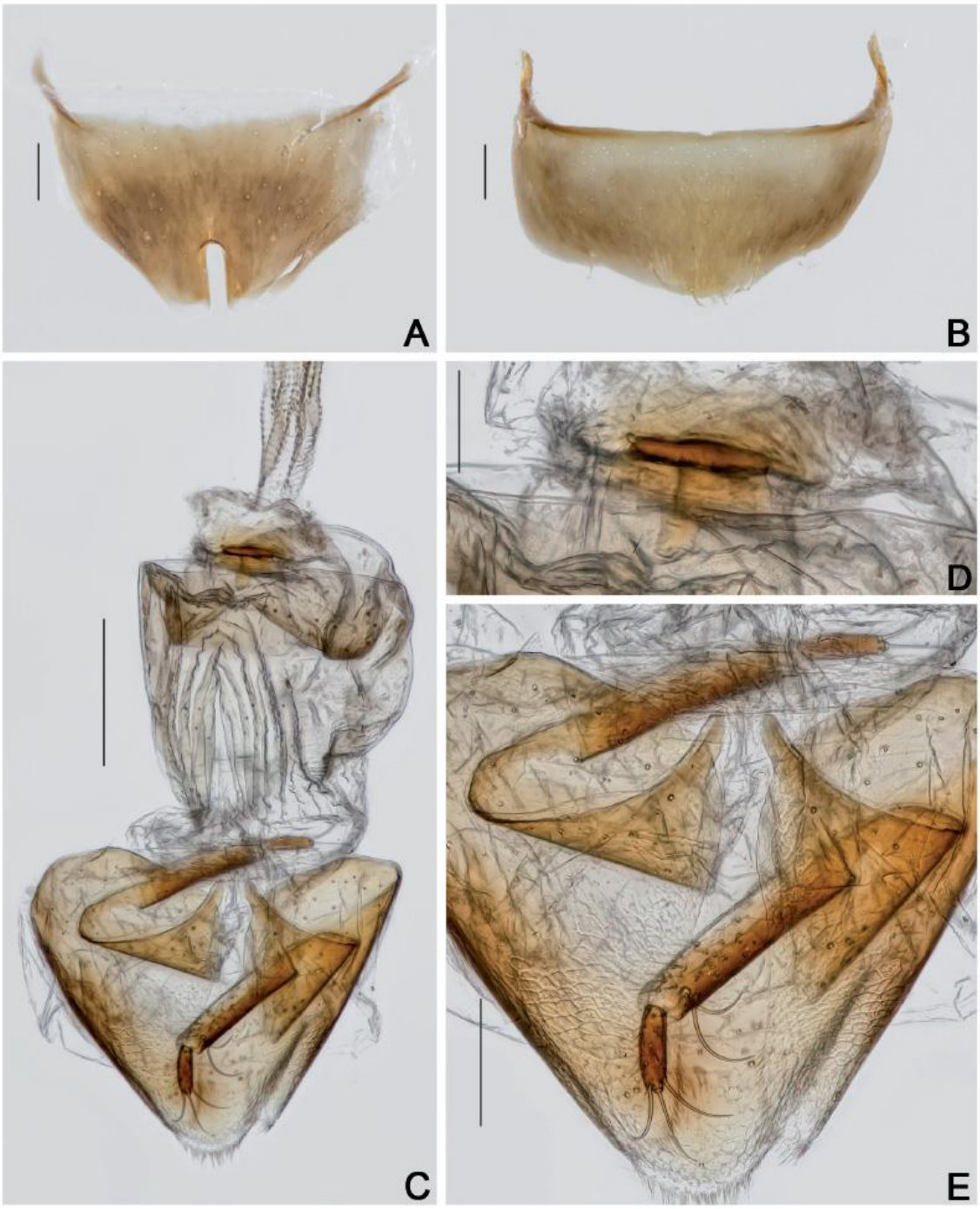

Fig. 21. *Cyparium lescheni* sp. nov., paratype, ♀ (CELC). **A**. Tergite VIII. **B**. Sternite VIII. **C**. Terminalia. **D**. Sclerite of vaginal plate. **E**. Ovipositor. Specimen collected at Mata da Biologia, Viçosa (MG, Brazil). Scale bars: A–B, E = 0.1 mm; C = 0.2 mm; D = 0.05 mm.

in *C. newtoni*. Tergite VIII in males is triangular in *C. lescheni* and straight apically in *C. newtoni*. Parameres in *C. newtoni* are longer and the sclerite of the internal sac is also different. Tergite VIII in females has an invagination in *C. lescheni*, while in *C. newtoni* it is entire.

Distribution

Known only from Mata da Biologia and Mata do Paraíso, campus of the Universidade Federal de Viçosa, Viçosa, state of Minas Gerais, Southeast Brazil (Fig. 46).

Cyparium loebli sp. nov.
urn:lsid:zoobank.org:act:88FF6EF0-5AED-4505-9E56-2200ED4ABEEF
Figs 4, 22–29, 46; Supp. file 1C

Diagnosis

TL: 2.53–2.78 mm in males and 2.34–2.68 mm in females. Pronotum, hypomeron and scutellum reddish brown (Fig. 22A). Elytra black, anterior region reddish brown (Fig. 22A). Hypomeron and mesanepisternum with strigulate microsculpture. Metaventrite smooth, coarsely punctate above intercoxal plates (Fig. 25D). Metanepisternum and metepimeron with imbricate microsculpture. Aedeagus apex long, parameres longish, weak sclerites in internal sac (Fig. 28A–E). Distal gonocoxites straight and slender (Fig. 29E).

Etymology

In homage to Dr Ivan Löbl (Muséum d'histoire naturelle, Genève, CH), for his remarkable contributions to the systematics of Scaphidiinae, which are the greatest source of information for our ongoing works on these beetles.

Material examined

Holotype

BRAZIL • ♂; Minas Gerais, Viçosa, EPTEA Mata do Paraíso; 12 Nov. 2019; LabCol leg.; "\\ Em *Xylodon flaviporus* \\ *Cyparium loebli* von Groll & Lopes-Andrade HOLOTYPUS" [red paper]; CELC (Supp. file 1C).

Paratypes

BRAZIL • 1 ♂, 1 ♀ (same pin); same collection data as for holotype; 8 Dec. 2014; I.S.C. Pecci-Maddalena leg.; CELC • 1 ♂, 2 ♀ (1 ♀, abdomen and head dissected, stored in glycerin); same collection data as for holotype, "Trilha dos Gigantes"; 15 Feb. 2015; S. Aloquio, A. Orsetti and M. Bento leg.; CELC • 2 specs; same collection data as for holotype; 19 Feb. 2015; FIT; A. Orsetti, S. Aloquio and M. Bento leg.; CELC • 1 ♂; same collection data as for holotype; S. Aloquio, A. Orsetti and M. Bento leg.; CELC • 6 ♂♂, 2 ♀♀ (1 ♂ entirely dissected, preserved in glycerin); same collection data as for holotype; "T. da Madeira"; 27 Feb. 2015; I.S.C. Pecci-Maddalena *et al*. leg.; CELC • 1 ♂, 1 ♀; same collection data as for holotype; CAMB • 1 ♀ (head dissected, preserved in glycerin); same collection data as for holotype; 13 Mar. 2015; S. Aloquio, A. Orsetti, C. Lopes-Andrade and M. Bento leg.; CELC • 1 ♂; same collection data as for holotype; 20 Mar. 2015; A. Orsetti and I. Gonçalves leg.; CELC • 6 ♂♂, 2 ♀♀ (2 ♂♂ dissected, preserved in glycerin); same collection data as for holotype; 9 Nov. 2016; I. Pecci-Maddalena and C. Lopes-Andrade leg.; "\\ ex *Psathyrella candolleana*"; CELC • 1 ♂, 1 ♀; same collection data as for holotype; CERPE • 2 ♂♂, 5 ♀♀ (1 ♀, abdomen dissected, preserved in glycerin); same collection data as for holotype; 19 Nov. 2019; LabCol leg.; "\\ em *Agaricus sylvaticus*"; CELC.

All paratypes additionally labelled "*Cyparium loebli* von Groll & Lopes-Andrade PARATYPUS [yellow paper]".

Description

MEASUREMENTS (holotype, in mm). TL 2.59, PL 1.00, PA 0.80, PB 1.72, EW 1.06, EL 1.86, IS 0.22, HW 0.72.

COLORATION. Black, iridescent (Fig. 22A–C). Frons dark brown; clypeus yellowish-brown; mouthparts yellow (Fig. 23A); antennomeres I–VI and apex of XI yellow; VII– basal part of XI darker (Fig. 23A–C). Pronotum, hypomeron and scutellum reddish brown (Fig. 22A). Elytra black, anterior region reddish brown (Fig. 22A). Meso- and metathorax in ventral view brown to dark brown. Procoxae dark ochre; meso- and metacoxae brownish red; femora dark brown, apex light brown; tibiae dark ochre, base and apex lighter; tarsi yellow (Fig. 22B–C). Ventrite 1 dark brown to brown; each next segment lighter; ventrites 5 and 6 yellowish. Variation: some paratypes with pronotum and base of elytra ochreous (Fig. 22D–F).

HEAD. Punctation dense, fine (Fig. 23A). Eyes wide and rounded (Fig. 23A). Labrum rectangular, lateral margins rounded, well delimited apically; central margins straight and wide; sclerotized portion inwardly curved; lateral setae well exceeding margins of labrum; densely porose centrally (Fig. 23D). Mandibles strongly curved and somewhat long apically; subapical serrations on left mandible conspicuous (Fig. 23E–F). Maxillae with palpomere III short; galea with a row of lateral setae; galea densely pubescent, lacinia moderately pubescent, wider than galea (Fig. 23G). Mentum forming a straight projection apically (Fig. 24A). Setae of labial palpomere II far exceeding palpomere III; palpomere III longish, with short apical setae (Fig. 24A–B). Post-gena microsculptured with close transversal lines; gula densely porose, but limited to central region; gula long and narrow (Fig. 24C). Antennal club well distinct; antennomere XI pentagonal, rounded apically (straight in some individuals); no notable difference between sexes (Fig. 23B–C).

PROTHORAX. Pronotum smooth, shining; punctuation dense, fine; pubescence short, fine (Fig. 24D–E); transverse, sub-straight laterally, forming an obtuse angle at lateral areas of posterior margin (Fig. 24E). Hypomeron with strigulate microsculpture. Notosternal suture straight, slightly inward directed (Fig. 24F). Profurca thin, only reaching half length of foramen (Fig. 24G). Prosternal process rounded (Fig. 25A).

MESOTHORAX. Mesonotum with prescutellar suture (= scutellar lines, Leschen & Löbl 2005) wavy (Fig. 25B). Scutellum tapering posteriorly (Fig. 25B). Anterior phragma large and obtuse (Fig. 25C). Mesanepisternum with strigulate microsculpture. Procoxal rests triangular, strongly curved posteriorly (Fig. 25D). Mesoventral and median lines wavy; area between median and mesocoxal lines not specially enlarged (Fig. 25D). Process of metaventrite curved at top and straight at base, forming a ridge (Fig. 25E).

METATHORAX. Metanotum with alacrista enlarged anteriorly and turned to sides; scutoscutellar suture curved; median membranous area wide and short (Fig. 25F). Metaventrite smooth, punctuation sparse and fine; coarsely punctate above intercoxal plates (Figs 22B, 25D). Mesocoxal line forming an angle between coxal cavities, and finely punctate under coxal cavities (Fig. 25D). Metanepisternum and metepimeron with imbricate microsculpture. Intercoxal plates smooth. Metendosternite with arms almost straight; 'stalk ridge' exceeding half length of stalk (Fig. 26A); ventral longitudinal flange curved in lateral view (Fig. 26B).

WINGS. Elytra slightly wider than longer; partially covering tergite VI (Fig. 26A); basal and lateral lines punctate (Fig. 24D); sutural line dashed; adsutural area with a row of setae; six rows of coarse punctures (not including sutural line), but rows 5 and 6 somewhat intermixed (Figs 22A, 26C); apical coarse punctation sparse; apical serrations small, sparse; pubescence short and fine (Fig. 26D). Epipleuron with diffuse, coarse, and close punctures. Hind wings fully developed (Fig. 26E).

LEGS. Pro-, meso- and metacoxae, and femora with strigulate microsculpture. Femora somewhat fusiform (Fig. 26F–H). Pro- and mesofemora sparsely and coarsely punctate; metafemora with shallow and fine

punctation. Mesotibia densely spinose, spines fine (Fig. 26G). Metatibiae sparsely spinose, spine fine (Fig. 26H).

ABDOMEN. Tergites VI–VIII with imbricate microsculpture (Fig. 27A). Tergite VII triangular; punctation sparse, coarse; pubescence sparse, fine (Fig. 27A). Ventrites (Fig. 27B) sparsely pubescent; with strigulate microsculpture. Ventrite 1 sparsely and coarsely punctate (Fig. 27C). Ventrites 2–5 moderately sparse and finely punctate. Metacoxal lines finely punctate.

Males

MEASUREMENTS (n = 1, paratype; in mm). Antennomeres (length(width)): 0.15(0.06), 0.11(0.05), 0.10(0.04), 0.08(0.04), 0.08(0.05), 0.06(0.06), 0.09(0.11), 0.08(0.12), 0.08(0.13), 0.08(0.14), 0.13(0.14);

Fig. 22. *Cyparium loebli* sp. nov. **A–C**. Holotype, ♂ (CELC). **A**. Dorsal view. **B**. Ventral view. **C**. Lateral view. **D–F**. Paratype, ♂ (CELC). **D**. Dorsal view. **E**. Ventral view. **F**. Lateral view. Specimens collected at Mata do Paraíso, Viçosa (MG, Brazil). Scale bars = 1.0 mm.

(n = 7, including the holotype; in mm): TL 2.53–2.78 (mean = 2.65, standard deviation ± 0.08), PL 1.00–1.08 (1.02 ± 0.03), PA 0.80–0.84 (0.82 ± 0.02), PB 1.60–1.80 (1.70 ± 0.06), SL 0.13–0.17 (0.15 ± 0.02), SW 0.13–0.16 (0.14 ± 0.01), EI 1.48–1.62 (1.52 ± 0.05), EL 1.74–1.90 (1.82 ± 0.05), EW 0.92–1.06 (0.98 ± 0.05), EH 0.43–0.71 (0.63 ± 0.10), HW 0.70–0.74 (0.72 ± 0.01), IS 0.20–0.23 (0.21 ± 0.01), WA 0.16–0.19 (0.17 ± 0.01), MC 0.68–0.74 (0.70 ± 0.02), MB 0.26–0.36 (0.32 ± 0.04), VL 0.52–0.56 (0.54 ± 0.02).

Pro- and mesotarsomeres I–III enlarged, with tenet setae (Fig. 26F–G). Tergite VIII heptagonal, acuminate posteriorly; punctuation fine, almost inconspicuous; subglabrous (Fig. 27D). Tergite IX with more or less bent ventral struts (Fig. 27E–F). Sternite VIII rectangular, with a small projection (Fig. 27G). Sternite IX triangular at ends and centrally constricted (Fig. 27F). Aedeagus sclerotized, enlarged at base, apex of median lobe long (Fig. 28A–C); openings in dorsal view long and somewhat enlarged, forming an acute angle (Fig. 28C); internal sac with weak irregular sclerites, with two hooks (Fig. 28D–E); parameres thin, longish (Fig. 28A–B).

Females

MEASUREMENTS (n = 1, paratype). Antennomeres (length(width)): 0.16(0.06), 0.10(0.05), 0.09(0.04), 0.07(0.04), 0.07(0.05), 0.05(0.06), 0.08(0.11), 0.08(0.13), 0.08(0.15), 0.08(0.15), 0.14(0.14); (n = 7,

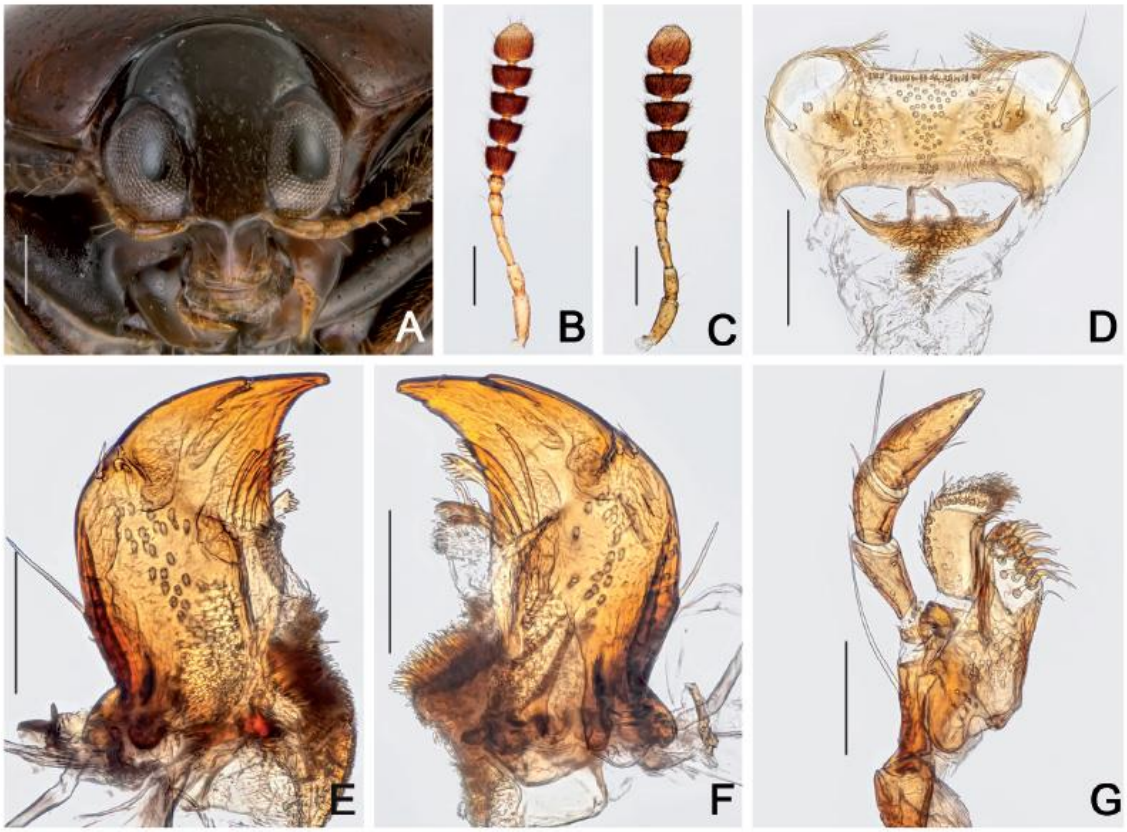

Fig. 23. *Cyparium loebli* sp. nov. **A**. Holotype, ♂ (CELC), frontal view. **B–C**. Antennae. **B**. Paratype, ♂ (CELC). **C**. Paratype, ♀ (CELC). **D–G**. Paratype, ♂ (CELC). **D**. Labrum. **E**. Left mandible. **F**. Right mandible. **G**. Maxilla. Specimens collected at Mata do Paraíso, Viçosa (MG, Brazil). Scale bars: A–C = 0.2 mm; D–G = 0.1 mm.

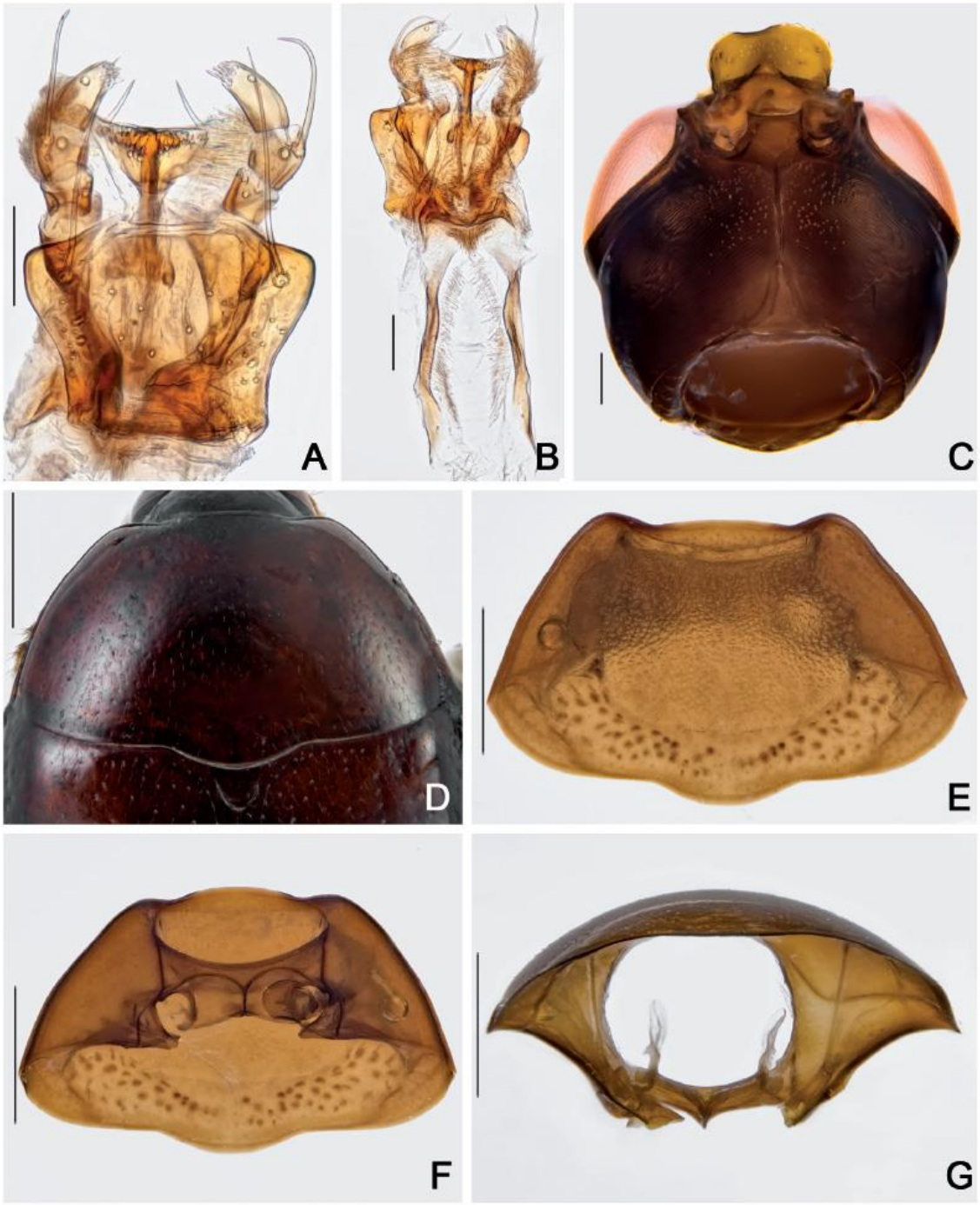

Fig. 24. *Cyparium loebli* sp. nov. **A–C, E–G**. Paratype, ♂ (CELC). **D**. holotype, ♂ (CELC). **A**. Labium. **B**. Hypopharynx. **C**. Head, ventral view. **D–E**. Pronotum, dorsal view. **F**. Prothorax, ventral view. **G**. Prothorax, inner view. Specimens collected at Mata do Paraíso, Viçosa (MG, Brazil). Scale bars: A–B = 0.05 mm; C = 0.1 mm; D–G = 0.5 mm.

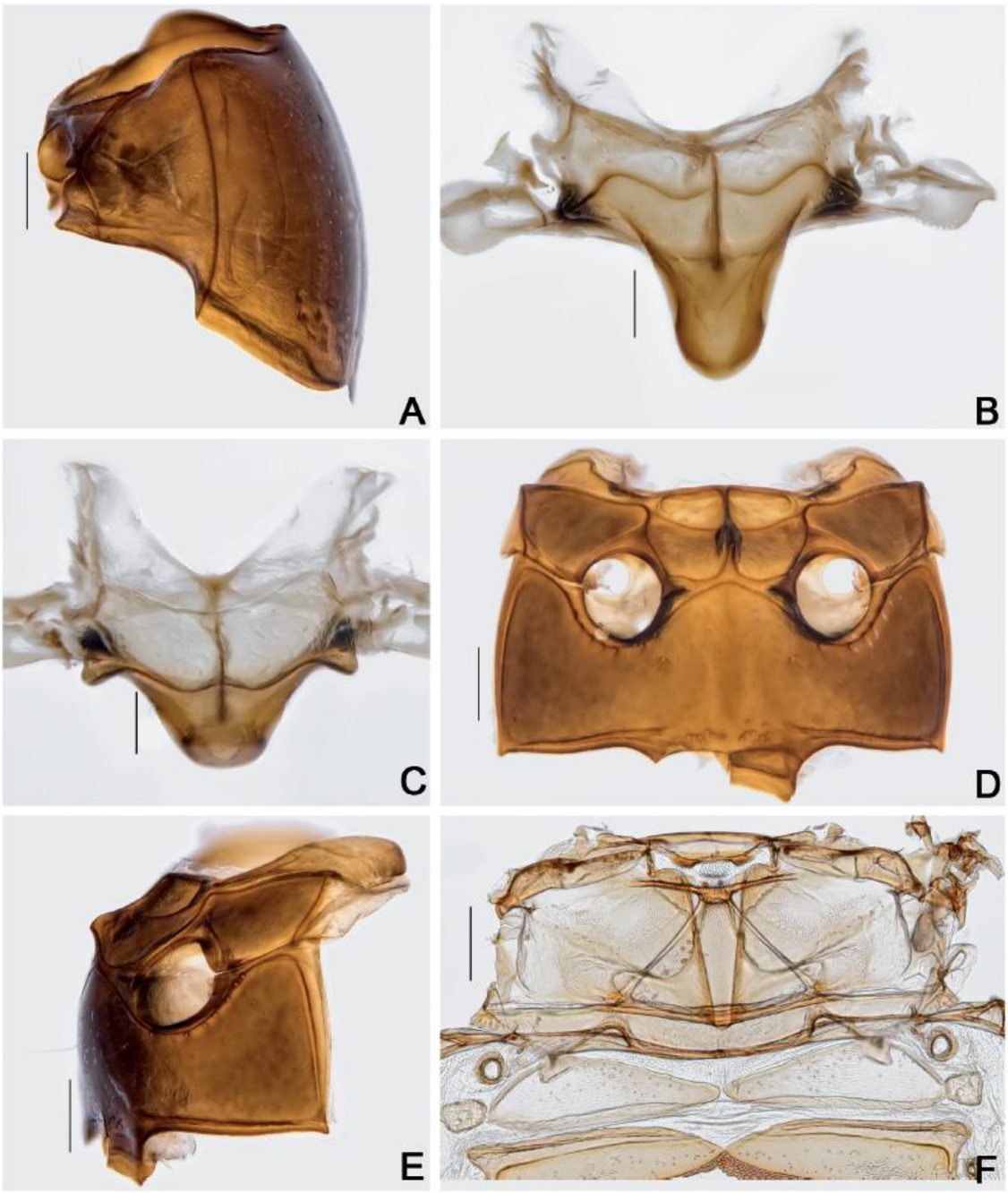

Fig. 25. *Cyparium loebli* sp. nov., paratype, ♂ (CELC). **A**. Prothorax, lateral view. **B–C**. Scutellar plate. **B**. Dorsal view. **C**. Apically slanted view. **D–E**. Meso- and metathorax. **D**. Ventral view. **E**. Lateral view. **F**. Metanotum. Specimen collected at Mata do Paraíso, Viçosa (MG, Brazil). Scale bars: A, D–F = 0.2 mm; B–C = 0.1 mm.

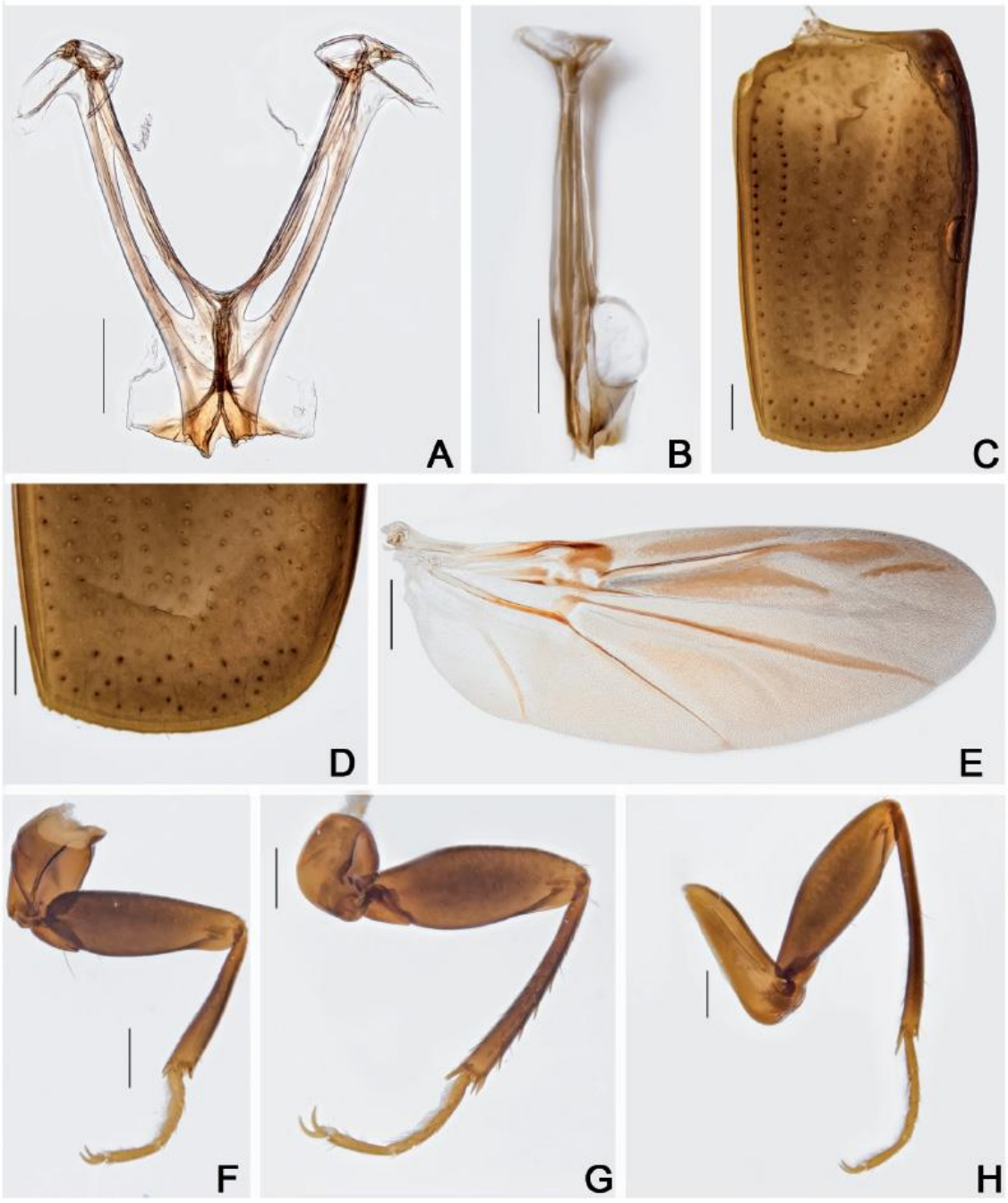

Fig. 26. *Cyparium loebli* sp. nov., paratype, ♂ (CELC). **A–B**. Metendosternite. **A**. Dorsal view. **B**. Lateral view. **C–D**. Elytron. **C**. Entire. **D**. Apex. **E**. Hind wing. **F–H**. Legs. **F**. Fore. **G**. Middle. **H**. Hind. Specimen collected at Mata do Paraíso, Viçosa (MG, Brazil). Scale bars: A–D, F–H = 0.2 mm; E = 0.5 mm.

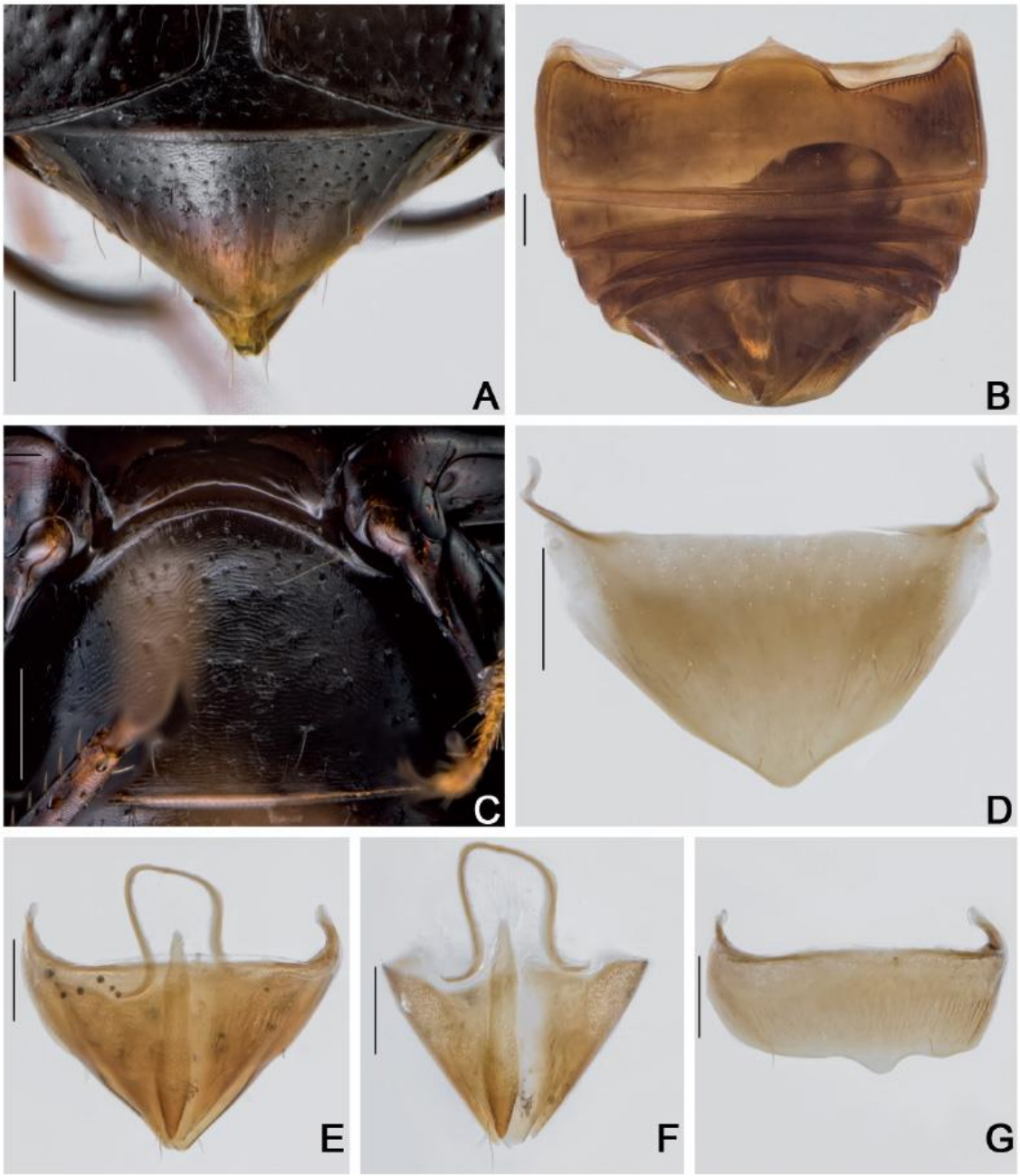

Fig. 27. *Cyparium loebli* sp. nov. **A–C**. Holotype, ♂ (CELC). **D–G**. Paratype, ♂ (CELC). **A**. Abdomen, dorsal view. **B**. Abdomen, ventral view. **C**. Ventrite 1. **D**. Tergite VIII. **E**. Terminalia. **F**. Tergite IX. **G**. Sternite VIII. Specimens collected at Mata do Paraíso, Viçosa (MG, Brazil). Scale bars = 0.2 mm.

Fig. 28. *Cyparium loebli* sp. nov., paratype, ♂ (CELC). **A–C**. Aedeagus. **A**. Lateral view. **B**. Frontal view. **C**. Dorsal view. **D–E**. Internal sac. **D**. Frontal view. **E**. Dorsal view. Specimen collected at Mata do Paraíso, Viçosa (MG, Brazil). Scale bars = 0.2 mm.

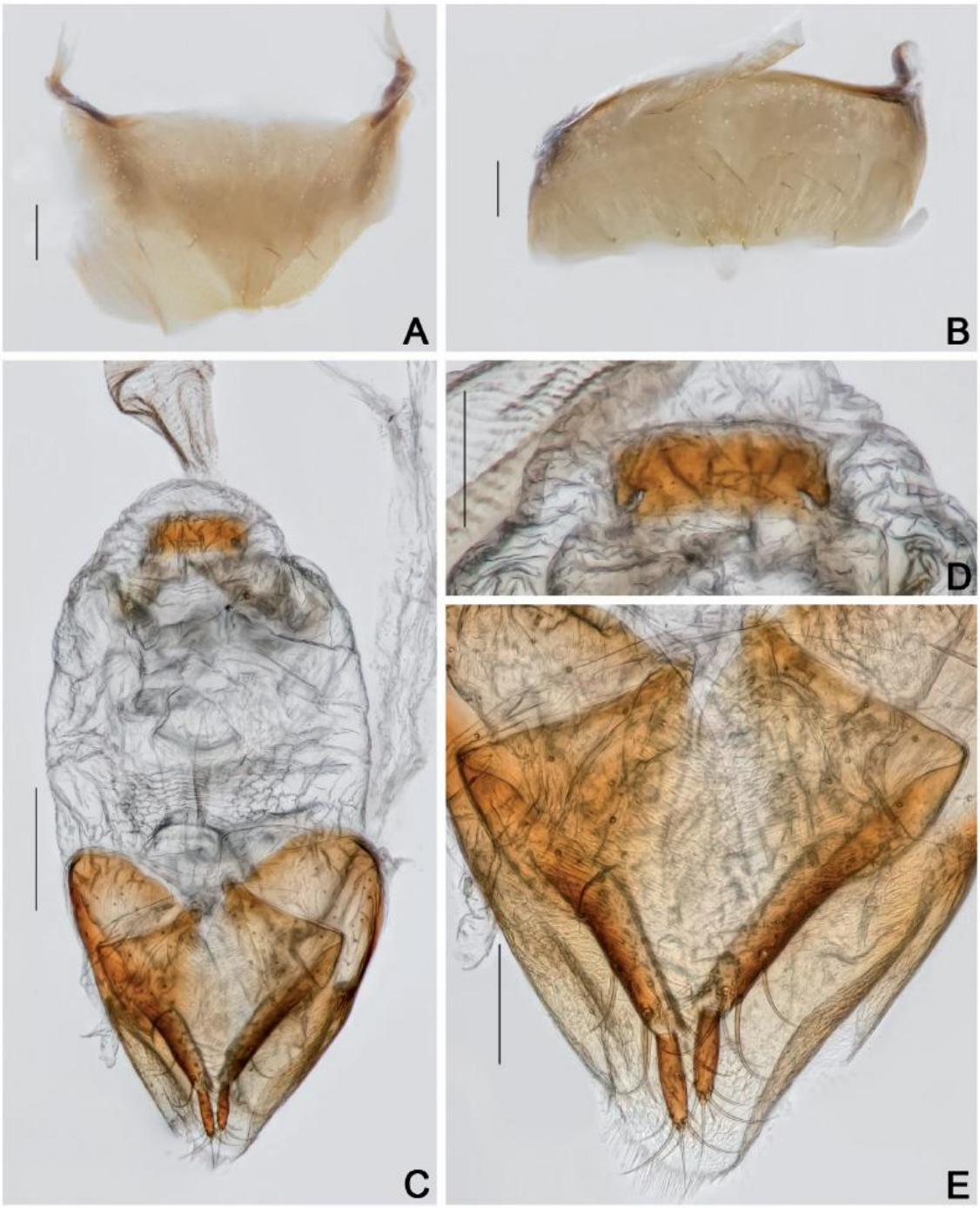

Fig. 29. *Cyparium loebli* sp. nov., paratype, ♀ (CELC). **A**. Tergite VIII. **B**. Sternite VIII. **C**. Terminalia. **D**. Sclerite of vaginal plate. **E**. Ovipositor. Specimen collected at Mata do Paraíso, Viçosa (MG, Brazil). Scale bars: A–B, D–E = 0.1 mm; C = 0.2 mm.

paratypes; in mm): TL 2.34–2.68 (mean = 2.57, standard deviation ± 0.12), PL 0.86–1.02 (0.96 ± 0.05), PA 0.76–0.86 (0.82 ± 0.04), PB 1.50–1.78 (1.68 ± 0.09), SL 0.13–0.17 (0.15 ± 0.01), SW 0.13–0.17 (0.14 ± 0.01), EI 1.40–1.64 (1.52 ± 0.08), EL 1.64–1.98 (1.83 ± 0.11), EW 0.86–1.06 (0.95 ± 0.07), EH 0.65–0.75 (0.69 ± 0.03), HW 0.66–0.74 (0.70 ± 0.02), IS 0.20–0.25 (0.23 ± 0.02), WA 0.17–0.19 (0.18 ± 0.01), MC 0.60–0.76 (0.71 ± 0.06), MB 0.29–0.36 (0.32 ± 0.03), VL 0.46–0.58 (0.54 ± 0.04).

Tergite VIII triangular; punctation inconspicuous; subglabrous (Fig. 29A). Sternite VIII rectangular with a distinct thin projection (Fig. 29B). Vagina and bursa copulatrix membranous without sclerites (Fig. 29C). Vaginal plate with an apical T-shaped sclerite (Fig. 29D). Spermatheca not detected. Distal gonocoxites straight, slender (Fig. 29C, E); gonostyli parallel, long, and slender (Fig. 29C, E).

Host fungi

Adults were collected from *Psathyrella candolleana* (1 record, 10 individuals), *Xylodon flaviporus* (Berk. & M.A. Curtis ex Cooke) Riebesehl & E.Langer (Hymenochaetales, Schizoporaceae) (1, 1) and *Agaricus sylvaticus* (1, 7).

Remarks

Similar to *C. lescheni* sp. nov., especially the teneral specimens, in the strigulate microsculpture of the hypomeron and metaventrite, reddish brown pronotum, and the size of the antennae, but differ in the comparatively larger body length and in the reddish brown anterior region of the elytra.

Distribution

Known only from Mata da Biologia and Mata do Paraíso, campus of the Universidade Federal de Viçosa, Viçosa, state of Minas Gerais, Southeast Brazil (Fig. 46).

Cyparium newtoni sp. nov.
urn:lsid:zoobank.org:act:8E4DB834-61A4-47B2-B9B3-2C0606708142
Figs 4, 30–37, 46; Supp. file 1D

Diagnosis

TL: 2.00–2.22 mm in males and 2.00–2.30 mm in females. Pronotum reddish brown (Fig. 32D). Elytra black (Fig. 30A). Hypomeron with strigulate microsculpture. Metaventrite smooth; coarsely punctate above intercoxal plates (Figs 30B, 33D). Intercoxal plates smooth. Apex of tergite VIII in males straight (Fig. 35D). Aedeagus openings in dorsal view narrow, forming an obtuse angle (Fig. 36C). Internal sac with a plate-like sclerite (Fig. 36D). Tergite VIII in females without apical invagination (Fig. 37A).

Etymology

In homage to Dr Alfred F. Newton (Field Museum, Chicago, USA) for his significant contribution to the systematics of Staphylinidae and more specifically of Scaphidiinae.

Material examined

Holotype

BRAZIL • ♂; Minas Gerais, Viçosa, EPTEA Mata do Paraíso; 19 Nov. 2019; LabCol leg.; "\\ em *Agaricus sylvaticus*\\ *Cyparium newtoni* von Groll & Lopes-Andrade HOLOTYPUS" [red paper]; CELC (Supp. file1D).

Paratypes

BRAZIL • 1 ♀; same collection data as for holotype; 19 Feb. 2015; S. Aloquio, A. Orsetti and M. Bento leg.; "\\ Trilha caminho das águas embaixo de casca de tronco caído"; CELC • 1 ♀; same collection

data as for holotype, "T. dos Gigantes"; 15 Feb. 2015; S. Aloquio, A. Orsetti and M. Bento leg.; CELC • 3 ♂♂, 1 ♀, 2 specs; same collection data as for holotype, "Trilha da Madeira"; 27 Feb. 2015; I.S.C. Pecci-Maddalena *et al*. leg.; CELC • 1 ♂, 1 ♀; same collection data as for holotype; CAMB • 2 ♂♂, 1 ♀; same collection data as for holotype; 13 Mar. 2015; S. Aloquio, A. Orsetti, C. Lopes-Andrade and M. Bento leg.; CELC • 5 ♂♂, 4 ♀♀ (2 ♂♂ dissected, preserved in glycerin); same collection data as for holotype; 9 Nov. 2016; I. Pecci-Maddalena and C. Lopes-Andrade leg.; "\\ ex. *Psathyrella candolleana*"; CELC • 2 ♂♂, 2 ♀♀ (1 ♂ dissected, preserved in glycerin); same collection data as for holotype; 21 Nov. 2019; LabCol leg.; "\\ Em *Agaricus dulcidulus* e *Leucocoprinus brebissoni*"; CELC • 1 ♂, 2 ♀♀, 1 spec. (1 ♂, abdomen dissected, preserved in glycerin); same collection data as for holotype; "\\ Em *Agaricus sylvaticus*"; CELC • 1 ♂, 1 ♀ (1 ♂, abdomen dissected, preserved in glycerin); Viçosa, Recanto das Cigarras, Mata da Biol.; 20 Nov. 2019; LabCol leg.; "Fungo 29 \\ Em *Entoloma* (*Inocephalus*) sp."; CELC • 2 ♂♂, 3 ♀♀, 1 spec. (1 ♂, entirely dissected, preserved in glycerin; 1 ♂, 1 ♀ (abdomen dissected, preserved in glycerin); same collection data as for preceding; "Fungo 08 \\ Em *Psathyrella* sp."; CELC • 1 ♂, 3 ♀♀; Viçosa, Mata da Biologia; 15 Oct. 2021; E. von Groll and A. Orsetti leg.; "Fungo 20 \\ Em *Agaricus* sp."; CELC.

All paratypes additionally labelled "*Cyparium newtoni* von Groll & Lopes-Andrade PARATYPUS [yellow paper]".

Description

MEASUREMENTS (holotype, in mm). TL 2.00, PL 0.72, PA 0.60, PB 1.30, EW 0.74, EL 1.44, IS 0.17, HW 0.56.

COLORATION. Frons dark brown; clypeus and mouthparts yellowish brown (Fig. 30D); antennomeres I–VI yellowish brown; VII–XI darker (Fig. 31A–C). Pronotum and hypomeron reddish brown (Fig. 30A–B). Scutellum ochre or black (Fig. 32D). Meso- and metathorax reddish-brown, each sclerite lighter laterally (Fig. 30B). Elytra black; epipleuron dark ochre (Fig. 30A). Coxae and trochanters dark ochre; femora dark ochre, apex lighter; tibiae dark ochre; lighter anteriorly and posteriorly; tarsi yellow (Fig. 30B–C). Tergite VIII yellow. Ventrite 1 dark ochre, 2–4 ochre, 5 and 6 yellow (Fig. 35C). Variation: few paratypes entirely dark brown, with lighter tarsi; others with reddish brown area less vibrant.

HEAD. Punctation dense, fine (Fig. 31A). Eyes globose in frontal view (Fig. 31A). Labrum rectangular, lateral margins rounded, well delimited apically; central margin straight; sclerotized portion inwardly curved; lateral setae extending well beyond margins of labrum; little porose centrally (Fig. 31D). Mandibles slightly curved; subapical serrations on left mandible conspicuous (Fig. 31E–F). Maxillary palps elongated; galea and lacinia moderately pubescent, lacinia elongated (Fig. 31G). Mentum slightly curved apically (Fig. 32A–B). Setae of labial palpomere II extending beyond palpomere III; palpomere III longish with short apical setae (Fig. 32A–B). Hypopharynx with wide and rounded sclerotized plate (Fig. 32A–B). Post gena microsculptured with transversal lines; few gular pores (Fig. 32C); gula narrow. Antennal club well distinct; antennomere XI longish, hexagonal (apex rounded in some specimens); antennal club different between sexes (Fig. 31B–C).

PROTHORAX. Pronotum smooth, shining; punctuation dense, fine; pubescence short, fine (Fig. 32D–E); transverse, sub-straight laterally, forming an obtuse angle at lateral areas of posterior margin (Fig. 32E). Hypomeron with strigulate microsculpture. Notosternal suture straight, inward directed (Fig. 32F). Profurca thin and elongated, slightly extending beyond half of foramen (Fig. 32G). Prosternal process acuminated (Fig. 33A).

MESOTHORAX. Mesonotum with prescutellar suture (= scutellar lines, Leschen & Löbl 2005) strongly wavy (Fig. 33B). Scutellum rounded posteriorly (Fig. 33B). Anterior phragma large and straight (Fig. 33C). Mesanepisternum with strigulate microsculpture. Procoxal rests wide; slightly curved posteriorly

(Fig. 33D). Mesoventral lines wavy and obtuse; median lines moderately wavy; area between median and mesoventral lines not specially enlarged (Fig. 33D). Process of metaventrite short, slightly curved at top and base, forming a small ridge (Fig. 33E).

METATHORAX. Metanotum with alacrista enlarged anteriorly and turned to the sides; scutoscutellar suture strongly curved; median membranous area wide and short (Fig. 33F). Metaventrite smooth; punctuation sparse, fine; coarsely punctate above intercoxal plates (Fig. 33D). Mesocoxal line not forming an angle between coxal cavities, just a simple triangle, and finely punctate under coxal cavities (Fig. 33D). Metanepisternum smooth; metepimeron with imbricate microsculpture. Intercoxal plates smooth.

Fig. 30. *Cyparium newtoni* sp. nov. **A–C**. Holotype, ♂ (CELC). **A**. Dorsal view. **B**. Ventral view. **C**. Lateral view. **D–E**. Paratype, unknown sex (CELC). **D**. Dorsal view. **E**. Lateral view. **F**. Paratype, ♀ (CELC), dorsal view. Specimens collected at Mata do Paraíso (A–C) and Mata da Biologia (D–F), Viçosa (MG, Brazil). Scale bars = 1.0 mm.

Metendosternite with arms almost straight; 'stalk ridge' not exceeding half of stalk (Fig. 34A); ventral longitudinal flange small, curved in lateral view (Fig. 34B).

WINGS. Elytra slightly wider than longer; partially covering tergite VI (Fig. 30A); basal and lateral lines punctate; sutural lines dashed (Fig. 32D); adsutural area with a row of setae; six rows of coarse punctures (not including sutural line) (Figs 30A, 34C); apical coarse punctation sparse; apical serrations almost inconspicuous (Fig. 34D); pubescence short and fine. Epipleuron with diffuse and coarse punctures. Hind wings fully developed (Fig. 34E).

LEGS. Pro-, meso- and metacoxae, and femora with strigulate microsculpture. Femora longish, somewhat fusiform (Fig. 34F–H). Pro- and mesofemora sparsely and coarsely punctate; metafemora with shallow and sparse punctuation. Mesotibiae densely spinose, spines fine (Fig. 34G); metatibiae sparsely spinose, spines fine (Fig. 34H).

ABDOMEN. Tergite VI–VIII with imbricate microsculpture (Fig. 35A). Tergite VII trapezoidal (Fig 35A) – triangular in some paratypes with tergite VIII not exposed; punctation sparse, fine; pubescence sparse, fine. Ventrites 1–5 (Fig. 35B) sparsely and finely punctate; pubescence sparse, fine; with strigulate microsculpture (Fig. 35C). Metacoxal lines finely punctate.

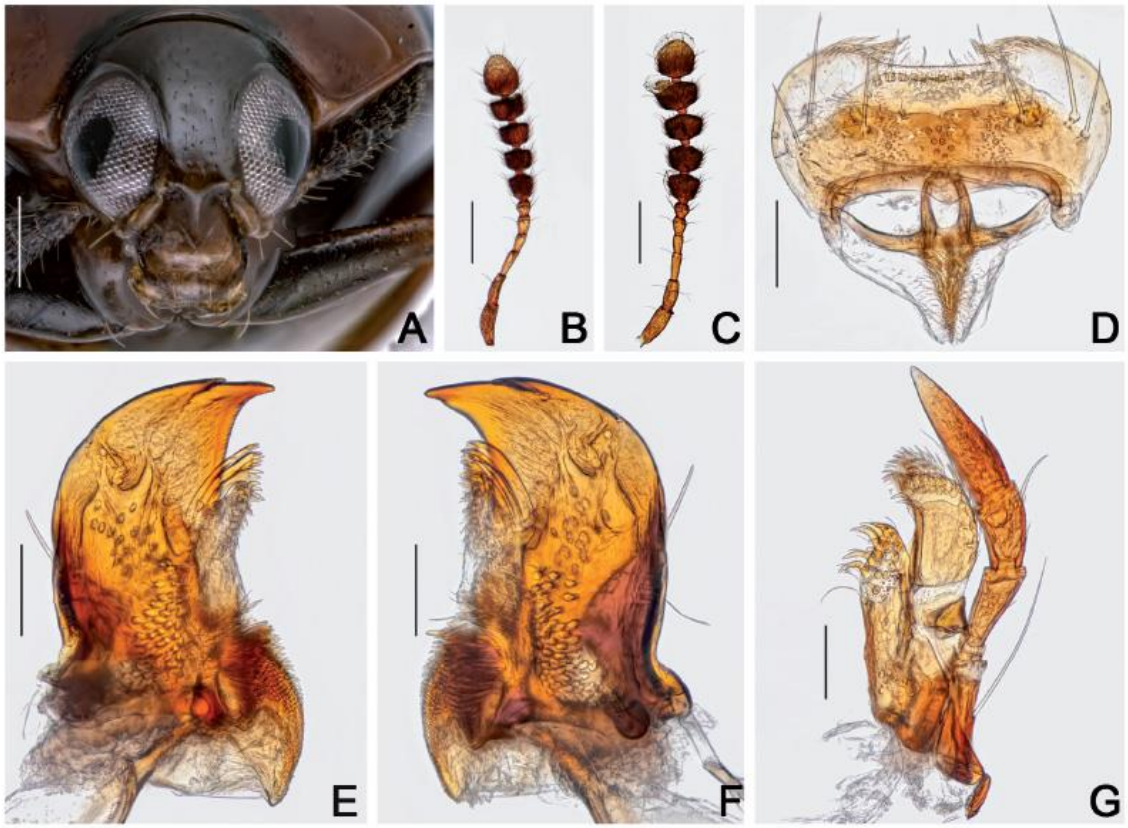

Fig. 31. *Cyparium newtoni* sp. nov. **A**. Holotype, ♂ (CELC), frontal view. **B–G**. Paratypes. **B**. Male antenna. **C**. Female antenna. **D**. Labrum. **E**. Left mandible. **F**. Right mandible. **G**. Maxilla. Specimens collected at Mata do Paraíso (A) and Mata da Biologia (B–G), Viçosa (MG, Brazil). Scale bars: A–C =1.0 mm; D–F = 0.2 mm; G–J = 0.05 mm.

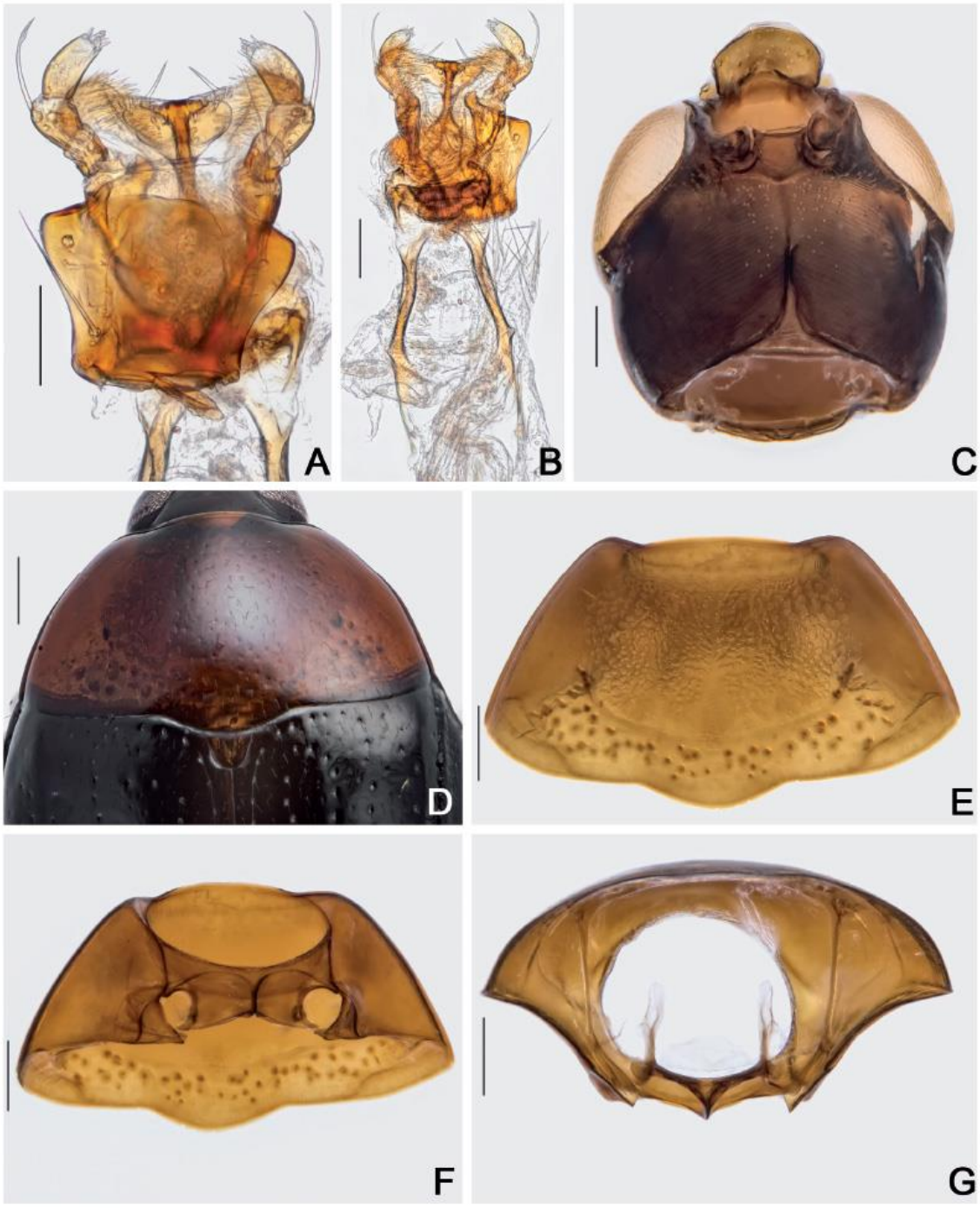

Fig. 32. *Cyparium newtoni* sp. nov. **A–C, E–G**. Paratype, ♂ (CELC). **A**. Labium. **B**. Hypopharynx. **C**. Head, ventral view. **D**. Holotype, ♂ (CELC), pronotum, dorsal view. **E–G**. Prothorax. **E**. Dorsal view. **F**. Ventral view. **G**. Inner view. Specimens collected at Mata da Biologia (A–C) and Mata do Paraíso (D–G), Viçosa (MG, Brazil). Scale bars: A–B = 0.05 mm; C = 0.1 mm; D–G = 0.2 mm.

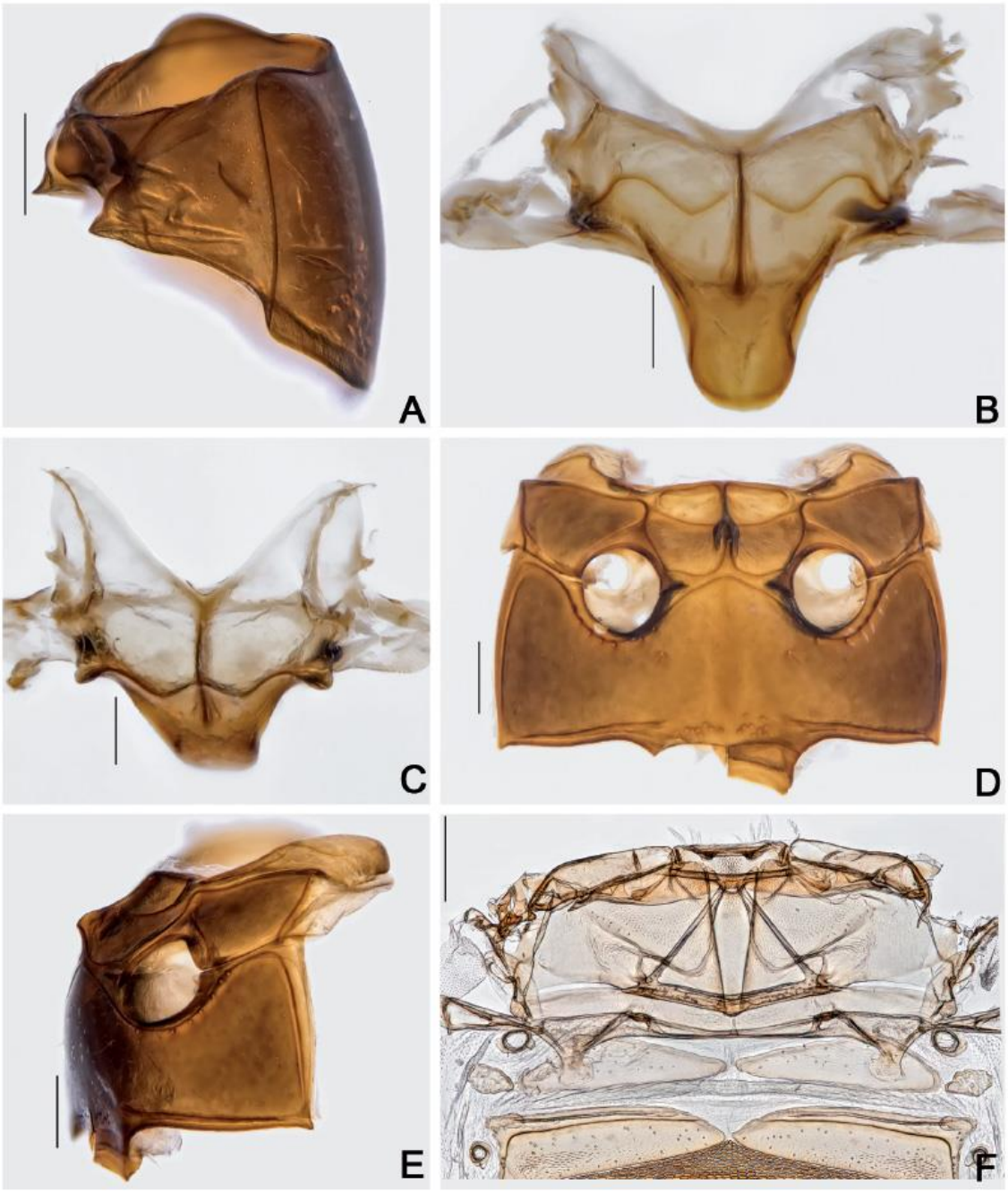

Fig. 33. *Cyparium newtoni* sp. nov., paratype, ♂ (CELC). **A**. Prothorax, lateral view. **B–C**. Scutellar plate. **B**. Dorsal view. **C**. Apically slanted view. **D–E**. Meso- and metathorax. **D**. Ventral view. **E**. Lateral view. **F**. Metanotum. Specimens collected at Mata do Paraíso (A. D–F) and Mata da Biologia (B–C), Viçosa (MG, Brazil). Scale bars: A, D–F = 0.2 mm; B–C = 0.1 mm.

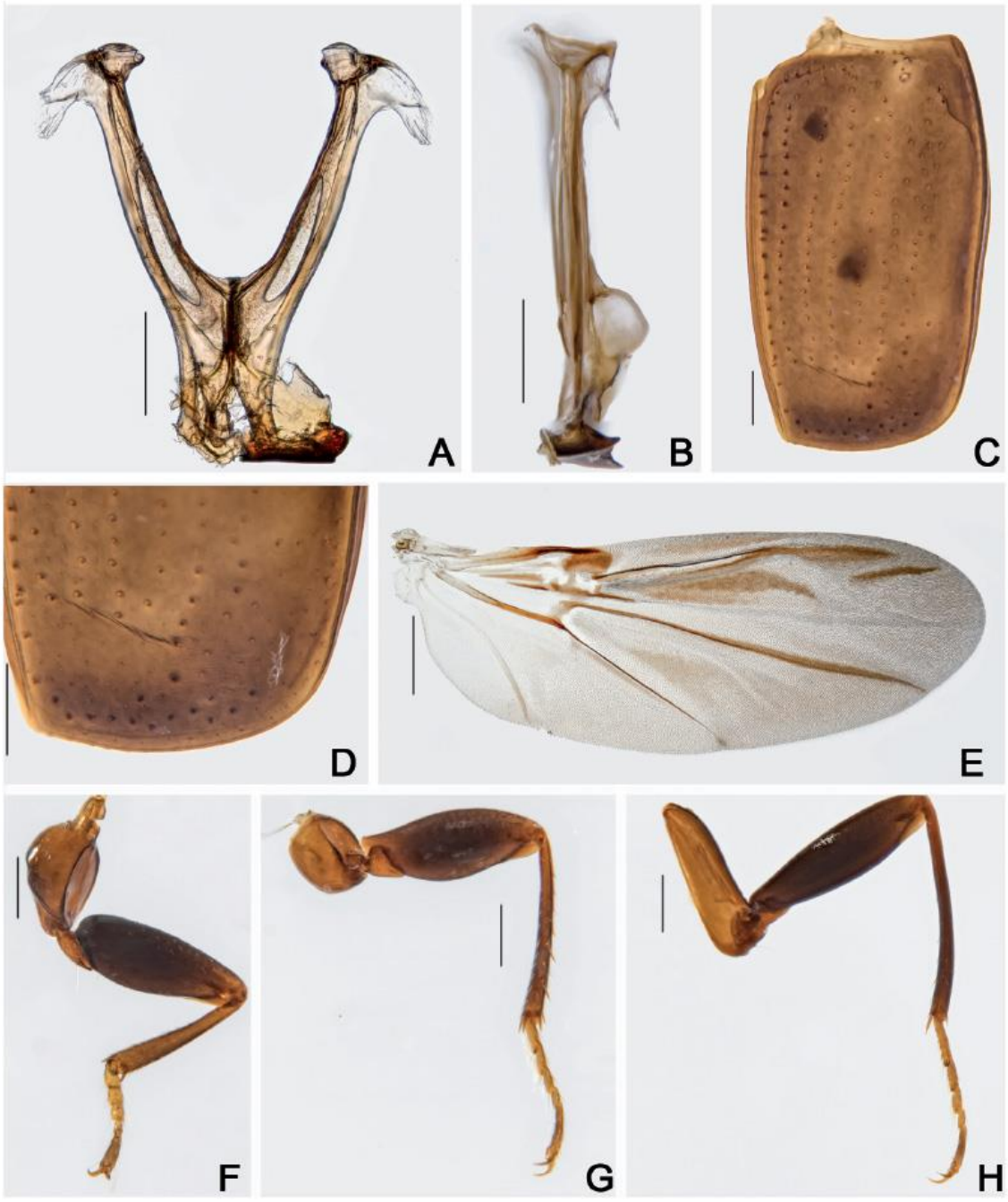

Fig. 34. *Cyparium newtoni* sp. nov., paratype, ♂ (CELC). **A–B**. Metendosternite. **A**. Dorsal view. **B**. Lateral view. **C–D**. Elytron. **C**. Entire. **D**. Apex. **E**. Hind wing. **F–H**. Legs. **F**. Fore. **G**. Middle. **H**. Hind. Specimens collected at Mata da Biologia, Viçosa (MG, Brazil). Scale bars: A–D, F–H = 0.2 mm; E = 0.5 mm.

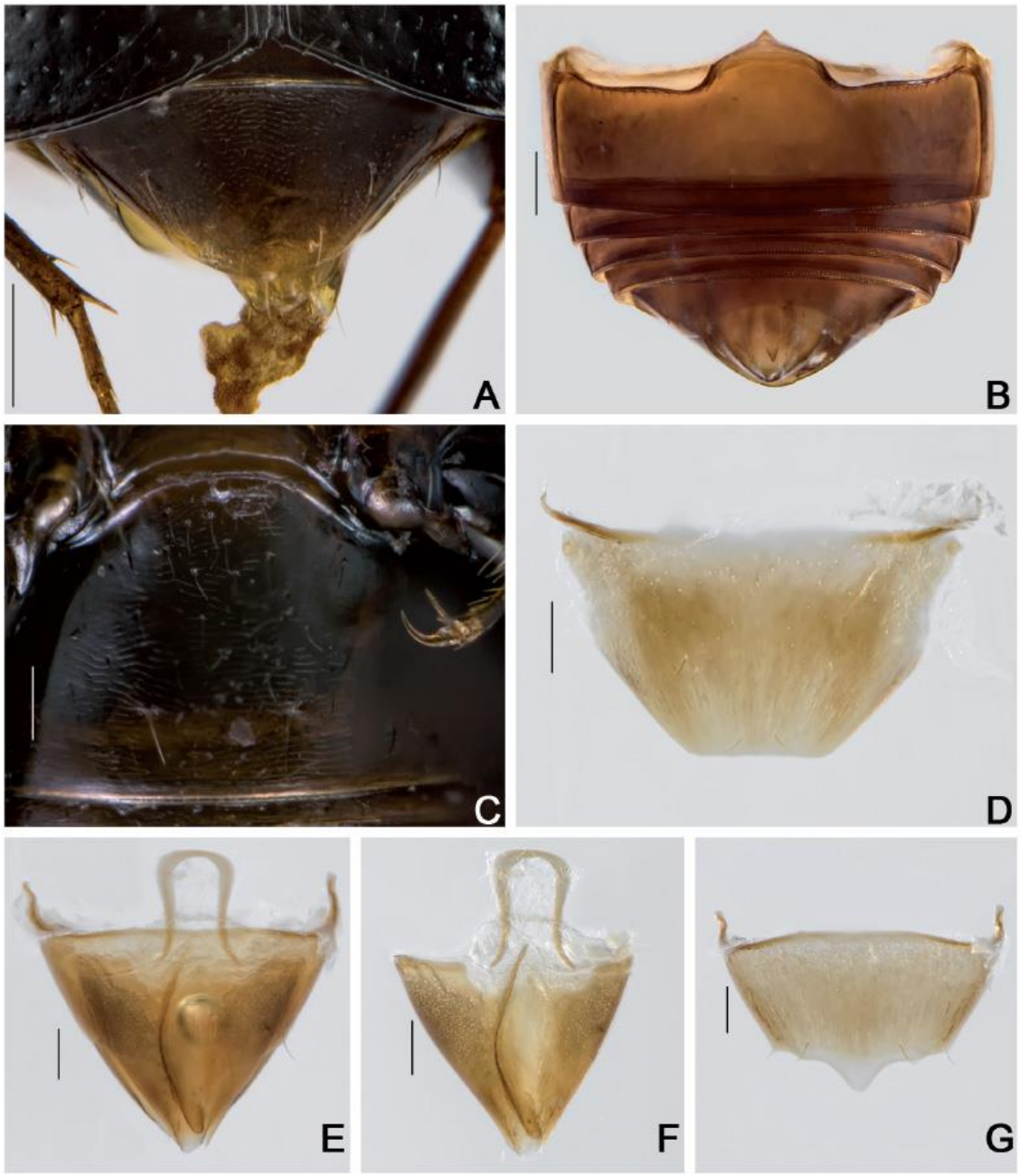

Fig. 35. *Cyparium newtoni* sp. nov. **A, C**. Holotype, ♂ (CELC). **B, D–G**. Paratype, ♂ (CELC). **A**. Abdomen, dorsal view. **B**. Abdomen, ventral view. **C**. Ventrite 1. **D**. Tergite VIII. **E**. Terminalia. **F**. Tergite IX. **G**. Sternite VIII. Specimens collected at Mata do Paraíso, Viçosa (MG, Brazil). Scale bars: A–B = 0.2 mm; C–G= 0.1 mm.

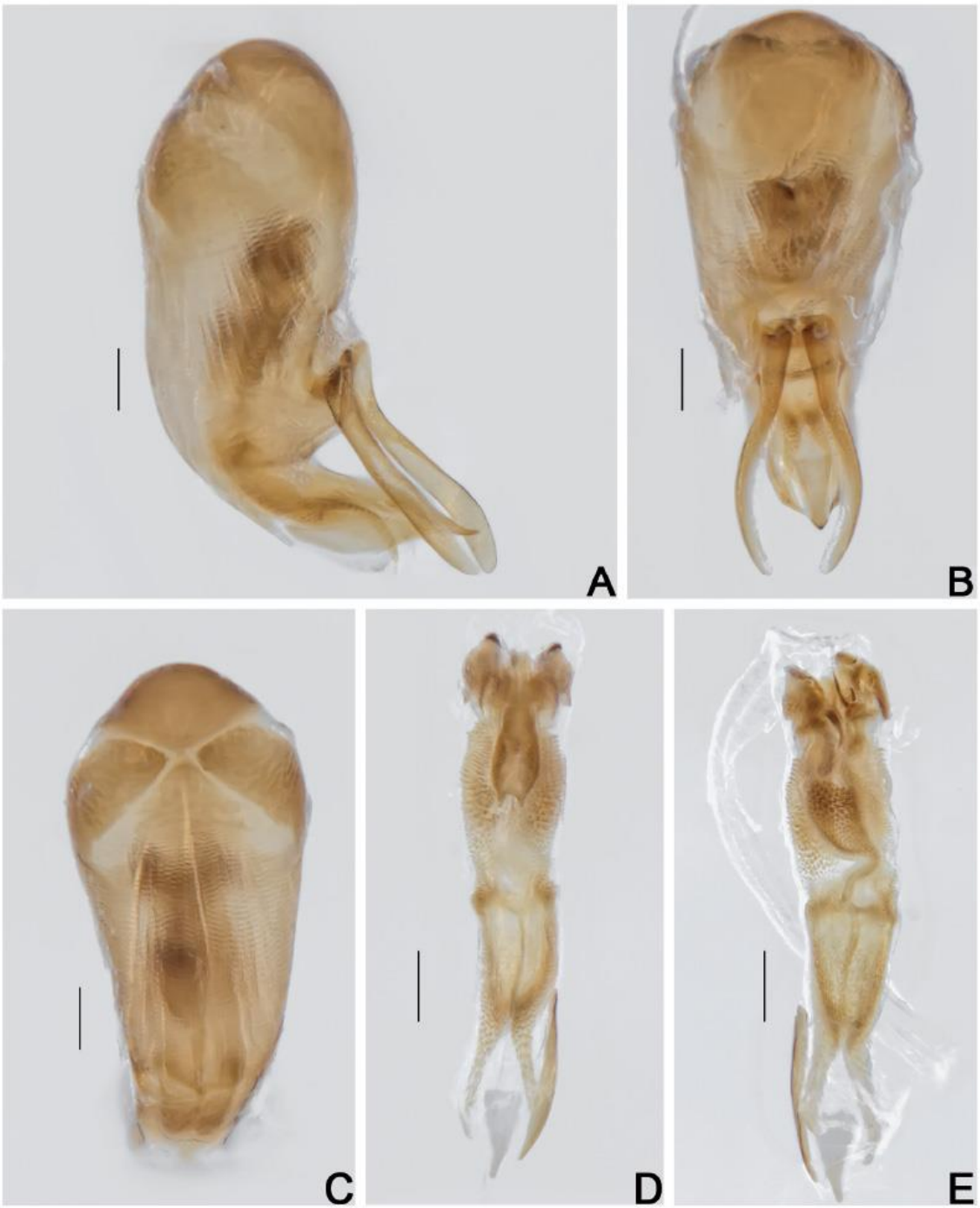

Fig. 36. *Cyparium newtoni* sp. nov., paratype, ♂ (CELC). **A–C**. Aedeagus. **A**. Lateral view. **B**. Frontal view. **C**. Dorsal view. **D–E**. Internal sac. **D**. Frontal view. **E**. Dorsal view. Specimen collected at Mata do Paraíso, Viçosa (MG, Brazil). Scale bars = 0.1 mm.

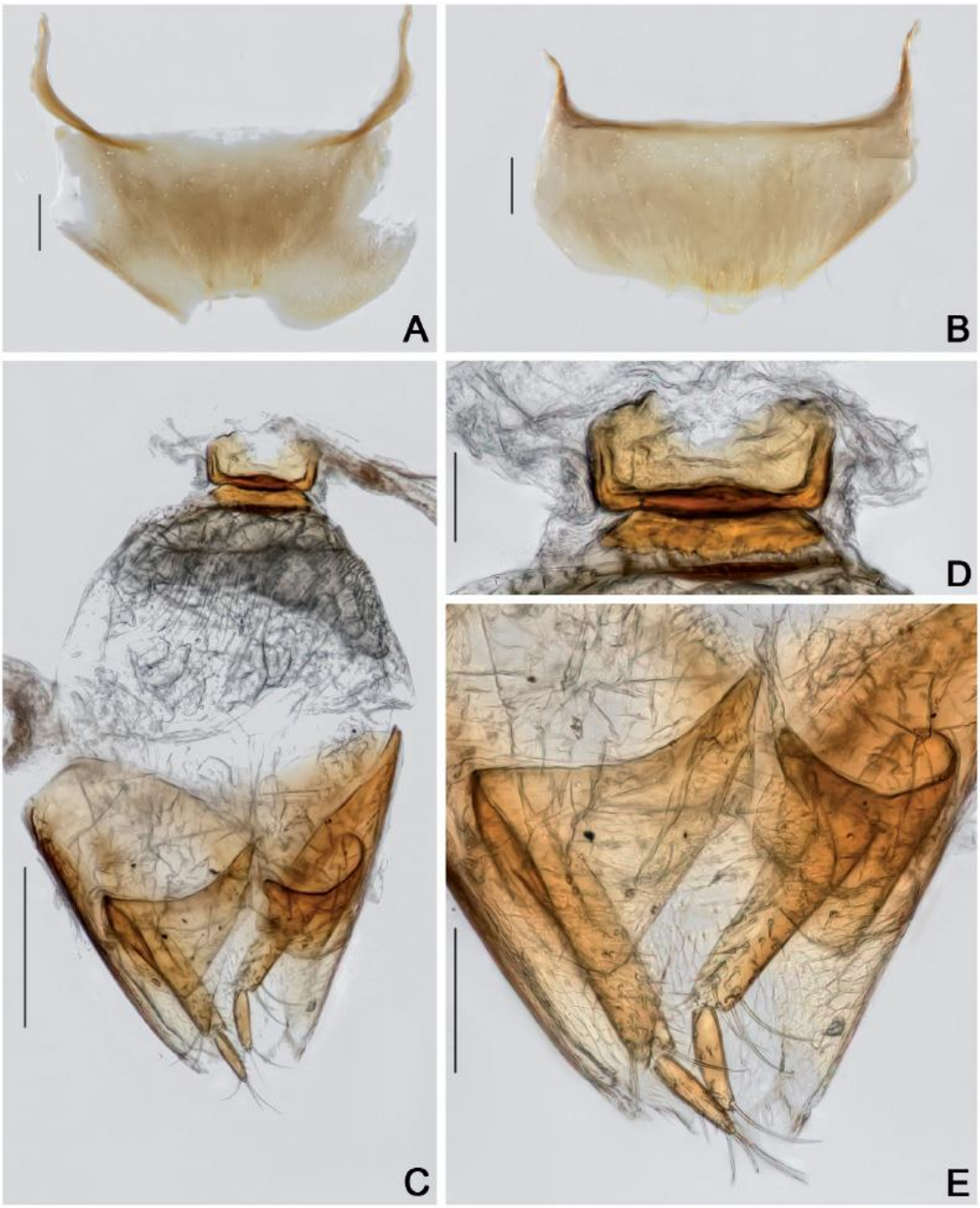

Fig. 37. *Cyparium newtoni* sp. nov., paratype, ♀ (CELC). **A**. Tergite VIII. **B**. Sternite VIII. **C**. Terminalia. **D**. Sclerite of vaginal plate. **E**. Ovipositor. Specimen collected at Mata da Biologia, Viçosa (MG, Brazil). Scale bars: A–B, E = 0.1 mm; C = 0.2 mm; D = 0.05 mm.

Males

MEASUREMENTS (n = 1, paratype; in mm). Antennomeres (length(width)): 0.13(0.06), 0.10(0.04), 0.08(0.03), 0.05(0.03), 0.06(0.04), 0.05(0.05), 0.08(0.09), 0.06(0.09), 0.07(0.10), 0.06(0.11), 0.13(0.11); (n = 7, including holotype; in mm): TL 2.00–2.22 (mean = 2.07, standard deviation ± 0.08), PL 0.70–0.80 (0.74 ± 0.03), PA 0.60–0.68 (0.63 ± 0.02), PB 1.28–1.40 (1.33 ± 0.04), SL 0.09–0.12 (0.10 ± 0.01), SW 0.10–0.12 (0.10 ± 0.01), EI 1.20–1.32 (1.25 ± 0.05), EL 1.40–1.54 (1.46 ± 0.05), EW 0.66–0.86 (0.77 ± 0.06), EH 0.50–0.62 (0.58 ± 0.04), HW 0.52–0.62 (0.57 ± 0.03), IS 0.17–0.18 (0.17 ± 0.00), WA 0.10–0.14 (0.13 ± 0.01), MC 0.52–0.61 (0.57 ± 0.02), MB 0.25–0.28 (0.27 ± 0.01), VL 0.42–0.56 (0.48 ± 0.04).

Antennal club less distinct than in females (Fig. 31B). Pro- and mesotarsomeres I–III enlarged, with tenet setae (Fig. 34F–G). Tergite VIII hexagonal, straight posteriorly; punctuation inconspicuous; subglabrous (Fig. 35D). Tergite IX with constricted ventral struts (Fig. 35E–F). Sternite VIII sub-rectangular, with projection (Fig. 35G). Sternite IX curved (Fig. 35F). Aedeagus sclerotized, apex of median lobe short (Fig. 36A,B); openings in dorsal view narrow, forming an obtuse angle (Fig. 36C); internal sac with weak irregular sclerites with two hooks and a central plate (Fig. 36D–E); parameres long, thin (Fig. 36B).

Females

MEASUREMENTS (n = 1, paratype; in mm). Antennomeres (length(width)): 0.13(0.05), 0.10(0.05), 0.09(0.03), 0.05(0.04), 0.06(0.04), 0.05(0.05), 0.08(0.10), 0.09(0.11), 0.09(0.13), 0.09(0.14), 0.13(0.12); (n = 7, paratypes; in mm): TL 2.00–2.30 (mean = 2.19, standard deviation ± 0.12), PL 0.76–0.84 (0.78 ± 0.03), PA 0.6–0.7 (0.64 ± 0.04), PB 1.30–1.48 (1.41 ± 0.07), SL 0.11–0.15 (0.12 ± 0.01), SW 0.11–0.14 (0.12 ± 0.01), EI 1.22–1.44 (1.34 ± 0.07), EL 1.44–1.64 (1.58 ± 0.06), EW 0.80–0.88 (0.83 ± 0.02), EH 0.57–1.07 (0.65 ± 0.18), HW 0.31–0.62 (0.55 ± 0.11), IS 0.16–0.18 (0.17 ± 0.01), WA 0.14–0.17 (0.15 ± 0.01), MC 0.56–0.65 (0.61 ± 0.03), MB 0.27–0.32 (0.30 ± 0.01), VL 0.45–0.52 (0.50 ± 0.03).

Antennal club more distinct than in males (Fig. 31B–C). Tergite VIII hexagonal; punctuation inconspicuous; subglabrous (Fig. 37A). Sternite VIII rectangular with a smooth projection (Fig. 37B). Vagina and bursa copulatrix membranous without sclerites (Fig. 37C). Vaginal plate with an apical sclerite (Fig. 37D). Spermatheca not detected. Distal gonocoxites straight and thin (Fig. 37C, E); gonostyli long, slender, larger at base (Fig. 37C, E).

Host fungi

Adults were collected from *Psathyrella candolleana* (1 record, 9 individuals), *Psathyrella* sp. (1, 6), *Agaricus* sp. (1, 4; von Groll *et al.* 2021: figs 1–4), *A. dulcidulus* (1, 4), *A. sylvaticus* (1, 5) and *Entoloma* (*Inocephalus*) sp. (1, 2).

Remarks

Extremely similar to *C. lescheni* sp. nov. (for comparison, see remarks under *C. lescheni* above and comparison of morphology below).

Distribution

Known only from Mata da Biologia and Mata do Paraíso, campus of the Universidade Federal de Viçosa, Viçosa, state of Minas Gerais, Southeast Brazil (Fig. 46).

Cyparium pici sp. nov.
urn:lsid:zoobank.org:act:7BE94FA9-A727-4779-B8FE-975D5C178ABC
Figs 5, 38–46; Supp. file 1E

Diagnosis

TL: 3.35–4.20 mm in males and 4.20–4.35 mm in females. Black. Antennae entirely yellow; club lighter (Fig. 38A). Anterior region of elytra reddish brown (Fig. 38A). Hypomeron and mesanepisternum with

close strigulate microsculpture. Metaventrite smooth; coarsely punctate above intercoxal plates (Fig. 38B, E). Ventrites 1–5 densely and coarsely punctate (Fig. 43C). Aedeagus strongly sclerotized, apex short; parameres short (Fig. 44A–B). Sclerites of internal sac strong (Fig. 44D–E). Distal gonocoxites short, straight and thick (Fig. 45E).

Etymology

In homage to Maurice Pic (1866–1957), who was responsible for gathering many specimens of scaphidiines deposited in museums, especially in the MNHN.

Material examined

Holotype

BRAZIL • ♂; Mato Grosso, Cotriguaçu, Faz. São Nicolau, matinha do Fernando [Fernando's woods]; 09°50′19″ S, 58°15′15″ W; FIT; 3 Nov. 2017; Vaz-de-Mello *et al*. leg.; "\\ *Cyparium pici* von Groll & Lopes-Andrade HOLOTYPUS" [red paper]; CEMT (Supp. file 1E).

Paratypes

BRAZIL • 8 ♂♂, 5 ♀♀ (1 ♂ entirely dissected, preserved in glycerin); same collection data as for holotype; CEMT • 3 ♂♂, 2 ♀♀ (2 ♂♂, 1 ♀, entirely dissected, preserved in glycerin; 1 ♀, abdomen dissected, preserved in glycerin); same collection data as for holotype; CELC.

All paratypes additionally labelled "*Cyparium pici* von Groll & Lopes-Andrade PARATYPUS [yellow paper]".

Description

Measurements (in mm). TL 3.45, PL 1.30, PA 1.12, PB 2.15, EW 1.42, EL 2.71, IS 0.28, HW 0.93.

Coloration. Black (Fig. 38A–C). Frons dark brown; clypeus light brown; mouth parts and antennae yellow, club lighter (Fig. 39A). Anterior region of elytra reddish brown (Fig. 38A); epipleuron dark ochre. Femora dark brown; tibiae lighter; tarsi yellow (Fig. 38B). Tergite VIII and ventrite 6 yellowish (Fig. 38B). Variation: (1) entirely light brown (Fig. 38D); (2) entirely dark brown with antennae, tarsi and tergite VIII yellow (Fig. 38E–F).

Head. Punctation dense, coarse (Fig. 39A). Eyes slightly wider than head, rounded (Fig. 39A). Labrum rectangular, lateral margins sub-straight, and well distinct from apical margin; central margin slightly curved centrally; sclerotized portion reaching apex; lateral setae slightly extending beyond margins; porose centrally (Fig. 39D). Left mandible slightly curved and right mandible more curved; subapical serrations on left mandible conspicuous (Fig. 39E–F). Maxillary palps elongated, palpomeres slender anteriorly; lacinia strongly robust, short and densely pubescent (Fig. 39G). Mentum with lateral areas strongly rounded and apex well delimited (Fig. 40A). Glossa heart-shaped (Fig. 40A). Setae of labial palpomere II slightly exceeding palpomere III; palpomere III longish, with short apical setae (Fig. 40A). Hypopharynx with wide and triangular sclerotized plate (Fig. 40B). Post gena microsculptured with very close transversal lines; densely porose, except at region of gula; gula triangular and narrow (Fig. 40C). Antennal club distinct; antennomere XI hexagonal, apex more or less acuminated, regardless of sex (Fig. 39B–C).

Prothorax. Pronotum smooth; punctuation dense, fine; pubescence short, fine (Fig. 40D); transverse, rounded laterally, forming a small obtuse angle at lateral areas of posterior margin (Fig. 40E). Hypomeron with close strigulate microsculpture. Notosternal suture straight (Fig. 40F). Profurca elongated, only reaching half length of foramen (Fig. 40G). Prosternal process short and round (Fig. 41A).

MESOTHORAX. Mesonotum with prescutellar suture (= scutellar lines, Leschen & Löbl 2005) wavy (Fig. 41B). Scutellum rounded posteriorly (Fig. 41B). Anterior phragma straight (Fig. 41C). Mesanepisternum with strigulate microsculpture. Procoxal rests triangular; slightly wavy posteriorly (Fig. 41D). Mesoventral and median lines strongly wavy; area between median and mesoventral lines enlarged (Fig. 41D). Process of metaventrite moderately long; apex more prominent, forming a ridge (Fig. 41E).

METATHORAX. Metanotum with alacrista triangular, small anteriorly and turned to posterior end; scutoscutellar suture not strongly wavy; median membranous area narrow and long (Fig. 41F). Metaventrite smooth; punctuation sparse, fine; coarsely punctate above intercoxal plates (Figs 38B, E, 41D). Mesocoxal line forming a smooth angle between coxal cavities; finely punctate under coxal cavities (Fig. 41D). Metanepisternum and metepimeron with imbricate microsculpture. Intercoxal plates

Fig. 38. *Cyparium pici* sp. nov. **A**–**C**. Holotype, ♂ (CEMT). **A**. Dorsal view. **B**. Ventral view. **C**. Lateral view. **D**. Paratype, ♀ (CEMT), dorsal view. **E**–**F**. Paratype, ♂ (CEMT). **E**. Dorsal view. **F**. Lateral view. Specimens collected at Cotriguaçu (MT, Brazil). Scale bars = 1.0 mm.

smooth. Metendosternite with arms slightly curved; 'stalk ridge' reaching half length of stalk (Fig. 42A); ventral longitudinal flange curved in lateral view (Fig. 42B).

WINGS. Elytra slightly wider than longer; covering just until tergite V (Fig. 38A, D); each elytron sub-rectangular (Fig. 42C); basal (Fig. 40D) and sutural lines dashed; adsutural area with a row of setae; six rows of coarse punctures (not including sutural line) (Figs 38A, D, 42C); lateral line punctate; apical coarse punctation moderately sparse; apical serrations almost inconspicuous (Fig. 42D); pubescence short and fine. Epipleuron with a row of sparse and coarse punctures. Hind wings fully developed (Fig. 42E).

LEGS. Pro-, meso- and metacoxae, and femora with strigulate microsculpture. Pro- and mesofemora fusiform (Fig. 42F–G); punctuation sparse, coarse; metafemora longish, punctuation sparse, shallow (Fig. 42H). Mesotibiae densely spinose, spines thick (Fig. 42G); metatibiae sparsely spinose, spines fine (Fig. 42H).

ABDOMEN. Tergites VI–VIII with narrow imbricate microsculpture; punctures dense, coarse; pubescence sparse, coarse (Fig. 43A). Ventrites 1–5 densely and coarsely punctate; pubescence moderately sparse, fine; close strigulate microsculpture (Fig. 43B–C). Metacoxal lines finely punctate.

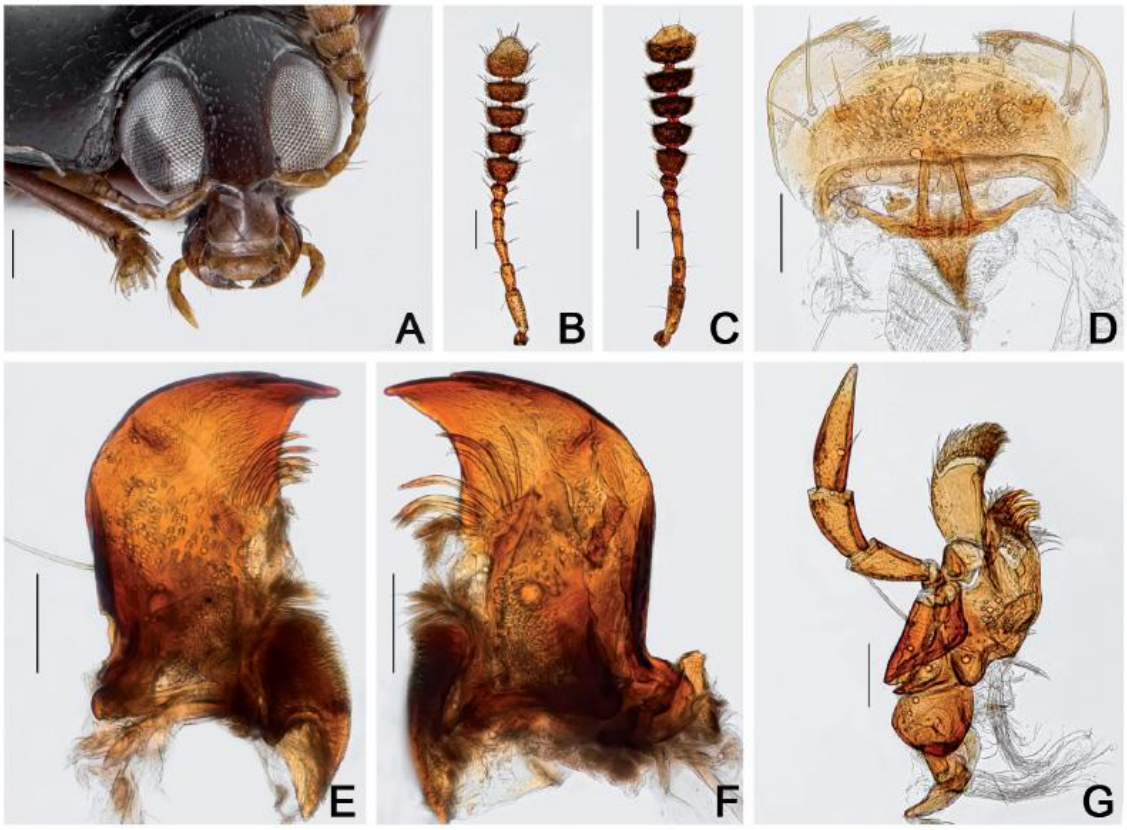

Fig. 39. *Cyparium pici* sp. nov. **A**. Holotype, ♂ (CEMT), frontal view. **B**–**G**. Paratypes (CELC). **B**. Male, antenna. **C**. Female antenna. **D**. Labrum. **E**. Left mandible. **F**. Right mandible. **G**. Maxilla. Specimens collected at Cotriguaçu (MT, Brazil). Scale bars: A–C = 0.2 mm; D–G = 0.1 mm.

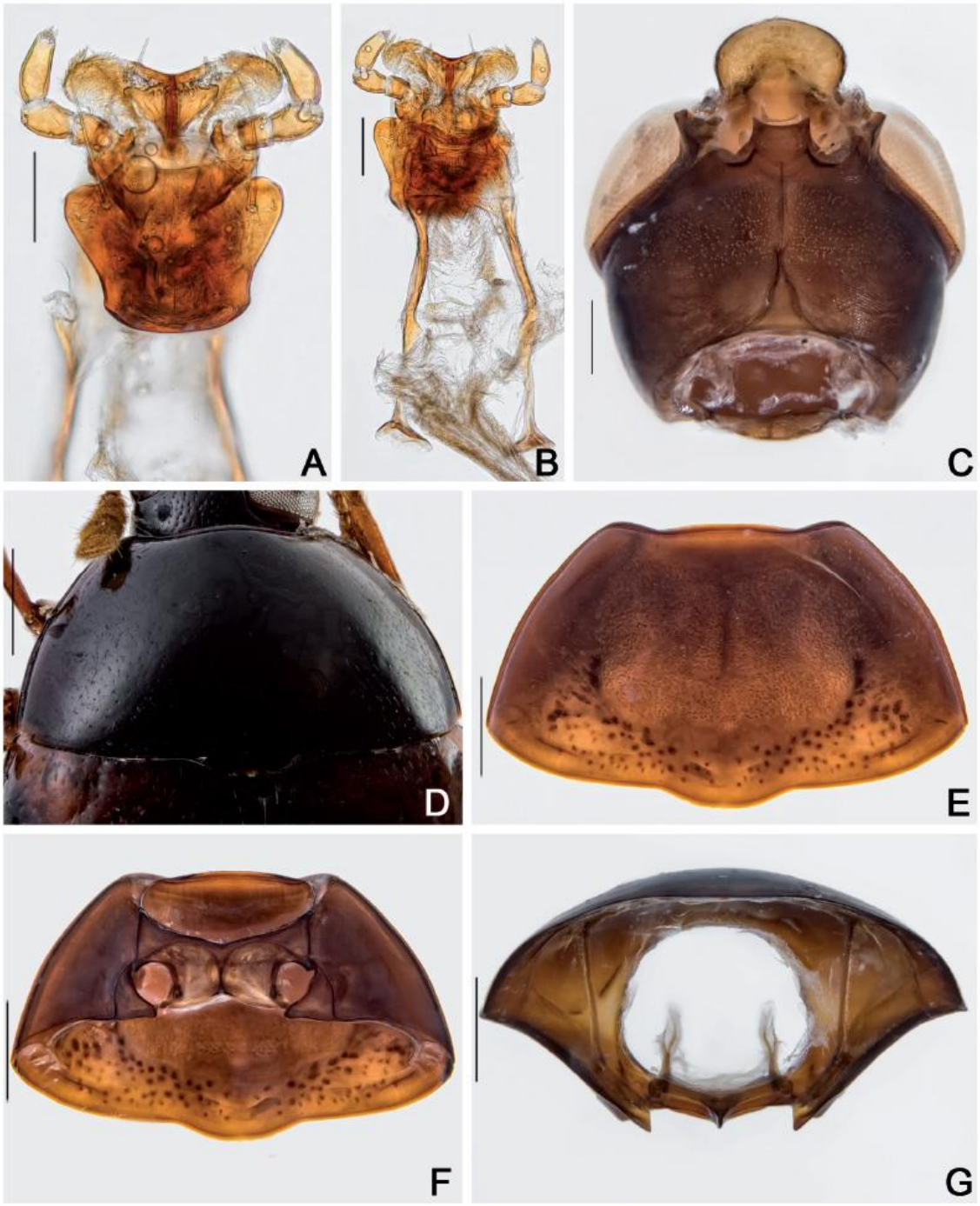

Fig. 40. *Cyparium pici* sp. nov. **A–C**. Paratype, ♂ (CELC). **A**. Labium. **B**. Hypopharynx. **C**. Head, ventral view. **D**. Holotype, ♂ (CEMT), pronotum, dorsal view. **E**. Paratype, ♂ (CEMT), pronotum, dorsal view. **F–G**. Paratype, ♂ (CELC), prothorax. **F**. Ventral view. **G**. Inner view. Specimens collected at Cotriguaçu (MT, Brazil). Scale bars: A–B = 0.1 mm; C = 0.2 mm; D–G = 0.5 mm.

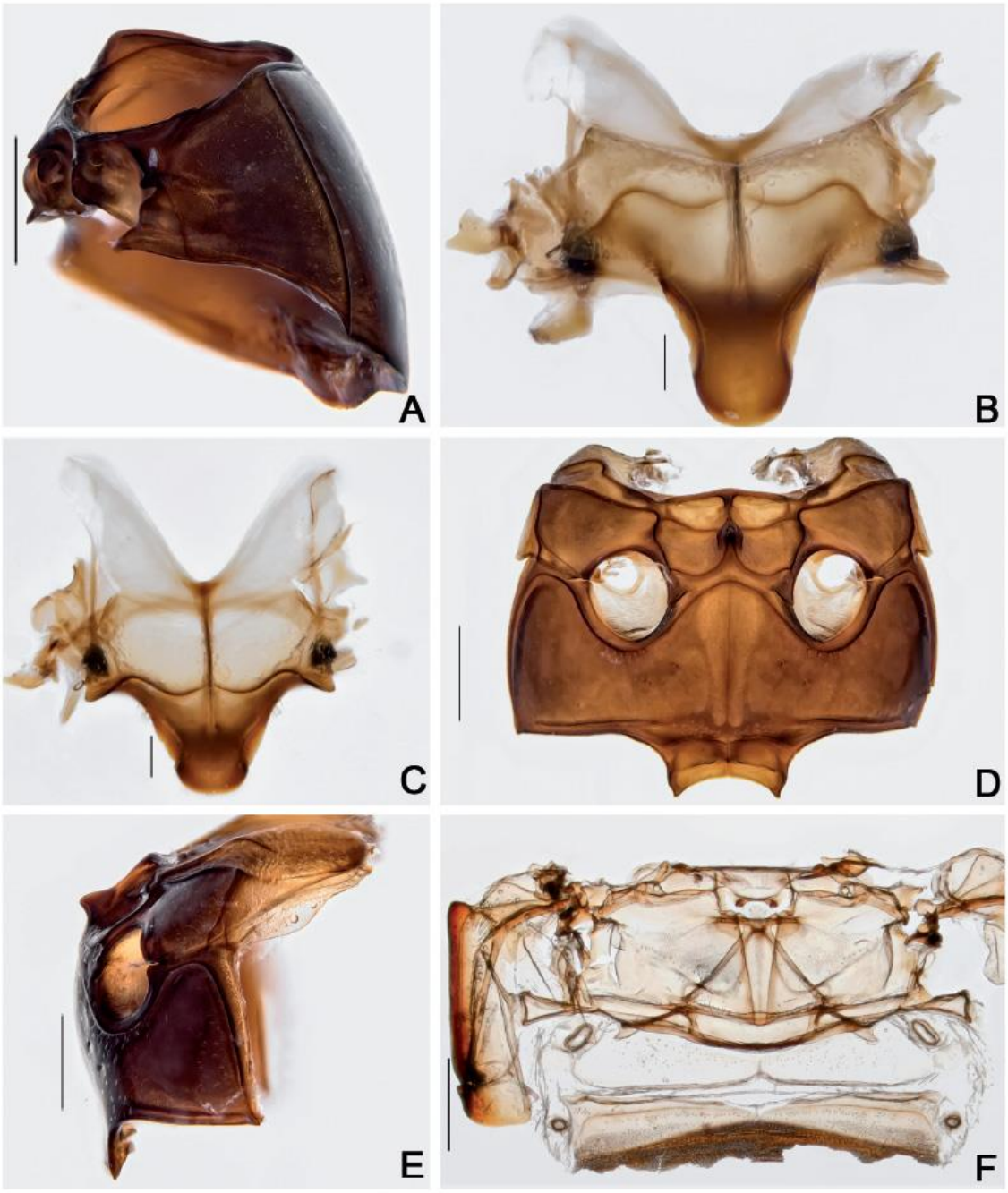

Fig. 41. *Cyparium pici* sp. nov., paratype, ♂ (CELC). **A**. Prothorax, lateral view. **B–C**. Scutellar plate. **B**. Dorsal view. **C**. Apically slanted view. **D–E**. Meso- and metathorax. **D**. Ventral view. **E**. Lateral view. **F**. Metanotum. Specimen collected at Cotriguaçu (MT, Brazil). Scale bars: A, D–F = 0.5 mm; B–C = 0.1 mm.

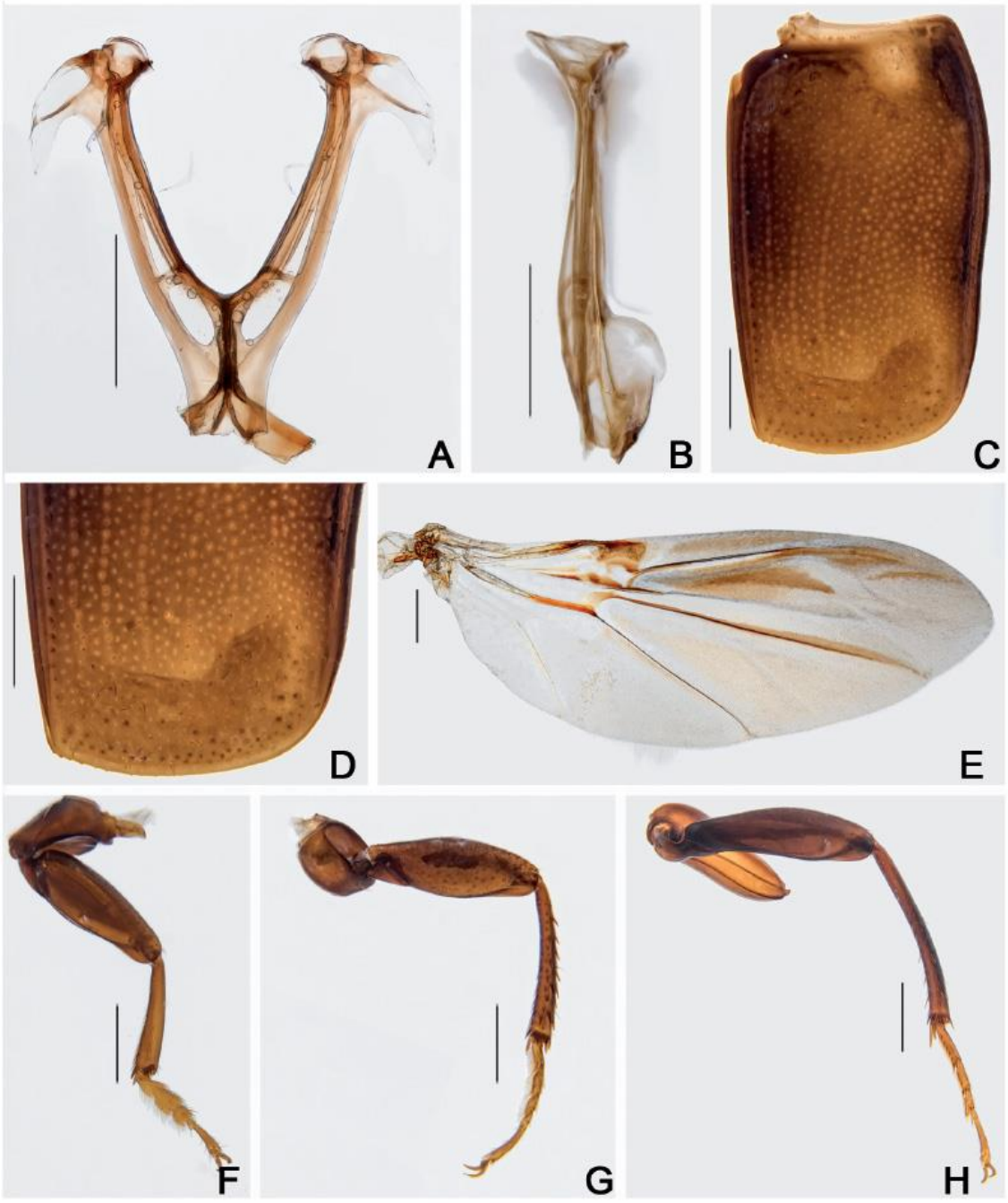

Fig. 42. *Cyparium pici* sp. nov., paratype, ♂ (CELC). **A–B**. Metendosternite. **A**. Dorsal view. **B**. Lateral view. **C–D**. Elytron. **C**. Entire. **D**. Apex. **E**. Hind wing. **F–H**. Legs. **F**. Fore. **G**. Middle. **H**. Hind. Specimen collected at Cotriguaçu (MT, Brazil). Scale bars = 0.5 mm.

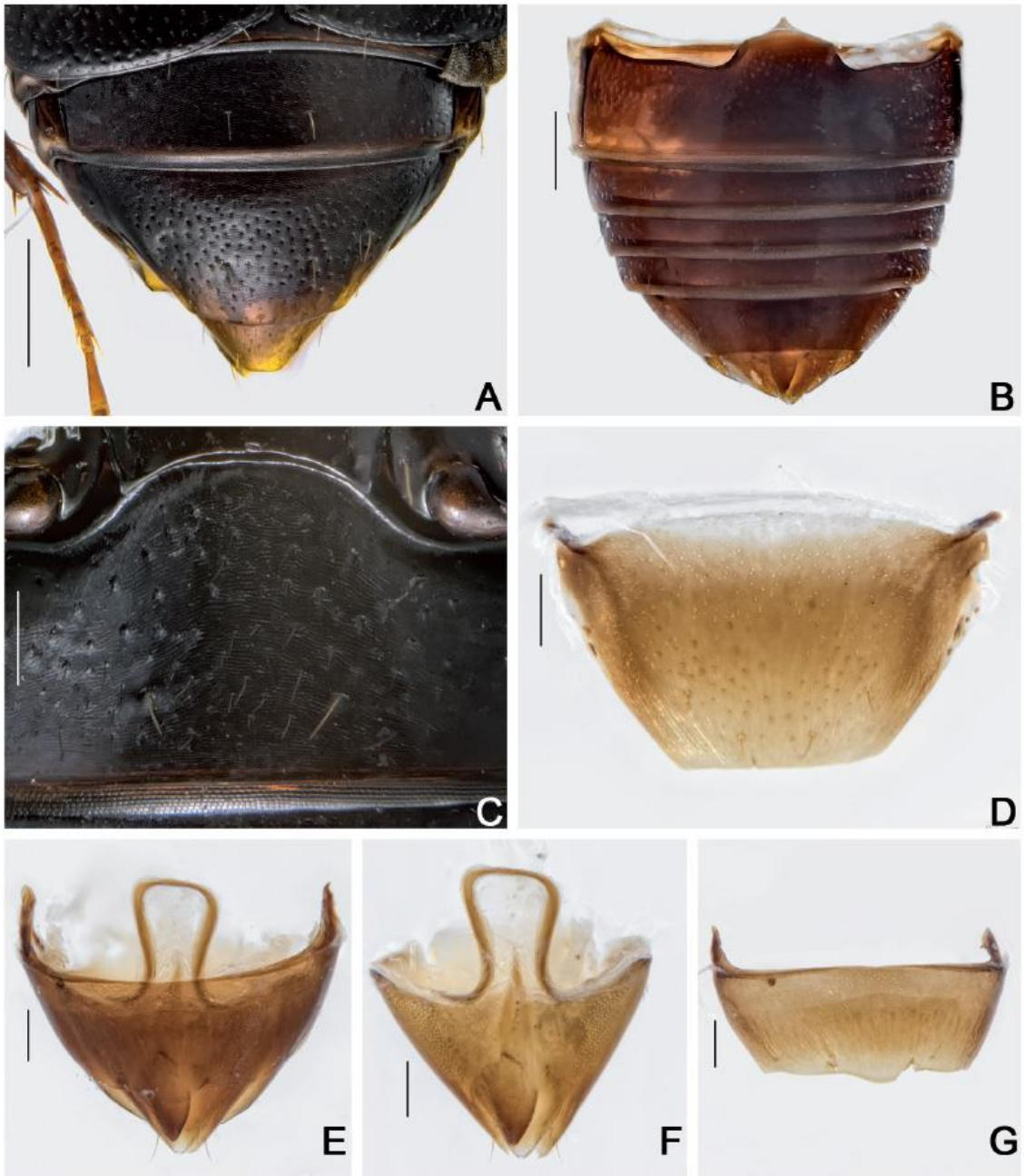

Fig. 43. *Cyparium pici* sp. nov. **A, C**. Holotype, ♂ (CEMT). **A**. Abdomen, dorsal view. **B**. Paratype, ♂ (CEMT), abdomen, ventral view. **C**. Ventrite 1. **D–G**. Paratype, ♂ (CELC). **D**. Tergite VIII. **E**. Terminalia. **F**. Tergite IX. **G**. Sternite VIII. Specimens collected at Cotriguaçu (MT, Brazil). Scale bars: A–B = 0.5 mm; C–G = 0.1.

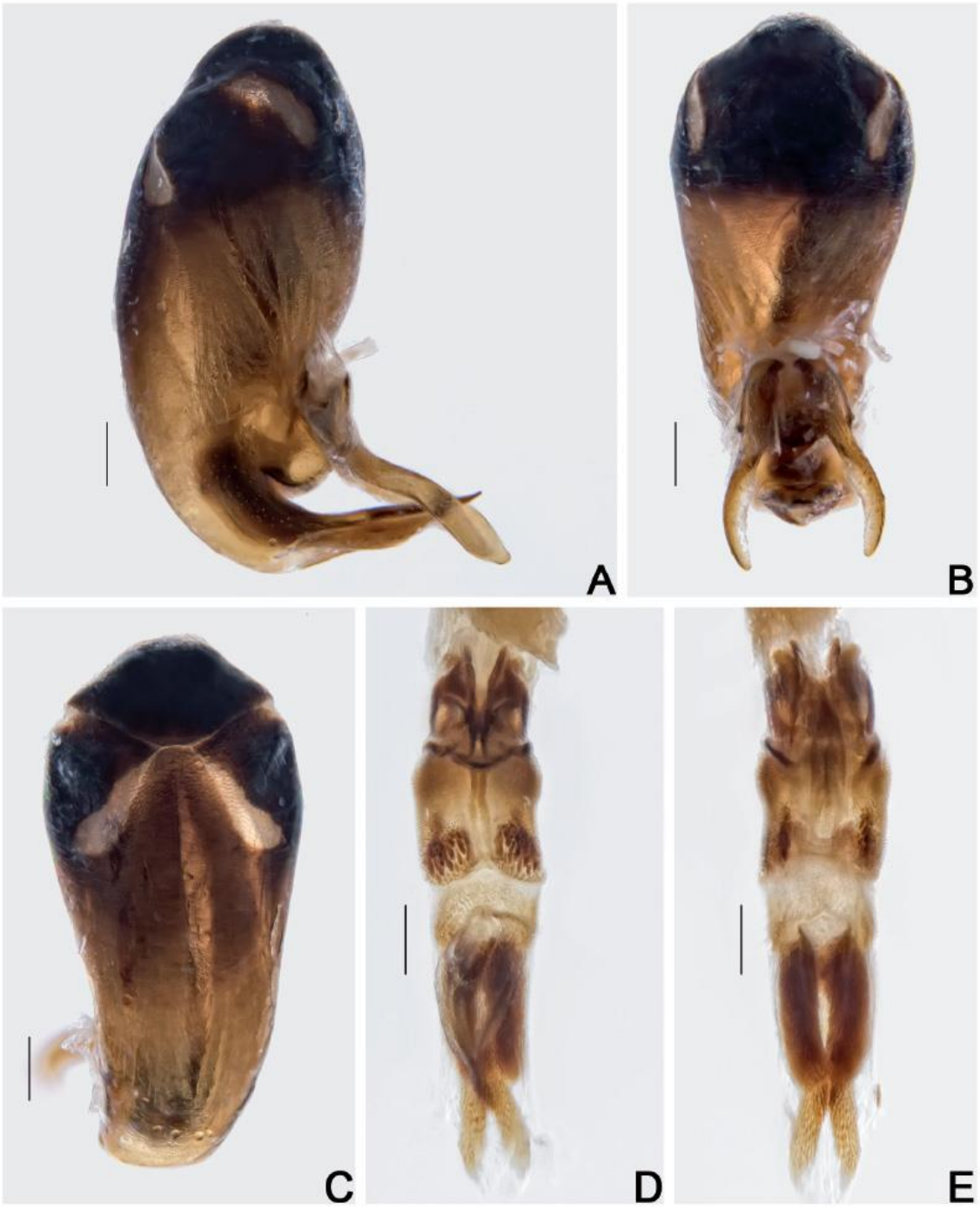

Fig. 44. *Cyparium pici* sp. nov., paratype, ♂ (CELC). **A**–**C**. Aedeagus. **A**. Lateral view. **B**. Frontal view. **C**. Dorsal view. **D**–**E**. Internal sac. **D**. Frontal view. **E**. Dorsal view. Specimen collected at Cotriguaçu (MT, Brazil). Scale bars = 0.2 mm.

Fig. 45. *Cyparium pici* sp. nov., paratype, ♀ (CELC). **A**. Tergite VIII. **B**. Sternite VIII. **C**. Terminalia. **D**. Sclerite of vaginal plate. **E**. Ovipositor. Specimen collected at Cotriguaçu (MT, Brazil). Scale bars = 0.1 mm.

Males

MEASUREMENTS (n = 1, paratype; in mm). Antennomeres (length(width)): 0.24(0.08), 0.14(0.07), 0.14(0.06), 0.11(0.06), 0.11(0.07), 0.08(0.09), 0.13(0.16), 0.12(0.18), 0.11(0.19), 0.11(0.20), 0.20(0.22); (n = 10, including the holotype, unless otherwise specified; in mm): TL 3.35–4.20 (mean = 3.75, standard deviation ± 0.32), PL 1.30–1.64 (1.45 ± 0.13), PA 1.07–1.32 (1.16 ± 0.07), PB 2.15–2.62 (2.36 ± 0.17), SL (n = 8) 0.13–0.23 (0.17 ± 0.03), SW (n = 8) 0.13–0.23 (0.18 ± 0.03), EI 1.85–2.28 (2.06 ± 0.15), EL (n = 9) 2.37–2.75 (2.60 ± 0.13), EW 1.37–1.65 (1.49 ± 0.08), EH 0.75–1.15 (0.96 ± 0.11), HW (n = 9) 0.91–1.08 (0.99 ± 0.06), IS (n = 9) 0.26–0.31 (0.28 ± 0.02), WA (n = 9) 0.21–0.30 (0.24 ± 0.03), MC 0.93–1.10 (1.03 ± 0.05), MB 0.37–0.50 (0.45 ± 0.04), VL 0.62–0.78 (0.70 ± 0.04).

Pro- and mesotarsomeres I–III enlarged, with tenet setae (Fig. 42F–G). Tergite VIII trapezoidal, straight posteriorly; triangular in some dry paratypes (Fig. 43D). Tergite IX with laterally curved ventral struts (Fig. 43E–F). Sternite VIII sub-rectangular, with a smooth projection (Fig. 43G). Sternite IX thick (Fig. 43F). Aedeagus strongly sclerotized, apex of median lobe short; openings in dorsal view moderately narrow, forming an acute angle, almost right (Fig. 44A–C); internal sac with strong and robust irregular sclerites (Fig. 44D–E), parameres short (Fig. 44A).

Females

MEASUREMENTS (n = 1, paratype; in mm). Antennomeres (length(width)): 0.25(0.09), 0.15(0.07), 0.15(0.06), 0.11(0.07), 0.10(0.08), 0.08(0.09), 0.13(0.15), 0.13(0.20), 0.11(0.22), 0.11(0.24), 0.19(0.26); (n = 6, paratypes; in mm): TL 4.20–4.35 (mean = 4.26 , standard deviation ± 0.06), PL 1.38–1.70 (1.62 ± 0.12),

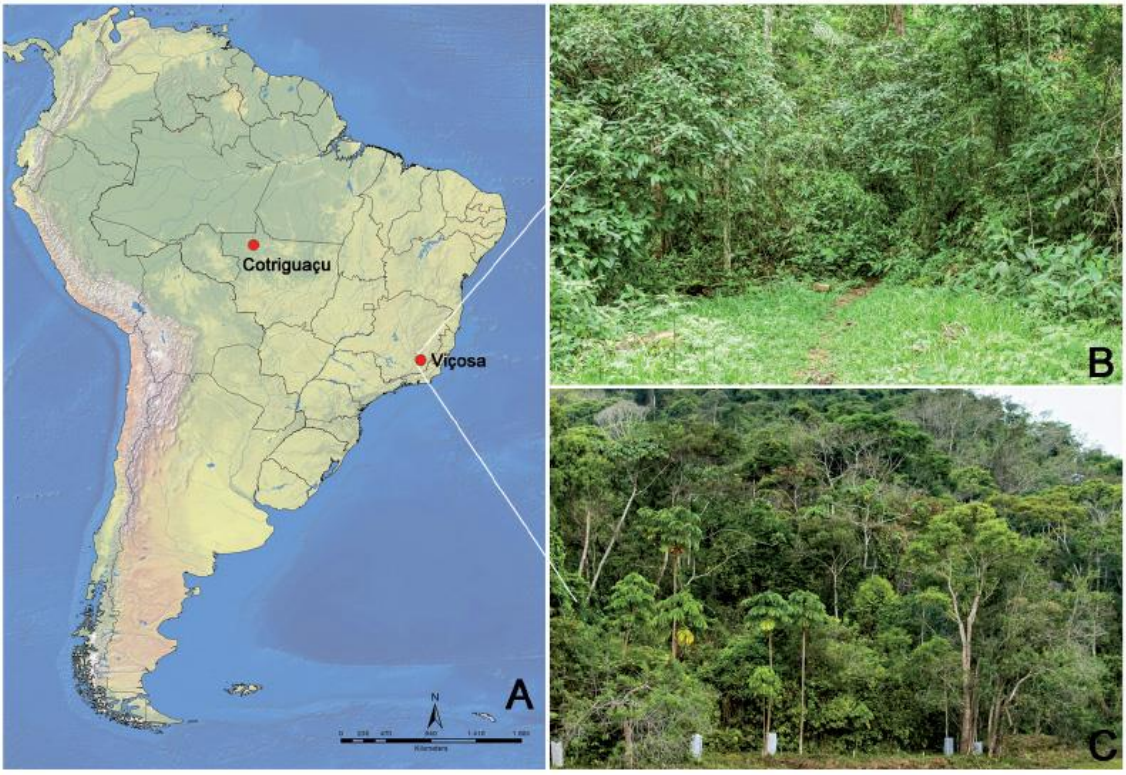

Fig. 46. A. Distribution map of species of *Cyparium* Erichson, 1845, South America. **B**. Mata da Biologia. **C**. Mata do Paraíso.

PA 1.22–1.35 (1.28 ± 0.05), PB 2.56–2.68 (2.62 ± 0.05), SL 0.15–0.25 (0.21 ± 0.03), SW 0.19–0.25 (0.22 ± 0.02), EI 2.25–2.47 (2.34 ± 0.10), EL 2.71–2.96 (2.79 ± 0.09), EW 1.62–1.80 (1.72 ± 0.06), EH 1.00–1.20 (1.10 ± 0.07), HW 1.05–1.15 (1.08 ± 0.03), IS 0.28–0.33 (0.31 ± 0.02), WA 0.22–0.28 (0.25 ± 0.02), MC 1.18–1.34 (1.26 ± 0.05), MB 0.56–0.62 (0.59 ± 0.03), VL 0.75–0.93 (0.85 ± 0.06).

Tergite VIII hexagonal (Fig. 45A), trapezoidal in dry specimens. Sternite VIII rectangular with a projection (Fig. 45B). Vagina and bursa copulatrix membranous; vagina without sclerites; bursa copulatrix with irregular sclerites (Fig. 45C). Vaginal plate with an apical M-shaped sclerite (Fig. 45D). Spermatheca not detected. Distal gonocoxites short, straight and thick; gonostyli somewhat thick, parallel (Fig. 45C–E).

Remarks

Similar in body length to *Cyparium rufohumerale*, but differs in the yellowish antennae (bicolored in *C. rufohumerale*) and in the comparatively larger reddish brown mark on the elytra (only at the humeral region in *C. rufohumerale*). Also similar to *C. humerale* in body length and the entirely yellow antennae, but differs in the non-triangular mark on the elytra and in the shorter elytra.

Distribution

Known only from Cotriguaçu, Faz. São Nicolau (09°50′19″ S, 58°15′15″ W), state of Mato Grosso, Midwest, Brazil (Fig. 46).

Redescriptions and new records

Cyparium collare Pic, 1920
Figs 4, 47–55; Supp. file 2B, Supp. file 3 (Figs 1A–4H)

Cyparium collare Pic, 1920a: 4. Syntypes: Muséum national d'histoire naturelle (MNHN), Paris, France.

Material examined

BRAZIL – **Sergipe** • 3 ♂♂; Sta Luzia do Itanhi, Faz. Crasto; 9–12 Sep. 1999; A. Bonaldo leg.; MCN 166400 (abdomen dissected), 166404, 166405 • 3 ♀♀; same collection data as for preceding; MCN 166398, 166401, 167484 • 2 ♂♂; Areia Branca, Est. Ecol. Serra de Itabaiana; 14–20 Sep. 1999; A. Bonaldo leg.; MCN 166402, 166403 (abdomen dissected, preserved in glycerin) • 1 ♀; same collection data as for preceding; MCN 166406. – **Minas Gerais** • 1 ♂; Viçosa, EPTEA Mata do Paraíso; 8 Dec. 2014; I. Pecci-Maddalena leg.; CELC • 3 ♂♂, 5 ♀♀ (1 ♀, abdomen dissected, preserved in glycerin); same collection data as for preceding; 6 Dec. 2018; LabCol leg; CELC • 7 ♂♂, 3 ♀♀ (1 ♀ entirely dissected, preserved in glycerin; 1 ♂, 1 ♀, abdomen dissected, preserved in glycerin); same collection data as for preceding; 5 Nov. 2019; LabCol leg.; "Fungo 02 \\ Em *Pleurotus pulmonarius*"; CELC • 1 ♀; same collection data as for preceding; "Fungo 03 \\ Em *Mycena* sp."; CELC • 14 ♂♂, 4 ♀♀ (1 ♂, 1 ♀ entirely dissected, preserved in glycerin; 1 ♂, 1 ♀, abdomen dissected, preserved in glycerin); same collection data as for preceding; "Fungo 01 \\ Em *Xerocomus* aff. *brasiliensis*"; CELC • 9 ♂♂, 3 ♀♀ (3 ♂♂ entirely dissected, preserved in glycerin); same collection data as for preceding; 7 Nov. 2019; LabCol leg.; "Fungo 17"; CELC • 1 ♂; same collection data as for preceding; "Fungo 14 \\ Em *Leucoagaricus rubrotinctus*"; CELC • 1 ♂, 1 ♀; same collection data as for preceding; "Fungo sem id"; CELC • 1 ♀; same collection data as for preceding; "Fungo A21 \\ Fotos: 712-713; 728-729, Em *Heimiomyces neovelutipes*"; CELC • 1 ♀; same collection data as for preceding; "Fungo Que"; CELC • 1 ♂, 2 ♀♀; same collection data as for preceding; 12 Nov. 2019; LabCol leg.; "Fungo 09"; CELC • 2 ♀♀ (1 ♀, abdomen dissected, preserved in glycerin); same collection data as for preceding; 13 Nov. 2019; LabCol leg.; "Fungo 18 \\ Em *Macrolepiota colombiana*"; CELC • 1 ♂; same collection data as for preceding; 14 Nov. 2019; "Fungo 22 \\ Em *Marasmiellus* sp."; CELC • 1 ♂; same collection data as for preceding; 19 Nov. 2019; "Fungo 18; Em *Marasmiellus cubensis*"; CELC • 1 ♀; same collection data as for preceding; "Fungo 16 \\ Em *Marasmiellus* sp."; CELC • 1 ♀; same collection data as for preceding; "Fungo 22 \\

Em *Leucoprinus ianthinus*"; CELC • 1 ♂, 2 ♀♀; same collection data as for preceding; "Fungo 13 \\ Em *Marasmiellus cubensis*"; CELC • 2 ♀♀; same collection data as for preceding; "Fungo 05 \\ Em *Marasmius* sp."; CELC • 2 ♀♀; same collection data as for preceding; "Fungo 24 \\ Em *Marasmiellus cubensis*"; CELC • 1 ♀; same collection data as for preceding; 21 Nov. 2019; LabCol leg.; "Fungo 38 \\ Em *Marasmiellus* sp."; CELC • 1 ♀; same collection data as for preceding; "Fungo 06 \\ Em *Agaricus dulcidulus* e *Leucocoprinus brebissoni*"; CELC • 5 ♂♂, 2 ♀♀ (1 ♂, abdomen dissected, preserved in glycerin); same collection data as for preceding; "Fungo 26 \\ Em *Lulesia lignicola*"; CELC • 2 ♀♀; same collection data as for preceding; "Fungo 16 \\ Em *Marasmius araucariae*"; CELC • 2 ♂♂, 3 ♀♀ (1 ♀, abdomen dissected, preserved in glycerin); same collection data as for preceding; "Fungo 12 \\ Em *Marasmiellus* aff. *ramealis*"; CELC • 1 ♀; same collection data as for preceding; "Fungo 52 \\ Em *Marasmiellus* sp."; CELC • 2 ♂♂, 1 ♀; same collection data as for preceding; "Fungo 41 \\ Em *Lepiota* sp."; CELC • 2 ♂♂; same collection data as for preceding; 26 Nov. 2019; LabCol leg.; "Fungo 23 \\ Em *Marasmiellus cubensis*"; CELC • 1 ♂; same collection data as for preceding; "Fungo 18 \\ Em *Entoloma* (*Inocephalus*) sp."; CELC • 2 ♀♀ (1 ♀, abdomen dissected, preserved in glycerin); same collection data as for preceding; "Fungo 46 \\ Em *Volvariella* sp."; CELC • 1 ♂, 1 ♀; same collection data as for preceding; "Fungo 24 \\ Em *Marasmius* sp."; CELC • 1 ♀; same collection data as for preceding; "Fungo 19 \\ *Pleteus* sp."; CELC • 1 ♂; same collection data as for preceding; "Fungo 37 \\ *Conocybe* sp."; CELC • 1 ♂; same collection data as for preceding; "Fungo 26 \\ Em *Leucocoprinus* sp."; CELC • 3 ♂♂; same collection data as for preceding; "Fungo 17"; CELC • 1 ♀; same collection data as for preceding; "Fungo 39 \\ Em *Marasmius hematocephalus*"; CELC • 2 ♂, 1 ♀ (1 ♂ entirely dissected, preserved in glycerin); same collection data as for preceding; 28 Nov. 2019; LabCol leg.; "fotos 1103-05 \\ Em *Marasmius* sp."; CELC • 1 ♂; same collection data as for preceding, "Trilha dos Gigantes"; 3 Feb. 2019; LabCol leg.; CELC • 1 ♀; Viçosa, Mata da Biologia; 3 May 2014; S. Aloquio leg.; "\\ ex. *Lepiota* sp."; CELC • 2 ♂♂, 2 ♀♀; Viçosa, Recanto das Cigarras, Mata da Biol.; 13 Nov. 2019; LabCol leg; "Fungo 11 \\ Em *Coprinellus disseminatus*"; CELC • 1 ♂; Viçosa, Mata da Biologia; 15 Oct. 2021; E. von Groll and A. Orsetti leg.; "Fungo 06"; CELC • 1 ♂, 1 ♀; same collection data as for preceding; "Fungo 26 \\ Em *Leucocoprinus cepistipes*"; CELC • 1 ♂, 1 ♀; same collection data as for preceding; 23 Nov. 2021; E. von Groll and G.L.N. Martins leg.; "\\ Em *Favolus tenuiculus*"; CELC • 8 ♂♂, 1 ♀; same collection data as for preceding; 26 Nov. 2021; "\\ Em *Favolus tenuiculus*"; CELC.

Diagnosis

TL: 2.60–3.40 mm in males and 2.56–3.52 mm in females. Pronotum reddish brown, elytra black (Fig. 47A). Eyes remarkably wider than head, rounded (Fig. 48A). Antennomere XI hexagonal, longish (Fig. 48B–C). Hypomeron only laterally with imbricate microsculpture. Metaventrite smooth, but laterally with imbricate microsculpture. Tergite VIII of males coarsely punctate (Fig. 52D). Rounded ventral struts (Fig. 52F). Aedeagus with short apex; openings in dorsal view thin, forming a wide acute angle; parameres short (Fig. 53A–C). Distal gonocoxites curved and thick (Fig. 54E).

Redescription

Coloration. Iridescent**.** Frons ochre, reddish brown; clypeus yellowish to ochre; mouthparts yellow-brown (Fig. 48A, Supp. file 3 (Figs 1D, 3D)); antennomeres I–VI and apex of XI yellow-brown; VII–X and basal part of XI darker (Fig. 48B). Pronotum and hypomeron reddish brown (Fig. 47A–B, Supp. file 3 (Figs 1E, 3E)). Scutellum reddish brown or black (Fig. 49D). Elytra black (Fig. 47A); epipleuron dark ochre. Mesanepisternum, metanepisternum and metepimeron dark ochre. Metaventrite dark brown, lighter laterally (Fig. 47B). Coxae and trochanters dark ochre; femora yellowish brown, apex yellow; tibiae and tarsi ochre (Fig. 47B–C). Tergite VI and VII black; tergite VIII yellow. Ventrites 1–4 dark brown; 5 and 6 yellow. Teneral specimens entirely light brown (Fig. 47D–E) or with pronotum lighter (Fig. 47F).

HEAD. Punctation dense, fine (Fig. 48A). Eyes remarkably wider than head, rounded (Fig. 48A). Labrum transverse, lateral areas rounded, not well marked at apex; central margin slightly curved; sclerotized portion rounded; lateral setae slightly exceeding margins of labrum; almost without pores centrally (Fig. 48D). Mandibles smoothly curved, subapical serrations on left mandible conspicuous (Fig. 48E–F). Maxillae with palpomere II long and thin; palpomere III somewhat globose; galea densely pubescent and lacinia moderately pubescent (Fig. 48G). Mentum laterally rounded, curved apically (Fig. 49A). Setae of labial palpomere II not exceeding palpomere III; palpomere III longish, with short apical setae (Fig. 49A–B). Post gena microsculptured with close transversal lines; gular pores limited to region next to eyes and submentum; gula triangular, small (Fig. 49C). Antennae not reaching or surpassing mesanepisternum, regardless of sex; antennal club smoothly delimited; antennomere XI hexagonal, longish (Fig. 48B–C).

Fig. 47. *Cyparium collare* Pic, 1920. **A–C**. ♂ (CELC). **A**. Dorsal view. **B**. Ventral view. **C**. Lateral view. **D–F**. ♀ (CELC). **D**. Dorsal view. **E**. Lateral view. **F**. Dorsal view. Specimens collected at Mata do Paraíso (A–C) and Mata da Biologia (D–F), Viçosa (MG, Brazil). Scale bars = 1.0 mm.

PROTHORAX. Pronotum smooth, shining; punctation dense, fine; pubescence short, fine (Fig. 49D); transverse, sub-straight laterally, almost forming a right angle at posterior margin (Fig. 49E). Hypomeron laterally with imbricate microsculpture. Notosternal suture with an angle, outward directed (Fig. 49F). Profurca thin, short, not exceeding half of foramen (Fig. 49G). Prosternal process apically wavy (Fig. 50A).

MESOTHORAX. Mesonotum with prescutellar suture (= scutellar lines, Leschen & Löbl 2005) wavy (Fig. 50B). Scutellum rounded posteriorly (Fig. 50B). Anterior phragma thin and somewhat straight (Fig. 50C). Mesanepistenum with shallow imbricate microsculpture, inconspicuous in some. Procoxal rests triangular, straight posteriorly (Fig. 50D). Mesoventral and median lines strongly wavy; area between median and mesocoxal lines large (Fig. 50D). Mesoventral process curved, forming a well-marked ridge (Fig. 50E).

METATHORAX. Metanotum with triangular alacrista, turned to the sides; scutoscutellar suture inconspicuous; median membranous area narrow and long (Fig. 50F). Metaventrite smooth, but with imbricate microsculpture laterally; punctation sparse, fine. Mesocoxal line forming an angle between coxal cavities; finely punctate under coxal cavities (Fig. 50D). Metanepisternum and metepimeron with imbricate microsculpture. Intercoxal plates smooth. Metendosternite with curved arms; 'stalk ridge'

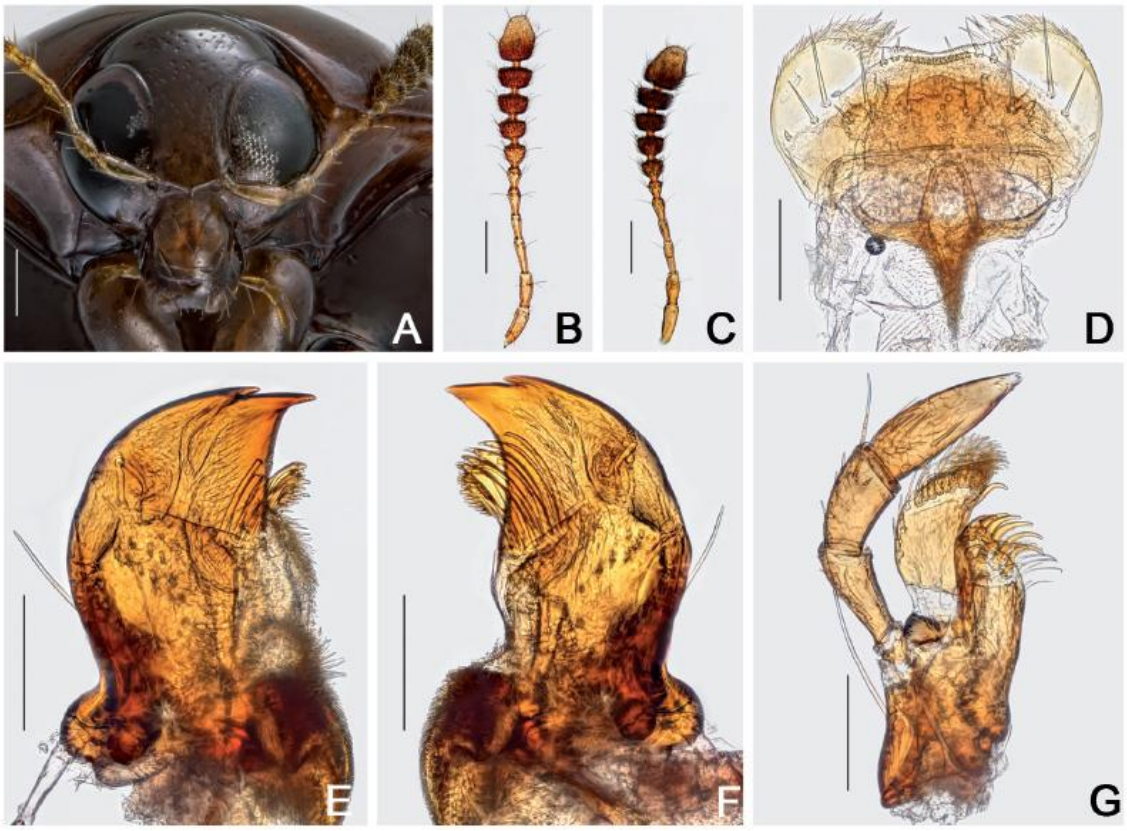

Fig. 48. *Cyparium collare* Pic, 1920. **A–B, D–G.** ♂ (CELC). **A**. Frontal view. **B**. Male antenna. **C**. Female antenna (CELC). **D**. Labrum. **E**. Left mandible. **F**. Rigth mandible. **G**. Maxilla. Specimens collected at Mata do Paraíso, Viçosa (MG, Brazil). Scale bars: A–C = 0.2 mm; D–G = 0.1 mm.

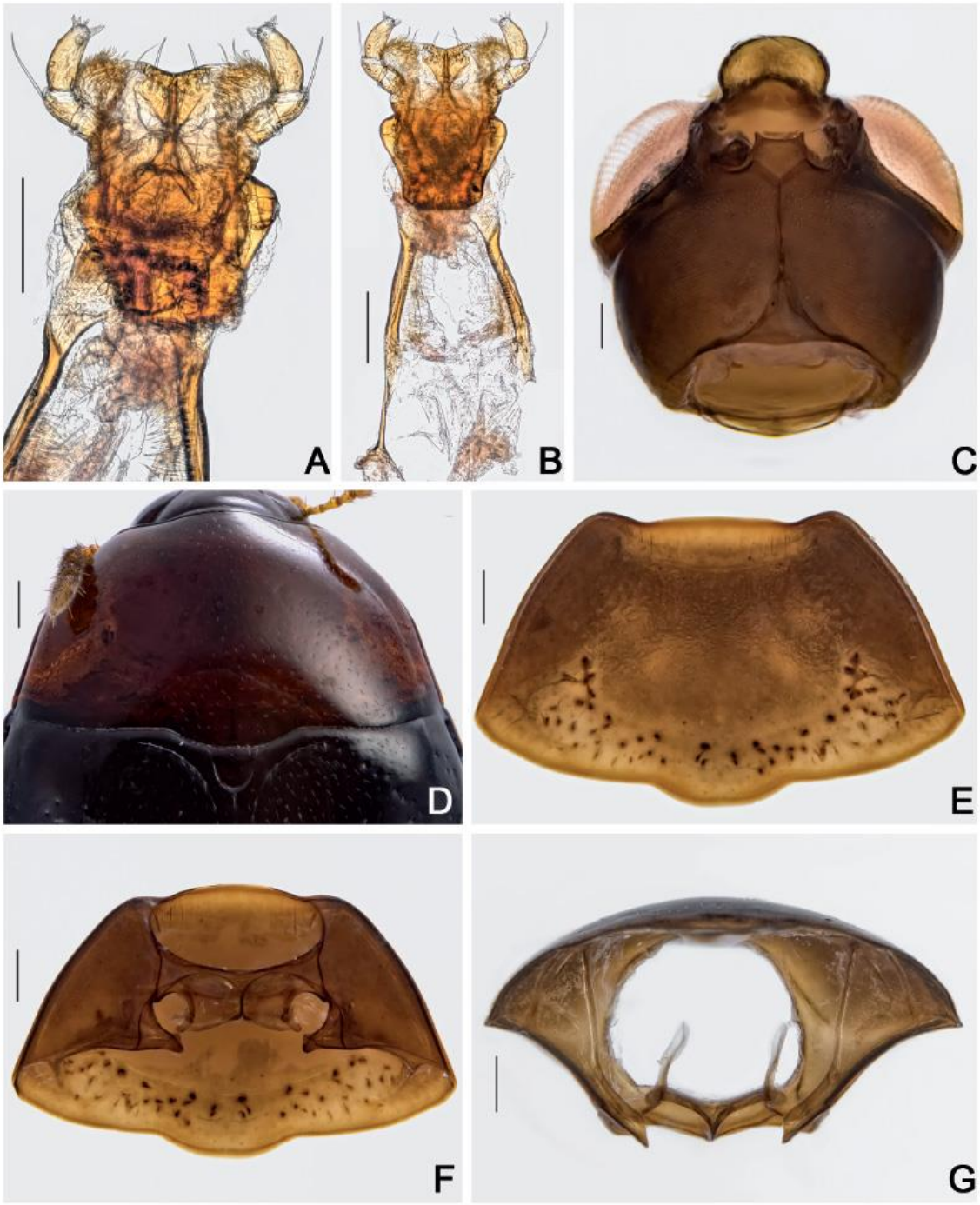

Fig. 49. *Cyparium collare* Pic, 1920, ♂♂ (CELC). **A**. Labium. **B**. Hypopharynx. **C**. Head, ventral view. **D**–**E**. Pronotum, dorsal view. **F**–**G**. Prothorax. **F**. Ventral view. **G**. Inner view. Specimens collected at Mata do Paraíso, Viçosa (MG, Brazil). Scale bars: A–C = 0.1 mm; D–G = 0.2 mm.

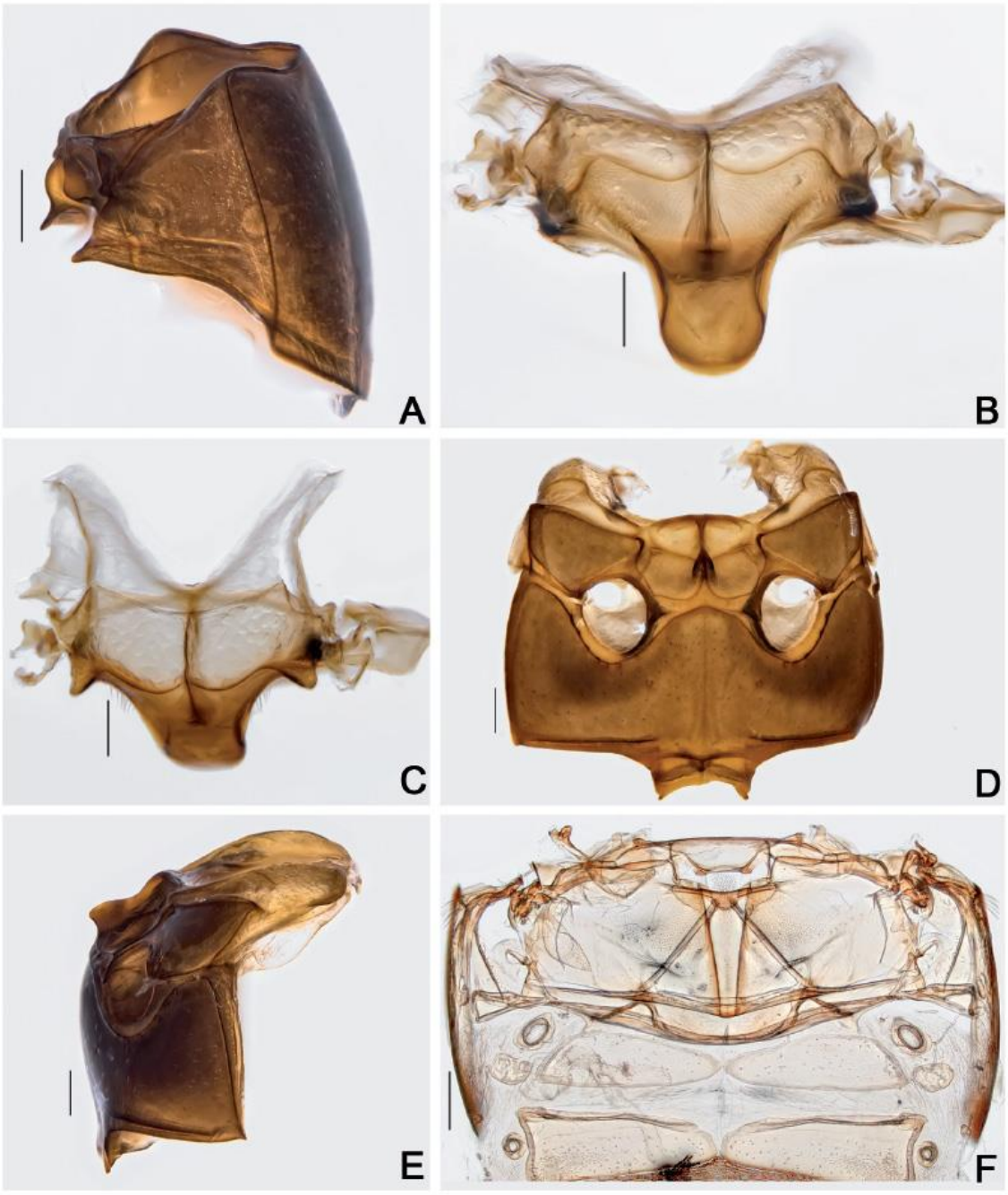

Fig. 50. *Cyparium collare* Pic, 1920, ♂ (CELC). **A**. Prothorax, lateral view. **B–C**. Scutellar plate. **B**. Dorsal view. **C**. Apically slanted view. **D–E**. Meso- and metathorax. **D**. Ventral view. **E**. Lateral view. **F**. Metanotum. Specimen collected at Mata do Paraíso, Viçosa (MG, Brazil). Scale bars: A, D–F = 0.2 mm; B–C = 0.1 mm.

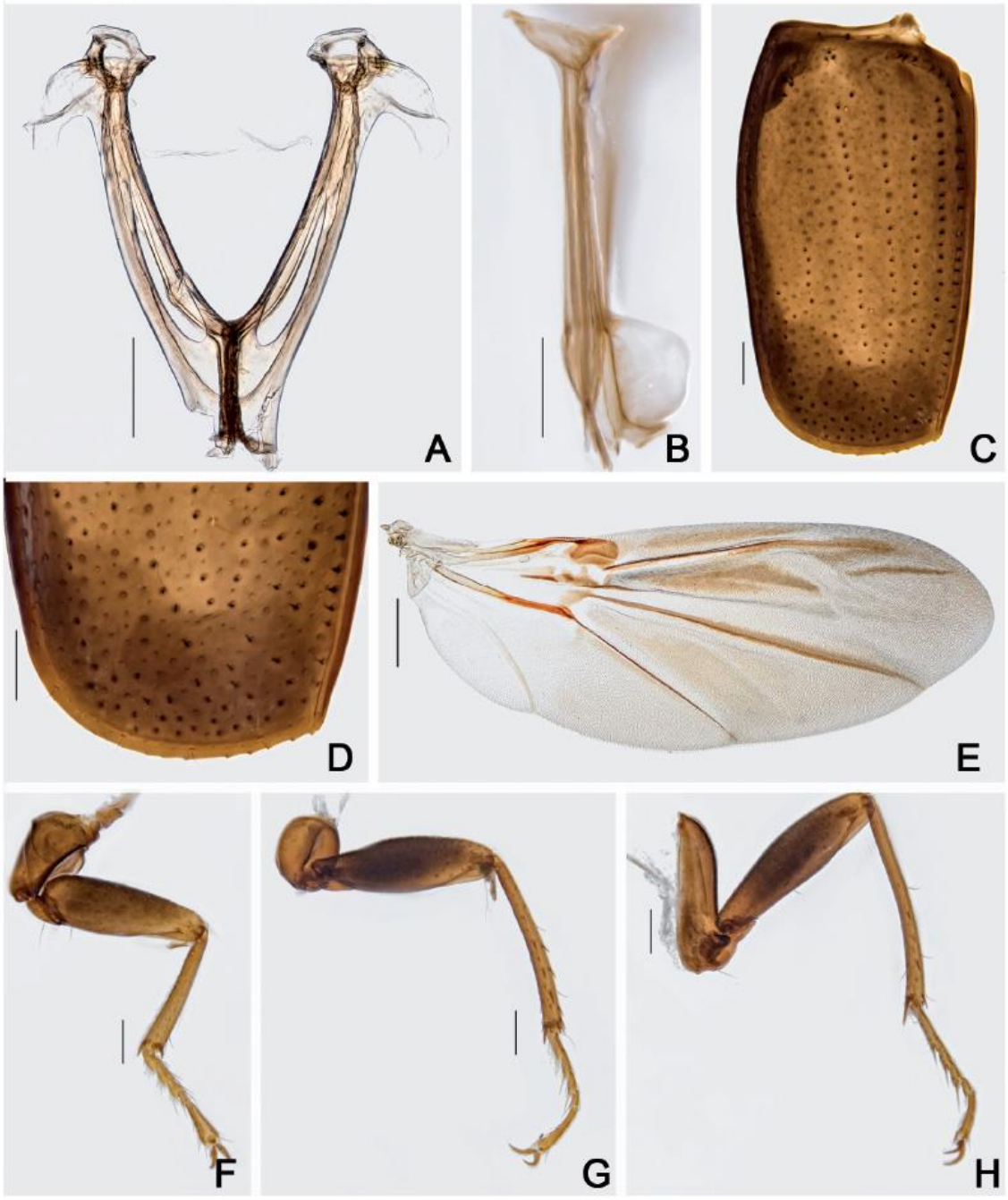

Fig. 51. *Cyparium collare* Pic, 1920, ♂ (CELC). **A–B**. Metendosternite. **A**. Dorsal view. **B**. Lateral view. **C–D**. Elytron. **C**. Entire. **D**. Apex. **E**. Hind wing. **F–H**. Legs. **F**. Fore. **G**. Middle. **H**. Hind. Specimen collected at Mata do Paraíso, Viçosa (MG, Brazil). Scale bars: A–D, F–H = 0.2 mm; E = 0.5 mm.

exceeding half length of stalk (Fig. 51A); ventral longitudinal flange wide and short in lateral view (Fig. 51B).

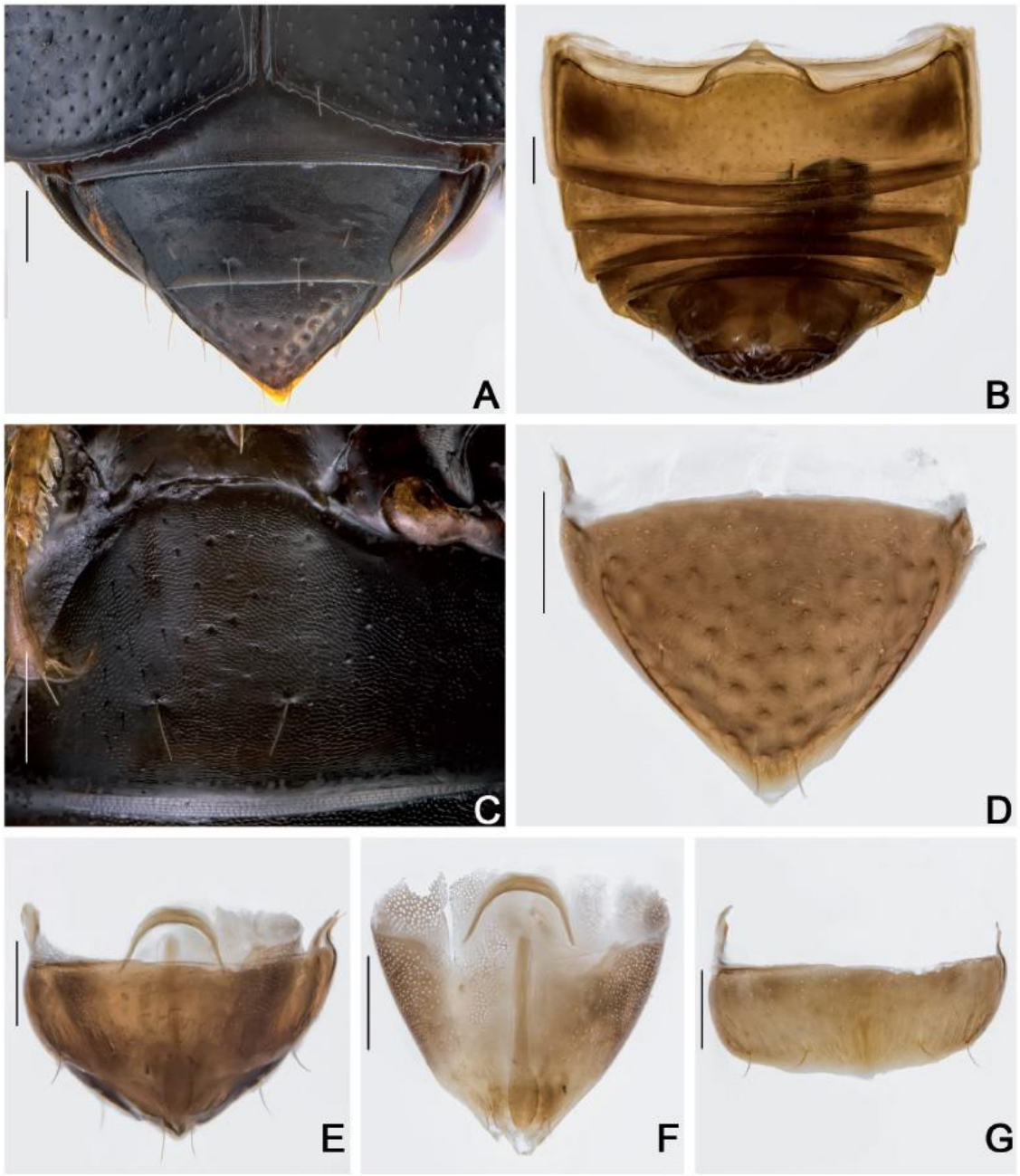

Fig. 52. *Cyparium collare* Pic, 1920, ♂♂ (CELC). **A**–**B**. Abdomen. **A**. Dorsal view. **B**. Ventral view. **C**. Ventrite 1. **D**. Tergite VIII. **E**. Terminalia. **F**. Tergite IX. **G**. Sternite VIII. Specimens collected at Mata do Paraíso, Viçosa (MG, Brazil). Scale bars = 0.2 mm.

Fig. 53. *Cyparium collare* Pic, 1920, ♂ (CELC). **A–C**. Aedeagus. **A**. Lateral view. **B**. Frontal view. **C**. Dorsal view. **D–E**. Internal sac. **D**. Frontal view. **E**. Dorsal view. Specimen collected at Mata do Paraíso, Viçosa (MG, Brazil). Scale bars = 0.1 mm.

Wings. Elytra slightly wider than long, partially covering tergite VI (Fig. 47A); basal (Fig. 49D) and sutural lines dashed and punctate; adsutural area with a row of setae, six rows of coarse punctures (not including sutural line) (Figs 47A, 51C); lateral lines punctate; apical coarse punctation dense; apical serrations moderately large, well visible (Fig. 51D); pubescence short, fine. Epipleuron with diffuse coarse punctures. Hind wings fully developed (Fig. 51E).

Legs. Pro-, meso- and metacoxae, and femora with strigulate microsculpture. Femora somewhat straight (Fig. 51F–H). Pro- and mesofemora sparsely and coarsely punctate; metafemora sparsely and finely punctate. Mesotibiae densely spinose, spines fine (Fig. 51G). Metatibiae sparsely spinose, spines fine (Fig. 51H).

Abdomen. Tergites VI–VIII with imbricate microsculpture; tergite VII trapezoidal; punctation sparse, fine; pubescence dense, fine (Fig. 52A). Ventrites 1–5 (Figs 52B, S5F) sparsely and coarsely punctate; pubescence sparse, fine; imbricate microsculpture anteriorly, and with strigulate microsculpture posteriorly (Fig. 52C). Metacoxal lines finely punctate.

Males

Measurements (n = 1; in mm). Antennomeres (length(width): 0.15(0.06), 0.13(0.05), 0.14(0.04), 0.09(0.04), 0.11(0.05), 0.08(0.06), 0.07(0.08), 0.07(0.11), 0.08(0.12), 0.08(0.13), 0.18(0.14); (n = 15, unless otherwise specified; in mm): TL 2.60–3.72 (mean = 3.16, standard deviation ± 0.34), PL 0.90–1.35 (1.12 ± 0.12), PA 0.75–1.00 (0.88 ± 0.07), PB 1.50–2.25 (1.90 ± 0.23), SL (n =14) 0.13–0.21 (0.16 ± 0.02), SW (n =14) 0.12–0.20 (0.16 ±0.02), EI 1.50–2.15 (1.84 ± 0.19), EL 1.77–2.55 (2.18 ± 0.23), EW 0.85–1.42 (1.12 ± 0.15), EH 0.30–0.95 (0.74 ± 0.20), HW 0.68–0.89 (0.79 ± 0.06), IS 0.15–0.25 (0.21 ± 0.02), WA 0.15–0.20 (0.18 ± 0.01), MC 0.70–1.15 (0.91 ± 0.12), MB 0.33–0.56 (0.44 ± 0.07), VL 0.46–0.75 (0.62 ± 0.08).

Pro- and mesotarsomeres I–III enlarged, with tenet setae (Fig. 51F–G). Tergite VIII triangular, acuminate posteriorly; punctation dense, coarse; subglabrous (Fig. 52A, D, Supp. file 3 (Figs 1F, 3G)). Tergite IX with rounded ventral struts (Fig. 52E–F, Supp. file 3 (Figs 1G, 4A–B)). Sternite VIII rectangular, short (Fig. 52G, Supp. file 3 (Figs 1H, 4C)). Sternite IX more or less spoon-like (Fig. 52F, Supp. file 3 (Figs 1G, 4B)). Aedeagus sclerotized enlarged at base, apex of median lobe short; openings in dorsal view thin, forming a very acute angle (Fig. 53A–C, Supp. file 3 (Figs 2A–C, 4D–F)); internal sac with irregular sclerites, crown-like (Fig. 53D–E, Supp. file 3 (Fig. 4G–H)); parameres short, curved and with denticular structures at base (Fig. 53A–B, Supp. file 3 (Figs 2A–B, 4D–E)).

Females

Measurements (n = 1; in mm). Antennomeres (length(width): 0.16(0.06), 0.12(0.06), 0.13(0.04), 0.08(0.04), 0.10(0.05), 0.06(0.06), 0.06(0.08), 0.08(0.10), 0.07(0.12), 0.08(0.14), 018(0.15); (n = 14, unless otherwise specified; in mm): TL 2.56–3.64 (mean = 3.15, standard deviation ± 0.30), PL 0.92–1.37 (1.14 ± 0.11), PA 0.77–1.02 (0.90 ± 0.06), PB 1.50–2.20 (1.92 ± 0.18), SL (n =12) 0.12–0.20 (0.16 ± 0.02), SW (n =12) 0.14–0.19 (0.16 ±0.01), EI (n =12) 1.52–2.12 (1.87 ± 0.16), EL (n =12) 1.85–2.52 (2.12 ± 0.19), EW 0.90–1.30 (1.14 ± 0.10), EH (n =12) 0.35–0.97 (0.75 ± 0.23), HW 0.65–0.88 (0.79 ± 0.02), IS 0.20–0.26 (0.22 ± 0.02), WA 0.15–0.22 (0.18 ± 0.02), MC (n =13) 0.72–1.06 (0.93 ± 0.09), MB 0.35–0.95 (0.49 ± 0.14), VL 0.52–0.77 (0.65 ± 0.07).

Tergite VIII triangular, rounded posteriorly; punctation dense, coarse; subglabrous (Fig. 54A). Sternite VIII rectangular with a sooth projection; with strigulate microsculpture (Fig. 54B). Vagina and bursa copulatrix membranous without sclerites; vaginal plate with an apical sclerite, more or less short; oviduct bilobed, each lobe bearing a filiform spermatheca (Fig. 54C–D, Supp. file 2B). Distal gonocoxites curved and thick; gonostyli long, slender (Fig. 54C, E).

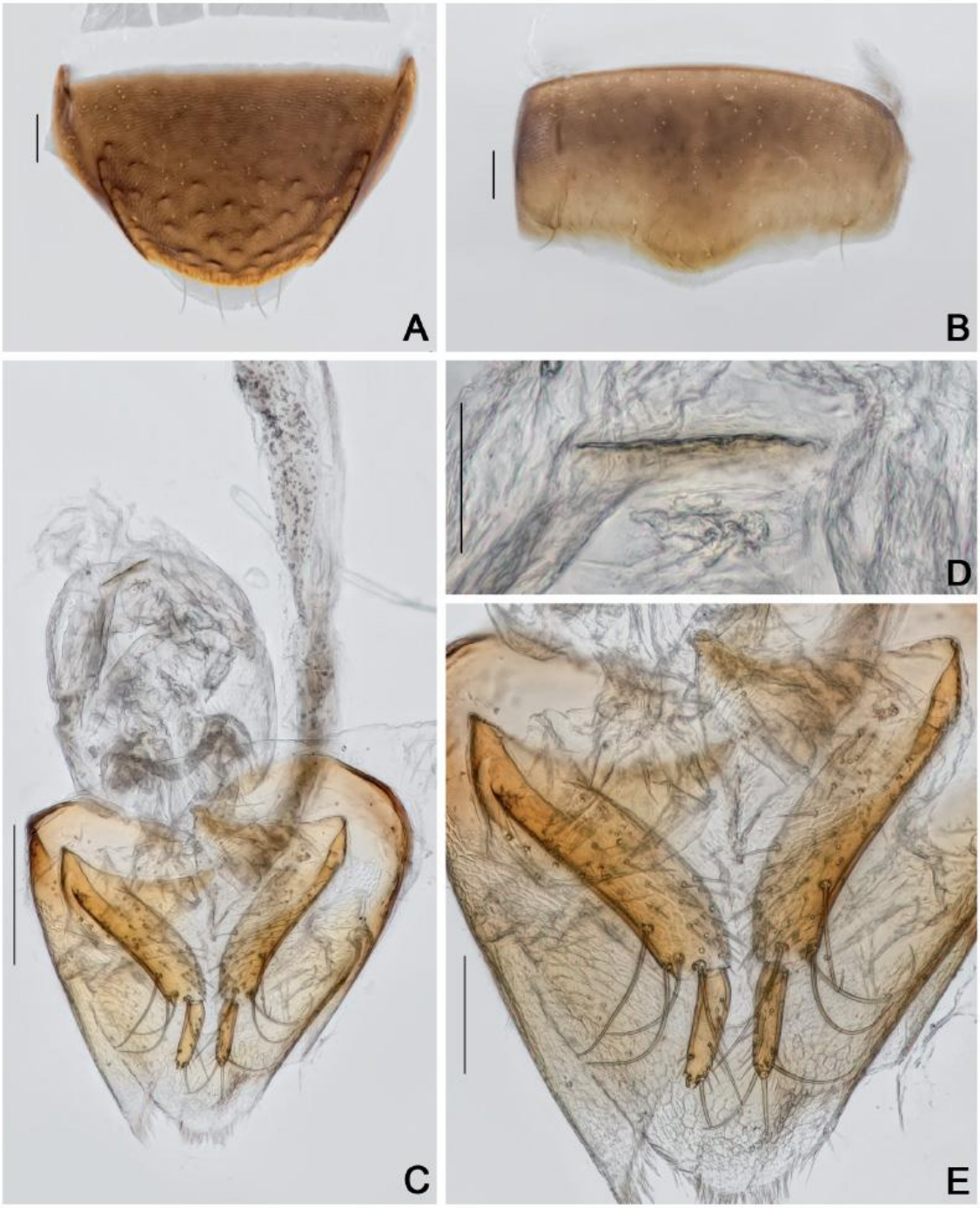

Fig. 54. *Cyparium collare* Pic, 1920, ♀ (CELC). **A**. Tergite VIII. **B**. Sternite VIII. **C**. Terminalia. **D**. Sclerite of vaginal plate. **E**. Ovipositor. Specimen collected at Mata do Paraíso, Viçosa (MG, Brazil). Scale bars: A–B, D–E = 0.1 mm; C = 0.2 mm.

Host fungi

Adults were collected from *Marasmiellus cubensis* (Berk. & M.A. Curtis) Singer (4 records, 8 individuals), *Marasmiellus* spp. (5, 6), *Marasmiellus* aff. *ramealis* (1, 5), cf. *Marasmiellus* sp. (yellow) (2, 5), cf. *Pleteus* sp. (1, 1), *Marasmius araucariae* Singer (1, 2), *Marasmius haematocephalus* (1, 1), *Leucocoprinus cepistipes* (1, 2), *Leucocoprinus ianthinus* (1, 1), *Leucoprinus* sp. (1, 1), *Inocybe* sp. (Agaricales, Inocybaceae) (1, 3), cf. *Valvariela* sp. (1, 2), *Leucoagaricus rubrotinctus* (Peck) Singer (1, 1), *Lepiota* sp. (Agaricales, Agaricaceae) (1, 3), *Macrolepiota colombiana* Franco-Mol. (Agaricales, Agaricaceae) (1, 2), *Heimiomyces neovelutipes* (Hongo) E.Horak (Agaricales, Mycenaceae) (1, 1), *Lulesia lignicola* B.E.Lechner & J.E.Wright (Agaricales) (1, 7), *Pleurotus pulmonarius* (Fr.) Quél. (Agaricales, Pleurotaceae) (2, 28), *Volvariella* sp. (Agaricales, Pleurotaceae) (1, 2), *Pluteus* sp. (Agaricales, Pleurotaceae) (1, 1), *Mycena* sp. (Agaricales, Mycenaceae) (1, 1), *Entoloma* (*Inocephalus*) sp. (1, 1), *Conocybe* sp. (Agaricales, Bolbitiaceae) (1, 1), *Coprinellus disseminatus* (Pers.) J.E.Lange (Agaricales, Psathyrellaceae) (1, 4), unidentified mushrooms (1, 18) and *Favolus tenuiculus* P.Beauv. (Polyporaceae, Polyporales).

Remarks

Images of the type series were requested from the MNHN, where these specimens were supposedly deposited (Löbl 2018a), but we were informed that they could not find any specimens. Nonetheless, we decided to treat the specimens that we examined as *C. collare* because their morphology and localities fit the original description and the known distribution of the species. Fourteen individuals of different body length and collected from different fungi at Viçosa, one from Areia Branca (SE) (Supp. file 3 (Figs 1–2)), and another one from Sta Luzia do Itanhi (SE) (Supp. file 3 (Figs 3–4)) were dissected. No differences were found in the terminalia, including the flagellum. Furthermore, no external differences were observed. The total body length is quite variable (2.60–3.72 mm). The three individuals from Areia Branca (SE) are the largest (3.64, 3.68 and 3.72 mm), while individuals collected at Viçosa (MG) and Sta Luzia do Itanhi (SE) are in the same size range (2.56–3.52 mm).

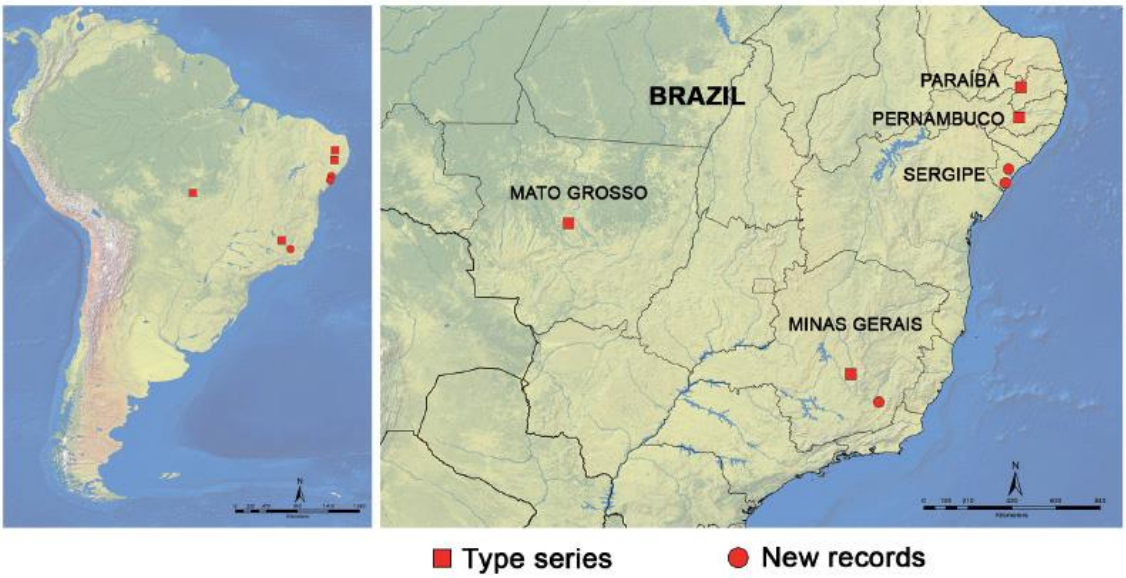

Fig. 55. *Cyparium collare* Pic, 1920, distribution. Squares = literature; circles = new records.

Distribution

Known from Brazil ["Matu Sinhos, Minas"; "Matto Grosso"; "Pery-Pery, Pernambuco"; "right bank of Parahyba"]. New records from Areia Branca and Santa Luzia do Itanhi, state of Sergipe, Northeast, Brazil, and from "Mata da Biologia" and "EPTEA Mata do Paraíso", campus of the Universidade Federal de Viçosa, Viçosa, Minas Gerais, Southeast Brazil (Fig. 55).

Cyparium oberthueri Pic, 1956
Figs 5, 56–64

Cyparium oberthüri Pic, 1956: 175. Syntypes: Muséum national d'histoire naturelle (MNHN), Paris, France.

Material examined

BRAZIL – **Minas Gerais** • 1 ♀; Viçosa, Mata da Biologia; 26 Oct. 2016; A. Orsetti and I. Pecci-Maddalena leg.; CELC • 7 ♂♂, 3 ♀♀ (2 ♂♂, entirely dissected, preserved in glycerin; 2 ♂♂, 1 ♀, abdomen dissected, preserved in glycerin); same collection data as for preceding; 26 Jun. 2019; von Groll and A. Orsetti leg.; CELC • 1 ♂, 2 ♀♀; Viçosa, EPTEA Mata do Paraíso; 9 Nov. 2016; I. Pecci-Maddalena and C. Lopes-Andrade leg.; "\\ ex *Psathyrella candolleana*"; CELC • 1 ♂; same collection data as for preceding; 12 Nov. 2019; LabCol leg; CELC.

Diagnosis

TL: 4.43–5.12 mm in males and 4.68–5.25 mm in females. Black (Figs 56A–C, 64A). Hypomeron with close strigulate microsculpture. Scutellum tapered posteriorly (Fig. 59B). Mesanepisternum long with imbricate microsculpture. Metaventrite smooth (Fig. 56B). Intercoxal plates with long imbricate microsculpture. Aedeagus poorly sclerotized, almost membranous, apex very long; parameres L-shaped, very long (Fig. 62A–D). Distal gonocoxites curved and tapered (Fig. 63C, E).

Redescription

Coloration. Black, iridescent (Figs 56A–C, 64A). Frons dark brown; clypeus light brown (Fig. 57A); mouth parts and antennomeres I–VI and apex of XI testaceous; antennomeres VII–X and base of XI dark (Fig. 57B). Coxae and femora dark-brown reddish; tibiae lighter; tarsi and tergite VIII yellow; ventrites 5 and 6 brown. Variation: specimens entirely light brown to brown (Fig. 56D–F).

Head. Punctation dense, fine (Fig. 57A); vertex with strigulate microsculpture. Eyes slightly wider than head, rounded apically (Fig. 57A). Labrum rectangular, lateral margins rounded, and well distinct from apical margin; posterior margin slightly curved centrally; sclerotized portion curved; lateral setae slightly exceeding margins; porose centrally (Fig. 57D). Mandibles curved, subapical serrations on left mandible conspicuous (Fig. 57E–F). Maxillary palps elongated, palpomere III tapering smoothly; galea and lacinia densely pubescent, lacinia robust (Fig. 57G). Mentum with lateral areas rounded and apex not well delimited; glossa concave (Fig. 58A). Setae of labial palpomere II exceeding palpomere III; palpomere III longish, with long apical setae (Fig. 58A). Hypopharynx with wide and rounded sclerotized plate (Fig. 58A–B). Post gena microsculptured with very close transversal lines; densely porose all over; gula triangular with concave lateral areas (Fig. 58C). Base of antennae long, antennal club distinct; antennomere XI hexagonal (Fig. 57B–C), no difference between males and females.

Prothorax. Pronotum smooth, densely and coarsely punctate; pubescence short, fine (Fig. 58D–E); transverse and slightly curved laterally, forming an obtuse angle at lateral areas of posterior margin (Fig. 58E). Hypomeron with close strigulate microsculpture. Notosternal suture straight and slightly

turned to lateral areas (Fig. 58F). Profurca elongated, extending half length of foramen (Fig. 58G). Prosternal process short and curved (Fig. 59A).

Mesothorax. Mesonotum with prescutellar suture (= scutellar lines, Leschen & Löbl 2005) wavy (Fig. 59B). Scutellum tapered posteriorly (Fig. 59B). Anterior phragma large and straight (Fig. 59C). Mesanepisternum with long imbricate microsculpture. Procoxal rests sub-squared, somewhat rounded posteriorly (Fig. 59D). Mesoventral and median lines somewhat wavy; area between median and mesoventral lines somewhat enlarged (Fig. 59D). Mesoventral process moderately short, with apex more prominent, forming a ridge (Fig. 59E).

Metathorax. Metanotum with alacrista triangular, posterior portion longish; turned just slightly to posterior end; scutoscutellar suture long and wavy (Fig. 59F). Metaventrite smooth; punctuation sparse, fine (Figs 56B, E, 59D). Mesocoxal line not forming an angle between coxal cavities, just a simple curve and finely punctate under coxal cavities (Fig. 59D). Metanepisternum and metepimeron with imbricate microsculpture. Intercoxal plates with long imbricate microsculpture. Metendosternite with arms close and somewhat straight; 'stalk ridge' not exceeding half length of stalk (Fig. 60A); ventral longitudinal flange longish and rounded in lateral view (Fig. 60B).

Wings. Elytra large, slightly wider than longer; covering tergite VI (Fig. 56A); basal (Fig. 58D) and sutural lines dashed; adsutural area with a row of setae; six rows of coarse punctures (not including sutural line) (Figs 56A, 60C); lateral line coarse punctate; apical coarse punctation dense; apical serrations small (Fig. 60D); pubescence short and fine. Epipleuron with a row of sparse and coarse punctures. Hind wings fully developed (Fig. 60E).

Legs. Pro-, meso- and metacoxae, and femora with strigulate microsculpture. Profemora fusiform; punctuation sparse, fine (Fig. 60F). Mesofemora longish; punctures sparse, coarse (Fig. 60G). Metafemora longish; punctuation sparse, fine (Fig. 60H). Mesotibiae densely spinose; spines thick (Fig. 60G); metatibia sparsely spinose, spines fine (Fig. 60H).

Abdomen. Tergites VI–VIII with narrow imbricate microsculpture (Fig. 61A). Tergite VII trapezoidal when tergite VIII not exposed and triangular when exposed; punctation inconspicuous; pubescence sparse, fine. Ventrites 1–5 with strigulate microsculpture (Fig. 61B). Ventrite 1 densely and coarsely punctate; pubescence sparse, fine (Fig. 61C). Ventrites 2–5 densely and finely punctate; pubescence moderately sparse, fine. Metacoxal lines finely punctate.

Males

Measurements (n = 1, in mm). Antennomeres (length(width)): 0.33(0.10), 0.16(0.08), 0.21(0.08), 0.18(0.08), 0.19(0.09), 0.13(0.11), 0.15(0.17), 0.11(0.18), 0.12(0.21), 0.12(0.23), 0.23(0.25); (n = 8, unless otherwise specified; in mm): TL 4.43–5.12 (mean = 4.91, standard deviation ± 0.21), PL 1.68–2.00 (1.88 ± 0.09), PA 1.2–1.4 (1.34 ± 0.06), PB 2.72–3.16 (3.04 ± 0.14), SL 0.20–0.27 (0.24 ± 0.02), SW 0.21–0.28 (0.23 ± 0.02), EI 2.56–3.00 (2.85 ± 0.14), EL 2.96–3.56 (3.39 ± 0.19), EW 1.72–2.00 (1.90 ± 0.09), EH 1.00–1.25 (1.16 ± 0.08), HW 1.01–1.17 (1.13 ± 0.05), IS 0.30–0.37 (0.32 ± 0.02), WA 0.22–0.30 (0.26 ± 0.03), MC (n = 5) 1.36–1.44 (1.41 ± 0.03), MB (n = 6) 0.64–0.72 (0.68 ± 0.03), VL (n = 6) 0.80–0.96 (0.84 ± 0.06).

Pro- and mesotarsomeres I–III enlarged, with tenet setae (Fig. 60F–G). Tergite VIII pentagonal, slightly acuminate posteriorly; punctation sparse, fine; subglabrous (Fig. 61D). Tergite IX with rectangular ventral struts (Fig. 61E–F). Sternite VIII sub-rectangular, with a smooth projection (Fig. 61G). Sternite IX thick, centrally constricted (Fig. 61F). Aedeagus poorly sclerotized, almost membranous, apex of median lobe very long (Fig. 62A–C); internal sac with irregular sclerites, with a large hook (Fig. 62D–E); parameres L-shaped, very long (Fig. 62A).

Females

MEASUREMENTS (n = 1, in mm). Antennomeres (length(width)): 0.28(0.10), 0.15(0.08), 0.20(0.07), 0.17(0.07), 0.17(0.08), 0.12(0.10), 0.14(0.16), 0.13(0.18), 0.11(0.20), 0.11(0.23), 0.22(0.23); (n = 6, unless otherwise specified; in mm): TL 4.68–5.25 (mean = 4.91, standard deviation ± 0.19), PL 1.76–2.04 (1.86 ± 0.09), PA 1.28–1.40 (1.34 ± 0.04), PB 2.84–3.28 (3.04 ± 0.15), SL 0.24–0.27 (0.25 ± 0.01), SW 0.21–0.30 (0.25 ± 0.03), EI 2.64–3.04 (2.82 ± 0.13), EL 3.16–3.60 (3.34 ± 0.15), EW 1.72–2.00 (1.90 ± 0.10), EH 1.15–1.40 (1.23 ± 0.08), HW 1.06–1.15 (1.11 ± 0.03), IS 0.30–0.35 (0.32 ± 0.01), WA 0.25–0.30 (0.26 ± 0.02), MC (n = 5) 1.32–1.52 (1.40 ± 0.07), MB (n = 5) 0.64–0.80 (0.74 ± 0.06), VL (n = 5) 0.88–1.04 (0.94 ± 0.06).

Fig. 56. *Cyparium oberthueri* Pic, 1956. **A**–**C**. Male specimen (CELC). **A**. Dorsal view. **B**. Ventral view. **C**. Lateral view. **D**–**F**. Different male specimen (CELC). **D**. Dorsal view. **E**. Ventral view. **F**. Lateral view. Specimens collected at Mata da Biologia (A–C) and Mata do Paraíso (D–F). Scale bars = 1.0 mm.

Tergite VIII triangular; punctation dense, fine; pubescence dense (Fig. 63A). Sternite VIII sub-rectangular with a triangular projection (Fig. 63B). Vagina and bursa copulatrix membranous, without sclerites (Fig. 63C). Vaginal plate with an apical rectangular sclerite (Fig. 63D) Spermatheca not detected. Distal gonocoxites curved and enlarged at base; gonostyli short, enlarged at base (Fig. 63C, E).

Host fungi

Adults were collected from *Psathyrella candolleana* (1 record, 3 individuals), unidentified mushroom ("*Lactarius*?") (1, 10).

Remarks

The dorsal photo of one specimen belonging to the type series (Fig. 64A) and the original description of *C. oberthueri* are consistent with the data of the specimens studied here. Furthermore, the itinerary of Philibert Germain (P. Germain) (Fig. 64C) was evaluated: in 1885 he was in Minas Gerais and in 1886 at "Province Matto Grosso" where the type series was collected (Fig. 64C) (Papavero 1971). The "Province Matto Grosso" at that time was a broad province that comprised what nowadays are the states of Mato Grosso, Mato Grosso do Sul and Rondônia. In 1887 he arrived in Cárceres (currently in the state of Mato Grosso) departing from Corumbá (currently Mato Grosso do Sul), and in 1889 he was in Cochabamba (Bolivia) (Fig. 64C) (Papavero 1971). It is likely that "Province Matto Grosso" refers to

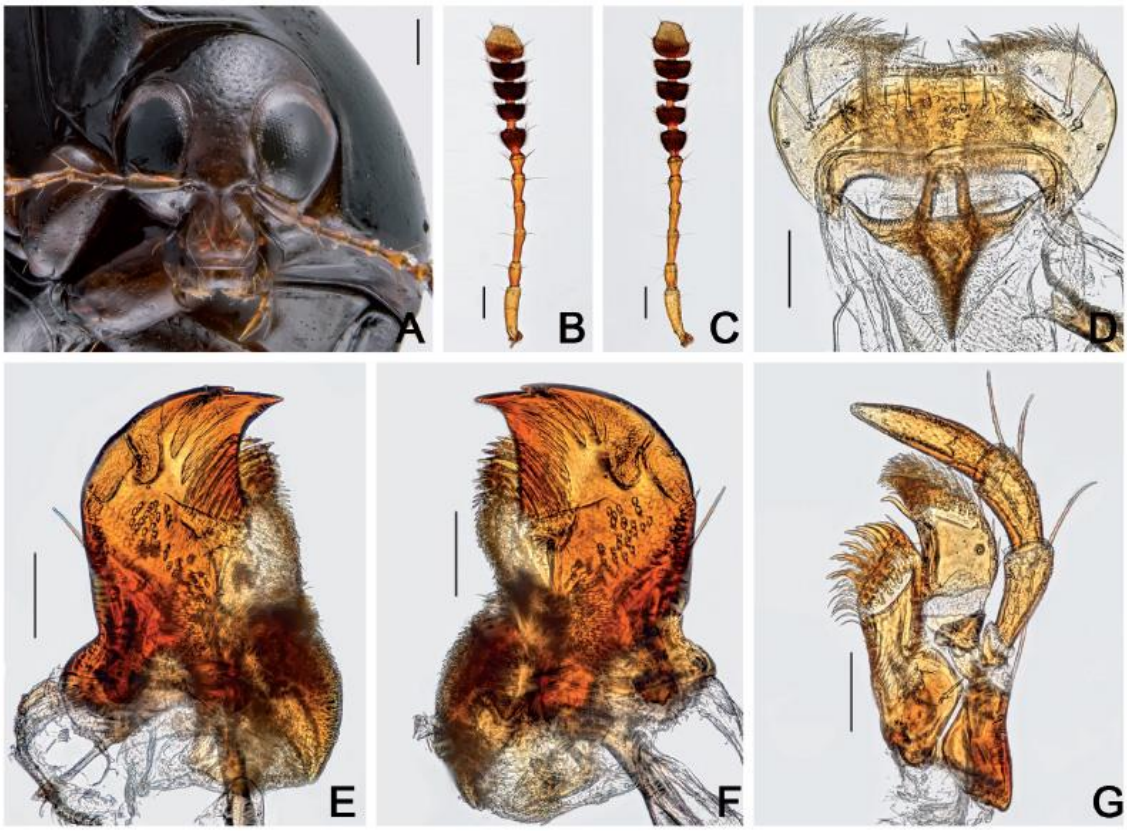

Fig. 57. *Cyparium oberthueri* Pic, 1956 (CELC). **A**. Frontal view. **B**. Male antenna. **C**. Female antenna. **D**. Labrum. **E**. Left mandible. **F**. Right mandible. **G**. Maxilla. Specimens collected at Mata da Biologia, Viçosa (MG, Brazil) (CELC). Scale bars: A–C = 0.2 mm; D–G = 0.1 mm.

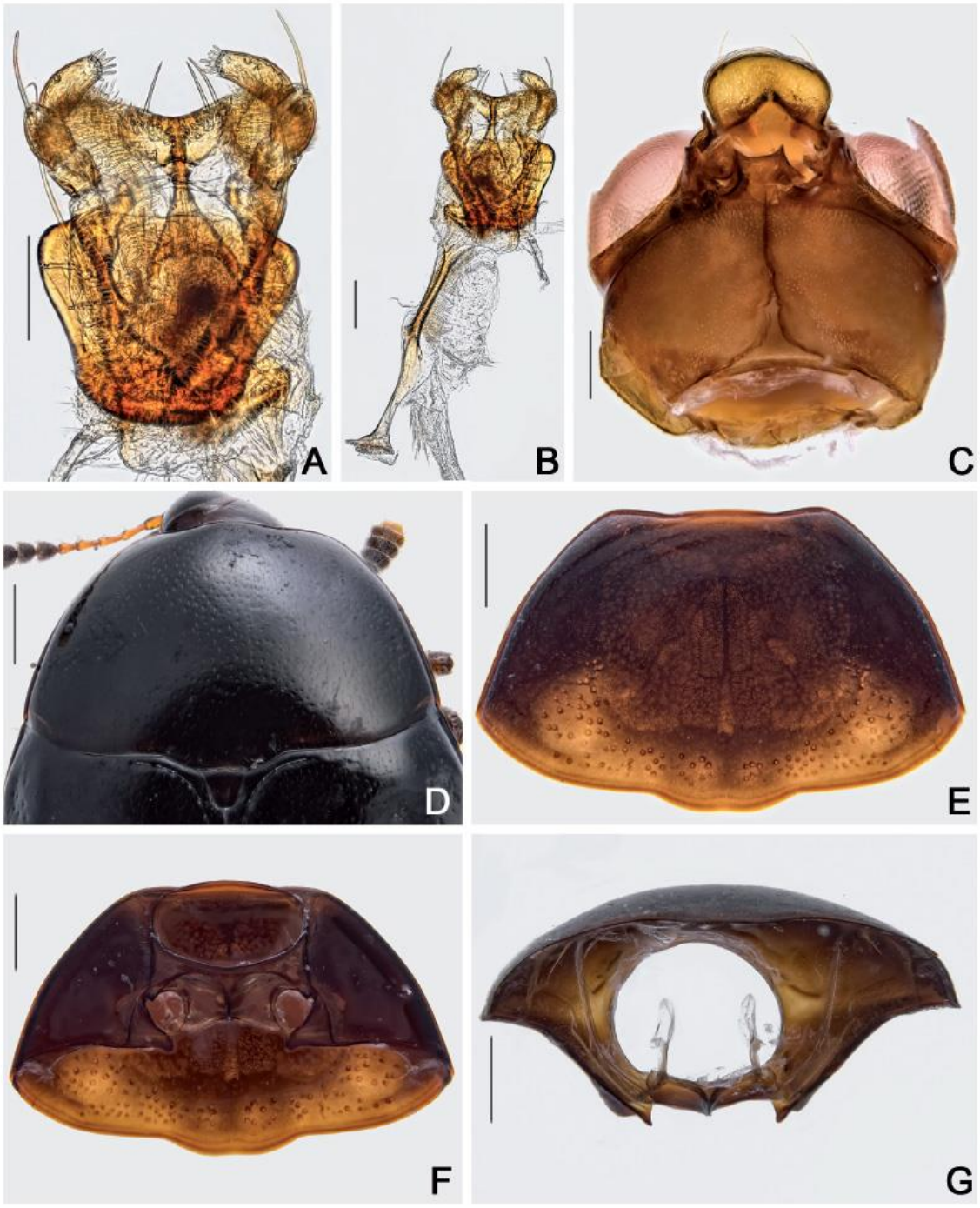

Fig. 58. *Cyparium oberthueri* Pic, 1956, ♂♂ (CELC). **A**. Labium. **B**. Hypopharynx. **C**. Head, ventral view. **D–E**. Pronotum, dorsal view. **F–G**. Prothorax. **F**. Ventral view. **G**. Inner view. Specimens collected at Mata da Biologia, Viçosa (MG, Brazil). Scale bars: A–B = 0.1 mm; C = 0.2 mm; D–G = 0.5 mm.

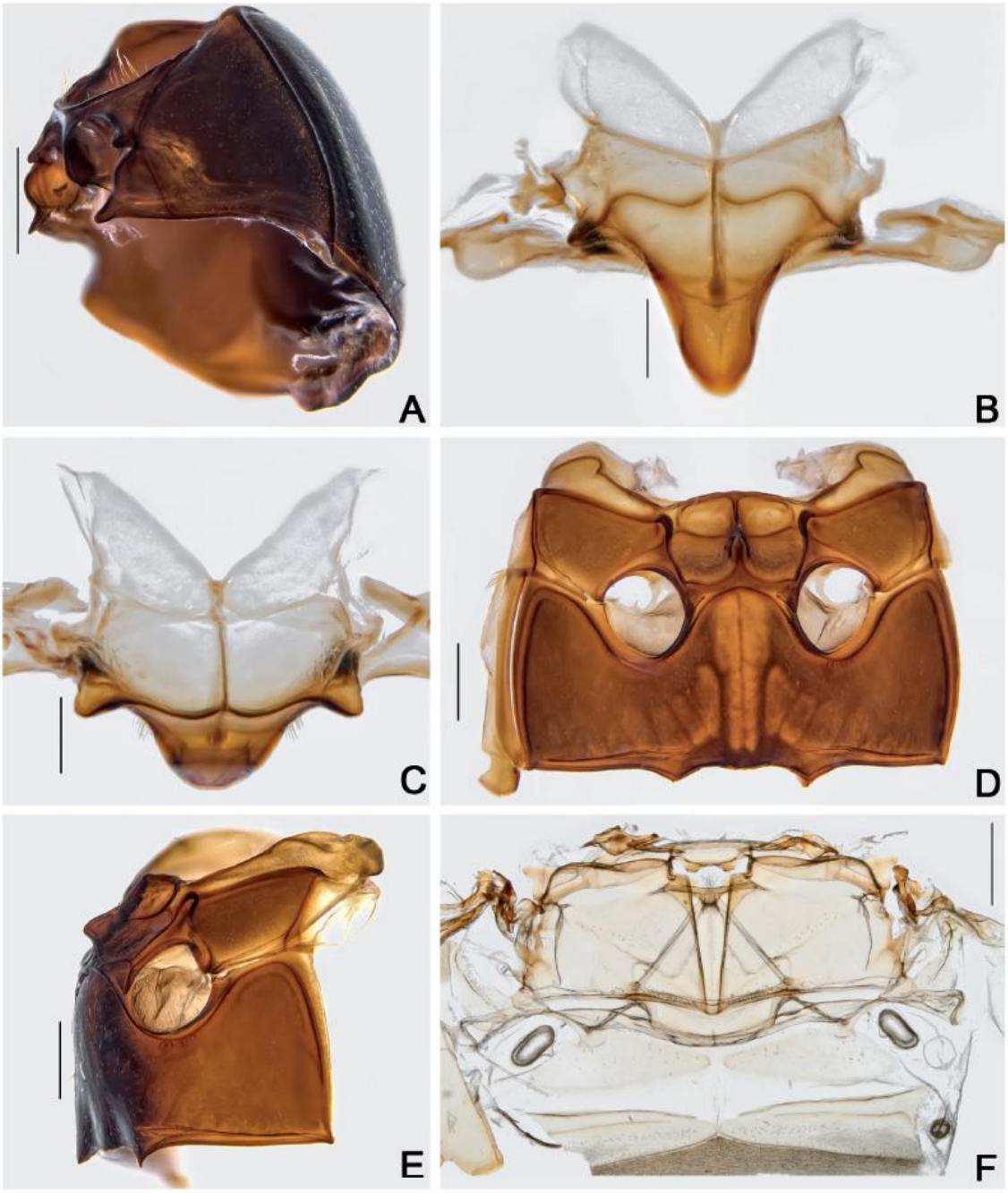

Fig. 59. *Cyparium oberthueri* Pic, 1956, ♂♂ (CELC). **A**. Prothorax, lateral view. **B–C**. Scutellar plate. **B**. Dorsal view. **C**. Apically slanted view. **D–E**. Meso- and metathorax. **D**. Ventral view. **E**. Lateral view. **F**. Metanotum. Specimens collected at Mata da Biologia, Viçosa (MG, Brazil) (CELC). Scale bars: A, D–F = 0.5 mm; B–C = 0.2 mm.

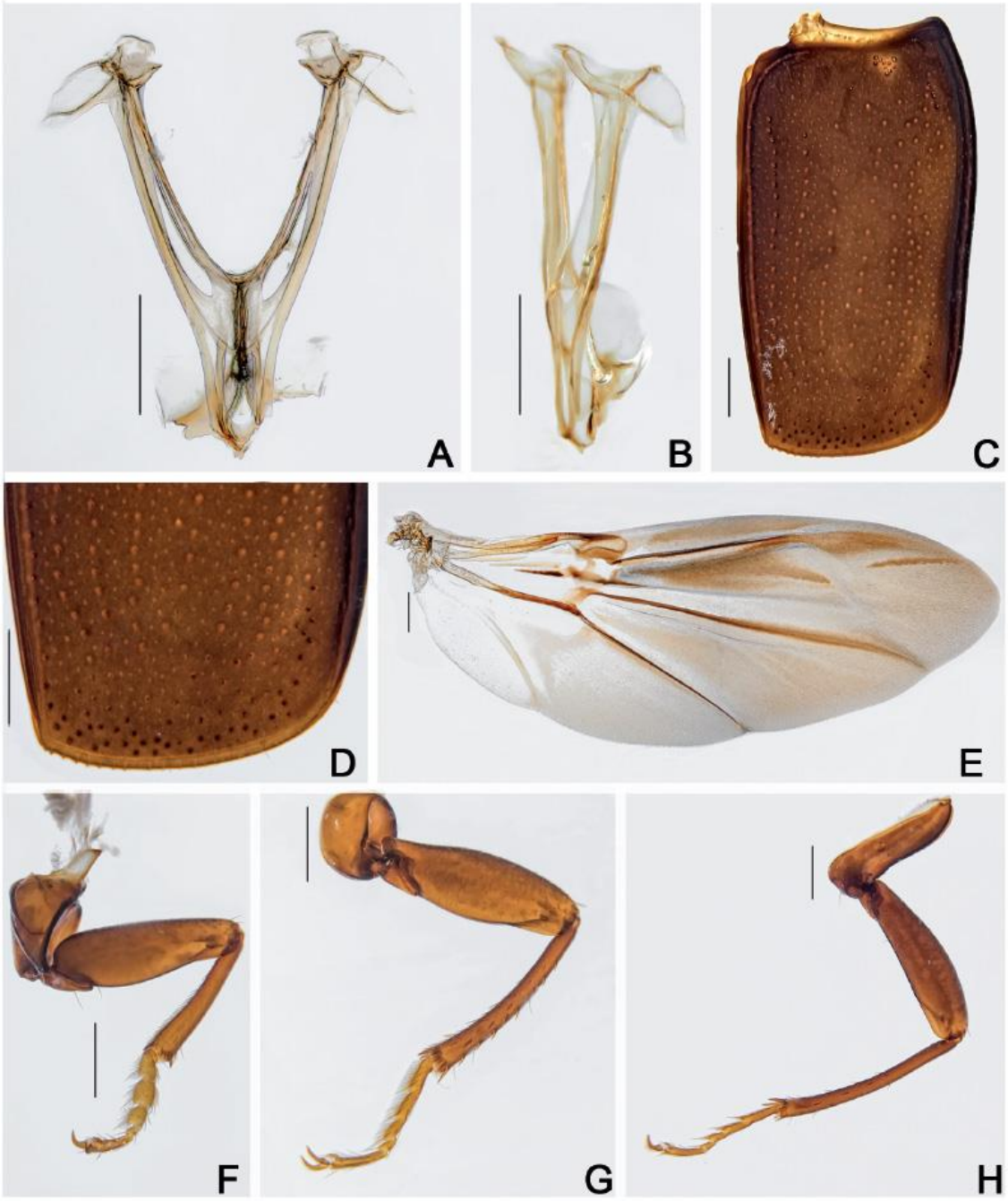

Fig. 60. *Cyparium oberthueri* Pic, 1956, ♂♂ (CELC). **A**–**B**. Metendosternite. **A**. Dorsal view. **B**. Lateral view. **C**–**D**. Elytron. **C**. Entire. **D**. Apex. **E**. Hind wing. **F**–**H**. Legs. **F**. Fore. **G**. Middle. **H**. Hind. Specimens collected at Mata da Biologia, Viçosa (MG, Brazil). Scale bars = 0.5 mm.

somewhere between what nowadays is the northern part of Mato Grosso do Sul, and the southern part of Mato Grosso. We do not know whether the type series was collected in the Cerrado biome or in riparian forest similar, or even linked, to areas of the Atlantic Forest biome. The specimens we examined are all from two Atlantic Forest remnants of Southeast Brazil, far away from the type locality, but they fit the

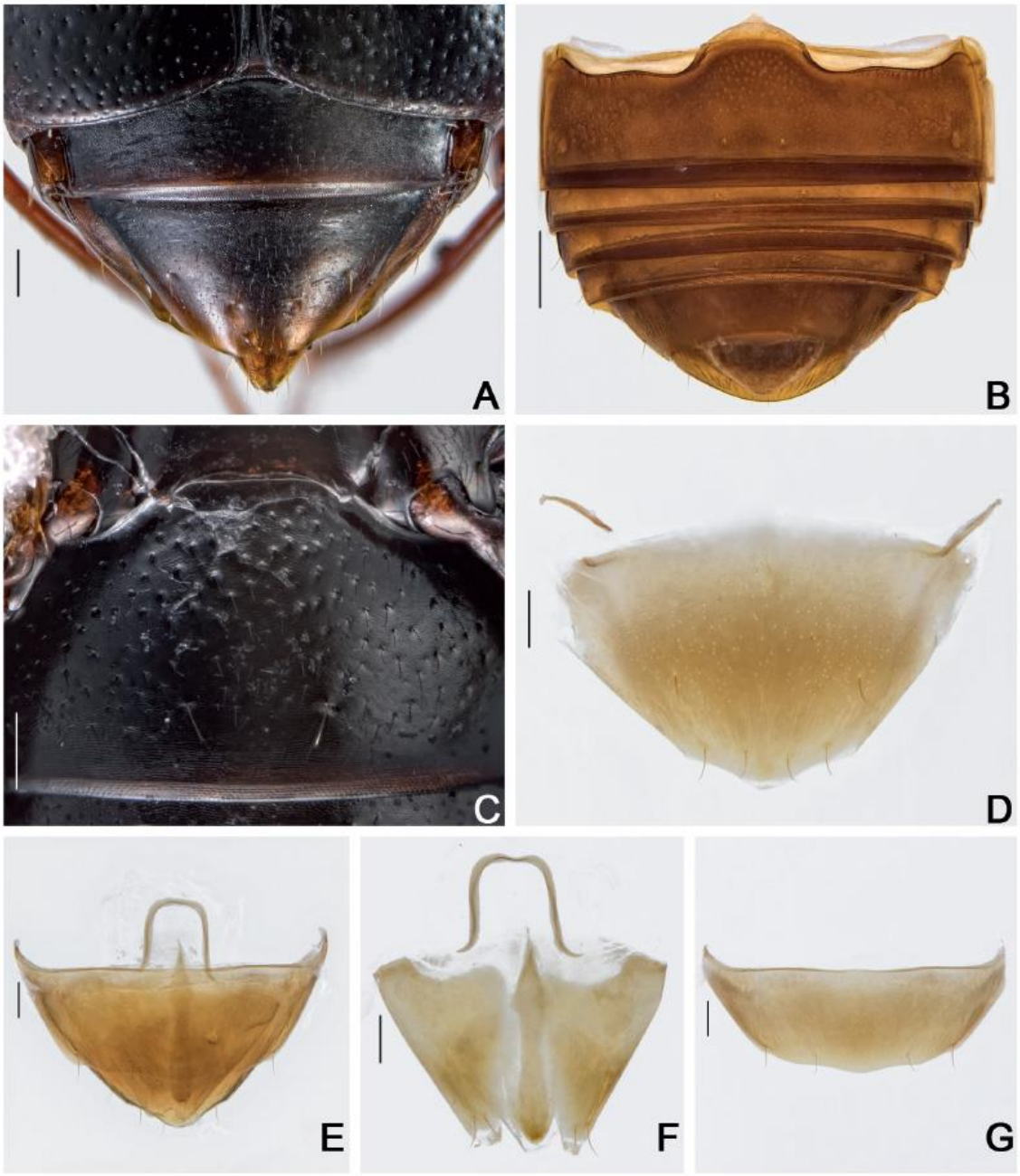

Fig. 61. *Cyparium oberthueri* Pic, 1956, ♂♂ (CELC). **A**–**B**. Abdomen. **A**. Dorsal view. **B**. Ventral view. **C**. Ventrite 1. **D**. Tergite VIII. **E**. Terminalia. **F**. Tergite IX. **G**. Sternite VIII. Specimens collected at Mata da Biologia, Viçosa (MG, Brazil). Scale bars: A, C–G = 0.2 mm; B = 0.5 mm.

Fig. 62. *Cyparium oberthueri* Pic, 1956, ♂ (CELC). **A–C**. Aedeagus. **A**. Lateral view. **B**. Frontal view. **C**. Dorsal view. **D–E**. Internal sac. **D**. Frontal view. **E**. Dorsal view. Specimen collected at Mata da Biologia, Viçosa (MG, Brazil). Scale bars = 0.2 mm.

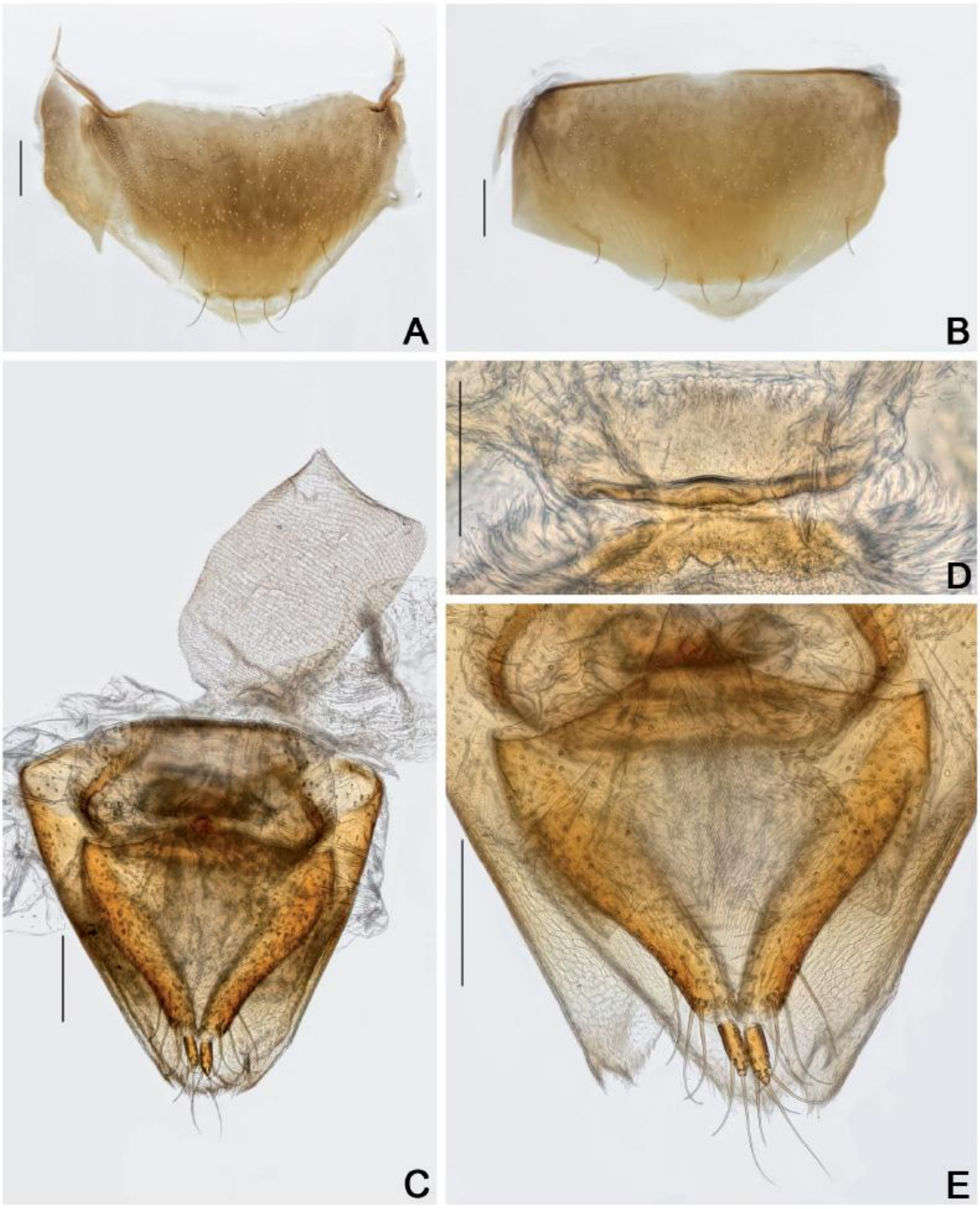

Fig. 63. *Cyparium oberthueri* Pic, 1956, ♀ (CELC). **A**. Tergite VIII. **B**. Sternite VIII. **C**. Terminalia. **D**. Sclerite of vaginal plate. **E**. Ovipositor. Specimen collected at Mata da Biologia, Viçosa (MG, Brazil). Scale bars: A–C, E = 0.2 mm; D = 0.1 mm.

original description and are morphologically similar to the available image of a syntype (Fig. 64A). At this moment, we prefer to call the specimens we have in hand as *C. oberthueri*, in the absence of any evidence to describe them as a new species.

Distribution

Known from "Prov. Matto Grosso", Midwest, Brazil (1886, P. Germain). New records from Viçosa, Minas Gerais, Southeast Brazil (Fig. 64C).

Fig. 64. *Cyparium oberthueri* Pic, 1956 (MNHN collection-Paris). **A**. Habitus. **B**. Labels. **C**. Distribution. Squares = P. Germain itinerary; circles = new records.

Discussion

There are two main problems in accurately identifying species of *Cyparium*. First, they are very similar to each other and morphological limits between species based on traditional characteristics (shape, size, colour pattern) are obscure. That is true for the species studied here and was previously pointed out by Leschen & Löbl (1995), who examined 48 species of the genus. Another important problem is that it is very common to observe intraspecific colour variation (e.g., in *C. lescheni* sp. nov., *C. newtoni* sp. nov., *C. oberthueri*; *C. terminale* as mentioned by Márquez (2007)), or species that were described based on teneral specimens like *C. palliatum* (as pointed out by Matthews (1888)). Therefore, the study of non-traditional characteristics, such as the morphology of mouthparts, meso- and metanotum, metendosternite, and male and female abdominal terminalia, among others, may help to circumvent these problems. Below we discuss some taxonomically important characteristics of *Cyparium* based on our results.

Cuticular microsculpture is shown to be very important for distinguishing species of *Cyparium*. It varies among the sclerites of the body, like the head and tergites (Table 1). This characteristic has not been very well studied in *Cyparium*, but it is well known in other genera, such as *Scaphisoma* Leach, 1815, *Brachynopus* Broun, 1881, and *Baeocera* Erichson, 1845 (Löbl & Leschen 2003; Löbl 2015, 2018b). For the species studied here, this microsculpture is imbricate or strigulate, and more or less separated; it covers the entire sclerite surface, or just a part of it. Most species of *Cyparium* studied here had different sets of cuticular microsculpture (Table 1), except for *C. loebli* sp. nov. and *C. pici* sp. nov. But even the latter two species showed some slight differences (microsculpture less spaced in *C. pici*).

Along with microsculpture, punctation also proved to be diagnostic. Elytron punctation is well known: it can have five to seven discal punctures (Ogawa *et al.* 2016). All species we studied here have six rows, but the latter two could be intermixed or not. Elytral apical punctation was also important, being more or less coarse and dense. The presence or absence of punctation on the metaventrite was diagnostic as well. Abdominal punctation was also diagnostic, like in the case of the coarse punctation on ventrite 1 in *C. pici*, and in tergite VII of *C. collare*.

Measurements of antennomeres are widely used to determine species in Scaphidiinae (Löbl & Leschen 2003; Ogawa & Sakai 2011; Ogawa *et al.* 2016; Löbl 2015, 2020; Löbl *et al.* 2021), and these were also taxonomically informative for the species of *Cyparium*. Measuring an entire antenna can be difficult, because it may be hidden, so we suggest focusing primarily on the last antennomere. The shape and colour (unicolorous/bicolored) of the last antennomere are quite variable between species, and it is usually easily visible even when the rest of the antenna is hidden.

Mouth parts are quite variable as well. The interspecific variation of the labrum shape came as a surprise, as can be seen, for instance, when comparing *C. achardi* sp. nov. and *C. loebli* (Figs 7G, 23D). The main differences in the remaining mouthparts are variations in proportions (length/width) and it is possible that noticing the structures alone, without others to compare, it would be difficult to describe them. The general shape of the mouthparts does not differ from that studied by Leschen & Löbl (1995, 2005) and Naomi (1988a, 1988b). Leschen & Löbl (1995) classified gular pores present in *Cyparium*, but the disposition and density of these pores were shown to be informative as well, as is the shape of the gula.

General pronotum shape is quite similar, but differences can be found in the proportions and shape of the anterior and posterior beads, and lateral areas. For example, in *C. achardi*, the anterior bead is less evident than in *C. pici*, and the shape of the former is also more squared, with the lateral areas less curved. We have not studied this structure in detail to separate species. However, it might be an interesting structure on which to conduct morphometric analysis. The same can be applied to the elytra, and also to the prosternal and mesoventral processes.

Table 1. Comparative morphology regarding the microsculpture of the various structures. Abbreviations: stri. = strigulate; imbr. = imbricate.

	Vertex	Hypomeron	Mesanepisternum	Metaventrite	Metanepisternum	Metepimeron	Ventrite 1
Cyparium achardi sp. nov.	–	–	–	–	imbr.	imbr.	stri.
Cyparium lescheni sp. nov.	–	stri.	stri.	stri.	imbr.	imbr.	stri.
Cyparium loebli sp. nov.	–	stri.	stri.	–	imbr.	imbr.	stri.
Cyparium newtoni sp. nov.	–	stri.	stri.	–	–	imbr.	stri.
Cyparium pici sp. nov.	–	stri.	stri.	–	imbr.	imbr.	stri.
Cyparium collare	–	imbr. (laterally)	imbr.	imbr. (laterally)	imbr.	imbr.	imbr.
Cyparium oberthueri	stri.	stri.	imbr.	–	imbr.	imbr.	stri.

The profurcae of scaphidiines are little studied. But comparing those of *Cyparium* to those of *Scaphisoma pandemum* von Groll & Lopes-Andrade, 2021 we noticed that the shape of the profurcae might be useful in generic diagnoses within Scaphidiinae. The profurcae of the seven species we studied were similar: short stalk and a longish apex (feather-shaped), but in *S. pandemum* the stalk is longer and the apex is rounded (von Groll & Lopes-Andrade 2021).

The sclerite between lateral area of mesanepisternum is considered to be a "not true mesepimeron" (Leschen *et al*. 1990). We consider this sclerite to be just a fold of the mesanepisternum (Fig. 3); on the other hand, the structure hidden by the elytra seems to be the mesepimeron (Fig. 9E). Nonetheless, we believe that this structure must be reviewed in *Cyparium*.

The metendosternite of Scaphidiinae has been illustrated for a few genera (Crowson 1938; Naomi 1989a; Leschen & Löbl 1995; von Groll & Lopes-Andrade 2021). Differences between genera are quite evident (e.g., arms longer and thinner, and stalk larger in *Scaphisoma* than in *Cyparium*), but among *Cyparium* species the differences are quite subtle: arms slightly curved, 'stalk ridge' occupying (or not) half of the stalk.

The metanotum of *S. pandemum* was illustrated and it is quite similar to those of the *Cyparium* species studied here. The metanotum studied here also presents a similar pattern as the metanotum of *Elodes pseudominuta* Klausnitzer, 1971 (Coleoptera, Scirtidae) (Friedrich & Beutel 2006): same alacrista, median membranous area and apodeme shapes. However, this structure is dissimilar to the reduced metanotum of the wingless *Trurlia* sp. (Staphylinidae, Scydmaeninae) (Jałoszyński 2009).

Venation of the hind wings was quite similar among species: CAS curved and smooth, MP_{1+2}, MSP, and RP_{3+4} well marked, and R_4 thin. Therefore, regarding the same genus they are not informative for diagnosis. Nonetheless, by comparing it with other genera it is possible to find differences. In *S. pandemum* the veins are more delicate and CAS less curved (von Groll & Lopes-Andrade 2021). The

venation of *Scaphidium* sp. and *Scaphium castanipes* Kirby, 1837 (Lawrence *et al.* 2021) differ from species of *Cyparium* mainly by the absence of MP_4, and MP_{1+2} and the straighter R_4.

The morphology of male aedeagus has been used in the taxonomy of Scaphidiinae (Leschen & Löbl 2005), as it is highly variable between species, but is quite similar within a species. Papers on *Cyparium* usually describe and illustrate it (Löbl 1984, 1999; Hwang & Ahn 2001; Fierros-López 2002; Márquez 2007; Ogawa & Sakai 2011; Ogawa *et al.* 2016). Although *Cyparium* have relatively homogeneous aedeagal characters (Leschen & Löbl 1995), there are numerous differences between the species that we have examined, like the morphologically similar *C. lescheni* and *C. newtoni*. Even the median lobe itself was enough to distinguish the species we have studied. Sometimes it is necessary to analyse the internal sac sclerites of scaphidiine beetles to search for diagnostic characteristics. We extracted and studied the internal sac of many *Cyparium* individuals, but did not find differences between the ones that had the same aedeagus shape, as in the case of specimens of *C. collare* from different localities. Although the ventral struts, sclerites VIII and IX, and tergite VIII are rarely illustrated, they were found to be very important for species delimitation, and may be diagnostic for some species, as in the case of *C. loebli* and *C. lescheni*.

Ogawa & Sakai (2011) emphasized that the vaginal plate is very useful to distinguish species of *Cyparium* and this is true for the species we have studied here. We found that the sclerite of the vaginal plate can be more or less developed; therefore, it cannot be analysed alone. The bursa copulatrix is a very variable structure, but some differences are only noticed when it is inflated. Unfortunately, we did not manage to keep the bursa inflated for the individuals we photographed for this work. But while we were testing techniques to dissect females on fresh collected specimens, we did manage to study inflated bursae, so it was possible to observe shape differences (e.g., *C. lescheni* Supp. file 2A and *C. collare* Supp. file 2B). Even though the spermatheca was not always detected, it does not mean that it does not exist; it is a very delicate and, usually, long structure that easily breaks. Every time it was observed, it was composed of a pair of filiform structures, similar to that of other species of *Cyparium* (Ogawa & Sakai 2011). We are working to improve techniques for dissecting females, but successful dissections seem to depend mostly on the degree of conservation of specimens. Distal gonocoxites and gonostyli are the best known structures of Scaphidiinae and are often illustrated (Ogawa & Sakai 2011; Ogawa & Löbl 2013, 2016; Ogawa *et al.* 2016). The main differences we found in these structures were the length in relation to width and the curvature, but sometimes the differences among species are more subtle than the ones regarding the vaginal plate. Therefore, we suggest studying all the female reproductive structures.

Specimens of *Cyparium* were collected from 39 different fungi: 36 Agaricales, one Hymenochaetales (*C. loebli* – probably incidental), one Polyporaceae (*C. collare*), and one unidentified mushroom ("*Lactarius*?", Russulales). The results corroborate with Newton (1984) and Kompantsev & Pototskaya (1987) who also mentioned species of *Cyparium* in Agaricales. *Cyparium lescheni*, *C. loebli*, and *C. newtoni* specimens were usually collected in large groups and sometimes cooccurring (especially the former and the latter); *C. oberthueri* beetles were also collected in groups, but apart from other species; *C. achardi* specimens were usually collected alone or in small groups, with four beetles each time at most; *C. collare* beetles were usually found alone or in small groups, but a few times they were found in large groups, usually with no other species; this is the most common species and seems to be the most generalist.

Conclusion

Cyparium now has 60 species; of these, 29 species are from the Neotropical region, thirteen from Brazil (Figs 4–5). Furthermore, by providing detailed morphological descriptions and redescriptions, along with illustrations, the morphology of *Cyparium* is somewhat better known now. Some of the structures and characteristics presented here can be used in future phylogenetic studies.

Acknowledgements

We thank the staff of Laboratório de Sistemática e Biologia de Coleoptera (UFV) for assistance in field collections at Viçosa. We also thank Luciano de A. Moura (MCNZ) and Fernando Z. Vaz-de-Mello (CEMT) for loaning specimens. We sincerely thank Azadeh Taghavian (MNHN) and Jiří Hájek (NMPC) for the images provided. We thank the doctoral qualifying committee (Angelico Asenjo, Andressa Paladini, Juares Fuhrmann and Igor de Souza Gonçalves), Dr Ivan Löbl, and the anonymous reviewer for the suggestions and corrections that helped to improve this manuscript. Financial support was provided by Conselho Nacional de Desenvolvimento Científico e Tecnológico (CNPq; research grant number 308432/2018-5 to the junior author), Fundação de Amparo à Pesquisa do Estado de Minas Gerais (FAPEMIG; Edital 02/2018—Programa Pesquisador Mineiro XII—PPM-00314-18) and Coordenação de Aperfeiçoamento de Pessoal de Nível Superior—Brasil (CAPES; Finance Code 001; doctorate degree grant to the senior author).

References

Achard J. 1921. Notes sur les Scaphidiidae du Musée de Leyde. *Zoologische Mededeelingen* 6: 84–91.

Achard J. 1922. Descriptions de scaphidides nouveaux (Col. Scaphidiidae). *Fragments entomologiques*: 35–45.

Ashe J.S. 1984. Description of the larva and pupa of *Scaphisoma terminatum* Melsh. and the larva of *Scaphium castanipes* Kirby with notes on their natural history (Coleoptera: Scaphidiidae). *The Coleopterists Bulletin* 38: 361–373.

Crowson R.A. 1938. The metendosternite in Coleoptera: a comparative study. *Transactions of the Royal Entomological Society of London* 87 (17): 397–415. https://doi.org/10.1111/j.1365-2311.1938.tb00723.x

Erichson W.F. 1845. *Naturgeschichte der Insecten Deutschlands. Erste Abteilung. Coleoptera. Dritter Band. Lieferung 1*. Nicolaische Buchhandlung, Berlin. https://doi.org/10.5962/bhl.title.8270

Fierros-López H.E. 2002. Descripción de dos especies nuevas de *Cyparium* Erichson 1845 (Coleoptera: Staphylinidae) de México. *Dugesiana* 9 (2): 7–14.

Friedrich F. & Beutel R.G. 2006. The pterothoracic skeletomuscular system of Scirtoidea (Coleoptera: Polyphaga) and its implications for the high-level phylogeny of beetles. *Journal of Zoological Systematics and Evolutionary Research* 44 (4): 290–315. https://doi.org/10.1111/j.1439-0469.2006.00369.x

Grebennikov V.V. & Newton A.F. 2012. Detecting the basal dichotomies in the monophylum of carrion and rove beetles (Insecta: Coleoptera: Silphidae and Staphylinidae) with emphasis on the oxyteline group of subfamilies. *Arthropod Systematics & Phylogeny* 70 (3): 133–165.

Harris R.A. 1979. A glossary of surface sculpturing. *Occasional Papers in Entomology* 28: 1-31.

Hübler N. & Klass K.D. 2013. The morphology of the metendosternite and the anterior abdominal venter in Chrysomelinae (Insecta: Coleoptera: Chrysomelidae). *Arthropod Systematics & Phylogeny* 71 (1): 3–41.

Hwang W. & Ahn K. 2001. New records of *Cyparium* Erichson and *Scaphidium* Olivier species in Korea (Coleoptera, Staphylinidae, Scaphidiinae). *Insecta Koreana* 18 (4): 369–372.

Jałoszyński P. 2009. *Trurlia*, a new Oriental genus of the tribe Cephenniini (Coleoptera: Scydmaenidae). *European Journal of Entomology* 106 (2): 261–274. https://doi.org/10.14411/eje.2009.034

Jałoszyński P. 2012. Taxonomy of '*Euconnus* complex'. Part I. Morphology of *Euconnus* s. str. and revision of *Euconnomorphus* Franz and *Venezolanoconnus* Franz (Coleoptera: Staphylinidae: Scydmaeninae). *Zootaxa* 3555 (1): 55–82. https://doi.org/10.11646/zootaxa.3555.1.3

Kirsch T. 1873. Beiträge zur Kenntniss der peruanischen Käferfauna auf Dr. Abendroth's Sammlungen basirt. *Berliner entomologische Zeitschrift* 17: 121–152.

Kompantsev A.V. & Pototskaya V.A. 1987. Novye dannye po lichikam zhukov-chelnovidok (Coleoptera, Scaphidiidae). *In*: Kompantsev A.V. & Pototskaya V.A. (eds) *Pototskaya Ekologiya i Morfologiya Nasekomychobyvateley Gribnych Substratov*: 87–100. Nauka, Mocow.

Lawrence J.F. & Newton Jr A.F. 1980. Coleoptera associated with the fruiting bodies of slime molds (Myxomycetes). *The Coleopterists' Bulletin* 34 (2): 129–143.

Lawrence J.F. & Ślipiński A. 2013. *Australian Beetles. Volume 1. Morphology, Classification and Keys*. CSIRO Publishing, Collingwood, Australia. https://doi.org/10.1071/9780643097292

Lawrence J.F., Zhou Y.-L., Lemann C., Sinclair B. & Ślipiński A. 2021. The hind wing of Coleoptera (Insecta): morphology, nomenclature and phylogenetic significance. Part 1. General discussion and Archostemata–Elateroidea. *Annales Zoologici* 71 (3): 421–606. https://doi.org/10.3161/00034541ANZ2021.71.3.001

Leschen R.A.B. 1994. Retreat-building by larval Scaphidiinae (Staphylinidae). *Mola* 4: 3–5.

Leschen R.A.B. & Löbl I. 1995. Phylogeny of Scaphidiinae with redefinition of tribal and generic limits (Coleoptera: Staphylinidae). *Revue suisse de Zoologie* 102 (2): 425–474. https://doi.org/10.5962/bhl.part.80472

Leschen R.A.B. & Löbl I. 2005. Phylogeny and classification of Scaphisomatini Staphylinidae: Scaphidiinae with notes on mycophagy, termitophily, and functional morphology. *Coleopterists Society Monographs* 3: 1–63. https://doi.org/10.1649/0010-065X(2005)059[0001:PACOSS]2.0.CO;2

Leschen R.A.B., Löbl I. & Stephan K. 1990. Review of the Ozark Highland *Scaphisoma* (Coleoptera: Scaphidiidae). *The Coleopterists' Bulletin* 44 (3): 274–294.

Löbl I. 1984. Les Scaphidiidae (Coleoptera) du nord-est de l'Inde et du Bhoutan I. *Revue suisse de Zoologie* 91(1): 57–107. https://doi.org/10.5962/bhl.part.81869

Löbl I. 1999. A review of the Scaphidiinae (Coleoptera: Staphylinidae) of the People's Republic of China, I. *Revue suisse de Zoologie* 106 (3): 691–744. https://doi.org/10.5962/bhl.part.80102

Löbl I. 2015. On the Scaphidiinae (Coleoptera: Staphylinidae) of the Lesser Sunda Islands. *Revue suisse de Zoologie* 122 (1): 75–120. Available from https://www.biodiversitylibrary.org/page/59078840 [accessed 5 Aug. 2022].

Löbl I. 2018a. *Coleoptera: Staphylinidae: Scaphidiinae*. World Catalogue of Insects, Vol. 16. Brill, Leiden, the Netherlands. https://doi.org/10.1163/9789004375956

Löbl I. 2018b. A review of Scaphisomatini from Sulawesi, with descriptions of ten new species (Coleoptera: Staphylinidae: Scaphidiinae). *Acta Entomologica Musei Nationalis Pragae* 58 (1): 151–165. https://doi.org/10.2478/aemnp-2018-0013

Löbl I. 2020. On the Scaphisomatini of Madagascar, and commentary on new trends in museums hampering taxonomic research. *Koleopterologische Rundschau* 90: 89–126.

Löbl I. & Leschen R.A.B. 2003. Scaphidiinae (Insecta: Coleoptera: Staphylinidae). *Fauna of New Zealand* 48: 1–94.

Löbl I. & Ogawa R. 2016. On the Scaphisomatini (Coleoptera, Staphylinidae, Scaphidiinae) of the Philippines, IV: the genera *Sapitia* Achard and *Scaphisoma* Leach. *Linzer biologische Beiträge* 48 (2): 1339–1492.

Löbl I., Leschen R.A.B & Warner W.B. 2021. Scaphisomatini of Arizona (Coleoptera, Staphylinidae, Scaphidiinae) collected by V-Flight Intercept traps. *Revue suisse de Zoologie* 128 (1): 173–185. https://doi.org/10.35929/RSZ.0043

Márquez J. 2007. Preliminary analysis of the colour variation in *Cyparium terminale* from Mexico, with comments on *C. palliatum*, and a new record for *C. yapalli* (Coleoptera: Staphylinidae, Scaphidiinae). *Entomological News* 118 (1): 1–10. https://doi.org/10.3157/0013-872X(2007)118[1:PAOTCV]2.0.CO;2

Matthews A. 1888. Fam. Scaphidiidae. *In*: *Biologia Centrali-Americana. Insecta, Coleoptera. Vol. 2, Part 1*: 158–181. [1887–1888]. Taylor & Francis, London. https://doi.org/10.5962/bhl.title.730

McKenna D.D., Farrell B.D., Caterino M.S., Farnum C.W., Hawks D.C., Maddison D.R., Seago A.E., Short A.E.Z., Newton A.F. & Thayer M.K. 2014. Phylogeny and evolution of Staphyliniformia and Scarabaeiformia: forest litter as a stepping stone for diversification of nonphytophagous beetles. *Systematic Entomology* 40 (1): 35–60. https://doi.org/10.1111/syen.12093

Naomi S. 1988a. Comparative morphology of the Staphylinidae and the allied groups (Coleoptera, Staphylinoidea): III. Antennae, labrum and mandibles. *Japanese Journal of Entomology* 56 (1): 67–77.

Naomi S. 1988b. Comparative morphology of the Staphylinidae and the allied groups (Coleoptera, Staphylinoidea): IV. Maxillae and labium. *Japanese Journal of Entomology* 56 (2): 241–250.

Naomi S. 1989a. Comparative morphology of the Staphylinidae and the allied groups (Coleoptera, Staphylinoidea): VII. Metendosternite and wings. *Japanese Journal of Entomology* 57 (1): 82–90.

Naomi S. 1989b. Comparative morphology of the Staphylinidae and the allied groups (Coleoptera, Staphylinoidea): X. Eighth and 10th segments of abdomen. *Japanese Journal of Entomology* 57 (4): 720–733.

Naomi S. 1990. Comparative morphology of the Staphylinidae and the allied groups (Coleoptera, Staphylinoidea): XI. Abdominal glands, male genitalia and female spermatheca. *Japanese Journal of Entomology* 58 (1): 16–23.

Newton A.F. Jr. 1984. Mycophagy in Staphylinoidea (Coleoptera). *In*: Wheeler Q. & Blackwell M. (eds) *Fungus/Insect Relationships. Perspectives in Ecology and Evolution*: 302–353. Columbia University Press, New York.

Newton A.F., Thayer M.K., Ashe J.S. & Chandler D.S. 2001. 22. Staphylinidae Latreille, 1802. *In*: Arnett R.H. Jr. & Thomas M.C. (eds) *American Beetles. Volume 1: Archostemata, Myxophaga, Adephaga, Polyphaga: Staphyliformia*: 272–418. CRC Press, Boca Raton, London, New York, Washington D.C.

Oberthür R. 1883. Scaphidiides nouveaux. *In*: *Coleopterorum Novitates. Recueil spécialement consacré à l'étude des coléoptères, Rennes* 1: 1–80. Available from https://www.biodiversitylibrary.org/page/60945290 [accessed 5 Aug. 2022].

Ogawa R. & Löbl I. 2013. A revision of the genus *Baeocera* in Japan, with a new genus of the tribe Scaphisomatini (Coleoptera, Staphylinidae, Scaphidiinae). *Zootaxa* 3652 (3): 301–326. https://doi.org/10.11646/zootaxa.3652.3.1

Ogawa R. & Löbl I. 2016. A review of the genus *Xotidium* Löbl, 1992 (Coleoptera, Staphylinidae, Scaphidiinae), with descriptions of five new species. *Deutsche entomologische Zeitschrift* 63 (1): 155–169. https://doi.org/10.3897/dez.63.8386

Ogawa R. & Sakai M. 2011. A review of the genus *Cyparium* Erichson (Coleoptera, Staphylinidae, Scaphidiinae) of Japan. *Japanese Journal of Systematic Entomology* 17: 129–136.

Ogawa R., Löbl I. & Maeto K. 2016. A new species of the genus *Cyparium* from northern Sulawesi, Indonesia (Coleoptera: Staphylinidae: Scaphidiinae). *Acta Entomologica Musei Nationalis Pragae* 56 (1): 195–201.

Omar M.B., Bolland L. & Heather W.A. 1979. A permanent mounting medium for fungi. *Bulletin of the British Mycological Society* 13 (1): 13–32. https://doi.org/10.1016/s0007-1528(79)80038-3

Papavero N. 1971. *Essays on the History of Neotropical Dipterology, with Special Reference to Collectors (1750–1905). Volume 1*. Museu de Zoologia, Universidade de São Paulo. https://doi.org/10.5962/bhl.title.101715

Pic M. 1916. Diagnoses spécifiques. *Mélanges exotico-entomologiques* 17: 8–20.

Pic M. 1920a. Nouveautés diverses. *Mélanges exotico-entomologiques* 32: 1–28.

Pic M. 1920b. Scaphidiides nouveaux de diverses origines. *Annali del Museo civico di Storia naturale di Genova* (3) 9: 93–97.

Pic M. 1931. Nouveautés diverses. *Mélanges exotico-entomologiques* 57: 1–36.

Pic M. 1947. [without tittle]. *Diversités entomologiques* 1: 1–16. https://doi.org/10.5962/bhl.title.107929

Pic M. 1956. Nouveaux coléoptères exotiques. *Bulletin de la Société entomologique de France* 60 [1955]: 173–175.

Reitter E. 1880. Die Gattungen und Arten der Coleopteren-Familie: Scaphidiidae meiner Sammlung. *Verhandlungen des naturforschenden Vereins in Brünn* 18 [1879]: 35–49.

Stephenson S.L., Wheeler Q.D., McHugh J. V. & Fraissinet P.R. 1994. New North American associations of Coleoptera with Myxomycetes. *Journal of Natural History* 28 (4): 921–936. https://doi.org/10.1080/00222939400770491

Tang L., Le L.Z. & He W.J. 2014. The genus *Scaphidium* in East China (Coleoptera, Staphylinidae, Scaphidiinae). *ZooKeys* 403: 47–96. https://doi.org/10.3897/zookeys.403.7220

von Groll E. & Lopes-Andrade C. 2021. *Scaphisoma pandemum* sp. nov. (Coleoptera: Staphylinidae: Scaphidiinae) from the Atlantic Forest of Southeast Brazil. *Zootaxa* 4999 (2): 143–156. https://doi.org/10.11646/zootaxa.4999.2.4

von Groll E., Aloquio S. & Lopes-Andrade C. 2021. A simple, low-cost device for collecting mushroom-dwelling Scaphidiinae (Coleoptera, Staphylinidae). *Zootaxa* 5071 (2): 296–298. https://doi.org/10.11646/zootaxa.5071.2.9

Zayas F. de 1988. *Entomofauna Cubana. Orden Coleoptera. Separata descripción de nuevas especies.* Editorial Cientifico-Técnica, La Habana.

Manuscript received: 28 December 2021
Manuscript accepted: 18 July 2022
Published on: 24 August 2022
Topic editor: Tony Robillard
Section editor: Max Barclay
Desk editor: Pepe Fernández

Brussels, Belgium; Natural History Museum of Denmark, Copenhagen, Denmark; Naturalis Biodiversity Center, Leiden, the Netherlands; Museo Nacional de Ciencias Naturales-CSIC, Madrid, Spain; Real Jardín Botánico de Madrid CSIC, Spain; Leibniz Institute for the Analysis of Biodiversity Change, Bonn – Hamburg, Germany; National Museum, Prague, Czech Republic.

Supplementary files

Supp. file 1. Holotypus labels. **A**. *Cyparium achardi* sp. nov. **B**. *C. lescheni* sp. nov. **C**. *C. loebli* sp. nov. **D**. *C. newtoni* sp. nov. **E**. *C. pici* sp. nov. https://doi.org/10.5852/ejt.2022.835.1909.7615

Supp. file 2. Female terminalia. **A**. *Cyparium lescheni* sp. nov. **B**. *C. collare* Pic, 1920. https://doi.org/10.5852/ejt.2022.835.1909.7617

Supp. file 3. Morphology of *Cyparium collare* Pic, 1920. https://doi.org/10.5852/ejt.2022.835.1909.7619

Fig 1. A–D. ♂ (SE, Areia Branca, MCN 166402). **A**. Dorsal view. **B**. Ventral view. **C**. Lateral view. **D**. Frontal view. **E–G**. ♂ (SE, Areia Branca, MCN 166403). **E**. Pronotum, dorsal view. **F**. Tergite VIII. **G**. Tergite IX. **H**. Sternite VIII. Scale bars: A–C = 1.0 mm; D, F–H = 0.2 mm; E = 0.5 mm.

Fig. 2. ♂ (SE, Areia Branca, MCN 166403), aedeagi. **A**. Lateral view. **B**. Frontal view. **C**. Dorsal view. Scale bars = 0.2 mm.

Fig. 3. A–F. ♂ (SE, Sta Luzia do Itanhi, MCN 166404). **A**. Dorsal view. **B**. Ventral view. **C**. Lateral view. **D**. Frontal view. **E**. Pronotum, dorsal view. **F**. Ventrite 1. **G**. ♂ (SE, Sta Luzia do Itanhi, MCN 166400), tergite VIII. Scale bars: A–C = 1.0 mm; D, F–G = 0.2 mm; E = 0.5 mm.

Fig. 4. ♂ (SE, Sta Luzia do Itanhi, MCN 166400). **A**. Terminalia. **B**. Tergite IX. **C**. Sternite VIII. **D–F**. Aedeagi. **D**. Lateral view. **E**. Frontal view. **F**. Dorsal view. **G–H**. Internal sac. **G**. Frontal view. **H**. Dorsal view. Scale bars = 0.2 in mm.

CAPÍTULO 4 – Rediscovery and redescription of *Scaphisoma nigrofasciatum* Pic (Coleoptera: Staphylinidae: Scaphidiinae): a remarkable new record from a distant continent

Publicado na revista *Zootaxa* 5375 (4): 565–573

https://doi.org/10.11646/zootaxa.5375.4.7

Zootaxa 5375 (4): 565–573
https://www.mapress.com/zt/

Article

ISSN 1175-5326 (print edition)
ZOOTAXA
ISSN 1175-5334 (online edition)

https://doi.org/10.11646/zootaxa.5375.4.7
http://zoobank.org/urn:lsid:zoobank.org:pub:31F699ED-89AB-441E-A67F-A10EB643A86A

Rediscovery and redescription of *Scaphisoma nigrofasciatum* Pic (Coleoptera: Staphylindae: Scaphidiinae): a remarkable new record from a distant continent

ELISA VON GROLL
Universidade Federal de Viçosa, Departamento de Biologia Animal, Campus Universitário, Viçosa - MG, 36570-900, Brazil
https://orcid.org/0000-0002-6563-8684; elisavgroll@gmail.com

Abstract

Scaphisoma nigrofasciatum Pic is a shining fungus beetle whose distribution was recorded from the Asian continent and three insular African countries. This paper presents a new record of this species from Brazil. In this paper, photographs of specimens from both Brazil and Asia are provided, accompanied by a brief new redescription. A preliminary hypothesis suggests that this species may have been introduced to Brazil alongside flamboyant trees.

Key words: India, Brazil, Pest, Fungi, Taxonomy, Shining fungus beetle

Introduction

Scaphisoma nigrofasciatum was originally described by Pic (1915). Initially, the description led to confusion regarding whether it was a form of *S. binotatum* Achard, 1915, or a valid species (Achard, 1915; Pic 1916; Scott 1922; Vinson 1943). This confusion was finally resolved by Löbl (1971), who not only provided a Lectotype but also compiled information about the species' distribution. Subsequent papers contributed additional records, and to this day, *S. nigrofasciatum* is known to inhabit three Asian countries (India, Nepal, and Sri Lanka) and three insular African countries (La Réunion, Mauritius, Seychelles) (Löbl 1971, 1977, 1979, 1986, 1990, 1992; Lecoq 2015).

In India, this species is considered a pest of cultivated mushrooms (Deepthi *et al.* 2004; Singh & Sharma 2016). Deepthi *et al.* (2004) observed groups of *S. nigrofasciatum* hiding between the gills of *Pleurotus ostreatus* (Jacq.) P. Kumm. 1871 (as *P. florida*) and many specimens feeding on the mycelium, stipe, and pileus of this economically important fungus. Singh and Sharma (2016) observed adults of *S. nigrofasciatum* laying eggs on decayed oyster mushrooms, with larvae infesting the soil.

In this paper, I aim to provide a concise redescription of *S. nigrofasciatum*, covering both males and females, including internal and external morphology and morphometry. Additionally, I present another noteworthy new record of this diminutive species.

Material and methods

Collections were performed in two urban locations in Minas Gerais (Brazil): (1) Viçosa (Vila Gianetti, 20°45′16"S, 42°52′21"W), and (2) Oratorios (20°25′55"S, 42°48′16"W), approximately 38.61 km from Viçosa. Both sites are situated in small cities surrounded by fragments of the Atlantic Forest. Beetles were collected manually or with mouth aspirator. Additional specimens were photographed but not collected in Vila Gianetti.

All Brazilian specimens are deposited at CELC (Coleção Entomológica do Laboratório de Sistemática e Biologia de Coleoptera da UFV, Viçosa, MG, Brazil). Asian beetles had previously been collected in Sri Lanka and India and were donated by Dr. Ivan Löbl to the FMNH (The Field Museum of Natural History).

Brazilian beetles and fungi were photographed using the following equipment: (1) Canon 5D + Canon macro lens 65mm / Canon EF 50mm for field photos; (2) Zeiss Discovery V20 stereo microscope + Zeiss AxioCam 506;

Accepted by J. Klimaszewski: 10 Nov. 2023; published: 24 Nov. 2023

(3) Zeiss AxioLab compound microscope + Canon EOS 1000D digital camera; (4) Samsung Smartphone. FMNH beetles were photographed using the Leica Z16 APO + Leica DFC450 Digital Camera system. All microscope images were stacked using Helicon Software.

Asian beetles had already been dissected by Dr. Löbl, and their genitalia and terminalia are preserved in Euparal and pinned alongside each specimen. For Brazilian specimens, dissected parts were preserved in microvials with glycerin.

Brazilian specimens were measured using a Zeiss Stemi 2000C stereo microscope equipped with a 2× objective lens. Antennae were photographed and digitally measured using tpsDig2 ver. 2.32 software. Range, mean, and standard deviation values were estimated using PAST. Asian specimens were digitally measured based on stereomicroscope photos, and antennomere width measurements were not possible. Therefore, only antennomere lengths are provided. Measurements follow von Groll & Lopes-Andrade (2021) (*), with some modifications (Tab 1, Fig. 1).

TABLE 1. Abbreviations and meanings of the measurements.

Figure	Abbr.	Meaning	Source
Fig. 2A	EI	elytral length—sutural line, including the scutellar shield	* (modified due mistake)
Fig. 2A	EL	elytral length—umeral region	* (modified due mistake)
Fig. 2A	EW	greatest right elytron width	*
Fig. 2A	PA	pronotal width at the anterior margin	*
Fig. 2A	PB	pronotal width at the posterior margin	*
Fig. 2A	PL	pronotal length along the midline	*
Fig. 2A	TL	total body length, not including head and abdomen	*
Fig. 2B	EH	elytral height in lateral view	this paper
Fig. 2B	MeL	mesepimeron length	this paper
Fig. 2B	MeW	mesepimeron width	this paper
Fig. 2B	VL2	first abdominal sternite at the lateral	this paper
Fig. 2C	HW	maximum width of the head including eyes	this paper
Fig. 2C	IS	interocular space	*, as GY
Fig. 2C	MC	mesothorax length in the midline	*
Fig. 2C	SY	shortest width between eyes above the antennae	*
Fig. 2C	WA	width between antennae	*
Fig. 2D	MA	length of metacoxal area	*
Fig. 2D	MA2	abdominal length bellow metacoxal area	this paper
Fig. 2D	MB	mesothorax length between fore and middle legs, not including mesocoxal areas	*
Fig. 2D	ML	length of mesocoxal area	*
Fig. 2D	VL	length of ventrite I in the midline	*

Results

Ten specimens of *Scaphisoma nigrofasciatum* were found feeding on a species of *Inonotus* P. Karst. 1879 (Hymenochaetaceae) in Viçosa, and one was collected in Oratórios feeding on the mushroom *Schizophyllum commune* Fr. 1821 (Schizophyllaceae). Four of these specimens were detailed studied and compared to Asian specimens. No morphological or morphometrical differences were found between both groups. In this sense, the redescription and comments are made based on Brazilian and Asian specimens, providing images for comparison.

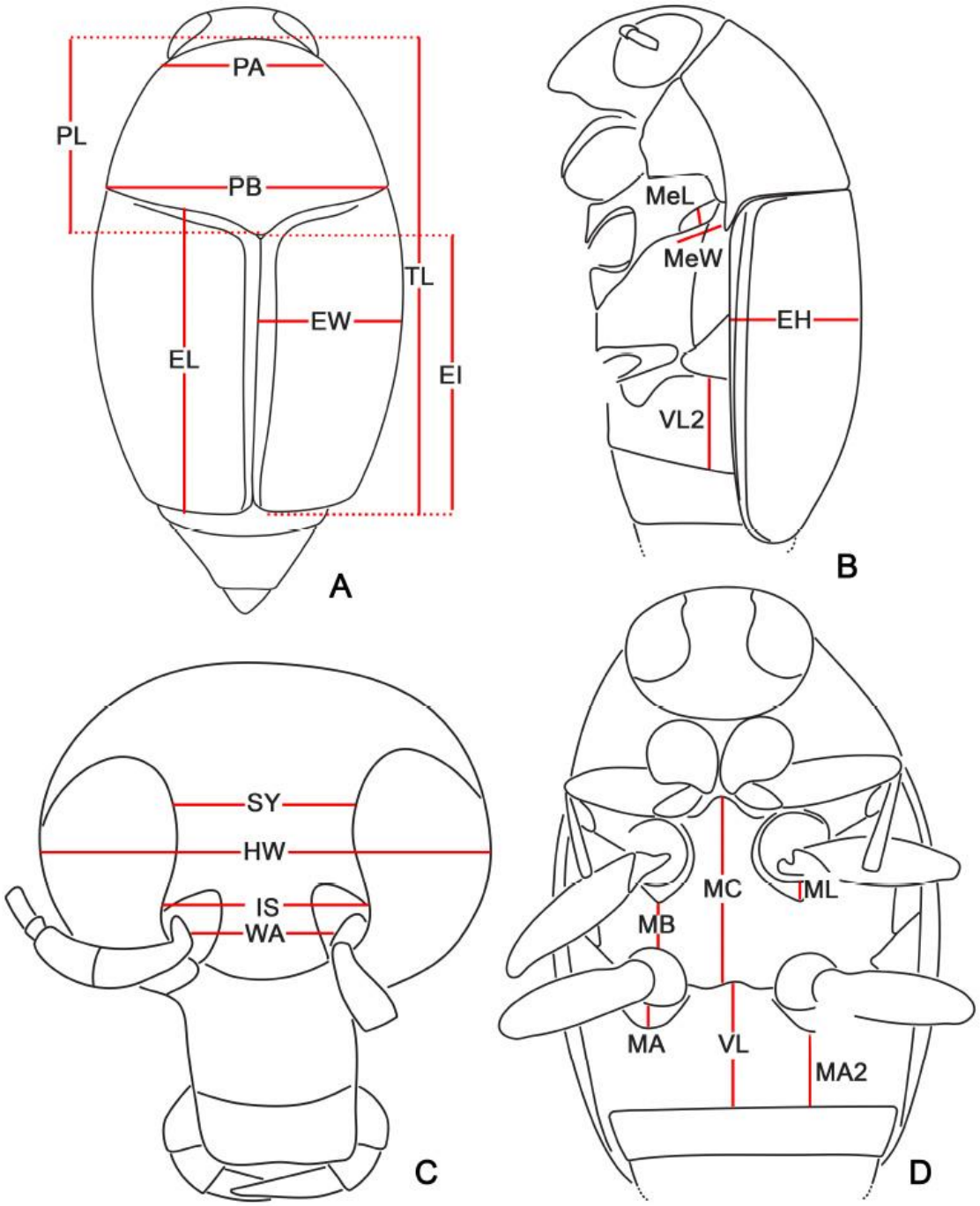

FIGURE 1. Measurements (modified from von Groll & Lopes-Andrade 2021): **A**, dorsal view; **B**, lateral view; **C**, head, frontal view; **D**, ventral view. Abbreviations: EH, elytral height, in lateral view; EI elytral length (including scutellum); EL, elytral length (umeral region); EW, greatest right elytron width; HW, maximum width of the head including eyes; IS, interocular space; MA, length of metacoxal area; MA2, abdominal length bellow metacoxal area; MB, mesothorax length between fore and middle legs, not including mesocoxal areas; MC, mesothorax length in the midline; MeL, mesepimeron length; MeW, mesepimeron width; ML, length of mesocoxal area; PA, pronotal width at the anterior margin; PB, pronotal width at the posterior margin; PL, pronotal length along the midline; SY, shortest width between eyes above the antennae; TL, total body length, not including head and abdomen; VL, length of ventrite I in the midline; VL2, first abdominal sternite at the lateral; WA, width between antennae.

Taxonomy

Scaphisoma nigrofasciatum Pic 1915
(Figs 2–6)

Scaphisoma nigrofasciatum Pic 1915: 31; Achard, 1915: 292 (synonym); Pic, 1916: 49 (valid species); Scott, 1922: 222, (characters); Vinson, 1943: 189 (characters); Löbl, 1971: 974 (lectotype fixed by inference, characters, records); Löbl, 1977: 42 (records); Löbl, 1979: 107 (records); Löbl, 1986: 347 (records); Löbl, 1990: 121 (records); Löbl, 1992: 534 (records); Deepthi *et al*., 2004 (fungal hosts); Lecoq, 2015: 210 (records); Singh and Sharma, 2016: 213 (fungal hosts).

Material examined (n=8, *= abdomen dissected and preserved in glycerin). **Brazil. Minas Gerais:** 2♂♂*, Viçosa, UFV, Vila Gianetti, 26.IV. 2022; E. von Groll leg., Falcon 23 / Em *Inonotus* sp.; (CELC); 1♀* ditto except, 25.III. 2022, E. von Groll leg., Falcon 29 / Em *Inonotus* sp.; 23.XI.2022 (CELC); 1♂*, Oratórios, 10-15.XII. 2021, G.L.N. Martins leg. (CELC). **Sri Lanka: Hanguranketa:** 2♂♂, 27.I.1970 MUSSARD BESUCHET LÖBL / PHOTOGRAPHED E. von Groll Scaphidiinae curation (terminalia embedded in Euparal) (FMNH 4431746-47). **India. Kerala:** 1♂, Cardamom H. Valara Fall 25.XI.72 Besuchet Löbl Mussard / *Scaphisoma nigrofasciatum* Pic det. Löbl 1977 / PHOTOGRAPHED E. von Groll Scaphidiinae curation (FMNH 4431745); 1♂, ditto except, 300m 27–29.XII.93, ca 50 km NW Pathanamthitta, 77°05'E, 9°25'N, Boukal B. & Kejval / PHOTOGRAPHED E. von Groll Scaphidiinae curation (terminalia embedded in Euparal) (FMNH 4431748).

Diagnosis. Length 1.40–1.64 mm. Light brown with squared, hollow black spots on each elytron, occasionally reduced. Pronotum features two lateral spots and two longitudinal bands, varying in intensity, sometimes faint. Parameres of the aedeagus possess a malleable membrane.

Redescription. Length 1.40–1.64 mm. Light brown, more vivid yellow when its alive (Fig. 2A–J). Elytra with squared, hollow black marks, varying in visibility and darkness (Fig. 2A–F). Pronotum with two small lateral black spots, and two central longitudinal bands–more or less marked (Fig. 2A,B—Q–S). Ventral view of the thorax with variable tonalities of brown, specimen-dependent (Fig. 2G,H). First abdominal ventrite darker than the remnants (Fig. 2G,H). Head smooth, finally punctate (Fig. 2I,J); clypeus strigulate microsculptured. Antennae long, IV antennomere 6–7x longer than wide (Fig. 2K–N). Last maxillary palpomere neraly 2x longer than previous (Fig. 2O,P). Pronotum densely punctate, with short and thin setae. Scutellum tip exposed. Elytra more densely and coarsely punctate (Fig. 2Q–S). Sutural striae entire, with a smooth and short curve at the basal region; basal striae absent. Hypomeron smooth, little setose (Fig. 2C). Mesepimeron about 4x wider than long (Fig. 2C,E). Metaventrite punctures fine laterally and very coarse centrally. Row of coarse punctures above the metacoxae present. Submesocoxal lines slightly arcuate; punctate. Submesocoxal area microsculptured; length = 0.06–0.07 mm (Fig. 2C–H). Legs long, slender (Fig. 2D–H). Abdomen, including pygidium, with strigulate microsculpture. Ventrite I densely pubescent; punctures fine laterally and coarse centrally. Submetacoxal lines punctate and arcuate ("check-shaped"); submetacoxal area microsculptured; length = 0.08–0.09 mm (Fig. 2C–H).

Males. Sternite VIII microsculptured; with a posterior round projection (Fig. 3A). Tergite VIII microsculptured; without a posterior projection (Fig. 3B). Tergite IX with translucid border; ventral struts strongly curved, oblong (Fig. 3C). Aedeagus large, strongly sclerotized; curved, in lateral view; anterior region of parameres distinctly sclerotized, bearing a pair of short frontal membranous prominences (Fig. 3A–O). Sclerite of the internal sac "flamingo-shaped" and with other irregular structures (Fig. 3P–R)

Measurements. Antennomeres, Brazil, males (length/width, n= "[#]"): I 7/5 [1]: II 7–8/4–5 [2]: III 2–3/2 [3]: IV 6–7/1 [3]: V 10–13/1–2 [3]: VI 10–11/2 [3]: VII 12–13/3 [3]: VIII 10–11/2 [3]: IX 12–13/3 [3]: X 11–12/2–3 [3]: XI 13–14/3 [2]. Antennomeres, Sri Lanka, male (length; in mm): I = 0.05, II = 0.07, III = 0.02, IV = 0.07, V = 0.11, VI = 0.11, VII = 0.10, VII I= 0.12, IX = 0.09, X = 0.11, XI = 0.13. Body measures, males (in mm; n = "[#]"): TL 1.44–1.64 (1.55 ± 0.08) [5], SY 0.19–0.19 (0.19 ± 0) [2], HW 0.47–0.50 (0.48 ± 0.02) [3], IS 0.23–0.25 (0.24 ± 0.01) [3], WA 0.12–0.16 (0.14 ± 0.02) [3], PL 0.55–0.67 (0.61 ± 0.05) [3], PA 0.44–0.59 (0.50 ± 0.06) [5], PB 0.88–1.02 (0.95 ± 0.05) [5], EI 0.90–1.05 (0.96 ± 0.05) [5], EL 0.98–1.17 (1.07 ± 0.07) [5], EW 0.45–0.66 (0.55 ± 0.08) [5], EH 0.35–0.48 (0.42 ± 0.07) [3], Me 0.29–0.31 (0.30 ± 0.01) [2], MeL 0.16–0.16 (0.16) [2], MeW 0.04–0.07 (0.06 ± 0.02) [2], MB 0.17–0.21 (0.18 ± 0.02) [3], MC 0.45–0.49 (0.46 ± 0.02) [3], ML 0.06–0.07 (0.06 ± 0.01) [3], MA 0.08–0.09 (0.09 ± 0.01) [4], MA2 0.14–0.15 (0.15 ± 0.01) [4], VL 0.26–0.34 (0.29 ± 0.04) [3], VL2 0.30–0.37 (0.33 ± 0.03) [4]

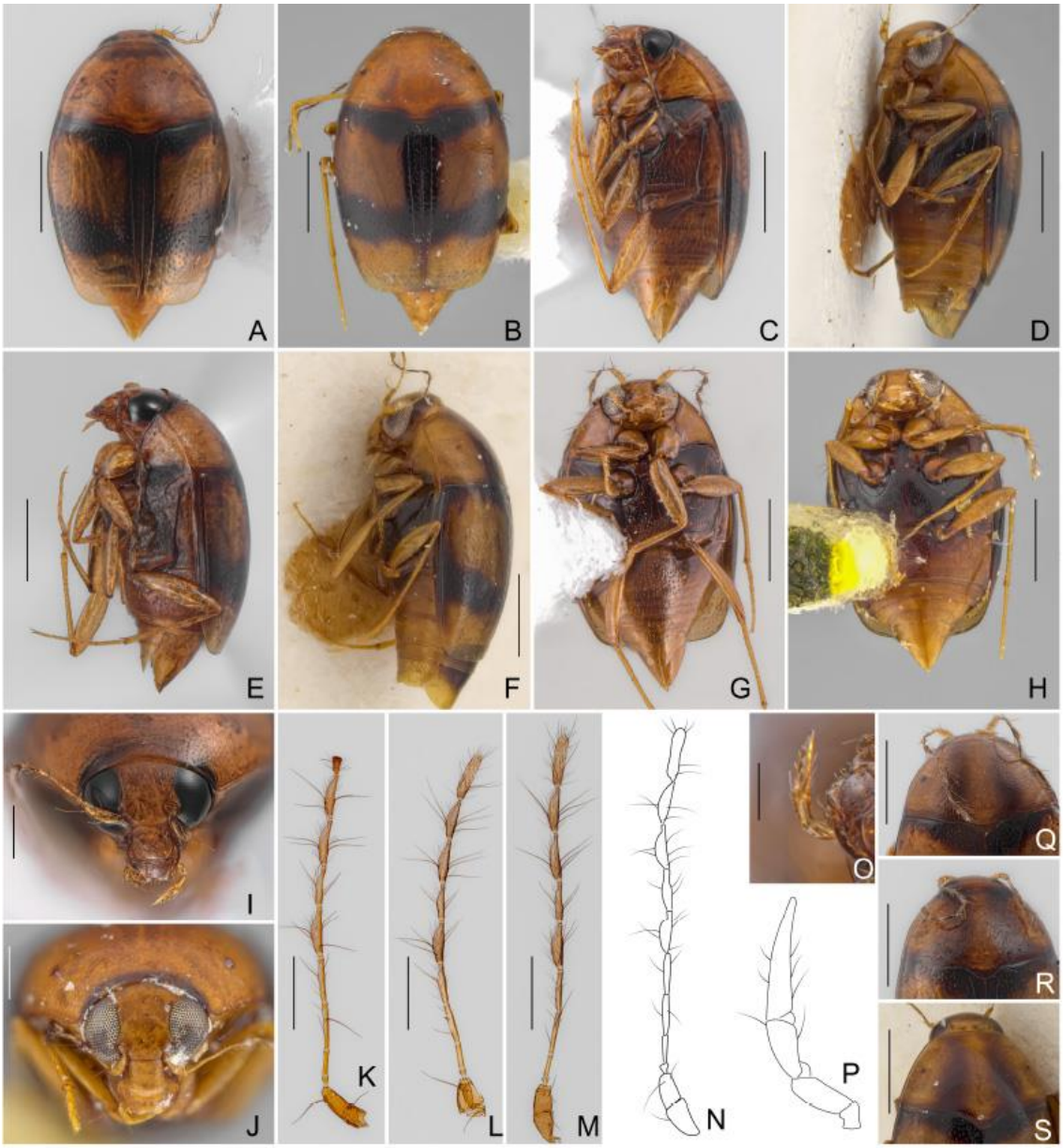

FIGURE 2. *Scaphisoma nigrofasciatum* Pic, 1915. Dorsal view: **A**, male, Brazil; **B**, male India (FMNH 4431748); lateral view: **C**, male, Brazil; **D**, male, Sri Lanka (FMNH 4431747); **E**, male, Brazil; **F**, male, Sri Lanka (FMNH 4431747); **G**, male, Brazil (Oratórios); **H**, male, India (FMNH 4431748); head, frontal view: **I**, male, Brazil; **J**, male India (FMNH 4431748); antenna: **K**, male, Brazil; **L**, female, Brazil; **M**, male, Brazil (Oratórios); **N**, illustration based on Scott 1922: Fig 18; maxillae: **O**, male, Brazil; **P**, illustration based on Scott 1922: Fig 19b; pronotum: **Q**, male, Brazil (Oratórios); **R**, female, Brazil; **S**, male, Sri Lanka (FMNH 4431746). Scale bars: A–H, Q–S: 0.5 mm; I–M: 0.2; P: 0.1 mm.

Females. Sternite VIII with large posterior projection; microsculptured (Fig. 4A). Tergite VIII lacking posterior projection; microsculptured (Fig. 4B). Distal gonocoxite very elongate; gonostylus slender; spermatheca not detected (Fig. 4C,D).

Measurements (n=1). Antennomeres (length/width): III 2/2: IV 7/1: V 10/2: VI 10/2: VII 12/3: VIII 10/2: IX 12/3: X 11/3: XI 13/3; (in mm): TL 1.53, HW 0.45, IS 0.24, WA 0.14, PL 0.63, PA 0.50, PB 0.92, SL0.03, SW 0.03, EI 0.99, EL 1.06, EW 0.55, EH 0.39, Me 0.29, MeL 0.16, MeW 0.05, MB 0.17, MC 0.41, ML 0.06, MA 0.09, MA2 0.15, VL 0.30, VL2 0.30.

Host fungi

In Brazil, specimens were collected from individuals of *Inonotus* sp., affixed on flamboyant trunks (*Delonix regia* (hook.) Raf.) (Fabaceae), along the sidewalk of an avenue (Fig. 5A–C). Additionally, one specimen was collected from *Schizophyllum commune* (Fig. 5D–E). In India, it is considered a pest of oyster mushrooms (*Pleurotus ostreatus*) (Deepthi *et al.*, 2004, Singh & Sharma, 2016).

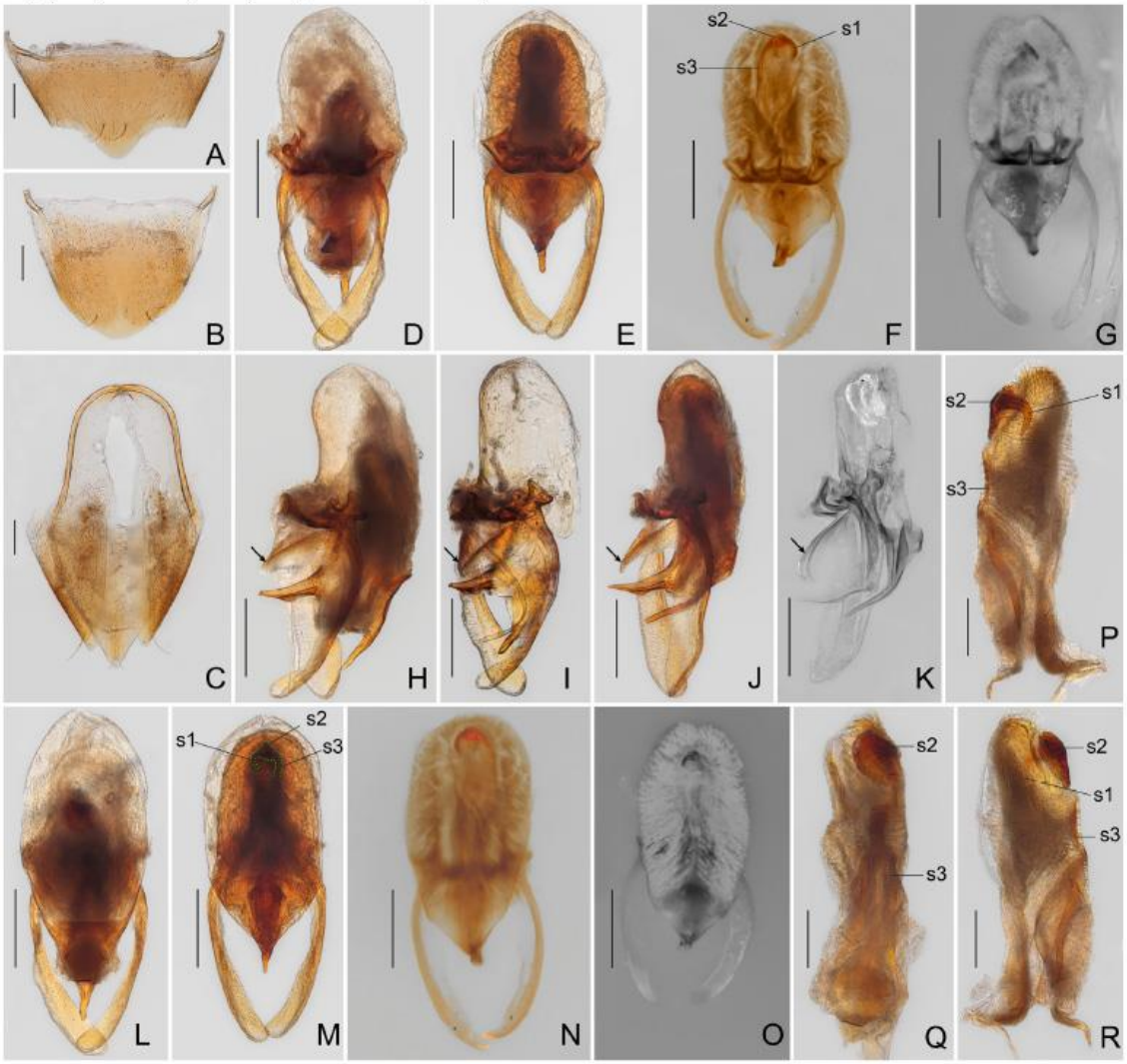

FIGURE 3. *Scaphisoma nigrofasciatum* Pic, 1915. Male: sternites, Brazil: **A**, sternite VIII; **B**, tergite VIII; **C**, tergite IX; aedeagi: frontal view: **D**, Brazil; **E**, Brazil (Oratórios); **F**, India (FMNH 4431745); **G**, Sri Lanka (FMNH 4431746); lateral view: **H**, Brazil, with sclerite; **I**, Brazil, sclerite removed; **J**, Brazil (Oratórios); **K**, Sri Lanka (FMNH 4431747); dorsal view: **L**, Brazil; **M**, Brazil (Oratórios); **N**, India (FMNH 4431745); **O**, India (FMNH 4431745); **P–R**, internal sac, Brazil. Scale bars: A–C, P–Q: 0.1 mm; D–O: 0.2 mm. s1: distal part of the sclerite; s2: middle part of the sclerite; s3: distal part of the sclerite. Arrows: prominences of the aedeagus.

Remarks

Similar to *S. pictum* Motschulsky, 1863 but smaller, with overlapping sizes; the aedeagus of *S. nigrofasciatum* does not form a posterior lobe. Female genitalia exhibit similarities to *S. pandemum* but with straighter and not centrally enlarged distal gonocoxites. Parameres longer compared to *S. binotatum*.

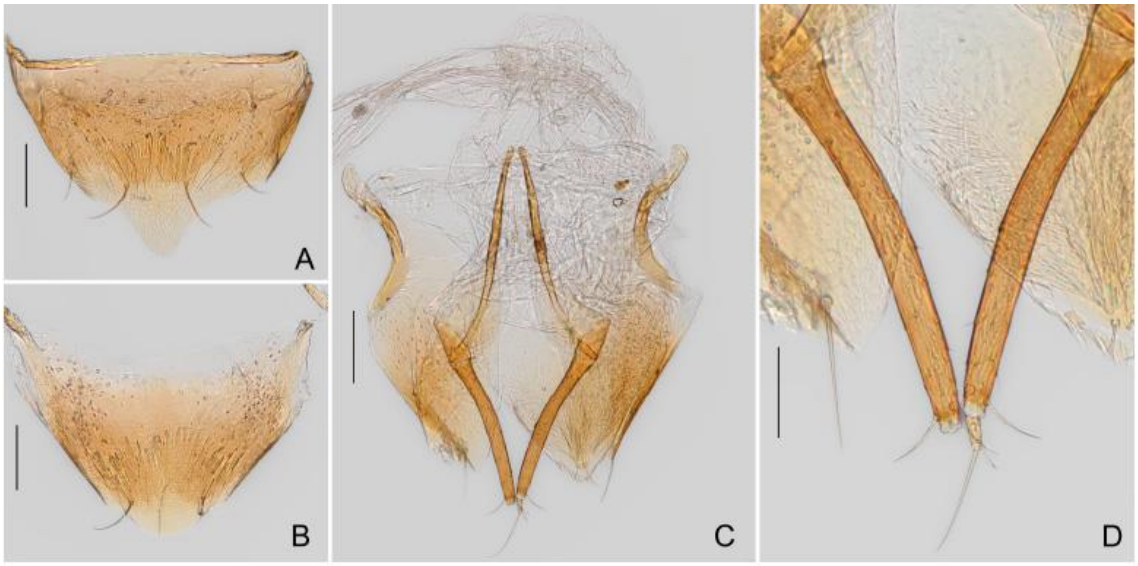

FIGURE 4. *Scaphisoma nigrofasciatum* Pic, 1915. Female: sternites: **A**, ventrite VIII; **B**, tergite VIII; **C**, terminalia; **E**, ovipositor. Scale bars: A–C: 0.1 mm; D: 0.05 mm.

FIGURE 5. A, Host fungus *Inonotus* sp. (Viçosa, Vila Gianetti); **B**, adult of *Scaphisoma nigrofasciatum* on the bottom face of the host; **C**, adult of *Scaphisoma nigrofasciatum* on the down surface of the host; *Schizophyllum commune* Fr. 1821: **D**, view from the top; **E**, gills. Scale bars: 1 cm.

Distribution

India: "Bengalien", Goa, Himachal Pradesh, Kerala, Tamil Nadu, Uttarakhand; Mauritius; Nepal; La Réunion; Seychelles; Sri Lanka; Brazil: Minas Gerais (Viçosa, Oratórios). Fig. 6.

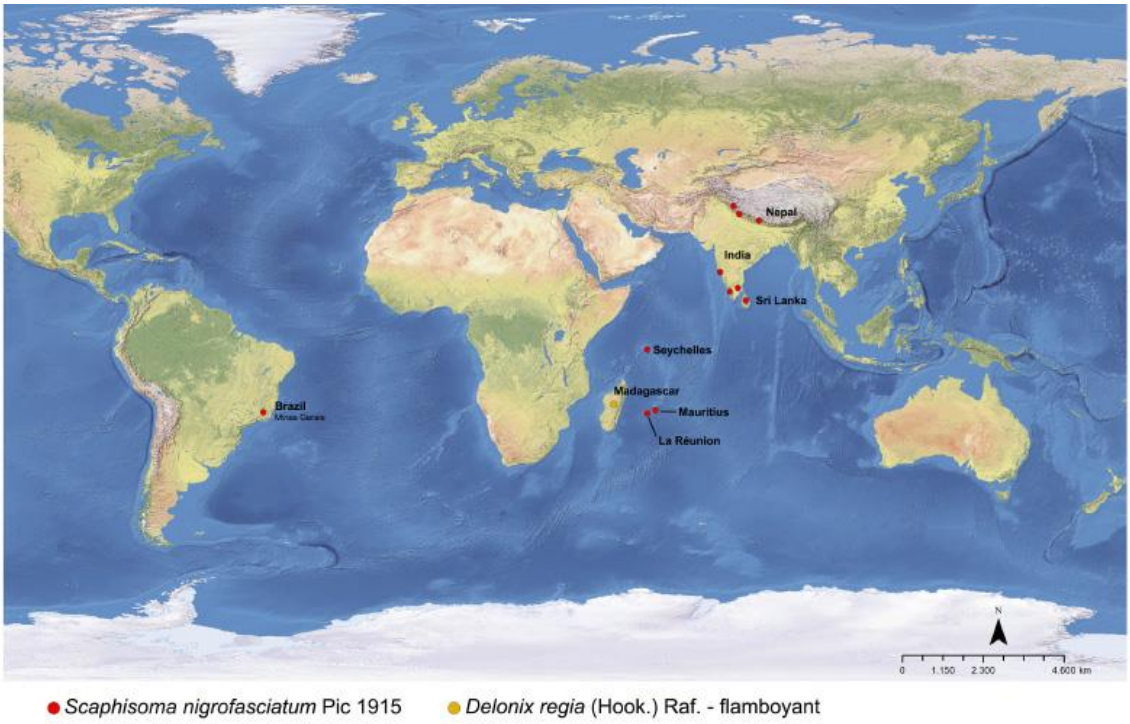

FIGURE 6. Distribution map of *Scaphisoma nigrofasciatum* Pic, 1915 (red dots) and original distribution of *Delonix regia* (hook.) Raf. (orange dot)

Discussion

In Viçosa, Brazil, the area where the beetles were observed is abundant with flamboyant trees, where the fungus *Inonotus* sp. is frequently found on the trunks. This tree originally is from Madagascar and was introduced to Brazil by João VI around the year 1800 (Fig. 6). The mushroom *Schizophyllum commune*, from which one specimen was collected, is recognized as a pioneer in decomposing organic matter. Like *P. ostreatus*, it is edible by humans but not actively cultivated. Furthermore, in some South Asian countries, *S. commune* is commonly used for medicinal purposes (Singh *et al.* 2021).

The primary question regarding distribution revolves around determining the original range of *S. nigrofasciatum*. Given the information provided above and the resemblance of *S. nigrofasciatum* to *S. pictum* and *S. binotatum* Achard, 1915 (two Asian species), it is very likely that the original distribution is in Asia, where the species was initially described. However, several unanswered questions remain.

One of the principal questions concerning Brazilian scaphidiines pertains to their distribution within the Neotropical Region. This subfamily has received limited study in this region, and most collections in Brazil are predominantly confined to Minas Gerais, where these beetles are exceptionally abundant. As a result, it is currently impossible to ascertain whether *S. nigrofasciatum* or any other scaphidiines collected in Minas Gerais also occur in other states or biomes. Prior studies have reported two species of *Cyparium* Erichson, 1845 (*C. collare* Pic, 1920, and *C. oberthueri* Pic, 1956) with a broader distribution in Brazil (von Groll & Lopes-Andrade, 2022), but these observations were made possible only through previous collections.

During the collections, various species of scaphidiines were also observed inhabiting the same fungus, representing different genera such as *Baeocera* Erichson, 1845, and *Toxidium* LeConte, 1860. Interestingly, all of these species exhibited skittish behavior, making it challenging to both photograph and collect them on the same day. Despite the relatively low number of dissected specimens, these observations strongly suggest that they are likely *S. nigrofasciatum*. However, to confirm this information and shed light on the original distribution of the species, DNA analysis would be highly beneficial.

One of the primary challenges encountered when comparing these species was the differing approaches to studying the aedeagal sclerite. While Dr. Löbl describes the sclerites within the aedeagi, I initially removed this structure for

examination. Fortunately, this time, this issue has been addressed. It has become evident that analyzing the sclerite is significantly more straightforward when it remains inflated and inside the aedeagi (Ivan Löbl, personal communication). Therefore, I recommend studying the sclerite using his method for greater accuracy and consistency.

Although *S. nigrofasciatum* is considered a pest of cultivated mushrooms in India, the same does not appear to be the case in Brazil. However, it is essential to note that mushroom cultivation in Brazil is still in its early stages, and the country has stringent regulations in place to ensure the safety of agricultural inputs.

Acknowledgments

I would like to express my gratitude to The Field Museum of Natural History, The Coleopterists Society, and Aperfeiçoamento de Nível Superior (CAPES) for their financial support. Special thanks to Ivan Löbl for providing the Indian specimens to the Field Museum, facilitating my study of this specimen. I extend my appreciation to the Collaborative Invertebrate Laboratories at the Field Museum, Corrie Moreau for granting access to imaging equipment (funded by the National Science Foundation and Negaunee Foundation), and Stephanie Ware for her valuable equipment training and support. I also acknowledge the insightful discussions with Alfred Newton, Margaret Thayer, Ivan Löbl, Bruno de Medeiros, Maureen Turcatel, and laboratory members at the Field Museum regarding specimen distribution. Furthermore, my gratitude goes to Jeferson Müller Timm for fungi identification.

References

Achard, J. (1915) Synonymie de quelques Scaphidiidae (Col.). *Bulletin de la Société entomologique de France*, 1915, 291–292. https://doi.org/10.3406/bsef.1915.25831

Deepthi, S., Suharban, M., Geetha, D. & Sudharma, K. (2004) Pests infecting oyster mushroom in Kerala and the seasonality of their occurrence. *Mushroom Research*, 13 (2), 76–81.

Lecoq, J.-C. (2015) Staphylinidae. *In*: Gomy, Y., Lemagnen, R. & Poussereau, J. (Eds.), *Les Coléoptères de l'île de La Réunion*. Editions Orphie, Saint-Denis, pp. 1–5 + 169–232.

Löbl, I. (1971) Scaphidiidae von Ceylon (Coleoptera). *Revue suisse de zoologie*, 78, 937–1006. https://doi.org/10.5962/bhl.part.97084

Löbl, I. (1977) Les Scaphidiidae (Coleoptera) de l'île de la Réunion. *Nouvelle Revue d'entomologie*, 7, 39–52.

Löbl, I. (1979) Die Scaphidiidae (Coleoptera) Südindiens. *Revue suisse de zoologie*, 86, 77–129. https://doi.org/10.5962/bhl.part.82281

Löbl, I. (1986) Contribution a la connaissance des Scaphidiidae (Coleoptera) du nordouest de l'Inde et du Pakistan. *Revue suisse de zoologie*, 93, 341–367. https://doi.org/10.5962/bhl.part.79699

Löbl, I. (1990) Contribution a la connaissance des *Scaphisoma* (Coleoptera, Scaphidiidae) de l'Himachal Pradesh, Inde. *Archives des sciences*, 43, 117–123.

Löbl, I. (1992) The Scaphidiidae (Coleoptera) of the Nepal Himalaya. *Revue suisse de zoologie*, 99, 471–627. https://doi.org/10.5962/bhl.part.79841

Pic, M. (1915) Diagnoses de nouveaux genres et nouvelles espèces de Scaphidiides. *L'Echange, Revue linnéenne*, 31, 30–32.

Pic, M. (1916) Notes relatives à divers Scaphidiidae (Col.). *Bulletin de la Société entomologique de France*, 1916: 49. https://doi.org/10.3406/bsef.1916.25862

Scott, H. (1922) The Percy Sladen Trust Expedition to the Indian Ocean in 1905, under the leadership of Mr. J. Stanley Gardiner, M.A. Vol. VII. no. IV- Coleoptera: Scydmaenidae, Scaphidiidae, Phalacridae, Cucujidae (Supplement), Lathridiidae, Mycetophagidae (including Propalticus), Bostrychidae, Lyctidae. *Transactions of the Linnean Society of London, 2nd Ser. Zoology*, 18 (1), 195–260, 19–22. https://doi.org/10.1111/j.1096-3642.1922.tb00550.x

Singh, S., Raj, C., Singh, H.K., Avasthe, R.K., Said, P., Balusamy, A., Sharma, S.K., Lepcha, S.C. & Kerketta, V. (2021) Characterization and development of cultivation technology of wild split gill *Schizophyllum commune* mushroom in India. *Scientia Horticulturae*, 289, 110–399. https://doi.org/10.1016/j.scienta.2021.110399

Singh, U A. & Sharma K. (2016) Pest of mushroom. *Advances in crop science and technology,* 4 (2), 213.

Vinson, J. (1943) The Scaphidiidae of Mauritius. *Mauritius Institut Bulletin* 2: 177–209.

von Groll, E. & Lopes-Andrade, C. (2021) *Scaphisoma pandemum* sp. nov. Coleoptera: Staphylinidae: Scaphidiinae) from the Atlantic Forest of Southeast Brazil. *Zootaxa,* 4999 (2), 143–156. https://doi.org/10.11646/zootaxa.4999.2.4

von Groll, E. & Lopes-Andrade, C. (2022) Contributions to the taxonomy of Neotropical *Cyparium* Erichson (Coleoptera: Staphylinidae: Scaphidiinae), with the description of five new species. *European Journal of Taxonomy,* 835, 1–97. https://doi.org/10.5852/ejt.2022.835.1909

CAPÍTULO 5 – New species of Scaphidiinae (Coleoptera: Staphylinidae) from remnants of the Atlantic Forest in Minas Gerais, southeastern Brazil, with host associations, and an illustrated key to the Brazilian genera

To be published in the European Journal of Taxonomy.

New species of Scaphidiinae (Coleoptera: Staphylinidae) from remnants of the Atlantic Forest in Minas Gerais, southeastern Brazil, with host associations, and an illustrated key to the Brazilian genera

Elisa VON GROLL

Programa de Pós-Graduação em Biologia Animal, Universidade Federal de Viçosa, Av. Peter Henry Rolfs, s/n, 36570-900, Viçosa, MG, Brasil

elisavgroll@gmail.com

https://orcid.org/0000-0002-6563-8684

Running title: **New Brazilian Scaphidiinae species (Coleoptera)**

The present paper has not been submitted to another journal, nor will it be in the 6 months after initial submission to EJT. All co-authors are aware of the present submission.

Abstract

Description 20 new species, distributed in five genera, of Scaphidiinae collected in remnants of Atlantic Forrest in Minas Gerais, southeast region of Brazil, are described, as follows: *Cyparium* sp. nov., *Alexidia* sp. nov. 1, *Alexidia* sp. nov. 2 *Baeocera* sp. nov. 1, *Baeocera* sp. nov. 2, *Baeocera* sp. nov. 3, *Baeocera* sp. nov. 4, *Baeocera* sp. nov. 5, *Baeocera* sp. nov. 6, *Scaphisoma* sp. nov. 1, *Scaphisoma* sp. nov. 2, *Scaphisoma* sp. nov. 3, *Scaphisoma* sp. nov. 4, *Toxidium* sp. nov. 1, *Toxidium* sp. nov. 2, *Toxidium* sp. nov. 3, *Toxidium* sp. nov. 4, *Toxidium* sp. nov. 5, *Toxidium* sp. nov. 6, *Toxidium* sp. nov. 7. Descriptions include host associations for all species, illustrations of the external and internal morphology of adult males and females, whenever it is possible. An illustrated key to the Brazilian genera and their respective diagnoses is provided.

Keywords: shining rove beetles, fungus, morphology, diversity, Neotropical Region.

Introduction

Scaphidiinae is a clade within the family Staphylinidae that includes more than 2,000 described species (Löbl 2018). These beetles are worldwide distributed, particularly in tropical and subtropical forests (Leschen & Löbl 1995). They are usually collected from fungi and slime molds, by sifting litter or by using flight intercept traps (Lawrence & Newton 1980; Newton 1984; Leschen 1994; Stephenson *et al.* 1994; Löbl & Leschen 2003b; Tang *et al.* 2014; Löbl 2018; Löbl *et al.* 2021).

Although the Neotropical Region has the main characteristics of housing scaphidiines, it encompasses about only 200 species (of the known 2,000). In Brazil, the situation is particularly worse, and despite the large forest areas, the country counts with only 41 known species, distributed among the following seven genera: *Cyparium* Erichson, 1845 (13 spp.), *Scaphidium* Olivier, 1790 (12 spp.), *Alexidia* Reitter, 1880 (1 sp.), *Amalocera* Erichson, 1845 (5 spp.), *Baeocera* (1 sp.), *Scaphisoma* Leach, 1815 (7 spp.), *Toxidium* LeConte, 1860 (1 sp.) (Löbl 2018; von Groll & Lopes-Andrade 2021, 2022; von Groll 2023).

Previous studies have shown that this low number is unrelated to the absence of these beetles in Brazil (von Groll & Lopes-Andrade 2021). This fact is more likely related to the lack of interest in studying them – as it is more common to find specimens of these beetles in miscellaneous collections, both alcohol or dry (pers. obs.). Nonetheless, the beetles in miscellaneous collections are usually collected using generic methods (e.g. FIT), which does not allow host associations.

In this paper, I aim to enhance understanding of the Brazilian shining fungus beetle's fauna, focusing on specimens collected directly from the hosts during 2018–2023 (with a few exceptions) in remnants of the Atlantic Forest in Minas Gerais, southeastern Brazil. Hence, at first, an illustrated key to the seven Brazilian genera is provided, along with descriptions of these genera. Furthermore, 20 new species distributed across five genera are described as follows: *Cyparium* (1 sp. nov.), *Alexidia* (2 spp. nov.), *Baeocera* (6 spp. nov.), *Scaphisoma* (4 spp. nov.), and *Toxidium* (7 spp. nov.). Descriptions include host information, colored plates illustrating the internal and external morphology of males and females (when available), and detailed measurements of the specimens. Finally, an updated checklist of the Brazilian species is provided.

Material and methods

The studied material is deposited at the Entomological Collection of the Laboratory of Systematics and Biology of Coleopter, UFV, Viçosa, Minas Gerais, Brazil (CELC). Specimens were collected during expeditions that took place between 2019 and 2023 in Viçosa, in the state of Minas Gerais, southeastern Brazil (with few exceptions):

(1) Viçosa, "Mata da Biologia" (20°45′32"S, 42°51′49"W; 75 ha. of Atlantic Forest) (Fig. 1A–D);
(2) Viçosa, "Vila Gianetti" (20°45′16"S, 42°52′21"W; sidewalk in front of an avenue) (Fig. 01A,B,E,F);
(3) Viçosa, "Estação de Pesquisa, Treinamento e Educação Ambiental Mata do Paraíso (EPTEA)" (20°48′05″ S, 42°51′58″ W; 194 ha. of Atlantic Forest) (Fig. 1A,B,G); and
(4) Parque Estadual da Serra do Brigadeiro, city of Araponga (20°39′54"S, 42°31′18"W; 14.984 ha. of Atlantic Forest) (Fig. 1A,B).

Scaphisomatiini beetles from Viçosa (*Alexidia*, *Baeocera*, *Scaphisoma*, and *Toxidium*) were collected using a DIY mouth aspirator (Fig. 1G) directly from the host. The single *Cyparium* specimen was collected manually. The collection method used to collect the specimens of *Toxidium* from Araponga is unknown. These specimens were included in this manuscript because other individuals belonging to the same species were collected during the same expeditions cited above.

After the collection, beetles were kept in the freezer for a few hours, mounted on card triangles, and then dried in a stove for approximately 24 hours. They were then labeled, sorted by genera, and kept in drawers containing camphor. Primary identifications were conducted using original descriptions and generic keys from the following Leschen & Löbl (2005), and supplemented by personal communication with Dr. Ivan Löbl.

For the dissections, beetles were immersed in warm water until the tissues were softened. Larger parts were separated and then, boiled in a solution of KOH for tissue clarification. After that, the structures were placed in 10% acetic acid and washed in water. Subsequently, the small structures were dissected and photographed in temporary slides using glycerin or KY®. After the process, the parts were washed and kept in genitalia vials or 0.2 ml Eppendorf's containing glycerin. Photographs follow von Groll & Lopes-Andrade (2022).

Measurements were taken using a Zeiss Stemi 2000C stereomicroscope equipped with a 2× objective lens and an ocular micrometer. Legs and antennae were photographed using a Zeiss AxioLab microscope equipped with a digital camera, and digitally measured, using the software tpsDig2 ver. 2.32. Range, mean and standard deviation values were estimated using PAST. Results of measurements are provided in ratio for the antennomeres, and millimeters (mm) for the others. Abbreviations follow von Groll (2023) and von Groll and Lopes-Andrade (2021).

Maps were generated using ArcGIS 10.8, and the coordinates were obtained via Google Earth Pro. Illustrations for the identification key were produced in Adobe Illustrator 2023, based on photos provided in this paper, except for (1) *Alexidia* sp., dorsal (based on a photo taken of a specimen deposited at CELC); (2) *Scaphidium peckorum* Fierros-López, 2005, frontal (based on a photo of the holotype deposited in the Field Museum of Natural History, available at https://collections-zoology.fieldmuseum.org/); and (3) antenna of *Scaphidium* (based on Fierros-López 2005, fig. 11). Plates were created using Adobe Photoshop CC 2018.

The following code is used in the "material examined" sections: "*", for specimens with the abdomen and genitalia removed, and "**" for entirely dissected beetles. All dissected parts are preserved genitalia vial or an Eppendorf, filled with glycerin, and pinned along with the beetle. All paratypes are labeled "PARATYPUS + '♂' / '♀'", or just "PARATYPUS" – when the sex is unknown – in yellow paper. All holotypes are labeled "HOLOTYPUS ♂", in red paper, except for *Alexidia* sp. 2, which still needs a "HOLOTYPUS ♀" label.

The key is based on Leschen and Löbl (1995, 2005), and the general descriptions for the Brazilian genera follow Löbl & Leschen (2003), Leschen & Löbl (2005), complemented by specific papers mentioned after each description. Terminology follows Ogawa & Löbl (2013) for external morphology, and male and female terminalia; Naomi (1988a, 1988b), Leschen *et al.* (1990), Leschen & Löbl (2005), Lawrence & Ślipiński (2013), and von Groll & Lopes-Andrade (2022) for external morphology; Harris (1979) for microsculpture; Jałoszyński (2012) for the internal structure of the prothorax; Friedrich & Beutel (2006) for the mesonotum; Lawrence *et al.* (2021) for the hind wing venation; Crowson (1938), Naomi (1989a), and Hübler & Klass (2013), von Groll & Lopes-Andrade (2022) for the metendosternite; Naomi (1989b) for the abdominal segments; and Naomi (1990) for male terminalia.

Results

Key to the Scaphidiinae genera occurring in Brazil.

1. Antennae robust; antennomeres 7–11 forming a distinct club (Fig. 2A,B) …….. 2

– Antennae slender; antennomeres 7–11 slender, forming a loose club (Fig. 2C,D) ……...3

2(1). Eyes emarginate near antennal insertion (Fig. 2E), tibiae smooth (not spinose) ……..……..…….…… *Scaphidium* Olivier, 1790.

– Eyes not emarginate near antennal insertion (Fig. 2F), tibiae spinose (Fig. 2G) …..……..…….. *Cyparium* Erichson, 1845.

3(1). Profemora with ctenidium (Fig. 2H) ……...…… 4

– Profemora without ctenidium ……...……5

4(3). Antennomere 3 short, triangular (Fig 2C); last apical palpomere normal (almost the same width as previous and gradually tapering towards the apex) (Fig. 2I) ……...…… *Scaphisoma* Leach, 1815.

– Antennomere 3 not distinctly shorter than 4 (Fig. 2D); last apical palpomere aciculate (much narrower than the previous or abruptly narrowed at the apex) (Fig. 2J) …….……..… *Baeocera* Erichson, 1845.

5(3). Body laterally compressed, strongly convex dorsally (in lateral view) (Fig. 2K); elytral basal striae absent; maxillary palpi normal (Fig. 2I) …….. …….……...……. *Toxidium* LeConte, 1860.

– Body not compressed laterally, and just normally convex dorsally (in lateral view); elytral basal striae present (Fig. 2L,M) ……. 6

6(5). Scutellum visible in dorsal view (Fig. 2L); mesotibiae with two inner apical spines (Fig. 2N); prothoracic corbiculum absent ……. *Amalocera* Erichson, 1845.

– Scutellum concealed in dorsal view (Fig. 2M); mesotibiae with just one inner apical spine (Fig. 2O); prothoracic corbiculum present (Fig. 2P) ……... *Alexidia* Reitter, 1880.

Descriptions of new species

Class Insecta Linnaeus, 1758

Order Coleoptera Linnaeus, 1758

Family Staphylinidae Latreille, 1802

Subfamily Scaphidiinae Latreille, 1806

Tribe Cyparіini Achard, 1924

Genus ***Cyparium*** Erichson

(Figs 2A,F,G, 3–5)

Cyparium Erichson, 1845: 3. Type species: *Cyparium palliatum* Erichson, 1845; by monotypy.
Yparicum Achard, 1920: 126. Type species: *Yparicum yunnanum* Achard, 1920; by monotypy.

Cyparium, the only genus of the Cyparіini tribe, comprises 68 species (63) and subspecies, with the majority found in the Neotropical Region (26), including 14 species described in Brazil. While it was once considered "notably absent from southern South America, the western part of the Palaearctic, and Australia" (Löbl & Leschen 2003b), it is now understood that the low number of species in Brazil is a result of the lack of studies/collections involving Scaphidiinae (von Groll & Lopes 2022). Throughout my field trips in Minas Gerais, Brazil, it was very common to collect specimens of *Cyparium*. Although this paper counts with the description of just one new species, it should be noted that several others have been collected and await to be studied.

General Description

HEAD. Mandible with two apical teeth and subapical serrations present on the left mandible. Maxillary palp normal. Galea narrow, with paniculate brush. Inner and basal setae of lacinia absent. Last labial palp straight. Eyes anteriorly entire, not notched. Antennae clubbed; antennomeres VII–XI symmetrical. PROTHORAX prothoracic corbiculum absent. Hypomeron visible in lateral view; apex acute and not extending beyond pronotum. MESOTHORAX. Mesoventral lines impunctate. Secondary lines present. Scutellum visible in dorsal view. Mesoventral process carinate. Mesepimeron absent. Meso- and metaventrite separate. METATHORAX. Submesocoxal lines parallel to coxae, punctate. Metaventral setose patch absent. Primary seta present. WINGS. Sutural and apical serrations of the elytra present. Lateral stria present. LEGS. Profemoral ctenidium absent. Tibiae spinose. Mesotibiae with two inner apical spines, equal in length. ABDOMEN. Submetacoxal bead on abdominal process absent. Submetacoxal space absent. (Leschen & Löbl 2005).

***Cyparium* sp. nov.**

(Figs 2A,F,G, 3–5)

Diagnosis

Body length: 4.40 mm, robust, black, laterals of pronotum, hypomere and humeral region reddish; very shining. Seven rows of coarse elytral punctures. Lacking microsculpture. Medium lobe strongly curved in lateral view; parameres thin.

Etymology

Material examined

Holotype

BRAZIL • ♂*; Minas Gerais, Viçosa, Mata da Biologia; 15 May. 2021; E. von Groll & A. Orsetti leg.; Fungo 44 / Em *Agaricales* indet. / Dissecado em 15.xii.2022 / HOLOTYPUS ♂; CELC. (Fig. 3D,E).

Description

COLORATION. Black. Humeral region, laterals of pronotum and hypomeron reddish (Figs 3A–C,F, 4A,B). Legs dark red-purplish (Fig 4C–E). Antennomeres I–VI and XI, mouthparts, and tarsi ochreous (Figs 3F, 4F–H).

HEAD. Frons with dense and coarse punctate; eyes prominent (Fig. 3F). Antennomeres VIII–XI wide; ratios: I 127/45: II 83/38: III 86/33: IV 63/36: V 55/40: VI 40/46: VII 69/85: VIII 62/93: IX 70/102: X 67/110: XI 103/112 (Fig. 3G).

THORAX. Pronotum coarse and shallowly punctate (less than frons) (Fig. 4A). Hypomeron smooth (Fig. 4B). Scutellum rounded posteriorly (Fig. 4A). Ventral sclerites of the thorax smooth and almost glabrous; metaventrite with few coarse punctures laterally (Figs 4B,C, 4B). Submesocoxal lines parallel to coxae, coarse punctate (Fig. 4B).

WINGS. Elytra rectangular, longer than larger; sutural and basal striae connected; basal stria punctate, reaching almost middle of elytra (Fig. 3A). Seven rows of coarse punctures (Fig. 3A). Epipleuron coarsely punctate (Fig. 4B). Apical spines small (Fig. 4K).

LEGS. Femora sparsely and coarsely punctate (Fig. 4C–E). Meso- and metatibiae curved (Fig. 4D,E), with two large apical spines (Fig. 4I,J).

ABDOMEN. Abdominal ventrite I coarsely punctate, denser laterally; submetacoxal bead with close and coarse punctures (Figs 3B,C, 4B). Propygidium and pygidium micropunctured and with coarse punctures; disc with strigulate microsculpture anteriorly (Fig. 4L). Sternite VIII rectangular with a rounded projection (Fig. 5A). Tergite VIII wide and rounded (Fig. 5B). Tergite IX with rectangular-shaped ventral struts (Fig. 5C). Tergite X (Fig 5D) longer than wider. Sternite IX thicker posteriorly (Fig. 5E).

Male

AEDEAGUS. Strongly sclerotized. Basal bulb robust; apical lobe curved, in lateral view (Fig. 5F–H); dorsal openings forming an upside-down triangle (Fig. 5H). Parameres thin and short (Fig. 5F,G). Internal sac with irregular sclerites (Fig. 5I–K).

MEASUREMENTS (n = 1; in mm): TL 4.40, SY 0.37, HW 1.09, IS 0.44, WA 0.27, PL 1.56, PA 1.41, PB 2.75, SL 0.24, SW 0.28, EI 2.70, EL 3.12, EW 1.60, EH 1.09, MSW 0.55, MEL 0.31, MEW 0.13, MB 0.71, MC 1.22, VL 1.00, VL2 0.66. Legs: PrF 1.53, PrT 0.91, MsF 1.34, MsT 1.09, MtF 1.59, MtT 1.56.

Host

Found alone under an undetermined mushroom on the border of the field trail (Fig 93A–B)**.**

Remarks

Humeral reddish area similar to *C. pici* von Groll & Lopes-Andrade, 2021 and *C. loebli* von Groll & Lopes-Andrade, 2021 but differ by the larger size and the pronotal lateral reddish marks. Pronotum similar to *C. anale* Reitter, 1880 but elytra different. Aedeagus similar to *C. pici* but less robust and sclerites in a different shape. Aedeagus is also similar to *C. lescheni* von Groll & Lopes-Andrade, 2021 but larger and more robust.

Distribution

Mata da Biologia, Universidade Federal de Viçosa, campus of Viçosa, state of Minas Gerais, Southeast Brazil (Fig. 1A–D).

Scaphidiini Latreille, 1806

Genus ***Scaphidium*** Olivier

(Fig. 2B,E)

Scaphidium Olivier, 1790: 20: 1. Type species: *Scaphidium quadrimaculatum* Olivier, 1790; fixation by Latreille, 1810.
Ascaphidium Pic, 1915a: 24. Type species: *Ascaphidium sikorai* Pic, 1915; by monotypy.
Cribroscaphium Pic, 1920b: 93 (subgenus of *Scaphidium*). Type species: *Scaphidium irregulare* Pic, 1920; by monotypy.
Hemiscaphium Achard, 1922a: 12. Type species: *Scaphidium striatipenne* Gestro, 1879; by original designation.
Hyposcaphidium Achard, 1922a: 12 (subgenus of *Scaphidium*). Type species: *Scaphidium rufopygum* Lewis, 1893, designated by Löbl, 2015: 21.
Isoscaphium Achard, 1922a: 12 (subgenus of *Scaphidium*). Type species: *Scaphidium quadriguttatum* Say, 1823, designated by Löbl, 2015: 21.
Pachyscaphidium Achard, 1922a: 12 (subgenus of *Scaphidium*). Type species: *Scaphidium arrowi* Achard, 1920; by monotypy.
Scaphidiolum Achard, 1922a: 12. Type species: *Scaphidium basale* Laporte, 1840; by original designation.
Scaphidopsis Achard, 1922a: 12. Type species: *Scaphidium pardale* Laporte, 1840; by original designation.
Falsoascaphidium Pic, 1923: 16. Type species: *Scaphidium subdepressum* Pic, 1921; by original designation.
Parascaphium Achard, 1923: 97. Type species: *Scaphium optabile* Lewis, 1893; by monotypy.

There are 13 known *Scaphidium* species to Brazil. During my field trips, it was possible to collect only one specimen, *Scaphidium* cf. *gounellei*. Nonetheless, this single specimen was not included in this manuscript.

General description

HEAD. Mandible with two apical teeth and serrations present. Maxillary palp normal. Galea wide with radulate brush. Inner and basal setae of lacinia present. Last labial palp straight. Eyes anteriorly notched. Antennae clubbed; antennomeres VII–XI symmetrical. PROTHORAX prothoracic corbiculum absent. Hypomeron visible in lateral view; apex subacute and not extending beyond pronotum. MESOTHORAX. Mesoventral lines impunctate. Secondary lines present. Scutellum visible in dorsal view. Mesoventral process carinate. Mesepimeron absent. Meso- and metaventrite separate. METATHORAX. Submesocoxal lines parallel to coxae. Metaventral setose patch present. Primary seta absent. WINGS. Sutural and apical serrations of the elytra present. Basal stria absent; lateral stria present. LEGS. Profemoral ctenidium absent. Tibiae smooth. Mesotibiae with two inner apical spines, equal in length. ABDOMEN. Submetacoxal bead on abdominal process absent. Submetacoxal space absent. (Leschen & Löbl 2005).

Tribe Scaphisomatini Casey, 1893

Genus ***Alexidia*** Reitter

(Figs 2M,O,P, 6–13)

Alexidia Reitter, 1880: 43. Type species: *Alexidia rogenhoferi* Reitter, 1880; by monotypy.

Alexidia comprises four species, all of them distributed at the Neotropical Region. Only *Alexidia plaumanni* Löbl & Leschen, 2003a is registered to Brazil (state of Santa Catarina). During my field trips, two species of *Alexidia* were discovered and are described here. *Alexidia* sp. nov. 1 is represented by 19 specimens, and *Alexidia* sp. nov. 2 by a single female. No more specimens belonging to this genus were collected.

General description

Body large, oval. HEAD. Labral setae present. Mandible apically bidentate (Fig. 7B,C). Maxillary palp aciculate (Fig. 7D). Galea wide, with radulate brush (Fig. 7D). Inner and basal setae of lacinia absent (Fig. 7D). Setae on adoral surface of hypopharynx spinose (Fig. 7E,F). Last labial palpomere curved (Fig. 7E,F). Submaxillary ducts present (Fig. 7G). Gular suture not reaching the submentum. Frontoclypeal suture present (Fig. 6H, 12E). Antennomeres III and IV elongate; VII–X with a long apical stalk (Figs 6J,K, 12F). PROTHORAX. Prothoracic corbiculum present (Fig. 7L). Hypomeron visible in lateral view; apex subacute and not extending beyond pronotum (Figs 6B, 12B). MESOTHORAX. Mesoventral lines impunctate and connected to the mesocoxal cavity (Fig. 8D). Median and secondary lines absent. Prepectus present. Scutellum concealed in dorsal view (Fig. 8A,B). Mesoventral process paxillate (Fig.8G). Meso- and metaventrite not fused (Fig. 8D). METATHORAX. Submesocoxal lines arcuate (Figs 8F, 12D). Metaventral setose patch absent (Fig. 8E). Intercoxal plates present. WINGS. Elytra lacking apical serrations (Figs 9H, 12H); basal and lateral striae present (Fig. 8A). LEGS. Profemoral ctenidium absent. Mesotibiae with a single inner apical spine (Fig. 9E) ABDOMEN. Submetacoxal bead meeting in the middle; punctate (Fig. 8E). Submetacoxal area absent. MALES. Aedeagal sclerites tripartite (Fig. 10E–J). (Löbl & Leschen 2003b; Leschen & Löbl 2005).

Alexidia **sp. nov. 1**

(Figs 6–11)

Diagnosis

Body length: 1.41–1.55 mm. Oval, in dorsal view, and convex in lateral. Brown to dark brown, edges of some sclerites reddish; shining. Sutural, basal, and lateral striae joined. Almost glabrous and lacking coarse punctures. Submetacoxal area short.

Etymology

Material examined

Holotype

BRAZIL • ♂; Minas Gerais, Viçosa, EPTEA Mata do Paraíso; 24 Mar. 2022; E. von Groll *et al.* leg.; Fungo 20 / Em *Ceratiomyxa fruticulosa* em Pinus / HOLOTYPE ♂; CELC. (Fig. 6D,E).

Paratypes

BRAZIL • 1 ex.; same locality as for holotype; 12 Nov. 2019; Leg. LabCol; Fungo 10 / Em *Ceratiomyxa fruticulosa*; CELC • 6♂♂, 7♀♀ (1♂*, 1♂**, 1♀**,); same locality as for holotype; 10 Mar. 2022; Leg. LabCol, Falcon 26 / Em *Ceratiomyxa fruticulosa* em Pinus; CELC • 1♂, 1♀; same locality as for holotype; 24 Mar. 2022; E. von Groll *et al.* leg.; Fungo 20 / Em *Ceratiomyxa fruticulosa* em Pinus; CELC • 1♂, 1♀; same locality as for holotype; 14 Apr. 2022 Leg. LabCol; Falcon 42 / Em *Ceratiomyxa fruticulosa* em Pinus; CELC.

Description

COLORATION. Dark brown, edges of some sclerites reddish; distal part of femora and tibiae lighter, tarsi, mouthparts and antennomeres I–VI yellow (Fig. 6A–C,H). Variation: light brown and not reddish (Fig. 6F,G).

HEAD. Frons smooth, subglabrous, devoid of punctures (Fig. 6H). Clypeus longer than wide (Fig. 6H,I). Labrum rounded apically (Fig. 7A). Mandible elongate (Fig. 7B,C). Last maxillary palpomere 1.70× longer than previous (Fig. 7D). Terminal labial palpomere not strongly curved (Fig. 7E,F). Mentum laterally constricted (Fig. 7F). Three submaxillary ducts (Fig. 7G). Gular region with strigulate microsculpture and few and sparse gular pores; gular suture short, more than 2× distant from the submentum (Fig. 7G). Antennomeres VIII, IX, and XI slender.

Antennomeres proportions (n = 2): I 98/32: II 88/36: III 56/16: IV 84/16: V 98/17: VI 89/17: VII 97/25: VIII 77/17: IX 112/27: X 105/35: XI 113/35 (Fig. 6J,K).

PROTHORAX. Smooth, lacking microsculpture (Figs 6A,F, 7H,I, 11A). Pronotum strongly curved, in lateral view (Figs 6B,G, 11B); punctation very fine; pubescence sparse and short; posterior angles not trespassing mesenepisternum. Hypomeron almost glabrous (Figs 6G, 11C). Notosternal suture curved inward (Fig. 7J). Prosternal process long and acute (Fig. 7K). Profurca thin and elongate (Fig. 7L). Prothoracic corbiculum shortly pubescent (Fig. 7L).

MESOTHORAX. Lacking microsculpture, almost glabrous (Figs 6B,G, 8E,F, 11B,C). Scutellar lines straight in the middle and forming two lateral lobes (Fig. 8C). Mesepimeron short and oblique (Fig. 8F). Procoxal rests triangular, wide (Fig. 8D). Mesoventral lines oblique (Fig. 8D). Median and secondary lines absent. Mesoventral process wavy (Fig. 8G).

METATHORAX. Metaventrite smooth, devoid of punctures; pubescence sparse (Figs 6B,G, 8E,F, 11B,C). Submesocoxal lines punctate; submesocoxal area micropunctured; length: 0.04–0.05 (Figs 6A,G, 8F, 11C). Metanepisternum mostly covered by elytra (Figs 6A,G, 8F, 11C). Metanotum with alacrista triangular and wide; median membranous area wide; scutoscutellar suture oval and flattened (Fig. 8H). Metepimeron distinct, smooth. Intercoxal plates rectangular (Figs 6A,G, 8F, 11B,C). Metendosternite thick, stalk, and ventral longitudinal flange elongate (Fig. 8I–K).

WINGS. Elytra wider anteriorly; shining; lacking microsculpture; finely punctate; moderately pubescent (Figs 6A,F, 8L,M, 11A). Sutural striae connected to the basal striae and then, to the lateral striae (Figs 6A,B,F,G, 7H). Adsutural area wider near the posterior 2/3. Epipleura impunctate (Fig. 8F). Hind wings fully developed (Fig. 9A).

LEGS (Figs 9B–G, 11D–I). Pro- and mesofemora sparse and coarsely punctate. Femora narrow. Meso- and metatibiae bearing a long apical spine.

ABDOMEN. Subglabrous, shining; primary setae present. Lateral of ventrite I and tergite VI with micropuncture (6B, 11B). Tergite VI bearing few setae (Figs 9H, 11J).

Males

Antennae slightly thinner than females (Fig. 6J). Pro- and mesotarsomeres I–III slightly widened, bearing tenent setae (Fig. 9C,E). Metatibia arcuate (Fig. 9F). Ventrite VIII with a short posterior projection (Fig. 9I); tergite VIII straight posteriorly (Fig. 9J); both tergite and ventrites VIII punctate and not microsculptured. Tergite IX with rounded ventral struts (Fig. 9K); sternite IX thick, with strigulate microsculpture (Fig. 9L); tergite X triangular (Fig. 9M).

AEDEAGUS (Fig 10A–J). Curved, in lateral view; basal bulb poorly sclerotized; apical lobe sclerotized. Parameres long and thin; sclerite tripartite and symmetrical (Fig. 10E–J).

MEASUREMENTS (n = 9, including the holotype, unless otherwise specified): TL (n = 8) 1.44–1.50 (1.46 ± 0.02), SY 0.17–0.20 (0.18 ± 0.01), HW 0.36–0.40 (0.39 ± 0.01), IS 0.18–0.22 (0.19 ± 0.01), WA 0.10–0.13 (0.12 ± 0.01), PL (n = 8) 0.54–0.60 (0.57 ± 0.02), PA 0.42–0.47 (0.44 ± 0.02), PB 0.93–0.97 (0.95 ± 0.01), EI 0.96–1.05 (1.00 ± 0.03), EL 1.05–1.12 (1.08 ± 0.03), EW 0.48–0.54 (0.50 ± 0.02), EH 0.42–0.49 (0.46 ± 0.02), MsW 0.20–0.26 (0.23 ± 0.02), MeL 0.06–0.12 (0.09 ± 0.02), MeW (n = 8) 0.03–0.04 (0.03 ± 0.006), MB 0.10–0.13 (0.12 ± 0.01), MC 0.30–0.35 (0.32 ± 0.02), ML 0.04–0.05 (0.04 ± 0.005), VL 0.25–0.28 (0.26 ± 0.01), VL2 (n = 8) 0.22–0.27 (0.25 ± 0.02); PrF 0.37–0.42 (0.40 ± 0.02), PrT 0.25–0.31 (0.29 ± 0.02), MsF 0.40–0.47 (0.44 ± 0.02), MsT 0.35–0.41 (0.38 ± 0.02), MtF 0.44–0.50 (0.49 ± 0.02), MtT 0.43–0.49 (0.47 ± 0.02).

Females (Fig. 11)

Tarsi not enlarged and lacking tenent setae (Fig. 11G–I). Ventrite VIII with a triangular projection (Fig. 11K); tergite VIII straight posteriorly (Fig. 11L) – both microsculptured. Spermatheca elongate and twisted, forming a circular structure; spermathecal duct filiform (Fig. 11M). Distal gonocoxite long and slender, somewhat arcuate (Fig. 11M,N). Gonostylus about 2× longer than wide, tapering posteriorly (Fig. 11M,N).

MEASUREMENTS (n = 9, in mm): TL 1.41–1.55 (1.50 ± 0.04), SY 0.15–0.19 (0.18 ± 0.01), HW 0.39–0.41 (0.40 ± 0.01), IS 0.18–0.21 (0.19 ± 0.01), WA 0.11–0.14 (0.12 ± 0.01), PL 0.54–0.63 (0.59 ± 0.03), PA 0.43–0.47 (0.45 ± 0.01), PB 0.88–0.98 (0.95 ± 0.03), EI 0.95–1.04 (1.01 ± 0.03), EL 1.03–1.14 (1.11 ± 0.03), EW 0.44–0.55 (0.51 ± 0.04), EH 0.43–0.49 (0.46 ± 0.02), MsW 0.20–0.27 (0.24 ± 0.02), MeL 0.05–0.13 (0.09 ± 0.02), MeW 0.02–0.04 (0.03 ± 0.01), MB 0.10–0.14 (0.12 ± 0.01), MC 0.29–0.38 (0.33 ± 0.03), ML 0.04–0.06 (0.05 ± 0.01), VL 0.25–0.33 (0.28 ± 0.02), VL2 0.24–0.28 (0.26 ± 0.01), PrF 0.39–0.42 (0.41 ± 0.01), PrT 0.28–

0.31 (0.30 ± 0.01), MsF 0.42–0.46 (0.45 ± 0.01), MsT 0.35–0.41 (0.38 ± 0.02), MtF 0.45–0.50 (0.48 ± 0.02), MtT 0.45–0.49 (0.48 ± 0.01).

Host

Collected from *Ceratiomyxa fruticulosa* T.Macbr., 1899. (Protozoa) a fallen *Pinus* sp. tree (Fig. 1G).

Remarks

Aedeagus similar to *A. plaumanni* but external morphology differs: smaller, metaventrite and abdomen not punctate, elytral punctation not coarse.

Distribution

Mata do Paraíso, Universidade Federal de Viçosa, campus of Viçosa, state of Minas Gerais, Southeast Brazil (Fig. 1A,B,G).

***Alexidia* sp. nov. 2**

(Figs 12, 13)

Diagnosis

Body length: 1.74 mm. Dark wine-brown; legs lighter; tarsi and posterior laterals of elytra yellow; very shining. Somewhat flattened in lateral view. Sutural, basal, and lateral striae joined. Antennomere IX distinctly enlarged. Spermatheca C-shaped. Gonostylus short.

Etymology

Material examined

Holotype

BRAZIL • ♀*; Minas Gerais, Viçosa, Recanto das Cigarras (Mata da Biol.).; 20 Nov. 2019; Leg. Labcol; Fungo 14 / Dissecado em 07 Oct. 2022 / CELC. Lacking the “HOLOTYPUS ♀” label.

Description

COLORATION. Dark wine-brown; frons, coxae, femora and tibiae lighter (Fig. 12A–C). Antennae, tarsi, posterior laterals of elytra, propygidium and pygidium yellow (Fig. 12A–H).

HEAD. Frons smooth, sparsely pubescent, devoid of punctures; one fovea above each eye (Fig. 12E). Clypeus longer than wide (Fig. 12E). Labrum rounded apically (Fig. 12E). Antennomere VIII wavy (Fig. 12F); antennomeres proportions (n = 1): II 106/39: III 66/18: IV 94/16: V 109/18: VI 94/20: VII 108/35: VIII 88/22: IX 124/38: X 112/42: XI 119/46.

PROTHORAX. Smooth, lacking microsculpture (Fig. 12A–D,G). Pronotum not strongly curved in lateral view (Fig. 12B); punctation very fine; pubescence somewhat dense; posterior angles not trespassing mesenepisternum (Fig. 12B). Hypomeron poorly pubescent (Fig. 12D).

MESOTHORAX (Fig. 12B–D). Lacking microsculpture. Mesoventral line oblique. Secondary lines absent (Fig 12D). Mesepimeron short and oblique (Fig 12D).

METATHORAX (Fig. 12B–D). Metaventrite smooth, devoid of punctures, and sparsely pubescent. Submesocoxal lines punctate; submesocoxal area length: 0.05 mm. Metanepisternum mostly covered by elytra. Metepimeron distinct, smooth.

WINGS (Fig. 12A–D,G,H). Elytra wider anteriorly; shining, lacking microsculpture, finely punctate, and moderately pubescent. Sutural striae reaching the basal striae, and then, to the lateral line – distinctly punctate (Fig. 12A,B). Epipleura impunctate. (Fig. 12D)

LEGS (Fig. 12B–D). Pro- and mesofemora with sparse and coarse punctures. Femora narrow. Meso- and metatibiae bearing a long apical spine.

ABDOMEN (Fig. 12B–D,H). Ventrite I impunctate, shining; primary setae present. Tergite VI with micropuncture and sparsely pubescent.

TERMINALIA. Ventrite VIII with a triangular projection (Fig. 13A); tergite VIII straight posteriorly (Fig. 13B) – both microsculptured. Bursa copulatrix spinose (Fig. 13C,D). Spermatheca large, C-shaped; spermathecal duct filiform (Fig. 13C). Distal gonocoxite thick on the posterior area, arcuate (Fig. 13C,D). Gonostylus very short (Fig. 13C,D).

MEASUREMENTS (n=1, holotype): TL 1.70, SY 0.22, HW 0.44, IS 0.22, WA 0.15, PL 0.65, PA 0.50, PB 1.10, EI 1.16, EL 1.26, EW 0.53, EH 0.50, MB 0.11, MC 0.40, ML 0.05, VL 0.50, VL2 0.31, PrF 0.47, PrT 0.34, MsF 0.48, MsT 0.42, MtF 0.55, MtT 0.53.

Host

Collected from an undetermined and young orange-white unknown fungus/myxomycete on a decaying tree (Fig. 93C).

Remarks

Similar to *Alexidia* sp. nov. 1 but larger, more elongate, and less curved, in lateral view. Elytra with distinct coloration on the posterior laterals. Antennomeres thicker. Adsutural area not distinctly wide, at the posterior 2/3. Spermatheca large and not twisted; distal gonocoxite more curved; gonostylus shorter.

Distribution

Mata da Biologia, campus of the Universidade Federal de Viçosa, campus of Viçosa, state of Minas Gerais, Southeast Brazil (Fig. 1A–D).

Genus ***Amalocera*** Erichson

(Fig. 2L,N)

Amalocera Erichson, 1845: 4. Type species: *Amalocera picta* Erichson, 1845; by monotypy.

Amalocera is represented by only five known species – all them registered for Brazil. Until the development of this paper, the CELC collection counted with only two specimens (male and female) of this genus. The two specimens belong to the same new species – not included here.

General description

Body wide. HEAD. Labral setae present. Mandible apically bidentate, with apical serrations. Maxillary palp normal. Galea wide, with radulate brush. Inner and basal setae of lacinia absent. Setae on adoral surface of hypopharynx absent. Last labial palpomere curved. Submaxillary ducts present. Gular suture not reaching the submentum. Frontoclypeal suture present. Eyes entire – not notched. Anetennae filiform, antennomeres III and IV elongate; VII–XI asymmetrical. PROTHORAX. Prothoracic corbiculum absent. Hypomeron visible in lateral view; apex subacute and not extending beyond pronotum. MESOTHORAX. Mesoventral lines impunctate and not connected to the mesocoxal cavity. Secondary and median lines absent.

Prepectus present. Scutellum quite visible, in dorsal view. Meso -and metaventrite partially fused. Mesoventral process carinate. Mesepimeron absent. METATHORAX. Submesocoxal lines parallel to coxae. Metaventral setose patch absent. Intercoxal plates present. Wings. Elytra with apical serrations; basal and lateral striae present and connected. Profemoral ctenidium absent. Metatibiae with a single spine. Mesotibiae with two apical spines, unequal in length. ABDOMEN. Submetacoxal bead punctate, meeting in the middle; submetacoxal space present; submetaxocal lines parallel to coxae. Primary setae of ventrite I absent. MALES. Tibiae bearing secondary sexual characteristics. (Leschen & Löbl 2005; Löbl 1974).

Genus ***Baeocera*** Erichson

(Figs 2D,J, 14–43)

Baeocera Erichson, 1845: 4. Type species: *Baeocera falsata* Achard, 1920.

Sciatrophes Blackburn, 1903: 100. Type species: *Sciatrophes latens* Blackburn, 1903; by monotypy.

Cyparella Achard, 1924: 28. Type species: *Scaphisoma rufoguttatum* Fairmaire, 1898; by original designation.

Amaloceroschema Löbl, 1967: 1 (as subgenus). Type species: *Baeocera freudei* Löbl, 1967; by original designation.

Eubaeocera Cornell, 1967: 2, Fig. 1. Type species: *Baeocera abdominalis* Casey, 1900; by original designation.

With over 300 described species, *Baeocera* is one of the largest Scaphidiinae genera that can be found on all continents. However, until now, Brazil counts with just one known species: *Baeocera freudei* Löbl, 1967 (state of Amazonas). In this work, six new species are described. These new species present very similar external morphology. Adding this characteristic to the fact that some species were collected together (same host and days), made it very hard to identify them. Moreover, it was especially difficult to identify the females of each species, since the most obvious diagnostic characters are related to the male terminalia. This situation was solved by complete dissections in order to compare a higher number of structures.

General description (* = variable characters within the genera, but not variable in the species below).

HEAD. Labral setae simple*. Mandible unidentate*. Last maxillary palpomere aciculate; galea narrow (longer than wide), with paniculate brush; lacinia lacking basal setae. Setae on

adoral surface of hypopharynx setose. Last labial palpomere straight and thin. Antennomere III and IV not shortened. Gular pores present. Frontoclypeal suture present. PROTHORAX. Hypomeron visible in lateral view*; pronotal angles acute and slightly extending the anapleural suture*. Prothoracic corbiculum present. MESOTHORAX. Mesoventral process paxillate. Mesoventral space (prepectus) absent. Mesoventral lines connected to the mesocoxal cavity; impunctate*. Secondary lines absent. Mesanepisternum finely and sparsely punctate and pubescent*. Mesepimeron exposed*. METATHORAX. Metanepisternum exposed. Submesocoxal lines present. Metacoxal process short*. Metaventral setose patch present*. WINGS. Hind wings developed. Elytral basal and sutural striae connected*; lateral striae present*; apical serrations present*. LEGS. Profemoral ctenidium present. Mesotibiae bearing outer spines and two ventral spines ABDOMEN. Submetacoxal lines parallel to coxae; punctate*. Membranes of abdominal ventrites with brick-walled pattern. (Löbl & Leschen 2003b; Leschen & Löbl 2005).

Baeocera sp. nov. 1

(Figs 14–18)

Diagnosis

Body length: 1.00–1.18 mm; somewhat narrow, in dorsal view (Figs 14A,F, 18A); moderately convex, in lateral view (Figs 14B,G, 18B). Brown to dark brown; mouthparts, antennae, and legs ochreous (Fig. 14A–C,F,G, 18A–C). Mesepimeron wide = 2.16/3× of mesanepisternum wide, and 3.60 wider than long (Fig. 16B,C). Submesocoxal lines arcuate and punctate (Fig. 16B,C, 18C). Metanepisternal suture straight (Fig. 16B) or moderately curved (16C, 18C); punctate. Basal striae connected to sutural and reaching about 2/3 of elytra (Fig. 15G). Femora with strigulate microsculpture (Figs 14C,G, 16J–L, 18D–F). Aedeagus with parameres with apex slightly thinner, sclerite of internal sac disform (Fig. 17G–K). Distal gonocoxite and gonostylus elongate (18M,N).

Etymology

Material examined

Holotype

BRAZIL • ♂; Minas Gerais, Viçosa, EPTEA Mata do Paraíso; 24 Mar. 2022; E. von Groll *et al.* leg.; Falcon 20 / Em *Ceratiomyxa fruticulosa* em Pinus / HOLOTYPUS ♂; CELC. (Fig. 14D,E).

Paratypes

BRAZIL • 2♂♂, 5♀♀. (1♂**, 1♀**); same data as for holotype; CELC.

Description

COLORATION. Dark brown; mouthparts, antennae, clypeus, and anterior part of femora dark ochreous; tibiae and tarsi light ochrous (Fig. 14A–C,H). Variation: all tonalities lighter (Fig. 14F,G).

HEAD (Figs 14H,I, 15A–F). Finely punctate; pubescence sparse; one fovea above each eye (Fig. 14H,I). Labrum slightly curved posteriorly (Fig. 15A). Mandibles not strongly curved (Fig. 15B,C). Last labial palpomere distinctly elongate and curved; mentum concave posteriorly (Fig. 15E). Gular pores absent; gular suture wide near the ostium; gular region with strigulate microsculpture (Fig. 15F). Antennae elongate (Fig. 14J,K), antennomere VII thin, longer than VIII, XI elongate and oval; antennomeres proportions (n = 2): I 76/30: II 69/30: III 35/14: IV 45/13: V 58/14: VI 51/14: VII 70/19: VIII 63/21: IX 77/28: X 75/34: XI 101/40.

PROTHORAX (Figs 15G–K). Punctation sparse and fine; pubescence sparse (Figs 14A, 15G, 18A). Hypomeron almost glabrous, with few coarse punctation (Fig. 16B), absent in some specimens (Fig. 16C). Prosternal process narrow and spinose (Fig. 15I). Profurca thin and elongate (Fig. 15K).

MESOTHORAX (Figs 15G,L–16C). Scutellum visible in dorsal view, wider than longer (Fig. 15G); tip rounded; scutellar lines oblong laterally (Fig. 15L). Mesoventral lines angulate; coxal rests large; median lines short and open (Fig. 15M). Mesepimeron about 3.60× wider than long, and occupying about 2.16/3 of mesanepisternum (Fig. 16B,C).

METATHORAX (Figs 15M, 16A–F). Metaventrite smooth, shining, and with little pubescence laterally (Fig. 16B,C). Submesocoxal lines arcuate and punctate; submesocoxal area length: 0.03–0.04 mm (Fig. 16B,C, 18C). Metanepisternal suture punctate, curvature variable (Fig.

16B,C, 18C). Metanotum with large alacrista; scutoscutellar suture not trespassing the apodeme (Fig. 16D). Stalk of metendosternite narrower than arms (Fig. 16E,F).

WINGS (Figs 14A,F, 16G–I, 18A). Elytra with coarse and sparse punctures; pubescence fine and sparse. Basal striae connected to sutural, impunctate, and reaching 1.5/3 of elytra (Fig. 15G). Lateral striae fine, impunctate, and slightly curved near the humeral region (Fig. 14B,G,18B).

LEGS. Elongate; femora with distinct strigulate microsculpture (Figs 14C,G, 16J–L, 18D–F).

ABDOMEN. Ventral surface shining, finely punctate; pubescence moderately dense and elongate (Figs 14B,G, 18B,C). Pro- and pygidium with fine and sparse pubescence (17A, 18J). Posterior area of ventrite I, ventrites II–VI, and tergites with imbricate microsculpture (Fig. 14B,G, 18C).

Males

Pro- and mesotarsomeres I–III slightly widened, bearing few and elongate tenent setae (Fig. 16J–O). Sternite VIII with a distinct elongate posterior projection (Fig. 17B). Tergite VIII triangular, with a smooth posterior projection (Fig. 17C). Tergite IX with ventral struts curved, and forming an acute angle (Fig. 17D). Sternite IX with elongate anterior sclerotized projection (Fig. 17D,E). Tergite X triangular (Fig. 17D,F).

AEDEAGUS (Fig. 17G–K). Median lobe poorly sclerotized and slightly curved, in lateral view (Fig17I). Parameres more sclerotized than apical lobe; almost parallel but apex slightly thinner. Sclerite of internal sac disform (Fig. 17G–K).

MEASUREMENTS (n = 3, including the holotype; in mm): TL 1.05–1.13 (1.08 ± 0.04), SY 0.11–0.13 (0.12 ± 0.01), HW 0.30–0.31 (0.30 ± 0.01), IS 0.13–0.14 (0.14 ± 0.01), WA 0.06–0.08 (0.07 ± 0.01), PL 0.40–0.45 (0.42 ± 0.03), PA 0.30–0.35 (0.32 ± 0.03), PB 0.59–0.60 (0.60 ± 0.01), SL 0.01–0.02 (0.02 ± 0.01), SW 0.04–0.05 (0.05 ± 0.01), EI 0.64–0.7 (0.67 ± 0.03), EL 0.75–0.78 (0.77 ± 0.02), EW 0.33–0.36 (0.35 ± 0.02), EH 0.26–0.35 (0.31 ± 0.05), MsW 0.18–0.20 (0.19 ± 0.01), MeL 0.03–0.04 (0.04 ± 0.01), MeW 0.13–0.15 (0.14 ± 0.01), MB 0.10–0.14 (0.13 ± 0.02), MC 0.24–0.27 (0.26 ± 0.02), ML 0.03–0.04 (0.04 ± 0.01), VL 0.13–0.16 (0.15 ± 0.02), PrF 0.32–0.33 (0.32 ± 0.01), PrT 0.25–0.26 (0.26 ± 0.01), MsF 0.33–0.36 (0.34 ± 0.02), MsT 0.30–0.31 (0.31 ± 0.01), MtF 0.39–0.40 (0.4 ± 0.01), MtT 0.34–0.37 (0.36 ± 0.02).

Females (Fig. 18A–N)

Ventrite and tergite VIII with a triangular posterior projection (Fig. 18K,L). Spermatheca elongate, filiform (Fig. 18M). Distal gonocoxite elongate and slightly curved; gonostylus 6× longer than wide (Fig. 18M,N).

MEASUREMENTS (n = 5; in mm): TL 1.00–1.18 (1.10 ± 0.06), SY 0.11–0.14 (0.13 ± 0.01), HW 0.29–0.32 (0.31 ± 0.01), IS 0.12–0.16 (0.14 ± 0.01), WA 0.07–0.08 (0.07 ± 0.01), PL 0.38–0.45 (0.42 ± 0.03), PA 0.29–0.39 (0.33 ± 0.04), PB 0.55–0.67 (0.62 ± 0.04), SL 0.01–0.02 (0.02 ± 0), SW 0.04–0.05 (0.05 ± 0.01), EI 0.64–0.74 (0.71 ± 0.04), EL 0.72–0.82 (0.79 ± 0.04), EW 0.30–0.41 (0.35 ± 0.05), EH 0.27–0.36 (0.30 ± 0.04), MsW 0.16–0.22 (0.18 ± 0.02), MeL 0.03–0.05 (0.04 ± 0.01), MeW 0.13–0.15 (0.14 ± 0.01), MB 0.11–0.14 (0.13 ± 0.01), MC 0.22–0.32 (0.28 ± 0.04), ML 0.04, VL 0.15–0.17 (0.16 ± 0.01), PrF 0.31–0.35 (0.33 ± 0.02), PrT 0.24–0.28 (0.26 ± 0.02), MsF 0.33–0.40 (0.36 ± 0.03), MsT 0.30–0.33 (0.31 ± 0.02), MtF 0.38–0.45 (0.41 ± 0.03), MtT 0.35–0.39 (0.37 ± 0.02).

Host

Collected together from *Ceratiomyxa fruticulosa* on a fallen *Pinus* sp. tree (Fig. 1G).

Remarks

Ovipositor similar to species of *Xotidium* Löbl, 1992 (Ogawa & Löbl 2016), like *Xotidium montanum* (Löbl, 1971), but differs by the genera due to the larger body and not approximate meso- and metacoxae. This species differs from the other species of *Baeocera* here described by the femora with strigulate microsculpture and by the elongate distal gonocoxite and gonostylus in females.

Distribution

Mata do Paraíso, Universidade Federal de Viçosa, campus of Viçosa, state of Minas Gerais, Southeast Brazil (Fig 1A–B).

Baeocera sp. nov. 2

(Figs 19–24)

Diagnosis

Body length: 1.09–1.31 mm; body oblong (Fig. 19A, 23A); dark brown (Fig. 19B). Antennae elongate, almost reaching the metacoxae (Fig. 20I). Mesepimeron about 4.5× wider than long (Fig. 20I). Submesocoxal lines slightly arcuate, punctate; submesocoxal area short (Fig. 20G,I). Basal striae entire (connected to the sutural and lateral ones) (Fig. 20A). Parameres of aedeagus enlarged posteriorly, in lateral view (Fig. 22C). Females with distal gonocoxite rounded cone-shaped, bearing one long apical seta; gonostylus absent (Fig. 24).

Etymology

Material examined

Holotype

BRAZIL • ♂; Minas Gerais, Viçosa, EPTEA Mata do Paraíso; 24 Mar. 2022; E. von Groll *et al.* leg.; Falcon 20 / Em *Ceratiomyxa fruticulosa* em Pinus / HOLOTYPUS ♂; CELC. (Fig. 19D,E).

Paratypes

BRAZIL • 7♂♂, 6♀♀ (3♂♂*, 2♂♂**, 1♀*); same data as for holotype; CELC • 8♂♂, 3♀♀ (1♂*, 1♀*); same collection data as for holotype; 26 Mar. 2022; Falcon 26 / Em *Ceratiomyxia fruticulosa* em Pinus; CELC • 5♂♂, 6♀♀ (1♂**, 1♀*); same collection data as for holotype; 31 Mar. 2022; E. von Groll *et al.* leg.; Falcon 19 / Em *Ceratiomyxia fruticulosa* no tronco caído; CELC • 1♂, 5♀♀ (1♀*); same collection data as for holotype; 14 Apr. 2022; Falcon 42; CELC • 3♂♂, 2♀♀ (2♂♂*, 2♀♀*); Minas Gerais, Viçosa, UFV, Mata da Biologia; 12 Apr. 2022; E. von Groll & G.J Figueiredo leg.; Falcon 04 / Em *Ceratiomyxia fruticulosa* no tronco caído; CELC • 1♂; same data collection as for previous; Falcon 01 / Em *Ceratiomyxia fruticulosa* no tronco caído; CELC.

Description

COLORATION. Dark brown; antennomeres I–VI, tibiae, tarsi, apex of each abdominal ventrites light ochreous; coxae, femora, and clypeus dark ochreous (Fig. 19A–C,F). Variation: all tonalites lighter.

HEAD (Fig. 19F–M). Frons finely punctate; pubescence sparse (Fig. 19F). Labrum slightly curved posteriorly (Fig. 19I). Mandibles strongly curved; tooth elongate (Fig. 19J,K). Last maxillary palpomere remarkably thin (Fig. 19L). Labial palpomere III shortened, wider than longer; IV almost straight, thin; posterior portion of mentum with three concavities: one large in the center and two small laterally (Fig. 19M). Antennae (Fig. 19G,H) elongate, almost reaching metacoxae (Fig. 20I); antennomeres thin, antennomere VII slightly oblong; proportions (n = 13): I 69/33: II 69/33: III 39/14: IV 48/14: V 59/14: VI 59/16: VII 58/22: VIII 78/26: IX 89/32: X 89/34: XI 95/35.

PROTHORAX (Fig. 20A–E). Shining, lacking microsculpture; punctation fine and moderately sparse. Pronotum with a distinct anterior bead (Fig. 20A). Prosternal process thick, in lateral view (Fig. 20C). Profurca slightly robust and elongate (Fig. 20E).

MESOTHORAX (Fig. 20F–I). Scutellum visible in dorsal view, wider than long (Fig. 20A); tip rounded (Fig. 20F). Mesoventral lines very curved; coxal rests large; median lines open (Fig. 20G). Mesepimeron about 4.5× wider than long, and occupying about 2.18/3 of mesanepisternum (Fig. 20I).

METATHORAX (Fig. 20G–L). Metaventrite smooth, shining, and with few pubescence laterally (Fig. 20I). Submesocoxal lines slightly arcuate coxae, punctate; submesocoxal area short, length: 0.02–0.04 mm (Fig. 20G–I, 23C). Metanepisternal suture punctate, curvature variable (Figs 20I, 23C). Metanotum with trapezoidal alacrista and scutoscutellar suture just slightly trespassing the apodeme (Fig. 20J). Metendosternite with stalk and arms similar in thickness (Fig. K,L).

WINGS (Figs 19A, 21A–C, 23A). Elytra with coarse and moderately sparse punctures. Basal striae connected to the sutural and lateral ones; all impunctate.

LEGS. Elongate, not microsculptured (Figs 21D–I, 23D–I).

ABDOMEN. Submetacoxal lines distinctly coarse punctate (Figs 20I, 23C). Ventral surface shining; pubescence sparse, denser posteriorly, punctures moderately coarse (Figs 19B,C, 23B). Ventrite 1 with (Fig. 19B) or without (Fig. 23B) a lateral curved impression – not related to sex, collection day, period of life (teneral). Pro- and pygidium with hardly visible micropuncture; sparsely pubescent (Fig. 21J).

Males

Pro- and metatibiae slightly curved (Fig. 21D,E). Pro- and mesotarsomeres I–III slightly widened, protarsomeres bearing few and elongate tenent setae (Fig. 21G,H). Both sternite and tergite VIII with triangular-rounded posterior projection (Fig. K,L). Tergite IX with ventral struts curved (Fig. 21M). Sternite IX oblong (Fig. 21M). Tergite X wide and triangular.

AEDEAGUS (Fig. 22A–H). Median lobe slightly curved, in lateral view (Fig. 22C,H), basal bulb poorly sclerotized, apical lobe moderately sclerotized, almost same length as basal bulb. Parameres more (Fig. 22C) or less (Fig. 22H) wide posteriorly, in lateral view. Sclerite of internal sac with two elongate and twisted sclerotized plates (Fig. 22E–G).

MEASUREMENTS (n = 14, including the holotype, unless otherwise specified; in mm): TL (n = 26) 1.11–1.27 (1.18 ± 0.04), SY 0.13–0.17 (0.14 ± 0.01), HW 0.31–0.36 (0.33 ± 0.01), IS (n = 13) 0.14–0.18 (0.16 ± 0.01), WA 0.08–0.12 (0.09 ± 0.01), PL 0.4–0.48 (0.44 ± 0.02), PA 0.35–0.42 (0.38 ± 0.02), PB 0.62–0.76 (0.68 ± 0.03), SL 0.01–0.02 (0.02 ± 0), SW 0.04–0.05 (0.05 ± 0), EI 0.71–0.83 (0.77 ± 0.04), EL 0.80–0.93 (0.86 ± 0.04), EW 0.33–0.43 (0.38 ± 0.03), EH 0.29–0.36 (0.33 ± 0.02), MsW 0.17–0.21 (0.19 ± 0.01), MeL 0.03–0.04 (0.03 ± 0), MeW 0.11–0.16 (0.14 ± 0.02), MB 0.11–0.16 (0.14 ± 0.01), MC 0.27–0.31 (0.29 ± 0.02), ML 0.03–0.04 (0.03 ± 0), VL 0.15–0.22 (0.18 ± 0.02), VL2 0.21–0.27 (0.24 ± 0.02), PrF 0.31–0.4 (0.36 ± 0.02), PrT 0.25–0.31 (0.28 ± 0.02), MsF 0.32–0.41 (0.37 ± 0.02), MsT 0.30–0.36 (0.32 ± 0.02), MtF 0.39–0.45 (0.42 ± 0.02), MtT 0.35–0.44 (0.39 ± 0.03).

Females (Figs 23, 24)

Sternite VIII with a wide and rounded posterior projection (Fig. 23J). Tergite VIII triangular, lacking posterior projection (Fig. 23K). Distal gonocoxite rounded cone-shaped, bearing one long apical seta, gonostylus absent (Figs 23L–24D).

MEASUREMENTS (n = 14, unless otherwise specified; in mm): TL (n = 22) 1.09–1.31 (1.22 ± 0.05), SY 0.13–0.17 (0.15 ± 0.01), HW 0.31–0.35 (0.33 ± 0.01), IS 0.15–0.2 (0.18 ± 0.02), WA 0.08–0.12 (0.10 ± 0.01), PL 0.43–0.50 (0.47 ± 0.02), PA 0.35–0.42 (0.39 ± 0.02), PB (n = 12) 0.65–0.75 (0.70 ± 0.03), SL 0.02–0.03 (0.02 ± 0), SW 0.04–0.06 (0.05 ± 0), EI 0.70–0.86 (0.8 ± 0.05), EL 0.81–0.95 (0.89 ± 0.04), EW 0.34–0.44 (0.38 ± 0.03), EH 0.29–0.39 (0.35 ± 0.03), MsW 0.17–0.22 (0.19 ± 0.01), MeL (n = 13) 0.03–0.04 (0.03 ± 0), MeW (n = 13) 0.13–0.17 (0.14 ± 0.01), MB 0.13–0.18 (0.15 ± 0.01), MC 0.27–0.32 (0.3 ± 0.01), ML 0.02–0.04 (0.03 ±

0), VL 0.11–0.22 (0.19 ± 0.03), VL2 0.22–0.27 (0.25 ± 0.02), PrF 0.34–0.41 (0.37 ± 0.02), PrT 0.26–0.32 (0.29 ± 0.02), MsF 0.36–0.4 (0.39 ± 0.01), MsT 0.31–0.36 (0.34 ± 0.02), MtF 0.41–0.47 (0.44 ± 0.02), MtT 0.35–0.45 (0.41 ± 0.02).

Host

Collected from *Ceratiomyxa fruticulosa* on a fallen *Pinus* sp. (Fig. 1G) and other two logs, also with *C. fruticulosa* (Fig. 93D).

Remarks

Similar to *Baeocera* sp. nov. 6, differs by the entire basal, antennae more elongate, antennomeres thinner, submesocoxal area very short; last maxillary palpomere much thinner compared to the previous one; parameres straight; and distinct shape of the ovipositor. The absence of gonostylus was also recorded by the *Baeocera lenta* species group (e.g. *Baeocera caliginosa* Löbl, 1984) (Ogawa & Löbl 2013) but *Baeocera* sp. nov. 2 differs by the much shorter distal gonocoxite.

Distribution

Mata do Paraíso and Mata da Biologia, Universidade Federal de Viçosa, campus of Viçosa, state of Minas Gerais, Southeast Brazil (Fig 1A–B).

Baeocera sp. nov. 3

(Figs 25–28)

Diagnosis

Small, body length: 1.11 mm. Not strongly oblong in dorsal view; dark brown (Fig. 25A). Mesepimeron wide = 2.25/3 of mesanepisternum wide, and 3.18× wider than long (Fig. 26I). Submesocoxal lines arcuate and punctate (Fig. 26G,I). Basal striae connected to sutural and reaching about 2.12/3 of elytra (Fig. 26A). Parameres thin, lobed posteriorly, tip oblong (Fig. 28H). Female unkown.

Etymology

Material examined

Holotype

BRAZIL • ♂*; Minas Gerais, Viçosa, EPTEA Mata do Paraíso; 10 Mar. 2022; E. von Groll *et al.* leg.; Falcon 26 / Em *Ceratiomyxia fruticulosa* em Pinus / Dissecado em 21.x.2022 / HOLOTYPUS ♂; CELC. (Fig. 25D,E).

Paratype

BRAZIL • 1♂**; same data as for holotype; CELC.

Description

COLORATION. Dark brown; mouthparts, antennomeres I–VI, and legs ochreous; tarsi, posterior part of abdominal ventrites yellow (Fig. 25A–C,F).

HEAD (Fig. 25F–O). Frons finely punctate; pubescence moderately dense (Fig. 25F). Labrum straight posteriorly; laterals rounded (Fig. 25J). Mandibles not strongly curved; tooth somewhat elongate (Fig. 25K,L). Maxillary palpomere III somewhat oblong (Fig. 25M). Labial palpomeres elongate and very thin; palpomere III curved; mentum concave posteriorly (Fig. 25N). Gular pores absent (Fig. 25O). Antennae (Fig. 25H,I) elongate, antennomeres III–VI thick; antennomere VII longer than VIII; XI elongate, with sides parallel; antennomeres proportions (n = 2): I 75/32: II 62/32: III 33/14: IV 47/14: V 51/15: VI 47/16: VII 57/22: VIII 50/23: IX 72/33: X 75/38: XI 110/34.

PROTHORAX (Fig. 26A–E,I). Punctation moderately sparse and fine; pubescence sparse (Fig. 26A). Pronotum constricted laterally. Hypomeron poorly pubescent (Fig. 26I). Prosternal process strongly acute, in lateral view (Fig. 26C). Profurca tapering apically (Fig. 26E).

MESOTHORAX (Fig. 26F–I). Scutellum visible in dorsal view, wider than longer; tip rounded (Fig. 26F). Mesoventral lines strongly curved (Fig. 26G). Mesepimeron about 3.18× wider than long, and occupying about 2.25/3 of mesanepisternum (Fig. 26I). Mesoventral process truncated, in lateral view (Fig. 26H).

METATHORAX (Fig. 26G–I). Metaventrite smooth, shining, pubescence moderately sparse laterally (Fig. 26I). Submesocoxal lines arcuate and punctate; submesocoxal area length: 0.05–0.06 mm (Fig. 26G–I). Metanepisternal suture dashed, curvature variable (Fig. 26H,I). Metanotum with alacrista trapezoidal-shaped, with distinct sides; scutoscutellar suture elongate

and slight trespassing the apodeme (Fig. 26J). Stalk of Metendosternite narrower than arms (Fig. 27A,B).

WINGS (Fig. 25A, 27C–D). Elytra tapering toward the apex; punctation moderately coarse and sparse. Basal striae connected to sutural, impunctate, and reaching about 2.12/3 of elytra (Fig. 26A). Lateral striae fine, impunctate, and curved near the humeral region (Fig. 26I).

LEGS. Thin, elongate, not microsculptured

ABDOMEN. Submetacoxal lines with sparse and coarse punctures (Figs 25B, 26I). Ventral surface shining; pubescence dense; punctures fine. Propygidium dense and coarsely punctate; micropunctured; pubescence dense (Fig. 28A).

Males

Pro- and mesotarsomeres I–III widened, bearing tenent setae (Fig. 27F–K). Sternite VIII with a large posterior projection (Fig. 28B). Tergite VIII with a small posterior projection (Fig. 28C). Tergite IX with strongly curved ventral struts (Fig. 28D). Sternite IX slightly constricted centrally, microsculptured (Figs. 28E). Tergite X triangular (Fig. 28F).

AEDEAGUS (Fig. 28G–Q). Median lobe poorly sclerotized; basal bulb longer than apical lobe; apex truncate (Fig. 28H). Parameres also poorly sclerotized, but more than median lobe; thin, with a lobe near the apex, tip wide (Fig. 28G,J, N,O). Sclerite of internal sac with distinct curvatures, flagellum thin (Fig. 28K–M,P,Q).

MEASUREMENTS (n = 2, including the holotype; in mm): TL 1.11, SY 0.10–0.10 (0.10 ± 0), HW 0.31–0.32 (0.32 ± 0.01), IS 0.15–0.16 (0.16 ± 0.01), WA 0.07–0.07 (0.07 ± 0), PL 0.43–0.44 (0.44 ± 0.01), PA 0.31–0.36 (0.34 ± 0.04), PB 0.63–0.67 (0.65 ± 0.03), SL 0.02–0.02 (0.02 ± 0), SW 0.04–0.04 (0.04 ± 0), EI 0.69–0.70 (0.70 ± 0.01), EL 0.76–0.78 (0.77 ± 0.01), EW 0.32–0.34 (0.33 ± 0.01), EH 0.30–0.33 (0.32 ± 0.02), MsW 0.15–0.16 (0.16 ± 0.01), MeL 0.04–0.05 (0.05 ± 0.01), MeW 0.12–0.12 (0.12 ± 0), MB 0.10, MC 0.27–0.28 (0.28 ± 0.01), ML 0.05–0.06 (0.06 ± 0.01), VL 0.13–0.15 (0.14 ± 0.01), PrF 0.29–0.30 (0.30 ± 0.01), PrT 0.24–0.24 (0.24 ± 0), MsF 0.32–0.37 (0.35 ± 0.04), MsT 0.29–0.29 (0.29 ± 0), MtF 0.38–0.38 (0.38 ± 0), MtT 0.35–0.36 (0.36 ± 0.01).

Host

Collected from *Ceratiomyxa fruticulosa* on a fallen *Pinus* sp. tree (Fig. 1G).

Remarks

Similar to *Baeocera* sp. nov. 4 but differs by the smaller size, femora not distinctly darker near the coxae; antennomeres slender, antennomere XI more elongate and with parallel sides; sternite VIII with wider apical projection, tergite IX with more parallel sides; and parameres lobeled.

Distribution

Mata do Paraíso, Universidade Federal de Viçosa, campus of Viçosa, state of Minas Gerais, Southeast Brazil (Fig. 1A–B).

***Baeocera* sp. nov. 4**

(Figs 29–33)

Diagnosis

Body length: 1.16–1.22 mm. Dark brown; legs ochreous, femora darker on the anterior 3/2 (Fig. 29B, 33G). Antennomeres IX–XI oblong (Fig. 29K–M). Mesepimeron wide = 1.85/3 of mesanepisternum wide, and 2.90× wider than long (Fig. 31D,E). Submesocoxal lines arcuate, punctate; submesocoxal area = 0.05 mm (Fig. 31B,D,E). Basal striae connected to sutural and reaching about 2/3 of elytra (Fig. 29F). Aedeagus with thin parameres, with a shallow lobe near the apex, in frontal view (Fig. 32L). Tergite VIII in females with posterior projection. Distal gonocoxite triangular, elongate (Fig. 33L,M).

Etymology

Material examined

Holotype

BRAZIL • ♂*; Minas Gerais, Viçosa, EPTEA Mata do Paraíso; 14 Apr. 2022; E. von Groll *et al.* leg.; Falcon 42 / Em *Ceratiomyxa fruticulosa* em Pinus / Dissecado em 21.x.2022 / HOLOTYPUS ♂; CELC. (Fig. 29D,E).

Paratypes

BRAZIL • 1♀**; same collection data as for holotype; 10 Mar. 2022; E. von Groll *et al.* leg.; Falcon 26 / Em *Ceratiomyxia fruticulosa* em Pinus; CELC • 1♀**; same collection data as for holotype; 24 Mar. 2022; E. von Groll *et al.* leg.; Falcon 20 / Em *Ceratiomyxia fruticulosa* em Pinus; CELC.

Description.

COLORATION. Dark brown; mouthparts and tarsi yellow; antennae, posterior area of femora, and tibiae, ochreous; frons, coxae, and anterior 2/3 of femora dark ochreous (Fig. 29A–C,F,G, 32A–D, 33G). Variations: (1): body lighter; (2) abdominal ventrites III–VI ochrous (Fig. 29G, 33H). The coloration can change depending on the angle of the photos; for example, "Fig. 29G" and "Fig. 33G" are images of the same specimen taken in different angles. In Fig. 33G the coloration is darker and more faithful.

HEAD (Figs 29H–30G). Frons with punctures sparse; one fovea above each eye. Labrum almost straight posteriorly (Fig. 30A). Maxillary palpomere III elongate and not distinctly curved; IV thin (Fig. 30D,G). Labial palpomere III short and curved; mentum slightly concave posteriorly (Fig. 30E,G). Gular pores sparse (Fig. 30F). Antennae not distinctly elongate (Fig. 29K–M). Antennomere VII slightly longer than VIII; IX–XI oblong; antennomeres proportions (n = 3): I 71/32: II 63/32: III 30/15: IV 39/14: V 45/14: VI 39/15: VII 46/22: VIII 44/22: IX 62/35: X 64/38: XI 90/40.

PROTHORAX (Fig. 30H–M). Punctation sparse; pubescence short. Hypomeron subglabrous, impunctate (Fig. 31D,E). Prosternal process acute, in lateral view (Fig. 30L). Profurca thin and short (Fig. 30M).

MESOTHORAX (Fig. 31A–E). Scutellum visible in dorsal view (Fig. 30H), wider than longer; slightly triangular (Fig. 31A). Mesoventral lines smoothly curved (Fig. 31B). Median lines curved and open (Fig. 31B). Mesepimeron 2.90× wider than long, and occupying about 1.85/3 of mesanepisternum; variations: 2.33× wider than long, and occupying about 2/3 of mesanepisternum (Fig. 31D,E). Mesoventral process oblong, in lateral view (Fig. 31C).

METATHORAX (Fig. 31B–C). Metaventrite smooth, shining, pubescence moderately sparse laterally. Submesocoxal lines strongly arcuate; punctate; submesocoxal area length: 0.05–0.06

mm (Fig. 31D,E). Metanepisternal suture dashed, more or less convex (Fig. 31D,E). Metanotum with alacrista trapezoidal-shaped, longer than wide; scutoscutellar suture lateral end at the same position as apodeme (Fig. 31F). Arms of metendosternite slightly thicker than stalk (Fig. 31G,H).

WINGS (Figs 29A,F,I–K). Elytra with sparse and fine punctures – similar to pronotum; pubescence short. Basal striae connected to sutural, impunctate, and reaching about 2/3 of elytra (Fig. 29F). Lateral striae fine, impunctate, and curved near the humeral region (Fig. 29C,G).

LEGS. Thin, elongate, not microsculptured (Fig. 32A–C, 33A–F)

ABDOMEN. Submetacoxal lines coarse punctate (Fig. 29B,G). Ventrite I shining; pubescence dense; finely punctate. Propygidium dense and coarsely punctate; micropunctured; pubescence dense (Figs 32D, 33H).

Males

Protibiae slightly curved (Fig. 32A). Pro- and mesotarsomeres I–III widened, bearing tenent setae (Fig. A–B). Sternite VIII with an acute posterior projection (Fig. 32E). Tergite VIII with a small projection (32F). Tergite IX with curved ventral struts (Fig. 32G). Sternite IX elongate and oblong posteriorly (Fig. 32H). Tergite X triangular (Fig. 32I).

AEDEAGUS (Fig. 32 J–O). Median lobe slightly curved, in lateral view; basal bulb similar in length as apical lobe, and poorly sclerotized; apical lobe more sclerotized (Fig. J–L). Parameres thin and parallel, with a shallow lobe near the apex, and apex oval, in frontal view (Fig. 32J). Sclerite of internal sac curved, flagellum thin and very elongate (Fig. 32M–O).

MEASUREMENTS (n = 1, holotype; in mm): TL 1.16, SY 0.12, HW 0.32, IS 0.14, WA 0.06, PL 0.49, PA 0.32, PB 0.66, SL 0.01, SW 0.04, EI 0.76, EL 0.81, EW 0.37, EH 0.32, MsW 0.17, MeL 0.04, MeW 0.16, MB 0.10, MC 0.27, ML 0.05, VL 0.14, PrF 0.27, PrT 0.20, MsF 0.32, MsT 0.28, MtF 0.37, MtT 0.32.

Females (Fig. 29L,M, 33)

Antennomeres VI–X thicker than males (Fig. 29L,M). Ventrite and tergite VIII with a triangular posterior projection (Fig. 33I,J). Spermatheca filiform (Fig. 33K). Distal gonocoxite triangular and distinctly longer than wide, gonostylus rectangular (Fig. 33K–M).

MEASUREMENTS (n = 2; in mm): TL 1.22, SY 0.11–0.11 (0.11 ± 0), HW 0.32–0.34 (0.33 ± 0.01), IS 0.15–0.16 (0.16 ± 0.01), WA 0.08–0.10 (0.09 ± 0.01), PL 0.47–0.51 (0.49 ± 0.03), PA 0.35–0.35 (0.35 ± 0), PB 0.69–0.70 (0.7 ± 0.01), SL 0.02–0.03 (0.03 ± 0.01), SW 0.05–0.06 (0.06 ± 0.01), EI 0.76–0.77 (0.77 ± 0.01), EL 0.83–0.85 (0.84 ± 0.01), EW 0.38–0.40 (0.39 ± 0.01), EH 0.36–0.38 (0.37 ± 0.01), MsW 0.17–0.18 (0.18 ± 0.01), MeL 0.03–0.04 (0.04 ± 0.01), MeW 0.12–0.17 (0.15 ± 0.04), MB 0.11–0.12 (0.12 ± 0.01), MC 0.27–0.28 (0.28 ± 0.01), ML 0.05–0.06 (0.06 ± 0.01), VL 0.18–0.19 (0.19 ± 0.01), PrF 0.29–0.29 (0.29 ± 0), PrT 0.21–0.22 (0.22 ± 0.01), MsF 0.34–0.35 (0.35 ± 0.01), MsT 0.24–0.27 (0.26 ± 0.02), MtF 0.36–0.37 (0.37 ± 0.01), MtT 0.31–0.32 (0.32 ± 0.01).

Host

Collected from *Ceratiomyxa fruticulosa* on a fallen *Pinus* sp. tree (Fig. 1G).

Remarks

Similar to *Baeocera* sp. nov. 5, differs from it by the smaller size, antennomeres VII–XI oblong, spoon-like sternite IX, parallel parameres, curved sclerite of internal sac, and more elongate distal gonocoxite in females.

Distribution

Mata do Paraíso, Universidade Federal de Viçosa, campus of Viçosa, state of Minas Gerais, Southeast Brazil (Fig 1A–B).

Baeocera sp. nov. 5

(Figs 34–38)

Diagnosis

Body length: 1.23–1.25 mm; moderately oblong. Dark brown. Antennomeres VII and VIII oblong, IX–XI distinctly larger than remaining (Fig. 34J,K). Mesepimeron wide = 2.19 of mesanepisternum wide, and 2.73× wider than long (Fig. 35N). Submesocoxal lines strongly arcuate, punctate (Fig. 35L,N). Basal striae connected to sutural and reaching about 2/3 of elytra (Fig. 34A,B, 35F). Aedeagus with parameres wavy (Fig. 37I). Internal sac formed by twisted sclerites that forms an elongate and just slightly curved shape; terminal part of the flagellum

extends at a right angle from the main part, forming a “L-shaped” structure (Fig. 37L–N). Tergite VIII in females with a small posterior projection (Fig. 38G). Distal gonocoxite triangular, moderately elongate (Fig. 38I).

Etymology

Material examined

Holotype

BRAZIL • ♂; Minas Gerais, Viçosa, EPTEA Mata do Paraíso; 24 Mar. 2022; E. von Groll *et al.* leg.; Falcon 20 / Em *Ceratiomyxia fruticulosa* em Pinus / HOLOTYPUS ♂; CELC. (Fig. 34D,E).

Paratypes

BRAZIL • 3♂♂ (1♂*, 1♂**); same collection data as for holotype; 10 Mar. 2022; E. von Groll *et al.* leg.; Falcon 26 / Em *Ceratiomyxia fruticulosa* em Pinus; CELC • 1♀*; same collection data as for holotype; Falcon 42 / Em *Ceratiomyxia fruticulosa* em Pinus; CELC.

Description.

COLORATION. Dark brown; clypeus, tip of elytra, and femora dark ochreous; antennomeres, mouthparts, tibiae, apex of each ventral ventrite, and tarsi yellow (Fig. 34A–C, 38A–D). Variations: brown, with ochrous parts being yellow.

HEAD (Figs 34H–35I). Frons with punctation sparse and fine. Labrum curved posteriorly (Fig. 35A). Maxillary palpomeres elongate and moderately thin (Fig. 35D). Labial palpomeres very think, curved, and elongate; mentum concave posteriorly (Fig. 35E). Antennomeres VII and VIII oblong (Fig. 34J,K); antennomeres proportions (n = 2): I 69/32: II 68/34: III 33/17: IV 36/16: V 42/16: VI 37/17: VII 47/27: VIII 45/29: IX 69/44: X 76/44: XI 110/44.

PROTHORAX (Fig. F–J). Punctation sparse and very fine; pubescence sparse. Hypomeron subglabrous, impunctate (Fig. 35N). Prosternal process distinctly elongate and spinose, in lateral view (Fig. 35H). Profurca thin (Fig. 35J).

MESOTHORAX (Fig. 35K–N). Scutellum visible in dorsal view (Fig. 35F), wider than longer; tip rounded (Fig. 35K). Mesoventral lines smoothy curved; median lines closed (Fig. 35L). Mesepimeron about 2.73× wider than long, and occupying about 2.19/3 of mesanepisternum (Fig. 35N). Mesoventral process with a posterior ridge, in lateral view (Fig. 35M).

METATHORAX (Figs 35L–36C). Metaventrite smooth, shining, pubescence moderately sparse laterally (Fig. 35N). Submesocoxal lines arcuate and punctate; submesocoxal area length: 0.04–0.06 mm (Fig. 35L–M). Metanepisternal suture punctate, more or less convex (Fig. 35N). Metanotum with alacrista trapezoidal-shaped; scutoscutellar suture trespassing the apodeme (Fig. 36A). Arms of metendosternite slightly ticker than stalk (Fig. 36B,C).

WINGS (Figs 34A–C,F,G, 36D–F). Elytra with coarse and sparse punctures – coarser than pronotum. Basal striae connected to sutural, impunctate, and reaching about 2/3 of elytra (Fig. 35F). Lateral striae fine, impunctate, and curved near the humeral region (Fig. 35N).

LEGS. Thin, elongate, not microsculptured (Figs 36G–L, 38C,D).

ABDOMEN. Ventrite 1 with (Fig. 34C) or without (Fig. 38B) a lateral curved impression – not related to sex, collection day, period of life (teneral). Submetacoxal lines coarse punctate (Figs 34B, 38B). Ventral surface shining; pubescence dense; punctures fine (Figs 34B, 38B). Propygidium dense and coarsely punctate; micropunctured; pubescence dense (Fig. 37A, 38E).

Males

Tibiae slightly arcuate (Fig. G–I). Pro- and mesotarsomeres I–III widened, bearing tenent setae (Fig. 35J–L). Sternite VIII with a large triangular posterior projection (Fig. 37B). Tergite VIII triangular, lacking posterior projection (Fig. 37C). Tergite IX with curved ventral struts (Fig. 37D,E). Sternite IX somewhat acute posteriorly, elongate (Fig. 37F). Tergite X triangular, wide (Fig. 37G).

AEDEAGUS (Fig. 37H–R). Median lobe with basal bulb membranous, oval, and longer than apical lobe; apical lobe bent, in lateral view (Fig. 37J,Q). Parameres thin and wavy, in frontal view (Fig. 37I,P). Internal sac formed by a twisted sclerite that forms an elongate and just slightly curved main structure; terminal part of the flagellum extending at a right angle from the main part, forming a “L-shaped” structure (Fig. 37L–N,Q,R).

MEASUREMENTS (n = 4, including the holotype, unless otherwise specified): TL 1.23–1.27 (1.25 ± 0.01), SY 0.10–0.11 (0.11 ± 0.01), HW 0.35–0.36 (0.35 ± 0.01), IS 0.16–0.18 (0.17 ± 0.01), WA 0.07–0.12 (0.09 ± 0.02), PL 0.51–0.55 (0.53 ± 0.02), PA 0.35–0.40 (0.37 ± 0.02), PB 0.72–0.76 (0.74 ± 0.02), SL 0.02–0.03 (0.02 ± 0.01), SW 0.04–0.05 (0.05 ± 0.01), EI 0.75–0.80 (0.78 ± 0.02), EL 0.87–0.90 (0.88 ± 0.01), EW 0.39–0.44 (0.41 ± 0.02), EH 0.32–0.38 (0.36 ± 0.03), MsW 0.19–0.20 (0.20 ± 0.01), MeL 0.03–0.05 (0.04 ± 0.01), MeW 0.14–0.15 (0.15 ± 0.01), MB 0.11–0.14 (0.13 ± 0.01), MC 0.26–0.3 (0.28 ± 0.02), ML 0.04–0.06 (0.05 ± 0.01), VL 0.16–0.17 (0.17 ± 0.01), PrF 0.31–0.32 (0.32 ± 0.01), PrT 0.23–0.25 (0.24 ± 0.01), MsF 0.34–0.35 (0.35 ± 0.01), MsT 0.28–0.32 (0.3 ± 0.02), MtF 0.39–0.41 (0.41 ± 0.01), MtT 0.32–0.37 (0.35 ± 0.02).

Female (Fig. 38)

Antennae thicker than male (Fig. 34K). Ventrite VIII with a triangular posterior projection (Fig. 38F). Tergite VIII elongate, bearing a small posterior triangular projection (Fig. 38G). Spermatheca filiform. Triangular distal gonocoxite; gonostylus rectangular (Fig. 38H,I).

MEASUREMENTS (n = 1; in mm): TL 1.25, SY 0.12, HW 0.34, IS 0.19, WA 0.11, PL 0.50, PA 0.36, PB 0.72, SL 0.02, SW 0.04, EI 0.77, EL 0.83, EW 0.40, EH 0.36, MsW 0.20, MeL 0.04, MeW 0.14, MB 0.12, MC 0.30, ML 0.05, VL 0.15, PrF 0.30, PrT 0.25, MsF 0.34, MsT 0.30, MtF 0.40, MtT 0.38.

Host

Collected from *Ceratiomyxa fruticulosa* on a fallen *Pinus* sp. tree (Fig. 1G).

Remarks

Similar to *Baeocera* sp. nov. 4 and *Baeocera* sp. nov. 6. Differs by oblong antennomeres VII and VIII; last labial palpomere thin and elongate; parameres distinctly wavy in frontal view, compared to *Baeocera* sp. nov. 4 and lacking the posterior constriction present in *Baeocera* sp. nov. 6, by the not elongate flagellum as in *Baeocera* sp. nov. 4 and less curved sclerite of internal sac. Females can be distinguished by the proportions of the distal gonocoxite: not distinctly elongate as in *Baeocera* sp. nov. 4, and not strongly robust as in *Baeocera* sp. nov. 6.

Distribution

Mata do Paraíso, Universidade Federal de Viçosa, campus of Viçosa, state of Minas Gerais, Southeast Brazil (Fig. 1A–B).

Baeocera sp. nov. 6

(Figs 39–46)

Diagnosis

Body length: 1.08–1.22 mm; oblong. Dark brown (Fig. 39A). Mesepimeron wide = 1.94/3 of mesanepisternum wide, and 2.75× wider than long (Fig. 40I,J). Submesocoxal lines strongly arcuate, punctate (Fig. 40G,I). Basal striae connected to sutural and reaching about 2/3 of elytra (Fig. 40A). Propygidium dense and coarsely punctate (Fig. 41J). Aedeagus with parameres strongly wavy, posteriorly constricted; sclerites twisted, hummingbird-shaped. Tergite VIII in females lacking posterior projection (Fig. 43L). Distal gonocoxite robust (Fig. 43M,N).

Etymology

Material examined

Holotype

BRAZIL • ♂; Minas Gerais, Viçosa, EPTEA Mata do Paraíso; 12 Nov. 2019; Leg. LabCol; Fungo 06 / Fotos: 0751-0753 / Em *Ceratiomyxia fruticulosa* / HOLOTYPUS ♂; CELC. (Fig. 39D,E).

Paratypes

BRAZIL • 2♂♂, 3♀♀ (1♂**, 1♀*, 1♀**); same data as for holotype; CELC • 1♀*; same collection data as for holotype; Fungo 31 / Em *Xylodon flaviporus*; CELC • 4♂♂ (1♂*), 1♀*, 2 exs; same collection data as for holotype; Fungo 10 / Em *Ceratiomyxia fruticulosa*; CELC • 1♂*, 1♀, 1 ex.; same collection data as for holotype; 14 Nov. 2019; Leg. LabCol; Fungo 34 / Fotos: 0783-0790; Em *Ceratiomyxa fruticulosa*; CELC • 1♂*, 1♀*; same collection data as for holotype; 24 Mar. 2022; E. von Groll *et al.* leg.; Falcon 20 / Em *Ceratiomyxia fruticulosa* em Pinus; CELC.

Description.

COLORATION. Dark brown, with reddish nuances, depending on the angle of observation; clypeus, coxae, tip of elytra, and anterior part of femora ochreous; antennomeres I–VI, mouthparts, tibiae, apex of each ventral ventrite, and tarsi yellow (Fig. 39A–C,F,G, 43A–C). Variations: sclerites more or less dark.

HEAD (Fig. 39F–N). Frons with punctation sparse, some coarser than other (Fig. 39F,G). Labrum straight posteriorly (Fig. 39J). Mandibles with tooth not distinctly elongate (Fig. 39K,L). Maxillary palpomere III somewhat oblong, IV thick (Fig. 39M). Labial palpomere III elongate; IV, thin and curved; mentum concave posteriorly (Fig. 39N). Antennomeres VII and XI elongate (Fig. 39H,I); antennomeres proportions (n = 6): I 74/30: II 57/27: III 31/14: IV 37/14: V 42/14: VI 39/16: VII 43/22: VIII 45/24: IX 71/36: X 73/38: XI 106/39.

PROTHORAX (Fig. 40A–E). Punctation sparse and fine; pubescence sparse and short. Hypomeron subglabrous, impunctate (Fig. 39B, 43B). Prosternal process distinctly elongate and spinose, in lateral view (Fig. 40C). Profurca short and thick (Fig. 40E).

MESOTHORAX (Fig. F–J). Scutellum visible in dorsal view, wider than long; tip rounded (Fig. 40A). Mesoventral lines curved; median lines short, straight, and open (Fig. 40G). Mesepimeron about 2.75× wider than long, and occupying about 1.94/3 of mesanepisternum (Fig. 40G–J). Mesoventral process with a small posterior ridge (Fig. 40H).

METATHORAX (Fig. 40G–N). Metaventrite smooth, shining, pubescence moderately sparse laterally (Fig. 40I,J). Submesocoxal lines strongly arcuate, punctate; submesocoxal area length: 0.04–0.07 mm (Fig. 40G–J). Metanepisternal suture dashed, with variable curvature (Fig. 40I,J). Metanotum with alacrista trapezoidal-shaped; scutoscutellar suture short, and not trespassing the apodeme (Fig. 40K,L). Stalk of metendosternite slightly narrower than arms (Fig. 40M,N).

WINGS (Fig. 39A, 41A–B, 43A). Elytra dense and coarsely punctured. Basal striae connected to sutural, impunctate, and reaching about 2/3 of elytra (Fig. 40A). Lateral striae fine, impunctate, and curved near the humeral region (Fig. 39B).

LEGS. Thin, elongate, not microsculptured (Figs 41D–I, 43D–I).

ABDOMEN. Submetacoxal lines with coarse punctures (Fig. 40I,J). Ventral surface shining; pubescence dense; punctures fine (Fig. 40I,J). Propygidium dense and coarsely punctate; micropunctured; pubescence dense (Fig. 41J, 43J).

Males

Pro- and mesotarsomeres I–III widened, bearing tenent setae (Fig. 41G–I). Sternite VIII with an elongate posterior projection (Fig. 41K). Tergite VIII triangular with a smooth and wide posterior projection (Fig. 41L). Tergite IX with curved ventral struts. Sternite IX constricted centrally (Fig. 41M). Tergite X triangular, wide (Fig. 41M).

AEDEAGUS (Fig. 42A–N). Median lobe with basal bulb larger than apical lobe; apical lobe bent and more sclerotized. Parameres distinctly sclerotized and wavy, in frontal view; with a constriction near the apex (Fig. 42B). Internal sac formed by a twisted sclerite that forms a short and curved main structure; terminal part of the flagellum extending obliquely from the main part, that resembles a hummingbird (Fig. 42E–G,J,N).

MEASUREMENTS (n = 9, including the holotype, unless otherwise specified; in mm): TL 1.08–1.22 (1.18 ± 0.04), SY (n = 8) 0.08–0.12 (0.11 ± 0.01), HW (n = 8) 0.30–0.35 (0.33 ± 0.02), IS (n = 8) 0.15–0.18 (0.17 ± 0.01), WA (n = 8) 0.06–0.10 (0.08 ± 0.01), PL 0.43–0.51 (0.47 ± 0.03), PA 0.33–0.39 (0.35 ± 0.02), PB 0.64–0.72 (0.68 ± 0.03), SL 0.02–0.03 (0.02 ± 0), SW (n = 8) 0.04–0.05 (0.04 ± 0), EI 0.68–0.78 (0.75 ± 0.03), EL 0.74–0.85 (0.82 ± 0.03), EW 0.34–0.40 (0.37 ± 0.02), EH 0.33–0.38 (0.36 ± 0.02), MsW 0.15–0.18 (0.17 ± 0.01), MeL 0.04–0.05 (0.04 ± 0), MeW 0.11–0.15 (0.13 ± 0.01), MB 0.09–0.12 (0.10 ± 0.01), MC 0.25–0.30 (0.28 ± 0.02), ML 0.05–0.07 (0.06 ± 0.01), VL 0.13–0.18 (0.15 ± 0.01), PrF 0.29–0.34 (0.31 ± 0.02), PrT 0.20–0.29 (0.24 ± 0.03), MsF (n = 8) 0.32–0.37 (0.35 ± 0.01), MsT 0.28–0.32 (0.3 ± 0.02), MtF 0.35–0.41 (0.39 ± 0.02), MtT 0.32–0.37 (0.35 ± 0.02).

Females (Fig. 43A–N)

Ventrite VIII with a triangular posterior projection (Fig. 43K). Tergite VIII triangular, lacking a posterior projection (Fig. 43L). Bursa copulatrix with small sclerites (Fig. 43N). Spermatheca filiform (Fig. 43M). Distal gonocoxite triangular, robust; gonostylus elongate (Fig. 43M,N).

MEASUREMENTS (n = 9, unless otherwise specified/ in mm): TL 1.11–1.25 (1.20 ± 0.04), SY 0.10–0.12 (0.11 ± 0.01), HW 0.32–0.36 (0.34 ± 0.01), IS 0.16–0.19 (0.17 ± 0.01), WA 0.07–

0.10 (0.08 ± 0.01), PL 0.43–0.51 (0.48 ± 0.03), PA 0.35–0.38 (0.36 ± 0.01), PB 0.64–0.76 (0.70 ± 0.04), SL (n = 7) 0.02–0.03 (0.02 ± 0), SW (n = 8) 0.03–0.06 (0.04 ± 0.01), EI 0.73–0.80 (0.76 ± 0.03), EL 0.78–0.88 (0.84 ± 0.03), EW (n = 8) 0.34–0.42 (0.38 ± 0.03), EH (n = 8) 0.34–0.42 (0.37 ± 0.03), MsW 0.14–0.20 (0.17 ± 0.02), MeL 0.04–0.05 (0.04 ± 0), MeW (n = 8) 0.10–0.15 (0.13 ± 0.02), MB 0.09–0.14 (0.11 ± 0.02), MC 0.24–0.32 (0.28 ± 0.03), ML 0.04–0.06 (0.05 ± 0.01), VL 0.12–0.17 (0.15 ± 0.02), PrF (n = 8) 0.26–0.32 (0.3 ± 0.02), PrT 0.20–0.25 (0.23 ± 0.02), MsF 0.32–0.36 (0.34 ± 0.01), MsT 0.27–0.30 (0.29 ± 0.01), MtF (n = 8) 0.35–0.41 (0.38 ± 0.02), MtT 0.31–0.36 (0.35 ± 0.02).

Host

Collected from *Ceratiomyxa fruticulosa* on a fallen *Pinus* sp., *Xylodon flaviporus* (Berk. & M.A. Curtis ex Cooke) Riebesehl & Langer 2017 (Schizoporaceae), and from unknown fungi on logs (Fig 1G).

Remarks

Similar to *Baeocera* sp. nov. 5 and *Baeocera* sp. nov. 4. Differs by the more robust body, coarser and denser elytral punctures; shape of antennomeres; parameres wavy and bearing a posterior constriction; tergite IX in females lacking a posterior projection, and distal gonocoxite less elongate.

Distribution

Mata do Paraíso and Mata da Biologia, Universidade Federal de Viçosa, campus of Viçosa, state of Minas Gerais, Southeast Brazil (Fig 1A–D).

Genus ***Scaphisoma*** Leach
(Figs 2C,H, 44–64)

Scaphisoma Leach, 1815: 89. Type species: *Silpha agaricina* Linnaeus, 1758; by monotypy.

Scaphosoma Agazzi, 1846: 332. *Caryoscapha* Ganglbauer, 1899: 343 (as subgenus of *Scaphisoma*). Type species: *Scaphisoma limbatum* Erichson, 1945; by monotypy.

Scaphiomicrus Cassey, 1900: 58. Type species: *Scaphisoma pusilla* LeConte, 1860; by original designation.

Pseudoscaphosoma Pic, 1915b: 31. Type species: *Pseudoscaphosoma testaceomaculatum* Pic, 1915; by original designation.

Scutoscaphosoma Pic, 1916a: 3 (as subgenus of *Scaphosoma*). Type species: *Scaphisoma* (*Scutoscaphosoma*) *rouyeri* Pic, 1916; by monotypy.

Scaphella Achard, 1924: 29. Type species: *Scaphisoma antennatum* Achard, 1920; by original designation.

Macrobaeocera Pic, 1925: 195. Type species: *Scaphisoma phungi* Pic, 1922, by monotypy.

Macroscaphosoma Pic, 1928a: 33. Type species: *Macroscaphosoma collarti* Pic, 1928, by monotypy.

Mimoscaphosoma Pic, 1928b: 49 (as subgenus of *Scaphisoma*). Type species: *Scaphisoma bruchi* Pic, 1928; by original designation.

Metalloscapha Löbl, 1975a: 384. Type species: *Metalloscapha papua* Löbl, 1975; by original designation.

[*Macroscaphosoma* Löbl, 1997: xi. Type species *Macroscaphosoma collarti* Pic, 1928 (credited to Löbl, 1970)]

Encompassing about 800 species, *Scaphisoma* is the largest Scaphidiinae genera. However, it is likely that this number, as with other Scaphidiinae genera, is still underestimated, especially in Brazil. The Brazilian fauna comprises only seven known species – a number that is now understood (pers. obs.) to be substantially divergent from reality. This number should increase exponentially if studies on Scaphidiinae continue. To exemplify, in fewer than 30 short field trips it was possible to collect more than 500 specimens; and about 200 still need to be studied.

General description (* = variable characters within the genera, but not variable in the species below).

HEAD. Labral setae simple*. Mandible unidentate; lacking serrations*. Maxillary palp normal; galea wide, with radulate brush; lacinia with basal setae. Setae on adoral surface of hypopharynx setose. Last labial palpomere curved and thick. Eyes notched*. Antennomere III short and triangular. Gular pores present*. Frontoclypeal suture present. PROTHORAX. Prepectus present. Hypomeron visible in lateral view; extending beyond pronotum*. Prothoracic angle acute. Prothoracic corbiculum absent. MESOTHORAX. Mesoventral process paxillate. Scutellum tip exposed*. Mesoventral lines not connecting to the mesocoxal cavity. Mesepimeron exposed*. Meso- and metaventrite fused. METATHORAX. Metepimeron and metenepisternum exposed; metepimeral lines impunctate. Intercoxal plates absent. Metacoxal process digitate.

Metaventral setose patch absent*. WINGS. Lateral striae present. Elytral apical serration present. Hind wings developed. LEGS. Profemoral ctenidium present. Mesotibiae with two apical spines ABDOMEN. Submetacoxal lines punctate*. Membranes of abdominal ventrites lacking brick-walled pattern. (Löbl & Leschen 2003b; Leschen & Löbl 2005).

Scaphisoma sp. nov. 1

(Figs 44–49, 94C–D)

Diagnosis

Body length: 1.25–1.41 mm. Blackish. Each elytron with a large dark ochreous macula near, apex yellow. Basal striae absent; adsutural area notably widened and not angulate, anteriorly. Clypeus, coxae, femora, metaventrite, and abdomen with strigulate microsculpture. Aedeagus with trifid apex. Females with distal gonocoxite thick.

Etymology

Material examined

Holotype

BRAZIL • ♂; Minas Gerais, Viçosa, UFV, Vila Gianetti; 24 Mar. 2022; E. von Groll leg.; Falcon 43 / Em *Inonotus* sp. (Hymenochaetaceae) / HOLOTYPUS ♂; CELC. (Fig. 44D,E)

Paratypes

BRAZIL • 2♂♂; 1♀ (1♂*); same collection data as for holotype; 10 Mar. 2022; E. von Groll leg.; Falcon 36/ Em *Inonotus* sp. (Hymenochaetaceae); CELC • 2♂♂; 3♀♀; same collection data as for holotype; 10 Mar. 2022; E. von Groll leg.; Falcon 42 / Em *Inonotus* sp. (Hymenochaetaceae); CELC • 4♂♂, 1 ex (1♂*, 1♂**); same collection data as for holotype; 24 Mar. 2022; E. von Groll leg.; Falcon 43 CELC • 1♂, 2♀♀ (1♀*); same collection data as for holotype; 23 Mar. 2022; E. von Groll leg.; Falcon 36 / Em *Inonotus* sp. (Hymenochaetaceae); CELC • 3♂♂, 1♀; same collection data as for holotype; 23 Mar. 2022; E. von Groll leg.; Falcon 42 / Em *Inonotus* sp. (Hymenochaetaceae); CELC • 1♀; same collection data as for holotype; 25 Mar. 2022 E. von Groll leg.; Falcon 29 / Em *Inonotus* sp. (Hymenochaetaceae); CELC • 2♂♂; 1♀; same collection data as for holotype; 01 Apr. 2022;

Falcon 03 / Em *Inonotus* sp.; CELC • 1♂, 1 ex.; same collection data as for holotype; 01 Apr. 2022; E. von Groll leg.; Falcon 26 / Em *Inonotus* sp.; CELC • 10♂♂, 17♀♀, 3 exs. (1♂*); same collection data as for holotype; E. von Groll leg.; 26 Apr. 2022 / Em *Inonotus* sp.; CELC.

Description.

COLORATION. Blackish; each elytron with a large dark reddish-ochreous macula, apex yellow; head, thoracic ventrites, and ventrite I dark ochrous-brown; legs, mouthparts, and apex of abdominal ventrites II–VII light ochrous (Figs 44A–C, 45A). Variations: (1) lighter coloration (Fig. 44F,G); (2) elytral macula absent (Fig. 44H–J).

HEAD (Fig. 45A–I). Wide (0.41–0.45 mm); punctures very fine; pubescence moderately sparse. Clypeus transverse microsculptured (Fig. 45A,B). Labrum shallowly concave posteriorly (Fig. 45E). Last labial palpomere not strongly curved; mentum practically square-shaped (Fig. 45I). Antennomeres VII–IX wide (Fig. 45C,D); antennomeres proportions (n = 3): I 81/46: II 68/39: III 25/16: IV 40/14: V 64/17: VI 71/21: VII 90/33: VIII 62/25: IX 82/31: X 84/29: XI 117/35.

PROTHORAX (Figs 45J–46B). Not microsculptured. Pronotum shining; punctures coarse, more notable near posterior bead; pubescence short and moderately dense (Fig. 45J). Hypomeron shining, glabrous; prothoracic angle extending about 2× the mesepimeron length beyond the anapleural line (Fig. 44B,G,I). Prosternal process arcuate (Fig. 45L). Profurca with robust and slightly curved stalk (Fig. 45B).

MESOTHORAX (Fig. 46C–F). Visible part of scutellum with length similar to width; tip acute (Figs 45J; 46C). Mesanepisternum moderately coarse punctate, densely pubescent (Fig. 46F). Mesepimeron about 4.20× wider than long (Fig. 46E,F). Procoxal rests wider than long; mesoventral lines coarse punctate; secondary lines absent (Fig. 46D). Mesoventral process with similar length sides, in lateral view (Fig. 46E).

METATHORAX (Fig. 46D–I). Metaventrite with strigulate microsculpture, finely punctate, and densely pubescent (Fig. 46F). Submesocoxal lines slightly arcuate, punctate; submesocoxal area length: 0.03–0.05 mm (Fig. 46D–F). Metanepisternum and metepimeron shining, bearing fine and dense pubescence (Fig. 46F). Metanotum alacrista longer than wide (Fig. 46G). Metendosternite with arms somewhat oblong (Fig. 46H–I).

WINGS (Figs 44A–C, 46J–L). Elytra elongate, narrowed posteriorly, coarse punctate – coarser than pronotum –, and moderately pubescent; lateral contours arcuate. Lateral ridge visible in dorsal view. Sutural stria strongly widened and not curved anteriorly; adsutural area wider anteriorly; basal stria absent (Fig. 44A). Lateral stria not curving at the humeral area (Fig. 44B).

LEGS. Femora with strigulate microsculpture (Fig. 44C). Metafemora fusiform (Fig. 47A–C, 49D–F).

ABDOMEN. Strigulate microsculptured (Figs 47G,H, 49J). Ventrite I with finely punctate and densely pubescent (Fig. 44B). Submetacoxal lines arcuate, punctate; submetacoxal area length = 0.07–0.10 mm (Fig. 47G). Tergite VI sparsely and finely punctate; pubescence sparse (Figs 47H, 49J).

Males

Pre- and mesotarsomeres I–III enlarged, with tenent setae (absent in mesotarsomere I) (Fig. 47D–F). Sternite and tergite VIII strigulate microsculptured. Sternite VIII with a shallow triangular projection (Fig. 47I). Tergite VIII straight posteriorly (Fig. 47J). Tergite IX with short-angled ventral struts (Fig. 47K). Sternite IX very elongate, fusiform (Fig. 47K). Tergite X triangular (Fig. 47L).

AEDEAGUS (Fig. 48A–J). Median lobe poorly sclerotized; basal bulb oval (when inflate) and longer than apical lobe; apical lobe slightly curved, in lateral view (Fig. 48C). Parameres more sclerotized near the basal bulb, elongate, and narrowed apically. Internal sac with symmetrical sclerites; sclerite with an apical forceps-shaped structure that connects to the aedeagus apex, forming a tripartite apex – this structure can be more or less closed.

MEASUREMENTS (n = 8, including the holotype, unless otherwise specified; in mm): TL 1.25–1.41 (1.31 ± 0.05), SY 0.16–0.2 (0.19 ± 0.02), HW 0.41–0.45 (0.42 ± 0.01), IS 0.18–0.23 (0.2 ± 0.01), WA 0.11–0.16 (0.14 ± 0.02), PL 0.50–0.55 (0.53 ± 0.02), PA 0.45–0.51 (0.49 ± 0.03), PB 0.74–0.88 (0.82 ± 0.04), SL (n = 4) 0.02–0.02 (0.02 ± 0), SW (n = 4) 0.01–0.02 (0.02 ± 0.01), EI 0.75–0.86 (0.8 ± 0.04), EL 0.86–0.99 (0.91 ± 0.04), EW 0.40–0.50 (0.44 ± 0.03), EH 0.28–0.36 (0.32 ± 0.02), Me 0.17–0.23 (0.2 ± 0.02), MeL 0.10–0.14 (0.12 ± 0.01), MeW 0.02–0.04 (0.03 ± 0.01), MB 0.14–0.20 (0.16 ± 0.02), MC 0.34–0.40 (0.37 ± 0.02), ML 0.03–0.05 (0.04 ± 0.01), MA 0.06–0.10 (0.08 ± 0.02), MA2 0.12–0.15 (0.13 ± 0.01), VL 0.23–0.27 (0.25 ± 0.01), VL2 0.24–0.28 (0.26 ± 0.01), PrF 0.34–0.35 (0.35 ± 0), PrT 0.23–0.26 (0.25 ± 0.01),

MsF 0.34–0.36 (0.35 ± 0.01), MsT 0.30–0.36 (0.33 ± 0.02), MtF 0.40–0.46 (0.43 ± 0.02), MtT 0.40–0.46 (0.43 ± 0.02).

Females (Fig. 49)

Ventrite VIII slightly convex posteriorly (Fig. 49K). Tergite VIII shallowly concave, posteriorly (Fig. 49L). Distal gonocoxite thick, slightly curved; gonostylus fusiform (Fig. 49M,N).

MEASUREMENTS (n = 8, unless otherwise specified; in mm): TL 1.25–1.41 (1.32 ± 0.05), SY 0.17–0.20 (0.18 ± 0.01), HW 0.42–0.45 (0.43 ± 0.01), IS 0.20–0.22 (0.21 ± 0.01), WA 0.12–0.16 (0.14 ± 0.01), PL 0.46–0.55 (0.52 ± 0.03), PA 0.45–0.54 (0.50 ± 0.03), PB 0.75–0.85 (0.81 ± 0.03), SL (n = 2) 0.02, SW (n = 2) 0.02–0.03 (0.03 ± 0.01), EI 0.76–0.89 (0.81 ± 0.04), EL 0.84–0.94 (0.90 ± 0.04), EW 0.44–0.46 (0.45 ± 0.01), EH 0.27–0.33 (0.31 ± 0.03), Me 0.18–0.22 (0.20 ± 0.01), MeL 0.09–0.13 (0.10 ± 0.02), MeW 0.03–0.04 (0.03 ± 0), MB 0.15–0.19 (0.17 ± 0.01), MC 0.33–0.38 (0.35 ± 0.02), ML 0.03–0.05 (0.04 ± 0), MA 0.07–0.08 (0.07 ± 0.01), MA2 0.12–0.16 (0.14 ± 0.01), VL 0.22–0.26 (0.24 ± 0.01), VL2 (n = 7) 0.24–0.27 (0.26 ± 0.01), PrF 0.32–0.37 (0.35 ± 0.01), PrT 0.24–0.27 (0.25 ± 0.01), MsF 0.34–0.37 (0.35 ± 0.01), MsT 0.29–0.34 (0.32 ± 0.02), MtF 0.40–0.44 (0.41 ± 0.02), MtT 0.40–0.44 (0.42 ± 0.01).

Host

Collected from *Inonotus* sp. (Hymenochaetaceae) (Figs 1A–B, E–F, 94A–D).

Remarks

The species belongs to the *Scaphisoma haemorrhoidale* group (Löbl 1970), being more similar in size and aedeagus shape to *S. jacobsoni* Löbl, 1975b. However, it differs by the quite widened adsutural area and sutural striae not angulate anteriorly. It is also similar to *S. jacqi* Löbl & Ramage, 2022 (Ramage & Löbl 2022), differing also by the sutural striae, adsutural area, and by the metaventrite with strigulate microsculpture.

Distribution

Universidade Federal de Viçosa, campus of Viçosa, state of Minas Gerais, Southeast Brazil (Figs 1A,B,E,F).

***Scaphisoma* sp. nov. 2**

(Figs 50–54)

Diagnosis

Body length: 1.09–1.36 mm. Brown to dark brown. Very shining, lacking microsculpture. Antennomere IX elongate. Submesocoxal lines slightly arcuate and punctate. Basal stria absent; sutural striae curved anteriorly. Aedeagus distinctly small; apical elongate and triangular; sclerite of internal sac simple. Distal gonocoxite in females elongate.

Etymology

Material examined

Holotype

BRAZIL • ♂; Minas Gerais, Viçosa, Mata da Biologia; 23 Nov. 2021; E. von Groll & G.L.N. Martins leg. / Em fungo branco ressupinado no tronco caído / HOLOTYPUS ♂; CELC. (Fig.).

Paratypes

BRAZIL • 12♂♂, 8♀♀, 2 exs (1♂*, 1♂**, 2♀♀**); same collection data as for holotype; 13 Nov. 2019; E. von Groll *et al.* leg.; Fungo 16 / Em fungo amarelado ressupinado em tronco caído indet.; CELC • 13♂♂, 3♀♀, 2 exs. (1♂*); same collection data as for holotype; 20 Nov. 2019; E. von Groll *et al.* leg.; Fungo 31 / Em fungo amarelado ressupinado em tronco caído indet.; CELC • 9♂♂, 4♀♀, 3 exs. (1♂*); same collection data as for holotype; 20 Nov. 2019; E. von Groll *et al.* leg.; Fungo 20 / Em fungo branco ressupinado em tronco indet.; CELC • 17♂♂, 10♀♀, 13 exs. (1♂*, 1♀*, 1♂**); same collection data as for holotype; 23 Nov. 2021; E. von Groll & G.L.N. Martins leg. / Em fungo branco ressupinado no tronco caído; CELC • 3♂♂, 2 exs (1♂*); same collection data as for holotype; EPTEA Mata do Paraíso; 12 Nov. 2019; Leg. LabCol; Fungo 02 / Em fungo branco ressupinado em tronco indet.; CELC • 2♂♂, 4♀♀, 2 exs. (1♀*); same collection data as for holotype; EPTEA Mata do Paraíso; 12 Nov. 2019; Leg. LabCol; Fungo 10 / Em *Ceratiomyxa fruticulosa*; CELC • 25♂♂, 17♀♀, 12 exs. (5♂♂**, 1♀**); same collection data as for holotype; EPTEA Mata do Paraíso; 14 Nov. 2019; Leg. LabCol; Fungo 07 / Em fungo branco ressupinado em tronco indet.; CELC • 3♂♂, 1♀, 1 exs. (1♂*); same collection data as for holotype; EPTEA Mata do Paraíso; 14. Nov. 2019; Leg. LabCol; Fungo 13 / Em fungo ressupinado indet. no tronco caído e em *Ceratiomyxa fruticulosa*

no solo; CELC • 6♂♂, 15♀♀, 3 exs. (2♂♂**, 2♀♀**); same collection data as for holotype; EPTEA Mata do Paraíso; 14. Nov. 2019; Leg. LabCol; Fungo 23 / Em fungo branco ressupinado em tronco indet.; CELC • 6♂♂, 4♀♀, 3 exs. (1♂*); same collection data as for holotype; EPTEA Mata do Paraíso; 26 Nov. 2019; Leg. LabCol; Fungo 27 / Em fungo branco ressupinado em tronco indet.; CELC.

Description

COLORATION. Dark brown. Antennae, mouthparts, legs, tip of elytra, and abdominal ventrites II–VI yellow (Fig. 50A–B,H). Variations: (1) light brown (Fig. 50F); (2) medium brown; (3) pronotum darker than elytra (Fig. 50G).

HEAD (Figs 50H–51E). Punctation very fine, sparse. finely punctate; pubescence sparse (Fig. 50H). Labrum conspicuously concave posteriorly (Fig. 51A). Last maxillary palpomere elongate, about 6× longer than wide (Fig. 51D). Last labial palpomere strongly curved; posterior-lateral sides of mentum concave (Fig. 51E). Antennomeres VIII–XI elongate; antennomeres proportions (n = 3): I 83/40: II 70/36: III 23/17: IV 48/14: V 72/18: VI 71/21: VII 96/30: VIII 79/21: IX 99/25: X 97/27: XI 124/30.

PROTHORAX (Fig. 51F–J). Pronotum smooth; punctures dense and moderately coarse; pubescence fine and short. Hypomeron shining, glabrous; posterior angle not extending much beyond the anapleural line (Fig. 52B). Prosternal process thich (Fig. 51H). Membranous part of profurca almost rounded (Fig. 51J).

MESOTHORAX (Fig. 51K–N). Visible part of scutellum longer than wide (Fig. 51F); scutellar lines rising laterally; tip acute (Fig. 51K). Mesepimeron about 3.70× wider than long (Fig. 51N). Mesoventral lines not curved; punctate; secondary lines absent; median lines short, opened (Fig. 51L). Mesoventral process elongate, in lateral view (Fig. 51M).

METATHORAX (Fig. 51L–52C). Metaventrite smooth, punctures fine and sparse; pubescence moderately long (Fig. 51N). Submesocoxal lines slightly arcuate; punctate; submesocoxal area length about 0.04 mm (Fig. 51L–N). Arms of metendosternite straight, forming an angle less than 40° (Fig. 52B,C).

WINGS (Figs 50A–C, 52A–F). Elytra not strongly narrowed apically; punctures coarser than pronotum, pubescence sparse and short. Sutural stria curved near the base; basal stria absent (Fig. 51F). Lateral stria slightly curving at the humeral area (Fig. 50B).

LEGS. Lacking microsculpture (Figs 52G–L, 54D–I).

ABDOMEN. Abdomen lacking microsculpture, smooth, ventrites with very fine punctures, pubescence like metaventrite (Figs 51N, 52M). Submetacoxal lines arcuate, with sparse punctures; submetacoxal area length = 0.05–0.07 mm (Fig. 52M). Tergite VI with micro- and coarse punctures (Fig. 52N, 54J).

Males

Pro- and mesotarsomeres I–III slightly wide, with few tenent setae (except for mesotarsomere I) (Fig. 52J–L). Sternite and tergite VIII lacking microsculpture. Sternite VIII with a small projection (Fig. 53A). Tergite VIII straight apically (Fig. 53B). Sternite IX elongate and with parallel sides (Fig. 53C).

Aedeagus (Fig. 53D–J) very small, hardly visible between terminal tergites and ventrites (Fig. 53D,E). Median lobe with elongate apical lobe and small and membranous basal bult; apical lobe sclerotized and triangular, in ventral and dorsal view (Fig. 53F,J). Parameres almost straight, forming an angle anteriorly, in frontal view (Fig. 53F). Internal sac filling the entire median lobe, lacking complex sclerites (Fig. 53G,I).

MEASUREMENTS (n = 5, including the holotype, unless otherwise specified; in mm): TL (n = 35) 1.09–1.31 (1.21 ± 0.06), SY 0.15–0.18 (0.16 ± 0.01), HW 0.36–0.44 (0.41 ± 0.03), IS 0.17–0.23 (0.19 ± 0.02), WA 0.11–0.14 (0.12 ± 0.01), PL 0.44–0.53 (0.47 ± 0.03), PA 0.44–0.51 (0.46 ± 0.03), PB 0.68–0.80 (0.76 ± 0.05), EI 0.71–0.84 (0.78 ± 0.05), EL 0.78–0.95 (0.86 ± 0.07), EW 0.36–0.44 (0.41 ± 0.03), EH 0.29–0.35 (0.32 ± 0.02), Me 0.19–0.22 (0.20 ± 0.02), MeL 0.09–0.12 (0.11 ± 0.01), MeW 0.02–0.03 (0.02 ± 0), MB 0.12–0.15 (0.13 ± 0.01), MC 0.27–0.35 (0.31 ± 0.04), ML 0.03–0.05 (0.04 ± 0.01), MA 0.06–0.07 (0.06 ± 0.01), MA2 0.12–0.17 (0.14 ± 0.02), VL2 0.19–0.26 (0.22 ± 0.03), VL 0.22–0.29 (0.26 ± 0.03), PrF 0.28–0.35 (0.32 ± 0.03), PrT 0.22–0.27 (0.24 ± 0.02), MsF 0.30–0.36 (0.33 ± 0.03), MsT 0.27–0.36 (0.30 ± 0.04), MtF 0.33–0.42 (0.37 ± 0.04), MtT 0.33–0.42 (0.37 ± 0.04).

Females (Fig. 54)

Sternite VIII with a small posterior projection (Fig. 54K). Tergite VIII with a small concavity posteriorly (Fig. 54L). Distal gonocoxite slender, curved; gonostylus small, rectangular (Fig. 54M,N).

MEASUREMENTS (n = 8; unless otherwise specified; in mm): TL (n = 34) 1.17–1.36 (1.26 ± 0.05), SY 0.16–0.18 (0.16 ± 0.01), HW 0.40–0.43 (0.41 ± 0.01), IS 0.19–0.21 (0.2 ± 0.01), WA 0.11–0.15 (0.12 ± 0.01), PL 0.46–0.56 (0.5 ± 0.04), PA 0.40–0.51 (0.46 ± 0.04), PB 0.70–0.83 (0.76 ± 0.04), EI 0.75–0.89 (0.82 ± 0.05), EL 0.84–0.96 (0.89 ± 0.05), EW 0.41–0.45 (0.44 ± 0.02), EH 0.31–0.34 (0.33 ± 0.01), Me 0.18–0.23 (0.21 ± 0.02), MeL 0.09–0.11 (0.1 ± 0.01), MeW 0.02–0.03 (0.02 ± 0), MB 0.11–0.16 (0.13 ± 0.02), MC 0.29–0.36 (0.32 ± 0.03), ML 0.03–0.05 (0.04 ± 0.01), MA 0.05–0.07 (0.06 ± 0.01), MA2 0.12–0.16 (0.15 ± 0.01), VL 0.22–0.26 (0.24 ± 0.02), VL2 0.25–0.29 (0.27 ± 0.01), PrF 0.31–0.35 (0.33 ± 0.01), PrT 0.21–0.25 (0.23 ± 0.01), MsF 0.32–0.36 (0.34 ± 0.02), MsT: 0.28–0.32 (0.3 ± 0.01), MtF (n = 7): 0.35–0.42 (0.39 ± 0.02), MtT (n = 7): 0.35–0.42 (0.39 ± 0.02).

Host

Collected from undetermined resupinate and/or crust fungi (Fig. 93F–J). Few specimens collected from a decomposing small log with *Ceratiomyxa fruticulosa*.

Remarks

Similar to *S. minutipenis* Löbl & Ogawa, 2016 due the color pattern, elongate sternite IX, small aedeagus, and internal sac without sclerite or flagellum; it can be easily distinguished by the smaller size, thinner antennomeres, submetacoxal lines more arcuate, submetacoxal area longer, and the absence of ventral abdominal microsculpture.

Distribution

Mata do Paraíso and Mata da Biologia, Universidade Federal de Viçosa, campus of Viçosa, state of Minas Gerais, Southeast Brazil (Fig 1A–D).

Scaphisoma sp. nov. 3

(Figs 55–59)

Diagnosis

Body length: 1.28–1.52 mm. Brown-reddish; pronotum darken than elytra. Pronotum and elytra iridescent. Elytra, thorax, legs, and abdomen with distinct strigulate microsculpture. Sutural striae parallel to the suture; basal striae absent. Submesocoxal lines nearly parallel; punctate. Submetacoxal lines arcuate. Parameres widened apically; sclerite of internal sac simple. Females with spermatheca large and twisted; distal gonocoxite curved.

Etymology

Material examined

Holotype

BRAZIL • ♂; Minas Gerais, Viçosa, Mata da Biologia; 30 Oct. 2019; E von Groll & I.S. Pecci-Madalena leg.; Fungo 25 / Em *Xylodon flaviporus* / HOLOTYPUS ♂; CELC. (Fig. 55D,E).

Paratypes

3♂♂, 4♀♀, 2 exs. (1♂**, 1♀*); same collection data as for holotype; 30 Oct. 2019; E von Groll & I.S. Pecci-Madalena leg.; Fungo 25 / Em *Xylodon flaviporus* / CELC • 2♂♂ (1♂*); same collection data as for holotype; 12 Nov. 2019; Leg. LabCol; Fungo 03 / Em fungo branco ressupinado em tronco indet.; CELC.

Description.

COLORATION. Elytra, thorax, and ventrite I reddish-brown; pronotum and posterior part of elytra darker (Fig. 55A–C); mouthparts, antennae, legs, apex of elytra, and abdominal segments III–VII yellow (Fig. 55C,H). Pronotum and elytra iridescent (Fig. 55F,G). Variations: (1) tonalities darker (Fig. 55F); (2) tonalities lighter (Fig. 55G); (3) iridescence covering more or less the structures; (4) ventrite also iridescent.

HEAD (Fig. 55H–56E). Front with punctures somewhat coarse; pubescence moderately sparse. Clypeus wider than long (Fig. 55I). Labrum shallowly concave posteriorly (Fig. 56A). Maxillary palpomeres conspicuously elongate (Fig. 56D). Last labial palpomere not strongly curved, thick; mentum elongate, with a posterior angulate concavity (Fig. 56E). Antennomere VII wide (Fig. 55J,K); antennomeres proportions (n = 2): II 73/45: III 34/18: IV 63/16: V 80/21: VI 81/21: VII 102/31: VIII 83/24: IX 110/33: X 105/32: XI 128/36.

PROTHORAX (Fig. 56F–J). Lacking microsculpture, smooth. Pronotum with punctures fine and moderately sparse; pubescence short and sparse (Fig. 56F). Hypomeron shining, glabrous; posterior angles angulate extending beyond the anapleural line (Fig 55B 56B). Prosternal process concave (Fig. 56H). Profurca short, curved (Fig. 56J).

MESOTHORAX (Fig. 56K–N). With strigulate microsculpture (Figs 56N, 59B). Visible part of scutellum longer than wide (Fig. 56F); scutellar line wavy; tip acute (Fig. 56K). Mesanepisternum with sparse pubescence (Figs 55B, 56N, 59B). Mesepimeron wide, 4.39× wider than long; almost uneven due to the strigulate microsculpture of the mesanepisternum (Fig. 56N). Mesoventral lines not curved; punctate; secondary and median lines absent (Fig. 56L). Mesoventral process longer than wide and curved, in lateral view (Fig. 56M).

METATHORAX (Figs 56L–57C). With strigulate microsculpture (Figs 56N, 56B). Metaventrite with moderately coarse punctures; pubescence sparse (Fig. 56N). Submesocoxal lines nearly parallel, punctate; submesocoxal length about 0.04 mm (Fig. 56L–N). Metanepisternum conspicuously wider near metacoxae (Fig. 56N). Metendosternite arms distinctly opened (Fig. 57B,C).

WINGS (Fig. 57D–G). Elytra with strigulate microsculpture (Fig. 57D–F); not strongly narrowed apically; punctation coarse – coarser than pronotum. One carina longitudinal carina on the disc of each elytron (Figs 55F,G, 59A), poorly visible (but present) on the holotype (Fig. 55A). Sutural striae slightly curved anteriorly; basal striae absent (Fig. 55A). Curvature of lateral striae shortened at the humeral area (Fig. 55B).

LEGS (Figs 56N, 57H–M, 59D–I) With strigulate microsculpture.

ABDOMEN. Ventrites with strigulate microsculpture; pubescence dense (Figs 55B,C, 58A, 59B,C). Submetacoxal lines arcuate and punctate; submetacoxal area length = 0.06 – 0.10 mm (Fig. 58A). Tergite VI and VII with imbricate microsculpture (Fig. 58B).

Males

Pro- and mesotarsomeres I–III widened, with dense tenent setae, especially mesotarsomeres (Fig. 57K–M). Sternite and tergite VIII with strigulate microsculpture. Sternite VIII with a smooth posterior projection (Fig. 58C). Tergite VIII slightly convex posteriorly (Fig. 58D).

Tergite IX with oblong ventral struts (Fig. 58E). Sternite IX wider posteriorly (Fig. 58F). Tergite X oblong (Fig. 58G).

AEDEAGUS (Fig. 58H–N). Basal bulb and apical lobe very distinct. Basal bulb remarkably rounded (Fig. 58H); apical lobe triangular, small, sclerotized, curved, and shorter than basal bulb (Fig. 58I). Parameres elongate; tip wide, in frontal view (Fig 58K). Internal sac membranous and following the median lobe shape: rounded with a projection (Fig. 58L,M).

MEASUREMENTS. (n = 6 including the holotype, unless otherwise specified; in mm): TL 1.28–1.45 (1.38 ± 0.07), SY (n = 5) 0.16–0.20 (0.19 ± 0.02), HW 0.40–0.45 (0.43 ± 0.02), IS 0.20–0.23 (0.21 ± 0.01), WA 0.12–0.15 (0.13 ± 0.01), PL 0.53–0.60 (0.56 ± 0.03), PA 0.44–0.55 (0.50 ± 0.04), PB 0.77–0.91 (0.84 ± 0.06), EI 0.79–0.94 (0.87 ± 0.06), EL 0.90–1.01 (0.95 ± 0.05), EW 0.40–0.54 (0.46 ± 0.05), EH 0.31–0.38 (0.34 ± 0.02), Me 0.18–0.25 (0.23 ± 0.02), MeL (n = 5) 0.13–0.14 (0.13 ± 0.01), MeW (n = 5) 0.03, MB 0.11–0.18 (0.14 ± 0.02), MC 0.31–0.39 (0.35 ± 0.03), ML 0.02–0.04 (0.03 ± 0.01), MA 0.06–0.10 (0.07 ± 0.02), MA2 0.13–0.19 (0.15 ± 0.02), VL 0.23–0.31 (0.26 ± 0.03), VL2 0.23–0.34 (0.27 ± 0.04), PrF 0.35–0.39 (0.37 ± 0.01), PrT 0.24–0.30 (0.27 ± 0.02), MsF 0.34–0.40 (0.37 ± 0.03), MsT 0.25–0.36 (0.31 ± 0.04), MtF 0.38–0.46 (0.43 ± 0.03), MtT 0.38–0.45 (0.42 ± 0.02).

Females (Fig. 59)

Sternite and tergite VIII. Sternite VIII with a wide projection (Fig. 59J). Tergite VIII bearing a very small projection (Fig. 59K). Spermatheca distinctly enlarged and twisted (Fig. 59L). Distal gonocoxite thick and curved; gonostylus very shortened (Fig. 59M).

MEASUREMENTS (n = 3; in mm; in mm): TL 1.48–1.52 (1.50 ± 0.02), SY 0.19–0.20 (0.19 ± 0.01), HW 0.45–0.47 (0.46 ± 0.01), IS 0.21–0.24 (0.22 ± 0.02), WA 0.14–0.16 (0.15 ± 0.01), PL 0.58–0.65 (0.62 ± 0.04), PA 0.45–0.55 (0.5 ± 0.05), PB 0.88–0.94 (0.9 ± 0.03), EI 0.92–0.99 (0.95 ± 0.04), EL 1.01–1.05 (1.03 ± 0.02), EW 0.48–0.58 (0.52 ± 0.05), EH 0.39–0.40 (0.39 ± 0.01), Me 0.26–0.27 (0.27 ± 0.01), MeL 0.13–0.15 (0.14 ± 0.01), MeW 0.03–0.04 (0.03 ± 0.01), MB 0.14–0.15 (0.14 ± 0.01), MC 0.34–0.4 (0.37 ± 0.04), ML 0.04–0.05 (0.04 ± 0.01), MA 0.07–0.11 (0.09 ± 0.02), MA2 0.15–0.18 (0.17 ± 0.02), VL 0.26–0.28 (0.27 ± 0.01), VL2 0.30–0.32 (0.31 ± 0.01), PrF 0.38–0.40 (0.39 ± 0.01), PrT 0.25–0.27 (0.26 ± 0.01), MsF 0.37–0.40 (0.39 ± 0.02), MsT 0.31–0.36 (0.34 ± 0.03), MtF 0.43–0.46 (0.45 ± 0.02), MtT 0.41–0.45 (0.43 ± 0.02).

Host

Collected from *Xylodon flaviporus* and an undetermined crust/resupinate fungus.

Remarks

Similar to *S. iridescens* Löbl & Ogawa, 2016 due to the presence of iridescence, similar sutural striae shape, and absence of basal ones; submesocoxal lines also similar in both species. Nonetheless, while *S. iridescens* presents the iridescence on the ventral surface, *Scaphisoma* sp. nov. 4 presents it on the dorsal surface (pronotum and elytra) – rarely ventrally and always dorsally. *Scaphisoma* sp. nov. 4 can also be easily distinguished by the smaller size, elytra with strigulate microsculptures, and different shape of parameres tha *S. iridescens*.

Distribution

Mata do Paraíso, Universidade Federal de Viçosa, campus of Viçosa, state of Minas Gerais, Southeast Brazil (Fig 1A–B).

***Scaphisoma* sp. nov. 4**

(Figs 59–64)

Diagnosis

Body length: 1.46–1.70 mm. Oblong; brown, appendages yellow. Last maxillary palpomere modified, flattened apically. Sutural stria present, connected to basal. Mesocoxal lines slightly arcuate; submesocoxal area very short. Metacoxal lines parallel to metacoxae; submetacoxal area very short. Males lacking tenent setae. Abdominal ventrite I with punctures coarse and dense; densely pubescent. Median lobe, parameres, and sclerite of internal sac elongate, and curved, in frontal view. Apex of parameres irregular denticulate. Distal gonocoxite fusiform.

Etymology

Material examined

Holotype

BRAZIL • ♂; Minas Gerais, Viçosa, Mata da Biologia; 12 Nov. 2020; Leg. E von Groll & G.L.N. Martins / Em fungo branco ressupinado em tronco caído / HOLOTYPUS ♂; CELC. (Fig. 60D,E).

Paratypes

BRAZIL • 4♂♂, 6♀♀, 6 exs. (1♂*, 1♀*, 1♂**, 1♀**); same collection data as for holotype; 12 Nov. 2020; Leg. E von Groll & G.L.N. Martins / Em fungo branco ressupinado em tronco caído; CELC • 5♂♂, 6♀♀, 12 exs (1♂*, 1♂**,1♀**); 15 Oct. 2021; E. von Groll & A. Orsetti leg.; Fungo 30 / Em fungo branco ressupinado no tronco caído; CELC.

Description.

COLORATION. Brown; antennae, legs, mouthparts, apex of elytra, and posterior bead of abdominal ventrites and tergites yellow (Fig. 60A–C,H, 63B). Variation: (1) lighter tonalities (Fig. 60F–G).

HEAD (Figs 60H–61E). Frons finely punctate; area between the antennae with coarse punctures; pubescence moderately dense (Fig. 60H). Clypeus widened posteriorly (Fig. 60I). Distance between antennal insertion less than 2× the size of the insertion, easily seen in dissected heads (Fig. 60I). Labrum conspicuously concave posteriorly (Fig. 61A). Mandibles not strongly curved, thick (Fig. 61B,C). Last maxillary palpomere with truncate apex (Fig. 61D). Last labial palpomere distinctly curved; mentum with sides similar in length (Fig. 61E). Antennomeres elongate (Fig. 60J,K); antennomeres proportions (n = 6): I 85/50: II 88/44: III 29/19: IV 38/15: V 78/18: VI 94/20: VII 117/37: VIII 90/23: IX 124/31: X 117/33: XI 123/30.

PROTHORAX (Fig. 61F–J). Pronotum with punctures fine and sparse; pubescence short, fine (Fig. 61F). Hypomeron shining, almost glabrous; posterior angle extending just a little beyond the anapleural line (Fig. 61C). Prosternal process forming a just slightly arcuate curvature (Fig. 61H). Profurca elongate, straight (Fig. 61J).

MESOTHORAX (Figs 61K–62C). Visible part of the scutellum with similar sides (Fig. 61F), tip not strongly acute (Fig. 61K). Mesoventral process short, in lateral view (Fig. 62B). Mesanepisternum with few punctures (Fig. 62C). Mesepimeron about 2.59× wider than long (Fig. 62C). Mesoventral lines straight, impunctate (Fig. 62A); secondary lines present, curved (Fig. 60B).

METATHORAX (Fig. 62A–F). Metaventrite with punctures moderately coarse, pubescence dense and thick (Fig. 62C). Submesocoxal lines slightly arcuate; submesocoxal area short, length = 0.03 mm (Fig. 62A–C, 64C). Metanepisternum less pubescent than metaventrite, wider near the metacoxae (Fig. 62C). Metepimeron densely pubescent. Metanotum with alacrista "P-shaped" laterally. Metendosternite with wide ventral lamina, arms forming an angle approximately of 40° (Fig. 62E,F).

WINGS (Fig. 62G–I). Elytra narrowed apically; punctation coarse and sparse. Sutural stria connected to basal (Fig. 61F). Adsutural area narrow (Fig. 60A). Basal stria impunctate and reaching 1/2 of elytral width. Lateral stria punctate, curved at the humeral area (Figs 60B, 64B).

LEGS (Figs 62J–O, 64D–I). Femora elongate and thin, not microsculptured. Apical spine of protibiae I longer than tarsomere I.

ABDOMEN. Ventrites conspicuously coarse and dense punctures and pubescence (Figs 6B,C,G, 64B). Submetacoxal lines parallel to coxae, coarse and densely punctate (Figs 62C, 63A). Submetacoxal area remarkably short: 0.01–0.04 mm (Fig. 62C). Tergite VI coarse punctate and densely pubescent; micropunctured (Fig. 63B, 64J).

Males

Tibiae slightly curved. Protarsomeres I–III just a slightly wider – visible only by microscope; lacking tenet setae (Fig. 62M–O). Sternite and tergite VIII lacking microsculpture and both with a wide apical projection (Fig. 63C,D). Tergite IX with ventral struts forming a flat plate (Fig. 63E). Sternite IX guitar-shape (Fig. 63F). Tergite X ellipsoidal (Fig. 63G).

AEDEAGUS (Fig. 63H–M). Median lobe with basal bulb membranous and rounded; apical lobe distinctly elongate and thin, longer than basal bulb (Fig. 63H–J,L,M); apical lobe and parameres curved in frontal view (Fig. 63J). Parameres more (Fig. 63M) or less (Fig. 63L) separated, with irregular denticulate apex, resembling to be broken (Fig. 63J). Internal sac thin, elongate, curved (Fig. 63K).

MEASUREMENTS (n = 8, including the holotype, unless otherwise specified; in mm): TL (n = 10) 1.52–1.66 (1.58 ± 0.04), SY 0.17–0.19 (0.18 ± 0.01), HW 0.49–0.5 (0.49 ± 0.01), IS 0.21–0.22 (0.22 ± 0), WA 0.13–0.15 (0.14 ± 0.01), PL 0.59–0.65 (0.62 ± 0.02), PA 0.50–0.56 (0.53 ± 0.02), PB 0.93–1.04 (0.96 ± 0.04), SL (n = 7) 0.01–0.03 (0.02 ± 0.01), EI 0.94–1.06 (1 ± 0.04),

EL 1.05–1.15 (1.1 ± 0.03), EW 0.54–0.59 (0.55 ± 0.02), EH 0.38–0.45 (0.41 ± 0.02), Me 0.23–0.27 (0.24 ± 0.01), MeL 0.03–0.05 (0.04 ± 0.01), MeW 0.10–0.12 (0.11 ± 0.01), MB 0.19–0.23 (0.21 ± 0.01), MC 0.30–0.37 (0.33 ± 0.03), ML 0.03–0.04 (0.03 ± 0.01), MA 0.02–0.03 (0.02 ± 0), VL 0.24–0.29 (0.26 ± 0.02); (n = 7): VL2 0.28–0.31 (0.29 ± 0.01), PrF 0.43–0.47 (0.45 ± 0.02), PrT 0.30–0.35 (0.31 ± 0.02), MsF 0.45–0.49 (0.47 ± 0.02), MsT 0.39–0.45 (0.43 ± 0.02), MtF 0.48–0.52 (0.5 ± 0.01), MtT 0.48–0.52 (0.5 ± 0.01).

Females (Fig. 64)

Sternite and tergite VIII with a wide apical projection (Fig. 64K,L). Tergite VIII imbricate microsculpture (Fig. 64L). Distal gonocoxite fusiform and curved; gonostylus wide, triangular (Fig. 64M,N).

MEASUREMENTS (n = 7, unless otherwise specified; in mm): TL (n = 12) 1.46–1.70 (1.62 ± 0.08), SY 0.16–0.19 (0.18 ± 0.01), HW 0.46–0.51 (0.49 ± 0.02), IS 0.2–0.24 (0.22 ± 0.01), WA 0.13–0.17 (0.15 ± 0.01), PL 0.59–0.68 (0.64 ± 0.03), PA 0.50–0.58 (0.54 ± 0.03), PB 0.89–1.06 (0.98 ± 0.06), SL 0.02–0.03 (0.02 ± 0), EI 0.95–1.13 (1.04 ± 0.06), EL 1.06–1.19 (1.13 ± 0.04), EW 0.54–0.6 (0.57 ± 0.02), EH 0.39–0.46 (0.43 ± 0.03), Me 0.24–0.27 (0.25 ± 0.01), MeL 0.04–0.05 (0.04 ± 0), MeW 0.10–0.11 (0.10 ± 0.01), MB 0.19–0.23 (0.21 ± 0.02), MC 0.30–0.39 (0.33 ± 0.04), ML 0.03–0.04 (0.03 ± 0.01), MA 0.01–0.04 (0.03 ± 0.01), VL 0.26–0.31 (0.28 ± 0.02), VL2 0.28–0.34 (0.30 ± 0.02), PrF 0.41–0.47 (0.45 ± 0.02), PrT (n = 6) 0.28–0.40 (0.32 ± 0.04), MsF 0.43–0.47 (0.46 ± 0.01), MsT 0.38–0.45 (0.42 ± 0.03), MtF 0.47–0.54 (0.5 ± 0.02), MtT 0.47–0.54 (0.50 ± 0.02).

Host

Collected from undetermined resupinate and/or crust fungi (Fig 93E–F).

Remarks

Punctation of submeso- and submetacoxal lines, sutural and basal striae similar to *S. repandum* Casey, 1893.Nonetheless, *Scaphisoma* sp. nov. 4 can be easily distinguish by the unusual shape of the last palpomere and more variable body size range.

Distribution

Mata da Biologia, Universidade Federal de Viçosa, campus of Viçosa, state of Minas Gerais, Southeast Brazil (Fig 1A–D).

Genus ***Toxidium*** LeConte

(Figs 2I,K, 65–91)

Toxidium LeConte, 1860: 324. Type species: *Toxidium gammaroides* LeConte, 1860, by monotypy.

Toxidium comprises only 34 described species, of which seven are from the Neotropical Region. Only *T. acuminatum* Pic, 1920c is reported to Brazil. In this paper, seven new species are described for Minas Gerais, Brazil. These new species represent just about half all new collected species.

General description (* = variable characters within the genera, but not variable in the species below)

Body compressed laterally. HEAD. Frontoclypeal suture present. Mandible with two apical teeth and subapical serrations. Labral setae simple. Maxillary palpomeres normal. Galea wide, with radulate brush. Eyes anteriorly notched. Antennomeres III and IV elongate. PROTHORAX. Hypomeron visible in lateral view, not extending beyond pronotum. Prothoracic carinae prominent. Prothoracic corbiculum absent. MESOTHORAX. Median lines absent. Mesoventral space (prepectus) present. Mesoventral lines impunctate, connecting to the mesocoxal cavity. Secondary lines present. Median lines absent. Mesoventral process paxillate. Mesepimeron absent. Meso- and metaventrite not fused. METATHORAX. Metanepisternum exposed. Mesocoxal lines parallel to the coxae, impunctate. Lacking metaventral setose patch. Intercoxal plates present. Metacoxae contiguous. WINGS. Hind wings developed. Elytral basal stria absent*. Sutural striae shortened*. Apical serrations on elytra absent. LEGS. Profemoral ctenidium absent. Mesotibiae with two apical spines. Metatarsi about as long as metatibiae. ABDOMEN. Submetacoxal space absent. Submetacoxal bead punctate. Membranes of abdominal ventrites with brick-walled pattern. (Löbl & Leschen 2003b; Leschen & Löbl 2005).

Toxidium **sp. nov. 1**

(Figs 65–70)

Diagnosis

Body length: 2.18–2.33 mm. Dark brown, some areas dark-reddish; femora and tibiae wine red; tarsi yellow. Shining; strongly curved in lateral view. Sutural striae covering about 4/5 from elytral apex; elytral punctation sparse. Pronotum length exceeding hypomeron. Metanepisternal suture almost straight. Metaventrite with few coarse punctures near the anapleural lines – absent in some specimens. Posterior region of abdominal ventrite I and ventrites II–VI with imbricate microsculpture. Parameres with a hock-shaped posterior projection. Sclerite of internal sac J-shaped. Distal gonocoxite remarkably elongate.

Etymology

Material examined

Holotype

BRAZIL • ♂; Minas Gerais, Araponga; Parque Estadual da Serra do Brigadeiro; em tronco; 25 Oct. 2015; Araújo, S.L. *et al.* leg / HOLOTYPUS ♂; CELC. (Fig. 65D,E).

Paratypes

BRAZIL • 1♂, 1♀ (1♂**, 1♀*); same collection data as for holotype; 25 Oct. 2015; Araújo, S.L. *et al.* leg.; CELC • 1♂*; Viçosa, EPTEA Mata do Paraíso; 07 Apr. 2022; E. von Groll & C. Lopes-Andrade leg.; Falcon 03 / Em Fungo branco ressupinado no tronco caído; CELC.

Description.

COLORATION. Dark brown; some areas dark-reddish; antennae, maxillary and labial palpomeres, tarsi, and apical ventral segments and elytra yellow; mouthparts, coxae, femora, and tibiae wine red (Fig. 65A–C,H) Variation: brown with lighter tonalities – not reddish (Fig. 65F,G).

HEAD (Figs 65H–66E). Frons densely and moderately coarse punctate; pubescence dense. Clypeus almost squared (Fig. 65I). Mandibles strongly curved (Fig. 66B,C). Last maxillary palpomere about 4× longer than wide; lacinia with moderately dense apical and basal pubescence (Fig. 66D). Last labial palpomere short and thick; mentum concave posteriorly (Fig. 66E). Gular pores absent; gular region strigulate microsculptured. Antennomere XI elongate (Fig. 65J–L); antennomeres proportions (n = 3) I 115/47: II 106/52: III 85/21: IV 125/19: V 138/21: VI 115/22: VII 150/36: VIII 97/24: IX 134/40: X 130/37: XI 155/39.

PROTHORAX (Fig. 66F–J). Pronotum strongly convex in lateral view (Fig. 65B); anterior bead (Fig. 66G) not visible in dorsal view (Fig. 66F) due to the curvature; shining; punctures moderately coarse and sparse; pubescence moderately sparse. Posterior angle trespasses the hypomeron and does not reach the anapleural line, in lateral view (Fig. 65G). Prosternal process spinose (Fig. 66H). Notosternal suture slightly curved (Fig. 66I). Profurca slightly curved and tapering towards the apex (Fig. 66J).

MESOTHORAX (Fig. 67A–E). Scutellum not visible in dorsal view (Fig. 66F); mesonotum strongly sclerotized (Fig. 67A); tip rounded. Mesanepisternum with finely punctate; pubescence moderately dense (Fig.67D). Mesoventral lines straight (fig. 57B); secondary lines curved (Fig. 67D). Mesoventral process with an apical ridge curved downwards, in lateral view (Fig. 67C).

METATHORAX (Fig. 67B–H). Metaventrite shining, finely punctate, almost glabrous, and with coarse punctures near the anapleural line (Fig. 57D) – sometimes absent (Fig. 67E); central region with imbricate microsculpture (Fig. 67D). Submesocoxal lines arcuate, slightly wavy, laterally, and connected at the midline, forming a very acute angle; submesocoxal area with imbricate microsculpture; length: 0.07–0.09 mm (Fig. 67B,D). Metanepisternal suture impunctate, strongly marked, and straight; metanepisternum mostly covered by the elytra (Fig. 67C–E). Metanotum with triangular and small alacrista; scutoscutellar suture laterally curved, trespassing the apodeme (Fig. 67F). Stalk of metendosternite distinctly narrow anteriorly and widening towards the arms (Fig. 67G).

WINGS (Fig. 65A–C, 67I–L). Elytra with punctures moderately coarse and denser than pronotum. Sutural striae shortened, extending from apex up to about 4/5 of sutural length (Fig. 66F). Lateral striae fine, impunctate, and curved near the humeral region (Fig. 65B).

LEGS (Fig. 68A–F). Meso- and metafemora and tibiae very elongate and slender; with imbricate microsculpture.

ABDOMEN. Ventral surface almost glabrous; posterior area of ventrite I, ventrites II–VI, with imbricate microsculpture (Fig. 67D,E). Pro- and pygidium with sparse pubescence and conspicuously microsculptured (Fig. 68H).

Males

Protarsomeres I–III widened, bearing tenent setae (Fig. 68D). Sternite VIII elongate, bearing a wide posterior projection (Fig. 68I). Tergite VIII narrow, with a small posterior projection (Fig. 68J). Tergite IX with ventral struts strongly curved (Fig. 68K). Sternite IX with laterals slightly curved (Fig. 68L). Tergite X triangular (Fig. 68M).

AEDEAGUS (Fig. 69). Median lobe with basal bulb and apical lobe almost indistinct, just slightly curved in lateral view, and membranous. Apical lobe triangular, in frontal/dorsal view. Parameres bearing a curved and elongate posterior projection (Fig. 69C,G). Sclerite of internal sac J-shaped (Fig. 69D,H).

MEASUREMENTS (n = 3, including the holotype, unless otherwise specified; in mm): TL 2.18–2.33 (2.25 ± 0.08), SY 0.27–0.30 (0.28 ± 0.02), HW 0.86–0.89 (0.88 ± 0.02), IS 0.33–0.43 (0.39 ± 0.05), WA 0.22–0.25 (0.24 ± 0.02), PL 0.84–1.00 (0.93 ± 0.08), PA 0.59–0.61 (0.60 ± 0.01), PB 1.02–1.20 (1.10 ± 0.09), EI 1.48–1.52 (1.49 ± 0.02), EL 1.58–1.68 (1.62 ± 0.05), EW 0.53–0.55 (0.54 ± 0.01), EH 0.70–0.78 (0.73 ± 0.05), MB 0.12–0.15 (0.14 ± 0.02), MC 0.11–0.16 (0.13 ± 0.02), MeW (n = 1) 0.35–0.35 (0.35 ± 0), ML 0.07–0.09 (0.08 ± 0.01), VL 0.25–0.27 (0.26 ± 0.01), VL2 0.43–0.43 (0.43 ± 0), PrF 0.59–0.63 (0.61 ± 0.02), PrT (n = 2) 0.42–0.43 (0.43 ± 0.01), MsF 0.67–0.75 (0.70 ± 0.04), MsT 0.60–0.65 (0.62 ± 0.03), MtF 0.72–0.77 (0.75 ± 0.03), MtT 0.57–0.78 (0.68 ± 0.11).

Females (Fig. 70)

Ventrite VIII with a thin posterior projection (Fig. 70A). Tergite VIII with a small posterior projection (Fig. 70B). Distal gonocoxite very long, slightly tapering posteriorly; gonostylus elongate and slightly oblong (Fig. 70D,E).

MEASUREMENTS (n = 1): TL 2.30, SY 0.30, HW 0.89, IS 0. 43, WA 0.25, PL 1.04, PA 0.63, PB 1.17, EI 1.56, EL 1.64, EW 0.52, EH 0.73, MB 0.14, MC 0.11, MeW 0.38, ML 0.07, VL 0.27, VL2 0.45, PrF 0.64, PrT 0.45, MsF 0.72, MsT 0.58, MtF 0.76, MtT 0.7.

Host

In Viçosa, collected from undetermined crust/resupinate fungi on logs.

Remarks

Despite *Toxidium* sp. nov. 1 presents all necessary characteristics to belong this genus, the morphology of this species is quite discrepant. It can be easily recognized by the shorter hypomeron compared to pronotum, pronotum strongly curved, in lateral view, and by the projections on the parameres. Nonetheless, the sclerite of the internal sac resembles the ones found in Toxidium sp. nov. 2, *Toxidium* sp. nov. 5, and *Toxidium* sp. nov. 7.

Distribution

Mata do Paraíso, Universidade Federal de Viçosa, campus of Viçosa and from Araponga, state of Minas Gerais, Southeast Brazil (Fig 1A–B).

Toxidium sp. nov. 2

(Figs 71–73)

Diagnosis

Body length: 1.90 mm. Reddish-brown; legs ochreous. Sutural striae covering about 3.69/5 from elytral apex. Posterior angle of pronotum not reaching the anapleural line. Submesocoxal area and anterior area of metaventrite with strigulate microsculpture. Metanepisternum conspicuously wider anteriorly. Sclerite on internal sac of aedeagus J-shaped, longer side 2.5× longer than shorter.

Etymology

Material examined

Holotype

BRAZIL • ♂*; Minas Gerais, Viçosa, EPTEA Mata do Paraíso; 17 Mar. 2022; E. von Groll *et al.* leg.; Falcon 12 / Em Fungo branco ressupinado no tronco caído / Dissecado em 11.nov.2022 / HOLOTYPUS ♂; CELC (Fig. 71D,E).

Description.

COLORATION. Reddish-brown, redder near sutures; shining; posterior area of clypeus, coxae, femora, and tibiae ochreous; antennae, mouthparts, tip of elytra, tarsi, and apex of abdominal ventrites yellow (Fig. 71A–C, 72A–F).

HEAD. Frons with punctures dense and fine – few coarser punctures near the frontoclypeal suture; pubescence dense (Fig. 71F). Antennomeres IV–VI distinctly thin (Fig. 71H), proportions: I 114/50: II 106/50: III 72/16: IV 86/13: V 103/11: VI 98/13: VII 117/27: VIII 88/23: IX 116/34: X 114/38: XI 143/46.

PROTHORAX (Fig. 71A–C,G). Somewhat elongate, smooth. Pronotum fine and moderately dense punctured. Lateral carinae dashed, visible in lateral view (Fig. 71B). Hypomeron with punctures very fine and poorly pubescent (Fig. 71B). Posterior angles of pronotum slightly acute, and not reaching the anapleural line (Fig. 71B).

MESOTHORAX. Tip of scutellum exposed, slightly longer than wide (Fig. 71G). Mesanepisternum very finely punctate; pubescence sparse (Fig. 71B). Mesoventral lines slightly curved, secondary lines straight (Fig. 72A).

METATHORAX. Metaventrite with imbricate microsculpture between submesocoxal lines and metanepisternal suture; almost glabrous and impunctate (Fig. 72D). Submesocoxal lines punctate; submesocoxal area imbricate microsculptured; length: 0.10 mm (Fig. 72A). Metanepisternum triangular; conspicuously wider anteriorly, pubescence denser near the metanepisternal suture (Fig. 72A).

WINGS. Elytra with coarse punctures – coarser than pronotum –, pubescence moderately dense (Fig. 71A). Sutural striae shortened, extending from apex up to about 3.69/5 of sutural length (Fig. 71A). Lateral striae impunctate, just slightly curved at the humeral region (Fig. 71B).

LEGS (Fig. 72C–E) With imbricate microsculpture.

ABDOMEN. Shining. Ventrite I with micropuncture only near the submetacoxal bead (Fig. 72D). Propygidium micropunctured (Fig. 72F).

MALE CHARACTERISTICS. Protarsomeres I–III widened, bearing tenent setae (Fig. 72C). Sternite VIII with a posterior triangular projection (Fig. 72G). Tergite IX with ventral struts slightly curved (Fig. 72H). Sternite IX rounded posteriorly (Fig. 72I). Tergite X triangular, angulate posteriorly (Fig. 72J).

AEDEAGUS (Fig. 73) poorly sclerotized. Basal bulb and apical lobe similar in length. Apical lobe triangular (Fig. 73). Parameres wavy, in lateral view (Fig. 73C). Sclerite of the internal sac J-shaped, longer side 2.5× longer than shorter.

MEASUREMENTS (n = 1, holotype; in mm): TL 1.90, SY 0.200, HW 0.81, IS 0.33, PL 0.84, PA 0.55, PB 0.98, EI 1.20, EL 1.26, EW 0.52, EH 0.58, MB 0.13, MC 0.16, MeW 0.3, ML 0.10, VL 0.25, VL2 0.37, PrF 0.5, PrT 0.35, MsF 0.56, MsT 0.46, MtF 0.59, MtT 0.55.

Host

Collected from an undetermined crust/resupinate fungus.

Remarks

Similar to *Toxidium* sp. nov. 4 but differ by the absence of coarse punctures on the metaventrite, elytra with shallow punctures and less pubescent than *Toxidium* sp. nov. 4, and by the curved sclerite of internal sac.

Distribution

Mata do Paraíso, Universidade Federal de Viçosa, campus of Viçosa, state of Minas Gerais, Southeast Brazil (Fig 1A–B).

***Toxidium* sp. nov. 3**

(Figs 74–76)

Diagnosis

Body length: 1.88 mm. Brown. Ventral side almost glabrous. Sutural striae covering 4.44/5 from elytral apex. Metaventrite I with few coarse punctures next to the submesocoxal lines. Metanepisternal suture wavy. Abdominal ventrite I with micropunctures on the central region. Parameres of the aedeagus wavy, in lateral view; sclerite asymmetrical.

Etymology

Material examined

Holotype

BRAZIL • ♂*; Minas Gerais, Viçosa, Mata da Biologia; 23 Nov. 2021; E. von Groll & G.L.N. Marins leg. / Em Fungo branco ressupinado no tronco caído / Dissecado em 12.xi.2022 / HOLOTYPUS ♂; CELC (Fig. 74D,E).

Description.

COLORATION. Brown; mouthparts, antennae, and tibiae yellow; anterior part of femora dark ochreous; posterior tip of femora, tibiae, elytral apex, and apex of each abdominal ventrite, ochrous (Fig. 74A–C,F).

HEAD. Fron with punctures moderately sparse and coarse, and with some micropunctures; pubescence moderately dense (Fig. 74F). Antennomere XI elongate; antennomeres proportions (Fig. 74H): II 107/41: III 69/20: IV 90/18: V 104/18: VI 100/16: VII 121/36: VIII 90/22: IX 115/35: X 115/36: XI 157/42.

PROTHORAX. Smooth; punctures fine; pubescence moderately sparse (Fig. 74G). Hypomeron with punctures very fine and pubescence sparse (Fig. 74B). Posterior angle of pronotum somewhat acute, almost reaching the anapleural line (Fig. 74B).

MESOTHORAX. Tip of scutellum very little exposed (Fig. 74G). Mesanepisternum finely punctate; very little pubescence (Fig. 74B). Mesoventral lines slightly wavy; secondary straight (Fig. 74B, 75A).

METATHORAX. Metaventrite smooth, shining, with few lateral pubescence; punctures inconspicuous; few coarse punctures next to the submesocoxal lines (Fig. 74B). Submesocoxal lines somewhat straight laterally, and connected at the midline, forming an obtuse angle; submesocoxal area length: 0.09 mm (Fig. 74B). Metanepisternal suture wavy (Fig. 75A).

WINGS (Fig. 74A–C, 75B). Elytra moderately dense and coarse punctate – more than pronotum. Sutural striae just slightly shortened, extending from apex up to about 4.44/5 of sutural length (Fig. 74A). Lateral striae impunctate, slightly curved at the humeral region, and reaching the elytral border (Fig. 74B).

LEGS. With imbricate microsculpture (Fig. 75S,D).

ABDOMEN. Central region of ventrite I and propygidium micropunctured; ventral surface almost glabrous (Figs 74B, 75D). Pro- and pygidium with some coarse punctures, moderately pubescent, and micropunctured (Fig. 75E).

Male

Protarsomeres I–III widened, bearing tenent setae (Fig. 75C). Sternite VIII shortened, bearing a triangular posterior projection (Fig. 75F). Tergite VIII with a rounded posterior projection (Fig. 75G). Tergite IX with ventral struts almost straight (Fig. 75H). Sternite IX widened posteriorly (Fig. 75I). Tergite X triangular (Fig. 75J).

AEDEAGUS (Fig. 76). Basal bulb longer than apical lobe; apical lobe curved, just slightly sclerotized. Parameres wavy and strigulate microsculptured (Fig. 76B); sclerite of internal sac asymmetrical (Fig. 76D–G).

MEASUREMENTS (n = 1, holotype; in mm): TL 1.88, SY 0.24, HW 0.78, IS 0.34, WA 0.17, PL 0.82, PA 0.53, PB 1.02, EI 1.22, EL 1.36, EW 0.55, EH 0.55, MB 0.24, MC 0.11, ML 0.09, PrF 0.49, PrT 0.34, MsF 0.59, MsT 0.44, MtF 0.60, MtT 0.54.

Host

Collected from an undetermined crust fungus (Fig. 93E–F).

Remarks

Similar to *Toxidium* sp. nov. 7 but differs by the shorter submesocoxal area, ventrite I not microsculptured, and by the dilatated parameres, in lateral view, and by the not curved sclerite of internal sac.

Distribution

Mata da Biologia, Universidade Federal de Viçosa, campus of Viçosa, state of Minas Gerais, Southeast Brazil (Fig. 1A–D).

Toxidium sp. nov. 4

(Figs 77–79)

Diagnosis

Body length: 1.90 mm. Dark-brown. Dorsal surface pubescence very dense. Metaventrite coarsely punctate between submesocoxal lines and metenepisternum. Metanepisternum triangular, wider anteriorly. Aedeagus with parameres remarkably wavy, in lateral view. Sclerite of internal sac arrow-shaped.

Etymology

Material examined

Holotype

BRAZIL • ♂*; Minas Gerais, Viçosa, Mata da Biologia; 15 Oct. 2021; E. von Groll & A. Orsetti leg.; Fungo 30 / Em Fungo branco ressupinado no tronco caído / Dissecado em 11.nov.2022 / HOLOTYPUS ♂; CELC (Fig. 77D,E).

Description.

COLORATION. Dark-brown; clypeus, coxae, femora, and tibiae dark ochreous; antennae, mouthparts, tip of elytra, and apex of each abdominal ventrite yellow (Fig. 77).

HEAD. Frons with fine and dense punctures; pubescence dense; clypeus micropunctured. Antennomeres III–VI somewhat thicker, IX about 3,20× longer than VIII, XI, oblong (Fig. 77H); proportions: I 115/38: II 101/45: III 58/18: IV 76/16: V 90/18: VI 88/18: VII 110/32: VIII 70/21: IX 110/33: X 115/35: XI 146/47.

PROTHORAX. Pronotum not strongly curved; finely and densely punctate, pubescence very dense (Fig. 77G). Posterior angles of pronotum slightly acute, reaching the anapleural line (Fig. 77B).

MESOTHORAX. Tip of scutellum exposed (as long as wide) (Fig. 77G). Mesanepisternum with inconspicuous punctation, pubescence sparse (Fig. 77B). Secondary lines straight, not connected to the mesocoxal cavities (Fig. 77B).

METATHORAX. Metaventrite with conspicuous coarse punctures between submesocoxal lines and metanepisternal suture; almost glabrous (Figs 77B, 78A). Submesocoxal lines not wavy;

submesocoxal area with imbricate microsculpture; length: 0.09 mm (Fig. 78A). Metanepisternal suture curved anteriorly; metanepisternum triangular, wider anteriorly (Fig. 78A).

WINGS. Elytra densely and coarsely punctate – coarser than pronotum; pubescence dense (Fig. 77A,G). Sutural striae not strongly shortened, extending from apex up to about 4.10/5 of sutural length (Fig. 77A). Lateral striae impunctate, slightly curved at the humeral region (Fig. 77B).

LEGS (Fig. 78C,D). With imbricate microsculpture.

ABDOMEN. Ventral surface shining, almost glabrous (Fig. 77B). Ventrite I with micropuncture at the middle. Propygidium micropunctured (Fig. 78E).

Male

Protarsomeres I–III widened, bearing tenent setae (Fig. 78C). Sternite VIII elongate, with a very short posterior projection (Fig. 78F). Tergite VIII straight posteriorly (Fig. 78G). Tergite IX with ventral struts thick and slightly curved (Fig. 78H). Sternite IX oblong (Fig. 78I). Tergite X triangular and rounded posteriorly (Fig. 78J).

AEDEAGUS (Fig. 79). Median lobe slightly sclerotized; basal bulb longer than apical lobe; apical lobe bent (Fig. 79B). Parameres remarkably wavy and wide, in lateral view (Fig. 79D). Sclerite of the internal sac arrow-shaped (Fig. 79E,F).

MEASUREMENTS (n = 1, holotype; in mm): TL 1.88, SY 0.20, HW 0.75, WA 0.11, PL 0.88, PA 0.52, PB 0.95, EI 1.20, EL 1.32, EW 0.55, EH 0.55, MB 0.12, MC 0.14, MeW 0.30, ML 0.09, VL 0.23, VL2 0.35, PrF 0.5, PrT 0.35, MsF 0.57, MsT 0.42, MtF 0.54, MtT 0.53.

Host

Collected from undetermined crust/resupinate fungus (Fig. 94E–F).

Remarks

Parameres dilatated and sclerite of internal sac incurved as *T. robustum* Pic, 1930. Nonetheless, *Toxidium* sp. nov. 4 can be easily distinguished by the longer sutural striae and absence of basal striae.

Distribution

Mata da Biologia, Universidade Federal de Viçosa, campus of Viçosa, state of Minas Gerais, Southeast Brazil (Fig. 1A–D).

Toxidium sp. nov. 5

(Figs 80–82)

Diagnosis

Body length: 1.45 mm. Brown. Posterior angle of pronotum not acute and not trespassing the anapleural line; lateral carina wavy. Metaventrite with coarse and dense punctures under the anapleural lines and next to the metanepisternal suture. Metanepisternum entirely hidden beneath elytra. Submesocoxal area short = 0.04 mm. Parameres of aedeagus oar-shaped, in lateral view; sclerite of internal sac strongly curved.

Etymology

Material examined

Holotype

BRAZIL • ♂*; Minas Gerais, Viçosa, EPTEA Mata do Paraíso; 12 Nov. 2019; Leg. LabCol; Falcon 01 / Em tronco pequeno caído com hifa indet. / Dissecado em 12.xi.2022 / HOLOTYPUS ♂; CELC (Fig. 80D,E).

Description.

COLORATION. Brown, ventral sclerites lighter near the sutures; posterior 1/2 of clypeus, tip of elytra, coxae, femora, and tibiae ochreous; mouthparts, antennae, tarsi, and apex of each abdominal ventrite yellowish (Fig. 80A–C,F).

HEAD. Frons sparsely punctate and pubescent; punctation fine, with some coarser sparsely distributed. Antennomeres elongate (Fig. 80H); proportions: I 81/41: II 86/42: III 49/15: IV 79/13: V 93/14: VI 87/16: VII 113/24: VIII 84/20: IX 116/28: X 108/33: XI 137/42.

PROTHORAX. Pronotum with pubescence and punctures moderately dense (Fig. 80G). Hypomeron with punctures very fine and pubescence sparse (Fig. 80B). Prothoracic carina

wavy, in lateral view (Fig. 80B). Posterior angles of pronotum not acute and not reaching the anapleural lines (Fig. 80B).

MESOTHORAX. Tip of scutellum exposed (longer than wide). Mesanepisternum finely punctate, pubescence sparse. Secondary lines wavy and connected to the mesocoxal cavities (Fig. 80B).

METATHORAX. Metaventrite lacking microsculpture, shining, almost glabrous; densely and coarsely punctate under the anapleural lines and next to the metanepisternal suture (Fig. 81A). Submesocoxal lines parallel to the coxae; submesocoxal area micropunctured and short, length: 0.04 mm (Figs 80B, 81A). Metanepisternum completely hidden under elytra (Figs 80B, 81A).

WINGS (Figs 80A–B, 81B) Elytra with coarse and moderately sparse punctures. Sutural striae shortened, extending from apex up to about 4/5 of sutural length (Fig. 80A). Lateral striae impunctate, slightly curved at the humeral region (Fig. 80B).

LEGS (Fig. 81C,D) Meso- and metafemora thin, with imbricate microsculpture.

ABDOMEN. Ventral surface smooth, shining, almost glabrous (Fig. 80B). Propygidium micropunctured and sparsely pubescent (Fig. 81E).

Male

Protarsomeres I–III widened, bearing tenent setae (Fig. 81C). Sternite VIII with a shallow posterior projection (Fig. 81F). Tergite VIII convex posteriorly (Fig. 81G). Tergite IX with curved ventral struts (Fig. 81H). Sternite IX oblong (Fig. 81I). Tergite X rounded curved (Fig. 81J).

AEDEAGUS (Fig. 82) poorly sclerotized. Median lobe lacking obvious divisions between apical lobe and basal bulb; apical lobe membranous and curved backwards (Fig. 82C). Parameres without sclerotized anterior portion (that connects to the median lobe); and oar-shaped, in lateral view (Fig. 82C). Sclerite of internal sac strongly curved (Fig. 82C).

MEASUREMENTS (n = 1, holotype; in mm): TL 1.46, SY 0.17, HW 0.44, WA 0.07, PL 0.61, PA 0.41, PB 0.74, EI 0.95, EL 0.99, EW 0.36, EH 0.46, MB 0.12, MC 0.04, ML 0.04, VL 0.17, PrF 0.35, PrT 0.29, MsF 0.42, MsT 0.33, MtF 0.52, MtT 0.43.

Host

Collected from a rotten small log, covered with undetermined hypha.

Remarks

Similar to *Toxidium* sp. nov. 7 but differs by the presence of dense and coarse lateral punctuation on the metaventrite, metenepisternum covered by elytra, and by the shape of the median lobe, parameres, and much longer sclerite of internal sac.

Distribution

Mata do Paraíso, Universidade Federal de Viçosa, campus of Viçosa, state of Minas Gerais, Southeast Brazil (Fig 1A–B).

***Toxidium* sp. nov. 6**

(Figs 83–88)

Diagnosis

Body length: 2.08 – 2.25 mm. Dark reddish-brown. Posterior angle of pronotum slightly trespassing the anapleural line. Metaventrite with some coarse punctures next to the submesocoxal lines. Metanepisternal suture sinuous. Sutural striae shortened, covering about 3/5 from elytral apex. Elytra densely pubescent. Aedeagus with parameres strigulate near the middle; sclerite of internal sac elongate and curved. Distal gonocoxite elongate, curved. Gonostylus tapering posteriorly.

Etymology

Material examined

Holotype

BRAZIL • ♂; Minas Gerais, Viçosa, EPTEA Mata do Paraíso; 05 Nov. 2019; Leg. LabCol; Fungo 13 / Em *Hyphodontia* / HOLOTYPUS ♂; CELC. (Fig. 83D,E)

Paratypes

BRAZIL • 2♂♂, 3♀♀ (1♂**, 1♀**); same collection data as for holotype; 05 Nov. 2019; Leg. LabCol; Fungo 13 / Em *Hyphodontia*; CELC • 2♀♀ (1♀*); same collection data as for holotype; 11 Fev. 2015; S. Aloquio, A. Orsetti, C. Lopes-Andrade & M. Bento leg.; CELC.

Description.

COLORATION. Dark reddish-brown; frons, femora, and tibiae dark ochrous; antennae, mouthparts, tarsi, apex of abdominal ventrites, and tip of elytra yellow (Fig. 83A–C). Variations: (1) reddish tonality less visible (Fig. 83F); (2) reddish tonality more visible (Fig. 83G).

HEAD (FIG. 83H–84E). Frons with punctation dense and fine – some punctures coarser near the eyes. Clypeus squared, with coarse punctures (Fig. 83H,I). Labrum concave posteriorly; labral setae simple (Fig. 84A). Mandibles not strongly curved (Fig. 84B,C). Last maxillary palpomere about 3.90× longer than wide; lacinia poorly pubescent (Fig. 84D). Last labial palpomere somewhat elongate and curved; mentum concave posteriorly (Fig. 84E). Gular pores absent; gular region with strigulate microsculpture (Fig. 84F). Antennomeres slender (Fig. 83J,K); antennomeres proportions (n = 2): I 112/48: II 104/52: III 66/20: IV 88/17: V 110/18: VI 95/20: VII 126/39: VIII 86/23: IX 122/37: X 124/40: XI 168/41.

PROTHORAX (Figs 84G–K, 85D,E). Smooth, shining. Pronotum shining, punctures fine and moderately dense (Fig. 84G). Posterior angle acute, slightly trespassing the anapleural line (Fig. 85D). Hypomeron finely punctate; pubescence moderately dense (Fig. 85D,E). Notosternal suture concave (Fig. 84J). Prosternal process strongly spinose (Fig. 84I). Profurca short and sinuous (Fig. 84K).

MESOTHORAX (Fig. 85A–E). Lacking microsculpture, shining (Fig. 85D,E). Scutellar plate strongly sclerotized and large; scutellum triangular, with sides slightly convex (Fig. 85A); just a little part of the scutellum exposed, longer than wide (Fig. 84G). Mesanepisternum with inconspicuous punctures, pubescence moderately dense (Fig. 85D,E). Mesoventral and secondary lines connected to the with mesocoxal cavity (Fig. 85B). Mesoventral process with a small ridge upwards, in lateral view (Fig. 85C). Mesofurca sinuous (Fig. 85G).

METATHORAX (Fig. 85B–J). Lacking microsculpture, shining. Metaventrite with very inconspicuous punctures and pubescence sparsely pubescent (Fig. 85D,E); variation: some specimens with more or less coarse punctures next to the submesocoxal lines (Fig. 85E).

Submesocoxal area elongate; length: 0.10–0.15 mm (Fig. 85B). Metanepisternal suture convex, impunctate; metanepisternum wider at the anterior part (Fig. 85D,E). Metanotum with triangular alacrista; scutoscutellar suture laterally acute, trespassing the apodeme (Fig. 85F). Arms of metendosternite wider at the connection to the stalk (Fig. 85H–J).

WINGS (Fig. 83A–C,F,G, 85K–M). Elytra with coarse and dense punctures – more than pronotum; pubescence dense. Sutural striae shortened, extending from apex up to about 3/5 of sutural length (Fig. 83A). Lateral striae fine, impunctate, smoothly curved at the humeral region (Fig. 83B).

LEGS (Fig. 86A–F) With imbricate microsculpture. Femora and tibiae long and slender.

ABDOMEN. Smooth, shining. Each ventral segment with a row of apical setae (Fig. 83C). Tergites micropunctured (Figs 86G, 88A).

Males

Protarsomeres I–III widened, bearing tenent setae (Fig. 86D). Sternite VIII with a triangular posterior projection (Fig. 86J). Tergite VIII with a tiny small posterior projection (Fig. 86K). Tergite IX with ventral struts somewhat curved (Fig. 86I,L). Sternite IX slightly acute posteriorly (Fig. 86M). Tergite X rounded posteriorly (Fig. 86N).

AEDEAGUS (Fig. 87). Median lobe strongly curved, in lateral view; basal bulb longer than apical lobe (Fig. 87B). Parameres thick, with a small projecting, followed by a constriction at the posterior 2/3, in frontal view (Fig. 87C). Sclerite of internal sac elongate and curved (Fig. 87E).

MEASUREMENTS (n = 3, including the holotype; in mm): TL 2.08–2.18 (2.12 ± 0.05), SY 0.22–0.25 (0.24 ± 0.02), HW 0.83–0.86 (0.85 ± 0.02), IS 0.30–0.35 (0.33 ± 0.03), WA 0.16–0.17 (0.17 ± 0.01), PL 0.82–0.92 (0.87 ± 0.05), PA 0.55–0.58 (0.56 ± 0.02), PB 1.11–1.16 (1.14 ± 0.02), EI 1.32–1.40 (1.37 ± 0.05), EL 1.44–1.50 (1.47 ± 0.03), EW 0.47–0.52 (0.50 ± 0.03), EH 0.56–0.69 (0.61 ± 0.07), MB 0.14–0.15 (0.14 ± 0.01), MC 0.16–0.19 (0.18 ± 0.02), MeW 0.32–0.34 (0.33 ± 0.01), ML 0.10–0.12 (0.11 ± 0.01), VL 0.31–0.33 (0.32 ± 0.01), VL2 0.42–0.47 (0.44 ± 0.03), PrF 0.52–0.57 (0.54 ± 0.03), PrT 0.33–0.43 (0.39 ± 0.05), MsF 0.60–0.62 (0.61 ± 0.01), MsT 0.49–0.53 (0.52 ± 0.02), MtF 0.63–0.65 (0.64 ± 0.01), MtT 0.60–0.65 (0.62 ± 0.03).

Females (Fig. 88)

Sternite and tergite VIII with imbricate microsculpture. Sternite VIII with an acute posterior projection (Fig. 88B). Tergite VIII straight posteriorly (Fig. 88C). Spermatheca elongate and twisted (Fig. 88D). Distal gonocoxite elongate, curved, gonostylus tapering posteriorly (Fig. 88E–H).

MEASUREMENTS (n = 5, unless otherwise specified; in mm): TL 2.18–2.25 (2.20 ± 0.04), SY 0.24–0.26 (0.25 ± 0.01), HW 0.83–0.88 (0.86 ± 0.02), IS 0.35–0.39 (0.37 ± 0.02), WA 0.15–0.18 (0.16 ± 0.01), PL 0.8–0.94 (0.86 ± 0.07), PA 0.58–0.63 (0.60 ± 0.02), PB 1.14–1.22 (1.18 ± 0.03), EI 1.34–1.50 (1.42 ± 0.08), EL 1.48–1.60 (1.52 ± 0.05), EW 0.47–0.53 (0.51 ± 0.03), EH 0.63–0.69 (0.66 ± 0.03), MB 0.13–0.19 (0.15 ± 0.02), MC 0.16–0.23 (0.18 ± 0.03), MeW 0.30–0.35 (0.33 ± 0.02), ML 0.10–0.15 (0.11 ± 0.02), VL 0.31–0.40 (0.34 ± 0.04), VL2 0.41–0.45 (0.43 ± 0.01), PrF 0.51–0.59 (0.55 ± 0.03), PrT 0.37–0.39 (0.38 ± 0.01), MsF 0.60–0.65 (0.62 ± 0.02), MsT 0.49–0.55 (0.51 ± 0.03), MtF 0.60–0.66 (0.64 ± 0.02), MtT 0.58–0.63 (0.61 ± 0.02).

Host

Collected from *Hyphodontia* sp. (Hymenochaetaceae).

Remarks

Resembles to *Toxidium* sp. nov. 2 but differs by the shorter sutural striae, oblong metenepisternum, and by the presence of a constriction on the apical portion of the parameres, also by the more rounded curvature on the sclerite of the internal sac.

This species can be recognized by the large size, elongate submesocoxal area, and the curvature of the metanepisternal suture.

Distribution

Mata do Paraíso, Universidade Federal de Viçosa, campus of Viçosa, state of Minas Gerais, Southeast Brazil (Fig 1A–B).

Toxidium sp. nov. 7

(Figs 89–92)

Diagnosis

Body length: 1.56–1.70 mm. Dark-brown, elytra apex yellow-ochreous. Sutural striae covering about 4.20/5 from elytral apex. Metaventrite I with few coarse punctures next to the submesocoxal lines. Ventrite I imbricate microsculptured. Parameres with poorly sclerotized lobe at the central region. Sclerite if internal sac D-shaped. Distal gonocoxite slightly fusiform. Gonostylus elongate.

Etymology

Material examined

Holotype

BRAZIL • ♂*; Minas Gerais, Viçosa, UFV, Vila Gianetti; 03 Dez. 2022; E. von Groll leg. / Em *Inonotus* sp. (Hymenochaetaceae) / Dissecado em 15.xii.2022 / HOLOTYPUS ♂; CELC. (Fig. 89D,E).

Paratypes

BRAZIL • 1♂, 1♀ (1♂*, 1♀*); same collection data as for holotype; 03 Dez. 2022; E. von Groll leg. / Em *Inonotus* sp. (Hymenochaetaceae); CELC.

Description

COLORATION. Brown; antennae, clypeus, mouthparts, tarsi, apex of abdominal ventrites, and tip of elytra light ochreous; femora and tibiae ochreous (Fig. 89A).

HEAD. Punctations moderately dense and coarse, some punctures coarser. Antennomeres very elongate (Fig. 89J,K); proportions (n = 3): I 89/42: II 83/40: III 60/17: IV 76/16: V 89/16: VI 85/16: VII 99/28: VIII 71/19: IX 95/30: X 94/33: XI 126/36.

PROTHORAX (Figs 89L, 90A–C). Pronotum elongate, slightly tapering towards to the head, not strongly curved, in lateral view (Fig. 89B); punctures moderately coarse; pubescence moderately sparse. Posterior angle of pronotum somewhat acute, and almost at the same position as anapleural line (Fig. 90A–C).

MESOTHORAX (Fig. 90A–C). Very small part of scutellum exposed (longer than wide), hardly visible. Mesanepisternum finely punctate; pubescence sparse. Secondary lines connected to the mesocoxal cavities.

METATHORAX (Fig. 90A–C). Metaventrite lacking microsculpture, almost glabrous; with coarse punctures next to the submesocoxal lines – density variable. Submesocoxal lines slightly truncate laterally; connected at midline, forming an acute angle (Fig. 90E); submesocoxal area: 0.07–0.08 mm. Metanepisternal suture almost straight or sinuous, impunctate; metanepisternum mostly covered by the elytra.

WINGS (Fig. 89A–C,F–H,D). Elytra with moderately sparse punctures, some coarser than other, both coarser than on pronotum. Sutural striae not strongly shortened, extending from apex up to about 4.20/5 of sutural length; variation: female with shorter striae, occupying 2.33/5 of sutural length. Lateral striae impunctate, slightly opening at the humeral region (Fig. 89B).

LEGS (Figs 90E,F, 92A,B). With imbricate microsculpture.

ABDOMEN. Sparsely pubescent. Anterior 2/3 of ventrite I (Figs 89B, 90A–C, 92C,D), and tergites (Fig. 90G), with imbricate microsculpture; remaining ventrites without microsculpture.

Males

Sternite VIII shortened, with acute posterior projection (Fig. 90H). Tergite VIII without posterior projection (Fig. 90I). Tergite IX with ventral struts short and almost straight (Fig. 90J). Sternite IX acute posteriorly (Fig. 90K). Tergite X triangular (Fig. 90L).

AEDEAGUS (Fig. 91). Basal bulb 2× longer than apical lobe; apical lobe bent (Fig. 91B). Parameres thin, bearing a poorly sclerotized lobe (Fig. 91B); sclerite of internal sac curved, D-shaped (Fig. 91D).

MEASUREMENTS (n = 2, including the holotype, unless otherwise specified; in mm): TL 1.56–1.60 (1.58 ± 0.03), SY 0.19–0.19 (0.19 ± 0), HW 0.42–0.43 (0.43 ± 0.01), IS 0.14–0.15 (0.14 ± 0.01), WA 0.26–0.27 (0.27 ± 0.01), PL 0.64–0.65 (0.64 ± 0.01), PA 0.40–0.41 (0.41 ± 0.01), PB 0.76–0.79 (0.78 ± 0.02), EI 1.03–1.06 (1.05 ± 0.02), EL 1.11–1.14 (1.13 ± 0.02), EW 0.41–0.41 (0.41 ± 0), EH 0.40–0.41 (0.41 ± 0.01), MB 0.10–0.10 (0.1 ± 0), MC 0.29–0.33 (0.31 ± 0.03), MeW 0.25–0.25 (0.25 ± 0), ML 0.08, VL 0.20–0.21 (0.21 ± 0.01), VL2 0.32–0.32 (0.32 ± 0),

PrF 0.40–0.41 (0.41 ± 0.01), PrT 0.31–0.33 (0.32 ± 0.01), MsF 0.46, MsT 0.36–0.37 (0.37 ± 0.01), MtF 0.47–0.50 (0.49 ± 0.02), MtT 0.45–0.49 (0.47 ± 0.03).

Female (Fig. 92)

Sternite and tergite VIII with imbricate microsculpture**.** Sternite VIII with an acute posterior projection (Fig. 92E). Tergite VIII lacking projections (Fig. 92F). Distal gonocoxite slightly fusiform, gonostylus elongate (Fig. 92G,H).

MEASUREMENTS (n = 1; in mm): TL 1.70, SY 0.22, HW 0.46, IS 0.17, WA 0.30, PL 0.69, PA 0.44, PB 0.78, EI 1.13, EL 1.20, EW 0.43, EH 0.43, MB 0.12, MC 0.34, MeW 0.26, ML 0.07, VL 0.20, VL2 0.36, PrF 0.43, PrT 0.31, MsF 0.49; MsT 0.38, MtF 0.50, MtT 0.45.

Host

Collected from *Inonotus* sp., located on a tree in front of an avenue (Figs 1E–F, 94A–B).

Remarks

Similar to *Toxidium* sp. nov. 3, differing by the more elongate body, longer submesocoxal area – reaching half of the metaventrite, presence of microsculpture on the ventrite I, tergite IX less sclerotized, median lobe with shorter apex, thinner parameres, and shape of sclerite. Although the female present a larger size and shorter sutural striae, the specimen presents all the other characteristics of the species.

Distribution

Universidade Federal de Viçosa, campus of Viçosa, state of Minas Gerais, Southeast Brazil (Fig. 1A–B,E–F).

Discussion

With the addition of these 20 new species, Brazil now counts with 62 species of Scaphidiinae. Nonetheless, this number is still quite inferior to the real potential of the country. During my 22 collections in Viçosa (MG) (that resulted in the species described in this paper), I managed

to collect approximately 350 more specimens that still need to be studied. There is no doubt that many of these specimens represent new species.

Considering that collections in only three areas in one city led to so many new species, it is possible to assume that Brazil, a country with six biomes (Amazon, Caatinga, Cerrado, Pantanal, Atlantic Forest, and Pampa), with 59% of its area covered by forests, and known for its megadiversity, has the potential to hold a much higher Scaphidiinae abundance and diversity. It is important to note that the lack of these beetles in pinned or dry collections does not reflect their absence in nature – not even in museums or academic collections. This situation is more related to the difficulty in collecting these animals, the greater interest in other groups, and also by the taxonomists decrease (Löbl *et al.* 2023). For instance, it is more common to find small beetles (of any family) in alcohol or entomological envelopes in most collections.

Even though shining fungus beetles can be collected by intercept traps, Winkler, and sifting litter (Löbl & Leschen 2003b; Tang *et al.* 2014; Löbl *et al.*, 2021), the specific and active collection is very important to collect these beetles (von Groll *et al.* 2021; von Groll & Lopes-Andrade 2021). Although this method requires time and willingness, with fewer results compared to intercept traps, this is the only way to make host associations (Löbl & Leschen 2003b).

One of the findings regarding beetle × host interactions was that specimens of *Alexidia* showed to be strongly associated with the myxomycete *Ceratiomyxa fruticulosa*. Also, the presence of corbiculum (= setose pockets; = setose cavities (Newton 19840)) corroborates with this relation. The corbiculum has already been hypothesized to function as mycangia or spore-retaining and aid in the dispersal of host spores (Newton 1984). The structure is also present in the genus *Baeocera*, a genus well-known for feeding on slime mold bodies (Newton 19840).

Two additional peculiar morphological characteristics were observed. The first can be seen in *Scaphisoma* sp. nov. 4 *Scaphisoma* is characterized by the normal last maxillary palpomere ("tapering"; "typically as wide as the penultimate segment" Löbl & Leschen 2003b; Leschen & Löbl 2005). This characteristic is true for the four new species, but the discrepancy relies on the truncate apex of the last palpomere of *Scaphisoma* sp. nov. 4, a characteristic contrasting with the usual acute apex. This species presents other not very typical characteristics – but also described for other known species – such as the absence of the tenent setae on male tarsomeres, submetacoxal area very short, and distinct parameres.

The second peculiar characteristic found during this study can be observed in *Toxidium* sp. nov. 1. This species is the most distinct one among the other described in this manuscript. The most discrepant characteristic is the posterior region of the hypomeron, shorter than the posterior end of the pronotal angle – better observed in lateral view. Nonetheless, this genus still needs a revision based on more species. Despite the low number of described species, this genus (and/or similar ones) is well-represented in many museums (pers. obs.).

It is notably that this study brings descriptions more detailed than expected for new species. This more complete morphological study was conducted in order to investigate other possible characteristics that might facilitate the species delimitation. In this sense, it is possible to affirm that even similar species can be distinguished by some differences on the mouth parts, metendosternite, profurca, and other structures. However, for a precise comparison, it is almost mandatory to dissect/measure more than one specimen of each species. This is recommended because most of the differences are regarding width, length, angles, and other very subtle aspects.

Nonetheless, the already known characteristics are still the most significant ones to solve identifications: antennomeres length/width, submesocoxal and -metacoxal lines shape and length, and aedeagus shape. However, the terminal ventrites and tergites VIII–X, and the female terminalia also exhibit very significative diagnostic characteristics. Furthermore, more than distinguishing similar species, this comprehensive analysis was even more helpful in order to relate the females of each species, especially when more than one species was collected together.

An example of this situation can be seen on *Baeocera* sp. nov. 4, *Baeocera* sp. nov. 5, *Baeocera* sp. nov., 6 and by *Baeocera* sp. nov. 3. These four species are quite similar and it was necessary to study the metendosternite, mouth parts, and other not so usual diagnostic characteristics in order to determine the female of each species. Also, although the importance of female terminalia is not always recognized, in a few cases it can be used to form groups of species (Ogawa & Sakai 2011; Ogawa & Löbl 2013).

This was true for the six new *Baecoera* species. Taking the females characteristics into consideration, the six new species can be separated in three groups: (1) *Baeocera* sp. nov. 1, with elongate distal gonocoxite; (2) *Baeocera* sp. nov. 2, with short distal gonocoxite absence of gonostylus (also described for the *lenta* species group of *Baeocera* (Ogawa & Löbl 2013))

and; (3) *Baeocera* sp. nov. 4, *Baeocera* sp. nov. 5 *Baeocera* sp. nov. 6, and possible *Baeocera* sp. nov. 3, characterized by the "unusual shape of the ovipositor with elongate distal gonocoxites", also found on *B. frater* species group (Ogawa & Löbl 2013).

Yet, regarding the females', the terminalia of *Alexidia* and *Toxidium* are described for the first time. With respect to *Alexidia*, the most significant differences rely on the spermathecal and gonostylus shape. Regarding *Toxidium*, females present a very similar terminalia morphology, but at the same time, they are still easily distinguishable due to the variations being very clear (e.g. distal gonocoxite elongate but more curved in *Toxidium* sp. nov. 6; sternite VIII in *Toxidium* sp. nov. 7 short).

Nonetheless, males terminalia are still the best morphologic diagnostic characteristics. Naturally, it also faces some situations. The main one I faced during the production of this manuscript was the intentionally dissection of internal sac (e.g. von Groll 2023). It is somewhat complicate to compare an internal sac that has been removed to the ones that has not been removed (method more commonly used). Not removing the internal sac can facilitate the observation of position of the internal sac and its sclerites; besides being a less destructive method. Sometimes the internal sac is already extroverted what can cause some confusion as well.

Scaphidiinae beetles were easily collected in forests and even in the city of Viçosa (e.g. *Scaphisoma* sp. nov. 1). Viçosa (MG) is a small city surrounded by preserved remnants of Atlantic Forest, which might explain the facility to find these beetles. It is not known, however, if these beetles are common all over the country, like in other Biomes in Brazil, and areas more or less preserved. A first step to solve this question is to visit the miscellaneous collections in order to investigate if these beetles were collected via more comprehensive methods, such as Winkler and FIT traps.

Hopefully, this study will be of interest to the Scaphidiinae fauna, especially in the Neotropical Region, where they have been poorly studied over the years. Since 2000, Hugo Eduardo Fierros-López has published consistent papers on this subfamily in this region, in addition to a paper regarding the genus *Alexidia* (Löbl & Leschen 2003a). In addition, it is very important to perform larger molecular and morphological analyses to gain a better understanding of this group.

Checklist of the Brazilian species of Scaphidiinae:

1. *Cyparium achardi* von Groll & Lopes-Andrade, 2022. Brazil (Minas Gerais)
2. *Cyparium collare* Pic, 1920a. Brazil (Minas Gerais, Mato Grosso, Pernambuco)
3. *Cyparium ferrugineum* Pic, 1920a. Brazil (Piauí, Pernambuco, Mato Grosso)
4. *Cyparium grilloi* Pic, 1920b. Brazil (Paraná)
5. *Cyparium grouvellei* Pic, 1920a. Brazil
6. *Cyparium lescheni* von Groll & Lopes-Andrade, 2022. Brazil (Minas Gerais).
7. *Cyparium loebli* von Groll & Lopes-Andrade, 2022. Brazil (Minas Gerais).
8. *Cyparium newtoni* von Groll & Lopes-Andrade, 2022. Brazil (Minas Gerais).
9. *Cyparium oberthüri* Pic, 1956. Brazil (Mato Grosso, Minas Gerais).
10. *Cyparium pici* von Groll & Lopes-Andrade, 2022. Brazil (Mato Grosso)
11. *Cyparium pygidiale* Achard, 1922b. Brazil (Goias)
12. *Cyparium ruficolle* Achard, 1922b. Brazil (Mato Grosso)
13. *Cyparium rufohumerale* Pic, 1931. Brazil.
14. *Cyparium* sp. nov. 1 von Groll, 2024. Brazil (Minas Gerais).
15. *Scaphidium bipunctatum* Redtenbacher, 1868. Brazil (Rio de Janeiro).
16. *Scaphidium bisbimaculatum* Pic, 1917. Brazil (Espirito Santo).
17. *Scaphidium castaneum* Perty, 1830. Brazil.
18. *Scaphidium cerasinum* Oberthür, 1883. Brazil (Tocantins, Amazonas).
19. *Scaphidium exclamans* Oberthür, 1883. Brazil (São Paulo) ; Paraguai.
20. *Scaphidium fasciatomaculatum* Oberthür, 1883. Brazil (Amazonas); Ecuador, Peru.
21. *Scaphidium fascipenne* Reitter, 1880. Brazil.
22. *Scaphidium gounellei* Pic, 1920a. Brazil.
23. *Scaphidium pantherinum* Oberthür, 1883. Brazil («Rio Negro» Paraná).
24. *Scaphidium pardale pardale* Laporte, 1840. French Guiana, Brazil.
25. *Scaphidium pardale* ssp. *nigripenne* Oberthür, 1883. Brazil
26. *Scaphidium testaceum* Reitter, 1880. Brazil.
27. *Scaphidium undulatum* Pic, 1915c. Brazil
28. *Alexidia plaumanni* Löbl & Leschen, 2003a. Brazil (Santa Catarina).
29. *Alexidia* sp. nov. 1 von Groll, 2024. Brazil (Minas Gerais)
30. *Alexidia* sp. nov. 2 von Groll, 2024. Brazil (Minas Gerais)
31. *Amalocera basipennis* Löbl, 1974. Brazil (Ega?????)
32. *Amalocera dentifera* Löbl, 1974. Brazil (Santa Catarina).

33. *Amalocera paulistana* Achard, 1922b. Brazil ("near São Paulo")
34. *Amalocera picta* Erichson, 1845. Brazil.
35. *Amalocera tibialis* Löbl, 1974. Brazil (Minas Gerais).
36. *Baeocera freudei* Löbl, 1967. Brazil (Amazonas)
37. *Baeocera* sp. nov. 1 von Groll, 2024. Brazil (Minas Gerais).
38. *Baeocera* sp. nov. 2 von Groll, 2024. Brazil (Minas Gerais).
39. *Baeocera* sp. nov. 3 von Groll, 2024. Brazil (Minas Gerais).
40. *Baeocera* sp. nov. 4 von Groll, 2024. Brazil (Minas Gerais).
41. *Baeocera* sp. nov. 5 von Groll, 2024. Brazil (Minas Gerais).
42. *Baeocera* sp. nov. 6 von Groll, 2024. Brazil (Minas Gerais).
43. *Scaphisoma brunneipenne* Pic, 1916b. Brazil (Santa Catarina)
44. *Scaphisoma elongatum* Waterhouse, 1879. Brazil (Rio de Janeiro).
45. *Scaphisoma pandemum* Groll & Lopes-Andrade, 2021. Brazil (Minas Gerais).
46. *Scaphisoma nigrofasciatum* Pic, 1915b. Brazil (Minas Gerais). India, Mauritius, Nepal, La Réunion, Seychelles, Sri Lanka. (von Groll, 2023)
47. *Scaphisoma phalacroide* Pic, 1920b. Brazil (São Paulo).
48. *Scaphisoma rubripes* Pic, 1920a. Brazil.
49. *Scaphisoma testaceiventre* Pic, 1928c. Brazil (São Paulo).
50. *Scaphisoma tropicum andreinii* Pic, 1920b. Brazil (São Paulo).
51. *Scaphisoma* sp. nov. 1 von Groll, 2024. Brazil (Minas Gerais).
52. *Scaphisoma* sp. nov. 2 von Groll, 2024. Brazil (Minas Gerais).
53. *Scaphisoma* sp. nov. 3 von Groll, 2024. Brazil (Minas Gerais).
54. *Scaphisoma* sp. nov. 4 von Groll, 2024. Brazil (Minas Gerais).
55. *Toxidium acuminatum* Pic, 1920c. Brazil.
56. *Toxidium* sp. nov. 1 von Groll, 2024. Brazil (Minas Gerais).
57. *Toxidium* sp. nov. 2 von Groll, 2024. Brazil (Minas Gerais).
58. *Toxidium* sp. nov. 3 von Groll, 2024. Brazil (Minas Gerais).
59. *Toxidium* sp. nov. 4 von Groll, 2024. Brazil (Minas Gerais).
60. *Toxidium* sp. nov. 5 von Groll, 2024. Brazil (Minas Gerais).
61. *Toxidium* sp. nov. 6 von Groll, 2024. Brazil (Minas Gerais).
62. *Toxidium* sp. nov. 7 von Groll, 2024. Brazil (Minas Gerais).

Conclusion

In this study, 19 new species of Sacphidiinae are described. As a result, the fauna of Brazilian shining rove beetles has increased from 41 to 60 known beetles. Detailed illustrations and descriptions of males and females, along with host data, represent a small but important step in understanding the diversity of this subfamily in Brazil.

Acknowledgments

I would like to thank Dr. Ivan Löbl (MHNG) for the fundamental assistance. I am also grateful for the valuable suggestions of the dissertation members committee: Gervasio S. Carvalho (retired professor), Jéssica Herzog Vianna (UEPA), Vinicius S. Ferreira (SDEI), and Gabriel Biffi (USP). I also thank the Department of Animal Biology (UFV) for allowing me to use the laboratory and the specimens. Financial support was provided by CAPES (Coordenação de Aperfeiçoamento de Pessoal de Nível Superior).

References

Achard J. 1920. Notes sur les Scaphidiidae de la faune Indo-Malaise. *Annales de la Société entomologique de Belgique* 60: 123–136.

Achard J. 1922a. Essai de groupement des espèces du genre *Scaphidium* Ol. (Col. Scaphidiidae). *Fragments entomologiques*: 10–13.

Achard, J. 1922b. Descriptions de scaphidides nouveaux (Col. Scaphidiidae). *Fragments entomologiques*: 35–45.

Achard J. 1923. Revision des Scaphidiidae de la faune japonaise. *Fragments entomologiques*: 94–120.

Achard J. 1924. Essai d'une subdivision nouvelle de la famille des Scaphidiidae. *Annales de la Société entomologique de Belgique* 65: 25–31.

Agassiz L. 1846. Nomenclatoris zoologici index universalis continens nomina systematica classium, ordinum, familiarum et generum animalium omnium, tam viventium quam fossilium, secundum ordinem alphabeticum unicum disposita, adjectis homonymiis plantarum, nec non variis adnotationibus et emendationibus. *In*: Agassiz L. (ed.) *Nomenclator Zoologicus, continens nomina systematica generum animalium tam viventium quam fossilium, secundum ordinem alphabeticum disposita, adjectis auctoribus, libris, in quibus reperiuntur, anno editionis, etymologia et familiis, ad quas pertinent, in singulis classibus*. Fasc. 12: viii + 393 pp. Soloduri: Jent et Gassmann. https://doi.org/10.5962/bhl.title.15763

Blackburn T. 1903. Further notes on Australian Coleoptera, with descriptions of new genera and species. *Transactions of the Royal Society of South Australia* 27: 91–182.

Casey T.L. 1893. Coleopterological Notices V. Scaphidiidae. *Annals of the New York Academy of Sciences* 7: 510–533. https://doi.org/10.1111/j.1749-6632.1893.tb55411.x

Casey T.L. 1900. Review of the American Corylophidae, Cryptophagidae, Tritomidae and Dermestidae, with other studies. *Journal of the New York Entomological Society* 8: 51–172.

Cornell J.F. 1967. A taxonomic study of *Eubaeocera* new genus (Coleoptera: Scaphidiidae) in North America north of Mexico. *The Coleopterists Bulletin* 21: 1–17.

Crowson R.A. 1938. The Metendosternite in Coleoptera: a comparative study. *Transactions of the Royal Entomological Society of London* 87 (17): 397–415. https://doi.org/10.1111/j.1365-2311.1938.tb00723.x

Erichson W.F. 1845. *Naturgeschichte der Insecten Deutschlands. Erste Abteilung. Coleoptera. Dritter Band. Lieferung 1*. Nicolaische Buchhandlung, Berlin. https://doi.org/10.5962/bhl.title.8270

Fairmaire L. 1898. Matériaux pour la faune coléoptérique de la région malgache, 5e note. *Annales de la Société entomologique de Belgique* 42: 222–260.

Friedrich F. & Beutel R. G. 2006. The pterothoracic skeletomuscular system of Scirtoidea (Coleoptera: Polyphaga) and its implications for the high-level phylogeny of beetles. *Journal of Zoological Systematics and Evolutionary Research* 44 (4): 290–315. https://doi.org/10.1111/j.1439-0469.2006.00369.x

Ganglbauer L. 1899. *Die Käfer von Mitteleuropa. Die Käfer des österreichisch-ungarischen Monarchie, Deutschlands, der Schweiz, sowie des französischen und italienischen Alpengebietes. Dritter Band. Staphylinoidea. Vol. 2: Scydmaenidae, Silphidae, Clambidae, Leptinidae, Platypsyllidae, Corylophidae, Sphaeriidae, Trichopterygidae, Hydroscaphidae, Scaphidiidae, Histeridae. Familienreihe Clavicornia. Sphaeritidae, Ostomidae, Byturidae, Nitidulidae, Cucujidae, Erotylidae, Phalacridae, Thorictidae, Lathridiidae, Mycetophagidae, Colydiidae, Endomychidae, Coccinellidae*. Carl Gerold's Sohn.

Gestro R. 1879. Note sopre alcuni coleotteri dell'Arcipelago Malese e specialmente delle isole della Sonda. *In*: *Annali del Museo civico di Storia naturale di Genova* [1879–1880] 15: 49–62.

Harris R.A. 1979. A glossary of surface sculpturing. *Occasional papers in Entomology* 28: 1–31.

Hübler N. & Klass K.D. 2013. The morphology of the metendosternite and the anterior abdominal venter in Chrysomelinae (Insecta: Coleoptera: Chrysomelidae). *Arthropod Systematics & Phylogeny* 71 (1): 3–41. https://doi.org/10.3897/asp.71.e31762

Jałoszyński P. 2012. Taxonomy of' *Euconnus* complex'. Part I. Morphology of *Euconnus* s. str. and revision of *Euconnomorphus* Franz and *Venezolanoconnus* Franz (Coleoptera: Staphylinidae: Scydmaeninae). *Zootaxa* 3555 (1): 55–82. https://doi.org/10.11646/zootaxa.3555.1.3

Laporte F.L.N. de Caumont (Comte de Castelnau). 1840. *Histoire naturelle des insectes coléoptères; avec une introduction renfermant l'anatomie et la physiologie des animaux articulés, par M. Brullé; ouvrage accompagné de 155 planches gravées sur acier représentant plus de 800 sujets. Vol. 10*. P. Duménil, Paris.

Latreille P.A. 1802. *Histoire naturelle générale et particulière des crustacés et des insectes: ouvrage faisant suite aux Oeuvres de Leclerc de Buffon, et partie du Cours complet d'histoire naturelle rédigé par CS Sonnini*. *Vol. 73*. https://doi.org/10.5962/bhl.title.15764

Latreille P.A. 1806. *Genera Crustaceorum et Insectorum, secundem ordinem naturalem in familias dispositas, iconibus exemplisque plurimus explicata. Vol 2: [1807]*. Amand Koenig, Paris. https://doi.org/10.5962/bhl.title.65741

Latreille P.A. 1810. *Considérations générales sur l'ordre naturel des animaux composant les classes des crustacés, des arachnides, et des insectes; avec un tableau méthodique de leurs genres, disposés en familles.* Schoell, Paris. https://doi.org/10.5962/bhl.title.39620

Lawrence J.F. & Newton Jr. A.F. 1980. Coleoptera associated with the fruiting bodies of slime molds (Myxomycetes). *The Coleopterists Bulletin* 34: 129–143.

Lawrence J.F. & Ślipiński A. 2013. *Australian Beetles. Vol. 1. Morphology, Classification and Keys*. CSIRO Publishing, Collingwood. https://doi.org/10.1071/9780643097292

Lawrence J.F., Zhou Y.-L. Lemann C., Sinclair B. & Ślipiński A. 2021. The Hind Wing of Coleoptera (Insecta): Morphology, Nomenclature and Phylogenetic Significance. Part 1. General Discussion and Archostemata–Elateroidea. *Annales Zoologici* 71 (3): 421–606. https://doi.org/10.3161/00034541ANZ2021.71.3.001

Leach W.E. 1815. Entomology. *In*: Brewster, D. (ed.). *Edingburg Encyclopaedia* 9: 57–172.

LeConte J.L. 1860. Synopsis of the Scaphidiidae of the United States. *Proceedings of the Academy of Natural Sciences of Philadelphia*: 321–324.

Leschen R.A.B. & Löbl I. 2005. Phylogeny and classification of Scaphisomatini Staphylinidae: Scaphidiinae with notes on mycophagy, termitophily, and functional

morphology. *Coleopterists Society Monographs* 3: 1–63. https://doi.org/10.1649/0010-065X(2005)059[0001:PACOSS]2.0.CO;2

Leschen R.A.B. 1994. Retreat-building by larval Scaphidiinae (Staphylinidae). *Mola* 4: 3–5.

Leschen R.A.B. & Löbl I. 1995. Phylogeny of Scaphidiinae with redefinition of tribal and generic limits (Coleoptera: Staphylinidae). *Revue suisse de Zoologie* 102 (2): 425–474. https://doi.org/10.5962/bhl.part.80472

Leschen R.A.B., Löbl I. & Stephen K. 1990. Review of the Ozark Highland *Scaphisoma* (Coleoptera: Scaphidiidae). *The Coleopterists Bulletin* 44: 274–294.

Lewis G. 1893. On some Japanese Scaphidiidae. *Annals and Magazine of Natural History* (6) 11: 288–294.

Linnaeus C. 1758. *Systema Naturae per regna tria naturae secundum classes, ordines, genera, species, cum characteribus, differentiis, synonymis, locis. tomus I. Editio decima, reformata.* Laurentii Salvii, Holmiae. https://doi.org/10.5962/bhl.title.542

Löbl I. & Leschen R.A.B. 2003a. Redescription and new species of *Alexidia* (Coleoptera: Staphylinidae: Scaphidiinae). *Revue suisse de zoologie* 110: 315–324. https://doi.org/10.5962/bhl.part.80187

Löbl I. & Leschen R.A.B. 2003b. Scaphidiinae (Insecta: Coleoptera: Staphylinidae). *Fauna of New Zealand* 48: 1–94.

Löbl I. 1967. Beitrag zur Kenntnis der neotropischen Arten der Gattung *Baeocera* Er. *Opuscula zoologica* 97: 1–3.

Löbl I. 1970. Revision der paläarktischen Arten der Gattungen *Scaphisoma* Leach und *Caryoscapha* Ganglbauer der Tribus Scaphisomini (Col. Scaphidiidae). *Revue suisse de zoologie* 77: 727–799. https://doi.org/10.5962/bhl.part.75925

Löbl I. 1971. Scaphidiidae von Ceylon (Coleoptera). *Revue suisse de zoologie* 78: 937–1006.

Löbl I. 1974. New Species of the Genus *Amalocera* Erichson from Brazil (Coleoptera, Scaphidiidae). *Studies on the Neotropical Fauna* 9: 39–45.

Löbl I. 1975a. Beitrag zur Kenntnis der Scaphidiidae (Coleoptera) von Neuguinea. *Revue suisse de Zoologie* 82: 369–420. https://doi.org/10.5962/bhl.part.78265

Löbl I. 1975b. Beitrag zur Kenntnis der orientalischen Scaphisomini (Coleoptera, Scaphidiidae). Mitteilungen der Schweizerischen entomologischen Gesellschaft 48: 269–290.

Löbl I. 1984. Contribution à la connaissance des Baeocera du Japon (Coleoptera, Scaphidiidae). *Archives des sciences* 37: 181–192.

Löbl I. 1992. The Scaphidiidae (Coleoptera) of the Nepal Himalaya. *Revue suisse de zoologie* 99: 471–627. https://doi.org/10.5962/bhl.part.79841

Löbl I. 1997. *Catalogue of the Scaphidiinae (Coleoptera: Staphylinidae)*. Muséum d'histoire naturelle, Geneve. https://doi.org/10.1163/9789004375956_002

Löbl I. 2015. Staphylinidae: Scaphidiinae. *In*: Löbl I. & Löbl D. (eds). *Catalogue of Palaearctic Coleoptera. Vol 2: Revised and Updated Edition. Hydrophiloidea – Staphylinoidea*: 21. Brill, Leiden/Boston. https://doi.org/10.1163/9789004296855

Löbl I. 2018. *Coleoptera: Staphylinidae: Scaphidiinae*. Brill, Leiden, The Netherlands. https://doi.org/10.1163/9789004375956

Löbl I., Leschen R.A.B & Warner W.B. 2021. Scaphisomatine of Arizona (Coleoptera, Staphylinidae, Scaphidiinae) collected by V-Flight Intercept traps. *Revue suisse de Zoologie* 128 (1): 173–185. https://doi.org/10.35929/RSZ.0043

Löbl I. & Ogawa R. 2016. On the Scaphisomatini (Coleoptera, Staphylinidae, Scaphidiinae) of the Philippines, IV: the genera Sapitia Achard and Scaphisoma Leach. *Linzer biologische Beiträge* 48 (2): 1339–1492.

Naomi S. 1988a. Comparative Morphology of the Staphylinidae and the Allied Groups (Coleoptera, Staphylinoidea): III. Antennae, Labrum and Mandibles. *Japanese journal of entomology* 56 (1): 67–77.

Naomi S. 1988b. Comparative Morphology of the Staphylinidae and the Allied Groups (Coleoptera, Staphylinoidea): IV. Maxillae and Labium. *Japanese journal of entomology* 56 (2): 241–250.

Naomi S. 1989a. Comparative Morphology of the Staphylinidae and the Allied Groups (Coleoptera, Staphylinoidea): VII. Metendosternite and Wings. *Japanese journal of entomology* 57 (1): 82–90.

Naomi S. 1989b. Comparative Morphology of the Staphylinidae and the Allied Groups (Coleoptera, Staphylinoidea): X. Eighth and 10th Segments of Abdmen. *Japanese journal of entomology* 57 (4): 720–733.

Naomi S. 1990. Comparative Morphology of the Staphylinidae and the Allied Groups (Coleoptera, Staphylinoidea): XI. Abdominal Glands, Male Genitalia and Female Spermatheca. *Japanese journal of entomology* 58 (1): 16–23. https://doi.org/10.5109/2464

Newton A.F. Jr. 1984. Mycophagy in Staphylinoidea (Coleopetra). *In*: Wheeler Q. & Blackwell M. (eds) *Fungus/insect relationships. Perspectives in ecology and evolution*: 302–353. Columbia University Press, New York.

Oberthür R. 1883. Scaphidiides nouveaux. *In*: *Coleopterorum Novitates. Recueil spécialement consacré à l'étude des coléoptères, Rennes* 1: 1–80. https://doi.org/10.1002/mmnd.48018830243 Pp. 5–16

Ogawa R. & Löbl I. 2013. A revision of the genus *Baeocera* in Japan, with a new genus of the tribe Scaphisomatini (Coleoptera, Staphylinidae, Scaphidiinae). *Zootaxa* 3652: 301–326. https://doi.org/10.11646/zootaxa.3652.3.1

Ogawa R. & Löbl I. 2016. A review of the genus *Xotidium* Löbl, 1992 (Coleoptera, Staphylinidae, Scaphidiinae), with descriptions of five new species. *Deutsche Entomologische Zeitschrift* 63 (1): 155–169. https://doi.org/10.3897/dez.63.8386

Ogawa R. & Sakai, M. 2011. A review of the genus *Cyparium* Erichson (Coleoptera, Staphylinidae, Scaphidiinae) of Japan. *Japanese Journal of Systematic Entomology* 17: 129–136.

Olivier G.-A. 1790. *Entomologie, ou Histoire Naturelle des Insectes, Avec leurs caracteres, génériques et spécifiques, leur description, leur synonymie, et leur figure enluminée. Vol 2*: *Coléoptéres* Baudouin, Paris. https://doi.org/10.5962/bhl.title.61905

Perty J.A.M. Insecta Brasiliensia, *In*: Perty J.A.M. 1830. *Delectus animalium articulatorum, quae in itinere per Brasiliam annis MDCCCXVII-MDCCCXX jussu et auspiciis Maximiliani Josephi I. Bavariae regis augustissimi peracto collegerunt Dr. J.B. de Spix et Dr. C.F. Ph. de Martius*: 1–60. Munich, Impensis Editoris.

Pic M. 1915a. Nouvelles especes de diverses familles. *Mélanges exotico-entomologiques* 15: 1–24.

Pic M. 1915b. Diagnoses de nouveaux genres et nouvelles espèces de Scaphidiides. *L'Echange, Revue linnéenne* 31: 30–32.

Pic M. 1915c. Diagnoses de nouveaux genres et nouvelles espèces de Scaphidiides. *L'Echange, Revue linnéenne* 31: 35–36.

Pic M. 1916a. Notes et descriptions abrégées diverses. *Mélanges exotico-entomologiques* 17: 2–8.

Pic M. 1916b. Diagnoses spécifiques. *Mélanges exotico-entomologiques* 17: 8–20.

Pic M. 1917. Descriptions abrégées diverses. *Mélanges exotico-entomologiques* 26: 2–24.

Pic M. 1920a. Nouveautés diverses. *Mélanges exotico-entomologiques* 32: 1–28.

Pic M. 1920b. Scaphidiides nouveaux de diverses origines. *Annali del Museo civico di Storia naturale di Genova* 9 (3): 93–97

Pic M. 1920c. Coléoptères exotiques en partie nouveaux. *L'Echange, Revue linnéenne* 36: 22–24.

Pic M. 1921. Nouveautés diverses. *Mélanges exotico-entomologiques* 33: 1–32.

Pic M. 1922. Nouveautés diverses. *Mélanges exotico-entomologiques* 36: 1–32.

Pic M. 1923. Nouveautés diverses. *Mélanges exotico-entomologiques* 38: 1–32.

Pic M. 1925. Notes sur les coléopteres scaphidiides. *Annales de la Société entomologique de Belgique* 64 [1924]: 193–196.

Pic M. 1928a. Scaphidiidae du Congo Belge. *Revue de Zoologie et de Botanique africaines* 16: 33–44.

Pic M. 1928b. Nouveaux coléopteres de la République Argentine. *Revista de la Sociedad entomologica argentina* 2: 49–52.

Pic M. 1928c. Nové druhy koleopter z Brasilie. Nouveaux coléoptères du Brésil. *Sborník entomologického oddělení Národního musea v Praze* 6: 74–76.

Pic M. 1930. Coléoptères asiatiques nouveaux. *Sborník entomologického oddělení Národního musea v Praze* 8: 58–59.

Pic M. 1931. Nouveautés diverses. *Mélanges exotico-entomologiques* 57: 1–36.

Pic M. 1956. Nouveaux coléoptères exotiques. *Bulletin de la Société entomologique de France* 60 [1955]: 173–175. https://doi.org/10.3406/bsef.1955.18803

Ramage T. & Löbl I. 2022. A new species of *Scaphisoma* Leach from the Society Islands with commentary on Staphylinidae of the French Polynesia (Coleoptera, Staphylinidae, Scaphidiinae). *Bulletin de la Société entomologique de France* 127 (1): 55–60. https://doi.org/10.32475/bsef_2224

Redtenbacher L. 1868. Coleopteren. *In*: Redtenbacher L., Sichel J., Mayr, G.L., & Brauer F. (eds) *Reise der Österreichischen Fregatte Novara um die Erde in den Jahren 1857, 1858, 1859 unter den Befehlen des Commodore B. von Wüllerstorf-Urbair. Zoologischer Theil. Zweiter Band:*. I–249, Vienna.

Reitter E. 1880. Die Gattungen und Arten der Coleopteren-Familie: Scaphidiidae meiner Sammlung. *Verhandlungen des Naturforschenden Vereins in Brünn* 18 [1879]: 35–49.

Say T. 1823. Description of coleopterous insects collected in the late expedition to the Rocky mountains, performed by order of Mr. Calhoun, Secretary of War, under the command of Major Long. *Journal of the Academy of Natural Sciences Philadelphia* 3 (1): 139–216.

Stephenson S.L., Wheeler Q.D., McHugh J.V. & Fraissinet P.R. 1994. North American associations of Coleoptera with Myxomycetes. *Journal of Natural History* 28(4): 921–936. https://doi.org/10.1080/00222939400770491

Tang L., Li L.-Z. & He W.-J. 2014. The genus *Scaphidium* in East China (Coleoptera, Staphylinidae, Scaphidiinae). *ZooKeys* 403: 47–96. https://doi.org/10.3897/zookeys.403.7220

von Groll E. & Lopes-Andrade C. 2021. *Scaphisoma pandemum* sp. nov. (Coleoptera: Staphylinidae: Scaphidiinae) from the Atlantic Forest of Southeast Brazil. *Zootaxa* 4999 (2): 143–156. https://doi.org/10.11646/zootaxa.4999.2.4

von Groll E. & Lopes-Andrade C. 2022. Contributions to the taxonomy of Neotropical *Cyparium* Erichson (Coleoptera: Staphylinidae: Scaphidiinae), with the description of five new species. *European Journal of Taxonomy* 835: 1–97. https://doi.org/10.5852/ejt.2022.835.1909

von Groll E. 2023. Rediscovery and redescription of *Scaphisoma nigrofasciatum* Pic (Coleoptera: Staphylindae: Scaphidiinae): a remarkable new record from a distant continent. *Zootaxa* 5375 (4): 565–573. https://doi.org/10.11646/zootaxa.5375.4.7

Waterhouse F.H. 1879. Descriptions of new Coleoptera of geographical interest, collected by Charles Darwin, Esq. *Journal of the Linnaean Society, Zoology* 14: 530–534. https://doi.org/10.1111/j.1096-3642.1879.tb02449.x

Figure captions

Fig. 1. Collection sites. **A–B.** Distribution maps of Scaphidiinae. **A.** South America. **B.** Minas Gerais (part). **C–D.** Entrance of Mata da Biologia (Viçosa, MG). **E–F.** Vila Gianetti (Viçosa, MG). **G.** Collecting from *Ceratiomyxa fruticulosa* on a fallen tree (Mata do Paraíso, Viçosa, MG).

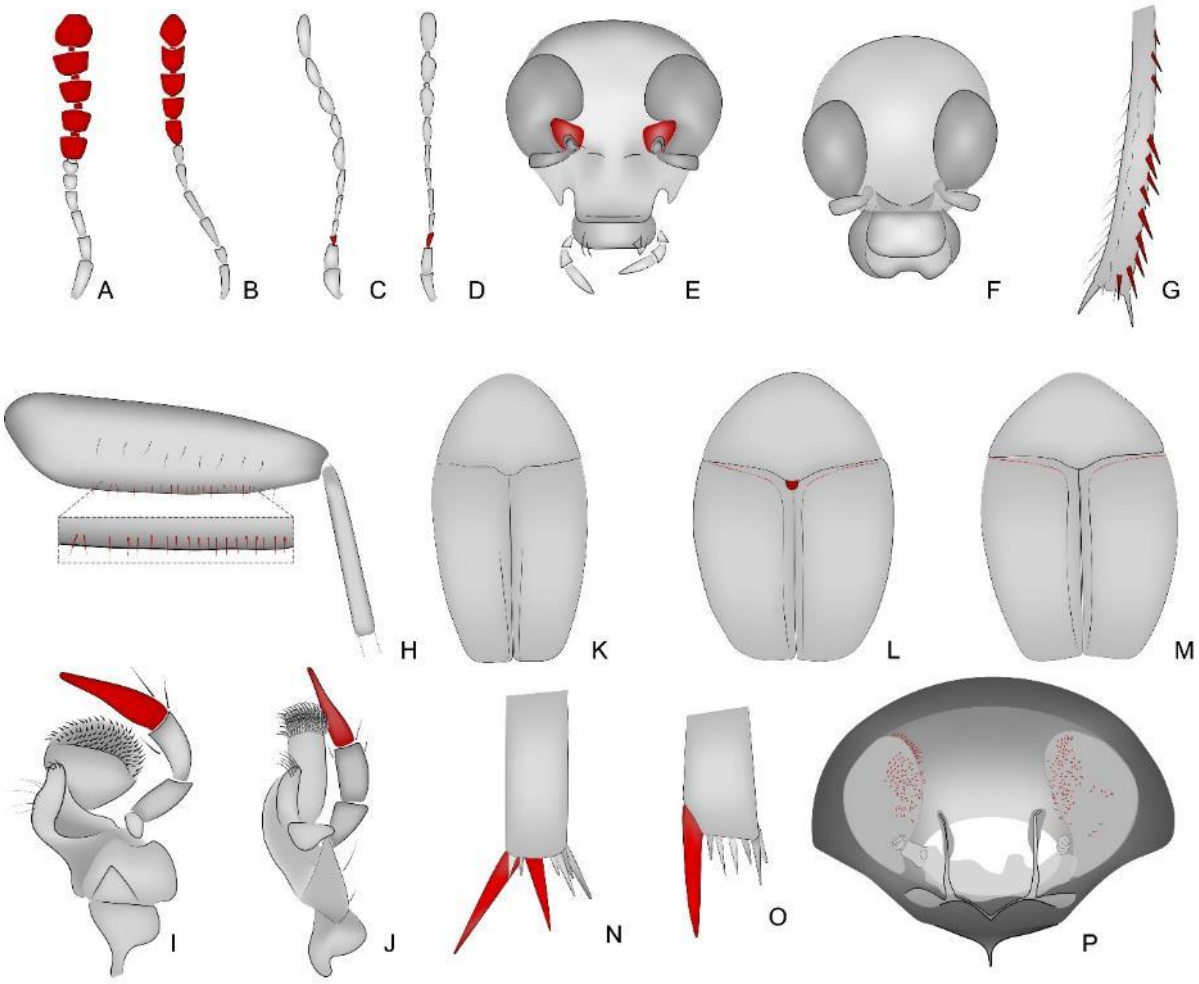

Fig. 2. Scaphidiinae morphology. In red: pertinent characteristics. **A–D.** Antennae. **A.** *Cyparium* sp. nov. **B.** *Scaphidium* sp., adapted from Fierros-López (2005). **C.** *Scaphisoma* sp. nov. 1. **D.** *Baeocera* sp. nov. 2. **E–F.** Head, frontal view. **E.** *Scaphidium peckorum* Fierros-López, 2005. **F.** *Cyparium* sp. nov. **G.** *Cyparium* sp., tibiae. **H.** *Scaphisoma* sp. nov. 1., ctenidium. **I–J.** Mandible. **I.** *Toxidium* sp. nov. 6. **J.** *Baeocera* sp. nov. 1. **K–M.** *Habitus*, dorsal view. **K.** *Toxidium* sp. nov. 6. **L.** *Amalocera* sp. **M.** *Alexidia* sp. nov. 1. **N–O.** Inner spines of mesotibiae. **N.** *Amalocera* sp. **O.** *Alexidia* sp. nov. 1. **P.** *Alexidia* sp. nov. 1, prothoracic corbiculum.

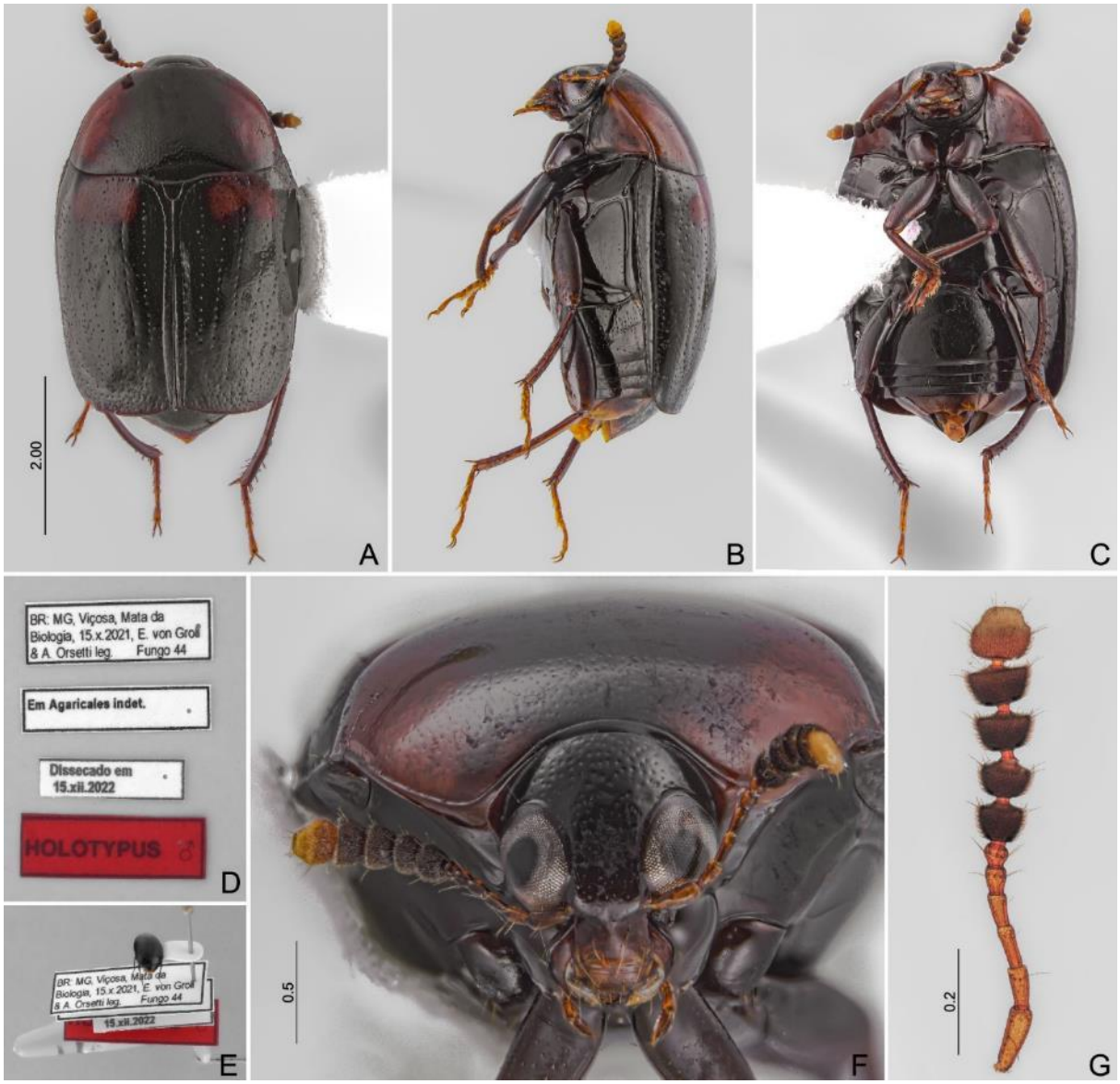

Fig. 3. *Cyparium* sp. nov. Holotype, ♂. **A.** Dorsal view. **B.** Lateral view. **C.** Ventral view. **D.** Labels. **E.** Pinned. **F.** Frontal view. **G.** Antennae. CELC. Scales in mm.

Fig. 4. *Cyparium* sp. nov. Holotype, ♂. **A.** Prothorax, dorsal view. **B.** Oblique view. **C–E.** Legs. **C.** Fore. **D.** Middle. **E.** Fore. **F–H.** Tarsi. **F.** Pro. **G.** Meso. **H.** Meta. **I.** Apical spine of mesotibiae. **J.** Apical spine of metatibiae. **K.** Apex of elytra. **L.** Abdomen, dorsal view. CELC. Scales in mm.

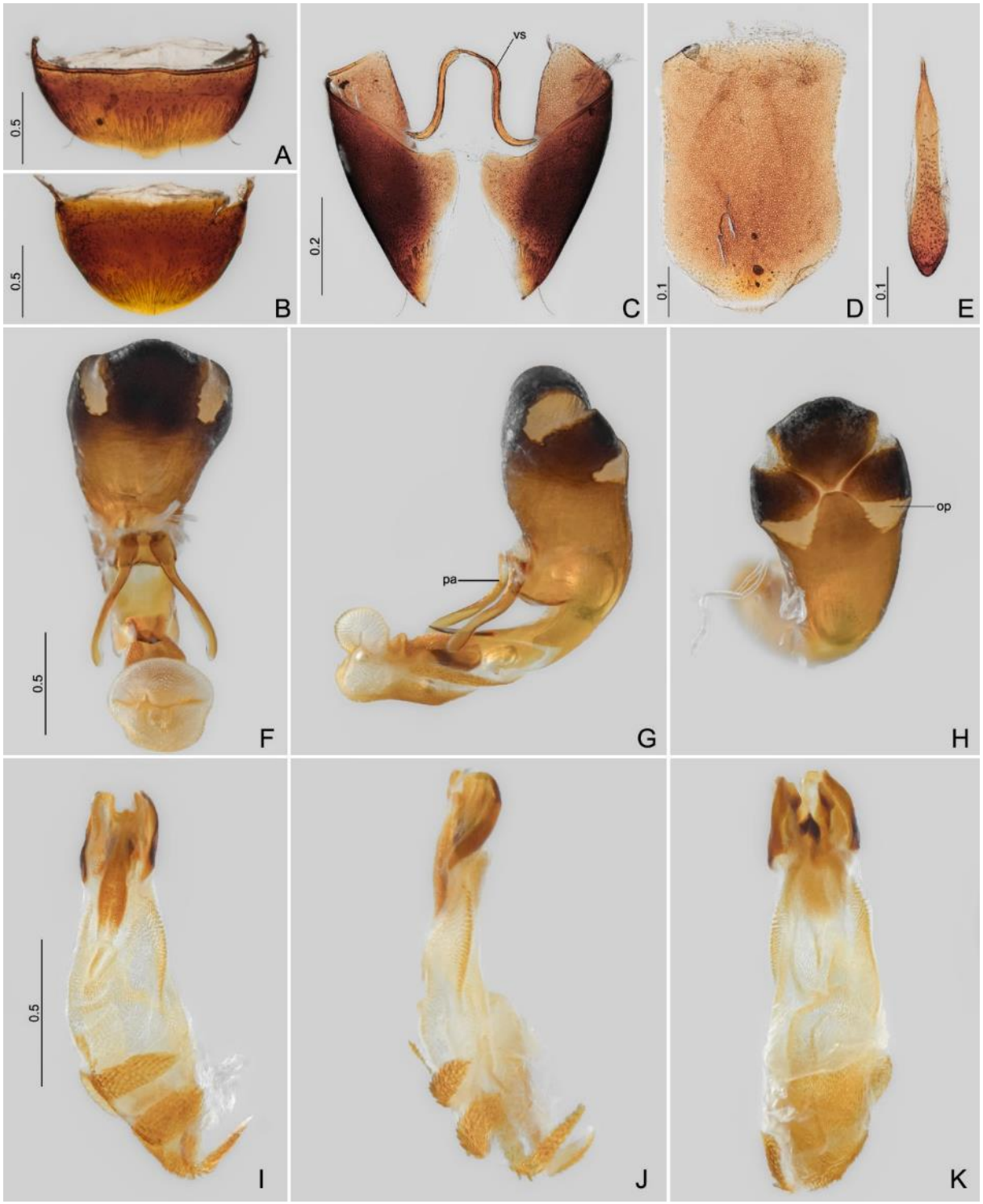

Fig. 5. *Cyparium* sp. nov. Holotype, ♂. **A.** Sternite VIII. **B.** Tergite VIII. **C.** Tergite IX. **D.** Tergite X. **E.** Sternite IX. **F–H.** Aedeagi: **F.** Frontal view. **G.** Lateral view. **H.** Dorsal view. **I–K.** Sclerite of the internal sac. **I.** Frontal view. **J.** Lateral view. **K.** Dorsal view. CELC. Abbreviations: pa = parameres; op = opening; vs = ventral strut. Scales in mm.

Fig. 6. *Alexidia* sp. nov. 1. **A–E.** Holotype, ♂. **A.** Dorsal view. **B.** Lateral view. **C.** Ventral view. **D.** Labels. **E.** Pinned. **F–G.** Paratype, teneral (#09). **F.** Dorsal view. **G.** Lateral view. **H.** Head, frontal view (holotype, ♂). **I.** Dissected head, frontal view (paratype, ♂ #05). **J–K.** Antennae. **J.** Paratype, ♂ (#11). **K.** Paratype, ♀ (#07). CELC. Scales in mm.

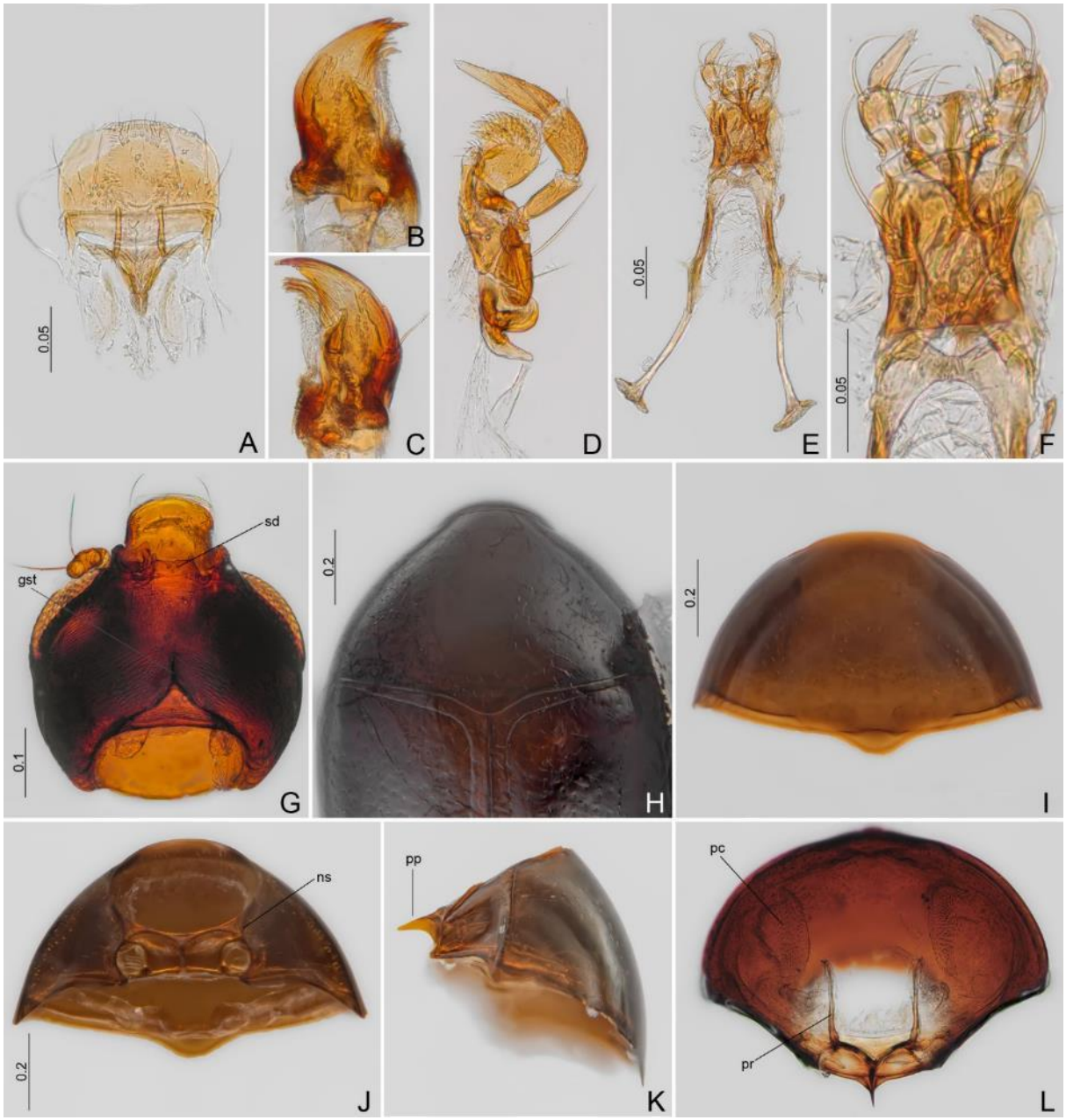

Fig. 7. *Alexidia* sp. nov. 1. **A–G.** Paratype, ♂ (#05). **A.** Labrum. **B–C.** Mandibles. **D.** Maxilla. **E–F.** Labium. **G.** Dissected head, ventral view. **H.** Prothorax, dorsal view (holotype, ♂). **I–K.** Prothorax, paratype, ♂ (#05). **I.** Dorsal view. **J.** Ventral view. **K.** Lateral view. **L.** Prothorax, inner view (paratype, #08). CELC. Abbreviations: gst = gular suture; ns, notosternal suture; pc = prothoracic corbiculum; pp = prosternal process; pr = frofurca; sd = submaxillary duct. Scales in mm.

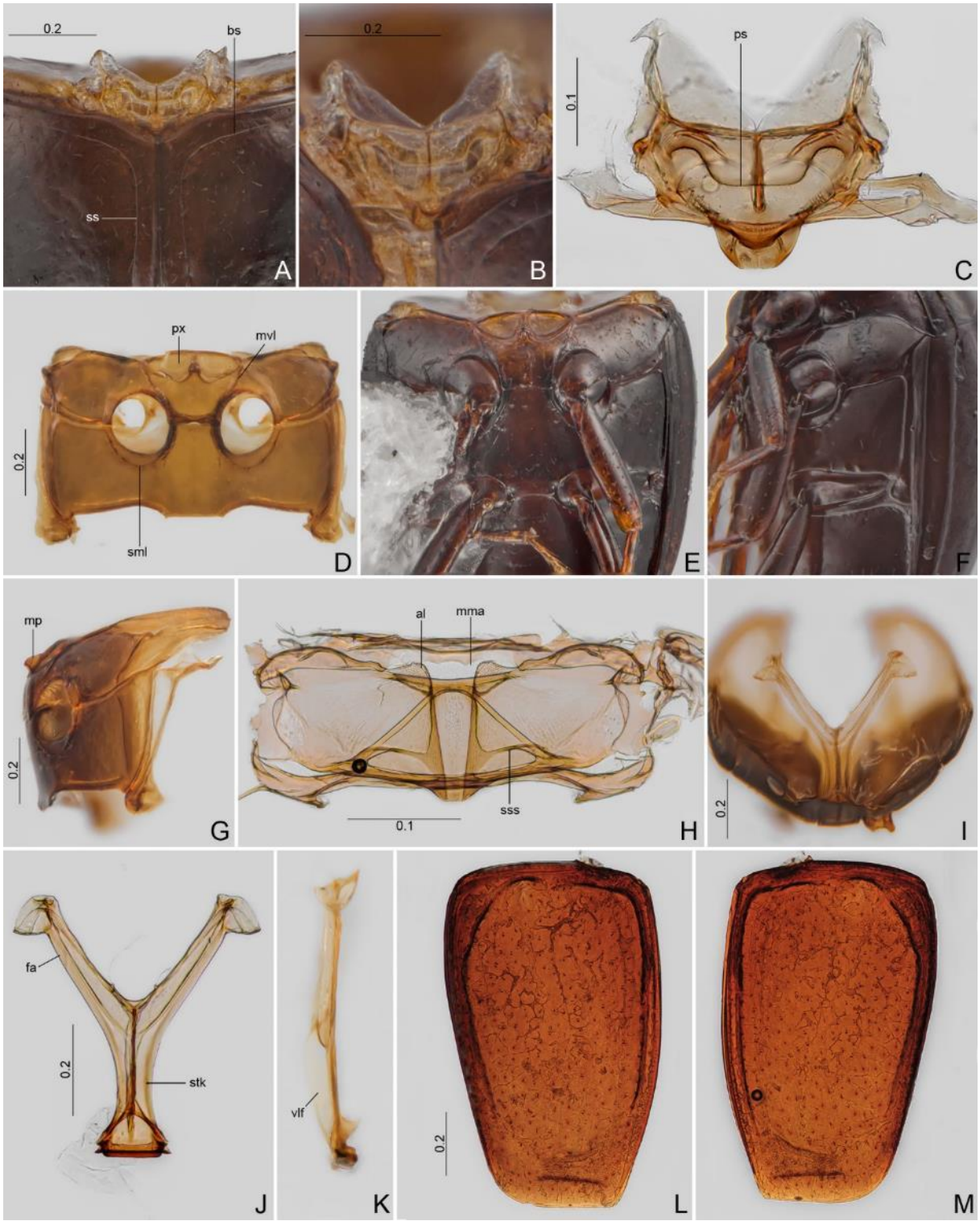

Fig. 8. *Alexidia* sp. nov. 1. **A–C.** Scutellar shield. **A–B.** Paratype #08. C. Paratype, ♂ (#11). **D–G.** Meso- and metathorax. **D.** Dissected, ventral view (paratype, ♂, #11). **E.** Ventral view (paratype #08). **F.** Oblique view (holotype, ♂). **G.** Lateral view (paratype, ♂ #11). **H.** Metanotum (paratype, ♂ #11). **I–K.** Metendosternite. **I.** Connected to the thorax (paratype, ♂ #05). **J.** Dorsal view (paratype, ♂ #11). **K.** Lateral view (paratype, ♂ #11). **L–M.** Elytra (paratype, ♂ #05). CELC. Scales in mm.

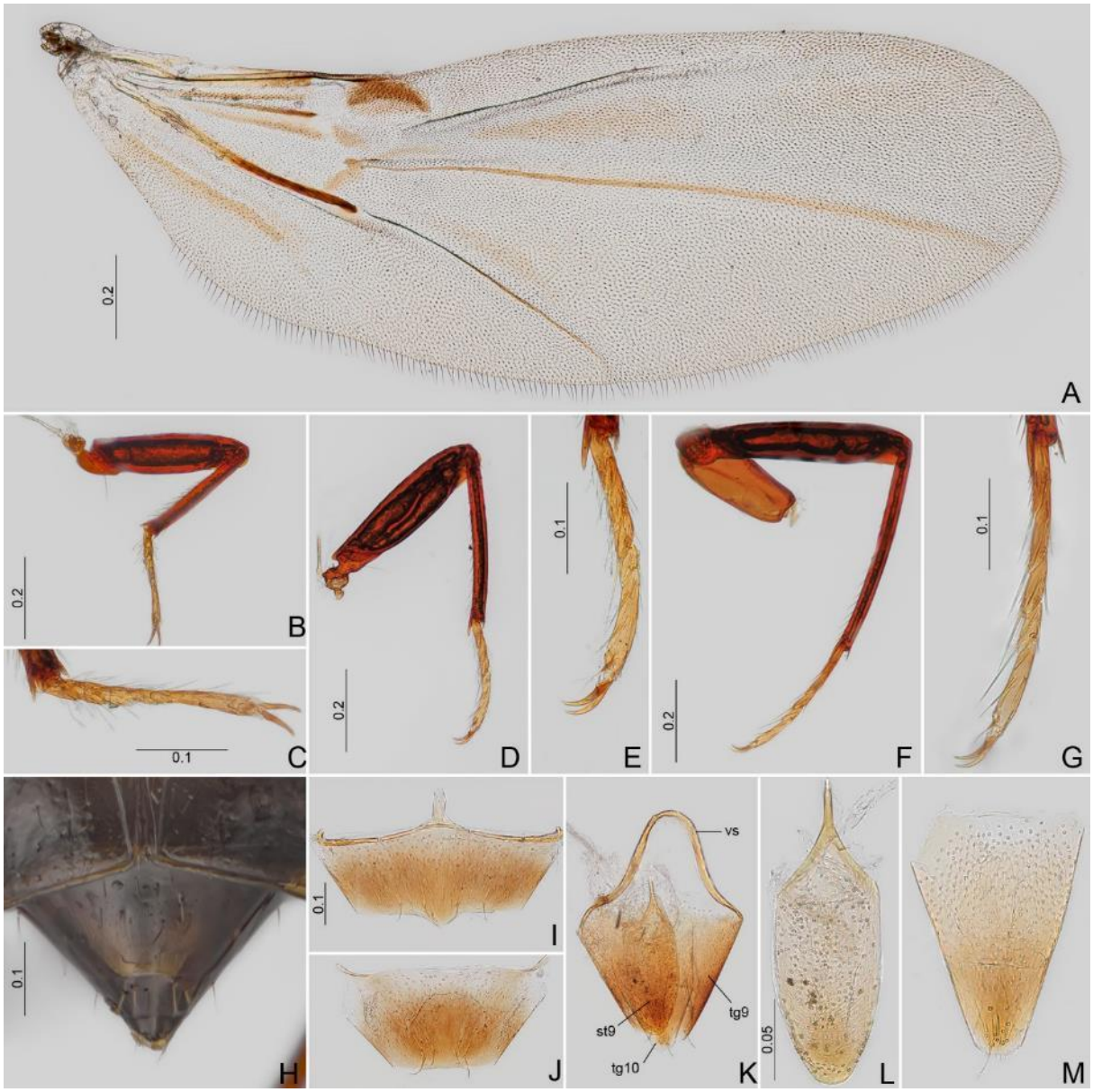

Fig. 9. *Alexidia* sp. nov. 1. **A–G.** Paratype, ♂ (#11). **A.** Hind wing. **B.** Foreleg. **C.** Protibiae. **D.** Middle leg. **E.** Mesotibiae. **F.** Hind leg. **G.** Metatibiae. **H.** Abdomen, dorsal view (holotype, ♂). **I–M.** Paratype, ♂ (#05). **I.** Sternite VIII. **J.** Tergite VIII. **K.** Tergite IX. **L.** Sternite IX. **M.** Tergite X. CELC. Abbreviations: st9 = sternite IX; tg9 = tergite IX; tg10 = tergite X; vs = ventral struts. Scales in mm.

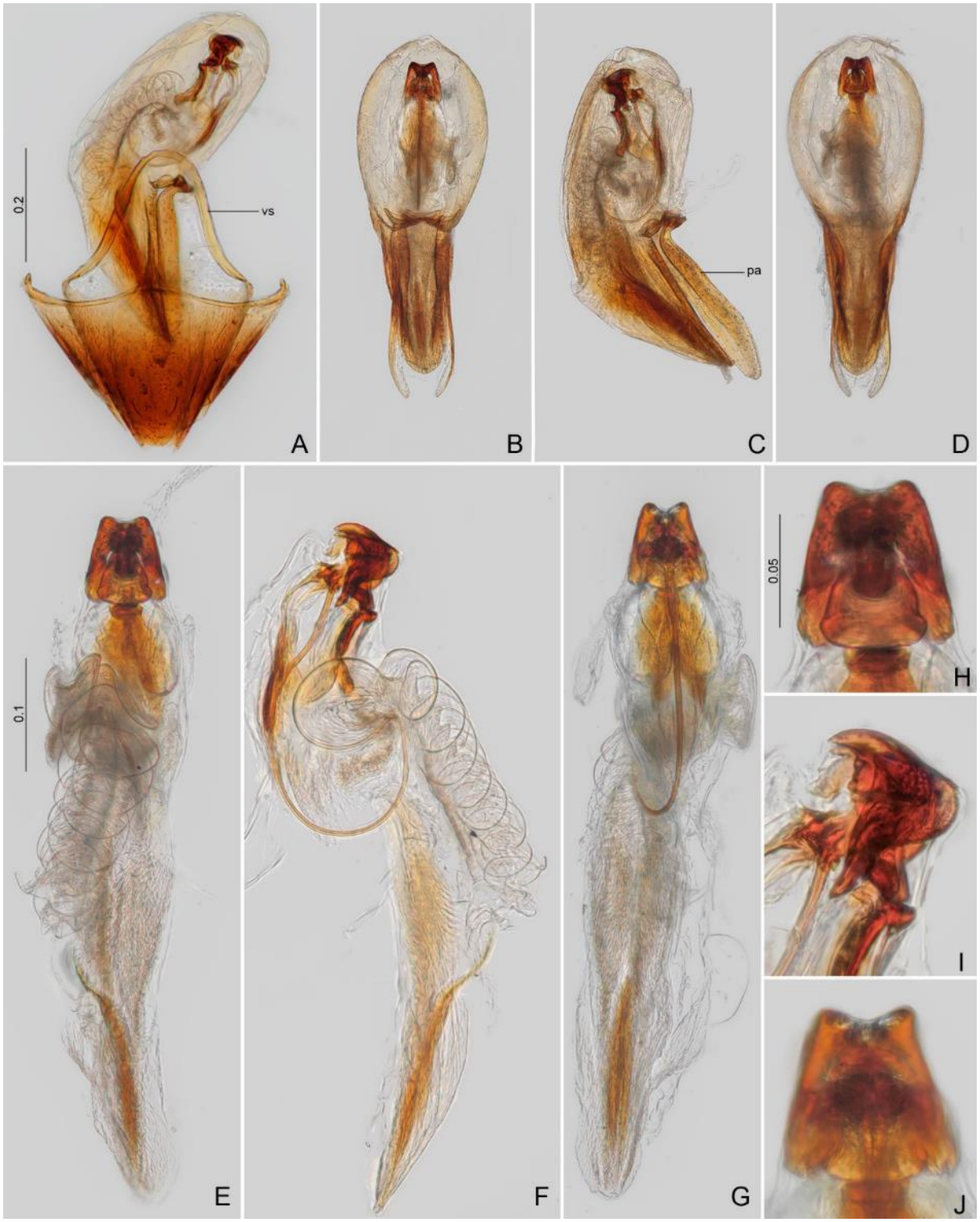

Fig. 10. *Alexidia* sp. nov. 1. **A–J**, paratype, ♂ (#05). **A.** Terminalia. **B–D.** Aedeagi: **B.** Frontal view. **C.** Lateral view. **D.** Dorsal view. **E–G.** Sclerite of the internal sac: **E.** Frontal view. **F.** Lateral view. **G.** Dorsal view. **H–J.** Detail of sclerite of the internal sac: **H.** Frontal view. **I.** Lateral view. **J.** Dorsal view. CELC. Abbreviations: pa = parameres; vs = ventral struts. Scales in mm.

Fig. 11. *Alexidia* sp. nov. 1. **A–B.** Paratype, ♀. **A.** Dorsal view. **B.** Lateral view. **C.** Oblique view. **D–F.** Legs. **D.** Fore. **E.** Midle. **F.** Hind. **G–I.** Tarsi. **G.** Pro. **H.** Meso. **I.** Meta. **J.** Abdomen, dorsal view. **K.** Sternite VIII. **L.** Tergite VIII. **M.** Genitalia. **N.** Ovipositor. CELC. Abbreviations: dg = distal gonocoxites; gs = gonostyli; sd = spermathecal duct; sp = spermatheca. Scales in mm.

Fig. 12. *Alexidia* sp. nov. 2, Holotype, ♀. **A.** Dorsal view. **B.** Lateral view. **C.** Ventral view. **D.** Oblique view. **E.** Head, frontal view. **F.** Antenna. **G.** Prothorax, dorsal view. **H.** Elytral apex. CELC. Scales in mm.

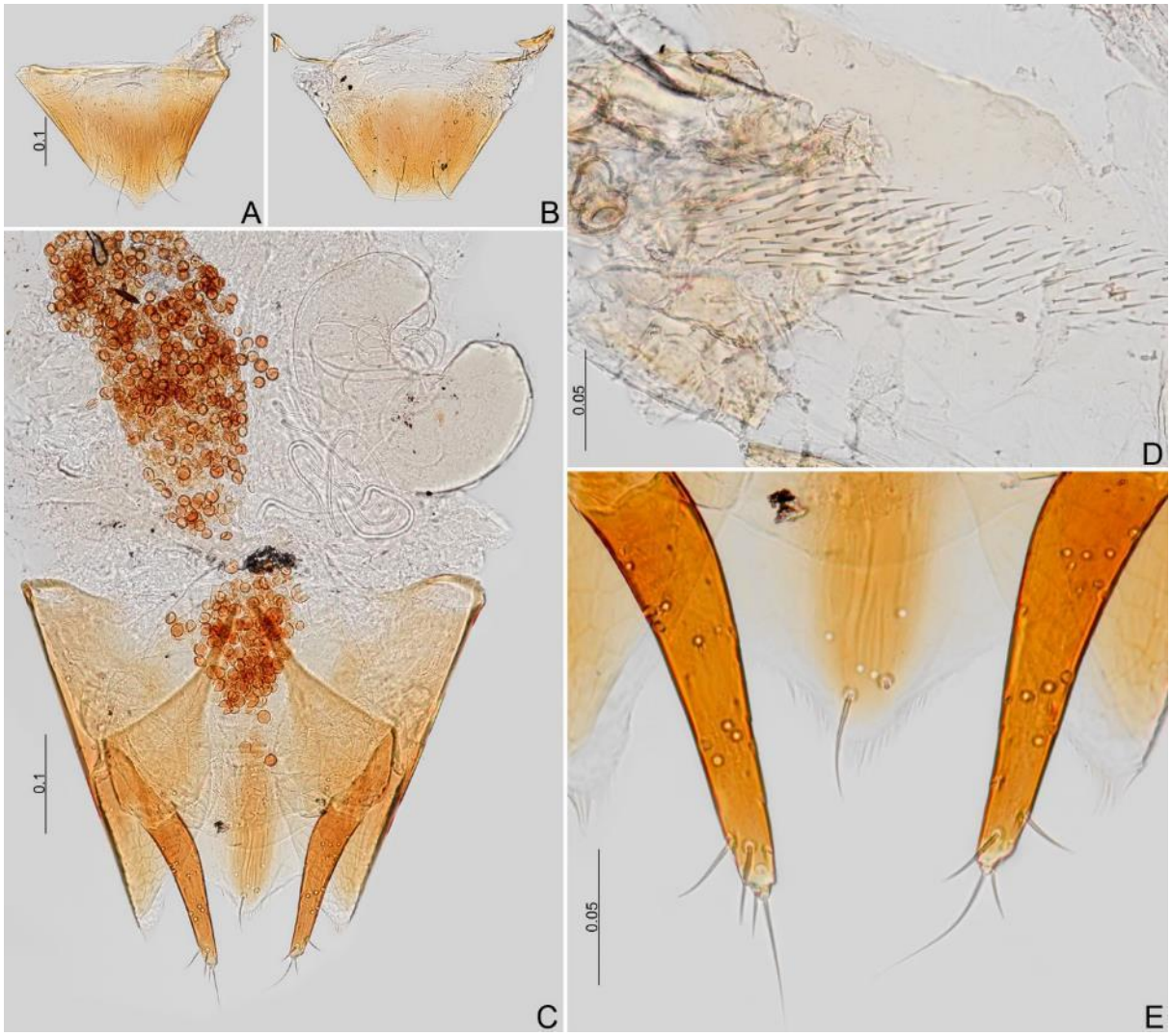

Fig. 13. *Alexidia* sp. nov. 2, holotype, ♀. **A.** Sternite VIII. **B.** Tergite VIII. **C.** Genitalia. **D.** Bursa copulatrix. **E.** Ovipositor. CELC. Scales in mm.

Fig. 14. *Baeocera* sp. nov. 1. **A–E.** Holotype, ♂. **A.** Dorsal view. **B.** Lateral view. **C.** Ventral view. **D.** Labels. **E.** Pinned. **F–G.** Paratype, ♀ (#51), teneral. **F.** Dorsal view. **G.** Lateral view. **H.** Head, frontal view (holotype, ♂). **I.** Head, frontal view, dissected (paratype, ♂, #102), arrow: fovea. **J–K.** Antennae. **J.** Paratype, ♂ (#102). **K.** Paratype, ♀ (#49). CELC. Abbreviation: mta = metanepisternum. Scales in mm.

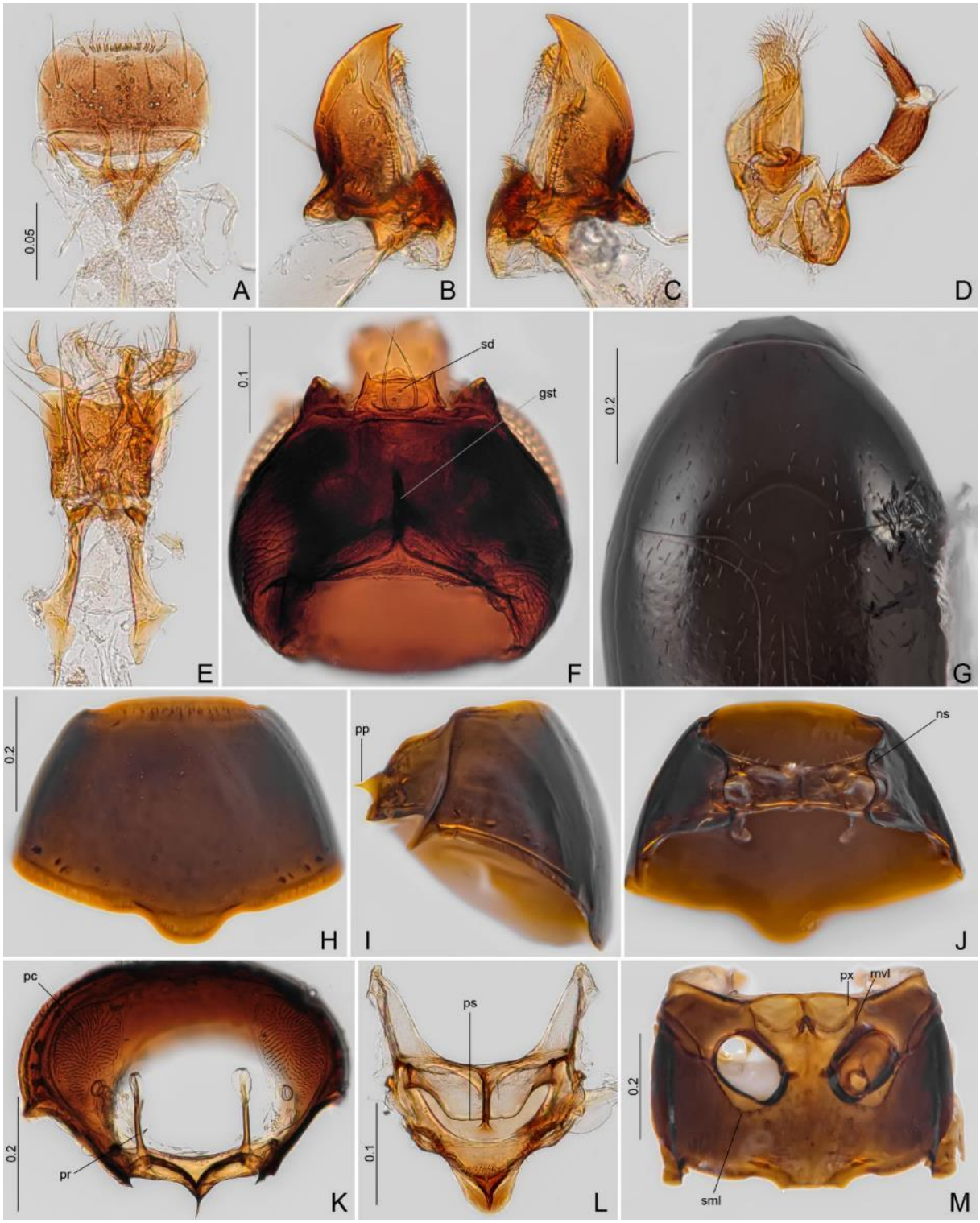

Fig. 15. *Baeocera* sp. nov. 1. **A.** Labrum (paratype, ♂, #102). **B–C.** Mandibles (paratype, ♀, #49). **D–F.** Paratype, ♂ (#102). **D.** Maxilla. **E.** Labium. **F.** Head, ventral view. **G.** Prothorax, dorsal view (holotype, ♂). **H–M.** Paratype, ♂ (#102). **H–K.** Prothorax. **H.** Dorsal view. **I.** Lateral view. **J.** Ventral view. **K.** Inner view. **L.** Scutellar shield. **M.** Meso- and metathorax, ventral view. CELC. Abbreviations: gst = gular suture; mvl = mesoventral line; ns = notosternal suture; pc = prothoracic corbiculum; pp = prosternal process; pr = profurca; ps = prescutellar line; px = procoxal rest; sd = submaxillary duct; sml = submesocoxal line. Scales

in mm.

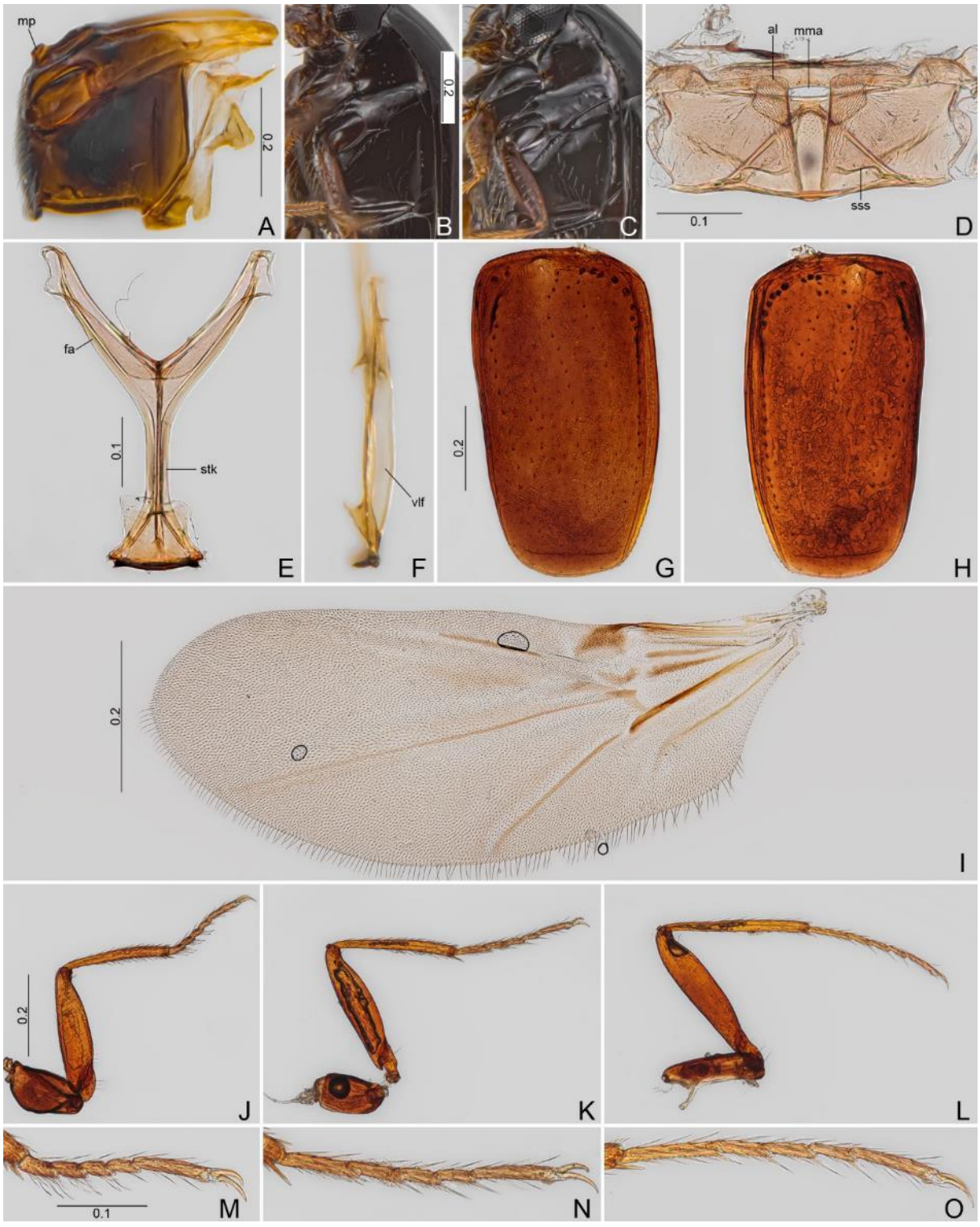

Fig. 16. *Baeocera* sp. nov. 1. **A–C.** Meso- and metathorax, lateral view. **A.** Lateral view, dissected (paratype, ♂, #102). **B.** Holotype, ♂. **C.** Paratype, ♀ (#53). **D.** Metanotum (paratype, ♂, #102). **E–F.** Metendosternite (paratype, ♀, #49). **E.** Dorsal view. **F.** Lateral view. **G–O.** Paratype, ♂ (#102). **G–H.** Elytra. **I.** Hind wing. **J–L.** Legs. **J.** Fore. **K.** Middle. **L.** Hind. **M–O.** Tarsi. **M.** Pro. **N.** Meso. **P.** Meta. Abbreviations: al = alacrista; fa = furcal arm; mma = median membranous area; mp = mesoventral process; sss = scutoscutellar suture; stk = stalk; vlf = ventral longitudinal flange. CELC. Scales in mm.

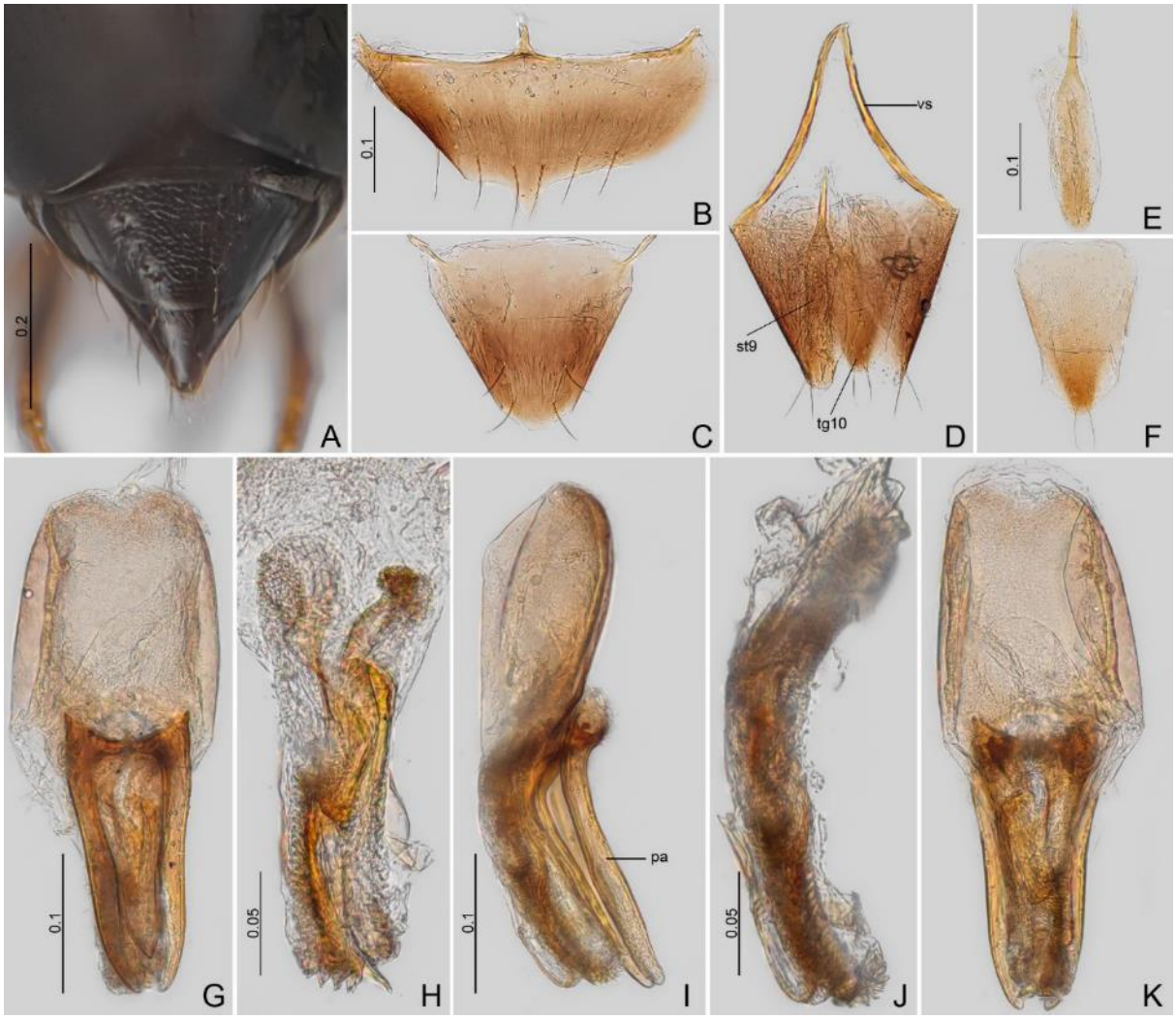

Fig. 17. *Baeocera* sp. nov. 1. **A.** Abdomen, dorsal view (holotype, ♂). **B–K.** Paratype, ♂ (#102): **B.** Sternite VIII. **C.** Tergite VIII. **D.** Tergite IX. **E.** Sternite IX. **F.** Tergite X. **G–K.** Aedeagi. **G.** Frontal view. **H.** Sclerite of internal sac, frontal view. **I.** Lateral view. **J.** Sclerite of internal sac, lateral view. **K.** Dorsal view. Abbreviations: pa = parameres; st9 = sternite IX; tg10 = tergite X; vs = ventral struts. CELC. Scales in mm.

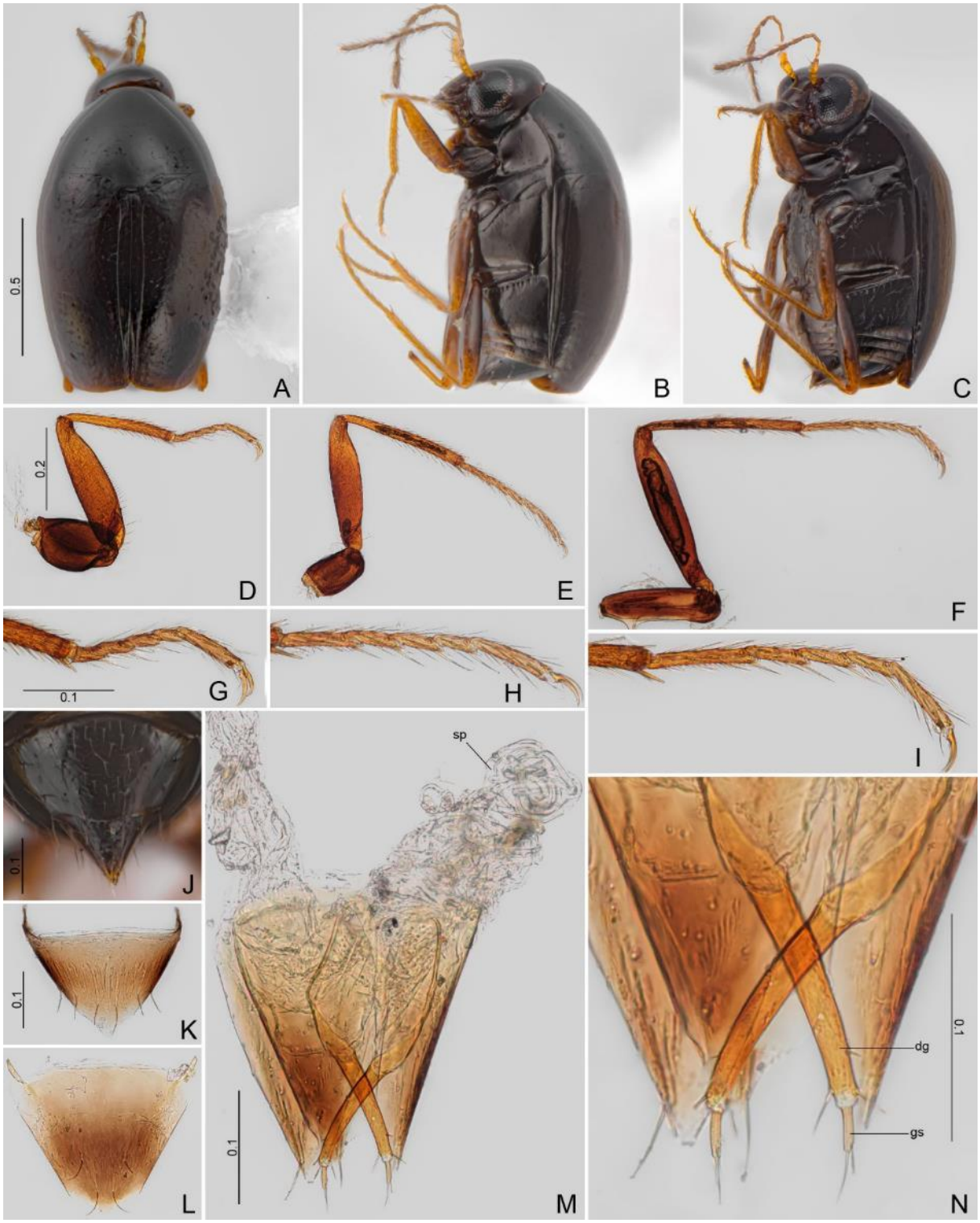

Fig. 18. *Baeocera* sp. nov. 1. **A–C.** Paratype, ♀ (#49). **A.** Dorsal view. **B.** Lateral view. **C.** Oblique view. **D–N.** Paratype, ♀ (#53). **F.** Legs. **D.** Fore. **E.** Middle. **F.** Hind. **G–I.** Tarsi. **G.** Pro. **H.** Meso. **I.** Meta. **J.** Abdomen, dorsal view. **K.** Sternite VIII. **L.** Tergite VIII. **M.** Terminalia. **N.** Ovipositor. CELC. Abbreviations: dg = distal gonocoxites; gs = gonostyli; sp = spermatheca. Scales in mm.

Fig. 19. *Baeocera* sp. nov. 2. **A–F.** Holotype, ♂. **A.** Dorsal view. **B.** Lateral view, arrow: lateral impression. **C.** Ventral view. **D.** Labels. **E.** Pinned. **F.** Head, frontal view. **G–H.** Antennae. **G.** Paratype, ♂ (#95). **H.** Paratype, ♀ (#103). **I–M.** Paratype, ♂. **I.** Labrum, arrow: lateral concavities. **J–K.** Mandibles. **L.** Maxilla. **M.** Labium. CELC. Scales in mm.

Fig. 20. *Baeocera* sp. nov. 2. **A.** Prothorax, dorsal view (holotype, ♂). **B–H.** Paratype, ♂ (#95). **B–E.** Prothorax. **B.** Dorsal view. **C.** Lateral view. **D.** Ventral view. **E.** Inner view. **F.** Scutellar shield. **G–J.** Meso- and metathorax (paratype, ♂, #95). **G.** Ventral view. **H.** Lateral view. **I.** Oblique view (holotype, ♂). **J–L.** Paratype, ♂ (#95). **J.** Metanotum. **K–L.** Metendosternite. **K.** Dorsal view. **L.** Lateral view. Abbreviation: ml = median line. CELC. Scales in mm.

Fig. 21. *Baeocera* sp. nov. 2. **A–I.** Paratype, ♂. **A–B.** Elytra. **C.** Hind wing. **D–F.** Legs. **D.** Fore. **E.** Middle. **F.** Hind. **G–I.** Tarsi. **G.** Pro. **H.** Meso. **I.** Meta. **J.** Abdomen, dorsal view (holotype, ♂). **K–M.** Paratype, ♂ (#95). **K.** Sternite VIII. **L.** Tergite VIII. **M.** Tergite IX. CELC. Scales in mm.

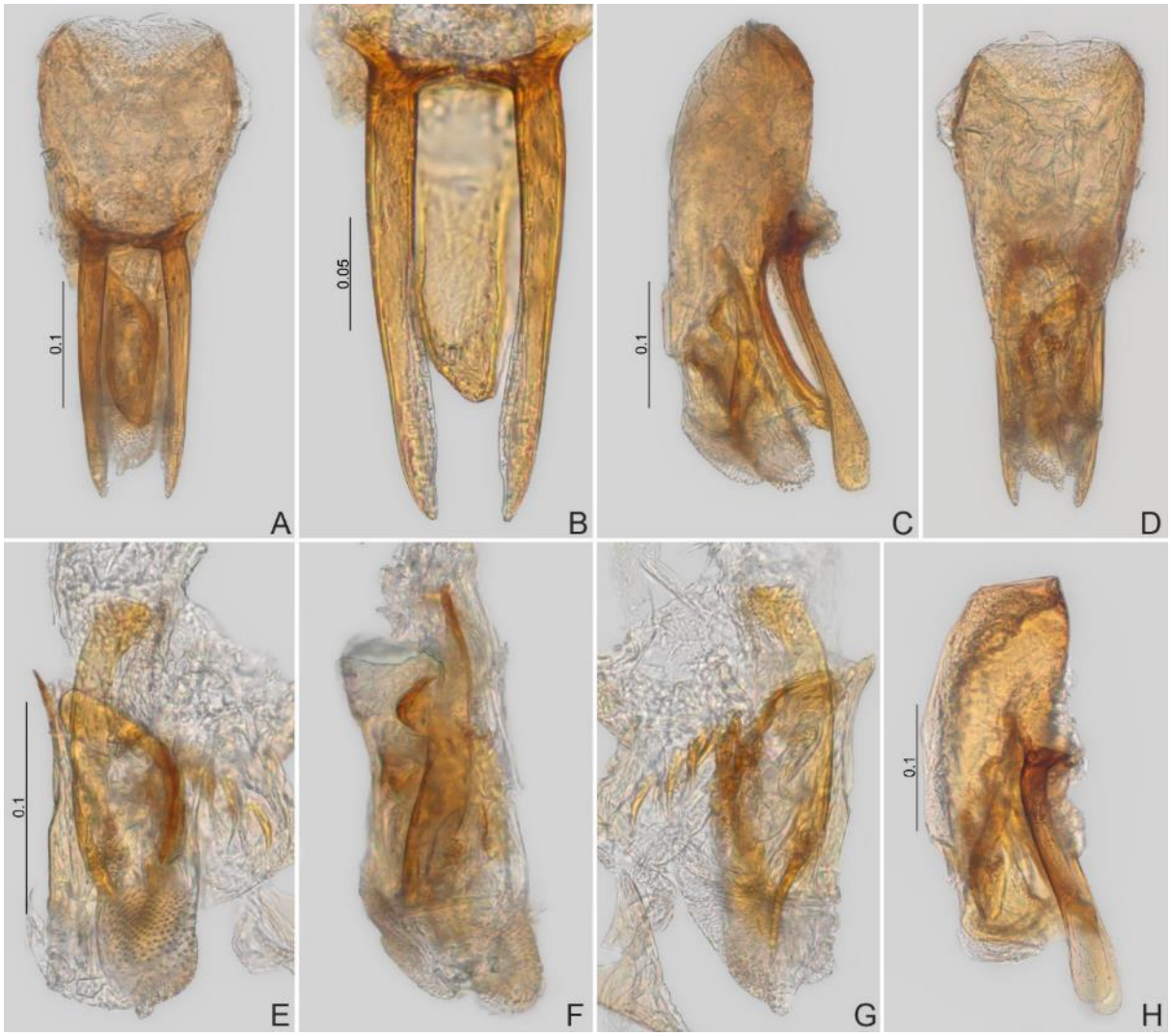

Fig. 22. *Baeocera* sp. nov. 2. **A**–**G**. Paratype, ♂ (#95). **A–D.** Aedeagi **A.** Frontal view. **B.** Parameres, frontal view. **C.** Lateral view. **D.** Dorsal view. **E–G.** Sclerite of internal sac. **E.** Frontal view. **F.** Lateral view. **G.** Dorsal view. **H.** Aedeagi, lateral view (paratype, ♂, #86). CELC. Scales in mm.

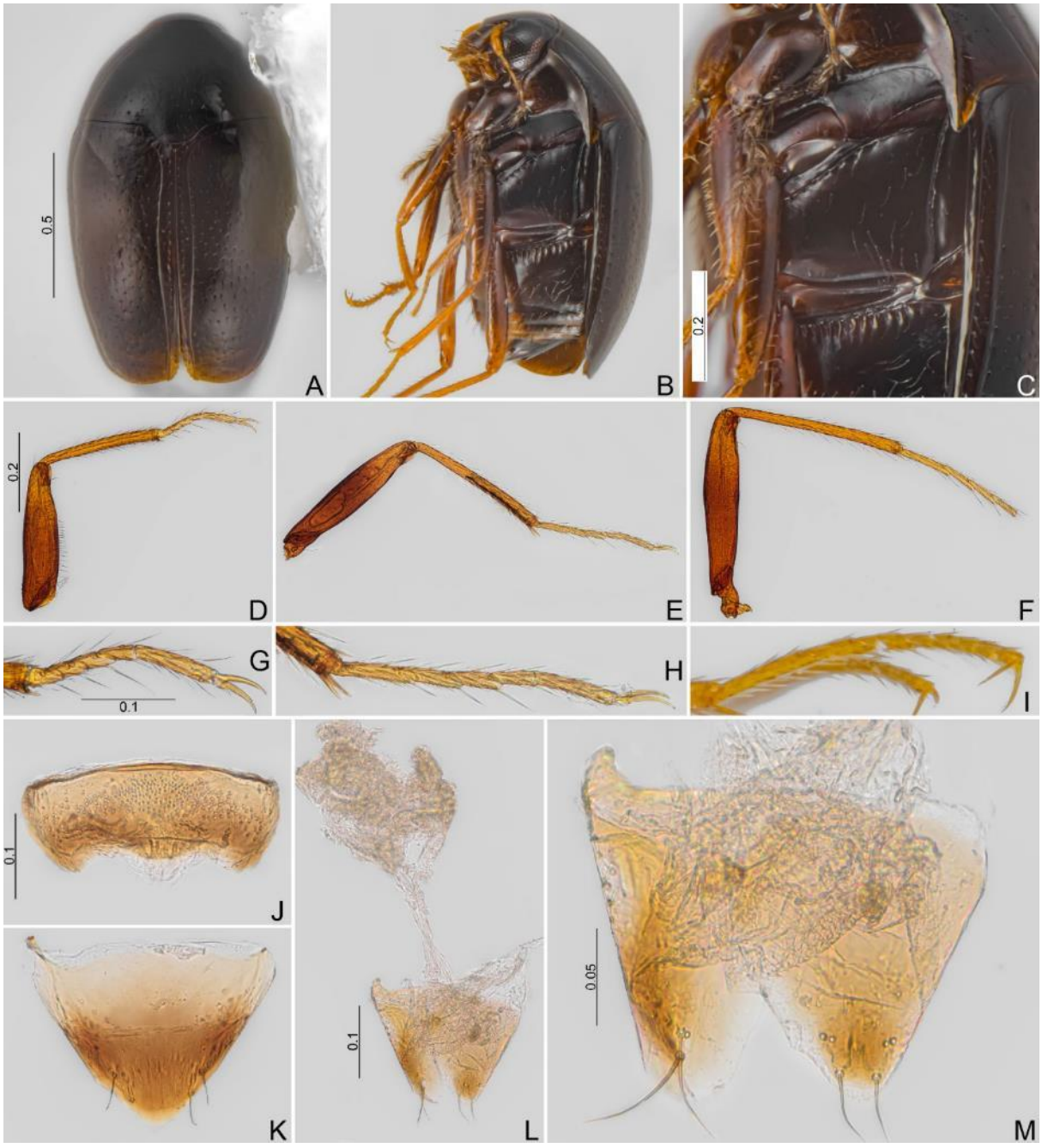

Fig. 23. *Baeocera* sp. nov., paratype, ♀ (#103). **A.** Dorsal view. **B.** Oblique view. **C.** Thorax, oblique view. **D–F.** Legs. **D.** Fore. **E.** Middle. **F.** Hind. **G–I.** Tarsi. **G.** Pro. **H.** Meso. **I.** Meta. **J.** Sternite VIII. **K.** Tergite VIII. **L.** Genitalia. **M.** Ovipositor. CELC. Scales in mm.

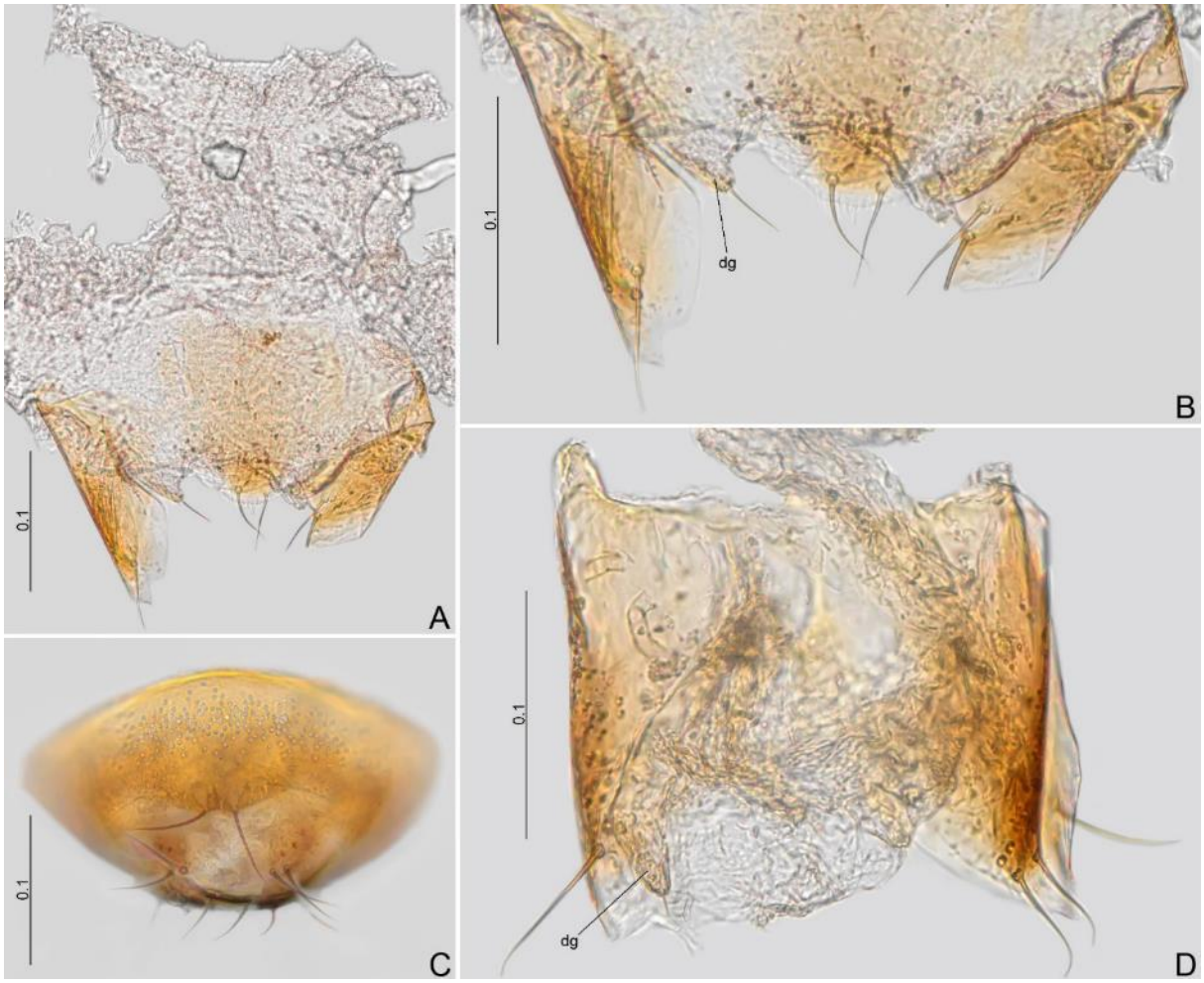

Fig. 24. *Baeocera* sp. nov. 2., paratypes, ♀♀. **A.** Genitalia (#134). **B.** Ovipositor (#134). **C.** Apex, abdomen with genitalia (#126). **D.** Genitalia (#23). CELC. Abbreviation: dg = distal gonocoxite. Scales in mm.

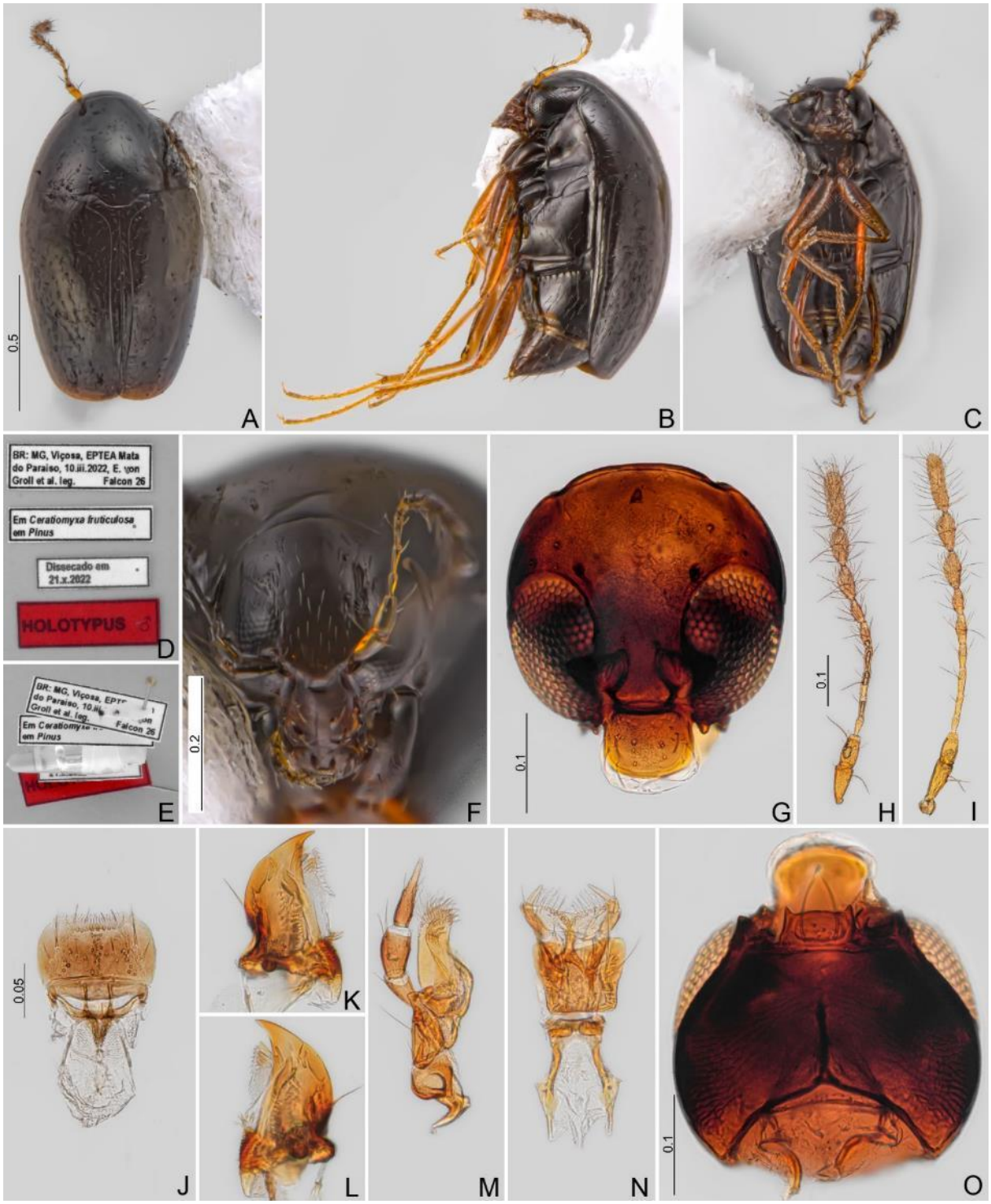

Fig. 25. *Baeocera* sp. nov. 3. **A–F.** Holotype, ♂. **A.** Dorsal view. **B.** Lateral view. **C.** Ventral view. **D.** Labels. **E.** Pinned. **F.** Head, frontal view. **G.** Head, frontal view (paratype, ♂, #33). **H–I.** Antennae. **H.** Holotype, ♂. **I.** Paratype, ♂ (#33). **J–O.** Paratype, ♂ (#33). **J.** Labrum. **K–L.** Mandibles. **M.** Maxilla. **N.** Labium. **O.** Head, ventral view. CELC. Scales in mm.

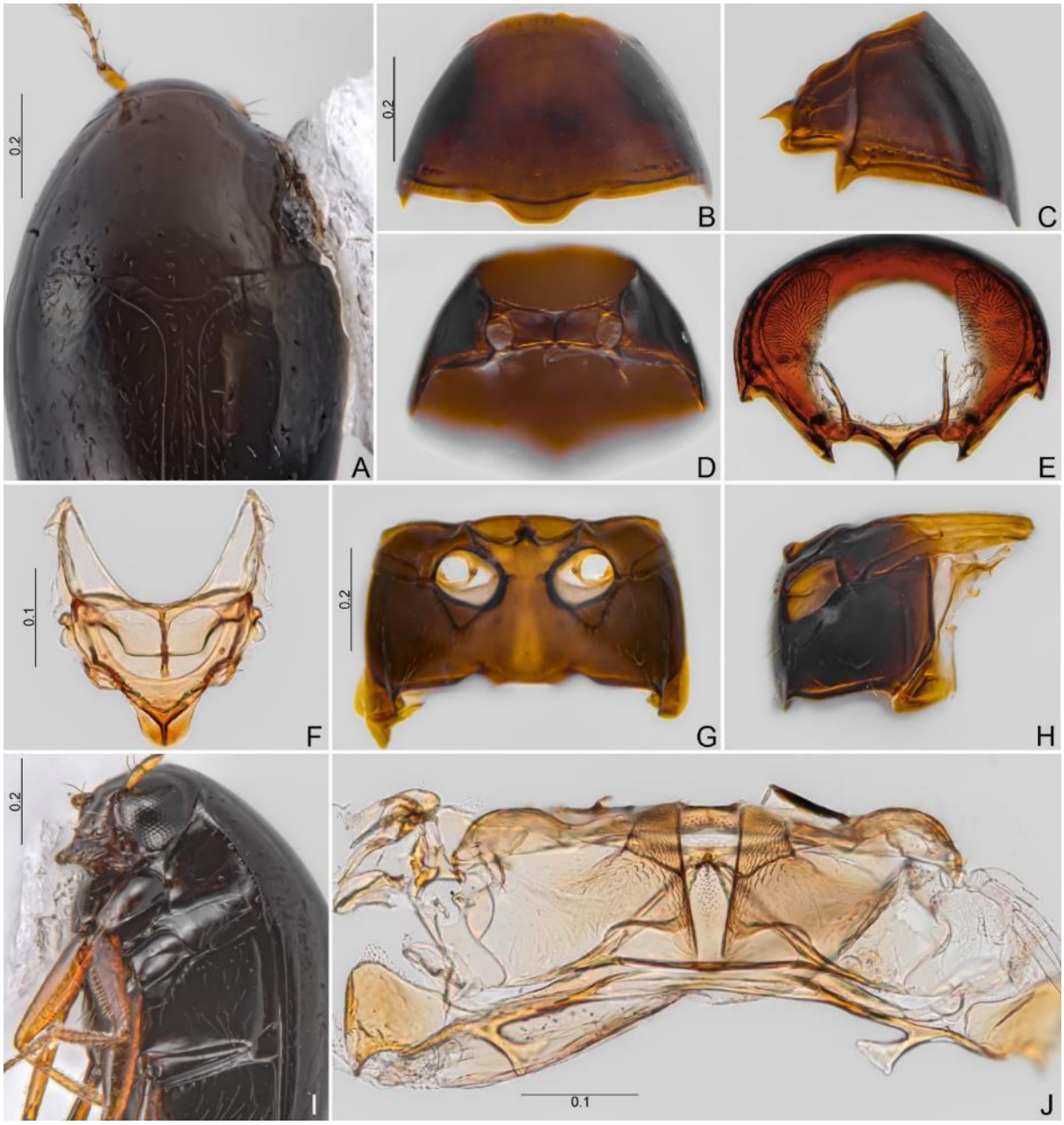

Fig. 26. *Baeocera* sp. nov. 3. **A.** Prothorax, dorsal view (holotype, ♂). **B–H.** Paratype, ♂ (#33). **B–E.** Prothorax. **B.** Dorsal view. **C.** Lateral view. **D.** Ventral view. **E.** Inner view. **F.** Scutellar shield. **G–I.** Meso- and metathorax. **G.** Ventral view. **H.** Lateral view. **I.** Oblique view (holotype, ♂). **J.** Metanotum (paratype, ♂, #33). CELC. Scales in mm.

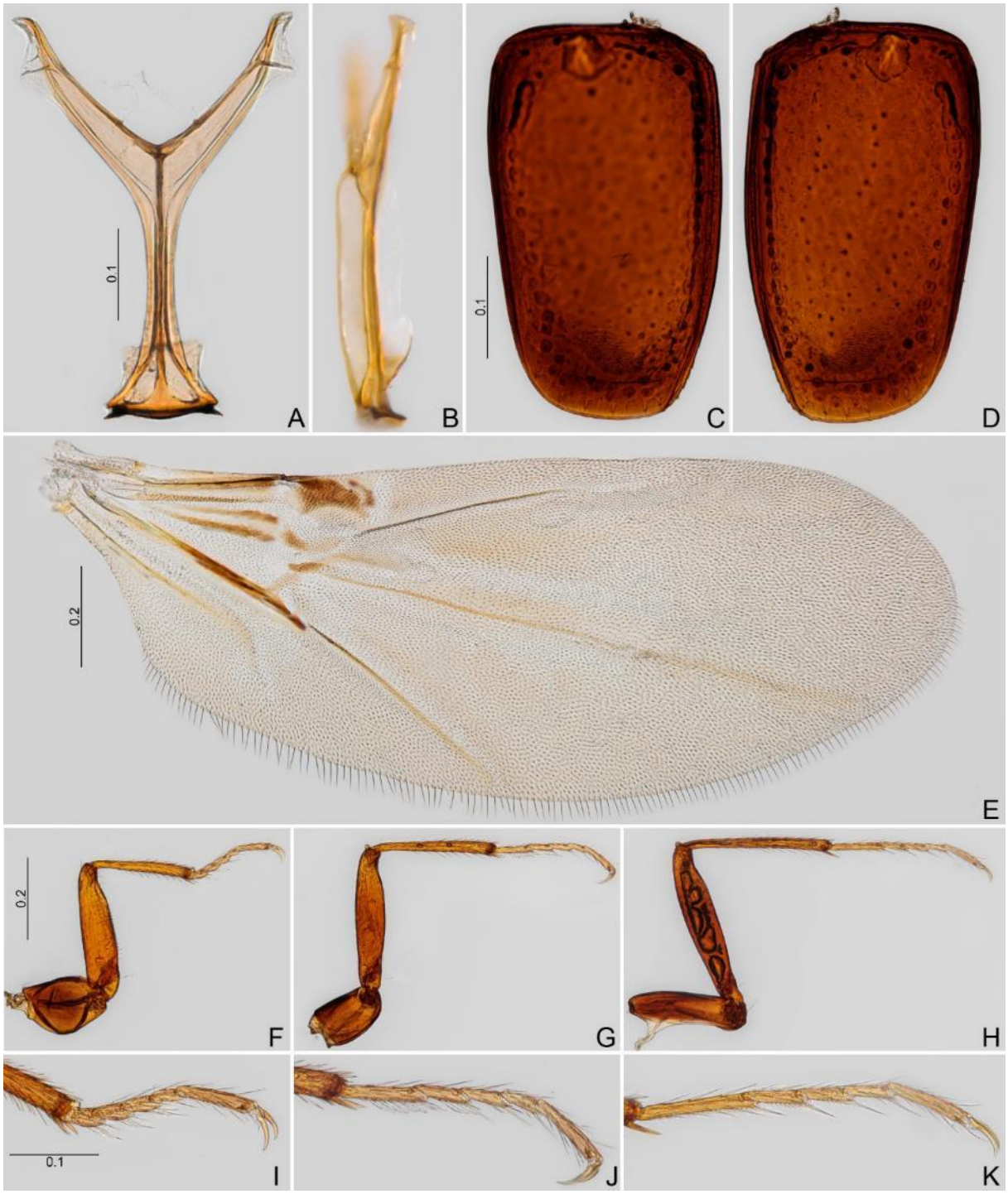

Fig. 27. *Baeocera* sp. nov. 3, paratype, ♂ (#33). **A–B.** Metendosternite. **A.** Dorsal view. **B.** Lateral view. **C–D.** Elytra. **E.** Hind wing. **F–H.** Legs. **F.** Fore. **G.** Middle. **H.** Hind. **I–K.** Tarsi. **I.** Pro. **J.** Meso. **K.** Meta. CELC. Scales in mm.

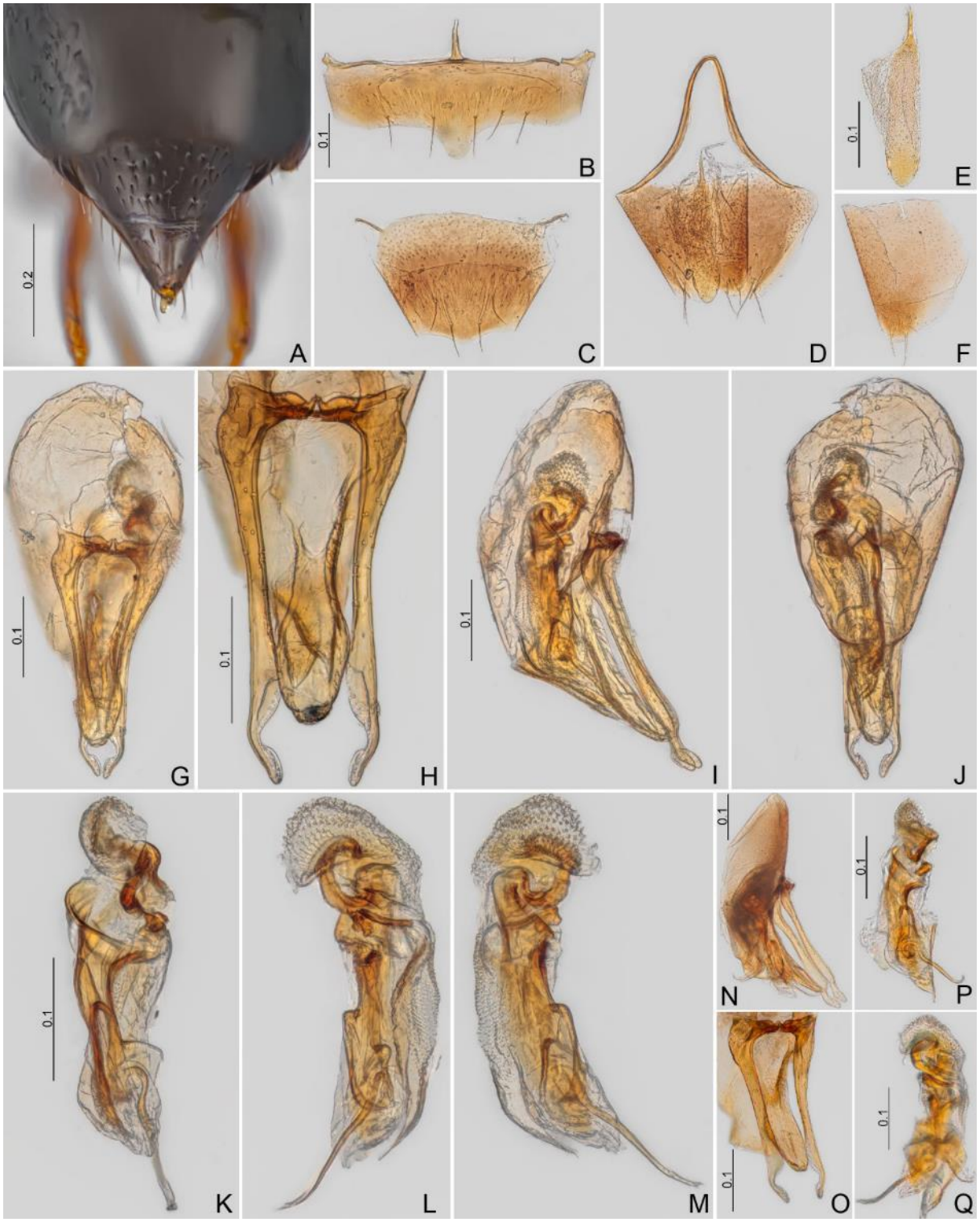

Fig. 28. *Baeocera* sp. nov. 3. **A–M.** Holotype, ♂. **A.** Abdomen, dorsal view. **B.** Sternite VIII. **C.** Tergite VIII. **D.** Tergite IX. **E.** Sternite IX. **F.** Tergite X. **G–J.** Aedeagi. **G.** Frontal view. **H.** Parameres, ventral view. **I.** Lateral view. **J.** Dorsal view. **K–M.** Sclerites of internal sac. **K.** Frontal view. **L.** Lateral view-1. **M.** Lateral view-2. **N–Q**. Aedeagi (paratype, ♂, #33). **N.** Lateral view. **O.** Parameres, oblique view. **P.** Sclerite, oblique view. **Q.** Sclerite, lateral view. CELC. Scales in mm.

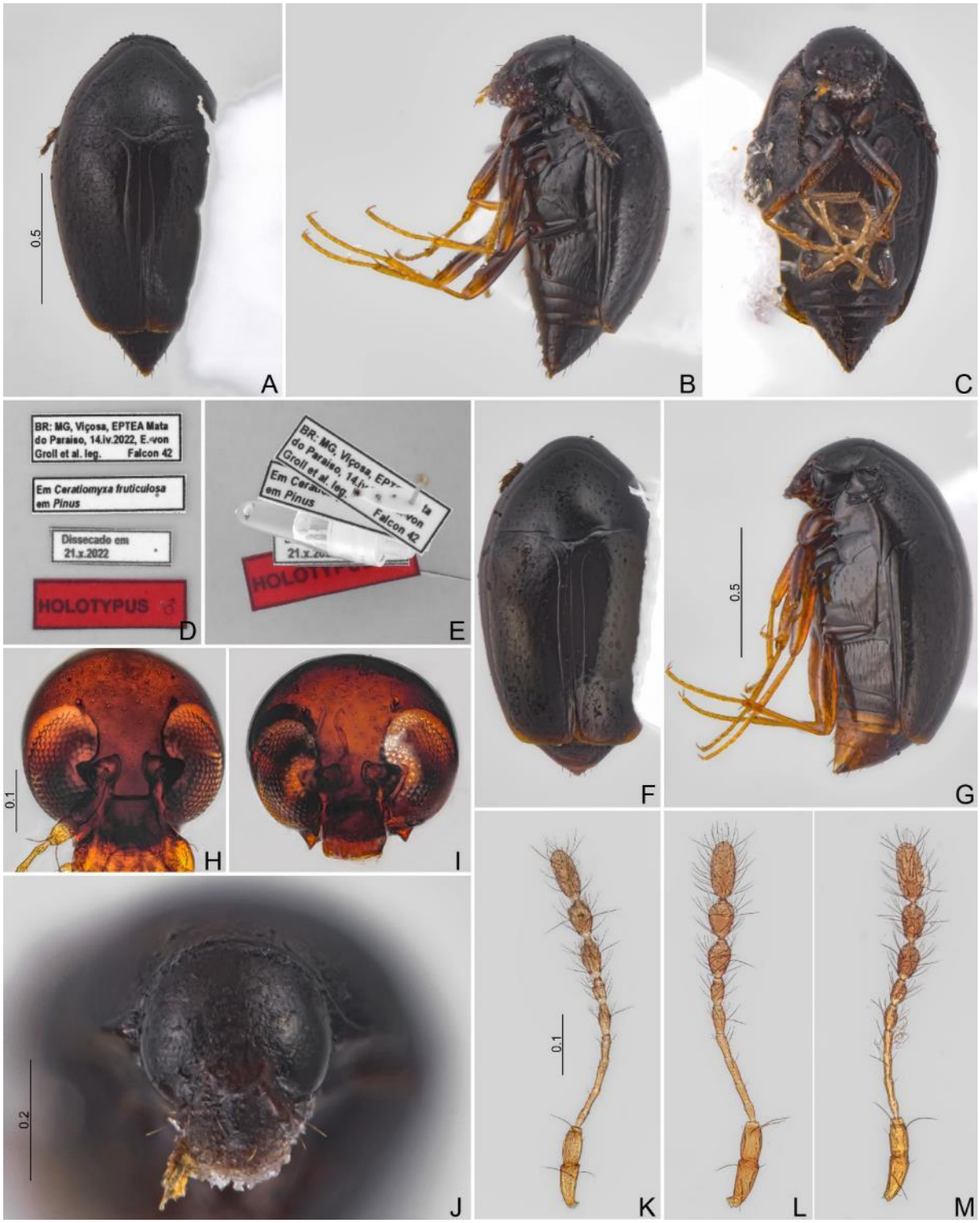

Fig. 29. *Baeocera* sp. nov. 4. **A–E.** Holotype, ♂. **A.** Dorsal view. **B.** Lateral view. **C.** Ventral view. **D.** Labels. **E.** Pinned. **F–G.** Paratype, ♀ (#52). **F.** Dorsal view. **G.** Lateral view. **H.** Head, frontal view (holotype, ♂). **I.** Head, frontal view, dissected (paratype, ♀, #31). **J.** Head, frontal view (holotype, ♂). **K–M.** Antennae: **K.** Holotype, ♂. **L.** Paratype, ♀ (#31). **M.** Paratype, ♀ (#52). CELC. Scales in mm.

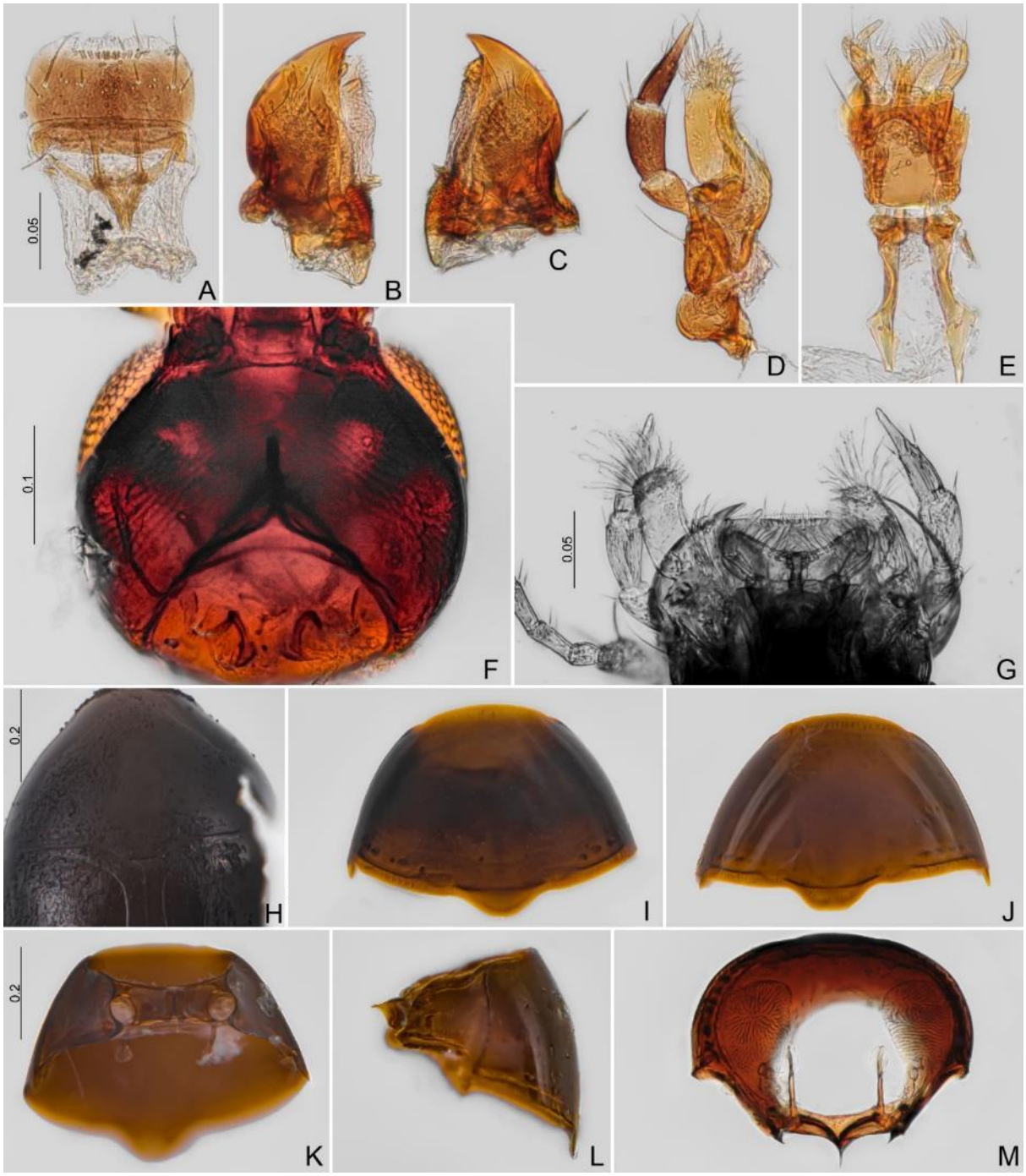

Fig. 30. *Baeocera* sp. nov. 4. **A–E.** Paratype, ♀ (#31). **A.** Labrum. **B–C.** Mandibles. **D.** Maxilla. **E.** Labium. **F–I.** Holotype, ♂. **F.** Head, ventral view. **G.** Mouth parts. **H.** Prothorax, dorsal view. **I.** Prothorax, dorsal view, dissected. **J–M.** Prothorax (paratype, ♀, #31)). **J.** Dorsal view. **K.** Ventral view. **L.** Lateral view. **M.** Inner view. CELC. Scales in mm.

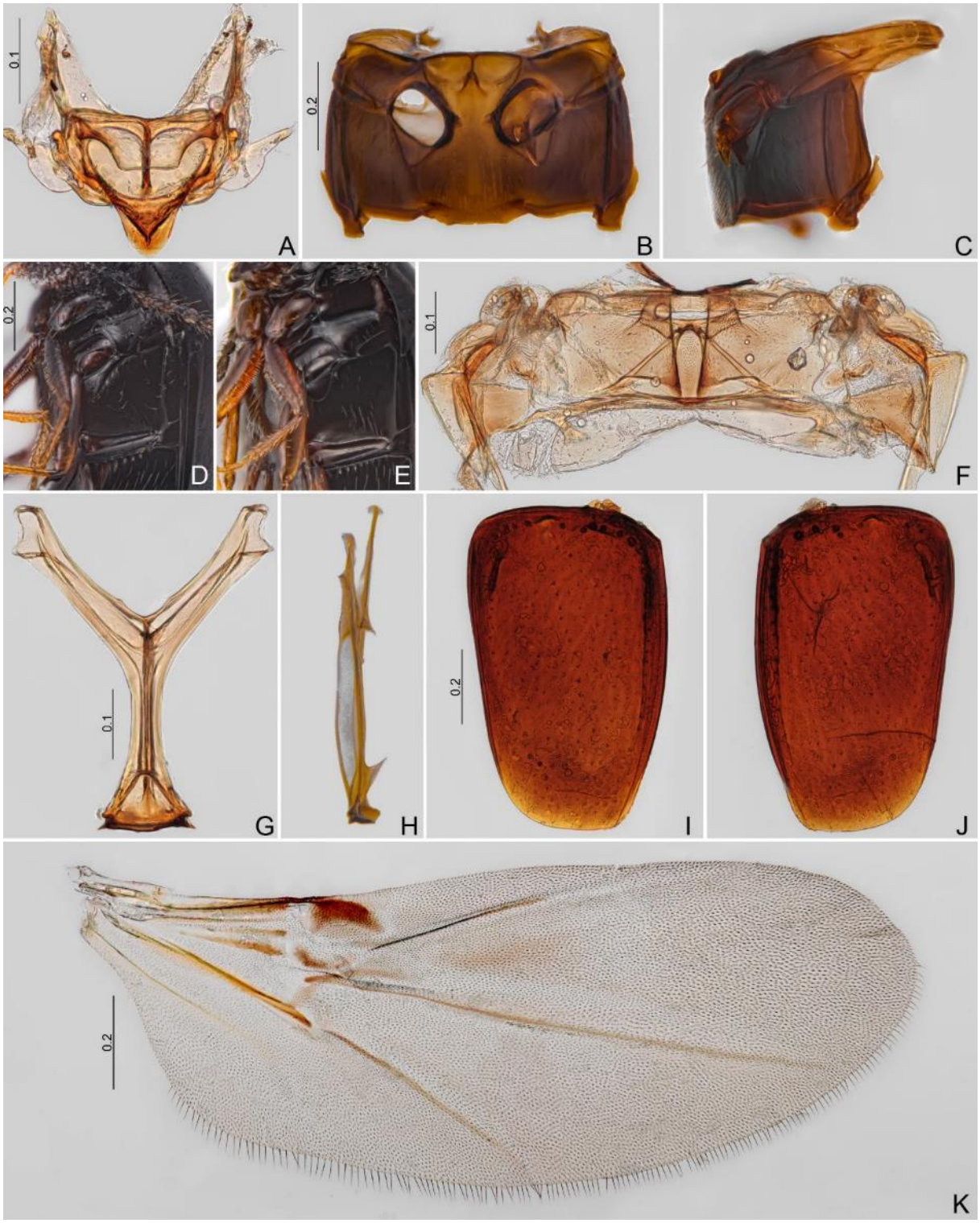

Fig. 31. *Baeocera* sp. nov. 4. **A–C.** Paratype, ♀ (#31). **A.** Scutellar shield. **B–E.** Meso- and metathorax. **B.** Ventral view. **C.** Lateral view. **D.** Oblique view (holotype, ♂). **E.** Oblique view (paratype, ♀, #52). **F–K.** Paratype, ♀ (#31). **F.** Metanotum. **G–H.** Metendosternite. **G.** Dorsal view. **H.** Lateral view. **I–J.** Elytra. **K.** Hind wing. CELC. Scales in mm.

Fig. 32. *Baeocera* sp. nov. 4, holotype, ♂. **A–C.** Legs. **A.** Fore. **B.** Middle. **C.** Hind. **D.** Abdomen, dorsal view. **E.** Sternite VIII. **F.** Tergite VIII. **G.** Tergite IX. **H.** Sternite IX. **I.** Tergite X. **J–L.** Aedeagi. **J.** Frontal view. **K.** Lateral view. **L.** Dorsal view. **M–O.** Sclerites of internal sac. **M.** Frontal view. **N.** Lateral view-1. **O.** Lateral view-2. CELC. Scales in mm.

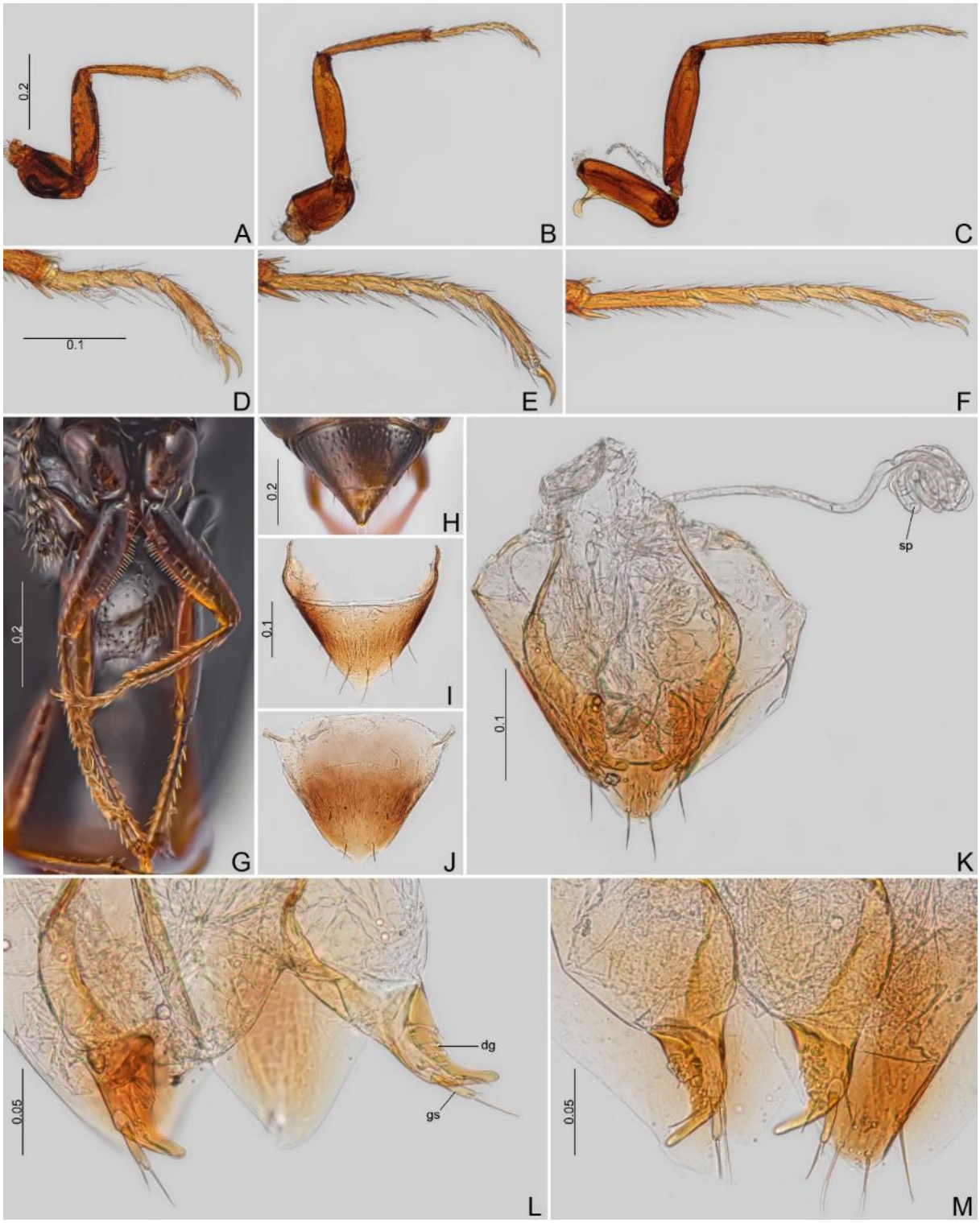

Fig. 33. *Baeocera* sp. nov. 4. **A–F.** Paratype, ♀ (#31). **A–C.** Legs: **A.** Fore. **B.** Middle. **C.** Hind. **D–F.** Tarsi: **D.** Pro. **E.** Meso. **F.** Meta. **G–H.** Paratype, ♀, (#52). **G.** Forelegs. **H.** Abdomen, dorsal view. **I–L.** Paratype, ♀ (#31). **J.** Sternite VIII. **J.** Tergite VIII. **K.** Genitalia. **L.** Ovipositor, specimen. **M.** Ovipositor (paratyepe, ♀, #52). CELC. Abbreviations: dg = distal gonocoxites; gs = gonostyli; sp = spermatheca. Scales in mm.

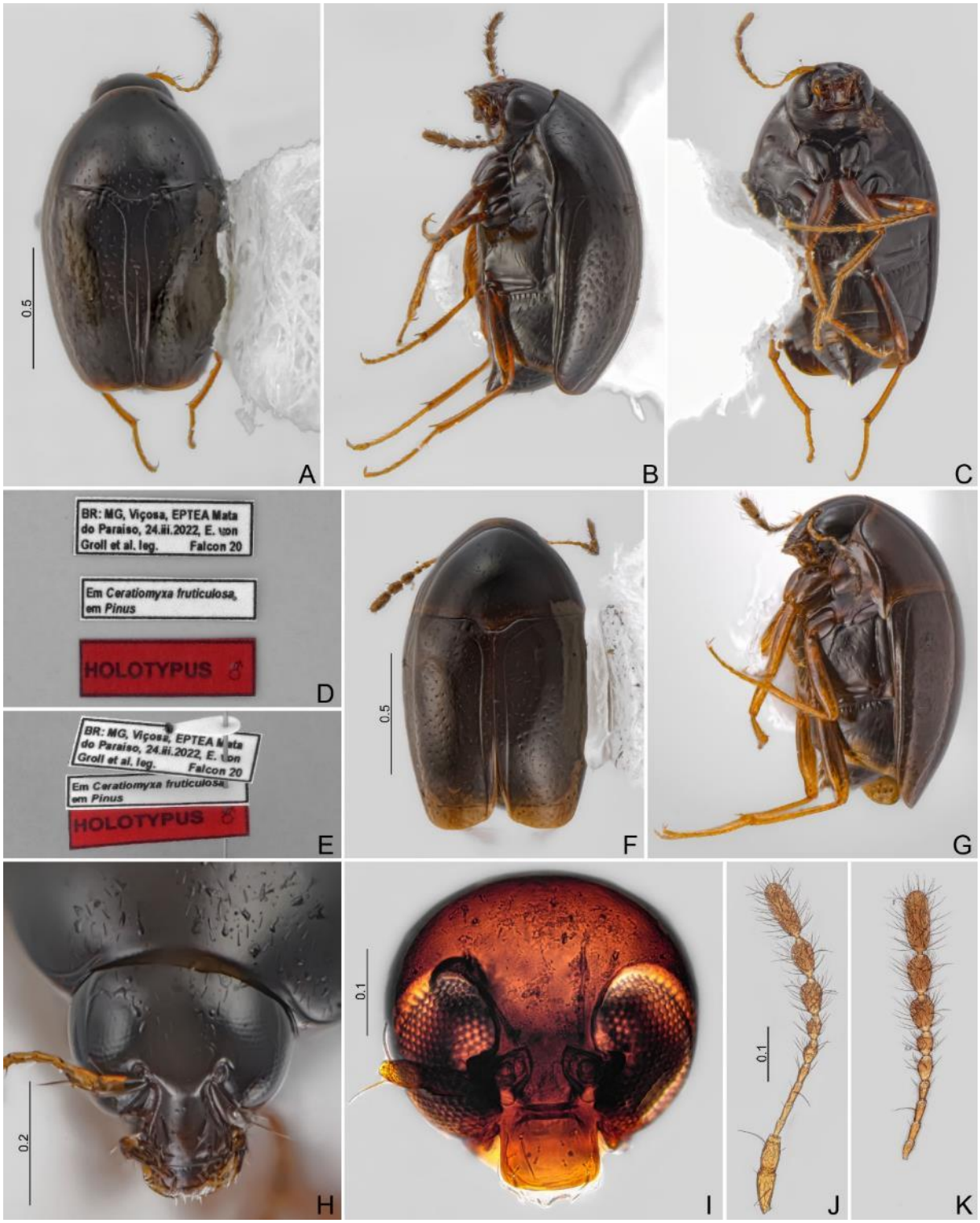

Fig. 34. *Baeocera* sp. nov. 5. **A–E.** Holotype, ♂. **A.** Dorsal view. **B.** Lateral view. **C.** Ventral view. **D.** Labels. **E.** Pinned. **F–G.** Paratype, ♂ (#36), teneral. **F.** Dorsal view. **G.** Lateral view. **H–I.** Head, frontal view. **H.** Holotype, ♂. **I.** Paratype, ♂ (#35). **J–K.** Antennae. **J.** Paratype, ♂ (#35). **K.** Paratype, ♀ (#57). CELC. Scales in mm.

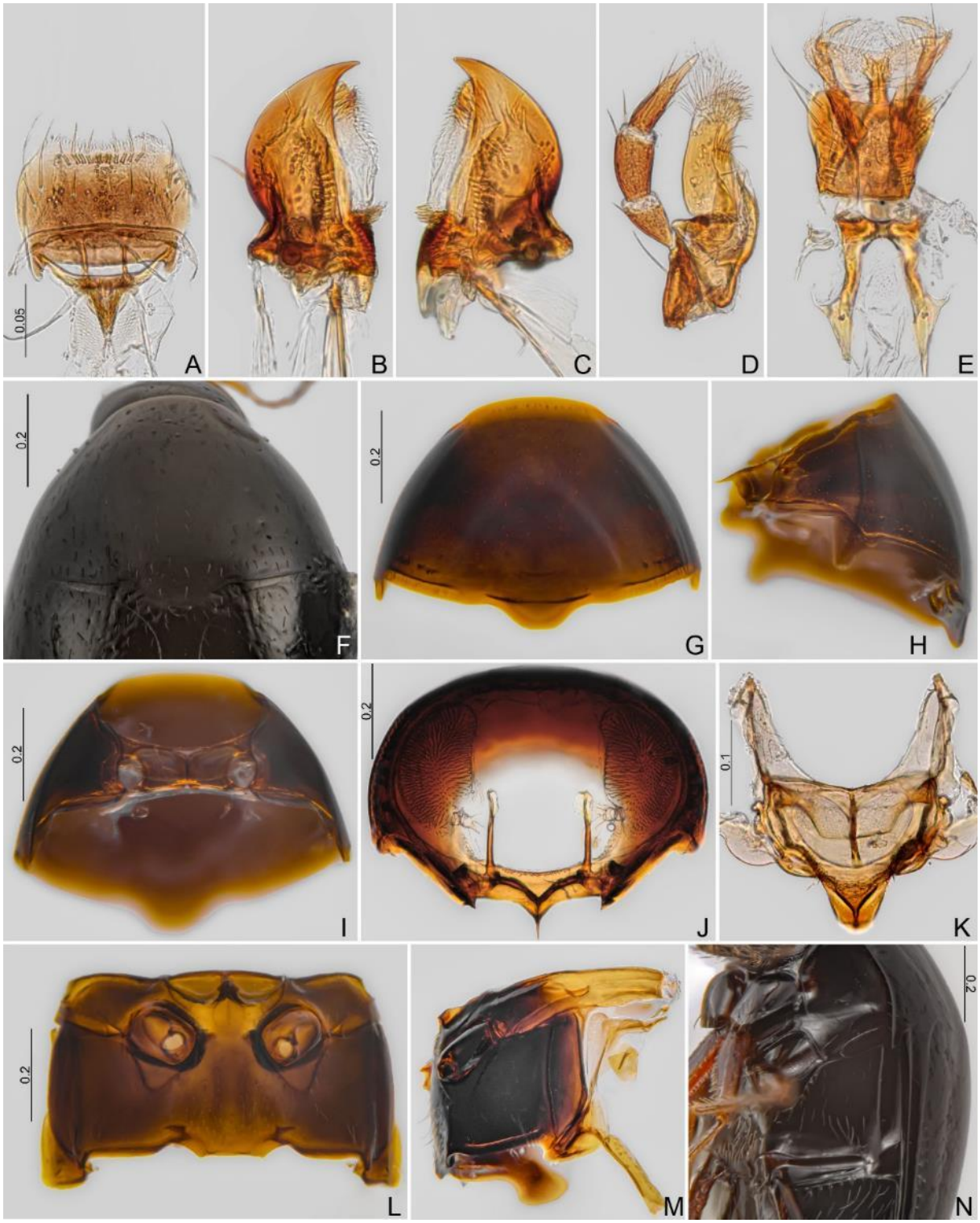

Fig. 35. *Baeocera* sp. nov. 5. **A–E.** Paratype, ♂ (#35). **A.** Labrum. **B–C.** Mandibles. **D.** Maxilla. **E.** Labium. **F.** Prothorax, dorsal view (holotype, ♂). **G–M.** Paratype, ♂ (#35). **G–J.** Prothorax. **G.** Dorsal view. **H.** Lateral view. **I.** Ventral view. **J.** Inner view. **K.** Scutellar shield. **L–N.** Meso- and metathorax. **L.** Ventral view. **M.** Lateral view. **N.** Oblique view (holotype, ♂). CELC. Scales in mm.

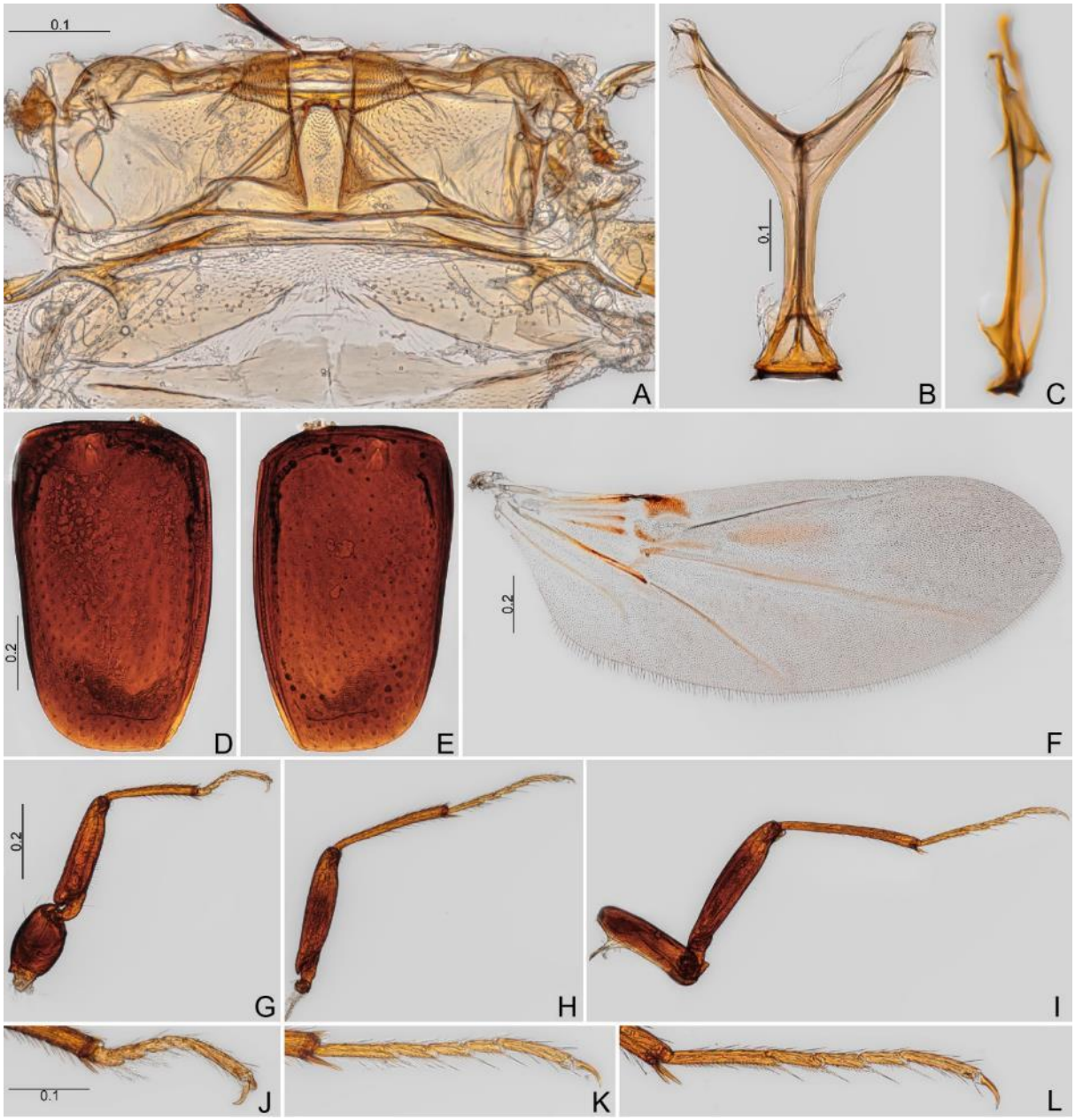

Fig. 36. *Baeocera* sp. nov. 5, paratype, ♂ (#35). **A.** Metanotum. **B–C.** Metendosternite. **B.** Dorsal view. **C.** Lateral view. **D–E.** Elytra. **F.** Hind wing. **G–I.** Legs. **G.** Fore. **H.** Middle. **I.** Hind. **J–L.** Tibiae. **J.** Pro. **K.** Meso. **L.** Meta. CELC. Scales in mm.

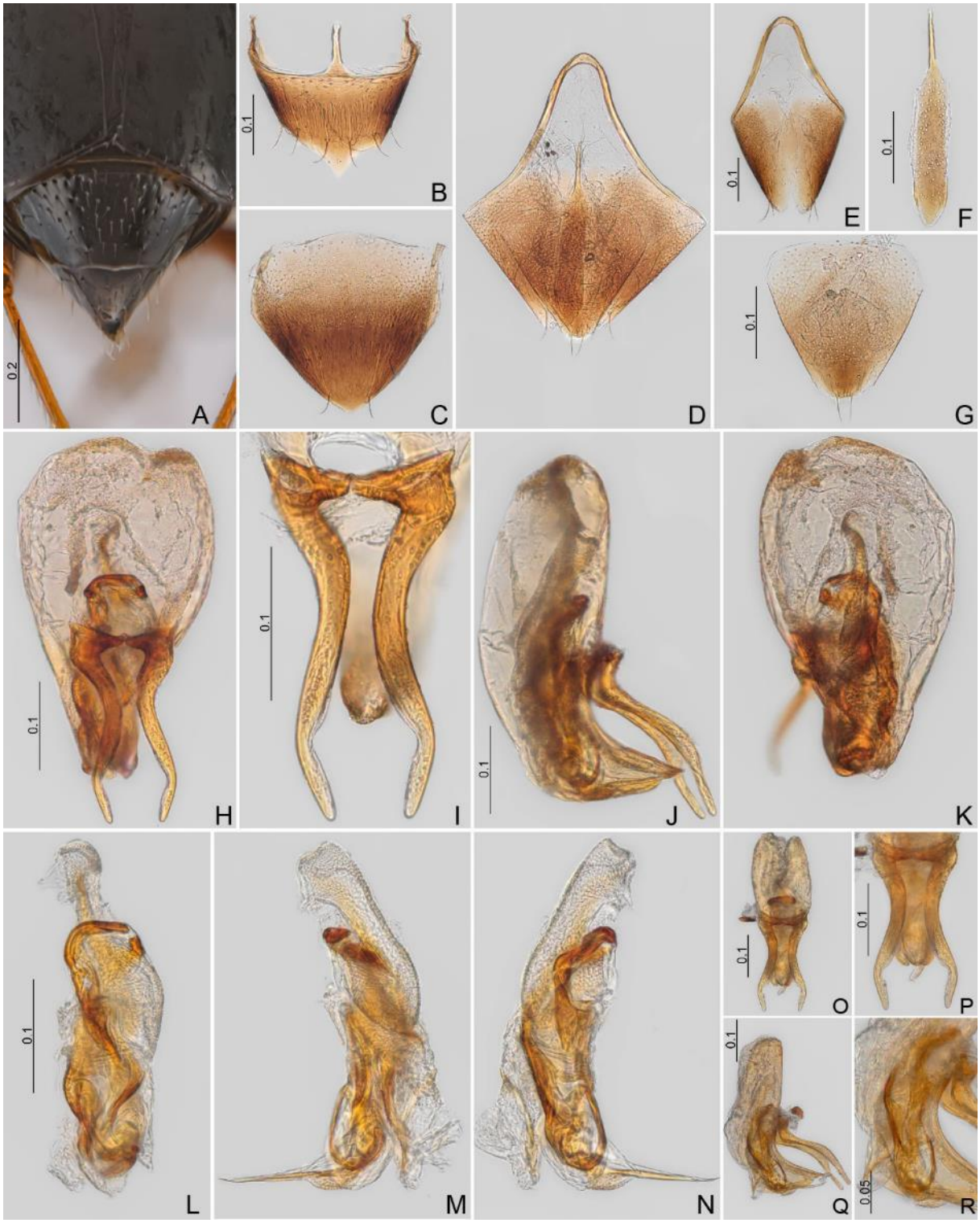

Fig. 37. *Baeocera* sp. nov. 5. **A.** Abdomen, dorsal view (holotype, ♂). **B–N.** Paratype, ♂ (#35). **B.** Sternite VIII. **C.** Tergite VIII. **D.** Tergite IX. **E.** Terminalia. **F.** Sternite IX. **G.** Tergite X. **H–K.** Aedeagi. **H.** Frontal view. **I.** Parameres, ventral view. **J.** Lateral view. **K.** Dorsal view. **L–N.** Sclerites of internal sac. **L.** Frontal view. **M.** Lateral view-1. **N.** Lateral view-2. **O–P.** Aedeagi (paratype, ♂, #30). **O.** Frontal view. **P.** Parameres, frontal view. **Q.** Lateral view. **R.** Lateral view (sclerite). CELC. Scales in mm.

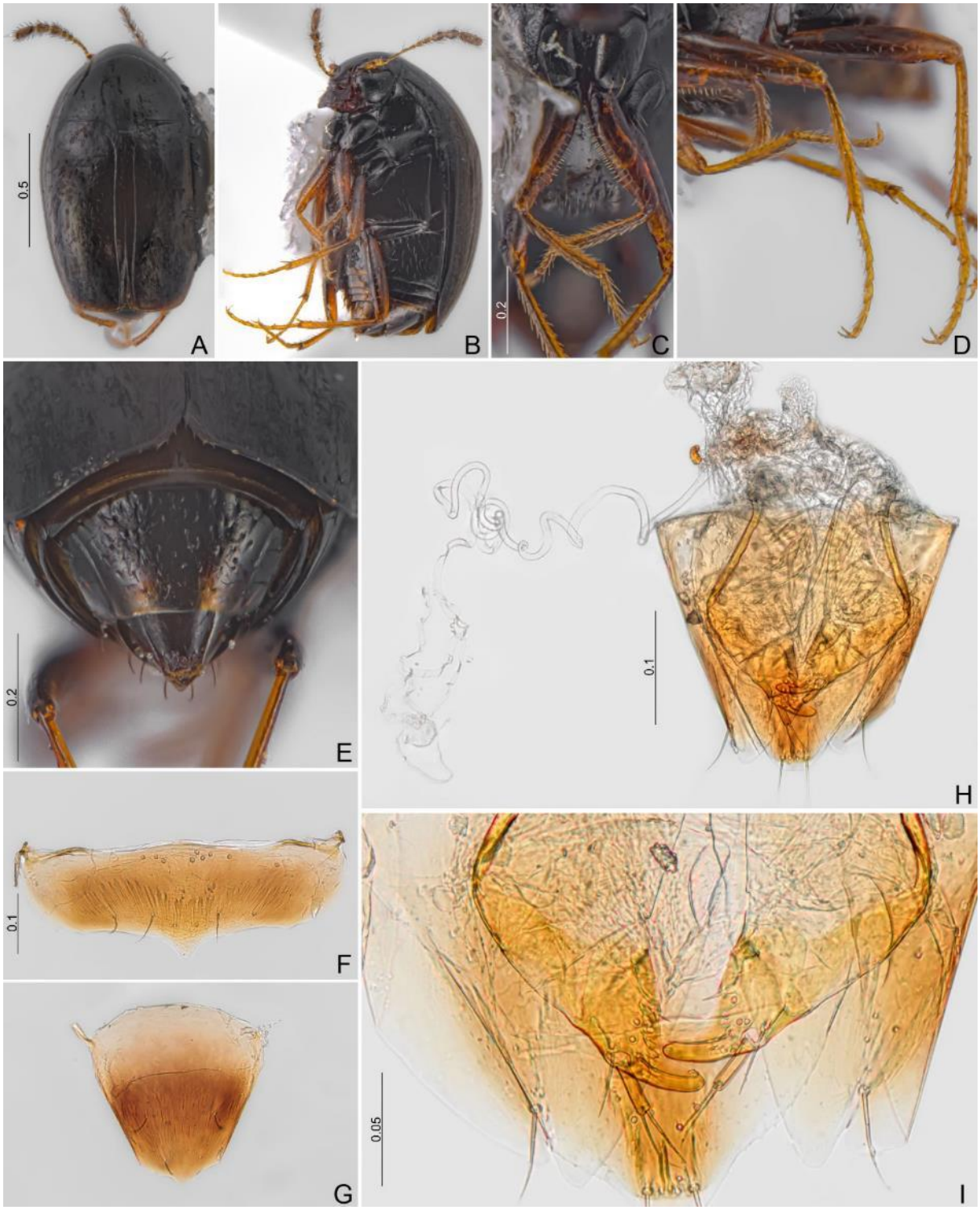

Fig. 38. *Baeocera* sp. nov. 5, paratype, ♀ (#57). **A.** Dorsal view. **B.** Oblique view. **C.** Forelegs. **D.** Middle and hind legs. **E.** Abdomen, dorsal view. **F.** Sternite VIII. **G.** Tergite VIII. **H.** Genitalia. **I.** Ovipositor. CELC. Scales in mm.

Fig. 39. *Baeocera* sp. nov. 6. **A–F.** Holotype, ♂. **A.** Dorsal view. **B.** Lateral view. **C.** Ventral view. **D.** Labels. **E.** Pinned. **F.** Head, frontal view. **G.** Head, frontal view, (paratype, ♀, #48). **H–I.** Antennae. **H.** Paratype, ♂ (#09). **I.** Paratype, ♀ (#22). **J–M.** Paratype, ♂ (#13). **J.** Labrum. **K–L.** Mandibles. **M.** Maxilla. **N.** Labium (paratype, ♀, #16). CELC. Scales in mm.

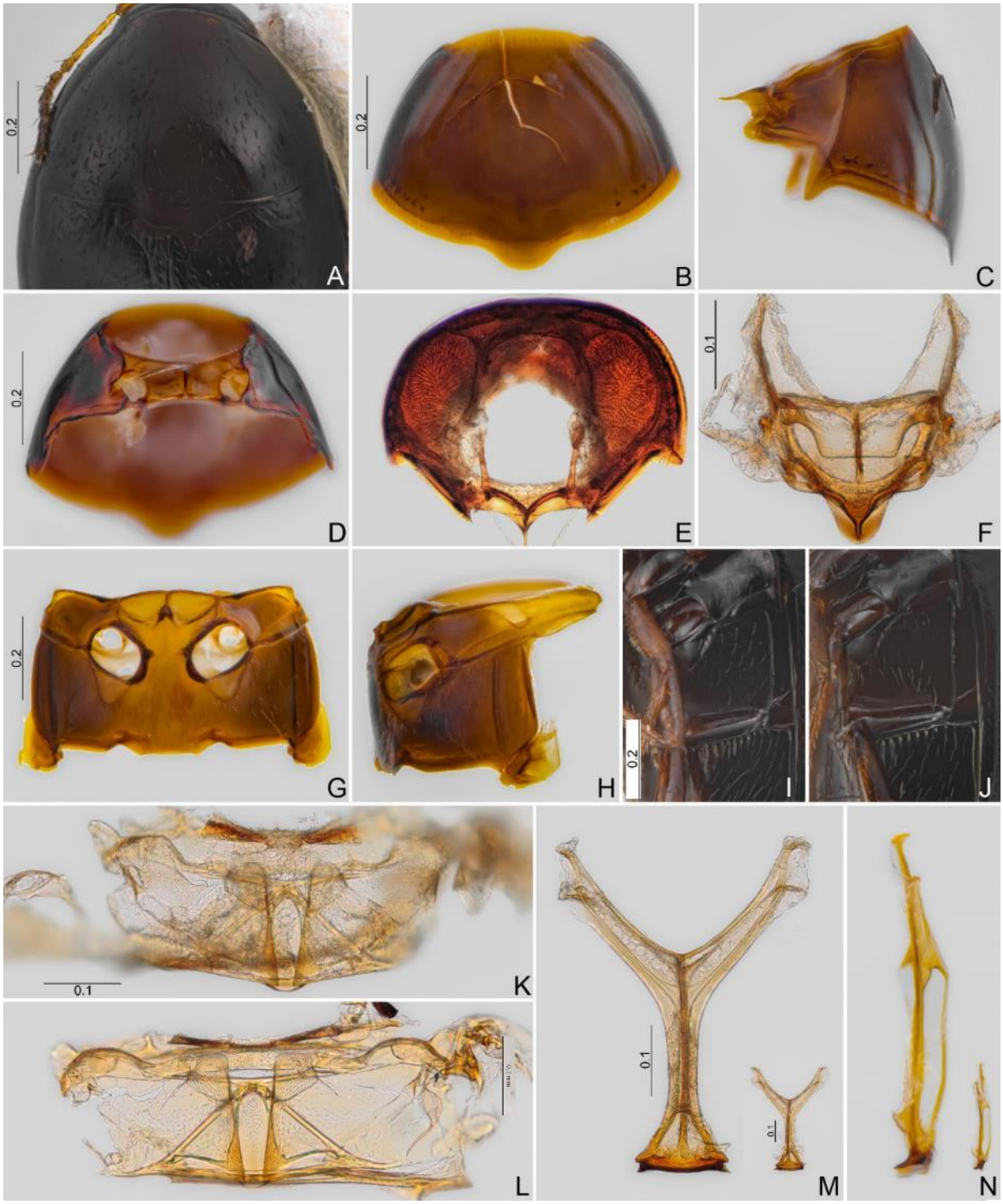

Fig. 40. *Baeocera* sp. nov. 6. **A.** Prothorax, dorsal view (holotype, ♂). **B–H.** Paratype, ♂ (#13). **B–E.** Prothorax. **B.** Dorsal view. **C.** Lateral view. **D.** Ventral view. **E.** Inner view. **F.** Scutellar shield. **G–J.** Meso- and metathorax. **G.** Ventral view. **H.** Lateral view. **I.** Oblique view (holotype, ♂). **J.** Oblique view (paratype, ♂, #55). **K–L.** Metanotum. **K.** Paratype, ♂ (#13). **L.** Paratype, ♀ (#16). **M–N.** Metendosternite (paratypes; large figures = ♂, #13; small = ♀, #16). **M.** Dorsal view. **N.** Lateral view. CELC. Scales in mm.

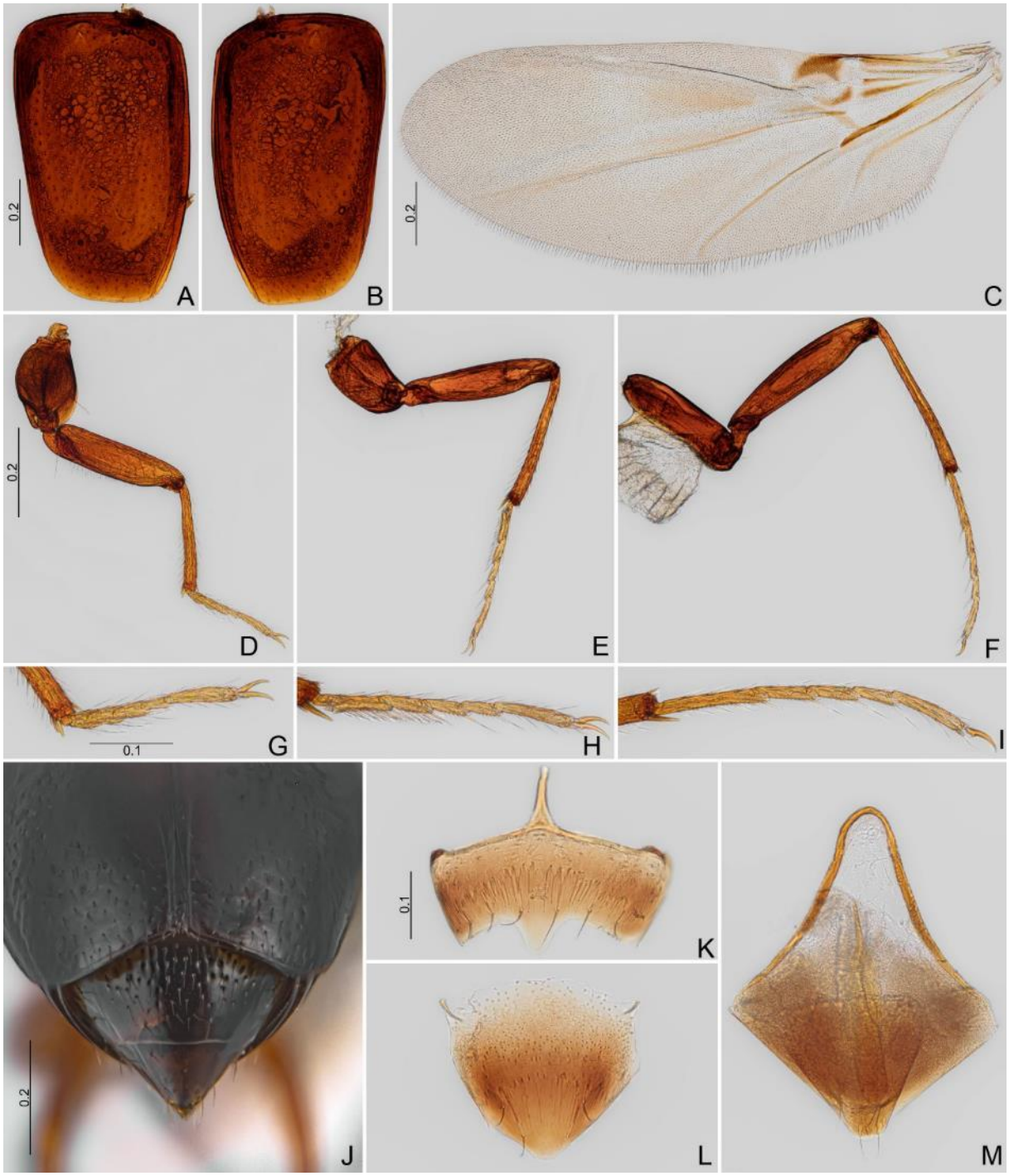

Fig. 41. *Baeocera* sp. nov. 6. **A–B.** Elytra (paratype, ♀, #16). **C–I.** Paratype, ♂ (#13). **C.** Hind wing. **D–F.** Legs. **D.** Fore. **E.** Middle. **F.** Hind. **G–I.** Tarsi. **G.** Pro. **H.** Meso. **I.** Meta. **J.** Abdomen, dorsal view (holotype, ♂). **K–M.** Paratype, ♂ (#09). **K.** Sternite VIII. **L.** Tergite VIII. **M.** Tergite IX. CELC. Scales in mm.

Fig. 42. *Baeocera* sp. nov. 6. **A–G.** Paratype, ♂ (#13). **A–D.** Aedeagi. **A.** Frontal view. **B.** Parameres, frontal view, arrow: constriction. **C.** Lateral view. **D.** Dorsal view. **E–G.** Sclerite of internal sac. **E.** Frontal view. **F.** Lateral view-1. **G.** Lateral view-2. **H–J.** Paratype, ♂ (#09). **H.** Frontal view. **I.** Lateral view. **J.** Sclerite of internal sac, lateral view. **K–N.** Paratype, ♂ (#55). **K.** Tergite IX. **L.** Aedeagi, frontal view. **M.** Aedeagi, lateral view. **N.** Sclerite of internal sac, lateral view. CELC. Scales in mm.

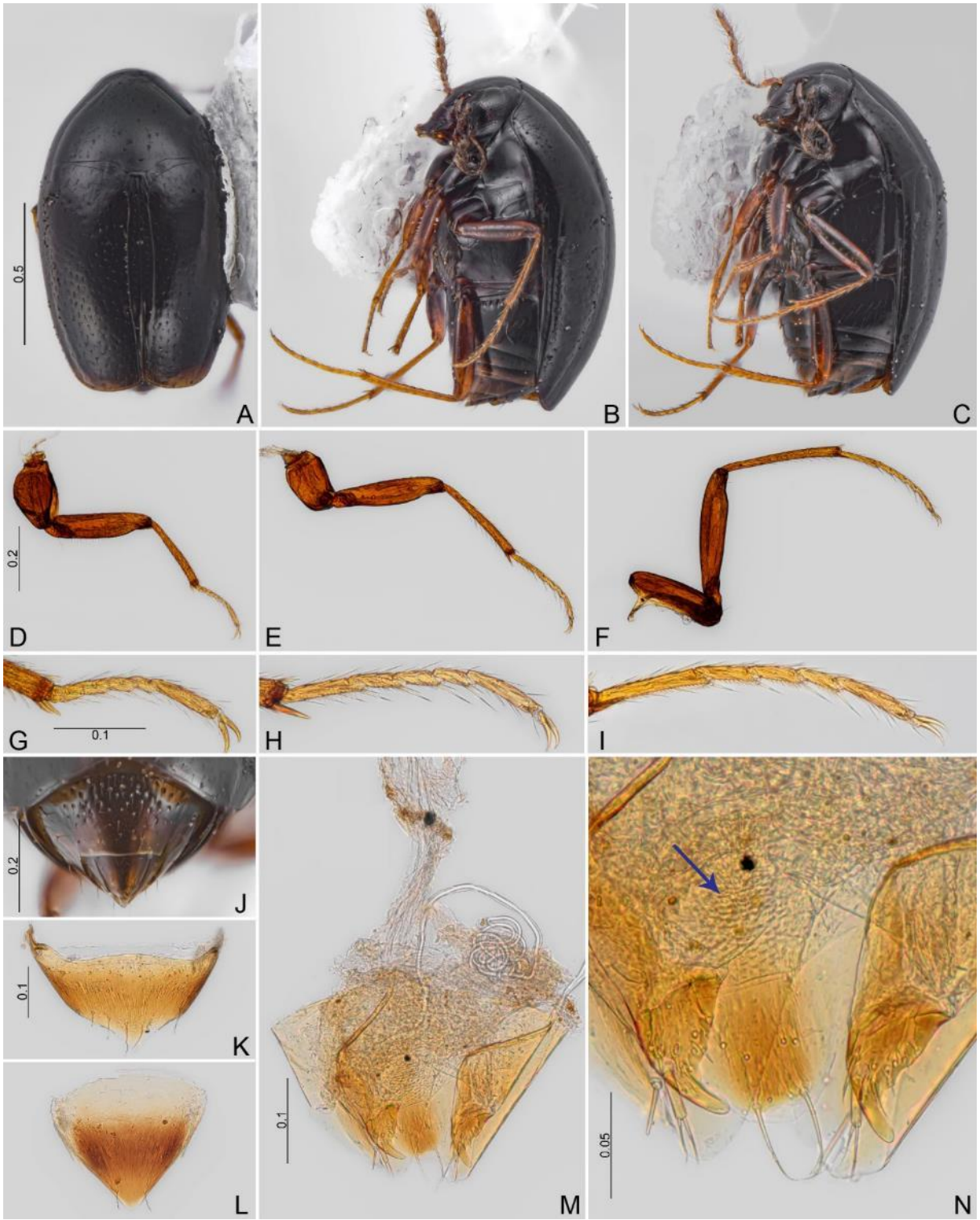

Fig. 43. *Baeocera* sp. nov. 6. **A–C.** Paratype, ♀ (#12). **A.** Dorsal view. **B.** Lateral view. **C.** Oblique view. **D–I.** Paratype, ♀ (#16). **D–F.** Legs. **D.** Fore. **E.** Middle. **F.** Hind. **G–I.** Tibiae. **G.** Pro. **H.** Meso. **I.** Meta. **J.** Abdomen, dorsal view (paratype, ♀, #12). **K–N.** Paratype, ♀ (#16). **K.** Sternite VIII. **L.** Tergite VIII. **M.** Genitalia. **N.** Ovipositor, arrow: sclerites. CELC. Scales in mm.

Fig. 44. *Scaphisoma* sp. nov. 1. **A–E.** Holotype, ♂. **A.** Dorsal view. **B.** Lateral view. **C.** ventral view. **D.** Labels. **E.** Pinned. **F–G.** Paratype, ♂ (#37). **F.** Dorsal view. **G.** Lateral view. **H–J.** Paratype, ♂ (#40). **H.** Dorsal view. **I.** Lateral view. **J.** Ventral view. CELC. Scales in mm.

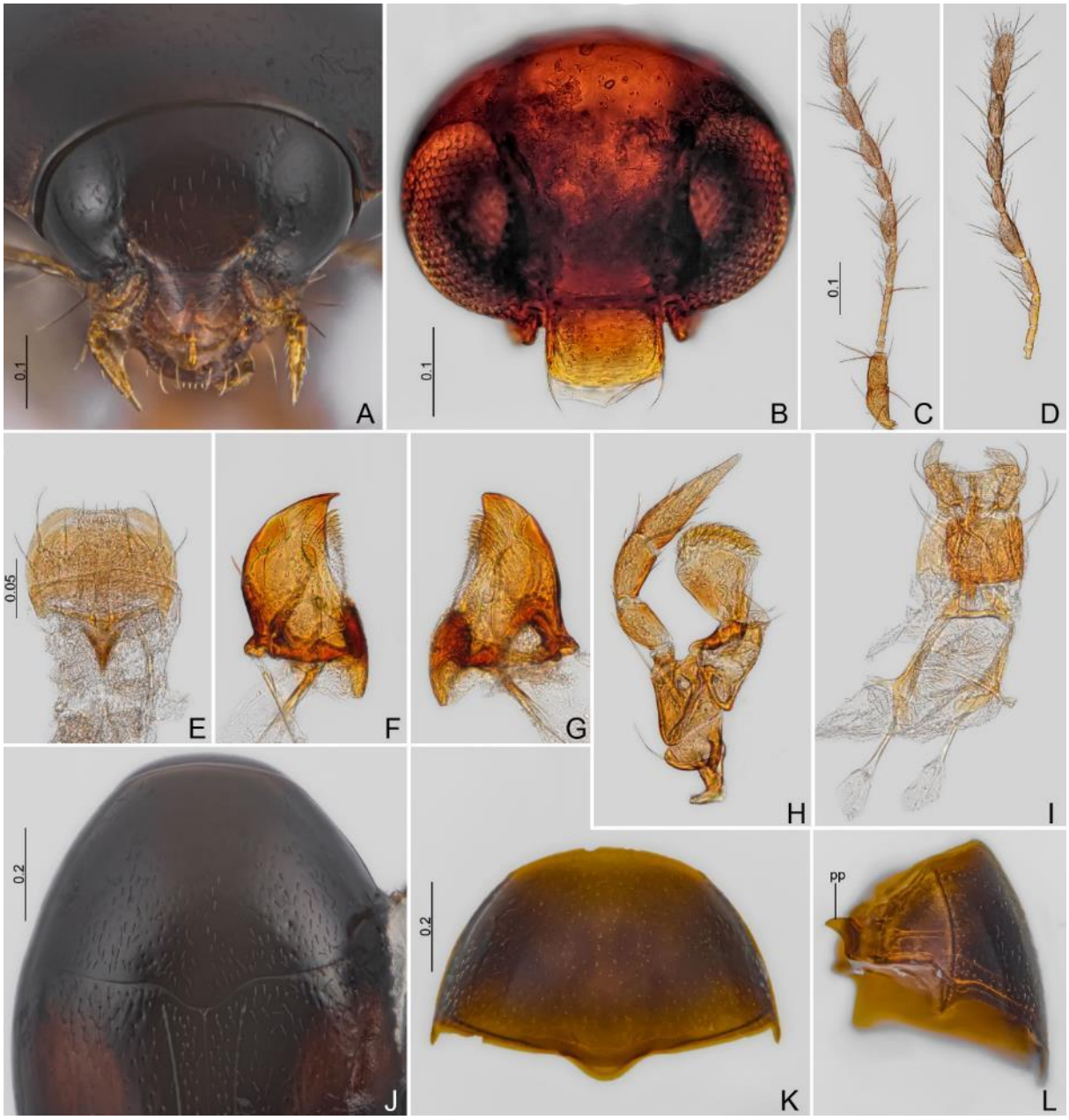

Fig. 45. *Scaphisoma* sp. nov. 1. **A.** Head, frontal view (holotype, ♂). **B.** Head, frontal view (paratype, ♂, #58). **C–D.** Antennae. **C.** Paratype, ♂ (#58). **D.** Paratype, ♀ (#55). **E–I.** Paratype, ♂ (#58). **E.** Labrum. **F–G.** Mandibles. **H.** Maxilla. **I.** Labium. **J.** Prothorax, dorsal view (holotype, ♂). **K–L.** Prothorax (paratype, ♂, #58). **K.** Dorsal view. **L.** Lateral view. CELC. Scales in mm. Abbreviation: pp = prosternal process.

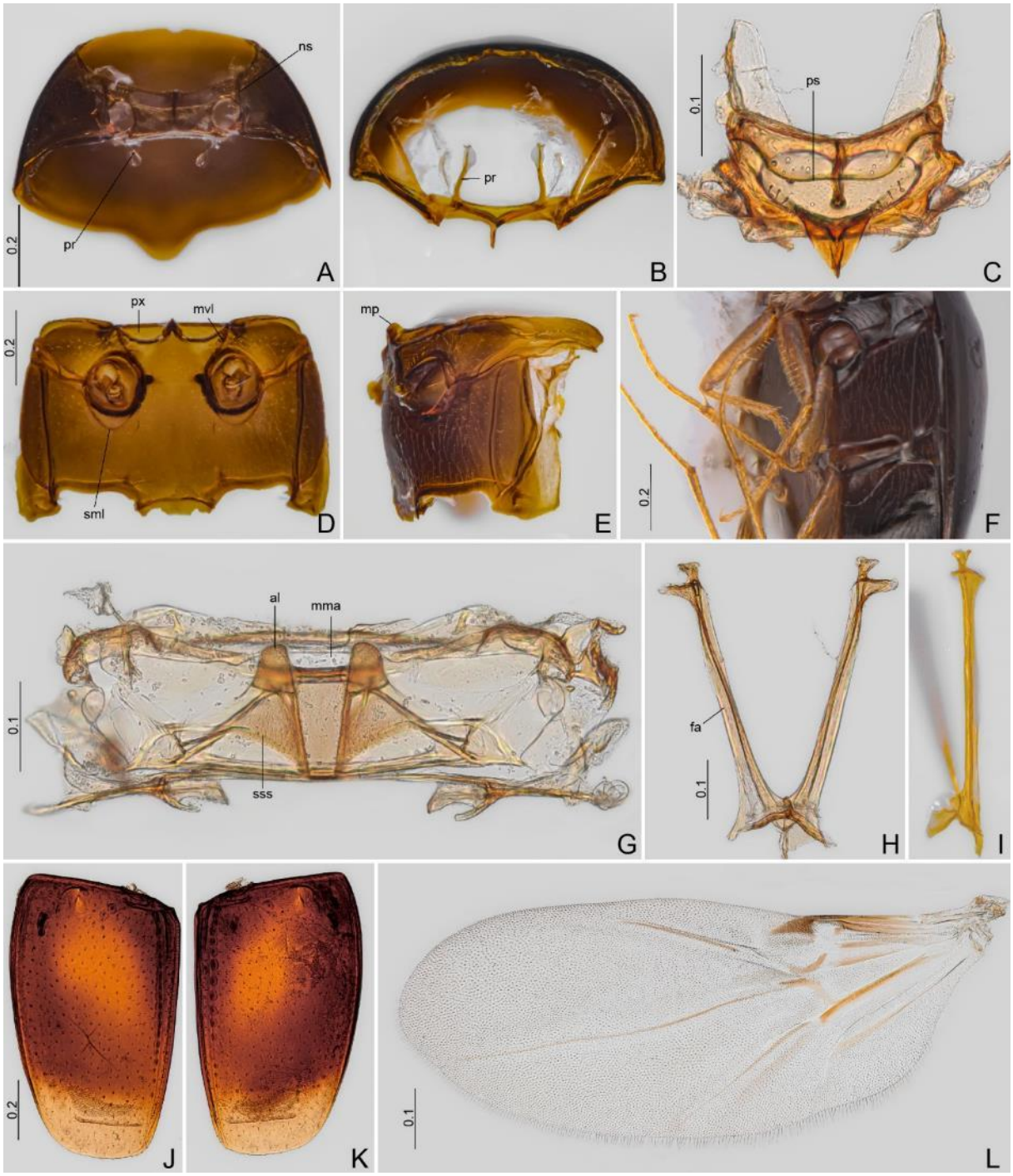

Fig. 46. *Scaphisoma* sp. nov. 1. **A–E.** Paratype, ♂ (#58). **A–B.** Prothorax. **A.** Ventral view. **B.** Inner view. **C.** Scutellar shield. **D–E.** Meso- and metathorax. **D.** Ventral view. **E.** Lateral view. **F.** Oblique view (holotype, ♂). **G–L.** Paratype, ♂ (#58). **G.** Metanotum. **H–I.** Metendosternite. **H.** Dorsal view. **I.** Lateral view. **J–K.** Elytra. **L.** Hind wing. CELC. Scales in mm. Abbreviations: al = alacrista; fa = furcal arm; mma = median membranous area; mp = mesoventral process; mvl = mesoventral line; ns, notosternal suture; pr = profurca; ps = prescutellar line; px = procoxal rest; sml = submesocoxal line; sss = scutoscutellar suture.

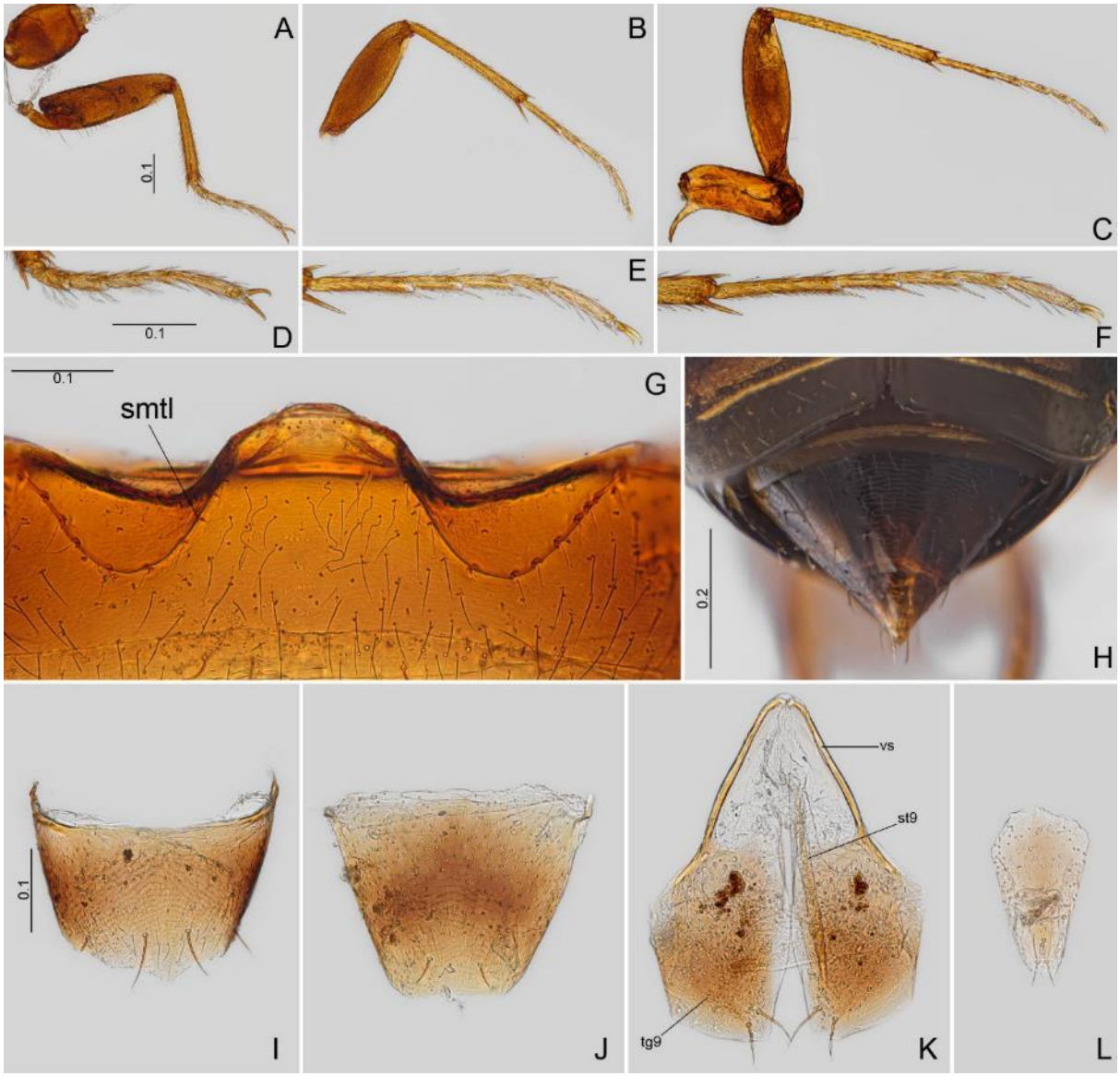

Fig. 47. *Scaphisoma* sp. nov. 1. **A–G.** Paratype, ♂ (#58). **A–C.** Legs. **A.** Fore. **B.** Middle. **C.** Hind. **D–F.** Tibiae. **D.** Pro. **E.** Meso. **F.** Meta. **G.** Ventrite. **H.** Abdomen, dorsal view (holotype, ♂). **I–L.** Paratype, ♂ (#58). **I.** Sternite VIII. **J.** Tergite VIII. **K.** Tergite IX. **L.** Tergite X. CELC. Scales in mm. Abbreviations: smtl = submetacoxal line; st9 = sternite IX; tg9 = tergite IX; vs = ventral struts.

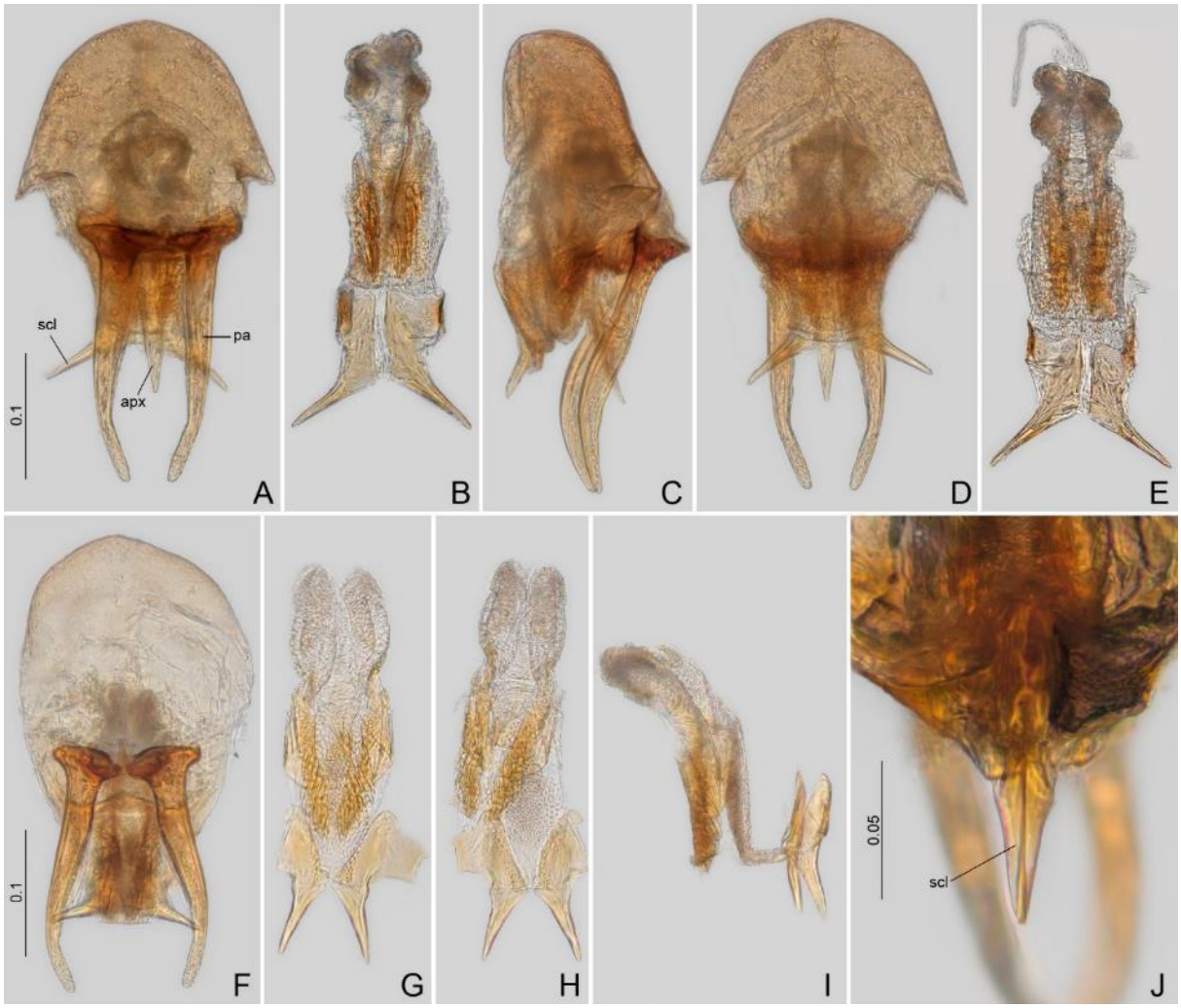

Fig. 48. *Scaphisoma* sp. nov. 1, Aedeagus. **A–E.** Paratype, ♂ (#58). **A.** Frontal view. **B.** Sclarite of internal sac, frontal view. **C.** Lateral view. **D.** Dorsal view. **E.** Sclerite of internal sac, dorsal view. **F–I.** Paratype, ♂ (#57). **F.** Frontal view. **G–J.** Sclerite of internal sac. **G.** Frontal view. **H.** Doral view. **I.** Lateral view. **J.** Paratype, ♂ (#16), dorsal view. CELC. Scales in mm. Abbreviations: apx = apex of aedeagi; pa = parameres; scl = sclerite of internal sac.

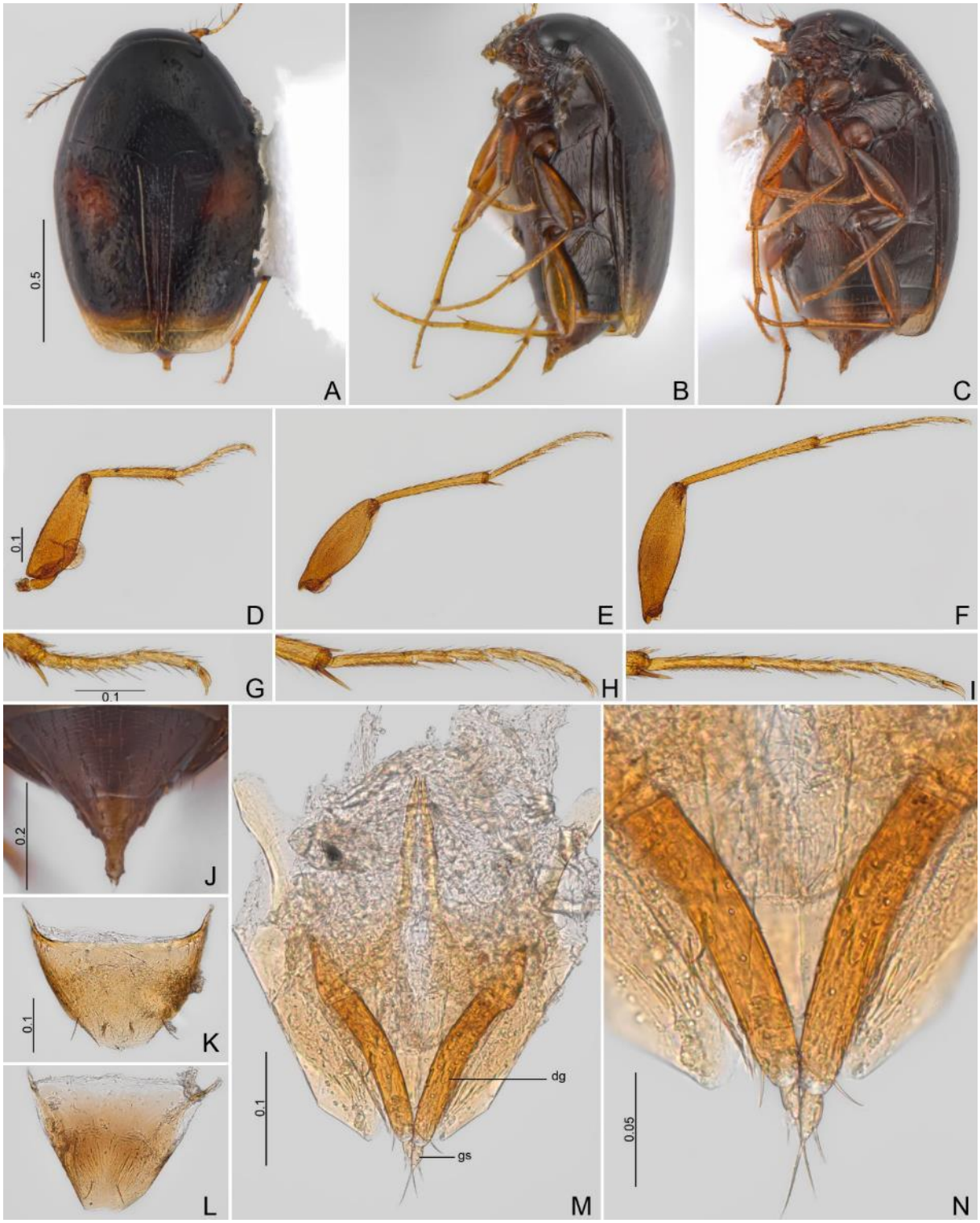

Fig. 49. *Scaphisoma* sp. nov. 1. **A–C.** Paratype, ♀ (#13). **A.** Dorsal view. **B.** Lateral view. **C.** Ventral view. **D–I.** Paratype, ♀ (#55). **D–F.** Legs. **D.** Fore. **E.** Middle. **F.** Hind. **G–I.** Tarsi. **G.** Pro. **H.** Meso. **I.** Meta. **J.** Abdomen, dorsal view (paratype, ♀, #13). **K–N.** Paratype, ♀ (#55). **K.** Sternite VIII. **L.** Tergite VIII. **M.** Genitalia. **N.** Ovipositor. CELC. Scales in mm. Abbreviations: dg = distal gonocoxites; gs = gonostyli.

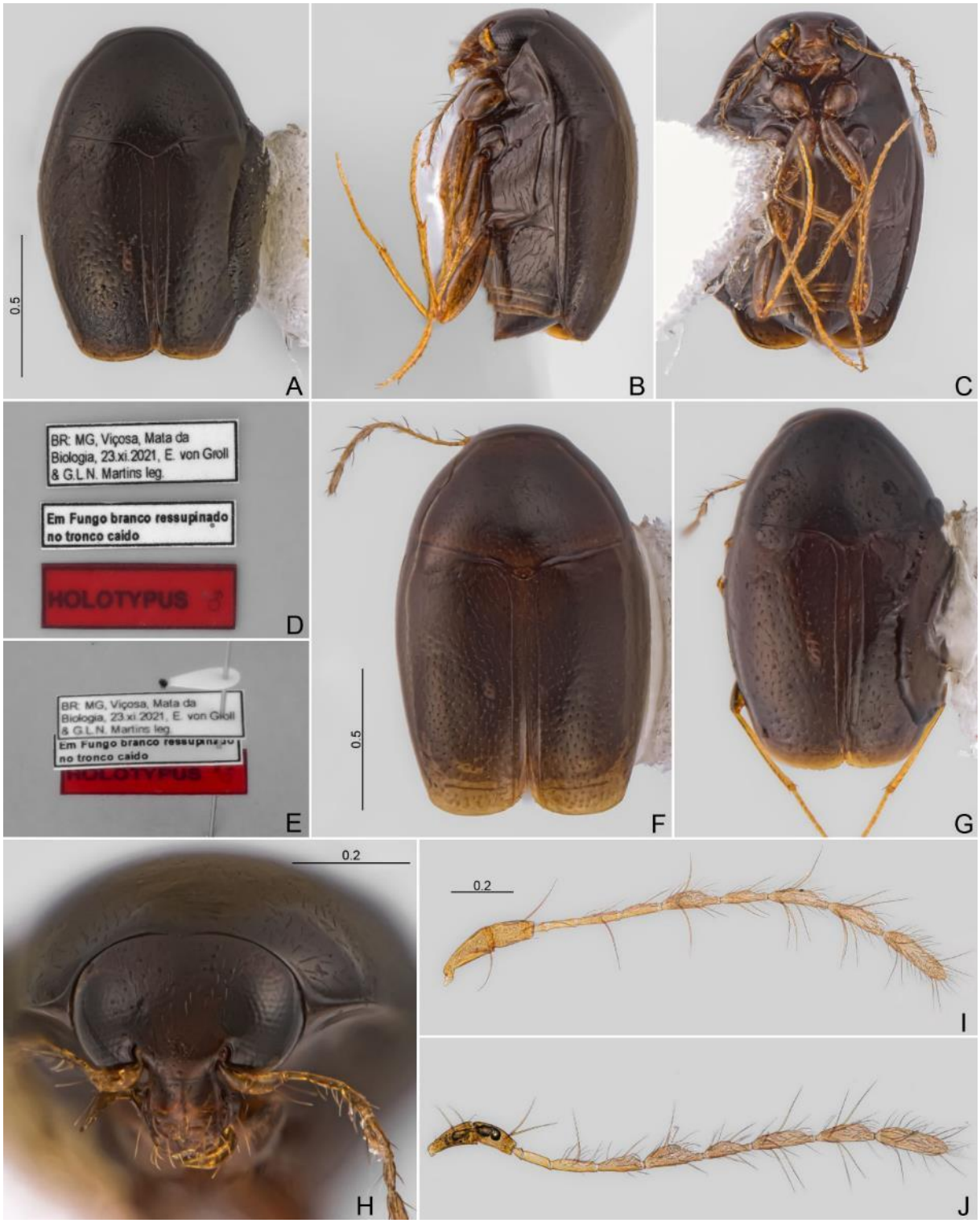

Fig. 50. *Scaphisoma* sp. nov. 2. **A–E.** Holotype, ♂. **A.** Dorsal view. **B.** Lateral view. **C.** Ventral view. **D.** Labels. **E.** Pinned. **F.** Paratype (#50). **G.** Paratype, ♀ (#55). **H.** Head, frontal view (holotype, ♂). **I–J.** Antennae. **I.** Paratype, ♂ (#SD54). **J.** Paratype, ♀ (#07). CELC. Scales in mm.

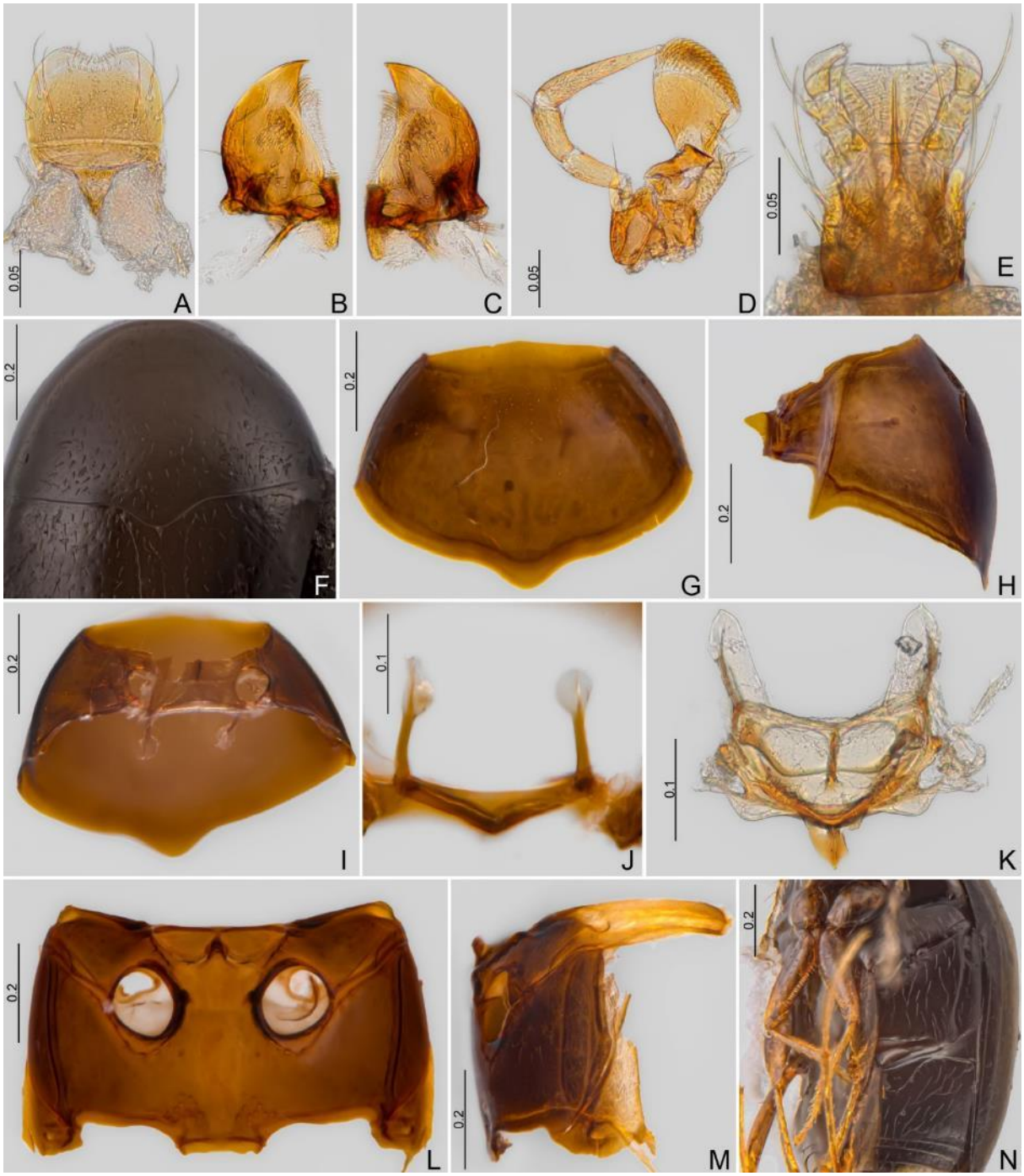

Fig. 51. *Scaphisoma* sp. nov. 2. **A.** Labrum (paratype, ♂, #SD36). **B–C.** Mandibles (paratype, ♂, #SD75). **D–E.** (paratype, ♂ (#SD36). **D.** Maxilla. **E.** Labium. **F.** Prothorax, dorsal view (holotype, ♂). **G–M.** Paratype, ♂ (#SD36). **G–J.** Prothorax. **G.** Dorsal view. **H.** Lateral view. **I.** Ventral view. **J.** Profurca. **K.** Scutellar shield. **L–N.** Meso- and metathorax. **L.** Ventral view. **M.** Lateral view. **N.** Oblique view (holotype, ♂). CELC. Scales in mm.

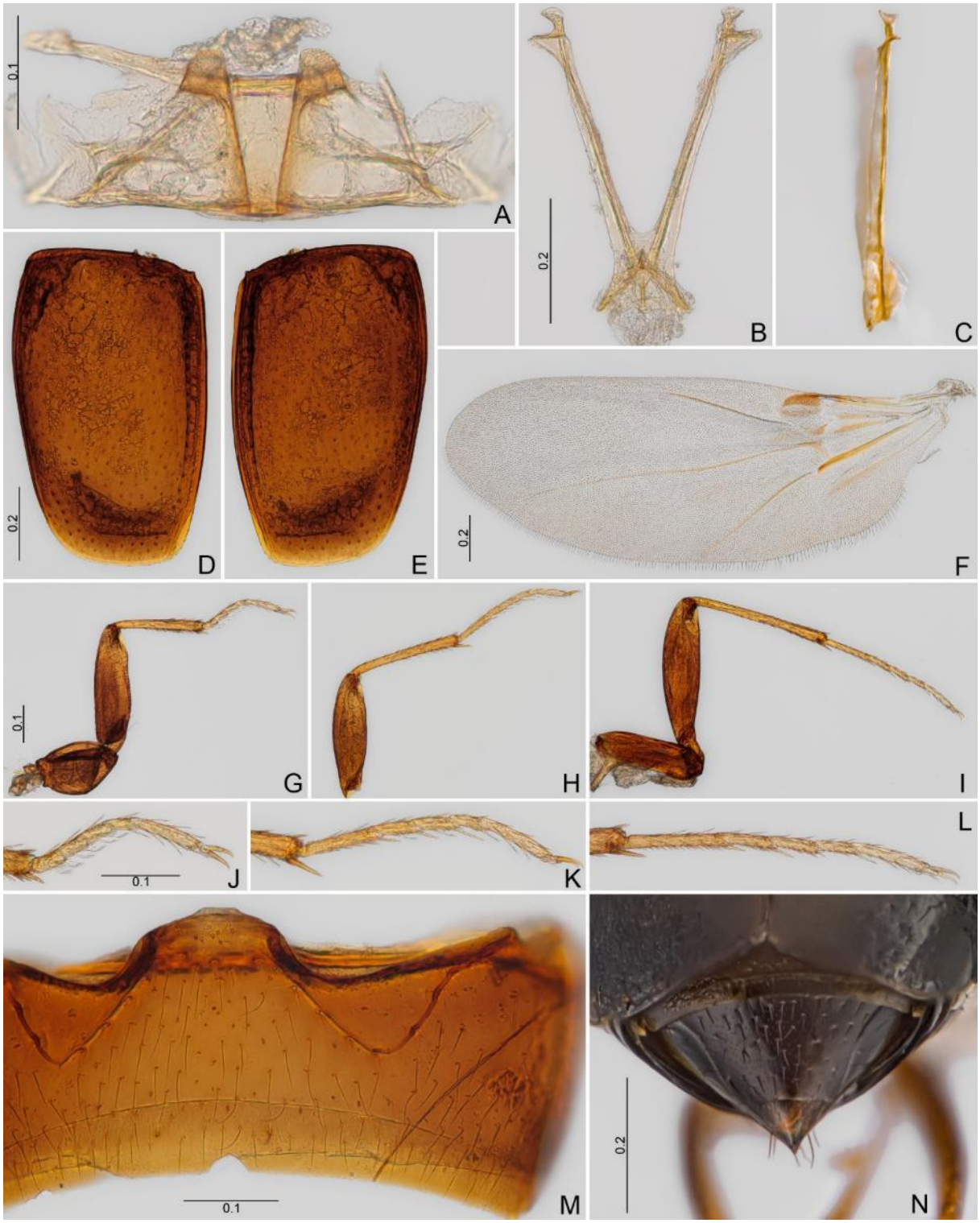

Fig. 52. *Scaphisoma* sp. nov. 2. **A–M**. Paratype, ♂ (#SD36). **A.** Metanotum. **B–C.** Metendosternite. **B.** Dorsal view. **C.** Lateral view. **D–E.** Elytra. **F.** Hind wing. **G–I.** Legs. **G.** Fore. **H.** Middle. **I.** Hind. **J–L.** Tibiae. **J.** Pro. **K.** Meso. **L.** Meta. **M.** Ventrite I. **N.** Abdomen, dorsal view (holotype, ♂). CELC. Scales in mm.

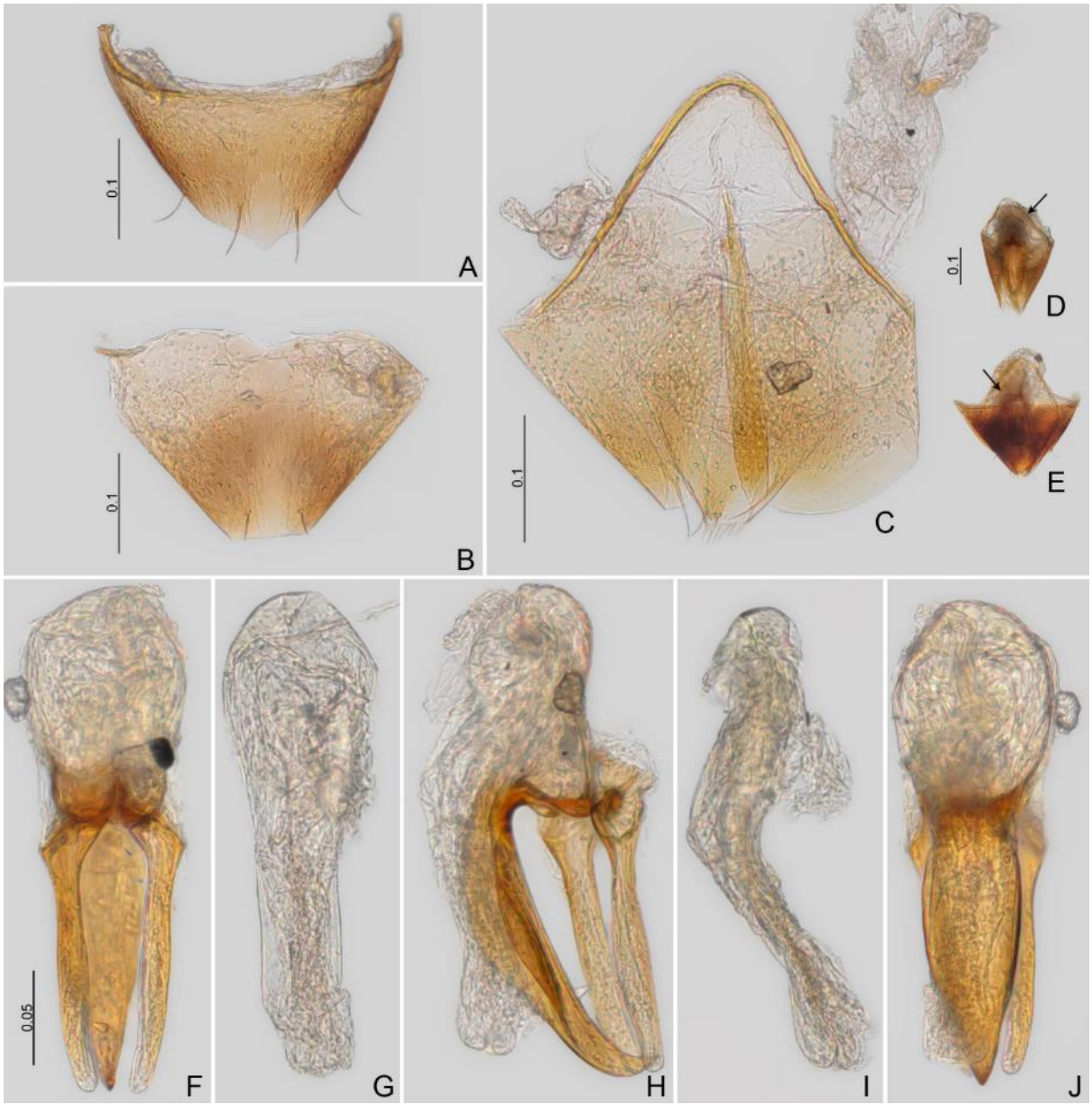

Fig. 53. *Scaphisoma* sp. nov. 2. **A–C.** Paratype, ♂ (#SD36). **A.** Sternite VIII. **B.** Tergite VIII. **C.** Tergite and sternite IX. **D–E.** Terminalia not dissected, arrow: aedeagus. **D.** Paratype, ♂ (#SD14). **E.** Paratype, ♂ (# 109). **F–J.** Paratype, ♂ (#SD36). **F–H.** Aedeagi. **F.** Frontal view. **G.** Sclerite of internal sac, frontal view. **H.** Lateral view. **I.** Sclerite of internal sac, lateral view. **J.** Dorsal view. CELC. Scales in mm.

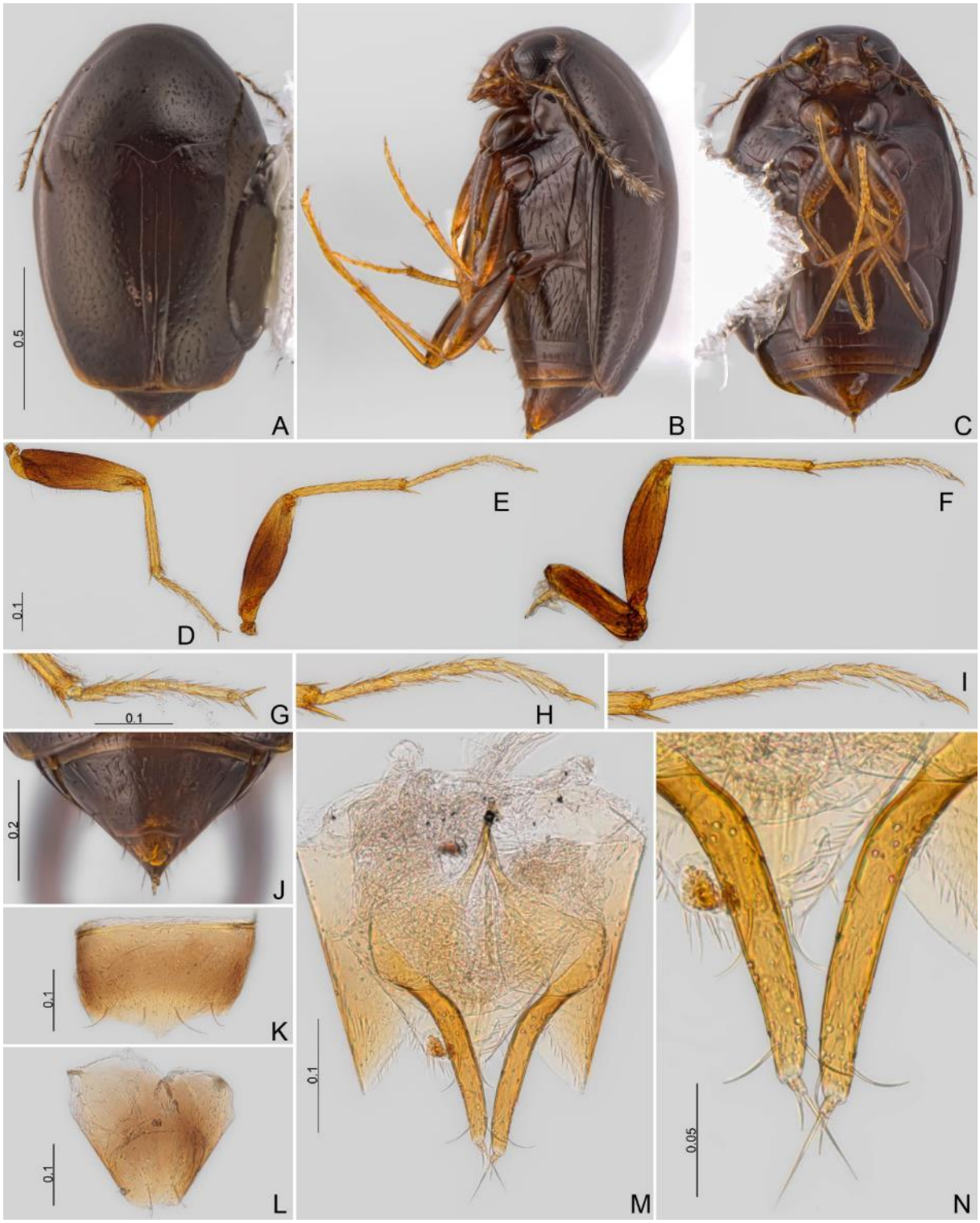

Fig. 54. *Scaphisoma* sp. nov. 2. **A–C.** Paratype, ♀ (#33). **A.** Dorsal view. **B.** Lateral view. **C.** Ventral view. **S–I.** Paratype, ♀ (#07). **D–F.** Legs. **D.** Fore. **E.** Middle. **F.** Hind. **G–I.** Tarsi. **G.** Pro. **H.** Meso. **I.** Meta. **J.** Abdomen, dorsal view. (paratype ♀, #33). **K–N.** Paratype, ♀ (#07). **K.** Sternite VIII. **L.** Tergite VIII. **M.** Genitalia. **N.** Ovipositor. CELC. Scales in mm.

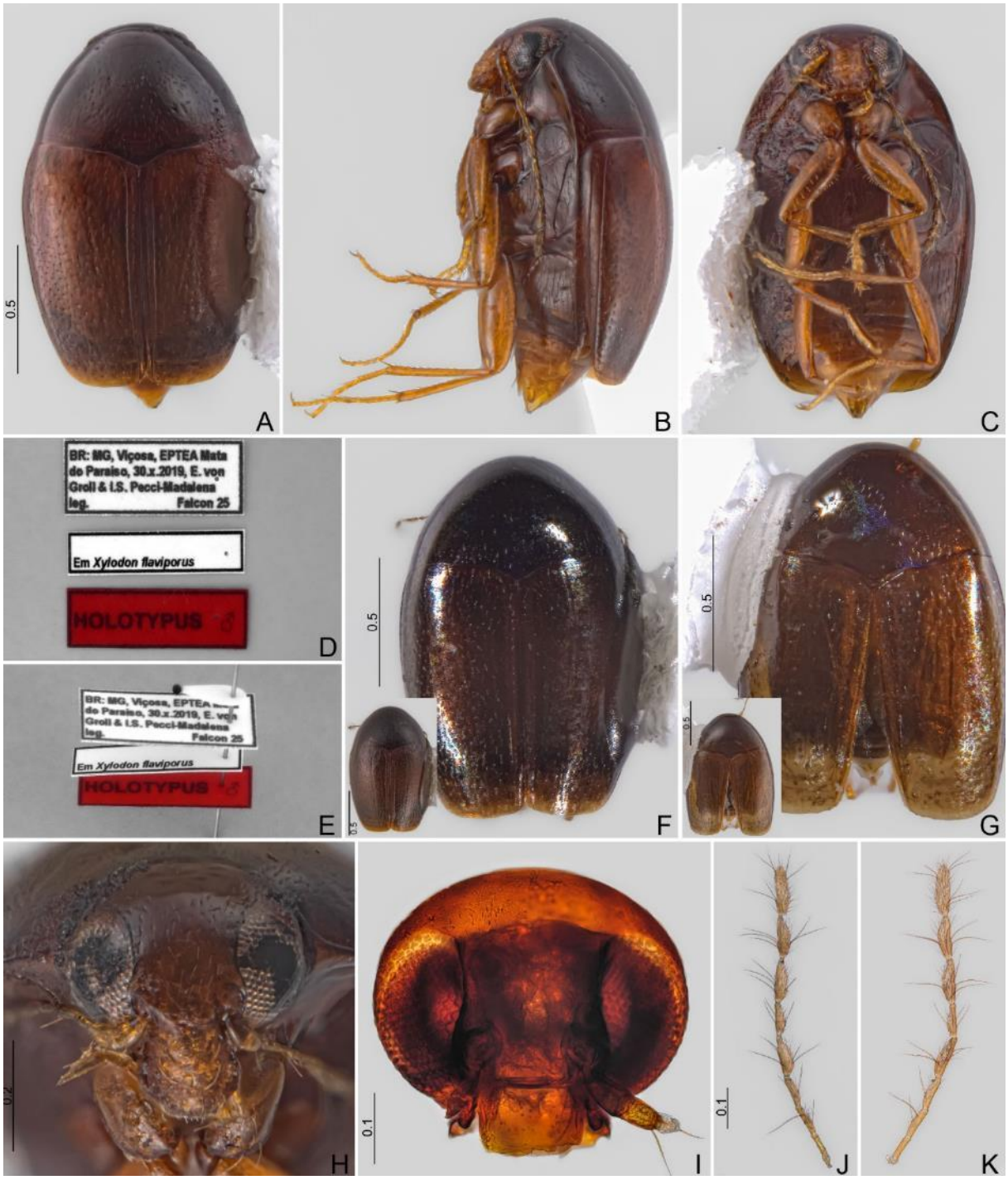

Fig. 55. *Scaphisoma* sp. nov. 3. Holotype, ♂. **A.** Dorsal view. **B.** Lateral view. **C.** Ventral view. **D.** Labels. **E.** Pinned. **F.** Paratype, ♂ (#67). **G.** Paratype (#72). **H–I.** Head, frontal view. **H.** Holotype, ♂. **I.** Paratype, ♂ (#69). **J–K.** Antennae. **J.** Paratype, ♂ (#69). **K.** Paratype, ♀ (#75). CELC. Scales in mm.

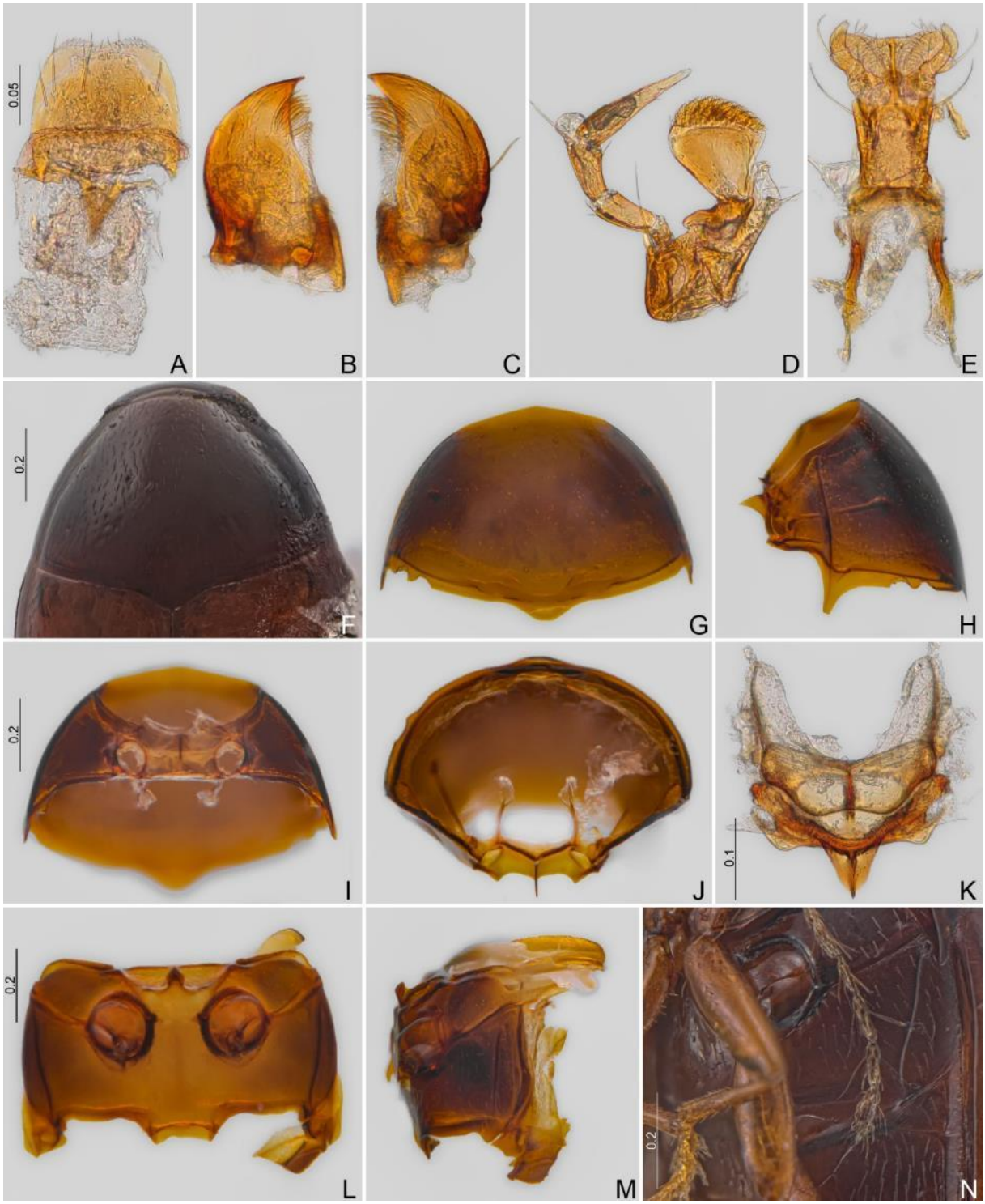

Fig. 56. *Scaphisoma* sp. nov. 3. **A–E.** Paratype, ♂ (#69). **A.** Labrum. **B–C.** Mandibles. **D.** Maxilla. **E.** Labium. **F.** Prothorax, dorsal view (holotype, ♂). **G–M.** Paratype, ♂ (#69). **G–J.** Prothorax. **G.** Dorsal view. **H.** Lateral view. **I.** Ventral view. **J.** Inner view. **K.** Scutellar shield. **L–N.** Meso- and metathorax. **L.** Ventral view. **M.** Lateral view. **N.** Oblique view (holotype, ♂). CELC. Scales in mm.

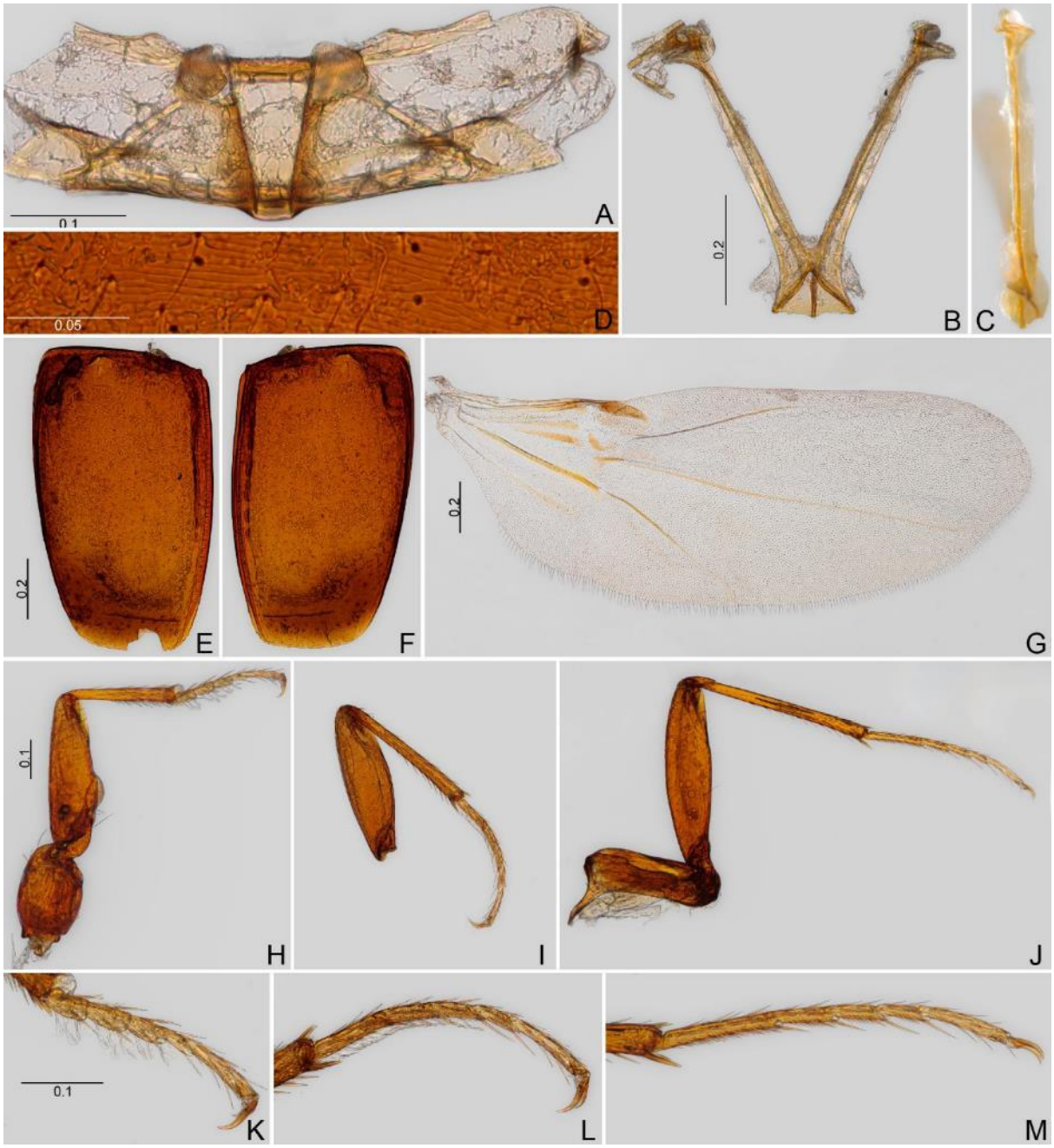

Fig. 57. *Scaphisoma* sp. nov. 3, paratype, ♂ (#69). **A.** Metanotum. **B–C.** Metendosternite. **B.** Dorsal view. **C.** Lateral view. **D–F.** Elytra. **D.** Detail. **E.** Left. **F.** Right. **G.** Hind wing. **H–J.** Legs. **H.** Fore. **I.** Middle. **J.** Hind. **K–M.** Tibiae. **K.** Pro. **L.** Meso. **M.** Meta. CELC. Scales in mm.

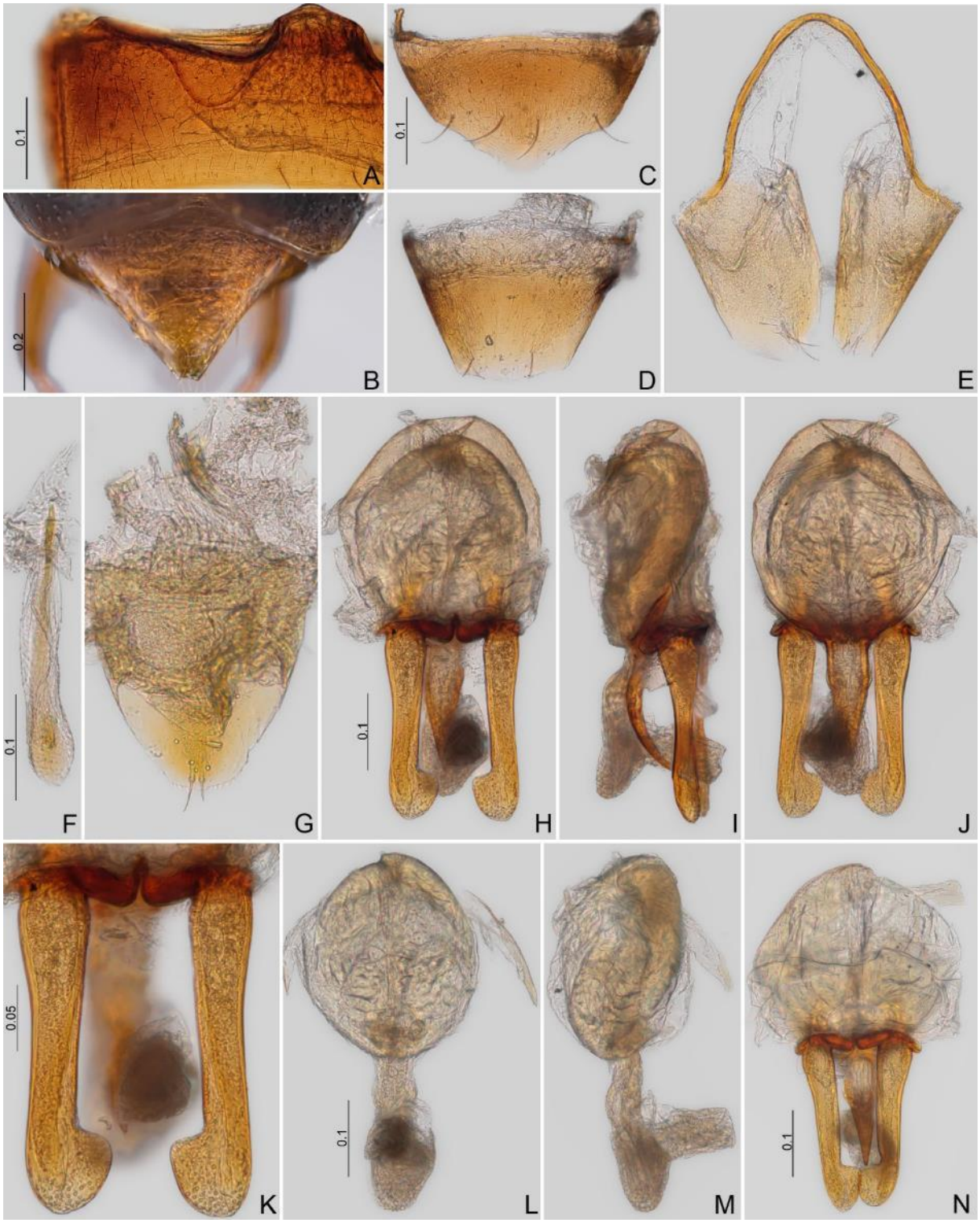

Fig. 58. *Scaphisoma* sp. nov. 3. **A.** Ventrite I (paratype, ♂, #69). **B.** Abdomen, dorsal view (holotype, ♂). **C–M.** Paratype, ♂ (#69). **C.** Sternite VIII. **D.** Tergite VIII. **E.** Tergite IX. **F.** Sternite IX. **G.** Tergite X. **H–N.** Aedeagi. **H.** Frontal view. **I.** Lateral view. **J.** Dorsal view. **K.** Parameres, frontal view. **L–M.** Sclerite of internal sac. **L.** Frontal view. **M.** Lateral view. **N.** Frontal view (paratype, ♂, #67). CELC. Scales in mm.

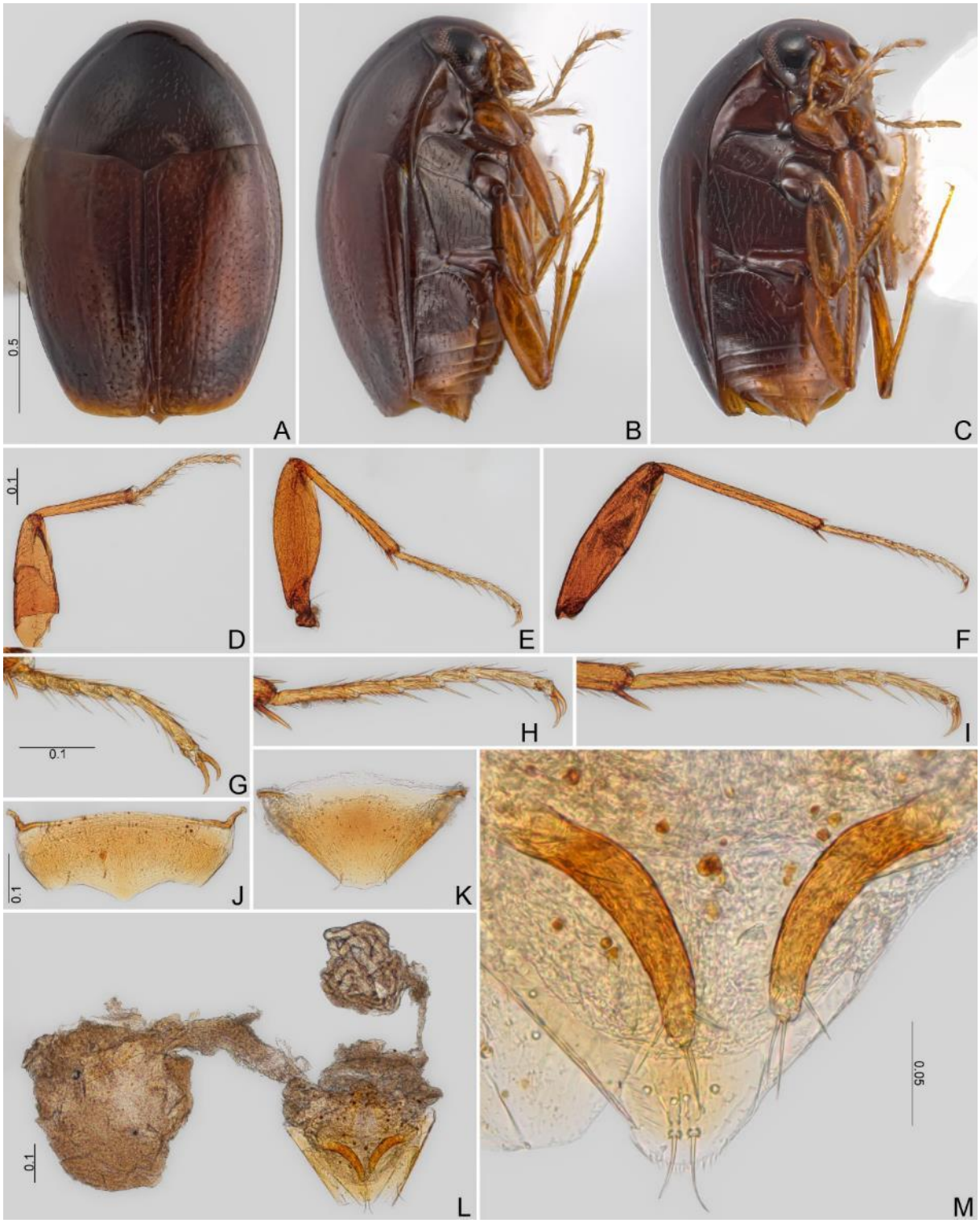

Fig. 59. *Scaphisoma* sp. nov. 3. A–C. Paratype, ♀ (#74). **A.** Dorsal view. **B.** Lateral view. **C.** Oblique view. D–M. Paratype, ♀ (#75). **D–F.** Legs. **D.** Fore. **E.** Middle. **F.** Hind. **G–I.** Tarsi. **G.** Pro. **H.** Meso. **I.** Meta. **J.** Sternite VIII. **K.** Tergite VIII. **L.** Genitalia. **M.** Ovipositor. CELC. Scales in mm.

Fig. 60. *Scaphisoma* sp. nov. 4. **A–E.** Holotype, ♂. **A.** Dorsal view. **B.** Lateral view. **C.** ventral view. **D.** Labels. **E.** Pinned. **F–G.** Paratype, teneral (#223). **F.** Dorsal view. **G.** Lateral view. **H–I.** Head, frontal view. **H.** Holotype, ♂. **I.** Paratype, ♂ (#236). **J–K.** Antennae. **J.** Paratype, ♂ (#236). **K.** Paratype, ♀ (#220). CELC. Scales in mm.

Fig. 61. *Scaphisoma* sp. nov. 4. **A–E.** Paratype, ♂ (#236). **A.** Labrum. **B–C.** Mandibles. **D.** Maxilla. **E.** Labrum. **F.** Prothorax, dorsal view (holotype, ♂). **G–J.** Paratype, ♂ (#202). **G–J.** Prothorax. **G.** Dorsal view. **H.** Lateral view. **I.** Ventral view. **J.** Inner view. **K.** Scutellar shield (paratype, ♂, ##236). CELC. Scales in mm.

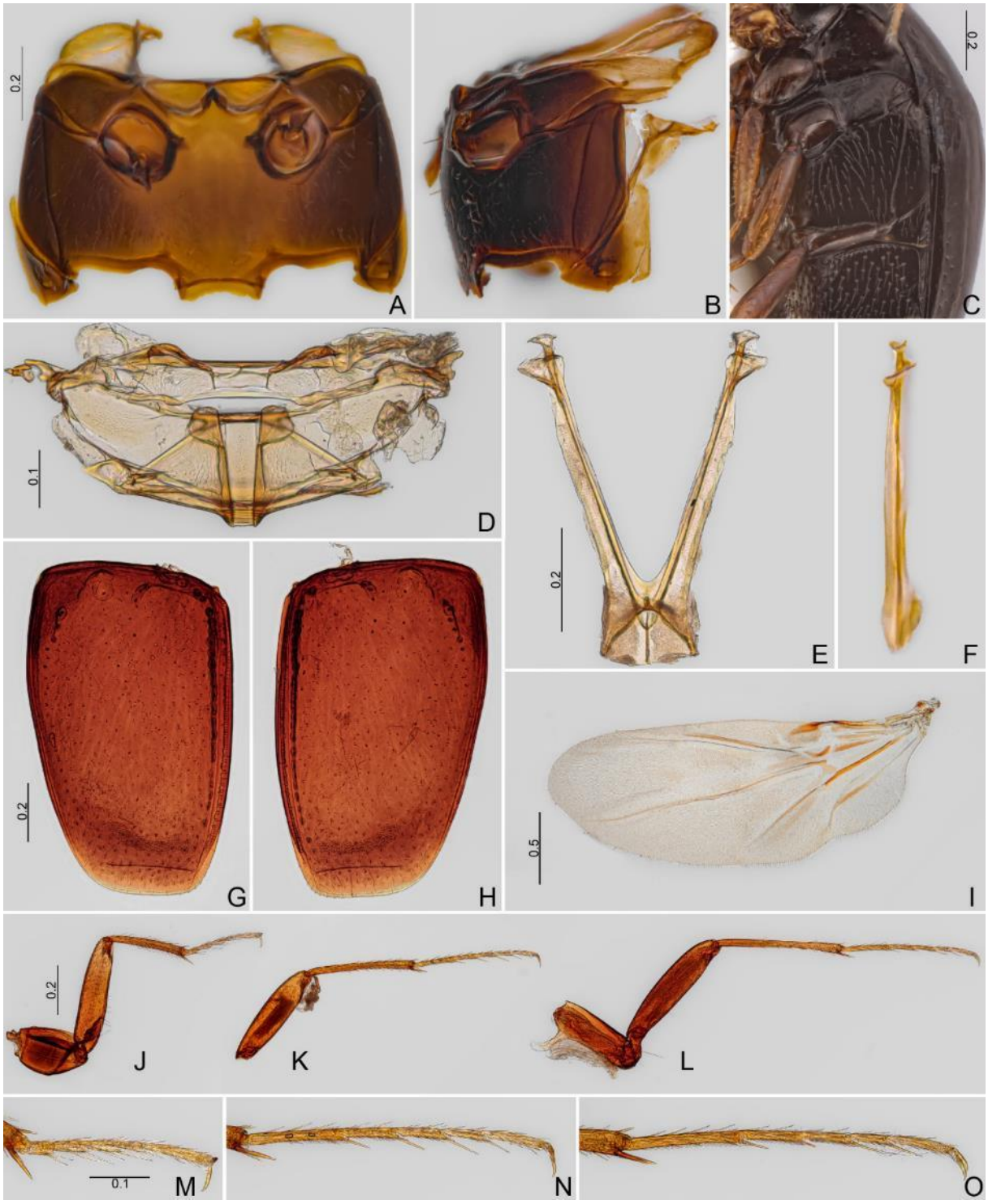

Fig. 62. *Scaphisoma* sp. nov. 4. **A–B.** Meso- and metathorax (paratype, ♂, #236). **A.** Ventral view. **B.** Lateral view. **C.** Oblique view (holotype, ♂). **D.** Metanotum (paratype, ♂, #236). **E–F.** Metendosternite (paratype, ♂, #202). **E.** Dorsal view. **F.** Lateral view. **G–O.** Paratype, ♂ (#236). **G–H.** Elytra. **I.** Hind wing. **J–L.** Legs. **J.** Fore. **K.** Middle. **L.** Hind. **M–O.** Tibiae. **M.** Pro. **N.** Meso. **O.** Meta. CELC. Scales in mm.

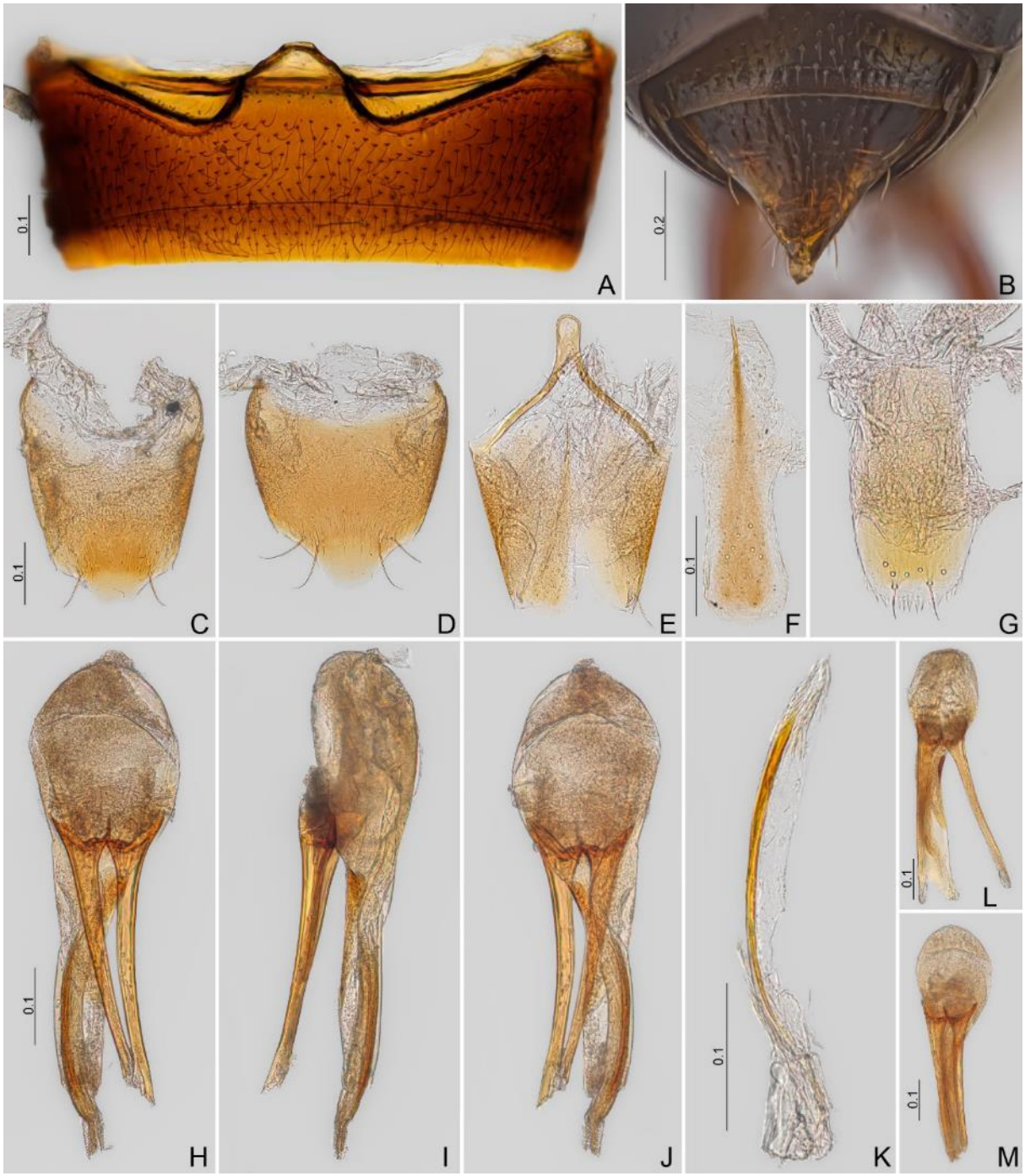

Fig. 63. *Scaphisoma* sp. nov. 4. **A.** Ventrite I (paratype, ♂, #236). **B.** Abdomen, dorsal view (holotype, ♂). **C–K.** Paratype, ♂ (#236). **C.** Sternite VIII. **D.** Tergite VIII. **E.** Tergite IX. **F.** Sternite IX. **G.** Tergite X. **H–M.** Aedeagus. **H.** Frontal view. **I.** Lateral view. **J.** Dorsal view. **K.** Sclerite of internal sac. **L.** Frontal view (paratype, ♂, #202). **M.** Frontal view (paratype, ♂, #215). CELC. Scales in mm.

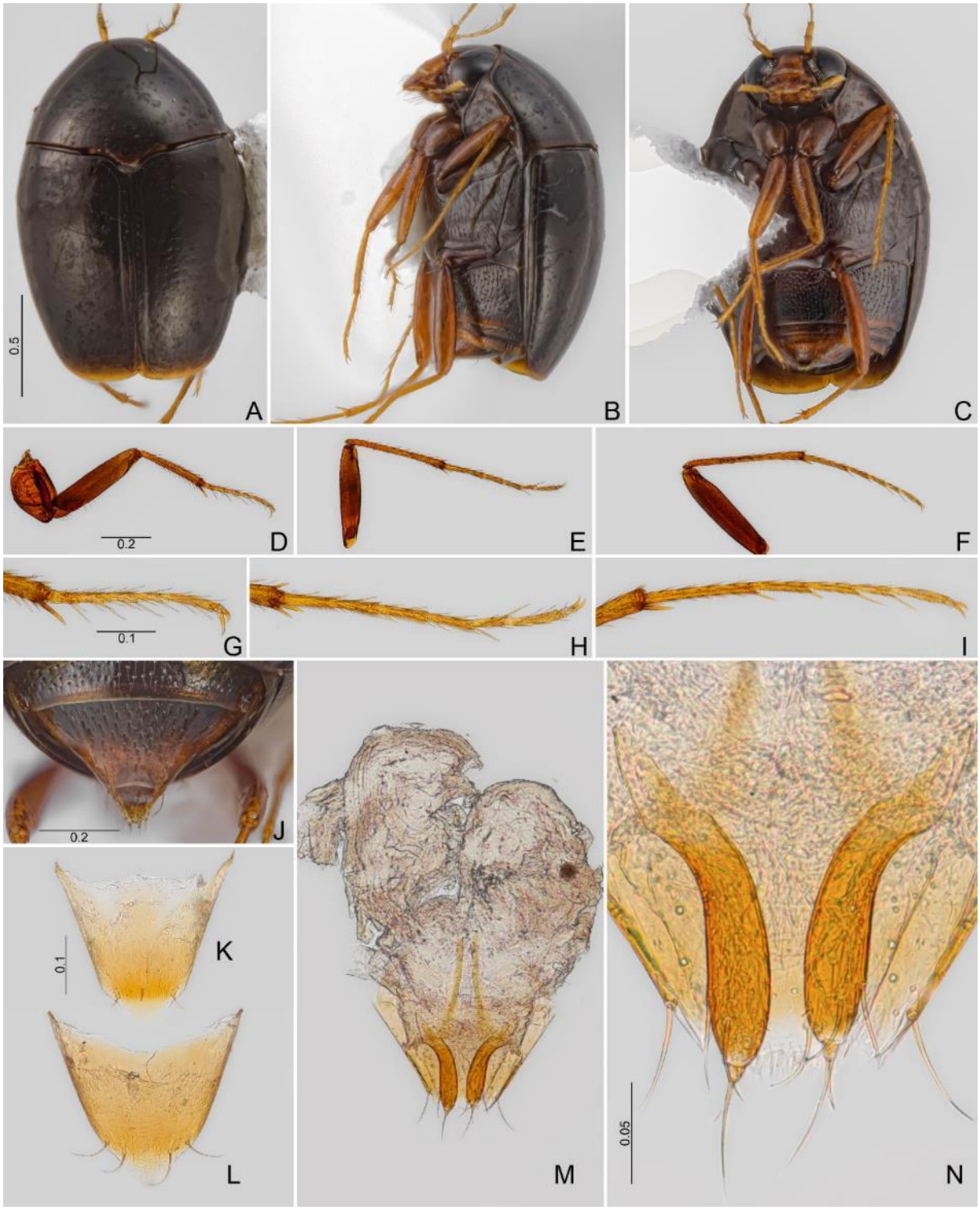

Fig. 64. *Scaphisoma* sp. nov. 4. Paratype, ♀ (#234). **A.** Dorsal view. **B.** Lateral view. **C.** Ventral view. D–I. Paratype, ♀ (#220). **D–F.** Legs. **D.** Fore. **E.** Middle. **F.** Hind. **G–I.** Tarsi. **G.** Pro. **H.** Meso. **I.** Meta. **J.** Abdomen, dorsal view (paratype, ♀, #234). **K–N.** Paratype, ♀ (#220). **K.** Sternite VIII. **L.** Tergite VIII. **M.** Genitalia. **N.** Ovipositor. CELC. Scales in mm.

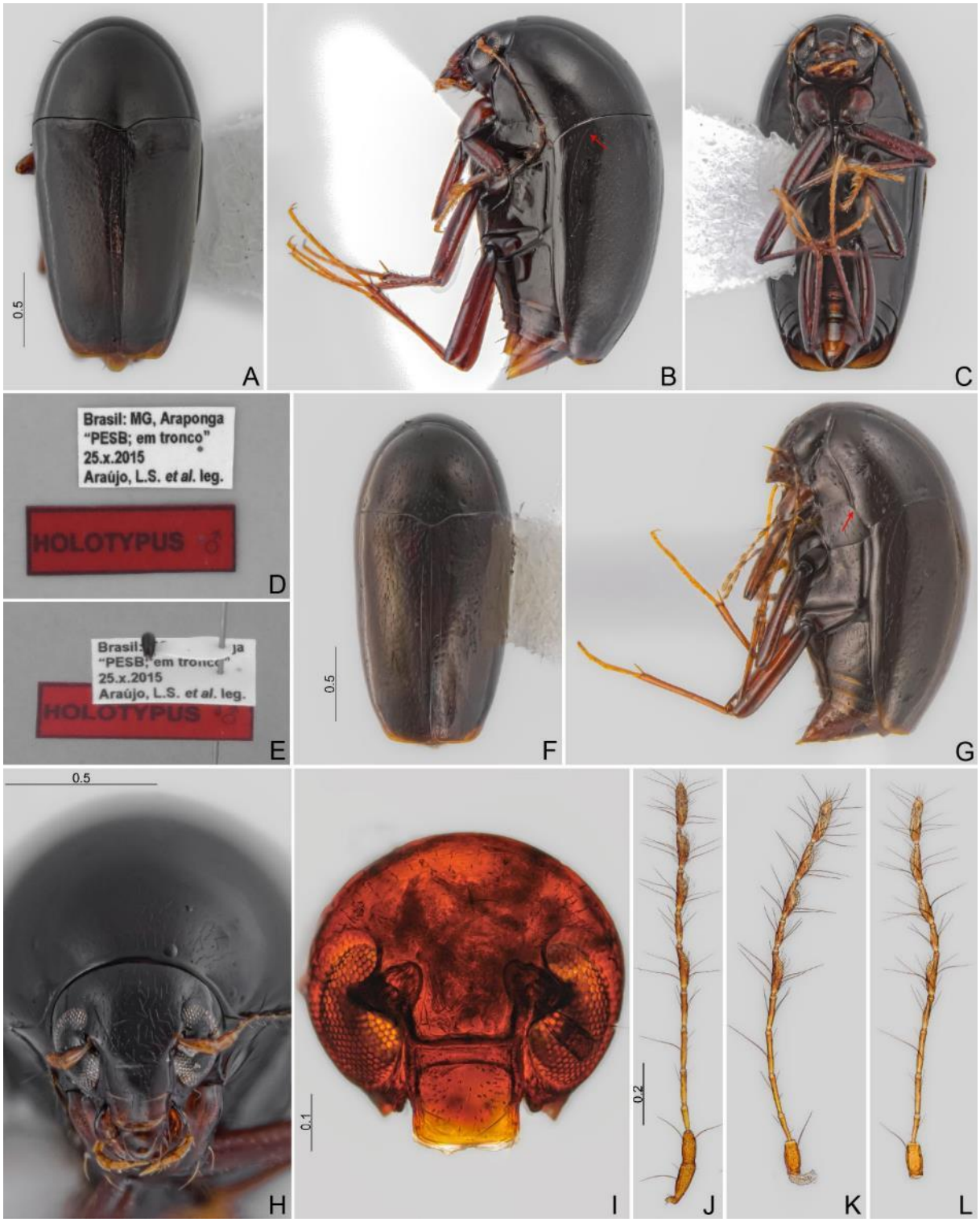

Fig. 65. *Toxidium* sp. nov. 1. **A–E.** Holotype, ♂. **A.** Dorsal view. **B.** Lateral view, arrow: curvature of lateral striae. **C.** ventral view. **D.** Labels. **E.** Pinned. **F–G.** Paratype, teneral (#09). **F.** Dorsal view. **G.** Lateral view, arrow: lateral carinae. **H–I.** Head, frontal view. **H.** Holotype, ♂. **I.** Paratype, ♂ (#12). **J–L.** Antennae. **J.** Paratype, ♂ (#12). **K.** Paratype, ♀ (#11). **L.** Paratype, ♂ (#09, Viçosa, MG). CELC. Scales in mm.

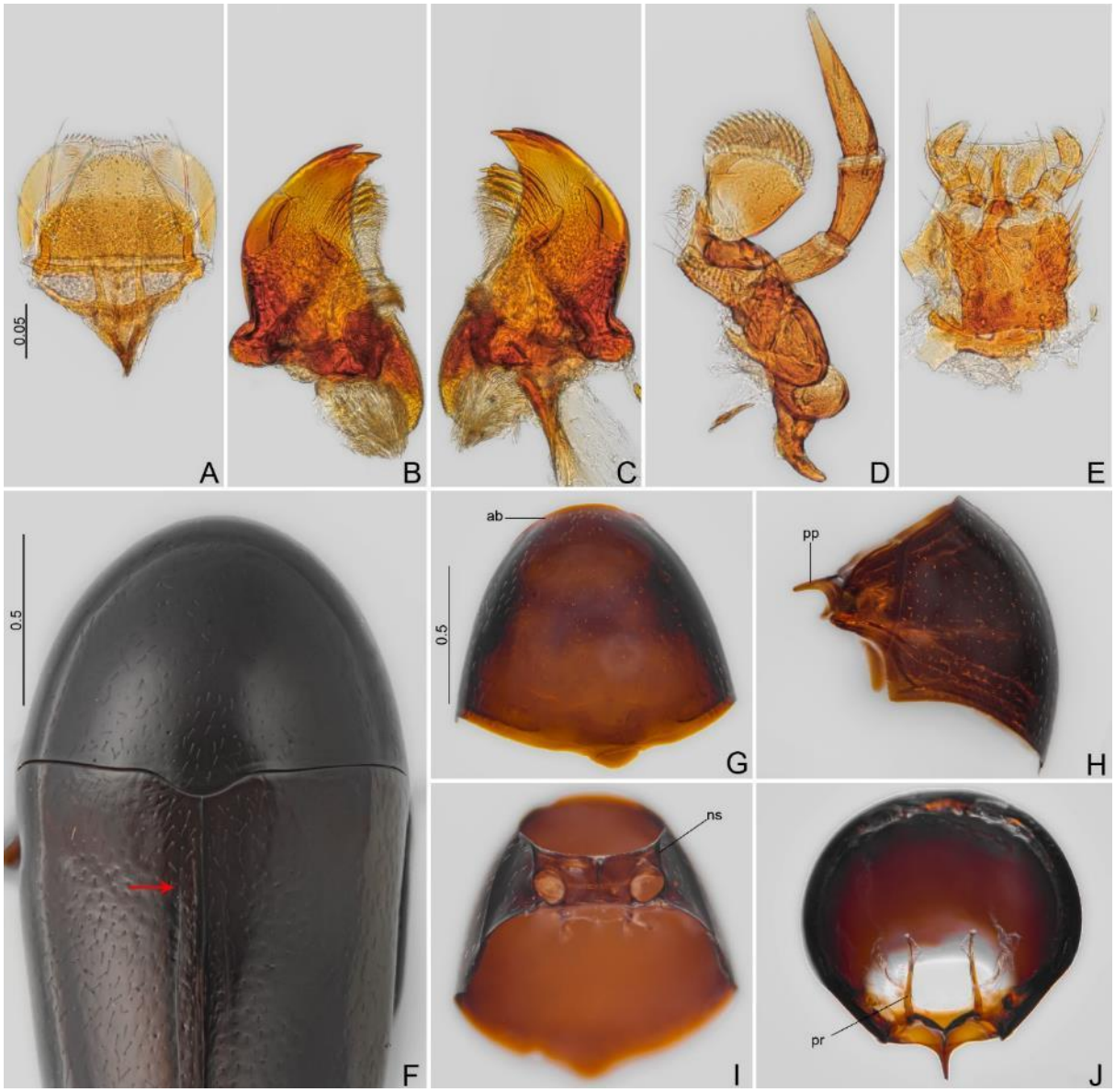

Fig. 66. *Toxidium* sp. nov. 1. **A–E.** Paratype, ♂ (#12). **A.** Labrum. **B–C.** Mandibles. **D.** Maxilla. **E.** Labium. **F.** Prothorax, dorsal view (holotype, ♂). **G–J.** Prothorax (paratype, ♂, #12). **G.** Dorsal view. **H.** Lateral view. **I.** Ventral view. **J.** Inner view. CELC. Scales in mm. Abbreviations: ab = anterior bead; ns = notosternal suture; pp = prosternal process; pr = profurca.

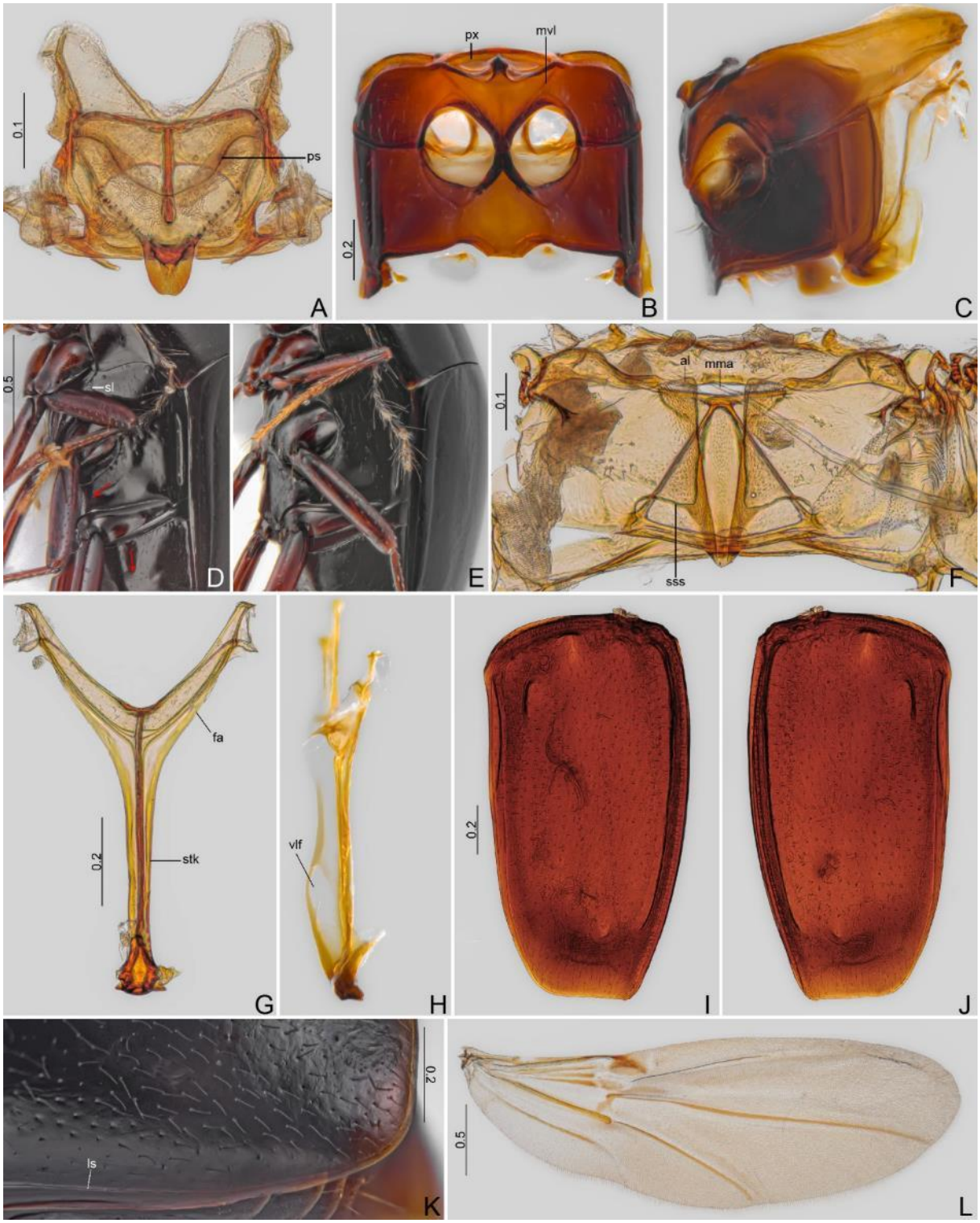

Fig. 67. *Toxidium* sp. nov. 1. **A–C.** Paratype, ♂ (#12). **A.** Scutellar shield. **B–E.** Meso- and metathorax. **B.** Ventral view. **C.** Lateral view. **D.** Oblique view (holotype, ♂), arrows: microsculptured areas. **E.** Oblique view (paratype, ♀, #11). **F.–J.** Paratype, ♂ (#12). **F.** Metanotum. **G–H.** Metendosternite. **G.** Dorsal view. **H.** Lateral view. **I–K.** Elytra. **I.** Left. **J.** Right. **K.** Lateral, apical area (holotype, ♂). **L.** Hind wing (paratype, ♂, #12). CELC. Scales in mm. Abbreviations: al = alacrista; fa = furcal arms; ls = lateral stria; mma = median membranous area; mvl = mesoventral line; ps = prescutellar line; px = procoxal rest; sl = sutural line; sss = scutoscutellar suture; stk = stalk; vlf = ventral longitudinal flange.

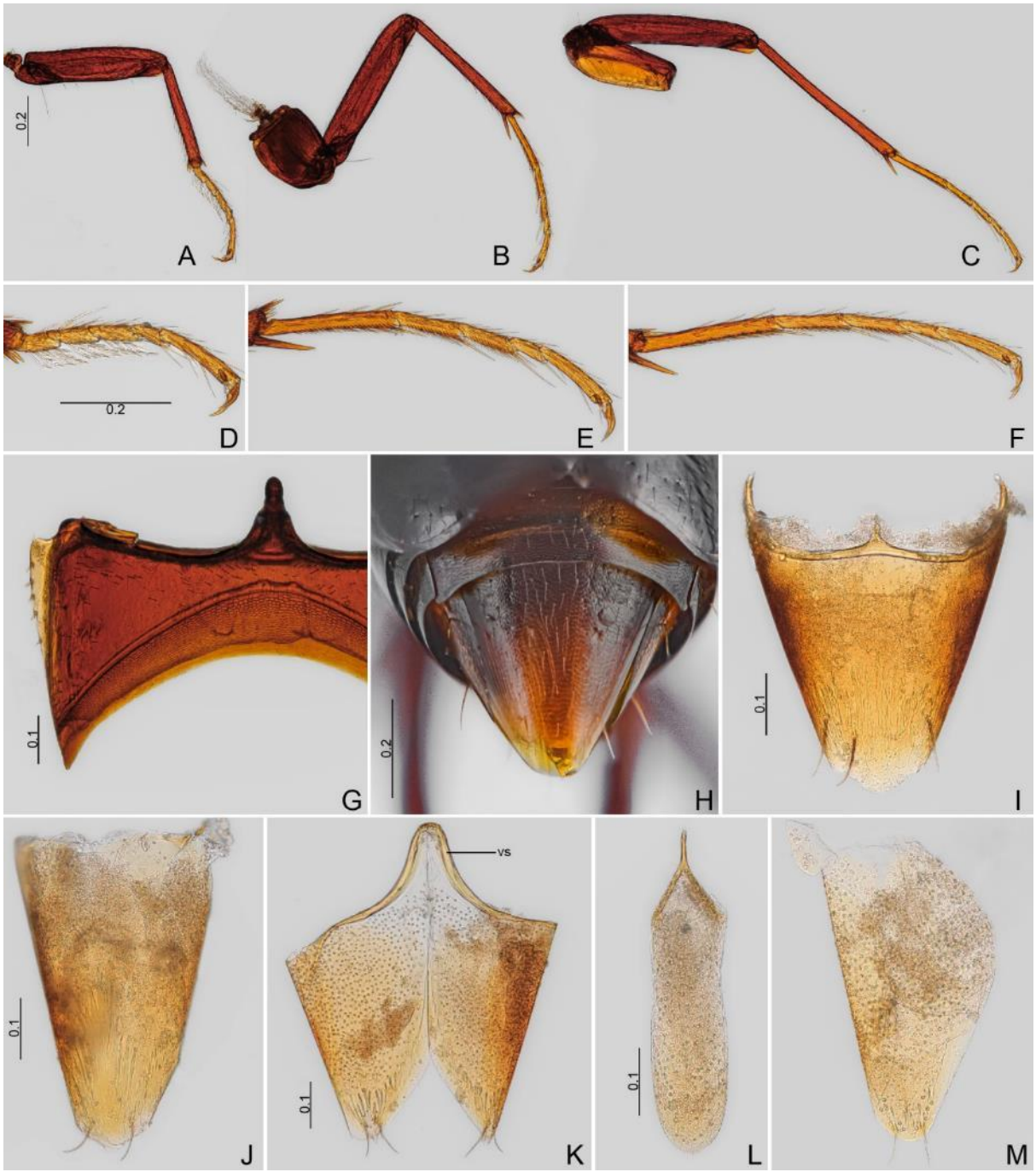

Fig. 68. *Toxidium* sp. nov. 1. **A–G.** Paratype, ♂ (#12). **A–C.** Legs. **A.** Fore. **B.** Middle. **C.** Hind. **D–F.** Tibiae. **D.** Pro. **E.** Meso. **F.** Meta. **G.** Ventrite I. **H.** Abdomen, dorsal view (holotype, ♂). **I–M.** Paratype, ♂ (#12). **I.** Sternite VIII. **J.** Tergite VIII. **K. K.** Tergite IX. **L.** Sternite IX. **M.** Tergite X. CELC. Scales in mm. Abbreviation = ventral strut.

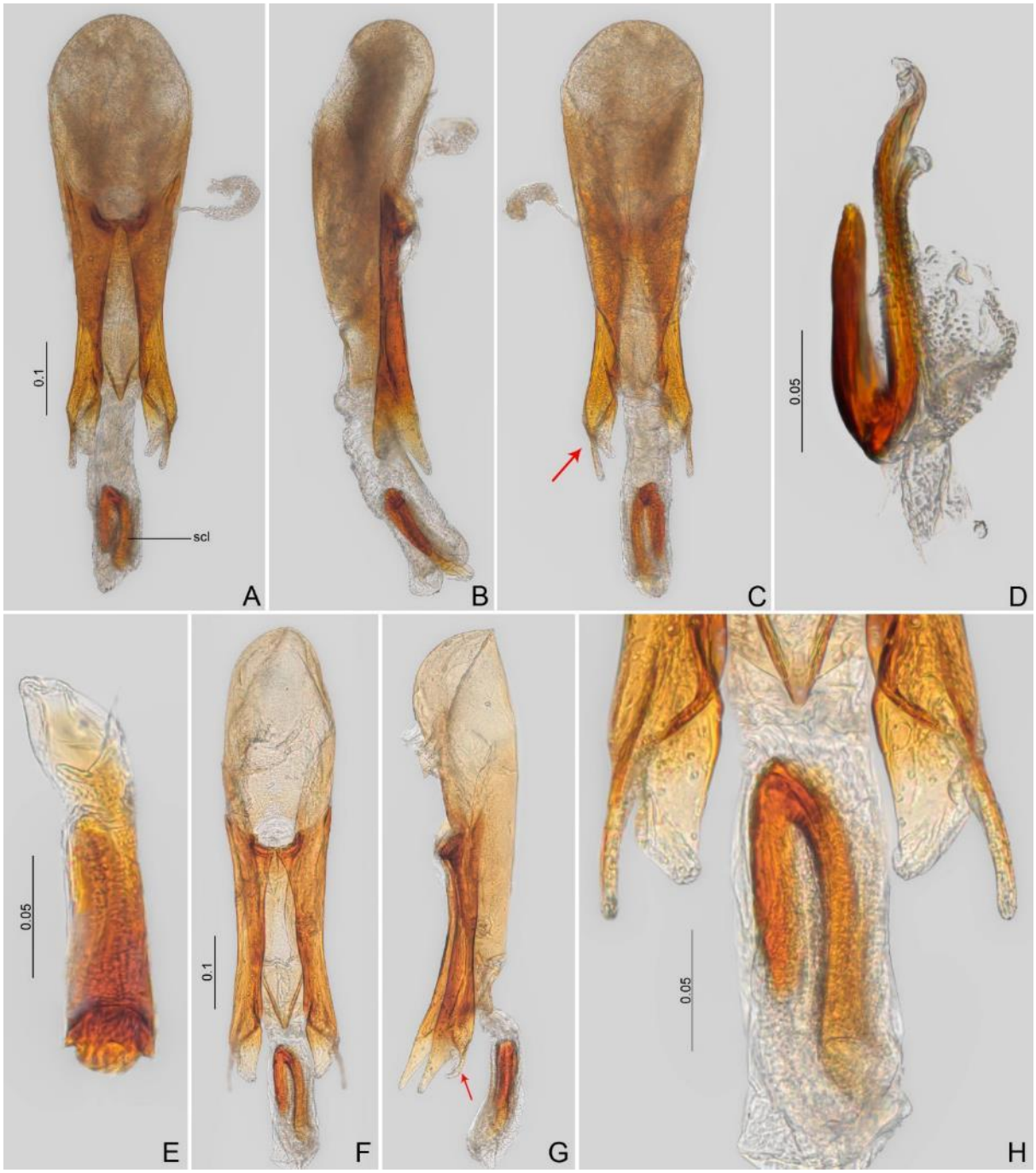

Fig. 69. *Toxidium* sp. nov. 1. **A–H.** Aedeagus. **A–E.** Paratype, ♂ (#12). **A.** Frontal view. **B.** Lateral view. **C.** Dorsal view, arrow: posterior projection. **D–E.** Sclerite of internal sac. **D.** Lateral view. **E.** Frontal view. **F–H.** Paratype, ♂ (#09, Viçosa, MG). **F.** Frontal view. **G.** Lateral view, arrow: posterior projection. **H.** Sclerite of internal sac. CELC. Scales in mm. Abbreviation = scl = sclerite of internal sac.

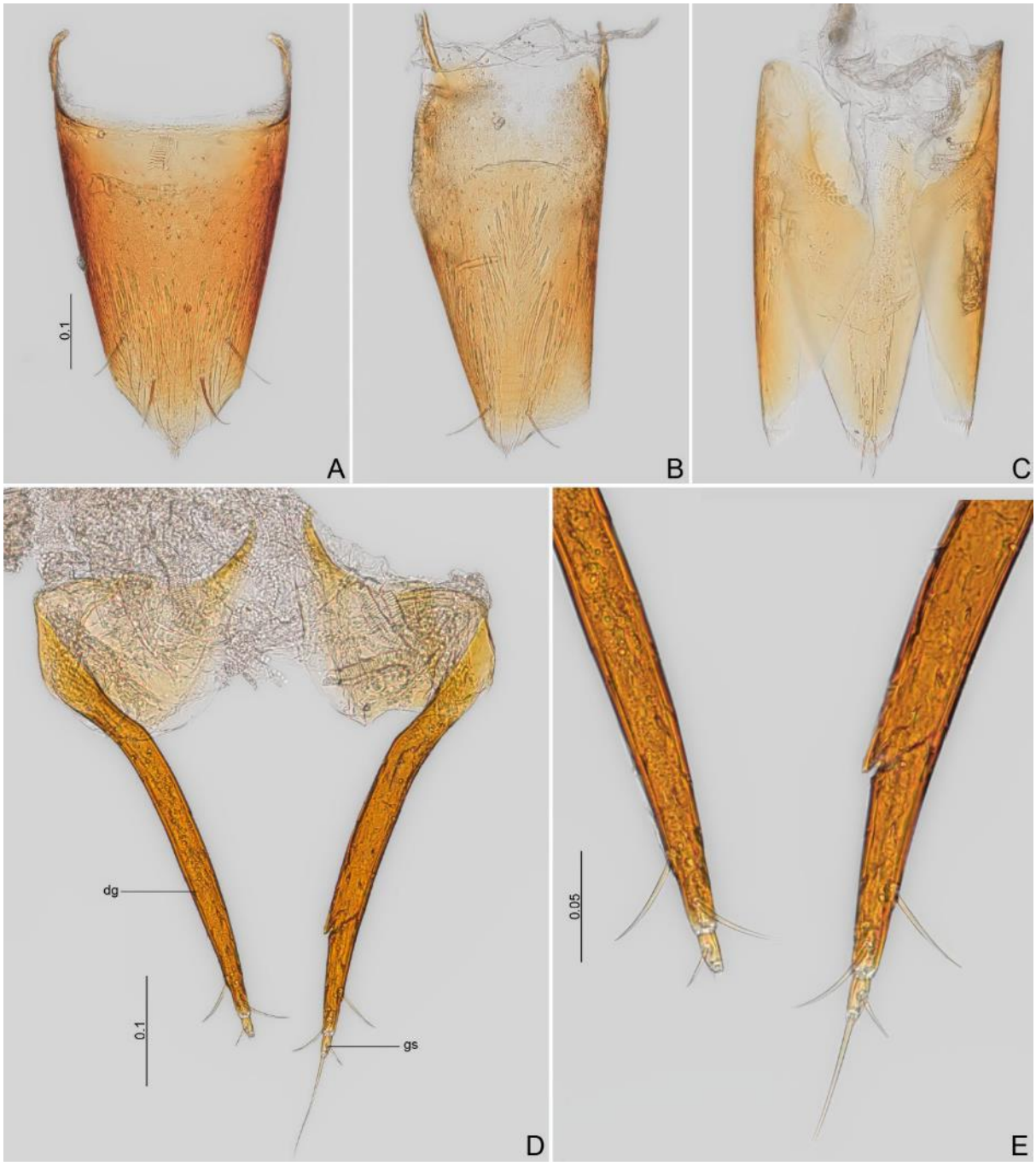

Fig. 70. *Toxidium* sp. nov. 1, paratype, ♀ (#11). **A.** Sternite VIII. **B.** Tergite VIII. **C.** Tergite IX. **D.** Genitalia. **E.** Ovipositor. CELC. Scales in mm. Abbreviations: dg = distal gonocoxites; gs = gonostyli.

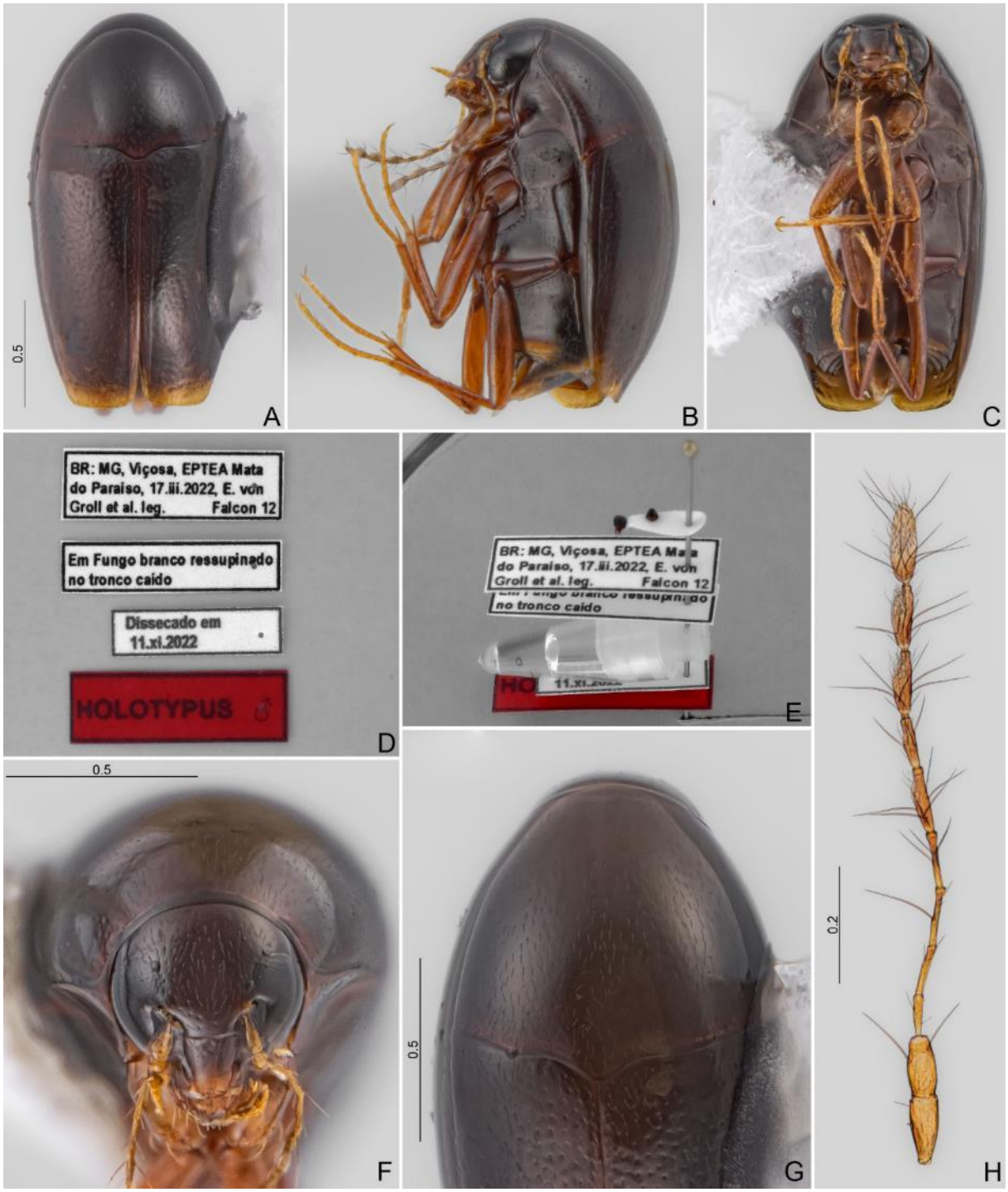

Fig. 71. *Toxidium* sp. nov. 2, holotype, ♂. **A.** Dorsal view. **B.** Lateral view. **C.** Ventral view. **D.** Labels. **E.** Pinned. **F.** Head, frontal view. **G.** Prothorax, dorsal view. **H.** Antenna. CELC. Scales in mm.

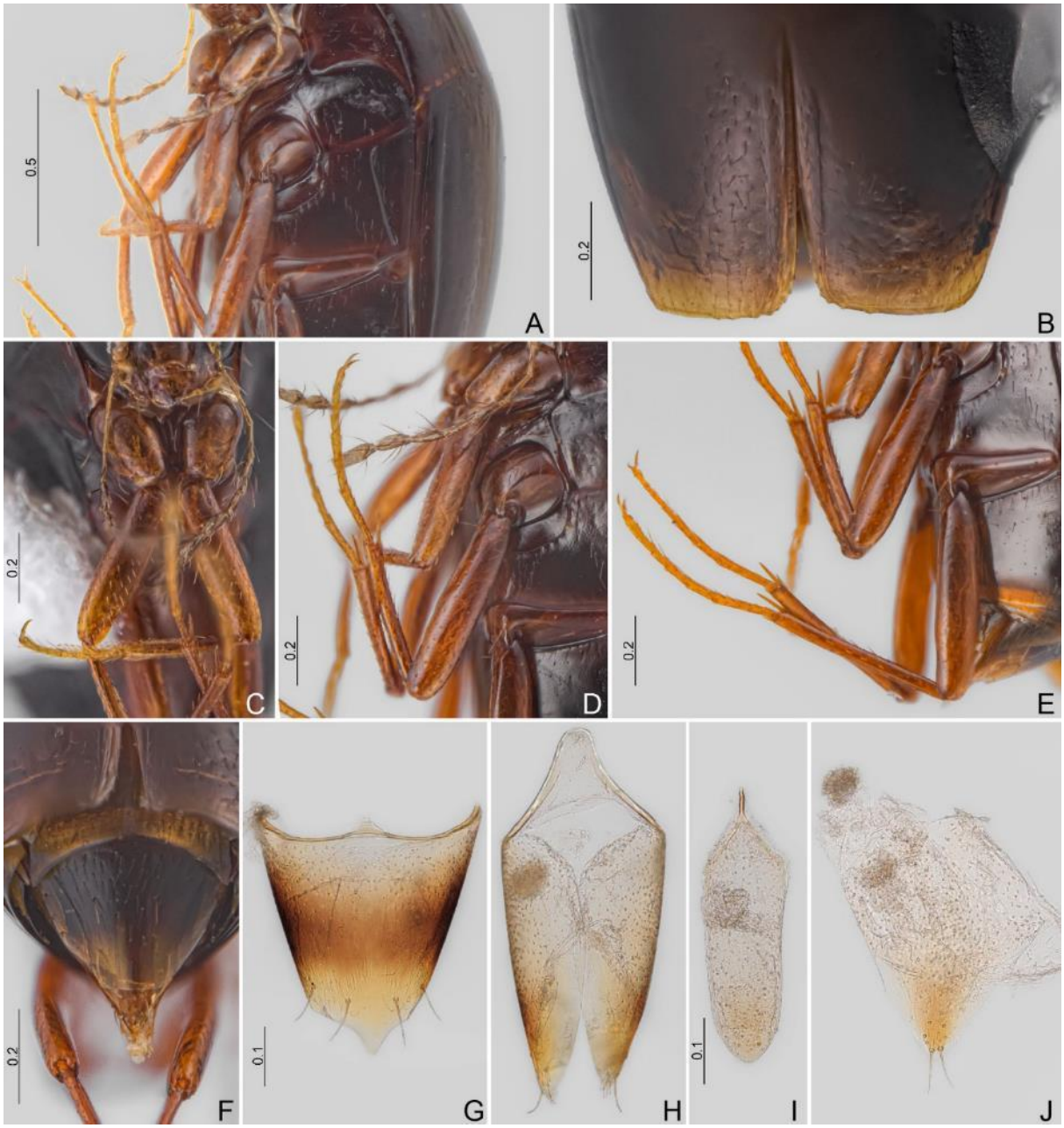

Fig. 72. *Toxidium* sp. nov. 2, holotype, ♂. **A.** Meso- and metathorax; oblique view. **B.** Elytra apex, dorsal view. **C–E.** Legs. **C.** Fore. **D.** Middle. **E.** Hind. **F.** Abdomen, dorsal view. **G.** Ventrite VIII. **H.** Tergite IX. **I.** Sternite IX. **J.** Tergite X. CELC. Scales in mm.

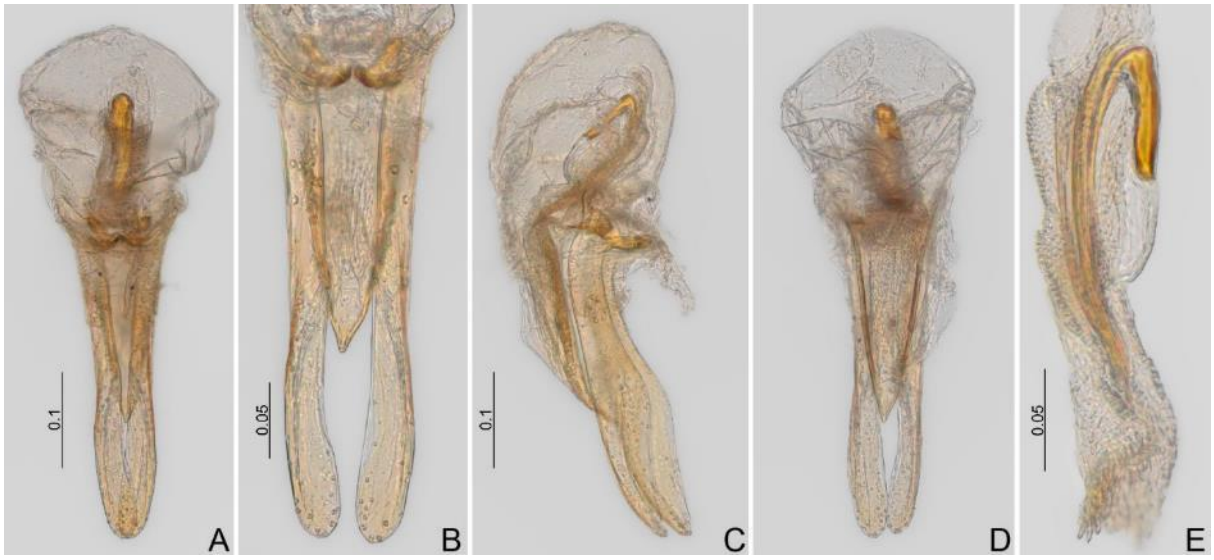

Fig. 73. *Toxidium* sp. nov. 2, holotype, ♂, aedeagi. **A.** Frontal view. **B.** Parameres, frontal view. **C.** Lateral view. **D.** Dorsal view. **E.** Sclerite of internal sac, lateral view. CELC. Scales in mm.

Fig. 74. *Toxidium* sp. nov. 3, holotype, ♂. **A.** Dorsal view. **B.** Lateral view. **C.** Ventral view. **D.** Labels. **E.** Pinned. **F.** Head, frontal view. **G.** Prothorax, dorsal view. **H.** Antenna. CELC. Scales in mm.

Fig. 75. *Toxidium* sp. nov. 3, holotype, ♂. **A.** Meso- and metathorax; oblique view. **B.** Elytra apex, dorsal view. **C–D.** Legs. **C.** Fore. **D.** Middle and hind. **E.** Abdomen, dorsal view. **F.** Ventrite VIII. **G.** Tergite VIII. **H.** Tergite IX. **I.** Sternite IX. **J.** Tergite X. CELC. Scales in mm.

Fig. 76. *Toxidium* sp. nov. 3, holotype, ♂, aedeagi. **A.** Frontal view. **B.** Lateral view. **C.** Dorsal view. **D–G.** Sclerite of internal sac. **D–E.** Frontal view. **F–G.** Lateral view. CELC. Scales in mm.

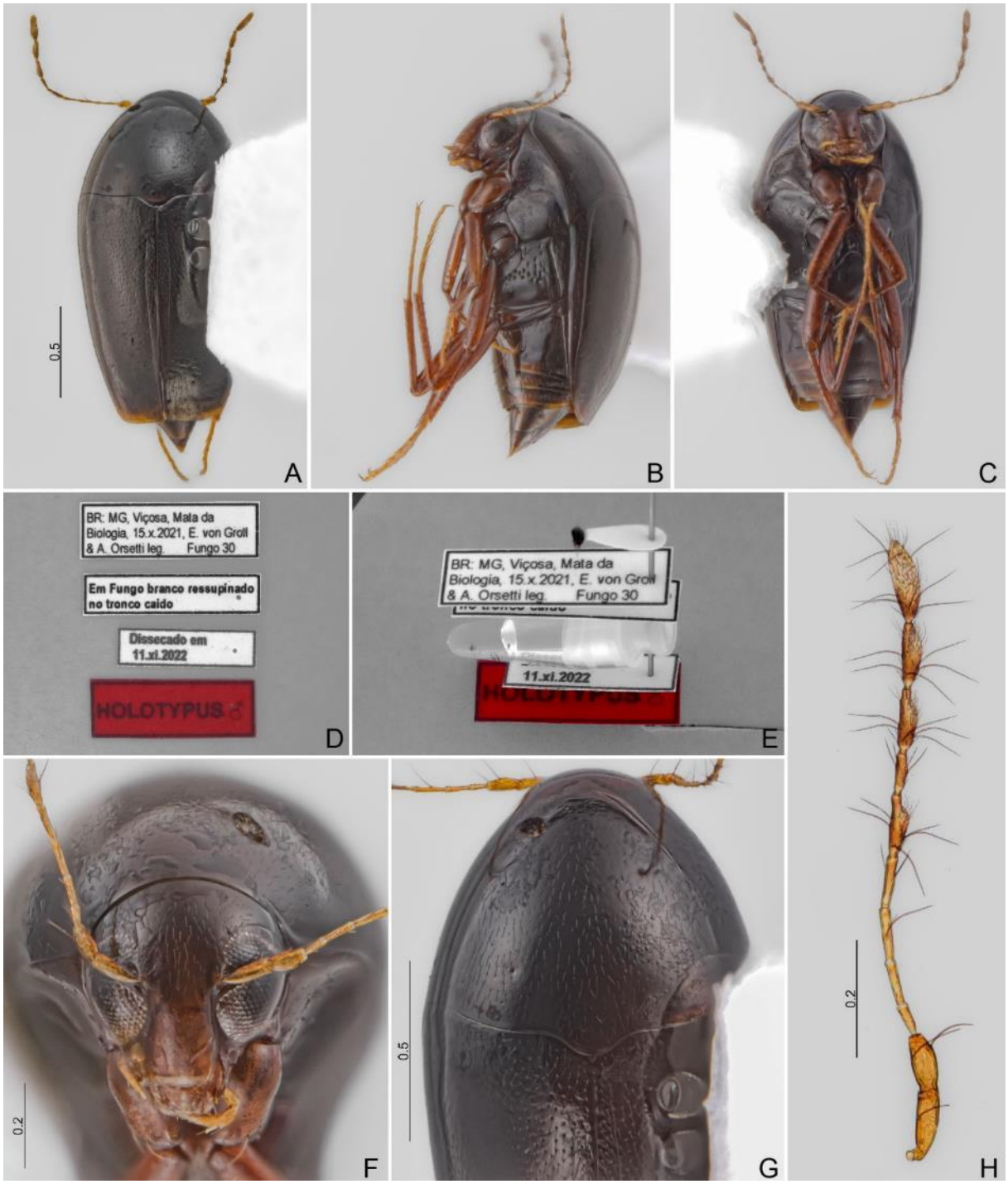

Fig. 77. *Toxidium* sp. nov. 4, holotype, ♂. **A.** Dorsal view. **B.** Lateral view. **C.** Ventral view. **D.** Labels. **E.** Pinned. **F.** Head, frontal view. **G.** Prothorax, dorsal view. **H.** Antenna. CELC. Scales in mm.

Fig. 78. *Toxidium* sp. nov. 4, holotype, ♂. **A.** Meso- and metathorax; oblique view. **B.** Elytra apex, dorsal view. **C–D.** Legs. **C.** Fore. **D.** Middle and hind. **E.** Abdomen, dorsal view. **F.** Ventrite VIII. **G.** Tergite VIII. **H.** Tergite IX. **I.** Sternite IX. **J.** Tergite X. CELC. Scales in mm.

Fig. 79. *Toxidium* sp. nov. 4, holotype, ♂, aedeagi. **A.** Frontal view. **B.** Lateral view. **C.** Dorsal view. **F.** Parameres, lateral view. **E–F.** Sclerite of internal sac. **E.** Frontal view. **F.** Lateral view. CELC. Scales in mm.

Fig. 80. *Toxidium* sp. nov. 5, holotype, ♂. **A.** Dorsal view. **B.** Lateral view. **C.** Ventral view. **D.** Labels. **E.** Pinned. **F.** Head, frontal view. **G.** Prothorax, dorsal view. **H.** Antenna. CELC. Scales in mm.

Fig. 81. *Toxidium* sp. nov. 5, holotype, ♂. **A.** Meso- and metathorax; oblique view. **B.** Elytra apex, dorsal view. **C–D.** Legs. **C.** Fore and middle. **D.** Hind. **E.** Abdomen, dorsal view. **F.** Ventrite VIII. **G.** Tergite VIII. **H.** Tergite IX. **I.** Sternite IX. **J.** Tergite X. CELC. Scales in mm.

Fig. 82. *Toxidium* sp. nov. 5, holotype, ♂, median aedeagi. **A.** Frontal view. **B.** Parameres, frontal view. **C.** Lateral view. **D.** Parameres, lateral view. **E–F.** Dorsal view. **G–H.** Sclerite of internal sac. **G.** Lateral view. **H.** Frontal view. CELC. Scales in mm.

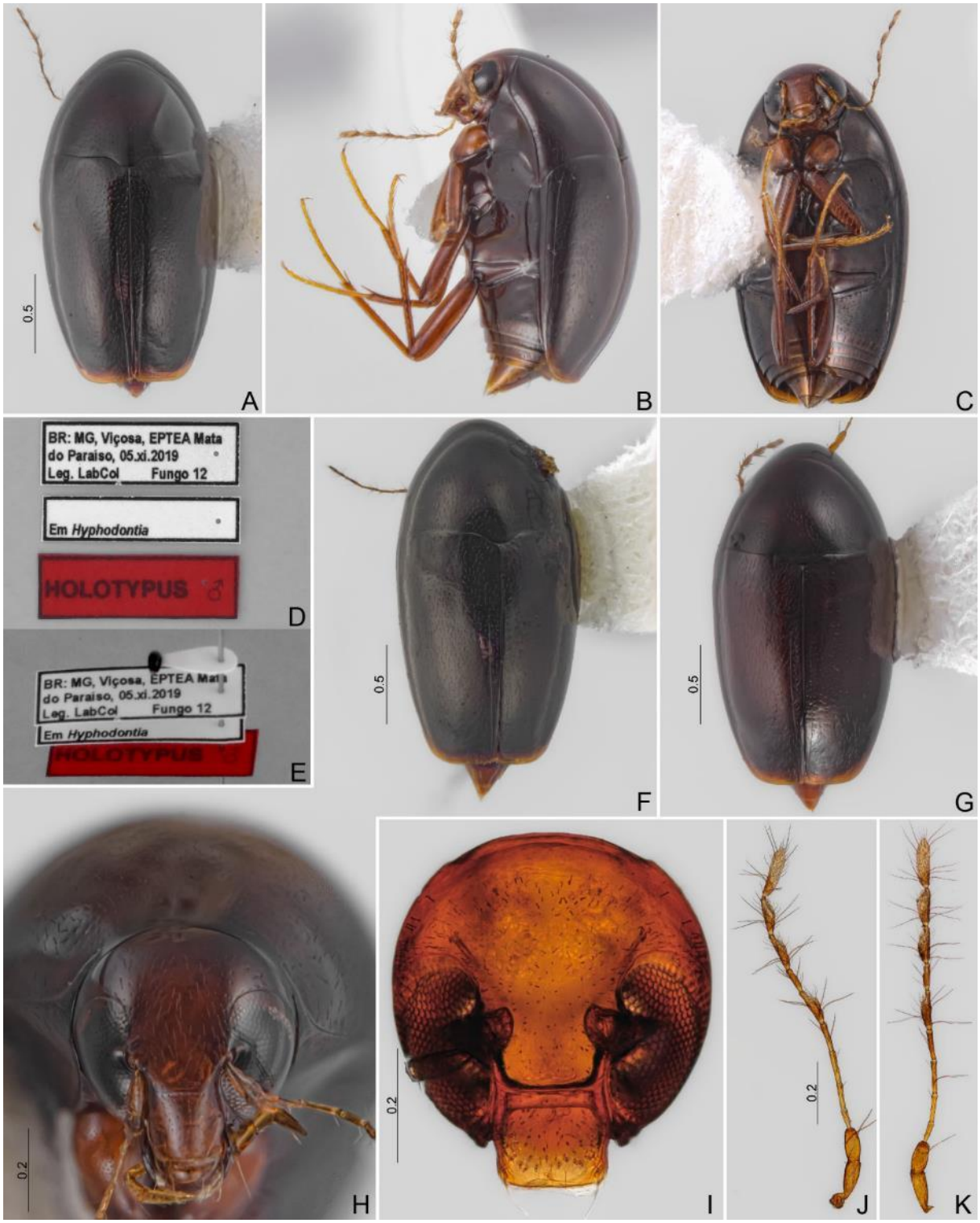

Fig. 83. *Toxidium* sp. nov. 6. **A–E.** Holotype, ♂. **A.** Dorsal view. **B.** Lateral view. **C.** Ventral view. **D.** Labels. **E.** Pinned. **F.** Paratype, ♀ (#01), dorsal view **G.** Paratype, ♂ (#05). **H–I.** Head, frontal view. **H.** Holotype, ♂. **I.** Paratype, ♀ (#05). **J–K.** Antennae. **J.** Paratype, ♂ (#04). **K.** Paratype, ♀ (#05). CELC. Scales in mm.

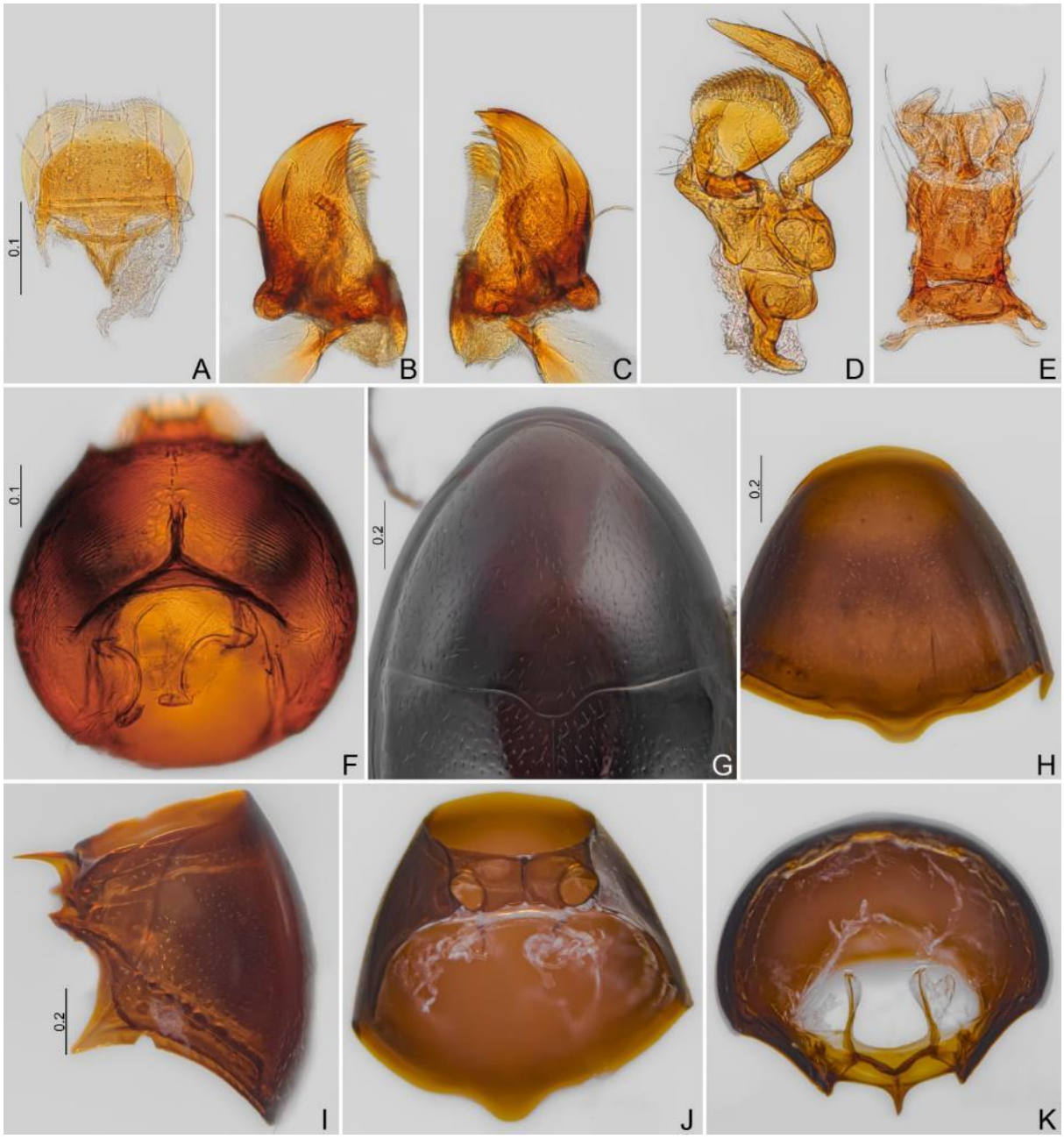

Fig. 84. *Toxidium* sp. nov. 6. **A–E.** Paratype, ♂ (#04). **A.** Labrum. **B–C.** Mandibles. **D.** Maxilla. **E.** Labium. **F.** Head, ventral view (paratype, ♀, #05). **G.** Prothorax, dorsal view (holotype, ♂). **H–K.** Prothorax (paratype, ♂, #04). **H.** Dorsal view. **I.** Lateral view. **J.** Ventral view. **K.** Inner view. CELC. Scales in mm.

Fig. 85. *Toxidium* sp. nov. 6. **A–C.** Paratype, ♂ (#04). **A.** Scutellar shield. **B–E.** Meso- and metathorax. **B.** Ventral view. **C.** Lateral view. **D.** Oblique view (holotype, ♂). **E.** Oblique view (paratype, ♀, #01). **F–I.** Paratype, ♂ (#04). **F.** Metanotum. **G.** XXXX. **H–J.** Metendosternite. **H.** Dorsal view. **I.** Lateral view. **J.** Dorsal view (paratype, ♀, #05). **K–M.** Paratype, ♂. **K–L.** Elytra. **M.** Hind wing. CELC. Scales in mm. Abbreviations: mr = mesofurca; mvl = mesoventral line; px = procoxal rest; sl = secondary line.

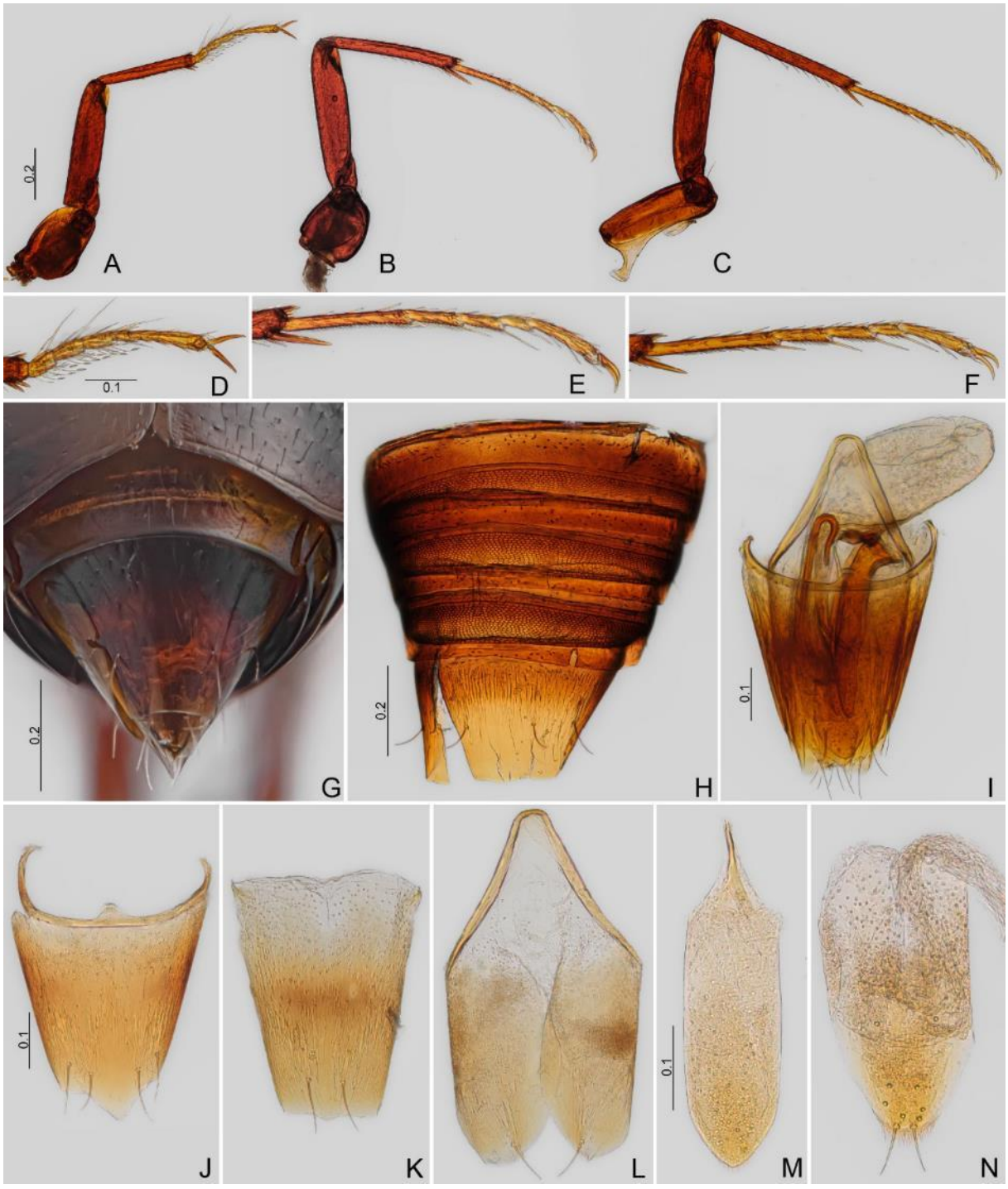

Fig. 86. *Toxidium* sp. nov. 6. **A–F.** Paratype, ♂ (#04). **A–C.** Legs. **A.** Fore. **B.** Middle. **C.** Hind. **D–F.** Tibiae. **D.** Pro. **E.** Meso. **F.** Meta. **F.** Abdomen, dorsal view (holotype, ♂). **H–N.** Paratype, ♂ (#04). **H.** Abdomen, dissected, ventral view. **I.** Terminalia. **J.** Sternite VIII. **K.** Tergite VIII. **L.** Tergite IX. **M.** Sternite IX. **N.** Tergite X. CELC. Scales in mm.

Fig. 87. *Toxidium* sp. nov. 6, paratype, ♂ (#04), aedeagi. **A.** Frontal view. **B.** Lateral view. **C.** Dorsal view. **F.** Parameres, ventral view. **E–F.** Sclerite of internal sac. **E.** Lateral view. **F.** Frontal view. CELC. Scales in mm.

Fig. 88. *Toxidium* sp. nov. 6. **A.** Abdomen, dorsal view (paratype, ♀, #01). **B–F.** Paratype, ♀ (#05). **B.** Sternite VIII. **C.** Tergite VIII. **D.** Terminalia. **E–F.** Ovipositor. **G–H.** Ovipositor (paratype, ♀, #07). CELC. Scales in mm.

Fig. 89. *Toxidium* sp. nov. 7. **A–E.** Holotype, ♂. **A.** Dorsal view. **B.** Lateral view. **C.** ventral view. **D.** Labels. **E.** Pinned. **F.** Dorsal view (paratype, ♂, #02) **G–H.** Paratype, ♀ (#03). **G.** Dorsal view. **H.** Lateral view. **I.** Head, frontal view (holotype, ♂). **J–K.** Antennae. **J.** Holotype, ♂. **K.** Paratype, ♀ (#03). **L.** Prothorax, dorsal view (holotype, ♂). CELC. Scales in mm.

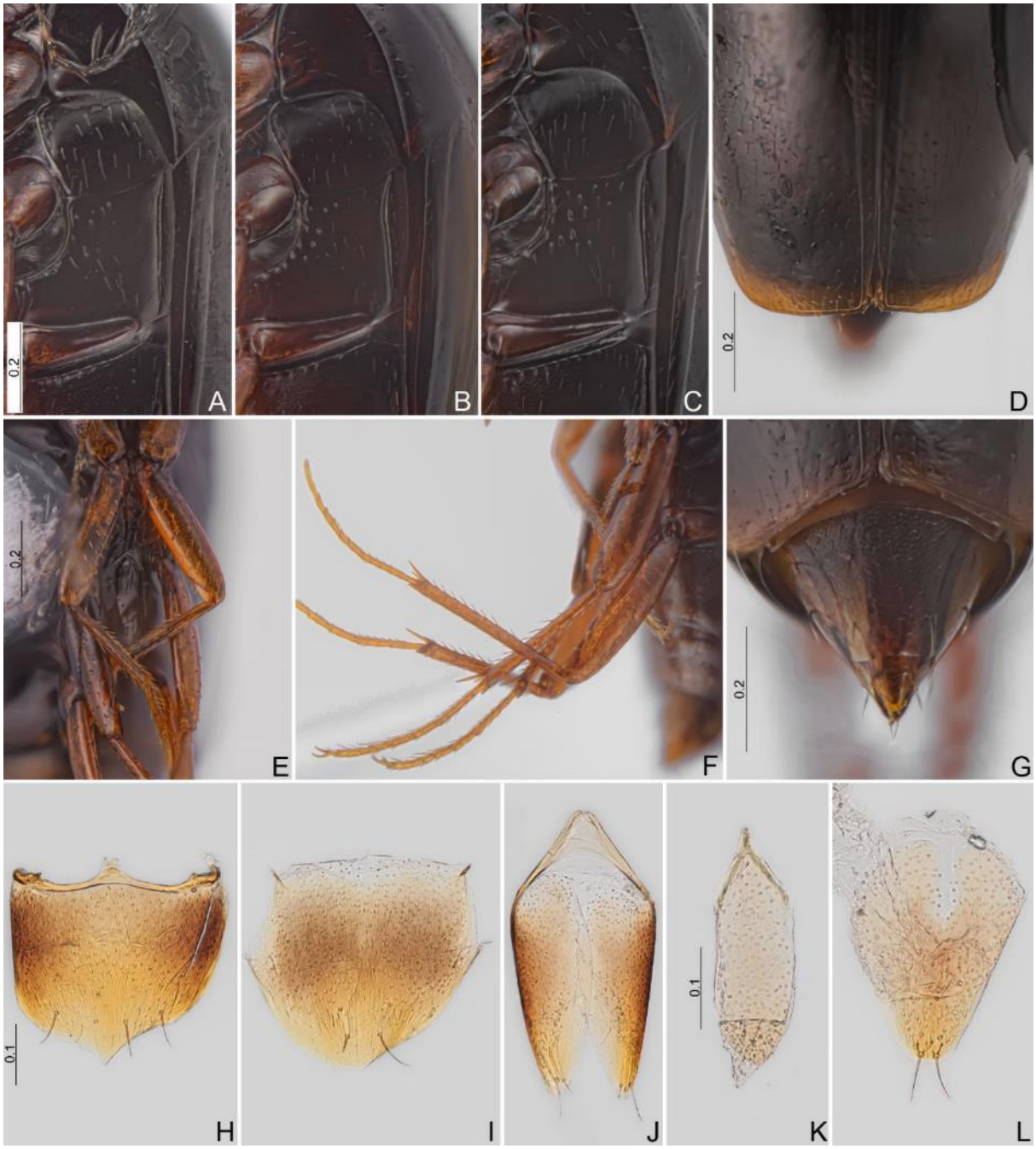

Fig. 90. *Toxidium* sp. nov. 7. **A–C.** Meso- and metathorax, oblique view. **A.** Holotype, ♂. **B.** Paratype, ♂ (# (#02). **C.** Paratype, ♀ (#03). **D–L.** Holotype, ♂. **D.** Elytra apex, dorsal view. **E–F.** Legs. **E.** Fore. **F.** Middle and hind. **G.** Abdomen, dorsal view. **H.** Sternite VIII. **I.** Tergite VIII. **J.** Tergite IX. **K.** Sternite IX. **L.** Tergite X. CELC. Scales in mm.

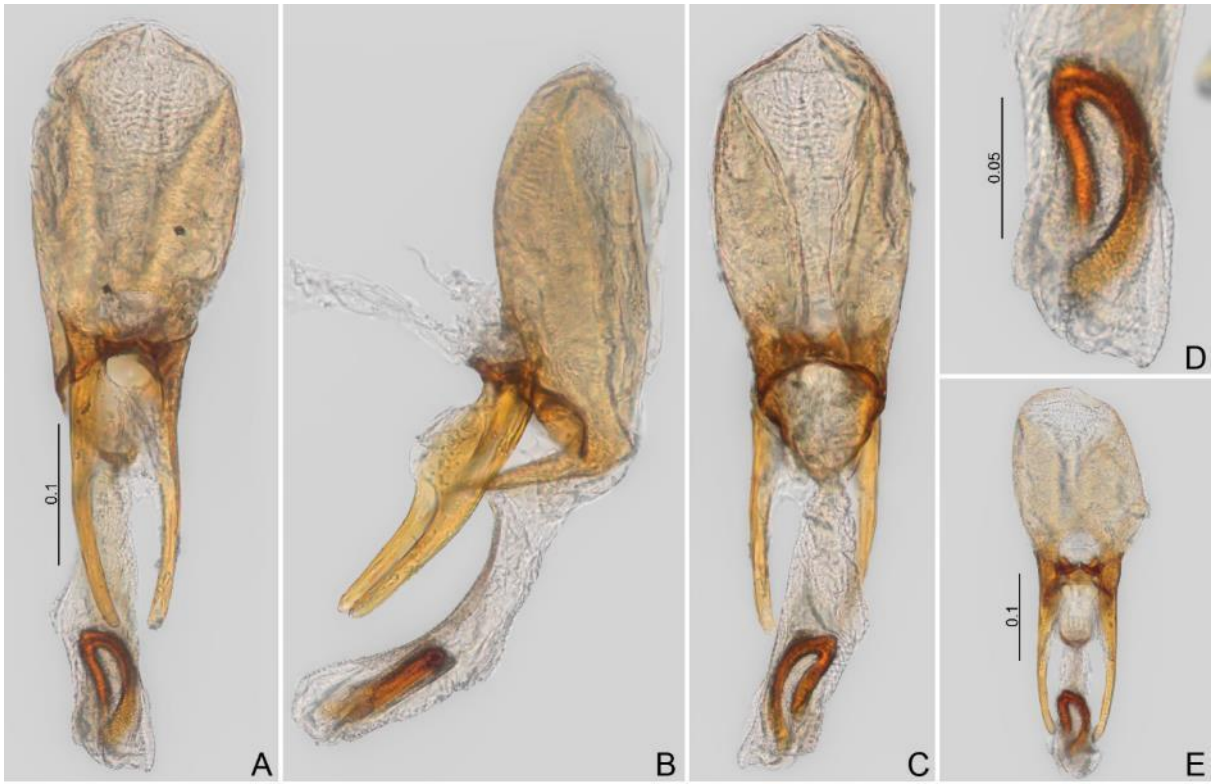

Fig. 91. *Toxidium* sp. nov. 7, aedeagus. **A–D.** Holotype, ♂. **A.** Frontal view. **B.** Lateral view. **C.** Dorsal view. **D.** Sclerite of internal sac. **E.** Aedeagi, frontal view (paratype, ♂, #02). CELC. Scales in mm.

Fig. 92. *Toxidium* sp. nov. 7, paratype ♀ (#03). **A–B.** Legs. **A.** Fore. **B.** Middle and hind. **C.** Ventrite I, detail, arrow: microsculpture. **D.** Abdomen, dorsal view. **E.** Sternite VIII. **F.** Tergite VIII. **G.** Genitalia. **H.** Ovipositor. CELC. Scales in mm.

Fig. 93. Scaphidiinae hosts (Mata da Biologia, Viçosa, MG). **A–B.** Mushroom. **C.** Unknown fungus / myxomycete. **D.** *Ceratyomyxa fruticulosa*. **E–F.** Resupinate/crust fungi 1. **G–H.** Resupinate/crust fungi 2. **I–J.** Resupinate/crust fungi 3.

Fig. 94. Scaphidiinae hosts (Viçosa, MG). **A–D.** *Inonotus* sp. (Vila Gianetti). (Hymenochaetaceae). **C–D.** *Scaphisoma* sp. nov. 1 on *Inonotus* sp. **E.** Resupinate/crust fungi (Mata da Biologia). **F.** Resupinate/crust fungi (Mata da Biologia).

4. GENERAL CONCLUSIONS

The thesis successfully achieved its objective: advancing knowledge of the Scaphidiinae subfamily. With the inclusion of the five papers, which encompasses both published and forthcoming works, the roster of Brazilian shining rove beetles was expanded by 26 species, of which 25 are new to science. Moreover, a substantial number of additional specimens have been collected and await examination, promising to increase the number of new species. The papers also contribute fresh insights into host fungi and myxomycete associations, as well as morphological characteristics, particularly those concerning the *Toxidum* and *Alexidia* ovipositor.

However, more than just offering some answers, this thesis also raises a series of questions. Following extensive collections of scaphidiines in Minas Gerais, Brazil, lingering queries revolve around the distribution of these species. Are their habitats more or less confined to specific states, ecoregions, or biogeographic areas? How do these beetles relate phylogenetically to species found in other regions, especially those that exhibit pronounced morphological similarities to those described in these papers? Although only the seven previously known genera were encountered during the field expeditions, the potential diversity of genera in Brazil remains uncertain. Additionally, aspects such as larval biology and behavior have yet to be explored.

It is my aspiration that through the dissemination of this study, including the detailed images and descriptions, I can stimulate greater interest in these tiny but interesting beetles. Luckily, this may, at least, encourage individuals to, at least, observe all kinds of fungi and slime mold to see if these beetles are there.

REFERENCES

ACHARD, J. Essai D'une Subdivision Nouvelle De La Famille Des Scaphidiidae. **Société entomologique de Belgique**, v. 65, p. 25–31, 1924.

ASHE, J. S. Description of the larva and pupa of *Scaphisoma terminatum* Melsh. and the larva of *Scaphium castanipes* Kirby with notes on their natural history (Coleoptera: Scaphidiidae). **The Coleopterists Bulletin**, v. 38, p. 361–373, 1984.

CASEY, T. L. Coleopterological Notices V. Scaphidiidae. **Annals of the New York Academy of Sciences**, v. 7, p. 510–533, 1893.

CSIKI, E. Catalogus Scaphidiidarum. **Rovartani Lapok**, v. 15, p. 151–174, 1908.

CSIKI, E. **Coleopterorum Catalogus. Pars 13: Scaphidiidae**. Berlin: W. Junk, 1910.

ERICHSON, W. F. **Naturgeschichte der Insecten Deutschlands. Erste Abteilung. Coleoptera. Dritter Band. Lieferung 1**. Berlin: Nicolaische Buchhandlung, 1845.

FIERROS-LÓPEZ, H. E. *Scaphidium mexicanum* Castelnau, 1840 (Coleoptera: Staphylinidae: Scaphidiinae). **Dugesiana,** v. 5, n. 2, p. 36–37, 1998.

FIERROS-LÓPEZ, H. E. Descripción de dos especies nuevas de *Cyparium* Erichson, 1845 (Coleoptera: Staphylinidae) de México. **Dugesiana**, v. 9, n. 2, p. 7–14, 2002.

FIERROS-LÓPEZ, H. E. Revisión del género *Scaphidium* Olivier, 1790 (Coleoptera, Staphylinidae) de México y Céntroamerica. **Dugesiana**, v. 12, p. 1–152, 2005.

FIERROS-LÓPEZ, H. E. Four new species of *Scaphisoma* Leach with maculate elytra (Coleoptera: Staphylinidae: Scaphidiinae) from Mexico, with new records and comments on *S. balteatum* Matthews. **Zootaxa**, v. 1279, n. 1, p. 53–53, 2006a.

FIERROS-LÓPEZ, H. E. Datos nuevos de distributión de algunas especies de Scaphidiinae Neotropicales (Coleoptera: Staphylinidae). **Dugesiana**, v. 13, p. 39–43, 2006b.

FIERROS-LÓPEZ, H. E. Description of Two New Species of *Baeocera* Erichson (Coleoptera: Staphylinidae: Scaphidiinae) from México. **Journal of the Kansas Entomological Society**, v. 83, n. 3, p. 201–207, 2010.

GEMMINGER, M.; HAROLD, E. **Catalogus coleopterorum hucusque descriptorum synonymicus et systematicus**. [*S. l.*]: Smithsonian Institution, 1868.

GREBENNIKOV, V. V.; NEWTON, A. F. Detecting the basal dichotomies in the monophylum of carrion and rove beetles (Insecta: Coleoptera: Silphidae and Staphylinidae) with emphasis on the Oxyteline group of subfamilies. **Arthropod Systematics & Phylogeny,** v. 70, n. 3, p. 133–165, 2012.

HANLEY, R. S. Immature stages of *Scaphisoma castaneum* Motschulsky (Coleoptera: Staphylinidae: Scaphidiinae), with observation on natural history, fungal hosts and development. **Proceedings of the Entomological Society of Washington**, v. 98, p. 36–43, 1996.

HANSEN, M. Phylogeny and classification of the staphyliniform beetle families (Coleoptera). **Biologiske Skrifter, Kongelige Danske Videnskabernes Selskab,** v. 48, p. 1–339, 1997.

KASULE, F. K. The subfamilies of the larvae of Staphylinidae (Coleoptera) with keys to the larvae of the British genera of Steninae and Proteininae. **Transactions of the Royal Entomological Society of London**, v. 118, n. 8, p. 261–283, 1966.

KASULE, F. K. The larval Characters of some subfamilies of British Staphylinidae (Coleoptera) with keys to the known genera. **Transactions of the Royal Entomological Society of London**, v. 120, n. 4, p. 115–138, 1968.

KOMPANTSEV, A. V.; POTOTSKAYA, V. A. Novye dannye po lichikam zhukov-chelnovidok (Coleoptera, Scaphidiidae). *In*: EKOLOGIYA I MORFOLOGIYA NASEKOMYCHOBYVATELEY GRIBNYCH SUBSTRATOV. [*S. l.*]: Nauka, Moskva, 1987. p. 87–100.

LATREILLE, P. A. **Genera Crustaceorum et Insectorum, secundem ordinem naturalem in familias dispositas, iconibus exemplisque plurimus explicata. Tomus secundus.** Paris: Amand Koenig, 1806-.

LAWRENCE, J. F.; NEWTON, A. F. Coleoptera associated with the fruiting bodies of slime molds (Myxomycetes). **The Coleopterists Bulletin**, v. 34, p. 129–143, 1980.

LAWRENCE, J. F.; NEWTON, A. F. Evolution and Classification of Beetles. **Annual Review of Ecology and Systematics**, v. 13, n. 1, p. 261–290, 1982.

LESCHEN, R. A. B. Retreat-building by larval Scaphidiinae (Staphylinidae). **Mola**, v. 4, p. 3–5, 1994.

LESCHEN, R. A. B.; LÖBL, I. Phylogeny of Scaphidiinae with redefinition of tribal and generic limits (Coleoptera: Staphylinidae). **Revue suisse de zoologie.**, v. 102, p. 425–474, 1995.

LESCHEN, R. A. B.; LÖBL, I. Phylogeny and classification of Scaphisomatini Staphylinidae: Scaphidiinae with notes on mycophagy, termitophily, and functional morphology. **Coleopterists Society Monographs**, v. 3, p. 1–63, 2005.

LÖBL, I. New species of the genus *Amalocera* Erichson from Brazil (Coleoptera, Scaphidiidae). **Studies on Neotropical Fauna**, v. 9, n. 1, p. 39–45, 1974.

LÖBL, I. Contribution to the knowledge of the genus Caryoscapha Ganglbauer (Coleoptera: Scaphidiidae). **The Coleopterists Bulletin**, v. 41, p. 385–391, 1987.

LÖBL, I. Catalogue of the Scaphidiinae (Coleoptera: Staphylinidae). **Instrumenta biodiversitatis**, v. 1, n. I–XII, p. 1–190, 1997.

LÖBL, I. **Coleoptera: Staphylinidae: Scaphidiinae**. [*S. l.*]: University of Illinois Urbana-Champaign, 2018.

LÖBL, I.; LESCHEN, R. A. B. Scaphidiinae (Insecta: Coleoptera: Staphylinidae). **Fauna of New Zealand**, v. 49, p. 1–94, 2003a.

LÖBL, I.; RICHARD. Redescription and new species of *Alexidia* (Coleoptera: Staphylinidae: Scaphidiinae). **Revue Suisse De Zoologie**, v. 110, p. 315–324, 2003b.

LÖBL, I.; LESCHEN, R. A. B.; WARNER, W. B. Scaphisomatini of Arizona (Coleoptera, Staphylinidae, Scaphidiinae) collected by V-Flight Intercept Traps. **Revue suisse de Zoologie**, v. 128, n. 1, 2021.

LÖBL, I.; OGAWA, R. On the Scaphisomatini (Coleoptera, Staphylinidae, Scaphidiinae) of the Philippines, IV: the genera *Sapitia* Achard and *Scaphisoma* Leach. **Linzer biologische**

Beiträge, v. 48, n. 2, p. 1339–1492, 2016.

MCKENNA, D. D.; FARRELL, B. D.; CATERINO, M. S.; FARNUM, C. W.; HAWKS, D. C.; MADDISON, D. R.; SEAGO, A. E.; SHORT, A. E. Z.; NEWTON, A. F.; THAYER, M. K. Phylogeny and evolution of Staphyliniformia and Scarabaeiformia: forest litter as a stepping stone for diversification of nonphytophagous beetles. v. 40, n. 1, p. 35–60, 2015.

MORRONE, J. J. Biogeographical regionalisation of the world: a reappraisal. **Australian Systematic Botany**, v. 28, n. 3, p. 81, 2015.

NAOMI, S. - I. The phylogeny and higher classification of the Staphylinidae and their allied groups (Coleoptera, Staphylinoidea). **Esakia**, v. 23, p. 1–27, 1985.

NEWTON, A. F. Jr. Scaphidiidae (Staphylinoidea). *In*: STEHR, F. W. (org.). **Immature Insects. Volume 2**. Dubuque: Kendall/Hunt Publishing Company, 1991. p. 337–339.

NEWTON JR., A. F. Mycophagy in Staphylinoidea (Coleopetra). *In*: WHEELER, Q.; BLACKWELL, M. (org.). **Fungus/insect relationships. Perspectives in ecology and evolution**. New York: Columbia University Press, 1984. p. 302–353.

NEWTON, A. F.; THAYER, M. K. Current classification and family-group names in Staphyliniformia (Coleoptera). **Fieldiana: Zoology N.S.**, v. 67, p. 1–92, 1992.

REITTER, E. Die Gattungen und Arten der Coleopteren-Familie: Scaphidiidae meiner Sammlung. **Verhandlungen des Naturforschenden Vereins in Brünn,** v. 18, n. 1879, p. 35–49, 1880.

STEPHENSON, S. L.; WHEELER, Q. D.; MCHUGH, J. V.; FRAISSINET. P. R. New North American associations of Coleoptera with Myxomycetes. **Journal of Natural History**, v. 28, n. 4, p. 921–936, 1994.

TANG, L.; LI, L.-Z.; HE, W.-J. The genus *Scaphidium* Olivier in East China (Coleoptera, Staphylinidae, Scaphidiinae). **ZooKeys**, v. 403, p. 47–96, 2014.

VON GROLL, E.; LOPES-ANDRADE, C. *Scaphisoma pandemum* sp. nov. (Coleoptera: Staphylinidae: Scaphidiinae) from the Atlantic Forest of Southeast Brazil. **Zootaxa**, v. 4999, n. 2, 2021.